

Hepatitis E: An overview and recent advances in vaccine research

Ling Wang, Hui Zhuang

Ling Wang, Hui Zhuang, Department of Microbiology, Peking University Health Science Center, Beijing 100083, China

Supported by the National Major Projects of National Committee of Science and Technology (2502AA2Z3342), and the Beijing Municipal Committee of Science and Technology (H020920020190)

Correspondence to: Hui Zhuang, Professor of Department of Microbiology, Peking University Health Science Center, Beijing 100083, China. zhuanghu@publica.bj.cninfo.net

Telephone: +86-10-82802221 **Fax:** +86-10-82801617

Received: 2003-11-22 **Accepted:** 2004-01-08

Abstract

Hepatitis E virus (HEV) is an unclassified, small, non-enveloped RNA virus, as a causative agent of acute hepatitis E that is transmitted principally via the fecal-oral route. The virus can cause large water-borne epidemics of the disease and sporadic cases as well. Hepatitis E occurs predominantly in developing countries, usually affecting young adults, with a high fatality rate up to 15-20% in pregnant women. However, no effective treatment currently exists for hepatitis E, and the only cure is prevention. But so far there are no commercial vaccines for hepatitis E available in the world. Although at least four major genotypes of HEV have been identified to date, only one serotype of HEV is recognized. So there is a possibility to produce a broadly protective vaccine. Several studies for the development of an effective vaccine against hepatitis E are in progress and the best candidate at present for a hepatitis E vaccine is a recombinant HEV capsid antigen expressed in insect cells from a baculovirus vector. In this article, the recent advances of hepatitis E and the development of vaccine research for HEV including recombinant protein vaccine, DNA vaccine and the recombinant hepatitis E virus like particles (rHEV VLPs) are briefly reviewed.

Wang L, Zhuang H. Hepatitis E: An overview and recent advances in vaccine research. *World J Gastroenterol* 2004; 10(15): 2157-2162

<http://www.wjgnet.com/1007-9327/10/2157.asp>

INTRODUCTION

Hepatitis E previously known as enterically transmitted non-A, non-B hepatitis, is an infectious viral disease with clinical and epidemiological features of acute hepatitis. It is a water-borne disease, transmitted primarily by contaminated water. There is also a possibility of zoonotic spread of the virus, since several non-human primates, pigs, cows, sheep, goats and rodents are susceptible to the infection^[1,2]. Hepatitis E virus (HEV) is a principal cause of acute hepatitis in adults throughout much of Asia, Middle East and Northern Africa^[3] and transmitted from person-to-person through the fecal-oral route. HEV had provisionally been classified into the *caliciviridae* family from 1988 to 1998, but now it is classified into the separate genus *Hepatitis E-like viruses*^[4-6] because the phylogenetic analysis of non-structural regions of the virus did not support the classification of HEV into the *Caliciviridae* family^[7]. Although at least four major genotypes have been

identified, only one serotype of HEV is recognized^[8-10]. HEV infection is endemic in developing countries where sanitary conditions are not well maintained. Over 50 outbreaks have been reported in Southeast and Central Asia, the Middle East, northern and western parts of Africa, and Mexico^[11-15]. Most of hepatitis E cases in developed countries have been linked to travel to endemic areas. However, recent studies revealed that hepatitis E also occurred in patients who had never been abroad^[16-18]. China is one of the high epidemic areas and there have been 11 hepatitis E epidemics reported to date. The largest one in the world occurred in Xinjiang Uighur Autonomous Region, the Northwest of China, during 1986-1988, with a total number of 119 280 cases and more than 700 deaths^[19-20]. Hepatitis E accounts for more than 50% of acute viral hepatitis in young adults of developing countries, although only 1% to 3% of non-pregnant patients progress to fatal fulminant hepatitis, the case-fatality rate can be as high as 20% among pregnant patients^[21], constituting a serious public health problem and stressing the need for development of an effective vaccine. The development of an attenuated or killed vaccine is not currently possible because of lacking an efficient cell culture system for replication of HEV^[22-27], although some cell lines have been reported for culturing and isolating HEV *in vitro*^[28,29]. Therefore, either a nucleic acid-based vaccine or a recombinant protein vaccine is needed. Compared with gene engineering vaccine for hepatitis B, the study of hepatitis E recombinant vaccine was only a recent endeavor, but some progress has been made^[30].

HEV GENOME

HEV genome consists of a linear, single-stranded, positive-sense RNA of approximately 7.5 kb containing a 3' poly (A) tail and 3' noncoding (NC) regions, and contains three overlapping open reading frames (ORFs). All three coding frames are used to express different proteins^[31-33] (Figure 1). ORF1 begins at the 5' end of the viral genome after a 27-bp non-coding sequence and extends 5 079 nt to the 3' end. ORF1 encodes a polyprotein of about 1 690 amino acids (aa) consisting of non-structural proteins that are involved in viral genome replication and viral protein processing, as its sequence contains motifs characteristic of viral methyltransferases, papain-like cysteineproteases, helicases and RNA-dependent RNA polymerases. In addition, ORF1 has two regions called Y and X domains of unknown function. The very short 5' NTR at the 5' end of the viral genome of 27-35 nucleotides is consistent with a capped genome. The ability of a monoclonal antibody to recognize 7-methylguanosine in RNA extracted from virions of different HEV genotypes suggests that HEV RNAs are capped^[34,35]. ORF3 is 369 nt long, located at the end of ORF1 and overlaps ORF1 at its 5' end by only 1 nt, and overlaps ORF2 by 328 nt. It encodes for a 123-aa protein (pORF3), which is expressed intracellularly. The studies of the biology of HEV replication have shown that pORF3 may be capable of associating with the liver cell cytoskeleton and appears to serve as a cytoskeletal anchor site, where pORF2 and RNA can bind to begin the process of viral nucleocapsid assembly^[36].

The ORF2 is located between 5 147 and 7 127 nt, consists of 1 980 nt and encodes 660 aa (71-88 kDa) most likely representing one or more structural or capsid protein(s)^[2,29-31].

However, the size of the ORF2 protein in native virions is not known^[37]. *In vitro* assays suggest that the -88 kDa of glycoprotein is co-translationally translocated across the endoplasmic reticulum and is expressed intracellularly as well as on the cell surface^[38]. ORF2 contains important epitopes that can induce neutralizing antibodies and has been the focus of vaccine development^[39]. Major epitopes appear to exist near the carboxyl ends of ORF2 and ORF3. Epitopes contained in ORF2 are more conserved (90.5%) than epitopes contained in ORF3 (73.5%) in different strains. Many different ORF2 antigens have been shown to induce antibody (Table 1). There are a number of reports suggesting that truncated ORF2 peptide of shorter length might be more antigenic than the full-length protein^[40-44]. However, in the majority of cases, it has not been shown that the resulting antibodies are neutralizing and, therefore, it is not known whether these antigens could serve as vaccine candidates. Only three ORF2 antigens (trpE-C2, Burma 62 kDa, Pakistan 55 kDa) thus far have been shown to induce antibodies that neutralize the virus^[33].

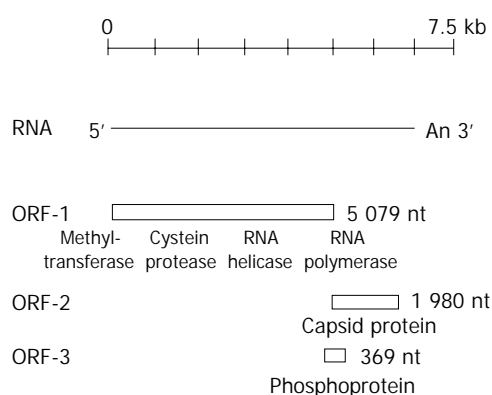


Figure 1 Genetic map of hepatitis E virus.

Table 1 HEV ORF2 antigenic peptides

HEV (origin)	Designation	Amino acid	
		N'	C'
Expressed in <i>E. coli</i>			
China	ORF2	1	660
Burma	TrpE-C2	221	660
Burma	SG3	328	654
China	ORF2.1	394	660
Mexico, Burma	3.2	612	654
Expressed in insect cells			
Burma	72 ku	1	660
Pakistan	63 ku	112	660
Burma	62 ku	112	636
Pakistan	55 ku	112	607
Pakistan	53 ku	112	578
Burma	50 ku	112	534
DNA vaccine			
Burma	pJHEV	1	660
China	pSVL-ORF3	1	123

HEV GENOTYPE

The genome sequence of HEV seems relatively stable^[45]. The genome of strains isolated from geographically distinct locations is generally more diverse. At present, no consensus exists on genotype classification. The detected HEV strains are currently genetically characterized in laboratories on the basis of ORFs regions^[32]. Recently, some research workers have

also started to characterize HEV strains antigenetically using specific antibodies produced by the recombinant expressed capsid proteins^[46,47]. On the basis of viruses having nucleotide divergence of not more than 20% of the nucleotides in the ORF2 region^[48], the genomes of several HEV strains from different parts of the world can be grouped into at least four major genotypes^[8,31,32,49]: Genotype 1 -including the isolates from South-East Asian (Burmese, some Indian strains), North and Central Asian (strains from China, Pakistan, Kyrgyzstan, and India), and North African strains; Genotype 2 -comprising the single North American (Mexico) isolate; Genotype 3 -consisting of the US and swine isolates; and Genotype 4 -including a subset of isolates from China and most isolates from Taiwan. Genetically heterogeneous isolates from several European countries have been designated new genotypes, but probably should be grouped with the US isolates into a large, heterogeneous group^[31,50]. Two novel isolates of HEV have recently been described in Argentina. Distinct from all previously described isolates, they represent two diverse subtypes of a new genotype of HEV^[51]. Despite the diversity of HEV genotype, no evidence has been found that heterogeneity results from the genetic diversity, thus HEV seems to exist as a single serotype^[8-10].

HEV VACCINE RESEARCHES

At present, no commercially available vaccines exist for the prevention of hepatitis E. However, several studies for the development of an effective vaccine against hepatitis E are in progress^[37,52-56]. Several lines of evidence have suggested the feasibility of a HEV vaccine. First, serum antibodies to HEV develop in response to naturally acquired and experimentally induced HEV infections in cynomolgus monkeys^[57]. Second, seroepidemiology of hepatitis E suggests that people previously infected with HEV are protected during epidemics of the disease^[58]. Finally, successful passive immune prophylaxis in animals indicated that effective vaccination against hepatitis E based on humoral immunity is possible^[59]. Although different geographical isolates of HEV have been identified, only one serotype has been recognized^[8]. So it may be possible to produce a broadly protective vaccine.

ORF2-encoded protein of HEV is the most promising subunit vaccine candidate because it possesses a good antigenicity. So far, HEV ORF2 gene or its fragments have been expressed in prokaryote cells^[56,60-64], insect cells^[37,65-68], yeast cells^[69-71], animal cells^[72], and plants (tomatoes)^[30], etc., and the expression products possess immunogenicity.

Expression in prokaryote cells

It was reported recently that the smallest fragment of ORF2, which is capable of combining the neutralizing antibody of HEV, is located between 452 and 617 aa. This fragment does not only induce neutralizing antibody, but also cross react to the antibody of other genotype^[22]. It was demonstrated that the 2/3 length of C-terminal region of HEV ORF2 contains epitopes, which are recognized by both acute-phase and convalescent-phase antibody to HEV and are likely to be associated with limited immunity to the infection, but these epitopes may be masked when larger portions of ORF2 are expressed as recombinant proteins^[64]. So far, many different length of ORF2 fragments have been expressed in *E. coli*^[56,63,64], but only a few expression products have been found with significant immunoactivity. The first candidate HEV vaccine was a recombinant fusion protein including 439 amino acids (221-660 aa). It comprised tryptophan synthetase and the carboxy terminal fragment of the ORF2 protein of the Burmese strain (genotype 1) and was expressed in *E. coli*. Two cynomolgus macaques were vaccinated with the fusion protein,

and neither of them developed hepatitis following experimental challenge. The animals challenged with the heterologous HEV, the Mexican strain (genotype 2), did get infected, but did not develop hepatitis^[73]. Another study also shows that the immunization with the bacterially expressed ORF2 peptide (pE2) corresponding to 394–607 aa, may prevent HEV infection in primates experimentally transmitted with the homologous strain of HEV^[56].

Expression in insect cells

It is thought that the best candidate at present for a hepatitis E vaccine is a recombinant HEV capsid antigen expressed in insect cells from a baculovirus vector^[25]. When ORF2 of genotype 1 strain is expressed from a baculovirus vector in insect cells, the initial 72-ku protein is quickly processed to smaller proteins, possibly via a protease encoded by the baculovirus^[66]. The most abundant proteins are 56 ku and 53 ku in size, respectively. However, the only neutralization epitope identified to date was mapped to a region of the ORF2 protein of Sar-55 between amino acids 578 and 607^[74]. Therefore, the 56 ku protein (112–607 aa) but not the 53 ku protein (112–578 aa) should contain this epitope. The recombinant 56 ku protein that is more soluble than the full-length protein was an efficient immunogen when adjuvanted with alum^[53,57]. Two 400 ng doses of the vaccine were injected to rhesus monkeys intramuscularly and high antibody titers (1:10 000) were achieved. The monkeys were protected against hepatitis E following intravenous challenge with 300 000 monkey infectious doses (MID₅₀) of the homologous (Sar-55) or 100 000 MID₅₀ of a heterologous HEV (Mexican 14)^[57]. To evaluate the immunogenicity and protective efficacy of the 53 kDa protein, the same research group immunized rhesus monkeys with the 53 ku vaccine, which was derived from processing of the ORF2 protein of Sar-55 and purified from the medium of recombinant baculovirus-infected insect cells and precipitated with alum. Two doses of vaccine containing 385 ng of alum-precipitated 53 ku protein were inoculated into the monkeys intramuscularly. The immunized monkeys were challenged with a high (1000 MID₅₀) or low (100 MID₅₀) dose of homologous virus. The result showed vaccination with the 53 ku protein greatly reduced virus shedding, but did not protect against hepatitis following the high dose challenge. Virus was not detected in the vaccinated animals following the low dose challenge, suggesting that sterilizing immunity might have been achieved. This study indicated that the 53 ku protein did not function as a better vaccine than did the 56 ku protein and actually appeared to have been less effective in preventing disease^[37]. The researches have shown that almost complete vaccine-induced protection lasts for at least 6 mo and partial protection persists for at least 1 year following vaccination^[75].

Expression in yeast and other cells

Recently, yeast expression system has been successfully used for production of vaccines, for example, the recombinant hepatitis B surface antigen^[76,77]. There are some advantages of using this expression system, such as the expression products similar to the natural protein, maintaining the biological activity of the production, to produce easily in large scale and so on^[78]. In recent studies, the ORF2 of HEV (69–660 aa and 112–660 aa) was successfully expressed in *pichia pastoris* and the expression products of recombinant protein (59 ku) was purified and immunized to rhesus monkeys. High titer of anti-HEV (1:8000) was detected in the immunized monkeys^[69–71,79]. Research on using plants for expression and delivery of oral vaccine has attracted much academic attention and has become a hot spot of study since 1990 when Curtiss *et al.*^[80] first reported the expression of *Streptococcus* mutants surface protein antigen A (SpaA) in tobacco, and great progress has

been made since then^[81]. In a recent study, the ORF2 partial gene of HEV named E2 (810 bp, 349–604 aa) was constructed into plasmid pCAMBIA1301 and yielded the reconstructed plant binary expression plasmid p1301E2^[62]. The p1301E2 was expressed in tomatoes and the recombinant antigen derived from them has normal immunoactivity. The transgenic tomatoes may hold a good promise for producing a new type of low-cost oral vaccine for hepatitis E^[30].

Subunit HEV vaccines

DNA immunization usually induces both cellular and antibody immune response. So it might provide a longer duration of protection. Therefore, it has become another focus of HEV vaccine research. Recombinant DNA vaccine is a recently developed new type of vaccine. Through directly injecting the recombinant plasmid DNA with the target gene into human or animals, the DNA will express the expected protein inside the host cells and therefore induce the immune responses to prevent and fight the disease. Recently, a new technology has been introduced for the development of subunit vaccines involving the direct injection of purified plasmid DNA containing protein coding sequences of interest and appropriate regulatory elements allowing expression in mammalian tissues. This novel technology has several potential advantages over other vaccine approaches^[82]. First, the antigens expressed in living cells are in their native form, improving processing and presentation and usually resulting in the activation of both arms of the immune system. Second, DNA can be made inexpensively, in large quantities, at high levels of purity, and is extremely stable. Third, the vector is unlikely to be, or to become, pathogenic, in contrast to live-virus vaccines, and there is little or no immune response to the vector.

In an early study, an HEV cDNA pSVL-ORF3 was constructed by inserting the full length of ORF3 fragment into prokaryotic expression vector pSVL. A total amount of 100 µg of the cDNA was injected to BALB/c mice intramuscularly and anti-HEV IgG was detected in 12 of the 16 immunized mice. However, no antibody was found in the mice injected with the empty vector. The result indicated that the recombinant HEV cDNA could induce the antibody response in mice^[83]. Later, another HEV cDNA pJHEV was constructed by inserting full length of ORF2 fragment. The HEV structural protein was expressed in Cos-7 cells under the control of a hCMV promoter. The successful construct was further tested in BALB/c mice for the induction of an ORF2 specific immune response. All the mice immunized with the cDNA were found seroconverted, but no anti-HEV responses induced in the mice of control group. Sera from the mice injected with pJHEV specifically recognized HEV ORF2 structural protein expressed in recombinant baculovirus in an enzyme-linked-immunosorbent assay (ELISA) and Western blot^[82]. Furthermore, it was also shown that the antiserum generated by the DNA vaccine could bind specifically to native HEV^[84]. Recently, a full-length HEV cDNA clone was constructed in a pSGI vector. The three ORFs were amplified separately and then reconstructed to the full-length clone. The *in vitro* transcribed RNA of the full-length cDNA clone was infective in a HepG2 tissue culture. Viral replication was detected for six passages with strand-specific PCR^[85].

The rHEV VLPs

In spite of the above vaccine candidates, recently the recombinant hepatitis E virus (rHEV) virus-like particles (VLPs) are also the focuses of vaccine research for hepatitis E. With 111 amino acids truncated at the N-terminal, when the capsid protein of HEV was expressed in the baculovirus expression system, it was spontaneously assembled into virus-like particles^[54]. Electron cryomicroscopy shows that these VLPs are formed with

60 copies of a 54 ku protein arranged in T=1 symmetry^[54, 86, 87]. As a mucosal immunogen, the VLPs have several advantages: they are composed of a single protein assembled into particles without nucleic acid, which makes them unable to replicate; they are easy to prepare and purify in large quantities, with a yield of approximately 1 mg /10⁷ insect cells; rHEV VLPs are antigenically similar to the native virions; they are highly immunogenic in experimental animals when injected parenterally; they are very stable at low pH such as in stomach; and oral delivery of rHEV VLPs could induce the same immune responses as occur in natural infection^[86,54].

In a previous study^[87], mice were orally inoculated with purified rHEV VLPs without adjuvant. Serum IgM response was obtained within 2 wk after the first administration. Serum IgG and IgA were detected by 4 wk, and the intestinal IgA response was found at 8 wk post-immunization. Therefore, the oral immunization of rHEV VLPs is capable of inducing both systemic and intestinal antibody responses. However, since mice are not susceptible to HEV, the same group recently immunized cynomolgus monkeys orally with 10 mg of purified rHEV VLPs, serum IgM, IgG, and IgA responses were observed. All these antibody responses were obtained without adjuvants. When the monkeys were challenged with native HEV by intravenous injection, they were protected against infection or developing hepatitis. These results suggested that rHEV VLPs could be a candidate for the oral hepatitis E vaccine^[88]. Some similar experiments have been described previously^[89-91].

PRE-CLINICAL AND CLINICAL TRIALS

So many vaccine candidates for hepatitis E have been explored as described above. But so far, there is only one HEV vaccine candidate progressed to the stage of clinical trials. That is the 56 ku (expressed in insect cells from a baculovirus vector) recombinant vaccine developed at the NIH, USA^[68]. In phase I trial, the vaccine was found to be safe and immunogenic in 88 American volunteers. A further phase I evaluation was performed in Nepal, where hepatitis E is endemic. Three doses of 5 µg and 20 µg, respectively, were injected into 22 Nepalese volunteers each at zero, one and six months. No serious adverse events were observed. By the second month, 43 of 44 volunteers had seroconverted to anti-HEV. By the 7th month, the remaining volunteers also developed antibody to HEV. The study indicated that the HEV vaccine candidate was safe and immunogenic. This same lot of vaccine is currently being used in phase II/III clinical trials in Nepal^[25], where as many as 90% of the jaundice cases are caused by HEV.

In recent pre-clinical trials, the vaccine used in the experiment was from the same lot that was prepared for the above clinical trials. The results indicated that two doses of HEV vaccine as small as 1 µg were highly effective in preventing not only hepatitis but also infection following intravenous administration of 10⁴ MID₅₀ of virulent virus. However, these doses of vaccine will not be sufficient for long-term protection. Other studies have shown that a third dose of vaccine at 6 or 12 mo following the first dose will enhance immunogenicity and/or efficacy^[75,92]. The study has also confirmed that the cross-protection against a Mexican genotype 2 isolate and extended the evidence for cross-protection to a US genotype 3 isolate of HEV. The results of this experiment have shown that the manufacture of a candidate hepatitis E vaccine can be scaled up to produce more clinical quality and that such a vaccine is highly immunogenic and effective for preventing hepatitis E in the pre-clinical trials. It is likely that protection against infection will be more effective following natural oral challenge with relatively small doses of HEV^[25].

CONCLUSIONS

Despite the achievements mentioned above, there are still many questions to be answered in future. For example, there is a study showing that acute hepatitis E can be induced by plasma transfusion from a donor with HEV viremia, which indicates the possibility of transfusion transmitted hepatitis E^[93]. Some similar studies also showed the possibility of post-transfusion hepatitis E^[94-97]. Therefore, effective measures for preventing post-transfusion hepatitis E must be taken. To achieve effective immunization, how should the HEV vaccine be given by, orally or intramuscularly? Will a monovalent vaccine protect against all HEV strains including HEV from animals and genotypes and provide a long-term immunity to hepatitis E? To facilitate vaccine development and to improve our knowledge about the mechanism of virus replication, an effective practical cell culture system should be established and demonstrated.

REFERENCES

- Harrison TJ. Hepatitis E virus-an update. *Liver* 1999; **19**: 171-176
- Aggarwal R, Krawczynski K. Hepatitis E: an overview and recent advances in clinical and laboratory research. *J Gastroenterol Hepatol* 2000; **15**: 9-20
- Perez-Gracia MT, Rodriguez-Iglesias M. Hepatitis E virus: current status. *Med Clin* 2003; **121**: 787-792
- Pringle CR. Virus taxonomy-San Diego 1998. *Arch Virol* 1998; **143**: 1449-1459
- Pringle CR. Virus taxonomy-1999. The universal system of virus taxonomy, updated to include the new proposals ratified by the International Committee on Taxonomy of Virus during 1998. *Arch Virol* 1999; **144**: 421-429
- Green KY, Ando T, Balayan MS, Berke T, Clarke IN, Estes MK, Matson DO, Nakata S, Neill JD, Studdert MJ, Thiel HJ. Taxonomy of the caliciviruses. *J Infect Dis* 2000; **181**(Suppl 2): S322-S330
- Berke T, Matson DO. Reclassification of the Caliciviridae into distinct genera and exclusion of hepatitis E virus from the family on the basis of comparative phylogenetic analysis. *Arch Virol* 2000; **145**: 1421-1436
- Schlauder GG, Mushahwar IK. Genetic heterogeneity of hepatitis E virus. *J Med Virol* 2001; **65**: 282-292
- Meng XJ, Purcell RH, Halbur PG, Lehman JR, Webb DM, Tsareva TS, Haynes JS, Thacker BJ, Emerson SU. A novel virus in swine is closely related to the human hepatitis E virus. *Proc Natl Acad Sci U S A* 1997; **94**: 9860-9865
- Wang Y, Zhang H, Ling R, Li H, Harrison TJ. The complete sequence of hepatitis E virus genotype 4 reveals an alternative strategy for translation of open reading frames 2 and 3. *J Gen Virol* 2000; **81**(Pt 7): 1675-1686
- Viswanathan R. A review of the literature on the epidemiology of infectious hepatitis. *Indian J Med Res* 1957; **45**(Suppl): 145-155
- Khuroo MS. Study of an epidemic of non-A, non-B hepatitis. Possibility of another human hepatitis virus distinct from post-transfusion non-A, non-B type. *Am J Med* 1980; **68**: 818-824
- Arora NK, Panda SK, Nanda SK, Ansari IH, Joshi S, Dixit R, Bathla R. Hepatitis E infection in children: study of an outbreak. *J Gastroenterol Hepatol* 1999; **14**: 572-577
- Naik SR, Aggarwal R, Salunke PN, Mehrotra NN. A large water-borne viral hepatitis E epidemic in Kanpur, India. *Bull World Health Organ* 1992; **70**: 597-604
- Velazquez O, Stetler HC, Avila C, Ornelas G, Alvarez C, Hadler SC, Bradley DW, Sepulveda J. Epidemic transmission of enterically transmitted non-A, non-B hepatitis in Mexico, 1986-1987. *JAMA* 1990; **263**: 3281-3285
- Schlauder GG, Dawson GJ, Erker JC, Kwo PY, Knigge MF, Smalley DL, Rosenblatt JE, Desai SM, Mushahwar IK. The sequence and phylogenetic analysis of a novel hepatitis E virus isolated from a patient with acute hepatitis reported in the United States. *J Gen Virol* 1998; **79**(Pt 3): 447-456
- Erker JC, Desai SM, Schlauder GG, Dawson GJ, Mushahwar IK. A hepatitis E virus variant from the United States: molecular characterization and transmission in cynomolgus macaques. *J Gen Virol* 1999; **80**(Pt 3): 681-690

- 18 **Takahashi K**, Iwata K, Watanabe N, Hatahara T, Ohta Y, Baba K, Mishiro S. Full-genome nucleotide sequence of a hepatitis E virus strain that may be indigenous to Japan. *Virology* 2001; **287**: 9-12
- 19 **Zhuang H**, Cao XY, Liu CB, Wang GM. Epidemiology of hepatitis E in China. *Gastroenterol Jpn* 1991; **26**(Suppl): 135-138
- 20 **Zhuang H**, Zhu WF, Li F, Zhu XJ, Li K, Cui YH, Zhu YH. Studies on hepatitis E. *Chin Med Sci J* 1999; **14**(Suppl): S47-50
- 21 **Skidmore S**. Overview of hepatitis E virus. *Curr Infect Dis Rep* 2002; **4**: 118-123
- 22 **Meng J**, Dai X, Chang JC, Lopareva E, Pillot J, Fieds HA, Khudyakov YE. Identification and characterization of the neutralization epitope(s) of the hepatitis E virus. *Virology* 2001; **288**: 203-211
- 23 **Schofield DJ**, Purcell RH, Nguyen HT, Emerson SU. Monoclonal antibodies that neutralize HEV recognize an antigenic site at the carboxyterminus of an ORF2 protein vaccine. *Vaccine* 2003; **22**: 257-267
- 24 **Meng J**, Dubreuil P, Pillot J. A new PCR-based seroneutralization assay in cell culture for diagnosis of hepatitis E. *J Clin Microbiol* 1997; **35**: 1373-1377
- 25 **Purcell RH**, Nguyen H, Shapiro M, Engle RE, Govindarajan S, Blackwelder WC, Wong DC, Prieels JP, Emerson SU. Pre-clinical immunogenicity and efficacy trial of a recombinant hepatitis E vaccine. *Vaccine* 2003; **21**: 2607-2615
- 26 **Zhang J**, Ge SX, Huang GY, Li SW, He ZQ, Wang YB, Zheng YJ, Gu Y, Ng MH, Xia NS. Evaluation of antibody-based and nucleic acid-based assays for diagnosis of hepatitis E virus infection in a rhesus monkey model. *J Med Virol* 2003; **71**: 518-526
- 27 **Grimm AC**, Fout GS. Development of a molecular method to identify hepatitis E virus in water. *J Virol Methods* 2002; **101**: 175-188
- 28 **Tam AW**, White R, Yarbough PO, Murphy BJ, McAttee CP, Lanford RE, Fuerst TR. *In vitro* infection and replication of hepatitis E virus in primary cynomolgus macaque hepatocytes. *Virology* 1997; **238**: 94-102
- 29 **Huang R**, Li D, Wei S, Li Q, Yuan X, Geng L, Li X, Liu M. Cell culture of sporadic hepatitis E virus in China. *Clin Diagn Lab Immunol* 1999; **6**: 729-733
- 30 **Ma Y**, Lin SQ, Gao Y, Li M, Luo WX, Zhang J, Xia NS. Expression of ORF2 partial gene of hepatitis E virus in tomatoes and immunoactivity of expression products. *World J Gastroenterol* 2003; **9**: 2211-2215
- 31 **Hepatitis E**. World health organization. *WHO/CDS/CSR/EDC/2001*: 12
- 32 **Worm HC**, van der Poel WH, Brandstatter G. Hepatitis E: an overview. *Microbes Infect* 2002; **4**: 657-666
- 33 **Emerson SU**, Purcell RH. Recombinant vaccines for hepatitis E. *Trends Mol Med* 2001; **7**: 462-466
- 34 **Magden J**, Takeda N, Li T, Auvinen P, Ahola T, Miyamura T, Merits A, Kaariainen L. Virus-specific mRNA capping enzyme encoded by hepatitis E virus. *J Virol* 2001; **75**: 6249-6255
- 35 **Kabrane-Lazizi Y**, Meng XJ, Purcell RH, Emerson SU. Evidence that the genomic RNA of hepatitis E virus is capped. *J Virol* 1999; **73**: 8848-8850
- 36 **Zafrullah M**, Ozdener MH, Panda SK, Jameel S. The ORF3 protein of hepatitis E virus is a phosphoprotein that associates with the cytoskeleton. *J Virol* 1997; **71**: 9045-9053
- 37 **Zhang M**, Emerson SU, Nguyen H, Engle RE, Govindarajan S, Gertin JL, Purcell RH. Immunogenicity and protective efficacy of a vaccine prepared from 53 kDa truncated hepatitis E virus capsid protein expressed in insect cells. *Vaccine* 2001; **20**: 853-857
- 38 **Zafrullah M**, Ozdener MH, Kumar R, Panda SK, Jameel S. Mutational analysis of glycosylation, membrane translocation, and cell surface expression of the hepatitis E virus ORF2 protein. *J Virol* 1999; **73**: 4074-4082
- 39 **Tam AW**, Smith MM, Guerra ME, Huang CC, Bradley DW, Fry KE, Reyes GR. Hepatitis E virus (HEV): molecular cloning and sequencing of the full-length viral genome. *Virology* 1991; **185**: 120-131
- 40 **Zhang Y**, McAttee P, Yarbough PO, Tam AW, Fuerst T. Expression, characterization, and immunoreactivities of a soluble hepatitis E virus putative capsid protein species expressed in insect cells. *Clin Diagn Lab Immunol* 1997; **4**: 423-428
- 41 **Ghabrah TM**, Tsarev S, Yarbough PO, Emerson SU, Strickland GT, Purcell RH. Comparison of tests for antibody to hepatitis E virus. *J Med Virol* 1998; **55**: 134-137
- 42 **Anderson DA**, Li F, Riddell M, Howard T, Seow HF, Torresi J, Perry G, Sumarsidi D, Shrestha SM, Shrestha IL. ELISA for IgG-class antibody to hepatitis E virus based on a highly conserved, conformational epitope expressed in *Escherichia coli*. *J Virol Methods* 1999; **81**: 131-142
- 43 **Li TC**, Zhang J, Shinzawa H, Ishibashi M, Sata M, Mast EE, Kim K, Miyamura T, Takeda N. Empty virus-like particle-based enzyme-linked immunosorbent assay for antibodies to hepatitis E virus. *J Med Virol* 2000; **62**: 327-333
- 44 **Obriadina A**, Meng J, Ulanova T, Trinta K, Burkov A, Fields H, Khudyakov Y. A new enzyme immunoassay for the detection of antibody to hepatitis E virus. *J Gastroenterol Hepatol* 2002; **17**(Suppl 3): S360-S364
- 45 **Arankalle VA**, Paranjape S, Emerson SU, Purcell RH, Walimbe AM. Phylogenetic analysis of hepatitis E virus isolates from India (1976-1993). *J Gen Virol* 1999; **80**(Pt 7): 1691-1700
- 46 **Riddell MA**, Li F, Anderson DA. Identification of immunodominant and conformational epitopes in the capsid protein of hepatitis E virus by using monoclonal antibodies. *J Virol* 2000; **74**: 8011-8017
- 47 **Wang Y**, Zhang H, Li Z, Gu W, Lan H, Hao W, Ling R, Li H, Harrison TJ. Detection of sporadic cases of hepatitis E virus (HEV) infection in China using immunoassays based on recombinant open reading frame 2 and 3 polypeptides from HEV genotype 4. *J Clin Microbiol* 2001; **39**: 4370-4379
- 48 **Anod T**, Noel JS, Fankhauser RL. Genetic classification of Norwalk-like viruses. *J Infect Dis* 2000; **181**(Suppl 2): S336-S348
- 49 **Wang Y**, Ling R, Erker JC, Zhang H, Li H, Desai S, Mushahwar IK, Harrison TJ. A divergent genotype of hepatitis E virus in Chinese patients with acute hepatitis. *J Gen Virol* 1999; **80**(Pt 1): 169-177
- 50 **Schlauder GG**, Desai SM, Zanetti AR, Tassopoulos NC, Mushahwar IK. Novel hepatitis E virus (HEV) isolates from Europe: evidence for additional genotypes of HEV. *J Med Virol* 1999; **57**: 243-251
- 51 **Schlauder GG**, Frider B, Sookoian S, Castano GC, Mushahwar IK. Identification of 2 novel isolates of hepatitis E virus in Argentina. *J Infect Dis* 2000; **182**: 294-297
- 52 **Purcell RH**, Emerson SU. Hepatitis E virus. In Knipe DM, Howley PM. *Fields Virology*, Fourth edition, V2 Lippincott and Wilkins, Philadelphia, PA 2001: 3051-3052
- 53 **Tsarev SA**, Tsareva TS, Emerson SU, Govindarajan S, Shapiro M, Gerin JL, Purcell RH. Recombinant vaccine against hepatitis E: dose response and protection against heterologous challenge. *Vaccine* 1997; **15**: 1834-1838
- 54 **Xing L**, Kato K, Li T, Takeda N, Miyamura T, Hammar L, Cheng RH. Recombinant hepatitis E capsid protein self-assembles into a dual-domain T=1 particle presenting native virus epitopes. *Virology* 1999; **265**: 35-45
- 55 **Yarbough PO**. Hepatitis E virus. Advances in HEV biology and HEV vaccine approaches. *Intervirology* 1999; **42**: 179-184
- 56 **Im SW**, Zhang JZ, Zhuang H, Che XY, Zhu WF, Xu GM, Li K, Xia NS, Ng MH. A bacterially expressed peptide prevents experimental infection of primates by the hepatitis E virus. *Vaccine* 2001; **19**: 3726-3732
- 57 **Tsarev SA**, Tsarva TS, Emerson SU, Govindarajan S, Shapiro M, Gerin JL, Purcell RH. Successful passive and active immunization of cynomolgus monkeys against hepatitis E. *Proc Natl Acad Sci U S A* 1994; **91**: 10198-10202
- 58 **Bryan JP**, Tsarev SA, Iqbal M, Ticehurst J, Emerson S, Ahmed A, Duncan J, Rafiqi AR, Malik IA, Purcell RH. Epidemic hepatitis E in Pakistan: patterns of serologic response and evidence that antibody to hepatitis E virus protects against disease. *J Infect Dis* 1994; **170**: 517-521
- 59 **Quiroga JA**, Cotonat T, Castillo I, Carreno V. Hepatitis E virus seroprevalence in acute viral hepatitis in a developed country confirmed by a supplemental assay. *J Med Virol* 1996; **50**: 16-19
- 60 **Zhang M**, Zhao H, Jiang Y. Expression of hepatitis E virus structural gene in *E. coli*. *Zhonghua Shiyan He Linchuang Bingduxue Zazhi* 1999; **13**: 130-132
- 61 **Bi S**, Lu J, Jiang L, Huang G, Pan H, Jiang Y, Zhang M, Shen X. Preliminary evidence that a hepatitis E virus (HEV) ORF2 recombinant protein protects cynomolgus macaques against challenge with wild-type HEV. *Zhonghua Shiyan He Linchuang Bingduxue Zazhi* 2002; **16**: 31-32
- 62 **Li SW**, Zhang J, He ZQ, Ge SX, Gu Y, Lin J, Liu RS, Xia NS. The

- study of aggregate of the ORF2 peptide of hepatitis E virus expressed in *Escherichia coli*. *Shengwu Gongcheng Xuebao* 2002; **18**: 463-467
- 63 **Li F**, Torresi J, Locarnini SA, Zhuang H, Zhu W, Guo X, Anderson DA. Amino-terminal epitopes are exposed when full-length open reading frame 2 of hepatitis E virus is expressed in *Escherichia coli*, but carboxy-terminal epitopes are masked. *J Med Virol* 1997; **52**: 289-300
- 64 **Li F**, Riddell MA, Seow HF, Takeda N, Miyamura T, Anderson DA. Recombinant subunit ORF2.1 antigen and induction of antibody against immunodominant epitopes in the hepatitis E virus capsid protein. *J Med Virol* 2000; **60**: 379-386
- 65 **Zhang M**, Yi Y, Zhan M, Liu C, Bi S. Expression of thermal stable, soluble hepatitis E virus recombinant antigen. *Zhonghua Shiyan He Linchuang Bingduxue Zazhi* 2002; **16**: 20-22
- 66 **Robinson RA**, Burgess WH, Emerson SU, Leibowitz RS, Sosnovtseva SA, Tsarev S, Purcell RH. Structural characterization of recombinant hepatitis E virus ORF2 proteins in baculovirus-infected insect cells. *Protein Expr Purif* 1998; **12**: 75-84
- 67 **McAtee CP**, Zhang Y, Yarbrough PO, Fuerst TR, Stone KL, Samander S, Williams KR. Purification and characterization of a recombinant hepatitis E protein vaccine candidate by liquid chromatography-mass spectrometry. *J Chromatogr B Biomed Appl* 1996; **685**: 91-104
- 68 **Stevenson P**. Nepal calls the shots in hepatitis E virus vaccine trial. *Lancet* 2000; **355**: 1623
- 69 **Tong YP**, Bi SL, Jiang YZ, Zhan MY. Intracellular expression of hepatitis E virus ORF2 protein in *pichia pastoris* and its purification. *Bingdu Xuebao* 2001; **17**: 34-37
- 70 **Tong YP**, Bi SL, Zhang MC, Lu J, Zhan MY. Extracellular expression of hepatitis E virus ORF2 protein in *pichia pastoris*. *Zhonghua Shiyan He Linchuangbing Duxue Zazhi* 2000; **14**: 391-392
- 71 **Tong YP**, Lu J, Jian YZ, Bi SL, Zhan MY. The application of recombinant HEV ORF2 protein expressed in yeast cells to the diagnosis of hepatitis E. *Zhonghua Shiyan He Linchuang Bingduxue Zazhi* 2001; **15**: 189-190
- 72 **Jameel S**, Zafrullah M, Ozdener MH, Panda SK. Expression in animal cells and characterization of the hepatitis E virus structural proteins. *J Virol* 1996; **70**: 207-216
- 73 **Purdy MA**, McCaustland KA, Krawczynski K, Spelbring J, Reyes GR, Bradley DW. Preliminary evidence that a trpE-HEV fusion protein protects cynomolgus macaques against challenge with wild-type hepatitis E virus (HEV). *J Med Virol* 1993; **41**: 90-94
- 74 **Schofield DJ**, Glamann J, Emerson SU, Purcell RH. Identification by phage display and characterization of two neutralizing chimpanzee monoclonal antibodies to the hepatitis E virus capsid protein. *J Virol* 2000; **74**: 5548-5555
- 75 **Zhang M**, Emerson SU, Nguyen H, Engle R, Govindarajan S, Blasckwelder WC, Gerin J, Purcell RH. Recombinant vaccine against hepatitis E: duration of protective immunity in rhesus macaques. *Vaccine* 2002; **20**: 3285-3291
- 76 **Torres J**, Earnest-Silveira L, Deliyannis G, Edgtton K, Zhuang H, Locarnini SA, Fyfe J, Sozzi T, Jackson DC. Reduced antigenicity of the Hepatitis B virus HBsAg protein arising as a consequence of sequence changes in the overlapping polymerase gene that are selected by lamivudine therapy. *Virology* 2002; **293**: 305-313
- 77 **Zhang YX**, Dai L, Sun XM. Kinetic aspect of hepatitis B surface antigen production in recombinant *Saccharomyces cerevisiae* fermentation. *Process Biochemistry* 2003; **38**: 1593-1598
- 78 **Romanos M**. Advances in the use of *pichia pastoris* for high-level gene expression. *Curr Opin Biotechnol* 1995; **6**: 527-533
- 79 **Lu J**, Tong YP, Jiang YZ, Bi SL. The application of recombinant HEV ORF2 protein expressed in yeast cells to the detection of serum antibody in experimental rhesus monkeys. *Zhonghua Shiyan He Linchuang Bingduxue Zazhi* 2001; **15**: 382-383
- 80 **Curtiss R 3rd**, Galan JE, Nakayama K, Kelly SM. Stabilization of recombinant avirulent vaccine strains *in vivo*. *Res Microbiol* 1990; **141**: 797-805
- 81 **Gao Y**, Ma Y, Li M, Cheng T, Li SW, Zhang J, Xia NS. Oral immunization of animals with transgenic cherry tomatillo expressing HBsAg. *World J Gastroenterol* 2003; **9**: 996-1002
- 82 **He J**, Hoffman SL, Hayes CG. DNA inoculation with a plasmid vector carrying the hepatitis E virus structural protein gene induces immune response in mice. *Vaccine* 1997; **15**: 357-362
- 83 **Lu FM**, Zhuang H, Zhu YH, Zhu XI. A preliminary study on immune response to hepatitis E virus DNA vaccine in mice. *Chin Med J* 1996; **109**: 919-921
- 84 **He J**, Binn LN, Caudill JD, Asher LV, Longer CF, Innis BL. Antiserum generated by DNA vaccine binds to hepatitis E virus (HEV) as determined by PCR and immune electron microscopy (IEM): application for HEV detection by affinity-capture RT-PCR. *Virus Res* 1999; **62**: 59-65
- 85 **Panda SK**, Ansari IH, Durgapal H, Agrawal S, Jameel S. The *in vitro*-synthesized RNA from a cDNA clone of hepatitis E virus is infectious. *J Virol* 2000; **74**: 2430-2437
- 86 **Li TC**, Yamakawa Y, Suzuki K, Tatsumi M, Razak MA, Uchida T, Takeda N, Miyamura T. Expression and self-assembly of empty virus-like particles of hepatitis E virus. *J Virol* 1997; **71**: 7207-7213
- 87 **Li T**, Takeda N, Miyamura T. Oral administration of hepatitis E virus-like particles induces a systemic and mucosal immune response in mice. *Vaccine* 2001; **19**: 3476-3484
- 88 **Li TC**, Suzaki Y, Ami Y, Dhole TN, Miyamura T, Takeda N. Protection of cynomolgus monkeys against HEV infection by oral administration of recombinant hepatitis E virus-like particles. *Vaccine* 2004; **22**: 370-377
- 89 **Rose RC**, Lane C, Wilson S, Suzich JA, Rybicki E, Williamson AL. Oral vaccination of mice with human papillomavirus virus-like particles induces systemic virus-neutralizing antibodies. *Vaccine* 1999; **17**: 2129-2135
- 90 **Ball JM**, Hardy ME, Atmar RL, Conner ME, Estes MK. Oral immunization with recombinant Norwalk virus-like particles induces a systemic and mucosal immune response in mice. *J Virol* 1998; **72**: 1345-1353
- 91 **Estes MK**, Ball JM, Guerrero RA, Opekun AR, Gilger MA, Pacheco SS, Graham DY. Norwalk virus vaccine: Challenges and progress. *J Infect Dis* 2000; **181**(Suppl 2): S367-373
- 92 **Safary A**. Perspectives of vaccination against hepatitis E. *Intervirology* 2001; **44**: 162-166
- 93 **Xia NS**, Zhang J, Zheng YJ, Qiu Y, Ge SX, Ye XZ, Ou SH. Detection of hepatitis E virus on a blood donor and its infectivity to rhesus monkey. *Zhonghua Ganzangbing Zazhi* 2004; **12**: 13-15
- 94 **Nicand E**, Grandadam M, Teyssou R, Rey JL, Buisson Y. Viremia and faecal shedding of HEV in symptom-free carriers. *Lancet* 2001; **357**: 68-69
- 95 **Arankalle VA**, Chobe LP. Retrospective analysis of blood transfusion recipients: evidence for post-transfusion hepatitis E. *Vox Sang* 2000; **79**: 72-74
- 96 **Arankalle VA**, Chobe LP. Hepatitis E virus: can it be transmitted parenterally? *J Viral Hepat* 1999; **6**: 161-164
- 97 **Gao DY**, Peng G, Zhu JM, Sun L, Zheng YJ, Zhang J. Investigation of sub-clinical infection of hepatitis E virus in blood donors. *Zhonghua Ganzangbing Zazhi* 2004; **12**: 11-12

Clinicopathologic analysis of esophageal and cardiac cancers and survey of molecular expression on tissue arrays in Chaoshan littoral of China

Min Su, Xiao-Yun Li, Dong-Ping Tian, Ming-Yao Wu, Xian-Ying Wu, Shan-Ming Lu, Hai-Hua Huang, De-Rui Li, Zhi-Chao Zheng, Xiao-Hu Xu

Min Su, Xiao-Yun Li, Dong-Ping Tian, Ming-Yao Wu, Xian-Ying Wu, Xiao-Hu Xu, Department of Pathology, Shantou University Medical College, Shantou 515031, Guangdong Province, China
De-Rui Li, Tumor Hospital of Shantou University Medical College, Shantou 515031, Guangdong Province, China
Shan-Ming Lu, First Affiliated Hospital of Shantou University Medical College, Shantou 515031, Guangdong Province, China
Hai-Hua Huang, Zhi-Chao Zheng, Second Affiliated Hospital of Shantou University Medical College, Shantou 515031, Guangdong Province, China

Supported by the National Natural Science Foundation of China, No. 30210103904 and Key Natural Science Foundation of Guangdong Province, No. A1080203 and Medical Research Foundation of Guangdong Province and Elitist Foundation of Guangdong, No. Q02109 and Development Foundation of Shantou University and Sir Li Ka-Ching Foundation

Correspondence to: Professor Min Su, Department of Pathology, Shantou University Medical College, 22 Xinling Road, Shantou 515031, Guangdong Province, China. minsu@stu.edu.cn

Telephone: +86-754-8900429 **Fax:** +86-754-8900429

Received: 2003-12-28 **Accepted:** 2004-02-03

Abstract

AIM: To investigate clinical and pathologic data of esophageal carcinoma (EC) and cardiac carcinoma (CC) among residents in Chaoshan region of China.

METHODS: Clinical and pathologic data of 9 650 patients with EC and 4 173 patients with CC in the Chaoshan population were collected and analyzed. Moreover, Chaoshan esophageal carcinoma tissue arrays were made for high-throughput study.

RESULTS: Male to female ratio was 3:1 in patients with EC and 4.75:1 in CC. The average age of the occurrence of EC was 54.6 years, and of CC was 58.1 years. For both EC and CC, age at diagnosis was a little younger in Chaoshan region than in most other areas. The most commonly affected site of esophageal carcinoma was the middle third of esophagus (72.0%); the second was the lower third (15.3%). The main gross type of esophageal carcinoma was ulcerative type (41.50%); the medullary type was the second (39.6%). Squamous cell carcinoma accounted for the overwhelming majority of esophageal cancer (96.4%); adenocarcinoma accounted for the overwhelming majority of cardiac carcinoma (94.5%). Chaoshan esophageal carcinoma tissue arrays were easily for high-throughput study, and tissue cores with a diameter of 1.5 mm could better keep more structure for molecular expression study.

CONCLUSION: Both EC and CC are common in males. The average occurrence age of EC and CC is younger in Chaoshan than in most other regions of China. The most commonly affected site of esophageal carcinoma was the middle third of esophagus (72.0%). Squamous cell

carcinoma accounted for the overwhelming majority of esophageal cancer; adenocarcinoma accounted for the overwhelming majority of cardiac carcinoma. Tissue arrays technology is applicable for rapid molecular profiling of large numbers of cancers in a single experiment.

Su M, Li XY, Tian DP, Wu MY, Wu XY, Lu SM, Huang HH, Li DR, Zheng ZC, Xu XH. Clinicopathologic analysis of esophageal and cardiac cancers and survey of molecular expression on tissue arrays in Chaoshan littoral of China. *World J Gastroenterol* 2004; 10(15): 2163-2167

<http://www.wjgnet.com/1007-9327/10/2163.asp>

INTRODUCTION

Esophageal cancer (EC) ranks among the 10 most common cancers in the world, and is almost uniformly fatal. Chaoshan area is a unique littoral high-risk area of EC in China, within which Nanao island has the highest risk, the second being Jieyang county. According to the report from the Department of Public Health, Guangdong Province in 1993, the mortalities of EC in Nanao island were: $108.68 \pm 7.88/100\ 000$ in standardized Chinese population, $145.44 \pm 10.49/100\ 000$ in standardized world population, $261.16 \pm 25.01/100\ 000$ in standardized world population between the age of 35-64. The annual average incidence rates in males and females were $132.19/100\ 000$ and $69.20/100\ 000$ in Nanao island from 1987 to 1992^[1].

The predominant inhabitants of Chaoshan are offsprings of immigrants who hundreds or thousands of years ago came from the Central Plains of China, now a world well-known high risk region for EC. Chaoshan residents who have a high risk of EC and cardiac carcinoma (CC) are a relatively isolated population who have kept the old Chinese language (Chaoshan dialect) and customs. It is important to see if there is any evidence for the reducing incidence and mortality of EC and CC in Nanao island so far^[2] as the incidences of EC and CC present a downward trend in most other high risk regions. This unique society provides us an unparalleled base for the genetic and also environmental study of esophageal carcinoma. In the current study, we explored the clinical and pathologic features of EC and CC.

In addition, scholars have discovered that many genes and signaling pathways are involved in EC and CC development^[3-7]. However, genetic tumor markers have not gained in EC and CC diagnostics and prognosis prediction. Identification and evaluation of new molecular parameters are of utmost importance in cancer research. Here we present a high-throughput approach to rapidly identify relevant molecular expression changes in Chaoshan EC tissue arrays.

MATERIALS AND METHODS

Clinical data

Data about age, gender, and X-ray or pathological diagnoses of 13 823 patients with carcinoma of esophagus (9 650 cases) or

cardia (4 173 cases) were collected from the Tumor Hospital (1978-1998), First Affiliated Hospital (1989-1998), and Second Affiliated Hospital (1983-1998) of Shantou University Medical College, the Central Hospital of Shantou and the Hospital of Jieyang.

Sample collecting and EC tissues arrays construction

Seventy esophageal squamous carcinoma tissue specimens were selected from Department of Pathology, Shantou University Medical College in 2002. The specimens were fixed in 40 g/L neutrally buffered formaldehyde, embedded in paraffin. Sections of 5 μ m stained with hematoxylin and eosin were obtained to confirm the diagnosis and to identify different viable, representative areas of the specimen. From these defined areas core biopsies were taken with a precision instrument. Sixty-eight EC and para-cancerous tissue cores with a diameter of 1.5 mm from each specimen were punched and arrayed in 8 \times 9 on a recipient paraffin block. Five- μ m sections of the EC tissue array block was cut and placed on adhesive coated slides (cooperated with Cybrdi, Dr. Li Jun).

Immunohistochemistry

The expression of Erk1/Erk2 MAPK signaling protein was analyzed using Erk1/Erk2 Mouse derived anti-activated MAP kinase monoclonal antibody (1:400, Sigma), HistostainTM-SP kit and DAB visualization methods according to the manufacture's instruction (China Beijing Zhongshan Biological Technology CO., LTD.) And the expression of epidermal growth factor receptors were primarily analyzed using phosphor-EGFR (Tyr845) rabbit polyclonal antibodies and HRP-linked anti-rabbit IgG (Cell Signaling Technology, Inc. #2231, #7074). Four conventional normal esophageal epithelium tissues from autopsy were used as normal tissue controls. The human breast cancer tissue was used as positive control. Negative control was designed using phosphate-buffered saline (PBS) instead of primary antiserum. The detailed immunohistochemical process was carried out according to the manufacture's instructions.

Assessment of staining

The positive immunohistochemical staining of Erk1/Erk2 proteins was shown as brown signals in the nuclei; and the immunohistochemical signals of phosphor-EGFR (Tyr845) was in membrane and cytoplasm. The percentage of positive stained

cells was evaluated for each tissue sample by counting all cells at 5 high power fields of micrometric rule (5 mm \times 5 mm). The cases having positive cancer cells or epithelium accounting for more than 75% of all cancer cells or epithelium on the slide were defined as a score of +++, 50-74% were defined as a score of ++, 25-49% were defined as a score of +, 1-5% were defined as a score of \pm , less than 1% were defined as a score of -.

Statistical analysis

Data were stored in a computer data base (FoxPro, version 2.5 b) and analyzed using a computer (Pentium 4) spread sheet (Microsoft Excel 97) and professional statistical computer software (SPSS, version 11.0 and SAS, version 6.08). $P < 0.05$ was taken as significant. Immunoreactivity was classified as continuous data (undetectable levels or 0% to homogeneous staining or 100%) for all markers.

RESULTS

Gender and age

Genders of the patients were recorded in 9 635 cases. The 8 665 EC cases had age records, the youngest and the oldest were 17 years and 91 years respectively, and 3714 CC cases had age records. The male to female ratio and average age of morbidity for EC and CC in Chaoshan region are shown in Table 1. Constituent ratio of EC, CC in every age group is shown in the histogram (Figure 1).

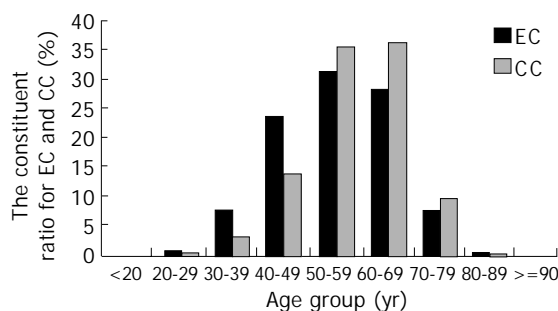


Figure 1 The histogram of the constituent ratio for EC and CC in Chaoshan region.

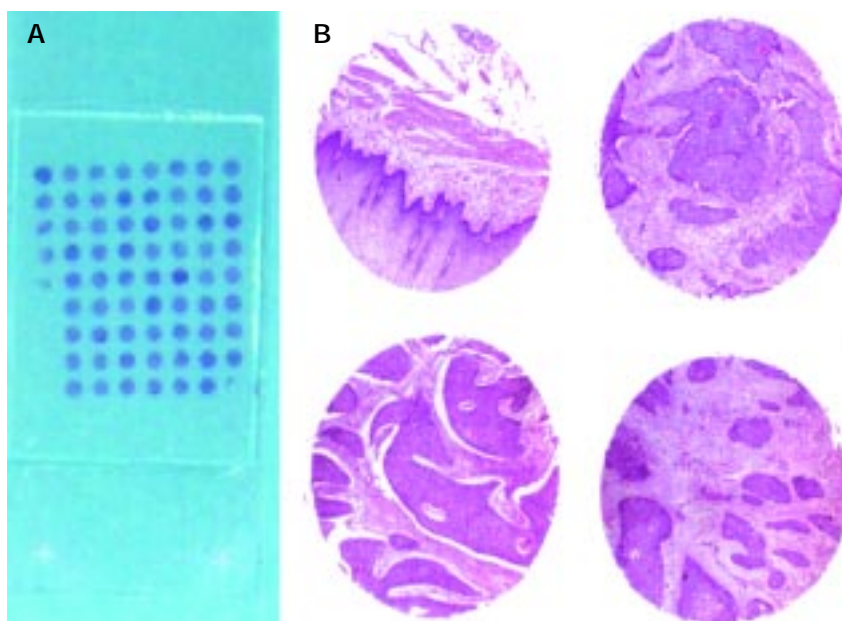


Figure 2 A: Overview of Chaoshan esophageal carcinoma tissue array (tissue cores with a diameter of 1.5 mm with 68 samples); B: Esophageal para-cancerous tissue and squamous carcinoma tissue (HE staining, original magnification: $\times 40$).

Table 1 Sex ratio, average age of morbidity for EC and CC in Chaoshan littoral region (mean±SD)

	<i>n</i>	Sex (male:female)	Age(yr)	<i>F</i>	<i>P</i>
EC	9 635	7 228:2 407(3.0:1)	54.61±10.73	103.24	<0.001
CC	4 167	3 442:725(4.75:1)	58.14±9.45		

EC:CC=2.31:1.

Pathology

The overwhelming majority of ECs were squamous cell carcinoma (96.4%); whereas CCs were composed mainly of adenocarcinomas (94.5%), and squamous cell carcinoma ranked second (4.4%). The detailed information of pathology is shown in Table 2.

Table 2 Pathology for EC and CC in Chaoshan littoral region (%)

	Site			Gross type				Histological type			
	U	M	L	UT	MT	ST	FT	SCA	ACA	UCA	O
EC	12.7	72.0	15.3	41.5	39.6	9.6	9.4	96.4	2.7	0.6	0.3
CC								4.4	94.5	0.9	0.2

Site (EC, *n*=6 384); Gross type (EC, *n*=1 193); Histological type (EC, *n*=7 272; CC, *n*=3 086); U: Upper third; M: Middle third; L: Lower third; UT: Ulcerative type; MT: Medullary type; ST: Scirrhus type; FT: Fungating type; SCA: Squamous cell carcinoma; ACA: Adenocarcinoma; UCA: Undifferentiated carcinoma; O: others.

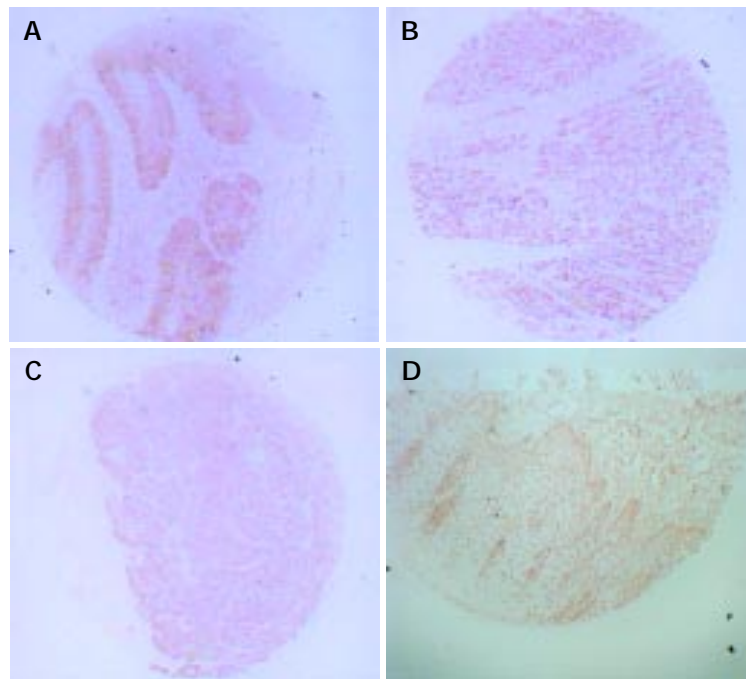


Figure 3 Phosphor-EGFR (Tyr845) expression on esophageal squamous carcinoma tissue (A, B, C) and esophageal para-cancerous tissue (D) (Cell Signaling Technology kit, original magnification: ×40).

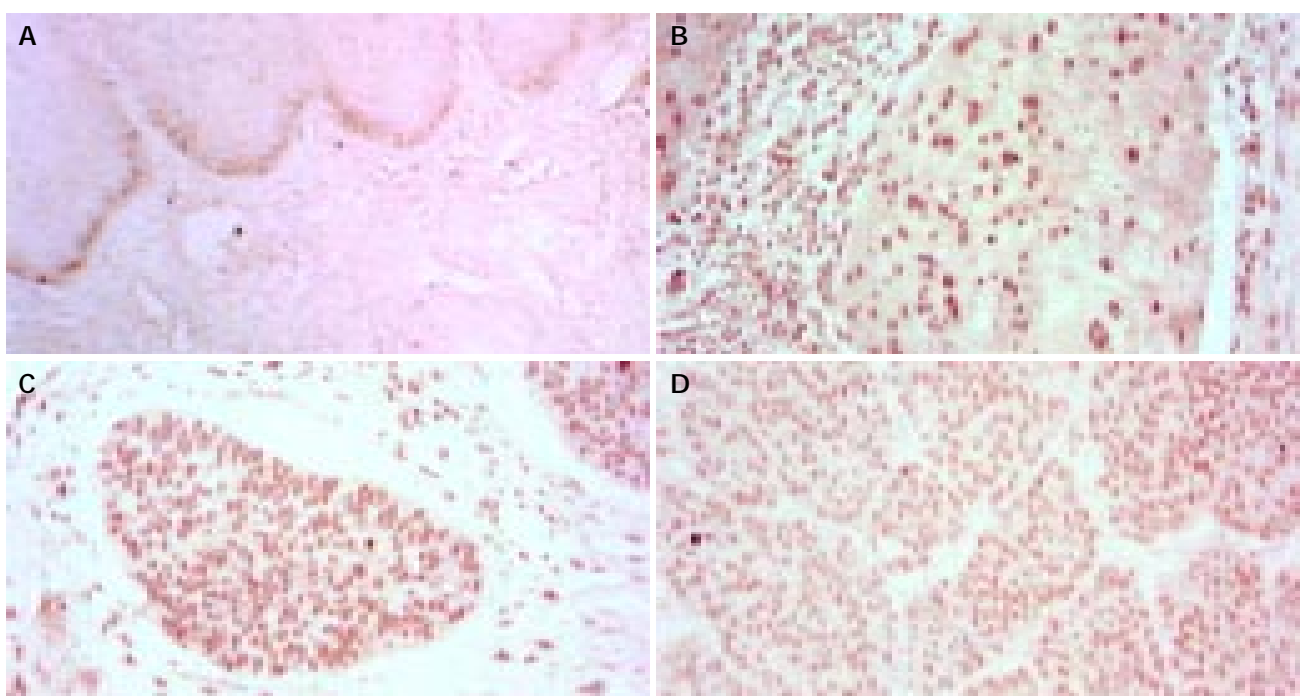


Figure 4 Erk1/Erk2 expression on normal esophageal squamous tissue (A, conventional tissue section, SP×100) and esophageal squamous carcinoma tissue (B, C, D tissue arrays) (SP×200).

Table 3 Expression of Erk1/Erk2 in esophageal squamous carcinoma tissue and para-cancerous tissue (% , mean±SD)

	Normal esophageal squamous cell (n=5)	Para-cancerous tissue (n=5)	Grade I (n=19)	Grade II (n=34)	Grade III (n=9)	F	P
Activated ERK1/ERK2	5.10±1.44	76.80±0.14	76.80±0.09	75.80±0.09	69.30±0.14	2.60	0.04

There was marked difference between normal esophageal epithelium and cancer tissues or para-cancerous tissue. But there was no marked difference among para-cancerous tissues and esophageal squamous carcinoma tissues ($F=1.463$, $P=0.236$).

Chaoshan EC tissues arrays and immunohistochemistry

Sections from tissue arrays were kept structure well for pathologic and immunohistochemical research (Figure 2). The expression of phosphor-EGFR(Tyr845) in esophageal squamous carcinoma tissue are relative diversity from \pm to $++++$, but no distinct differences among esophageal squamous carcinoma tissues according to grading (Figure 3). The expression of activated ERK in esophageal squamous carcinoma tissue and para-cancerous tissue are shown in Table 3 (Figure 4).

DISCUSSION

In data from Yangquan city of Shanxi Province (502 cases)^[8], the median age of EC patients was 59.17 years, 4.56 years older than that of Chaoshan EC patients. And also data from Linxian of Henan Province (2 601 cases)^[9], the proportion of EC patients from 20 to 30 years was 0.35%, from 30 to 40 was 5.19%; whereas both of the two proportions were lower than those from our data (0.70% and 7.70% respectively). In our data from Chaoshan region, the ulcerative type (41.5%) was the most common gross type of EC, which suggests that most EC patients were in the terminal stages when they arrived at hospitals.

Both preceding evidences indicated the average age of EC occurrence was younger in Chaoshan population than those in central plains of China. Synthetically analysis of two reports from Henan Province (1 045 cases and 1 332 cases respectively)^[9,10] showed the proportion of CC patients less than 50 years old was 15.56%, which was slightly lower than that from Chaoshan CC data (17.60%). The similar phenomena were seen in other papers^[11,12]. It might indicate that the age of incidence of cardiac cancer is also younger in Chaoshan region than in most other areas. Pathological analysis of 1 572 EC patients from Henan Province indicated histological type for the overwhelming majority of EC was squamous cell carcinoma (SCC), and the proportion of SCC (95.1%) was similar to that in our data (96.44%)^[13]. In comparison of the constituent ratios of histological types for cardiac carcinoma with data respectively from the Chinese Academy of Medical Science^[14], Erlangen - Nurnberg University in Germany^[15] and our data, it homoplasmically shows that adenocarcinoma accounts for the overwhelming majority of cardiac carcinoma, while the proportions of other histological types are relatively low.

Both data from Yangquan and Linxian^[16] also showed the middle third of esophagus was the most commonly affected site analogously, followed by the lower third and then the upper third, similar to our results.

Tissue array technology is applicable for rapid molecular profiling of large numbers of cancers in a single experiment. But a possible limitation of the tissue array technology is that the minute tissue samples acquired from the original tissues may not always be representative of the entire tumor, in light of the intratumor heterogeneity characteristic to most cancers. The comparisons between similarly acquired specimens from different stages of tumor progression placed on the same tissue microarray should be less problematic. If tumor arrays are used to investigate prevalence or prognostic significance of molecular changes, the critical issue is the extent to which minute tissue samples are representative of their donor tumors. The findings of this study suggest that significant results

can be obtained on tumor arrays issue cores with a diameter of 1.5 mm. Well and truly, one should consider the tumor tissue array technology as a rapid, high-throughput survey method to pinpoint the biologically most prevalent or clinically most promising genes and molecular markers for detailed studies combined with conventional tissue specimens.

The epidermal growth factor (EGF) peptide induces cellular proliferation through the epidermal growth factor receptor (EGFR), a M_r 170 000 single-pass transmembrane tyrosine kinase, which is believed to play important roles in the control of cell growth and differentiation. The EGFR activates ras and the MAP kinase pathway, ultimately causing phosphorylation of transcription factors such as c-Fos to create AP-1 and ELK-1 that contribute to proliferation. Gene amplification and overexpression of EGFR have been reported in various human tumors, including head and neck/oral cancer^[17-22].

Mitogen-activated protein kinase (MAPK) cascades have been shown to play a key role in transduction extracellular signals to cellular responses. Extracellular signal-regulated kinase (ERK) has been the best characterized MAPK and the Raf-MEK-ERK pathway represents one of the best characterized MAPK signaling pathway. The activated ERKs translocate to the nucleus and transactivate transcription factors, changing gene expression to promote growth, differentiation or mitosis^[23].

Our primary immunohistochemical study showed that phosphor-EGFR (Tyr845) and activated ERK were expressed in both para-cancerous and esophageal cancerous cells. The intensity of the expression was much higher in cancer than in normal tissue, suggesting that EGFR, Erk1/Erk2 MAPK signaling pathway might play an important role in the regulation of proliferation of esophageal cancer^[24,25].

In summary, Both EC and CC are common in males. The average age of occurrence is younger in Chaoshan than in most other regions of China. It is suggested that either genetic factors might play an important role in the pathogenesis of esophageal and cardiac cancers in Chaoshan or Chaoshan residents exposed themselves to some high risk environmental factors. Tissue microarrays technology is applicable for rapid molecular profiling of many tissue samples in a single experiment.

ACKNOWLEDGMENTS

The authors acknowledge the participation of the following members of the undergraduate scientific research group in Shantou University Medical College of China led by Professor Min Su: SM Ying, Y Ni, YS Gao, J Lin, JK Sun, BC Yuan, YF Li, XL Chen, JS X, Y F Chen, who helped us collect the case data of esophageal carcinoma and cardiac cancer. We express our special thanks to Professor Bruce AJ Ponder, Hutchison/MRC Research Centre, MRC Cancer Cell Unit and University of Cambridge, for his invaluable suggestions, Dr. John KL, for his kind assistance in the preparation of the grammatical structure of this paper.

REFERENCES

- 1 **Su M**, Lu SM, Tian DP, Zhao H, Li XY, Li DR, Zheng ZC. Relationship between ABO blood groups and carcinoma of esophagus and cardia in Chaoshan inhabitants of China. *World*

- J Gastroenterol* 2001; **7**: 657-661
- 2 **Li K**, Su M, Yu P. Mortality trends for malignancies in Nanao county of Guangdong province. *Zhongguo Zhongliu* 2001; **10**: 269-270
 - 3 **Su H**, Hu N, Shih J, Hu Y, Wang QH, Chuang EY, Roth MJ, Wang C, Goldstein AM, Ding T, Dawsey SM, Giffen C, Emmert Buck MR, Taylor PR. Gene expression analysis of esophageal squamous cell carcinoma reveals consistent molecular profiles related to a family history of upper gastrointestinal cancer. *Cancer Res* 2003; **63**: 3872-3876
 - 4 **Nie Y**, Liao J, Zhao X, Song Y, Yang GY, Wang LD, Yang CS. Detection of multiple gene hypermethylation in the development of esophageal squamous cell carcinoma. *Carcinogenesis* 2002; **23**: 1713-1720
 - 5 **Shinohara M**, Aoki T, Sato S, Takagi Y, Osaka Y, Koyanagi Y, Hatooka S, Shinoda M. Cell cycle-regulated factors in esophageal cancer. *Dis Esophagus* 2002; **15**: 149-154
 - 6 **Gibson MK**, Abraham SC, Wu TT, Burtness B, Heitmiller RF, Heath E, Forastiere A. Epidermal growth factor receptor, p53 mutation, and pathological response predict survival in patients with locally advanced esophageal cancer treated with preoperative chemoradiotherapy. *Clinical Cancer Research* 2003; **9**: 6461-6468
 - 7 **Arteaga CL**. Epidermal growth factor receptor dependence in human tumors: more than just expression? *The Oncologist* 2002; **7**(Suppl 4): 31-39
 - 8 **Li SK**, Mao XZ, Jia YT. Clinic analysis of 502 cases with esophageal carcinoma. *Zhongliu Yanjiu He Linchuang* 1996; **8**: 106-107
 - 9 **Wang LD**, Gao WJ, Yang WC, Li XF, Li J, Zou JX, Wang DC, Guo RX. Preliminary analysis of the statistics on 3933 cases with esophageal cancer and gastric cardia cancer from the subjects in the People's Hospital of Linzhou in 9 years. *J Henan Med Univ* 1997; **32**: 9-11
 - 10 Collaboration group of gastroscopy in some hospitals of Henan province. Occurrence condition of cardia carcinoma and endoscope classification of early cardia carcinoma in high and low incidence areas of esophageal carcinoma. *J Henan Med Collage* 1987; **22**: 207-210
 - 11 Collaboration group of endoscopy in Shanghai. Clinic analysis of 1451 cardia carcinomas diagnosed by gastroscopy. *Neijing* 1985; **2**: 32-34
 - 12 **Hansson LE**, Sparen P, Nyren O. Increasing incidence of carcinoma of the gastric cardia in Sweden from 1970 to 1985. *Br J Surg* 1993; **80**: 374-377
 - 13 **Xu JY**, Zhang JK, Wang RM. Control observation on esophageal carcinoma and esophagitis detected by endoscopy between high and low incidence areas of esophageal carcinoma. *Linchuang Xiaohuabing Zazhi* 1995; **7**: 101-103
 - 14 **Li L**, Pan GL, Huang GJ, Lu X. Pathomorphology characteristics of cardiac carcinoma. *Zhonghua Zhongliu Zazhi* 1984; **6**: 37-40
 - 15 **Husemann B**. Cardia carcinoma considered as a district clinical entity. *Br J Surg* 1989; **76**: 136-139
 - 16 **Liu FS**. Pathology of esophageal carcinoma. *Zhongliu Fangzhi Yanjiu* 1976; **3**: 234-238
 - 17 **Eriksen JG**, Steiniche T, Askaa J, Alsner J, Overgaard J. The prognostic value of epidermal growth factor receptor is related to tumor differentiation and the overall treatment time of radiotherapy in squamous cell carcinomas of the head and neck. *Int J Radiat Oncol Biol Phys* 2004; **58**: 561-566
 - 18 **Selvaggi G**, Novello S, Torri V, Leonardo E, De Giuli P, Borasio P, Mossetti C, Ardisson F, Lausi P, Scagliotti GV. Epidermal growth factor receptor overexpression correlates with a poor prognosis in completely resected non-small-cell lung cancer. *Ann Oncol* 2004; **15**: 28-32
 - 19 **Chan KS**, Carbajal S, Kiguchi K, Clifford J, Sano S, DiGiovanni J. Epidermal growth factor receptor-mediated activation of Stat3 during multistage skin carcinogenesis. *Cancer Research* 2004; **64**: 2382-2389
 - 20 **Shimizu M**, Suzui M, Deguchi A, Lim JT, Weinstein IB. Effects of acyclic retinoid on growth, cell cycle control, epidermal growth factor receptor signaling, and gene expression in human squamous cell carcinoma cells. *Clin Cancer Research* 2004; **10**: 1130-1140
 - 21 **Perez-Soler R**. HER1/EGFR targeting: refining the strategy. *Oncologist* 2004; **9**: 58-67
 - 22 **Dahlberg PS**, Ferrin LF, Grindle SM, Nelson CM, Hoang CD, Jacobson B. Gene expression profiles in esophageal adenocarcinoma. *Ann Thorac Surg* 2004; **77**: 1008-1015
 - 23 **Zhang W**, Liu HT. MAPK signal pathways in the regulation of cell proliferation in mammalian cells. *Cell Research* 2002; **12**: 9-18
 - 24 **Nemoto T**, Ohashi K, Akashi T, Johnson JD, Hirokawa K. Overexpression of protein tyrosine kinases in human esophageal cancer. *Pathobiology* 1997; **65**: 195-203
 - 25 **Trisciuglio D**, Iervolino A, Candiloro A, Fibbi G, Fanciulli M, Zangemeister-Wittke U, Zupi G, Del Bufalo D. Bcl-2 induction of urokinase plasminogen activator receptor expression in human cancer cells through Sp1 activation: involvement of ERK1/ERK2 activity. *J Biol Chem* 2004; **279**: 6737-6745

Edited by Zhu LH and Chen WW Proofread by Xu FM

Expression of cyclooxygenase-2 in human esophageal squamous cell carcinomas

Jian-Gang Jiang, Jiang-Bo Tang, Chun-Lian Chen, Bao-Xing Liu, Xiang-Ning Fu, Zhi-Hui Zhu, Wei Qu, Katherine Cianflone, Michael P. Waalkes, Dao-Wen Wang

Jian-Gang Jiang, Jiang-Bo Tang, Chun-Lian Chen, Bao-Xing Liu, Xiang-Ning Fu, Zhi-Hui Zhu, Dao-Wen Wang, Internal Medicine Department and Gene Therapy Center, Tongji Hospital, Tongji Medical College of Huazhong University of Science and Technology, Wuhan 430030, Hubei Province, China

Wei Qu, Michael P. Waalkes, Inorganic Carcinogenesis Section, Laboratory of Comparative Carcinogenesis, National Cancer Institute at the National Institute of Environmental Health Sciences, Research Triangle Park, North Carolina 27709, USA

Katherine Cianflone, Mike Rosenbloom Laboratory for Cardiovascular Research, McGill University Health Center, Montreal, Quebec H3A 1A1, Canada

Co-first-authors: Jian-Gang Jiang and Jiang-Bo Tang

Correspondence to: Dr. Dao-Wen Wang, Department of Internal Medicine and Gene Therapy Center, Tongji Hospital, Tongji Medical College of Huazhong University of Science and Technology, Wuhan 430030, Hubei Province, China. dwwang@tjh.tjmu.edu.cn

Telephone: +86-27-83662842 **Fax:** +86-27-83662842

Received: 2003-11-17 **Accepted:** 2004-01-08

Abstract

AIM: To determine whether cyclooxygenase-2 (COX-2) was expressed in human esophageal squamous cell carcinoma.

METHODS: Quantitative reverse transcription-polymerase chain reaction (RT-PCR), western blotting, immunohistochemistry and immunofluorescence were used to assess the expression level of COX-2 in esophageal tissue.

RESULTS: COX-2 mRNA levels were increased by >80-fold in esophageal squamous cell carcinoma when compared to adjacent noncancerous tissue. COX-2 protein was present in 21 of 30 cases of esophageal squamous cell carcinoma tissues, but was undetectable in noncancerous tissue. Immunohistochemistry was performed to directly show expression of COX-2 in tumor tissue.

CONCLUSION: These results suggest that COX-2 may be an important factor for esophageal cancer and inhibition of COX-2 may be helpful for prevention and possibly treatment of this cancer.

Jiang JG, Tang JB, Chen CL, Liu BX, Fu XN, Zhu ZH, Qu W, Cianflone K, Waalkes MP, Wang DW. Expression of cyclooxygenase-2 in human esophageal squamous cell carcinomas. *World J Gastroenterol* 2004; 10(15): 2168-2173 <http://www.wjgnet.com/1007-9327/10/2168.asp>

INTRODUCTION

Esophageal cancer is the fourth most prevalent malignancy in China. Although several factors have been implicated for the recent rise in the frequency of esophageal carcinoma, including diet, activation of *c-myc* oncogenes and inactivation of tumor suppressor genes (*p53*)^[1,2], the exact pathogenic mechanisms and promoting factors of this cancer remain to be

clarified. There is no effective strategy for treatment of this disease. Recently epidemiological studies suggest intake of nonsteroidal anti-inflammatory drugs (NSAIDs) such as aspirin and indomethacin can reduce the risk of colorectal cancer^[3,4]. Based on these findings, subsequent studies have addressed the role of COX enzyme as a target of these compounds.

COX is a rate-limiting enzyme involved in the conversion of arachidonic acid to prostaglandin H₂, the precursor of several molecules including prostaglandin (PG), prostacyclin, and thromboxane. Results from recent studies have established the presence of two distinct COX enzymes, a constitutive enzyme (COX-1) and an inducible form (COX-2). They share over 60% identity at the amino acid level and have similar enzymatic activities, but both isoforms are suggested to have different biological functions^[5-9]. COX-1 is constitutively expressed in most mammalian tissues and is thought to carry out "housekeeping" functions such as cytoprotection of the gastric mucosa, regulation of renal blood flow, and control of platelet aggregation. In contrast, COX-2 mRNA and protein are undetectable in normal tissues, but can be rapidly induced by proinflammatory or mitogenic stimuli including cytokines, endotoxins, interleukins, and phorbol ester^[10-12].

Multiple lines of experimental evidence have also suggested that COX-2 is involved in carcinogenesis. For example, COX-2 is up-regulated in transformed cells^[13] and in various forms of cancer^[14-17], whereas levels of COX-1 are relatively stable. Moreover, COX-2 knockout mice develop 75% fewer chemically-induced skin papillomas than control mice. Recently, it has been shown that selective COX-2 inhibitors may significantly suppress experimentally-induced colon carcinogenesis^[18,19]. Epidemiological studies have shown that intake of aspirin was associated with up to a 90% decreased risk of developing esophageal cancer^[20,21], and in induced esophageal carcinomas, indomethacin had antitumor activity^[22,23].

Here we investigated whether COX-2 was up-regulated in esophageal squamous cell carcinomas from Chinese patients. Our data show that levels of COX-2 are markedly increased in esophageal squamous cell carcinomas, which raises the possibility that selective inhibitors of COX-2 may be useful in the prevention or treatment of this important disease.

MATERIALS AND METHODS

Samples

We examined 30 cases of esophageal squamous cell carcinoma. Both tumor tissue and surrounding normal tissue were obtained from surgical patients with esophageal squamous cell carcinoma at Tongji Hospital during operations. The age of the patients was 57±9 years (mean±SD; range, 37 to 75 years). Of the patients, 23 were men and 7 were women. A small portion from each tissue sample was immediately frozen in liquid nitrogen and stored at -80 °C. Tissue samples were fixed in 40 g/L neutral buffered formaldehyde, processed through graded ethanol solutions, and embedded in paraffin and immunostained for COX-2. A subset of paired tumor tissues and surrounding normal tissue was further examined by RT-PCR and Western blotting.

RNA extraction

Protein and total RNA were extracted using TriZol Reagent (Life Technologies, GIBCO BRL). RT-PCR kit was purchased from Takara Bio Co., Ltd. COX-2 affinity-purified polyclonal antibodies were obtained from Santa Cruz Biotechnology, Inc. Rabbit anti-goat IgG conjugated with horse-radish peroxidase (HRPO) was obtained from KPL, Inc., USA. ImmunoResearch Lab Enhanced chemiluminescence assay was purchased from PIERCE, Inc. SDS-PAGE standard was obtained from Bio-Rad, Inc.

Western blotting for detection of COX-2

Protein in the various samples were extracted and purified by TriZol Reagent, and the protein concentration was evaluated by Bradford method. A portion of protein (20 μ g) extracted from each tissue sample was subjected to electrophoresis in 80 g/L polyacrylamide slab gels. After transfer to PVDF membrane and blocking with fat free milk powder, blots were probed with COX-2 antibodies (1:750), followed by incubation with HRPO-conjugated secondary antibody (rabbit anti-goat 1:800). COX-2 proteins were visualized by enhanced chemiluminescence.

Semi-quantitative RT-PCR

Total RNA was isolated and purified by TriZol Reagent, and the RNA concentration was determined. Semi-quantitative analysis of the expression of COX-2 mRNA was performed using the multiplex RT-PCR technique. In this assay, we used a housekeeping gene, glyceraldehyde-3-phosphate dehydrogenase (GAPDH), as an internal standard. A sample (1 μ g) of total RNA was reverse-transcribed using the Takara Bio RT-PCR kit according to the manufacturer's protocol. PCR was performed in a 25 μ L reaction mixture containing 5 μ L of cDNA template, 1 \times PCR buffer, 1.5 mmol/L MgCl₂, 0.8 mmol/L dNTPs, 100 nmol/L of each primer for COX-2 (sense primer, 5'-CCGAGGTGTATGTATGAGTG-3'; antisense primer, 5'-AGGAGAGGTTAGAGAAGG-3') or 100 nmol/L GAPDH (sense primer, 5'-CCTTGCCTCTCAGACAATGC-3'; antisense primer, 5'-CCACGACATACTCAGCAC-3') and 1 U of *Taq* DNA polymerase. The PCR primers used for detection of COX-2, and GAPDH yielded cDNA products of 314-bp and 340-bp, respectively. The conditions for PCR were one cycle of denaturing at 94 $^{\circ}$ C for 5 min, followed by 35 cycles of at 94 $^{\circ}$ C for 45 s, 56 $^{\circ}$ C for 45 s, 72 $^{\circ}$ C for 1 min with a final extension at 72 $^{\circ}$ C for 7 min. The electrophoresed PCR products were scanned by densitometry and the ratio of COX-2 to GAPDH was calculated in each sample.

Immunohistochemistry

Tissue sections (4 μ m thick) were deparaffinized in xylene and rehydrated. Heat antigen retrieval was performed as described previously^[24]. Slides were then processed for immunohistochemistry. In the primary antibody reaction step, slides were incubated with the COX-2 antibody (final concentration 5 μ g/mL) for 1 h at room temperature. For positive controls, sections of colon cancer expressing the COX-2 protein were included in each staining procedure. For negative controls, nonimmunized rabbit IgG or Tris-buffered saline was substituted for the primary antibody to distinguish false positive responses from nonspecific binding to IgG or the secondary antibody. In addition, preabsorbed antibody with an excess amount of immunogen abolished the staining. Staining was repeated twice to avoid possible technical errors and similar results were obtained in all cases.

Evaluation of COX-2 immunohistochemistry

All immunostained sections were coded and evaluated without

prior knowledge of the clinical or pathological parameters. In each section, five high-power fields were selected at random and a total number of at least 700 cells were evaluated. The results were expressed as the intensity of staining. The intensity of staining was judged relative to smooth muscle cells in the sample, and estimated on a scale 0-3 (0 negative; 1 weak; 2 moderate; and 3 strong). All slides were interpreted by two investigators on three different occasions. Their evaluations were similar and <10% disagreement between the investigators was noted. In case of major disagreement, the final evaluation of such sections was determined by consensus using a multihead microscope.

Immunofluorescence assay

Tissue samples were cut into 6 μ m crystal-sections, and processed with COX-2 specific antibody and fluorescein labeled secondary antibodies and all the sections were observed immediately under fluorescence microscope.

Statistical analysis

Statistical analysis was performed using SAS software. Results of immunohistochemistry were analyzed by Fisher's exact test. The correlation of RT-PCR and western blotting was analyzed by logistic regression analysis. $P < 0.05$ was considered statistically significant.

RESULTS

COX-2 mRNA expression in esophageal squamous cell carcinoma by semi-quantitative RT-PCR

To examine the level of COX-2 mRNA, RT-PCR was performed to estimate the expression of COX-2 in tumor tissues relative to that in the matched normal tissues, which was expressed as COX-2/GAPDH ratio. GAPDH was used as an internal control. Semiquantitative RT-PCR indicated that COX-2 mRNA was found in 21 of 30 esophageal squamous cell carcinomas. In surrounding normal tissue of esophageal squamous cell carcinoma, COX-2 mRNA could not be detected (Figure 1). In the 21 esophageal squamous cell carcinoma tissues, the COX-2/GAPDH ratios ranged from 0.6 to 1.0, levels of COX-2 mRNA were increased by >80-fold compared to adjacent noncancerous tissue.

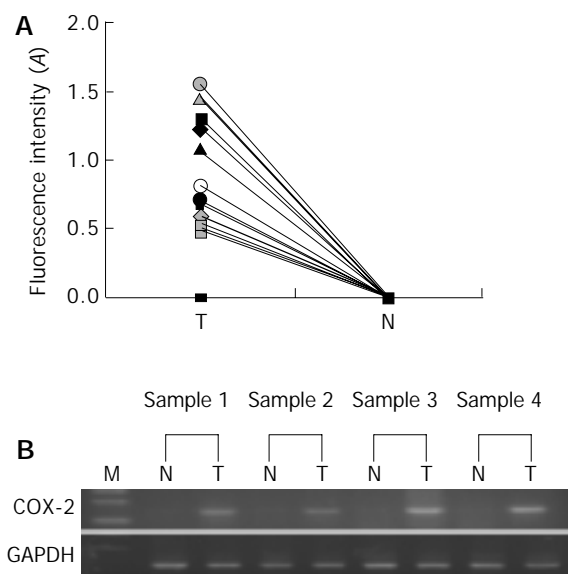


Figure 1 Semiquantitative result of RT-PCR analysis of COX-2 mRNA expression in squamous carcinoma tissues and matched normal tissues of the esophagus. A: Data are expressed as the fluorescence values of COX-2 band in tumor and nontumorous

tissue samples from 30 patients with esophageal squamous cell carcinoma. B: Representative results of semiquantitative RT-PCR, indicated COX-2 mRNA was found in esophageal squamous cell carcinoma samples (T), while in surrounding normal tissue (N), COX-2 mRNA could not be detected. The coamplified GAPDH gene served as an internal control. PCR product sizes are 314 bp for COX-2 and 340 bp for GAPDH. M indicates DNA marker. The samples in lanes 1N and 1T, 2N and 2T, 3N and 3T, 4N and 4T are paired samples from 4 patients, respectively.

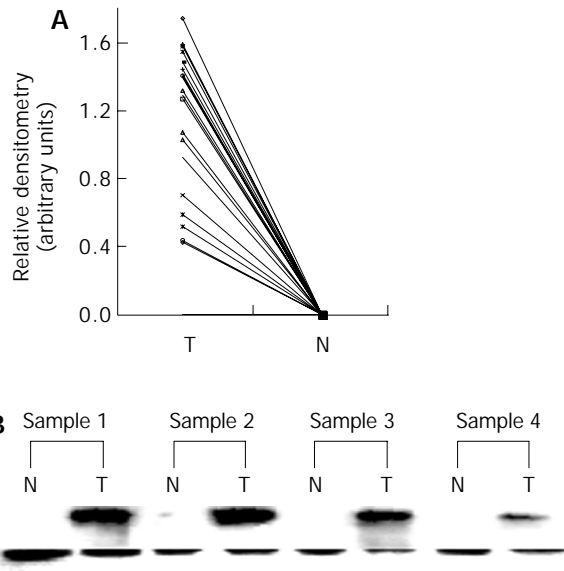


Figure 2 Western blot analysis of COX-2 in squamous carcinoma tissues and matched normal tissues of the esophagus. COX-2 expressions in representative tumor (T) and nontumorous (N) are shown. A: Data are expressed as the absorbency values of COX-2 band in tumor and nontumorous tissue samples from 30 patients with esophageal squamous cell carcinoma. B: Representative result of Western blot analysis. COX-2 protein was detected in tumor tissue but was undetectable in nontumorous tissue in the same patients. β -actin was used as an internal control. The samples in lanes 1N and 1T, 2N and 2T, 3N and 3T, 4N and 4T are paired samples from 4 patients, respectively.

Western blotting

To determine whether levels of COX-2 protein were also increased in esophageal squamous cell carcinomas, western blot analysis of paired tumorous and nontumorous tissue was performed. COX-2 protein was detected in tumor tissue from 21 of 30 patients but was undetectable in nontumorous tissue in the same patients. β -actin was used as an internal control

(Figure 2). Furthermore, the results of western blot analysis paralleled those of mRNA RT-PCR analysis. There was a significant positive correlation between western blot analysis and RT-PCR analysis results ($r=0.708$, $P<0.01$) (Figure 3).

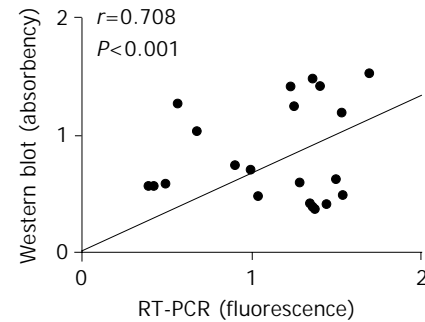


Figure 3 Correlation between western blot analysis and RT-PCR analysis results. The results showed that the expression of COX-2 in cancer tissues (western blot analysis) was highly correlated with by RT-PCR analysis (r value=0.708, $P<0.001$).

Table 1 Expression of COX-2 in esophageal squamous cell carcinomas detected by immunohistochemistry

	Intensity				
	0	1	2	3	
Tumor tissue	10	2	12	6	$P<0.05$
Normal tissue	27	3	0	0	

The intensity of staining was estimated on a scale 0–3. (0, negative; 1, weak; 2, moderate; and 3, strong).

COX-2 expression in esophageal squamous cell carcinoma by immunohistochemistry

Immunohistochemistry was performed to directly indicate cell specific COX-2 protein expression. In nontumorous tissue specimens, a weak COX-2 staining or no COX-2 staining was detected. In contrast, a moderate to strong expression of COX-2 was noted in many esophageal squamous cell carcinomas of the same patients. Specifically, a strong expression of COX-2 protein was present in 6 of 30 (20%) esophageal squamous cell carcinomas, moderate expression was present in 12 of 30 (40%), and weak expression was present in 2 of 30 (15%). The level of COX-2 expression in esophageal squamous cell carcinomas was significantly higher than that in surrounding normal tissue (Table 1). Expression of COX-2 was localized to tumor cells, not to surrounding stromal cells or infiltrating inflammatory cells (Figure 4).

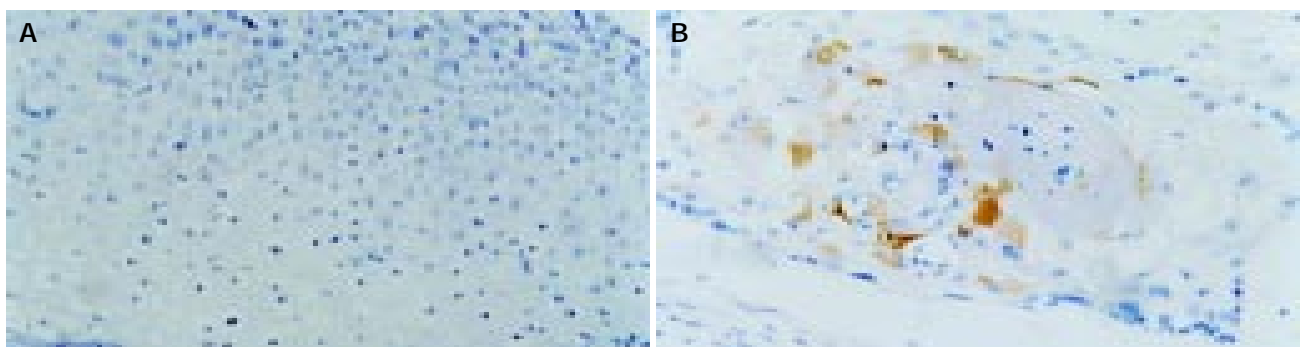


Figure 4 Representative results of immunohistochemical analysis of COX-2 in squamous carcinoma tissues and matched normal tissues of the esophagus from the same patient (Magnification x200). In normal esophageal tissue there is no positive staining for COX-2 (A) but in esophageal squamous cell carcinoma tissue, carcinoma cells display a strong staining for COX-2, which indicate COX-2 expression specifically in cancer tissues (B).

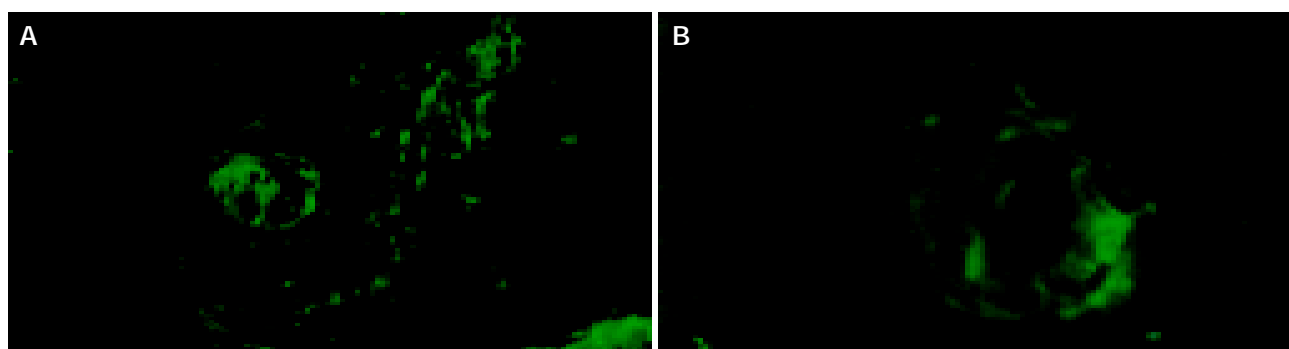


Figure 5 Immunofluorescence analysis of COX-2 in squamous carcinoma tissues (Magnification, x400). A and B are from 2 different patients with esophageal squamous cell carcinoma, Both display a strong green fluorescence staining for COX-2 in cancer-nests.

COX-2 expression in esophageal squamous cell carcinoma by immunofluorescence

Immunofluorescence was performed to directly indicate whether COX-2 protein was expressed in esophageal cancer. COX-2 expression was detected in esophageal squamous cell carcinomas. Immunofluorescence in esophageal squamous cell carcinomas displayed a cancer-nest structure (Figure 5).

DISCUSSION

Epidemiological studies indicate that the administration of nonsteroidal anti-inflammatory drugs (NSAIDs) results in a marked reduction in adenoma size and number and, not infrequently, leads to a complete regression of colonic polyps in patients with familial adenomatous polyposis^[25-27]. NSAIDs also reduce the risk of sporadic colorectal, breast, and lung cancers^[28,29]. These effects of NSAIDs on the inhibition of carcinogenesis have also been demonstrated in animal experiments, including pancreatic tumor model induced by N-nitrosobis (2-oxopropyl) amine in hamsters^[30]. Several lines of evidence indicate that the antitumor effects of NSAIDs may be due in part to the inhibition of COX-2 activity^[19,31-33]. Indeed, in carcinomas of the colon and lung and also in gastric and esophageal carcinomas, the level of COX-2 expression is significantly increased. These findings suggest that up-regulation of this enzyme might be a common mechanism for carcinogenesis of cells of an epithelial origin. Indeed, in the present large sampled study we found that COX-2 expression was increased at both the RNA and protein levels in a large proportion of esophageal squamous cell carcinoma compared with paired normal surrounding esophageal tissues by RT-PCR and Western blot analyses. RT-PCR analyses indicated that 21 of 30 (70%) esophageal squamous cell carcinoma cases displayed increased COX-2 mRNA. Furthermore, the results of mRNA analysis paralleled those of western blot and immunohistochemistry. Thus, approximately 67% of the carcinoma samples exhibited positive staining of COX-2 protein, whereas paired normal tissues showed little or no COX-2 staining. Up to 60% of carcinoma cases showed moderate to strong COX-2 immunostaining (intensity 2 or 3). Also, immunofluorescence demonstrated the expression of COX-2 in esophageal squamous cell cancer-nests. These findings suggest that COX-2 may also be a marker for the malignant potential of esophageal squamous cell carcinoma, although this function remains to be clarified. Taken into consideration of the limited number of specimens, a conservative interpretation of the increased COX-2 mRNA and protein expression is necessary. Examination of a larger number of paired samples of tumor tissue and nonmalignant mucosa from esophageal cancer patients, as well as normal mucosa from persons without esophageal cancer in future studies will be necessary to more clearly determine the status of COX-2 in normal esophageal mucosa and in

esophageal cancer. Because COX-2 was up-regulated at the transcriptional level, which can increase COX-2 protein expression, subsequent determination of COX-2 protein synthesis and bioactivity at the protein level is important. It is also important to study the possible link between the known genetic alterations and COX-2 in esophageal cancer. However, the present results indicate COX-2 is elevated in esophageal cancer in a fashion similar to that in intestinal tumors.

COX-2 could potentially cause carcinogenesis via multiple mechanisms, and the role of COX-2 in tumor development and progression *in vivo* is not known. The most obvious possibility is that overexpression of COX-2 leads to high levels of prostaglandins (PGs) in tumor tissue. This hypothesis is supported by the finding of elevated levels of PGs in cancer tissues, compared with corresponding normal tissues^[34,35]. PGs produced by COX-2 may subsequently facilitate tumor progression by acting as differentiation and growth factors, immunosuppressors and angiogenic agents^[36-38]. Additionally, it has been shown that elevated PGE₂ levels in COX-2 overexpression cancer cells correlate with the metastatic potential of the cancer cells, and can be reduced in a dose-dependent manner by COX inhibitors^[39]. On the other hand, there is also evidence that NSAIDs might exert their antineoplastic effect by a PG-independent pathway, and the COX-2 enzyme itself may promote cancer development and progression^[40]. Thus, NSAIDs suppressed proliferative activity in colon cancer cells devoid of cyclooxygenase and PGs^[31]. Moreover, in extrahepatic tissues in which cytochrome P450 content is low, COX may be important for generation of carcinogens. For example, several classes of chemical carcinogens, e.g., dihydrodiol derivatives of polycyclic aromatic hydrocarbons, aromatic amines and heterocyclic amines, are activated to mutagenic derivatives by COX^[41]. The generation of carcinogens by COX-2 may be important, therefore, for understanding the link between cigarette smoking or consumption of grilled or fried meat and esophageal cancer^[42]. Additional studies are needed to determine which of these mechanisms are more important in esophageal squamous cell carcinoma.

Selective inhibition of COX-2 in esophageal cancer cells induces apoptotic cell death and reduces proliferative activity and these effects correlate with the inhibition of PG synthesis. Similar results have been reported^[43-45]. The significance of COX-2 likely varies between different classes of tumors. We cannot conclude from this and other published data whether the antiproliferative and proapoptotic effects of COX-2 inhibition on esophageal cancer cells are exclusively mediated through the inhibition of PG synthesis or if other mechanisms are also involved. However, our data provide a theoretical basis for evaluation of long-term intake of COX inhibitors on reduction of the incidence of esophageal cancer. Defining actual response of individual tumors to COX-2 inhibitors *in vivo*, however,

awaits further evaluation, especially since the level of COX-2 expression varies substantially between different tumors. Based on our data, a more thorough study on COX-2 expression is needed in patients with esophageal squamous cell carcinoma. Patients with a high COX-2 expression may benefit from specific or nonspecific COX-2 inhibitor medication, such as aspirin, for potential carcinogenic prevention of these cancers. Long-term intake of COX-2 inhibitors may be recommended for family members, especially with a positive family history of esophageal squamous cell carcinoma.

Taken together, our study suggests that COX-2 may play a role in esophageal squamous cell carcinoma development and/or progression and COX-2 inhibitors may be potential agents for the prevention or treatment of human invasive esophageal squamous cell carcinoma. Therefore, long-term intake of NSAIDs, such as aspirin, might reduce the risk of esophageal squamous cell carcinoma. To verify this hypothesis studies to evaluate the efficacy of COX-2 inhibitors in relevant animal models of esophageal squamous cell carcinoma are needed. In addition, studies to define the possible role of COX-2 in esophageal squamous cell carcinoma and the mechanisms by which COX-2 inhibitors exert antitumor activity are essential.

ACKNOWLEDGEMENTS

We thank Drs. Fan Zhang and Chun-Xia Zhao for their technical assistance.

REFERENCES

- Ishizuka T, Tanabe C, Sakamoto H, Aoyagi K, Maekawa M, Matsukura N, Tokunaga A, Tajiri T, Yoshida T, Terada M, Sasaki H. Gene amplification profiling of esophageal squamous cell carcinomas by DNA array CGH. *Biochem Biophys Res Commun* 2002; **296**: 152-155
- Kajiyama Y, Hattori K, Tomita N, Amano T, Iwanuma Y, Narumi K, Udagawa H, Tsurumaru M. Histopathologic effects of neoadjuvant therapies for advanced squamous cell carcinoma of the esophagus: multivariate analysis of predictive factors and p53 overexpression. *Dis Esophagus* 2002; **15**: 61-66
- Greenberg ER, Baron JA, Freeman DH Jr, Mandel JS, Haile R. Reduced risk of large-bowel adenomas among aspirin users. *J Natl Cancer Inst* 1993; **85**: 912-916
- Giovannucci E, Egan KM, Hunter DJ, Stampfer MJ, Colditz GA, Willett WC, Speizer FE. Aspirin and the risk of colorectal cancer in women. *N Engl J Med* 1995; **333**: 609-614
- Hla T, Neilson K. Human cyclooxygenase-2 cDNA. *Proc Natl Acad Sci U S A* 1992; **89**: 7384-7388
- Kennedy BP, Chan CC, Culp SA, Cromlish WA. Cloning and expression of rat prostaglandin endoperoxide synthase (cyclooxygenase)-2 cDNA. *Biochem Biophys Res Commun* 1993; **197**: 494-500
- Feng L, Sun W, Xia Y, Tang WW, Chanmugam P, Soyoola E, Wilson CB, Hwang D. Cloning two isoforms of rat cyclooxygenase: differential regulation of their expression. *Arch Biochem Biophys* 1993; **307**: 361-368
- Smith WL, Meade EA, DeWitt DL. Pharmacology of prostaglandin endoperoxide synthase isozymes-1 and -2. *Ann N Y Acad Sci* 1994; **714**: 136-142
- Williams CS, DuBois RN. Prostaglandin endoperoxide synthase: why two isoforms? *Am J Physiol* 1996; **270**(3 Pt 1): G393-400
- DuBois RN, Tsujii M, Bishop P, Awad JA, Makita K, Lanahan A. Cloning and characterization of a growth factor-inducible cyclooxygenase gene from rat intestinal epithelial cells. *Am J Physiol* 1994; **266**(5 Pt 1): G822-G827
- Hempel SL, Monick MM, Hunninghake GW. Lipopolysaccharide induces prostaglandin H synthase-2 protein and mRNA in human alveolar macrophages and blood monocytes. *J Clin Invest* 1994; **93**: 391-396
- Prescott SM, White RL. Self-promotion? Intimate connections between APC and prostaglandin H synthase-2. *Cell* 1996; **87**: 783-786
- Subbaramaiah K, Telang N, Ramonetti JT, Araki R, DeVito B, Weksler BB, Dannenberg AJ. Transcription of cyclooxygenase-2 is enhanced in transformed mammary epithelial cells. *Cancer Res* 1996; **56**: 4424-4429
- Eberhart CE, Coffey RJ, Radhika A, Giardiello FM, Ferrenbach S, DuBois RN. Up-regulation of cyclooxygenase 2 gene expression in human colorectal adenomas and adenocarcinomas. *Gastroenterology* 1994; **107**: 1183-1188
- Ristimaki A, Honkanen N, Jankala H, Sipponen P, Harkonen M. Expression of cyclooxygenase-2 in human gastric carcinoma. *Cancer Res* 1997; **57**: 1276-1280
- Wilson KT, Fu S, Ramanujam KS, Meltzer SJ. Increased expression of inducible nitric oxide synthase and cyclooxygenase-2 in Barrett's esophagus and associated adenocarcinomas. *Cancer Res* 1998; **58**: 2929-2934
- Hida T, Yatabe Y, Achiwa H, Muramatsu H, Kozaki K, Nakamura S, Ogawa M, Mitsudomi T, Sugiura T, Takahashi T. Increased expression of cyclooxygenase 2 occurs frequently in human lung cancers, specifically in adenocarcinomas. *Cancer Res* 1998; **58**: 3761-3764
- Reddy BS, Rao CV, Seibert K. Evaluation of cyclooxygenase-2 inhibitor for potential chemopreventive properties in colon carcinogenesis. *Cancer Res* 1996; **56**: 4566-4569
- Kawamori T, Rao CV, Seibert K, Reddy BS. Chemopreventive activity of celecoxib, a specific cyclooxygenase-2 inhibitor, against colon carcinogenesis. *Cancer Res* 1998; **58**: 409-412
- Thun MJ, Namboodiri MM, Calle EE, Flanders WD, Heath CW Jr. Aspirin use and risk of fatal cancer. *Cancer Res* 1993; **53**: 1322-1327
- Funkhouser EM, Sharp GB. Aspirin and reduced risk of esophageal carcinoma. *Cancer* 1995; **76**: 1116-1119
- Rubio CA. Antitumoral activity of indomethacin on experimental esophageal tumors. *J Natl Cancer Inst* 1984; **72**: 705-707
- Rubio CA. Further studies on the therapeutic effect of indomethacin on esophageal tumors. *Cancer* 1986; **58**: 1029-1031
- Ciaparrone M, Yamamoto H, Yao Y, Sgambato A, Cattoretti G, Tomita N, Monden T, Rotterdam H, Weinstein IB. Localization and expression of p27KIP1 in multistage colorectal carcinogenesis. *Cancer Res* 1998; **58**: 114-122
- Giardiello FM, Hamilton SR, Krush AJ, Piantadosi S, Hylind LM, Celano P, Booker SV, Robinson CR, Offerhaus GJ. Treatment of colonic and rectal adenomas with sulindac in familial adenomatous polyposis. *N Engl J Med* 1993; **328**: 1313-1316
- Labayle D, Fischer D, Vielh P, Drouhin F, Pariente A, Bories C, Duhamel O, Troussot M, Attali P. Sulindac causes regression of rectal polyps in familial adenomatous polyposis. *Gastroenterology* 1991; **101**: 635-639
- Tonelli F, Valanzano R. Sulindac in familial adenomatous polyposis. *Lancet* 1993; **342**: 1120
- Thun MJ, Namboodiri MM, Heath CW Jr. Aspirin use and reduced risk of fatal cancer. *N Engl J Med* 1991; **325**: 1593-1596
- Schreinemachers DM, Everson RB. Aspirin use and lung, colon, and breast cancer incidence in a prospective study. *Epidemiology* 1994; **5**: 138-146
- Takahashi M, Furukawa F, Toyoda K, Sato H, Hasegawa R, Imaida K, Hayashi Y. Effects of various prostaglandin synthesis inhibitors on pancreatic carcinogenesis in hamsters after initiation with N-nitrosobis(2-oxopropyl)amine. *Carcinogenesis* 1990; **11**: 393-395
- Levy GN. Prostaglandin H synthases, nonsteroidal anti-inflammatory drugs, and colon cancer. *FASEB J* 1997; **11**: 234-247
- Takahashi M, Fukutake M, Yokota S, Ishida K, Wakabayashi K, Sugimura T. Suppression of azoxymethane-induced aberrant crypt foci in rat colon by nimesulide, a selective inhibitor of cyclooxygenase 2. *J Cancer Res Clin Oncol* 1996; **122**: 219-222
- Sano H, Kawahito Y, Wilder RL, Hashimoto A, Mukai S, Asai K, Kimura S, Kato H, Kondo M, Hla T. Expression of cyclooxygenase-1 and -2 in human colorectal cancer. *Cancer*

- Res* 1995; **55**: 3785-3789
- 34 **Bennett A**, Tacca MD, Stamford IF, Zebro T. Prostaglandins from tumours of human large bowel. *Br J Cancer* 1977; **35**: 881-884
- 35 **Maxwell WJ**, Kelleher D, Keating JJ, Hogan FP, Bloomfield FJ, MacDonald GS, Keeling PW. Enhanced secretion of prostaglandin E2 by tissue-fixed macrophages in colonic carcinoma. *Digestion* 1990; **47**: 160-166
- 36 **Marnett LJ**. Aspirin and the potential role of prostaglandins in colon cancer. *Cancer Res* 1992; **52**: 5575-5589
- 37 **Hla T**, Ristimaki A, Appleby S, Barriocanal JG. Cyclooxygenase gene expression in inflammation and angiogenesis. *Ann N Y Acad Sci* 1993; **696**: 197-204
- 38 **Qiao L**, Kozoni V, Tsioulas GJ, Koutsos MI, Hanif R, Shiff SJ, Rigas B. Selected eicosanoids increase the proliferation rate of human colon carcinoma cell lines and mouse colonocytes *in vivo*. *Biochim Biophys Acta* 1995; **1258**: 215-223
- 39 **Tsujii M**, Kawano S, DuBois RN. Cyclooxygenase-2 expression in human colon cancer cells increases metastatic potential. *Proc Natl Acad Sci U S A* 1997; **94**: 3336-3340
- 40 **Hanif R**, Pittas A, Feng Y, Koutsos MI, Qiao L, Staiano-Coico L, Shiff SJ, Rigas B. Effects of nonsteroidal anti-inflammatory drugs on proliferation and on induction of apoptosis in colon cancer cells by a prostaglandin-independent pathway. *Biochem Pharmacol* 1996; **52**: 237-245
- 41 **Eling TE**, Thompson DC, Foureman GL, Curtis JF, Hughes MF. Prostaglandin H synthase and xenobiotic oxidation. *Annu Rev Pharmacol Toxicol* 1990; **30**: 1-45
- 42 **Ahlgren JD**. Epidemiology and risk factors in pancreatic cancer. *Semin Oncol* 1996; **23**: 241-250
- 43 **Gierse JK**, Hauser SD, Creely DP, Koboldt C, Rangwala SH, Isakson PC, Seibert K. Expression and selective inhibition of the constitutive and inducible forms of human cyclo-oxygenase. *Biochem J* 1995; **305**(Pt 2): 479-484
- 44 **Ogino K**, Hatanaka K, Kawamura M, Katori M, Harada Y. Evaluation of the pharmacological profile of meloxicam as an anti-inflammatory agent, with particular reference to its relative selectivity for cyclooxygenase-2 over cyclooxygenase-1. *Pharmacology* 1997; **55**: 44-53
- 45 **Klein T**, Nusing RM, Wiesenber-Boettcher I, Ullrich V. Mechanistic studies on the selective inhibition of cyclooxygenase-2 by indanone derivatives. *Biochem Pharmacol* 1996; **51**: 285-290

Edited by Zhu LH Proofread by Chen WW and Xu FM

Gastric malignancies in Northern Jordan with special emphasis on descriptive epidemiology

Kamal E. Bani-Hani, Rami J. Yaghan, Hussein A. Heis, Nawaf J. Shatnawi, Ismail I. Matalaka, Amjad M. Bani-Hani, Kamal A. Gharaibeh

Kamal E. Bani-Hani, Rami J. Yaghan, Hussein A. Heis, Nawaf J. Shatnawi, Amjad M. Bani-Hani, Kamal A. Gharaibeh, Department of Surgery Princess Basma Teaching Hospital, Faculty of Medicine, Jordan University of Science & Technology, Irbid- Jordan

Ismail I. Matalaka, Department of Pathology, Princess Basma Teaching Hospital, Faculty of Medicine, Jordan University of Science & Technology, Irbid- Jordan

Correspondence to: Kamal E. Bani-Hani, Associate Professor of Surgery, Department of Surgery, Faculty of Medicine, Jordan University of Science and Technology, PO Box 3030, Irbid 22110, Jordan. banihani60@yahoo.com

Telephone: +962-79-5500014 **Fax:** +962-2-7060300

Received: 2004-02-06 **Accepted:** 2004-02-24

Abstract

AIM: To study the epidemiology of gastric malignancies in Jordan as a model for Middle East countries where such data is scarce.

METHODS: Pertinent epidemiological and clinicopathological data for 201 patients with gastric malignancy in north of Jordan between 1991 and 2001 were analyzed.

RESULTS: Male: female ratio was 1.8:1. The mean age was 61.2 years, and 8.5% of the patients were younger than 40 years of age. The overall age-adjusted incidence was 5.82/100 000 population/year. The age specific incidence for males raised from 1.48 in those aged 30-39 years to 72.4 in those aged 70-79 years. Adenocarcinomas, gastric lymphomas, malignant stromal tumors, and carcinoids were found in 87.5%, 8%, 2.5%, and 2% respectively. There was an average of 10.1-month delay between the initial symptoms and the diagnosis. Only 82 patients underwent "curative" gastrectomy. Among adenocarcinoma groups, Lauren intestinal type was the commonest (72.2%) and the distal third was the most common localization (48.9%). The mean follow up for patients with gastric adenocarcinoma was 25.1 mo (range 1-132 mo). The 5-year survival rates for stages I ($n=15$), II ($n=41$), III ($n=59$), and IV ($n=53$) were 67.3%, 41.3%, 5.7%, and 0% respectively ($P=0.0001$). The overall 5 year survival was 21.1%.

CONCLUSION: Despite low incidence, some epidemiological features of gastric cancer in Jordan mimic those of high-risk areas. Patients are detected and treated after a relatively long delay. No justification in favor of a possible gastric cancer screening effort in Jordan is supported by our study; rather, the need of an earlier diagnosis and subsequent better care.

Bani-Hani KE, Yaghan RJ, Heis HA, Shatnawi NJ, Matalaka II, Bani-Hani AM, Gharaibeh KA. Gastric malignancies in Northern Jordan with special emphasis on descriptive epidemiology. *World J Gastroenterol* 2004; 10(15): 2174-2178
<http://www.wjgnet.com/1007-9327/10/2174.asp>

INTRODUCTION

Gastric cancer (GC) is one of the most prevalent cancers and, today, is the second cause of cancer death worldwide^[1,2]. The pattern and incidence of GC vary widely between different parts of the world. Costa Rica and Japan have the first and second highest rates in the world with a death rate of 77.5 and 50.5 /100 000 population, respectively^[2,3]. In the United States 12 100 deaths from GC were expected during 2003 with a death rate of 6.8/100 000, and it was estimated that 224 00 (13 400 in men) new cases of GC were diagnosed in the same year^[4]. The risk of developing GC was relatively lower in the Middle East and North Africa compared to those of western countries^[1,5].

The epidemiology of GC has been widely studied in the Western world as well as in Japan^[6-12]. However, only few scattered reports from the developing world have been published^[13-17]. There is a lack of good descriptive data on GC from the Middle East countries, where both cancer registration and prevalence of risk factors are relatively unknown. Because of the decreasing trend that took place in the Western world as a result of possibly, socio-economic development and its consequences, it is important to gain an insight into what is happening in other parts of the world such as in the Middle East. This prompted us to report on the epidemiological and clinicopathological features of gastric malignancy in Jordan in comparison to other countries whenever possible. This could assist in the better understanding of the important risk factors, which contribute to the development of GC. This will also give a clue about whether or not screening programs are needed in our region.

MATERIALS AND METHODS

Patients

This is a retrospective study of gastric malignancy in the north of Jordan over an eleven-year period (Jan 1991 to Dec 2001). The population of Irbid province (north of Jordan) as determined in the last official census conducted in Jordan in 1994 was 745 774 out of which 385 264 (51.66%) were males. Fifty percent of the Jordanian population are below the age of 16 years^[18]. A total of 76% of the population live in cities and towns.

Initial data were obtained from the computer database at the Department of Pathology at Jordan University of Science and Technology. This is the only pathology center serving the area. Histologically confirmed primary gastric malignancy was found in 201 patients, including 176 patients with adenocarcinoma, 16 patients with primary gastric lymphoma (PGL), 5 patients with malignant gastric stromal tumors, and 4 patients with gastric carcinoids. Further information was obtained from the medical records of these patients at Princess Basma Teaching Hospital and Prince Rashed Teaching Hospital, the only two tertiary centers in Northern Jordan. All available endoscopy reports were reviewed. Patients and/or family members were contacted whenever possible.

A single pathologist reviewed all the histological slides. Gastric adenocarcinoma was classified into intestinal (IT), diffuse (DT), or mixed types according to the histological criteria

of Lauren^[19]. The site of the tumor was assessed pathologically in the resected specimens and endoscopically in the remaining cases, and was defined as that part of the stomach harboring the bulk of the tumor. Tumor staging in each patient was based on clinical information, preoperative radiological investigations, operative findings, and pathological examination. The staging was made in accordance with the TNM system endorsed by the Union Internationale Contre Le Cancer (UICC)^[20].

Vital status of patients was ascertained from death certificates or from families who were contacted.

All deaths within 30 d of surgery were considered surgical mortality. The incidence rates were adjusted to the world population. Our hospital based incidence data were matched with the Jordanian National Cancer Registry (JNCR) data only for the period 1996-2001, since the Registry was established in 1996. The survival rate was analyzed for each stage by the Kaplan-Meier method, and the survival curves were compared by the log-rank test using the Statistical Package for the Social Sciences Software Program (SPSS®, Inc., Chicago, Illinois, USA). Differences were considered statistically significant at $P < 0.05$.

RESULTS

During the study period 201 patients with primary gastric malignancy were identified, 128 (63.7%) patients were males with a male: female ratio of 1.8:1.

Sixty-five percent of the patients (131/202) were diagnosed during the second half of the study period. Analyses of the data from the JNCR, which was established in 1996, showed that all the 131 study patients diagnosed with gastric malignancy between 1st January 1996 and 31st December 2001 appeared in the registry and there were no additional patients from northern Jordan in the registry not identified by our study.

The overall age-adjusted incidence (world population) was 5.82/100 000 per year. Table 1 shows the age specific incidence

rate (ASIR) per 100 000 population by gender. The peak incidence was in the age group 60-69 years (39.8%), followed by the age group 70-79 (22.9%). Approximately 8.5% of the patients were younger than 40 years of age. The mean age for the whole group was 61.2 years (SD±12.3, range 24-91 years).

Presenting features for our patients are summarized in Table 2. Acute presentation was seen in 59 (29.4%) patients; 37 patients (18.4%) presented with upper gastrointestinal bleeding, 17 (8.5%) with gastric outlet obstruction, and in the remaining 5 (2.5%) patients perforation was the mode of presentation.

Table 2 Presenting features of patients with gastric malignancy

	Number of patients	%
Abdominal pain	144	71.6
Weight loss and/or anemia	130	64.7
Dyspepsia	98	48.8
Nausea, vomiting	96	47.8
Abdominal mass	62	30.8
Anorexia	58	28.9
Dysphagia	44	21.9
Gastrointestinal bleeding	37	18.4
Obstruction	17	8.5
Perforation	5	2.5

There was an average of 10.1-month delay (range 2-17 mo) between the initial symptoms and the diagnosis. In 119 patients this was a result of reluctance in seeking medical advice and/or delay in referring patients for endoscopy. However, in five patients the delay was caused by a false negative upper gastrointestinal endoscopy.

Table 3 shows the distribution of the different histological types according to age and sex. The histologic subtypes of the

Table 1 Age specific incidence rate per 100 000 population/year by age and gender

Age (yr) group	Male			Female		
	Population	No. of cancers ¹	ASIR ²	Population	No. of cancers ¹	ASIR ²
0-9	113 142	0	0	106 465	0	0
10-19	092 899	0	0	087 629	0	0
20-29	076 938	0	0	071 445	1	0.13
30-39	043 068	7	1.48	038 967	9	2.1
40-49	024 175	11	4.14	023 480	6	2.32
50-59	019 763	21	9.66	017 526	9	4.67
60-69	010 157	53	47.44	009 009	27	27.25
70-79	003 641	29	72.4	004 264	17	36.24
80	001 481	7	43	001 725	4	21.08
Total	385 264	128	3.02	360 510	73	1.84

¹Number of cancers during the 11-year study. ²Age specific incidence rate per 100 000 population/year.

Table 3 Histopathological distribution of gastric malignancies according to age and sex (%)

Histopathologic diagnosis	Age (yr)		Sex		Total
	Mean	Range	Male	Female	
Intestinal type adenocarcinoma	62.7	35-91	90(70.9)	37(29.1)	127(63.2)
Diffuse type adenocarcinoma	51.9	24-75	9(31)	20(69)	29(14.4)
Mixed type adenocarcinoma	64.3	51-72	11(57.9)	8(42.1)	19(9.5)
Adenosquamous carcinoma	82	82	1	-	1(0.5)
Primary gastric lymphoma	57.9	41-82	12(75)	4(25)	16(8)
Carcinoid	66	41-81	2(50)	2(50)	4(2)
Malignant stromal tumors	69.4	43-84	3(60)	2(40)	5(2.5)
Total	61.2	24-91	128(63.7)	73(36.3)	201(100)

Table 4 Distribution of gastric adenocarcinoma according to site (%)

Histopathological type	Proximal third	Middle third	Distal third	Entire stomach	Total
Intestinal type adenocarcinoma	22(17.3)	30(23.6)	70(55.1)	5(3.9)	127
Diffuse type adenocarcinoma	6(20.7)	7(24.1)	7(24.1)	9(31)	29
Mixed type adenocarcinoma	3(15.8)	5(26.3)	8(42.1)	3(15.8)	19
Adenosquamous carcinoma	-	-	1	-	1
Total	31(17.6)	42(23.9)	86(48.9)	17(9.7)	176

82 patients who had gastrectomy were correctly diagnosed in pre-gastrectomy endoscopic biopsies except in 2 cases, which were diagnosed as IT adenocarcinoma and turned out to be of the DT in subsequent examinations of the resected specimens. Pathological examination of the 65 resected IT and mixed adenocarcinomas revealed that 51 of the cancers were moderately differentiated, 10 were poorly differentiated and four were well differentiated.

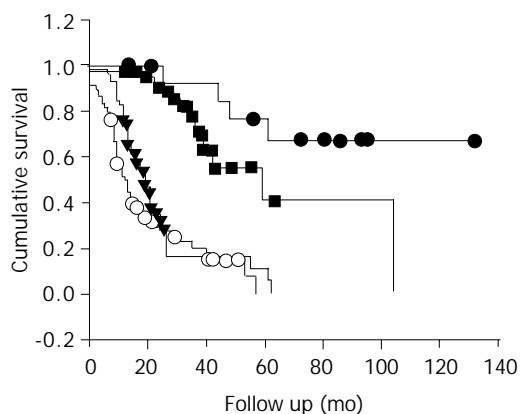
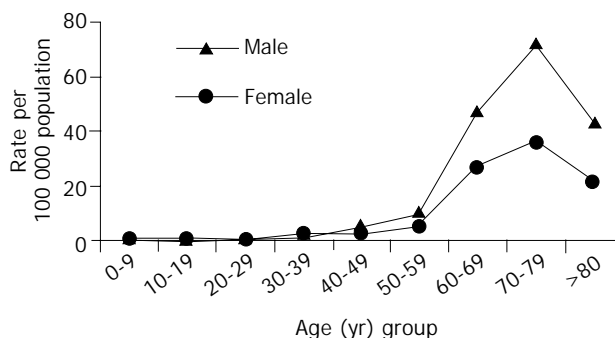
Table 4 shows the distribution of various histologic types of gastric adenocarcinoma according to the sites affected.

For gastric adenocarcinoma, using the TNM staging, 15 patients had stage I, 41 patients had stage II, 59 patients had stage III, and 53 patients had stage IV disease. In the remaining 8 patients, the stage could not be determined due to insufficient data (stage X).

Gastrectomy was performed for 82 patients (D1 in 63 and D2 in 19 patients). Palliative resection or bypass procedures were done for 95 patients, while 3 patients with PGL had chemotherapy only. The remaining 21 patients were too frail to be treated. No patients had D3 gastrectomy. None of the patients with adenocarcinoma was given adjuvant therapy. Postoperative morbidity occurred in 25.4% (45/177) of the patients. Eight patients died during the postoperative period giving a surgical mortality of 4.5% (8/177).

For the 176 patients with adenocarcinoma, the mean follow up until December 2002 was 25.1 mo (range 1-132 mo). At that time, vital status was available for 163 patients (92.6%). The remaining 13 patients (mean age 59.6 years; 11 males and 2 females) were lost to follow up at a mean of 28.2 mo (range 7-86 mo). The stages of the disease for these 13 patients were I, II, III, IV, and X in 1, 2, 4, 4, and 2 patients respectively.

Survival analysis included the 8 early postoperative deaths and the later non-cancer deaths. The median survival for stages II, III, and both stages IV and X was 59, 19, and 13 mo respectively. Figure 1 demonstrates the survival curves for stages I-IV using Kaplan-Meier method. The 5-year survival rates for stages I, II, III, and IV were 67.3%, 41.3%, 5.7%, and 0% respectively ($P=0.0001$). The overall 5 year survival was 21.1%.

**Figure 1** Survival rate of gastric adenocarcinoma patients according to stage using Kaplan-Meier analysis. (●) Stage I; $n=15$, (■) Stage II; $n=41$, (▼) Stage III; $n=59$, (○) Stage IV and X; $n=61$.**Figure 2** Age specific incidence rate per 100 000 population/year by gender.

DISCUSSION

There was consistency between our study and the data of the JNCR. The incidence was calculated and corrected for age in relation to the world population. The age-adjusted incidence of gastric malignancy in this study was 5.82/100 000 per year, which was significantly lower than those of developed countries but rather similar to most other Middle East countries^[1,2]. However, this incidence would rise sharply when the ASIR is calculated because of the specific pyramidal age distribution of our population where approximately 50% of our population are below the age of 16 years (1994 census). The ASIR for males per 100 000 population raised from 1.48 in those aged 30-39 years to 72.4 in those aged 70-79 years (Figure 2). Similarly, figures from the JNCR showed that during 1997, the ASIR raised sharply from 3.3 to 108 for the same gender and age groups^[18]. During the same year GC was the eighth commonest cancer, representing 4% of all cancer cases, and it accounted for 22% of all primary gastrointestinal tract cancers.

It is well known that the incidence of GC is decreasing globally. The apparent increase in diagnosing GC during the second half of the study period most likely reflects a better diagnostic yield after the relatively recent introduction of endoscopic services throughout the country rather than an actual increase in the incidence. Still the following two factors may play a role in this increasing trend. First, the rapid change in dietary habits Jordan is witnessing might constitute a risk factor. Vitamin C-rich fresh vegetables and fruits, starch, and natural unprocessed wheat products were the major constituents of Jordanian food. However, canned food, hot spices, pickles, and animal proteins are now dominating the Jordanian menu. It is known that the environmental risk factors for GC could be dietary in origin^[21,22]. Second, the already high prevalence of *Helicobacter pylori* in Jordan is increasing and the exposure time is also increasing with the improvement in life expectancy among Jordanians^[23,24]. It is proposed that Lauren's IT of GC is related to chronic *Helicobacter pylori* infection. Among our study group IT adenocarcinoma was the commonest histological subtype (63.2%).

Most resections were done with palliative intent. The low rate of gastrectomy with "curative" intent could be explained by the high proportion of patients with advanced GC at

presentation. However, we believe that surgical undertreatment might be a contributing factor. Our patients tended to present late as evidenced by the facts that there was a long interval between onset of symptoms and presentation, 29.4% presented acutely, and that only 40.8% (82/201) of them underwent D1 or D2 gastrectomy. This is not only due to insufficiency of current endoscopic services, but also due to the fact that many people in Jordan who have non-specific dyspeptic symptoms will seek the advice of non-physician personnel who will either prescribe herbal medicine for long term treatment or induce patches of second or third degree burns to the epigastric region using hot metals in order to ameliorate the deep seated pain! Subsequently some of these patients in whom the cause of dyspepsia is cancer will present to the hospital with late stage GC or one of its complications. In addition, the elderly people usually fail to make use of the available medical services due to inadequacy of primary health care in Jordan.

Some GC patterns in north of Jordan were similar to those reported from high-risk regions worldwide^[3,25]. In particular, the mean age was in the seventh decade, male to female ratio was 1.8:1, IT adenocarcinoma was more common than DT (4.4:1), and distal location was more frequent than proximal one (2.5:1). Since the demographic features among Jordanians are homogenous, we believe that these trends apply to whole Jordan. In contrary, in a low-risk area, such as Kenya, the DT is the commonest subtype^[26].

In our study, DT adenocarcinoma occurred in younger patients with a mean age of 51.9 years and was commoner in females with a male to female ratio of 0.45:1 (Table 3). Similar findings of diffuse tumors prevailing among young patients and women were reported from Sweden, Finland, Mexico and Taiwan^[6,8,16,17], but not from neighboring Saudi Arabia^[14,15].

Our survival rate for stages I and II is consistent with the rate reported in the Western literature^[27,28]. However, this rate was much lower for our patients with more advanced stages probably reflecting undertreatment at our institute. After the introduction of a specialized upper gastrointestinal unit at our hospital in January 2001, we have adopted a more radical approach.

In Western countries, PGL represented only 2% to 5% of gastric malignancies^[29], while it represented 8% of our series, which was similar to the 9% figure from neighboring Iraq^[30], but different from the 14-22% figure reported from Saudi Arabia^[14,15]. During the past three decades the site of PGL in the Middle East has changed^[31]. Small intestinal involvement became less common, and gastric involvement more frequent. This varying pattern seemed to be environmental in origin^[31]. Although the ratio of PGL to gastric adenocarcinoma among our patients was higher than in western series, a recent study from Jordan demonstrated that other patterns of PGL were mimicking those of the west^[32]. The stomach was the commonest site of involvement, accounting for 62% of all cases^[32].

Our rates for the gastric malignant stromal tumors and carcinoids are consistent with rates reported elsewhere^[33]. The survival rate for these patients was not calculated due to the small number of patients.

At the end of this discussion, we would like to highlight some of the shortcomings in our study. First, the incidence figures were calculated only after histological confirmation by endoscopy or surgery. In Jordan, hospital postmortem is rarely performed because of religious or social grounds. Additionally, only half of deaths are attended by medical workers personals. This means that some patients with GC were certainly not included in the incidence calculation. The limitation to histologically confirmed cases increases specificity but lowers the sensitivity in identifying cases to be included in the incidence figures. Cases admitted to hospitals with a suspicion of GC or deceased with a diagnosis of GC but without histological

confirmation were not considered in the estimation of incidence rates. Additionally as one third of our patients presented with an abdominal mass, and there was a 10-mo delay in diagnosis so the estimated incidence was lower than the real incidence because many patients did not reach the hospitals. Second, Lauren classification is known to be affected by a quite low reproducibility^[34]. Specifically, mixed cases might be classified as intestinal or as diffuse type, depending on the examined tissue areas endoscopically biopsied or from the surgical specimens.

In conclusion, the incidence of GC in Jordan is low, but increases appreciably with age. This, in addition to the fact that 50% of the Jordanian population are below the age of 16 years, shows that it does not seem justified introducing a screening program. However, general practitioners should be more liberal in referring patients for endoscopy and resist the temptation to treat dyspeptic patients with anti-ulcer therapy without an endoscopy. Open access endoscopy, greater efforts in patient education and improvement of the diagnostic technical skills may raise the chance of detecting GC early. Some patterns of GC in Jordan (age, sex, tumor location, and histological type) are similar to features from high-risk areas. Although this study clearly highlights the pertinent epidemiological and clinicopathological features of gastric malignancy in Jordan, further studies are needed to evaluate the treatment outcomes.

REFERENCES

- 1 **Parkin DM**, Pisani P, Ferlay J. Estimates of the worldwide incidence of 25 major cancers in 1990. *Int J Cancer* 1999; **80**: 827-841
- 2 **Parkin DM**, Pisani P, Ferlay J. Global cancer statistics. *CA Cancer J Clin* 1999; **49**: 33-64
- 3 **Sasagawa T**, Solano H, Mena F. Gastric cancer in Costa Rica. *Gastrointest Endosc* 1999; **50**: 594-595
- 4 **Jemal A**, Murray T, Samuels A, Ghafoor A, Ward E, Thun MJ. Cancer statistics, 2003. *CA Cancer J Clin* 2003; **53**: 5-26
- 5 **Pisani P**, Parkin DM, Bray F, Ferlay J. Estimates of the worldwide mortality from 25 cancers in 1990. *Int J Cancer* 1999; **83**: 18-29
- 6 **Ekstrom AM**, Hansson LE, Signorello LB, Lindgren A, Bergstrom R, Nyren O. Decreasing incidence of both major histologic subtypes of gastric adenocarcinoma—a population-based study in Sweden. *Br J Cancer* 2000; **83**: 391-396
- 7 **Kaneko S**, Yoshimura T. Time trend analysis of gastric cancer incidence in Japan by histological types, 1975-1989. *Br J Cancer* 2001; **84**: 400-405
- 8 **Lauren PA**, Nevalainen TJ. Epidemiology of intestinal and diffuse types of gastric carcinoma. A time-trend study in Finland with comparison between studies from high- and low-risk areas. *Cancer* 1993; **71**: 2926-2933
- 9 **Haugstvedt TK**, Viste A, Eide GE, Maartmann-Moe H, Myking A, Soreide O. Is Lauren's histopathological classification of importance in patients with stomach cancer? A national experience. Norwegian Stomach Cancer Trial. *Eur J Surg Oncol* 1992; **18**: 124-130
- 10 **Stelzner S**, Emmrich P. The mixed type in Lauren's classification of gastric carcinoma. Histologic description and biologic behavior. *Gen Diagn Pathol* 1997; **143**: 39-48
- 11 **Leocata P**, Ventura L, Giunta M, Guadagni S, Fortunato C, Discepoli S, Ventura T. Gastric carcinoma: a histopathological study of 705 cases. *Ann Ital Chir* 1998; **69**: 331-337
- 12 **Monferrer Guardiola R**, Peiro Gomez AM, Galiana Gil R, Montes Rotgla A, Lillo Sanchez A, Cuevas Campos A. Incidence of gastric cancer in the 02 health area of Castellon. *An Med Interna* 1996; **13**: 68-72
- 13 **Johnson O**, Ersumo T, Ali A. Gastric carcinoma at Tikur Anbessa Hospital, Addis Ababa. *East Afr Med J* 2000; **77**: 27-30
- 14 **Hamdi J**, Morad NA. Gastric cancer in southern Saudi Arabia. *Ann Saudi Med* 1994; **14**: 195-197
- 15 **Al-Mofleh IA**. Gastric cancer in upper gastrointestinal endos-

- copy population: prevalence and clinicopathological characteristics. *Ann Saudi Med* 1992; **12**: 548-551
- 16 **Mohar A**, Suchil-Bernal L, Hernandez-Guerrero A, Podolsky-Rapoport I, Herrera-Goepfert R, Mora-Tiscareno A, Aiello-Crocifoglio V. Intestinal type: diffuse type ratio of gastric carcinoma in a Mexican population. *J Exp Clin Cancer Res* 1997; **16**: 189-194
- 17 **Wu CW**, Tsay SH, Hsieh MC, Lo SS, Lui WY, P'eng FK. Clinicopathological significance of intestinal and diffuse types of gastric carcinoma in Taiwan Chinese. *J Gastroenterol Hepatol* 1996; **11**: 1083-1088
- 18 **Al-Kayed S**, Hijawi B. Cancer incidence in Jordan 1997 report. National Cancer Registry. The hashemite kingdom of Jordan. *Amman (HKJ), Ministry of Health* 1999
- 19 **Lauren P**. The two histological main types of gastric carcinoma: diffuse and so-called intestinal type carcinoma. *Acta Path Microbiol Scan* 1965; **64**: 31-49
- 20 Hermanek P, Sobin L. TNM classification of malignant tumors. 4th ed. *Berlin: Springer Verlag* 1987
- 21 **Ngoan LT**, Mizoue T, Fujino Y, Tokui N, Yoshimura T. Dietary factors and stomach cancer mortality. *Br J Cancer* 2002; **87**: 37-42
- 22 **Palli D**. Epidemiology of gastric cancer: an evaluation of available evidence. *J Gastroenterol* 2000; **35**: 84-89
- 23 **Bani-Hani KE**, Hammouri SM. Prevalence of *Helicobacter pylori* in Northern Jordan. Endoscopy-based study. *Saudi Med J* 2001; **22**: 843-847
- 24 **Latif AH**, Shami SK, Batchoun R, Murad N, Sartawi O. *Helicobacter pylori*: a Jordanian study. *Postgrad Med J* 1991; **67**: 994-998
- 25 **Correa P**. Clinical implications of recent developments in gastric carcinoma pathology and epidemiology. *Semin Oncol* 1985; **12**: 2-10
- 26 **Ogutu EO**, Lule GN, Okoth F, Musewe AO. Gastric carcinoma in the Kenyan African population. *East Afr Med J* 1991; **68**: 334-339
- 27 **Davis PA**, Sano T. The difference in gastric cancer between Japan, USA and Europe: what are the facts? what are the suggestions? *Crit Rev Oncol Hematol* 2001; **40**: 77-94
- 28 **Fuchs CS**, Mayer RJ. Gastric carcinoma. *N Engl J Med* 1995; **333**: 32-41
- 29 **Hertzer NR**, Hoerr SO. An interpretive review of lymphomas of the stomach. *Surg Gynecol Obstet* 1976; **143**: 113-124
- 30 **Al-Bahrani Z**, Al-Mondhiry H, Bakir F, Al-Saleem T, Al-Eshaiker M. Primary gastric lymphoma. Review of 32 cases from Iraq. *Ann R Coll Surg Engl* 1982; **64**: 234-237
- 31 **Taleb N**, Chamseddine N, Abi Gergis D, Chahine A. Non-Hodgkin's lymphoma of the digestive system. General epidemiology and epidemiological data concerning 100 Lebanese cases seen between 1965 and 1991. *Ann Gastroenterol Hepatol* 1994; **30**: 283-286
- 32 **Almasri NM**, al-Abbadi M, Rewaily E, Abulkhail A, Tarawneh MS. Primary gastrointestinal lymphomas in Jordan are similar to those in Western countries. *Mod Pathol* 1997; **10**: 137-141
- 33 **Hamilton SR**, Aaltonen LA, eds. World Health Organization classification of tumours. Pathology and genetics of tumours of the digestive system. *Lyon IARC Press* 2000
- 34 **Palli D**, Bianchi S, Cipriani F, Duca P, Amorosi A, Avellini C, Russo A, Saragoni A, Todde P, Valdes E. Reproducibility of histologic classification of gastric cancer. *Br J Cancer* 1991; **63**: 765-768

Edited by Zhu LH and Xu FM

Identification of tumor markers using two-dimensional electrophoresis in gastric carcinoma

Kai-Juan Wang, Run-Tian Wang, Jian-Zhong Zhang

Run-Tian Wang, Department of Epidemiology and Biostatistics, School of Public Health, Peking University, Beijing 100083, China

Kai-Juan Wang, Department of Epidemiology, School of Public Health, Zhengzhou University, Zhengzhou 450052, Henan Province, China

Jian-Zhong Zhang, National Institute for Communicable Disease Control and Prevention, Chinese Center for Disease Control and Prevention, Beijing 102206, China

Supported by the National Natural Science Foundation of China, No. 30070671

Correspondence to: Professor Run-Tian Wang, Department of Epidemiology and Biostatistics, School of Public Health, Peking University, Beijing 100083, China. kjwang@163.com

Telephone: +86-10-82801525

Received: 2004-02-20 **Accepted:** 2004-03-02

Abstract

AIM: To study the differential expression of proteins in normal and cancerous gastric tissues, and further identify new molecular markers for diagnosis and prognosis of gastric carcinoma, as well as develop new therapeutic targets of the disease.

METHODS: Matched pairs of tissues from 6 gastric cancer patients were analyzed for their two-dimensional electrophoresis (2DE) profiles. Soluble fraction proteins from human normal and cancerous gastric tissue were separated in the first dimension by isoelectric focusing on immobilized pH gradient (IPG, pH3-10) strips, and by 125 g/L sodium dodecyl sulfate polyacrylamide gel electrophoresis (SDS-PAGE) in the second dimension with silver nitrate staining. Protein differential expression was analyzed by use of image analysis software to find out candidates for gastric cancer-associated proteins.

RESULTS: Nine protein spots overexpressed in tumor tissues as compared with noncancerous regions. In the next step, 9 tumor-specific spots were cut off from Coomassie Brilliant Blue staining gels, digested in gel with L-1-tosylamide-2-phenylethyl chloromethyl ketone (TPCK)-trypsin. Protein identification was done by peptide mass fingerprinting with matrix assisted laser desorption/ionization-time of flight-mass spectrometry (MALDI-TOF-MS). In total, 5 tumor-specific protein spots corresponding to 5 different polypeptide chains were identified, including annexin V, carbonic anhydrase, prohibitin, fibrin beta and fibrinogen fragment D. Among these 5 spots, the potential significance of the differential expressions is discussed.

CONCLUSION Differential expression analysis of proteomes may be useful for the development of new molecular markers for diagnosis and prognosis of gastric carcinoma.

Wang KJ, Wang RT, Zhang JZ. Identification of tumor markers using two-dimensional electrophoresis in gastric carcinoma. *World J Gastroenterol* 2004; 10(15): 2179-2183
<http://www.wjgnet.com/1007-9327/10/2179.asp>

INTRODUCTION

Gastric cancer is a prevalent tumor worldwide. It is a multistage process involving multiple factors in aetiology and many gene-environment interactions. It is important to emphasize the heterogeneity of the histological background on which the tumor develops. Methods have been developed to identify tumor associated antigens such as molecular cloning in expression system or using a biochemical strategy based on the extraction of antigenic peptides bound to major histocompatibility complex class I molecules from tumor cells. These methods have allowed the recognition of certain human tumor antigens^[1]. Several tumor markers of gastric cancer have been identified^[2-4], including Lewis antigen, sulfomucin, CA50. However, no evidence has been obtained indicating that the detection of these markers precedes clinical diagnosis of gastric cancer. Proteomics studies of clinical tumor samples have led to the identification of cancer-specific protein markers, which provides a basis for developing new methods for early diagnosis and early detection of cancers as well as clues to understanding the molecular mechanism of cancer progression^[5]. In order to identify proteins that elicit humoral responses in gastric cancer patients, proteome-based approach was used. A number of proteins from gastric tumor tissues were separated by 2DE and identified by using mass spectrometry. It includes the systematic cataloging of protein expression on a large scale. Such studies could help elucidate the molecular mechanism of cellular events associated with cancer progression, such as cellular signaling^[6,7].

MATERIALS AND METHODS

Tissue samples and preparation^[8]

Six pairs of primary, and advanced poorly differentiated gastric adenocarcinoma tissues and corresponding adjacent noncancerous gastric tissues were obtained with informed consent from patients who underwent gastrectomy at the First Affiliated Hospital of Zhengzhou University and Beijing Cancer Hospital. Cancer samples were obtained from the "core" part of the tumor to avoid the adjacent noncancerous tissue. For each of the normal tissues, surface epithelium was selectively procured by dissection with special care for minimal contamination of nonepithelial cells, and samples were immediately snap-frozen in liquid nitrogen. They were classified histologically according to Lauren's classification after H & E staining.

Fragments of normal and malignant tissues were sharp dissected and homogenized with a homogenizer in 2 mL fresh lysis buffer [2 g/L dithiothreitol (Amersham Bioscience, USA), 200 mL/L trichloroacetic acid (Sigma, USA) and 800 g/L acetone], then placed into tubes at 4-8 °C for 8-10 h. The mixture was centrifuged at 1 000 r/min for 5 min to remove tissue and cell debris, then centrifuged in a Beckman TL-100 table top ultracentrifuge at 430 000 g in a TLA-100.2 rotor for 30 min at 4 °C. The supernatant was taken as soluble fraction. Protein was lyophilized, resuspended in isoelectric focusing gel rehydration solution {7 mol/L urea, 2 mol/L thiourea, 40 g/L 3-([3-cholamidopropyl] dimethylammonio)-1-propanesulfonate

(CHAPS), 50 mmol/L dithiothreitol, 20 g/L IPG buffer pH 3-10, L} and stored at -80 °C until use. These were used as the 2DE samples for the soluble fraction. Protein concentration of 2-DE samples was estimated according to a commercial Bradford reagent. BSA was used as standard.

2DE with IPG strips

First-dimension bioelectric focusing was carried out on Multiphor II system basically as described by the manufacturer Amersham Bioscience Inc. Samples containing up to 200 µg protein for analytical gels were diluted to up to 450 µL with dehydration solution (8 mol/L urea, 20 g/L CHAPS, 100 mol/L dithiothreitol, 5 g/L IPG buffer). Pre-cast Immobilized pH gradient (IPG) strip (24 cm, pH 3-10, linear gradient) was used for the first-dimensional separation. Strips were applied by overnight rehydration at 50 V, and for 1 h at 1 000 V. Then a gradient was applied from 1 000 to 8 000 V for 8 h to give a total of 180 000 Vh. All IEF steps were carried out at 20 °C. After the first-dimensional IEF, IPG gel strips were placed in an equilibration solution (6 mol/L urea, 200 g/L SDS, 300 g/L glycerol, 50 mol/L Tris-HCl, pH 8.8) containing 10 g/L dithiothreitol and shaken for 15 min. The gels were then transferred to the equilibration solution containing 25 g/L iodoacetamide to alkylate thiols and shaken for a further 15 min before being placed on a 125 g/L polyacrylamide gel slab. Separation in the second dimension was carried out using Tris-glycine buffer containing 1 g/L SDS, at a current setting of 5 mA/gel for the initial 0.5 h and 18 mA/gel thereafter and a temperature of 20 °C.

For silver staining, gels were immersed in ethanol: acetic acid: water (35:7:58) for 1.5 h, followed by washed twice in deionized water for 20 min. Gels were pretreated for 1 min in a solution of 0.2 g/L Na₂S₂O₃ and followed by 3 of 1-min washes in deionized water. Proteins were stained in a solution containing 2 g/L AgNO₃ and 0.075% formalin (37 g/L formaldehyde in water) for 20 min, and washed twice in deionized water for 1 min. Subsequently, gels were developed in a solution of 0.6 g/L formaldehyde, 20 g/L Na₂S₂O₃ and 0.004 g/L Na₂S₂O₃. When the desired intensity was attained, the developer was discarded and reaction stopped by 10 g/L EDTA-Na₂. For Coomassie Brilliant Blue staining of gels, gels were equilibrated in a solution containing 500 mL/L methanol, 50 mL/L acetic acid and 25 g/L Coomassie Brilliant Blue R-250. Gels were rinsed in 300 mL/L ethanol containing 70 mL/L acetic acid.

Protein patterns in the gels after silver staining were recorded as digitalized images using a high-resolution scanner. Gel image matching was done with PDQuest software.

In-gel protein digestion

Protein spots on Coomassie blue stained gel was performed essentially as described. After the completion of staining, the gel slab was washed twice with water for 10 min. The spots of interest were excised with a scalpel and put into 1.5 mL micro-tubes. The particles were washed twice with water and then twice with water/acetonitrile (1:1) for 15 min. The solvent volumes were about twice that of the gel. Liquid was removed, acetonitrile was added to the gel particles and the mixture was left for 2 h. After that, liquid was removed and the particles were rehydrated in 25 mmol/L NH₄HCO₃ for 5 min. Acetonitrile was added to produce a 1:1 mixture of 25 mmol/L NH₄HCO₃ / acetonitrile and the mixture was incubated for 15 min. All liquid was removed. Gel particles were dried in a vacuum centrifuge, reswelled in 10 mmol/L of dithiothreitol and 25 mmol/L of NH₄HCO₃, and incubated for 30 min at 56 °C to reduce the peptides. After chillness of tubes to room temperature and removal of the liquid, 55 mmol/L iodoacetamide in 25 mmol/L NH₄HCO₃ was added. The tubes were incubated for 30 min at room temperature in the dark to S-alkylate the peptides. Then

iodoacetamide solution was removed, the particles were washed with 25 mmol/L NH₄HCO₃ and acetonitrile, dried in a vacuum centrifuge, rehydrated in digestion buffer containing 50 mmol/L NH₄HCO₃ and 12.5 ng/µL trypsin (TPCK-treated, proteomics grade, Sigma, USA), incubated for 8-12 h at 37 °C. After digestion, 25 mmol/L NH₄HCO₃ was added, and the tube was incubated for 15 min. Acetonitrile was added and the tube was incubated for another 15 min. The supernatant was recovered, and the extraction was repeated twice with 50 g/L TFA/acetonitrile (1:1). The three extracts were pooled and dried in a vacuum centrifuge.

MALDI-TOF-MS analysis

One µL sample with 1 µL matrix solution CCA (α-cyano-4-hydroxycinnamic acid) was spotted on the target and dried. Dried spots were analyzed in an REFLEX-III (Bluker) MALDI-TOF mass spectrometer. The spectrometer was run in positive ion mode and in reflector mode with the setting: accelerating voltage, 20 kV; grid voltage, 76%; guide wire voltage, 0.01%; and a delay time of 150 ns. The low mass gate was set at 500 m/z.

Proteins were identified by peptide mass fingerprinting with the search programs Mascot (<http://www.matrixscience.com/cgi/index.pl?page=.1>). The following search parameters were applied: SWISS-PROT and NCBI were used as the protein sequence databases, a mass tolerance of 50 ppm and one incomplete cleavage were allowed; acetylation of the N-terminus, alkylation of lysine by carboxyamidomethylation were considered as possible modifications^[9].

RESULTS

Evaluation of the reproducibility

Mini 2DE gels (7 cm, pH3-10) were used to evaluate the reproducibility of the soluble protein preparations and to quantify the protein extracts for 2DE gel analysis. To ensure quality and reproducibility of results, 2DE maps (24 cm) were established from each sample based on silver staining of at least three independent gels, pairs of gels were run simultaneously with the same power supply and subjected to subsequent image analysis. Protein extracts prepared from tissues were compared in this way and found to be highly reproducible and similar amounts of total soluble protein were yielded when analyzed on the gels.

Overview analysis of the protein expression profiles of paired samples

2DE Gel separation of proteins from 6 pairs of normal and cancerous epithelial cells was procured from the same gastric carcinoma specimen respectively. A series of 2DE maps were constructed for the soluble fraction proteins of human gastric tissue. A representative 2DE gel images following silver staining of cancer tissues (Figure 1A) and normal tissues (Figure 1B) were produced in a 2DE imageMaster. Comparison of the differential protein expression between cancer and normal tissues shown in 2DE images was carried out using the AutoDetect Spots menu of PDQuest software. Figure 1A (from cancer tissues) contains a total of 356 spots, whereas Figure 1B (from normal tissues) contains a total of 382 spots. A total of 323 spots from cancer tissues could be matched to those from normal tissues. In total, we were able to identify 9 cancer-specific spots in 2DE gels. The positions of the identified proteins are shown in Figure 1A. These differences were observed in other cancerous samples. Because all of the identified spots were detectable with Coomassie Blue staining, they could be considered as abundant proteins.

Protein identification

The resulting spot identification was mapped onto the analytical

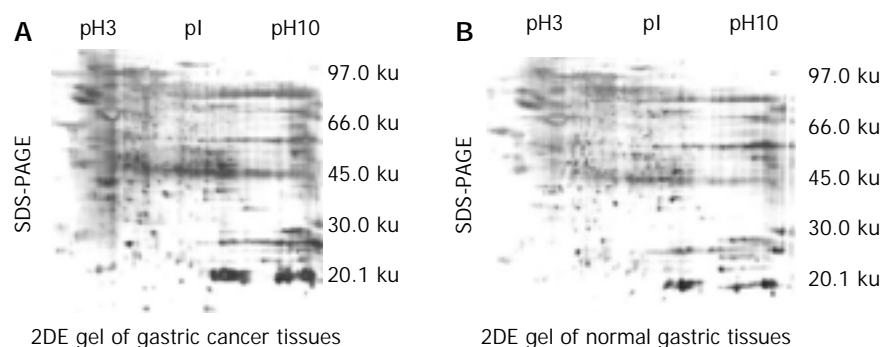


Figure 1 2DE maps of human gastric tissue from No.5 patient. A: was from gastric cancer. B: from normal gastric sample of the same patient. Proteins were separated on pH 3-10 linear IPG strip in the first dimension and 125 g/L SDS-PAGE in the second dimension, gels were silver stained. All labeled spots were tumor-specific.

gels stained by Coomassie Brilliant Blue. On the map, 9 cancer-specific spots were excised and subjected to in-gel digestion followed by peptide mass fingerprinting for protein identification. Figure 2 shows the identification of the spot No. 18 as an example. We identified proteins by peptide mass fingerprinting, MS-Fit of UCSF.

The criteria used to accept identifications included the extent of sequence coverage, the number of peptides matched, the probability score, and whether human protein appeared as the top candidates in the first pass search where no restriction was applied to the species of origin.

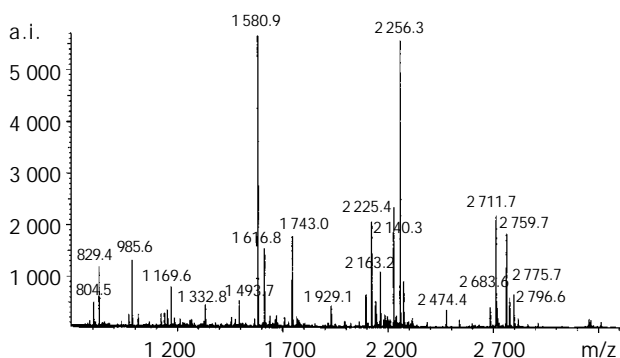


Figure 2 MALDI-TOF MS of tryptic digests of protein spot No. 18 resolved on 2DE gel, REFLEX III (BLUker). The data were collected on positive ion and reflector mode. Experimentally determined mass values are labeled on peptides. Spot 10 matched peptide 11; amino acid coverage, 60%; the spot was identified as carbonic anhydrase I.

The results of identification are summarized in the Appendix Table 1. For identified protein, probability based score greater than 73 was significant ($P < 0.05$). For example, in the case of annexin V, the protein score is 163. Some of these proteins, such as carbonic anhydrase I; chain B, crystal structure of fibrinogen fragment D; fibrin beta and prohibitin, have already been detected in gastric cancer tissues.

DISCUSSION

Proteome based profiling employs the measurement of protein expression pattern for the identification of individual proteins and clusters of proteins that mediate particular aspects in a physiological and pathophysiological process. The measurement of protein expression patterns of normal and disease tissues or cell populations will lead to the characterization of diagnostic and prognostic markers, and it can be further employed for the analysis of the disease stage which might also have an impact on the therapy. Thus, preferably small clusters of proteins represent the ideal diagnostic markers enabling an easier and more accurate diagnosis of diseases for better therapy^[10].

This study was based on an ongoing proteomic analysis of gastric cancer aiming at screening the protein markers in the proteome for diagnosis of gastric cancer. With the availability of high-throughput 2DE gels and initial screening by using automated procedures, identification of changes in the proteome in various tissues will be possible. The approach we described in this study has shown that high-throughput analysis will be a valuable tool. An effort is currently being made using proteome based techniques^[11]. 2DE pattern of normal and diseased tissues revealed a number of polypeptides

Table 1 Protein spots in GC searched by PeptIdent software in the SWISS-PROT database

Spot ID	SWISS-PROT ID	Peptide matched	Top score	Theoretic pI	Theoretic M_r	Sequence covered rate (%)	Protein name
17	gi999937	17/31	163	4.98	35 839	63	Annexin V
10	gi515109	11/24	116	6.63	28 778	60	Carbonic anhydrase I
5	gi2781208	15/43	105	5.84	38 081	55	Chain B, crystal structure of fibrinogen fragment D
12	gi223002	12/33	92	7.95	51 358	42	Fibrin beta
19	gi4505773	11/46	75	5.57	29 843	55	Prohibitin
4	gi2781208	9/31	67	5.84	38 081	37	Chain B, crystal structure of fibrinogen fragment D
18	gi15192925	8/29	63	6.90	31 032	46	Alcohol dehydrogenase
16	gi15895617	9/31	58	9.01	42 229	34	Sugar transaminase, involved in dTDP-4, 6-dideoxyglucose biosynthesis
11	gi1586816	10/35	55	9.33	42 071	27	Jerky gene

associated with gastric cancer, which were expressed in gastric cancer tissues, but absent in normal gastric tissues. Some of them might possibly be identified and serve as diagnostic and prognostic markers in gastric cancer.

In the preparation of 2DE maps presented in this study, tissue samples from different individuals were used without pooling of samples. The total homogenate was fractionated by ultracentrifugation into soluble fraction^[12]. In order to minimize the influence of the methodology, we attempted, when possible, to make protocols for 2DE PAGE alike. Our initial analyses of six normal tissue samples indicated the overall protein pattern remained very similar across the samples.

We identified nine protein spots which were expressed in cancerous tissues but absent in normal gastric tissues. Of the 9 position identifications, spots 4, and 5 were found as multiple spots on the 2DE gels. Those included the subunits of the proteins, both of which focused in several pI positions but had the same molecular mass. It indicated that these gene products were present as isoforms with post-translation modification^[13].

Annexins are Ca²⁺ and phospholipid binding proteins forming an evolutionarily conserved multigene family. For some annexins, it appears that they participate in the regulation of membrane organization and membrane traffic and the regulation of ion (Ca²⁺) currents across membranes or Ca²⁺ concentrations within cells. Some members of the family have been identified extracellularly where they can act as receptors for serum proteases on the endothelium as well as inhibitors of neutrophil migration and blood coagulation^[14]. Annexin V is used widely as a marker for apoptotic cells, the annexin V mutants showed defective homotypic cell adhesion and resistance to Ca²⁺-dependent apoptotic agents without exhibiting any changes in the generation of cytosolic Ca²⁺ fluxes^[15]. Annexin V also known as calphobindindin I, has been shown to be an endogenous inhibitor of protein kinase C, a key enzyme in cellular signal transduction. The inhibition of protein kinase C by annexin V is presumed to be ultimately related to carcinogenesis and studies have demonstrated that a decrease in the production of annexin V may lead to the dysregulated protein kinase C^[16,17]. Annexin V has been found in other cancer tissues or cell lines^[18,19], but its presence in gastric cancer has not be documented.

Carbonic anhydrase (CA) is the zinc-containing metalloenzyme that catalyzes the reversible hydration of CO₂. The role of the enzyme has been thoroughly investigated. The main functions of the enzyme are to produce HCO₃⁻ for the intermediate metabolism and to maintain pH, water, and ion equilibrium in the body^[20]. CAs show various levels of catalytic activity and binding to inhibitors. They have considerable diversity in tissue distribution and cellular localization, and they perform a variety of biological functions. CAI protein is associated with cell growth. It is likely expressed by rapidly proliferating tumor cells or cells that are about to enter the proliferative state, because the CA domain and other elements of the molecule take part in the regulation of cell growth in certain tumor cell types^[21].

The presence of fibrin (ogen) within the tumor stroma likely affects the progression of tumor cell growth and metastasis^[22]. The deposition of fibrin (ogen), along with other adhesive glycoproteins, into the extracellular matrix serves as a scaffold to support binding of growth factors and to promote the cellular responses of adhesion, proliferation, and migration during angiogenesis and tumor cell growth. Inappropriate synthesis and deposition of extracellular matrix constituents are linked to altered regulation of cell proliferation, leading to tumor cell growth and malignant transformation^[23,24]. Fibrin deposition occurs within the stroma of a majority of tumor types. Fibrin (ogen) content was significantly higher in malignant tumor patients than that in benign disease patients, significant

reduction was observed after treatment and became elevated again when there was recurrence or metastasis^[25]. Biggerstaff *et al.*^[26] suggested that coagulation activation and the subsequent increase in circulating fibrin may enhance platelet adhesion to circulating tumor cells and thereby facilitate metastatic spread. Assessment of fibrin (ogen) not only helps to diagnose cancers but also evaluates the therapeutic effect and prognosis^[27].

Prohibitin proteins have been implicated in cell proliferation, ageing and the maintenance of mitochondria integrity^[28], prohibitins are present in the inner mitochondrial membrane and always bound to each other. They are expressed during development and their expression levels are indicative of a role in mitochondrial metabolism^[29]. High level expression of the proteins is consistently seen in primary human tumors. The prohibitin protein has been found having various functions, including cell cycle regulation, apoptosis, assembly of mitochondrial respiratory chain enzymes and ageing. We are currently trying to identify the additional proteins whose expression is significantly altered in cancerous tissue.

This study also confirms that proteomic analysis is a powerful tool for the discovery of such molecular markers. Proteomic analysis allows the characterization of picoquantities of proteins with MS and changes in the levels inherent to the pathophysiology of any cell type, tissue, or whole organism. It is hoped that the identification of protein markers by this approach could discriminate cancerous from normal cells. As demonstrated here, proteomic analysis may be efficiently used to identify new indicators for the diagnosis and prognosis of cancer progression.

In conclusion, the differences of the proteins between normal gastric epithelial cell and malignant cells are complex. Our data only show a few of the highly expressed spots. Further basic and clinical investigation will be needed to demonstrate if these proteins could be markers for GC and to evaluate other non-constant spots in relation to the clinical condition of the patient.

ACKNOWLEDGEMENTS

The authors would like to thank Dr. Bo-Qing Li and Qing-Hua Zhou at Chinese Center for Disease Control and Prevention for their assistance in the experiments.

REFERENCES

- 1 **Lawrie LC**, Fothergill JE, Murray GI. Spot the differences: proteomics in cancer research. *Lancet Oncol* 2001; **2**: 270-277
- 2 **Zhang M**, Martin KJ, Sheng SJ, Sager R. Expression genetics: a different approach to cancer diagnosis and prognosis. *Trends Biotechnol* 1998; **16**: 66-71
- 3 **Torrado J**, Plummer M, Vivas J, Garay J, Lopez G, Peraza S, Carillo E, Oliver W, Muñoz N. Lewis antigen alterations in a population at high risk of stomach cancer. *Cancer Epidemiol Biomarkers Prev* 2000; **9**: 671-674
- 4 **Xu CT**, Pan BR, Zhang LZ, Li XX, Wang J. Significance of serum tumor markers CA50 and CEA in gastric cancer. *China J New Gastroenterol* 1996; **2**: 16-19
- 5 **Macgregor PF**, Squire JA. Application of microarrays to the analysis of gene expression in cancer. *Clin Chem* 2002; **48**: 1170-1177
- 6 **Gygi SP**, Corthals GL, Zhang Y, Rochon Y, Aebersold R. Evaluation of two-dimensional gel electrophoresis-based proteome analysis technology. *Proc Natl Acad Sci* 2000; **97**: 9390-9395
- 7 **Ni XG**, Zhao P, Liu Y, Zhao XH. Application of proteomic approach for solid tumor marker discovery. *Aizheng* 2003; **22**: 664-667
- 8 **Emmert-Buck MR**, Gillespie JW, Pawletz CP, Ornstein DK, Basrur VB, Appella E, Wang QH, Huang J, Hu N, Taylor P, Petricoin III EF. An approach to proteomic analysis of human tumors. *Mol Carcinog* 2000; **27**: 158-165
- 9 **Gorg A**, Obermaier C, Boguth G, Harder A, Scheibe B,

- Wildgruber R, Weiss W. The current state of two-dimensional electrophoresis with immobilized pH gradients. *Electrophoresis* 2000; **21**: 1037-1053
- 10 **Yu YL**, Yang PY, Fan HZ, Huang ZY, Rui YC, Yang PY. Protein expressions in macrophage-derived foam cells: comparative analysis by two-dimensional gel electrophoresis. *Acta Pharmacol Sin* 2003; **24**: 873-877
- 11 **Becamel C**, Galeotti N, Poncet J, Jouin P, Dumuis A, Bockaert J, Marin P. A proteomic approach based on peptide affinity chromatography, 2-dimensional electrophoresis and mass spectrometry to identify multiprotein complexes interacting with membrane-bound receptors. *Biol Proced Online* 2002; **4**: 94-104
- 12 **Mikami S**, Kishimoto T, Hori H, Mitsui T. Technical improvement to 2D-PAGE of rice organelle membrane proteins. *Biosci Biotechnol Biochem* 2002; **66**: 1170-1173
- 13 **Steel LF**, Shumpert D, Trotter M, Seeholzer SH, Evans AA, London WT, Dwek R, Block TM. A strategy for the comparative analysis of serum proteomes for the discovery of biomarkers for hepatocellular carcinoma. *Proteomics* 2003; **3**: 601-609
- 14 **Katayanagi K**, Van de Water J, Kenny T, Nakanuma Y, Ansari AA, Coppel R, Gershwin ME. Generation of monoclonal antibodies to murine bile duct epithelial cells: identification of annexin V as a new marker of small intrahepatic bile ducts. *Hepatology* 1999; **29**: 1019-1025
- 15 **Nimmo MC**, Carter CJ. The antiphospholipid antibody syndrome: A riddle wrapped in a mystery inside an enigma. *Clinical Applied Immunol Rev* 2003; **4**: 125-140
- 16 **Karube A**, Shidara Y, Hayasaka K, Maki M, Tanaka T. Suppression of calphobindin I (CPB I) production in carcinoma of uterine cervix and endometrium. *Gynecol Oncol* 1995; **58**: 295-300
- 17 **Shibata S**, Sato H, Ota H, Karube A, Takahashi O, Tanaka T. Involvement of annexin V in antiproliferative effects of gonadotropin-releasing hormone agonists on human endometrial cancer cell line. *Gynecol Oncol* 1997; **66**: 217-221
- 18 **Seow TK**, Ong SE, Liang RC, Ren EC, Chan L, Ou K, Chung MC. Two-dimensional electrophoresis map of the human hepatocellular carcinoma cell line, HCC-M, and identification of the separated proteins by mass spectrometry. *Electrophoresis* 2000; **21**: 1787-1813
- 19 **Xin W**, Rhodes DR, Ingold C, Chinnaiyan AM, Rubin MA. Dysregulation of the annexin family protein family is associated with prostate cancer progression. *Am J Pathol* 2003; **162**: 255-261
- 20 **Ivanov S**, Liao SY, Ivanova A, Danilkovitch-Miagkova A, Tarasova N, Weirich G, Merrill MJ, Proescholdt MA, Oldfield EH, Lee J, Zavada J, Waheed A, Sly W, Lerman MI, Stanbridge EJ. Expression of hypoxia-inducible cell-surface transmembrane carbonic anhydrases in human cancer. *Am J Pathol* 2001; **158**: 905-919
- 21 **Nogradi A**. The role of carbonic anhydrases in tumors. *Am J Pathol* 1998; **153**: 1-4
- 22 **Palumbo JS**, Kombrinck KW, Drew AF, Grimes TS, Kiser JH, Degen JL, Bugge TH. Fibrinogen is an important determinant of the metastatic potential of circulating tumor cells. *Blood* 2000; **96**: 3302-3309
- 23 **Stewart DA**, Cooper CR, Sikes RA. Changes in extracellular matrix (ECM) and ECM-associated proteins in the metastatic progression of prostate cancer. *Reprod Biol Endocrinol* 2004; **2**: 2
- 24 **Sahni A**, Odrlic T, Francis CW. Binding of basic fibroblast growth factor to fibrinogen and fibrin. *J Biol Chem* 1998; **273**: 7554-7559
- 25 **Holmbeck K**, Bianco P, Birkedal-Hansen H. MT1-mmp: a collagenase essential for tumor cell invasive growth. *Cancer Cell* 2003; **4**: 83-84
- 26 **Biggerstaff JP**, Seth NB, Meyer TV, Amirkhosravi A, Francis JL. Fibrin monomer increases platelet adherence to tumor cells in a flowing system: a possible role in metastasis? *Thromb Res* 1998; **92**: S53-S58
- 27 **Kim HK**, Lee KR, Yang JH, Yoo SJ, Lee SW, Jang HJ, Park SJ, Moon YS, Park JW, Kim CM. Plasma levels of D-dimer and soluble fibrin polymer in patients with hepatocellular carcinoma: a possible predictor of tumor thrombosis. *Thromb Res* 2003; **109**: 125-129
- 28 **McClung JK**, Jupe ER, Liu XT, Dell'Orco RT. Prohibitin: potential role in senescence, development, and tumor suppression. *Exp Gerontol* 1995; **30**: 99-124
- 29 **Nijtmans LGJ**, de Jong L, Artal Sanz M, Coates PJ, Berden JA, Back JW, Muijsers AO, van der Spek H, Grivell LA. Prohibitins act as a membrane-bound chaperone for the stabilization of mitochondrial proteins. *EMBO J* 2000; **19**: 2444-2451

Edited by Zhu LH Proofread by Chen WW and Xu FM

Therapeutic effects and prognostic factors in three-dimensional conformal radiotherapy combined with transcatheter arterial chemoembolization for hepatocellular carcinoma

De-Hua Wu, Li Liu, Long-Hua Chen

De-Hua Wu, Long-Hua Chen, Department of Radiation Oncology, Nanfang Hospital, First Military Medical University, Guangzhou 510515, Guangdong Province, China

Li Liu, Department of Pathology, First Military Medical University, Guangzhou 510515, Guangdong Province, China

Supported by the Natural Science Foundation of Guangdong Province, No. 013056

Correspondence to: Dr. Long-Hua Chen, Department of Radiation Oncology, Nanfang Hospital, First Military Medical University, Guangzhou 510515, Guangdong Province, China. flch@fimmu.com

Telephone: +86-20-61642136 **Fax:** +86-20-61642131

Received: 2003-12-10 **Accepted:** 2004-02-01

Abstract

AIM: To evaluate the therapeutic efficacy of three-dimensional conformal radiotherapy (3D-CRT) combined with transcatheter arterial chemoembolization (TACE) on the patients with hepatocellular carcinoma (HCC).

METHODS: Between 1998 and 2001, 94 patients with HCC received 3D-CRT combined with TACE. A total 63 patients had a Okuda stage I lesion and 31 patients had stage II. The median tumor size was 10.7 cm (range 3.0-18 cm), and liver cirrhosis was present in all the patients. There were 43 cases of class A and 51 class B. TACE was performed using lipiodol, 5-fluorouracil, cisplatin, doxorubicin hydrochloride and mitomycin, followed by gelatin sponge cubes. Fifty-nine patients received TACE only one time, while the others 2 to 3 times. 3D-CRT was started 3-4 wk after TACE. All patients were irradiated with a stereotactic body frame and received 4-8 Gy single high-dose radiation for 8-12 times at the isocenter during a period of 17-26 d (median 22 d).

RESULTS: The median follow-up was 37 mo (range 10-48 mo) after diagnosis. The response rate was 90.5%. The overall survival rate at 1-, 2-, and 3- year was 93.6%, 53.8% and 26.0% respectively, with the median survival of 25 mo. On univariate analysis, age ($P=0.026$), Child-Pugh classification for cirrhosis of liver ($P=0.010$), Okuda stage ($P=0.026$), tumor size ($P=0.000$), tumor type ($P=0.029$), albuminemia ($P=0.035$), and radiation dose ($P=0.000$) proved to be significant factors for survival. On multivariate analysis, age ($P=0.024$), radiation dose ($P=0.001$), and tumor size ($P=0.000$) were the significant factors.

CONCLUSION: 3D-CRT combined with TACE is an effective and feasible approach for HCC. Age, radiation dose and tumor size were found to be significant prognostic factors for survival of patients with HCC treated by 3D-CRT combined with TACE. Further study for HCC is needed to improve the treatment efficacy.

Wu DH, Liu L, Chen LH. Therapeutic effects and prognostic factors in three-dimensional conformal radiotherapy combined with transcatheter arterial chemoembolization for

hepatocellular carcinoma. *World J Gastroenterol* 2004; 10 (15): 2184-2189

<http://www.wjgnet.com/1007-9327/10/2184.asp>

INTRODUCTION

Hepatocellular carcinoma (HCC) is a major health threat in Africa and China where rates of hepatitis B infection have always been high^[1]. Although early diagnosis and curative surgical resection can achieve the best prognosis, the number of patients who could undergo resection is still limited, even for those with small tumors because of the unique characteristics of this tumor, such as multifocality, early vascular invasion, and concurrent liver cirrhosis^[2]. Nonsurgical therapies, such as percutaneous ethanol injection, transcatheter arterial chemoembolization (TACE), have been tried for unresectable HCC^[3,4]. TACE has achieved improved survival; however, the antitumor effect of TACE alone has frequently been incomplete, even after repeated treatments^[5,6]. Radiotherapy used for HCC has been attempted for more than 4 decades. Early trials adopted whole liver irradiation but the radiation dose was inadequate^[7]. Because of the unsatisfactory results obtained with this low-dose whole liver irradiation, doctors have not long applied it in their treatment of HCC. The advanced technique of three-dimensional conformal radiotherapy (3D-CRT), however, has made it possible to deliver a higher dose of radiation to part of the liver accurately without a significant dose increase in the other intra-abdominal critical structures. Several studies reported that 3D-CRT could tolerate higher radiation levels with a substantial tumor response^[8-17]. Their findings indicate that 3D-CRT can be an effective component of the treatment strategy for HCC. The principle for 3D-CRT was to escalate the radiation dose in an attempt to elevate the rate of tumor response without damaging the normal liver cells. Stereotactic radiosurgery or hypofractionated radiotherapy has 80-90% local control rate, even for so-called radioresistant tumors, such as renal cell carcinoma and melanoma^[18,19]. Because of its success, small-volume radiotherapy has been applied to extracranial lesions, such as lung and liver tumors^[20,21]. Although the role of 3D-CRT in the management of HCC has been increasingly recognized, there are still several questions to be solved, one of which involves the identification of prognostic factors so as to improve the therapeutic effects of the management for HCC after 3D-CRT combined with TACE. Another is how to assess the exact effectiveness and toxicity of 3D-CRT combined with TACE. In our department, 3D-CRT combined with TACE has been actively applied for the treatment of HCC since the 1998. In this retrospective study, we aimed to analyze the effects and prognostic factors affecting survival in 94 HCC patients treated with this therapy.

MATERIALS AND METHODS

Patients

The diagnosis of HCC was based on histological features or

on radiologic findings (liver tumor CT scan, as well as hypervascular mass in hepatic angiography) and on a serum alpha-fetoprotein (AFP) level exceeding 400 ng/mL. All tumors with an AFP less than 400 ng/mL underwent a biopsy for diagnosis. The exclusion criteria included were as follows: (1) the presence of extrahepatic metastasis; (2) liver cirrhosis of Child-Pugh class C; (3) tumors occupying more than two-thirds of the liver; and (4) a score of Karnofsky performance status of less than 60.

Table 1 Patient data before initiation of radiotherapy (*n*=94)

Data	<i>n</i> (%)
Age (yr)	
<60	78(83.0)
60	16(17.0)
Gender	
Male	84(89.4)
Female	10(10.6)
Alpha-fetoprotein	
>400 ng/mL	64 (68.1)
400 ng/mL	30(31.9)
Child-Pugh classification for cirrhosis of liver	
Class A	43(45.7)
Class B	51(54.3)
Karnofsky performance score	
>70	90(95.7)
<70	4(4.3)
Okuda stage	
I	63(67.0)
II	31(33.0)
Tumor size (cm)	
<5	17(18.1)
5-10	40(42.6)
>10	37(39.3)
Tumor type	
Massive	66(70.2)
Multinodular	28(29.8)
PVT	
Yes	12(12.8)
No	82(87.2)
Albuminemia	
<3 g/dL	15(16.0)
>3 g/dL	79(84.0)
Bilirubinemia	
<3 mg/dL	29(30.9)
>3 mg/dL	65(69.1)
Chronic hepatitis in serum virology	
Type B	90(95.7)
Type C	4(4.3)
Radiation dose	
60 Gy	34(36.2)
56 Gy	34(36.2)
48 Gy	26(27.6)
TACE	
1 fraction	59(62.8)
>1 fraction	35(37.2)

Ninety-four patients (84 male and female) who received 3D-CRT combined with TACE in our department between August 1998 and August 2001 were enrolled in this study. The patient data are shown in Table 1. Their median age was 51.5 years (range 23–73 years). Sixty-four patients had an serum AFP level >400 ng/mL. Liver cirrhosis was present in all patients, with 43 patients of Child-Pugh class's A. Most patients had good

performance status, and 90 patients had a Karnofsky performance score (KPS) of more than 70. The Okuda stage I was in 66 patients and II in 28 patients. The tumor size was calculated according to the mean of three orthogonal diameters on CT. It was <5 cm in 7 patients, 5-10 cm in 30 patients, and >10 cm in 57 patients, with the median tumor size of 10.7 cm (range 3.0-18 cm). The massive tumor was the most frequent type, which was found in 82 patients (87.2%). Portal vein thrombosis (PVT) was present in 12 patients (12.8%). Chronic hepatitis in serum virology was present in 90 patients with type B (95.7%), and in 4 patients with type C (4.3%).

TACE procedures

TACE was performed with the infusion of a mixture of 5–20 mL of iodized oil contrast medium (Lipiodol, Huaihai Pharmaceutical Factory, Shanghai, China), 1.0 g of 5-fluorouracil (5-Fu, Xudong Haipu Pharmaceutical Inc., Shanghai, China) and 40-60 mg of cisplatin (CDDP, Qilu Pharmaceutical Factory, Jinan, China) or 30-50 mg of doxorubicin hydrochloride (Adriamycin, Main Luck Pharmaceutical Inc., Shenzhen, China), and 10 mg of mitomycin (Mytomycin-C C, Kyowa Hakko Kogyo, Tokyo, Japan), followed by 1 mm×1 mm×10 mm of gelatin sponge cubes (Gelfoam, the 3rd Pharmaceutical Factory of Nanjing, Nanjing, China) embolization. To preserve liver function as much as possible, we performed superselective TACE for the feeding arteries of each intrahepatic tumor. When there was an arterial portal shunt or main branch PVT, we performed TACE without lipiodol to prevent severe damage to the normal liver. TACE procedures were performed with a 4-wk interval, and the patients received 1 to 3 times.

Radiotherapy

Radiation treatment was given to patients placed in a supine position, with both arms raised above the head and the head in a natural position. The patients were immobilized in this position using a vacuum pillow (TN-1, TOPSLANE, Shanghai, China) with an oxygen mask (3 000–5 000 cc/min) for respiratory suppression for CT simulator (PQS 2000, Picker, USA). CT data were all transferred to a 3D-radiation treatment planning system (STP 3.0, Leibinger, Freiburg, Germany) by the network. The hepatic tumor, liver, kidneys, spinal cord, and gastroduodenal intestine of each patient were contoured and reconstructed to form a 3D representation. The radiation treatment volumes and treatment angles were designed according to the beam's-eye view technique to minimize critical organ injury. Each beam's shape was designed using a multileaf collimator or custom-made block. Three-dimensional CT-based computerized treatment planning was used to determine the best combination of coplanar and noncoplanar portals. A dose-volume histogram (DVH) was generated from the stereotactic treatment planning system for each patient. Gross tumor volume (GTV) was defined as the hepatic tumor volume, visualized by three-dimensional computation of contrast CT-defined contours. Clinical target volume (CTV) was defined as GTV plus a 0.5 cm margin. Planning target volume (PTV) was defined as CTV plus a 0.5 cm margin at medial/lateral/ventral/dorsal sides, but plus a 1.5-2 cm margin at cranial/caudal sides to account for daily setup error and respiratory organ motion. Dose inhomogeneity of PTV should be within ±7% of isocenter dose. Normal liver was defined as the total liver volume minus the GTV. The average volume of GTV for these 94 patients was 979±623 mL. The average volume of whole liver was 1 790±645 mL. The number of portals used for radiation treatment ranged from 2 to 6, with a median of 5. Ultimately, the radiotherapy volume involved a portion of the liver, and whole liver radiation was always avoided. 3D-CRT was started within 3-4 wk after TACE using a 6-MV linear accelerator (CLINAC 600C/D, Varian Assoc, USA).

A dose of 4-8 Gy was applied each time and 3 times a week to deliver a total dose of 48-60 Gy. The total dose was determined by the fraction of the nontumorous liver receiving >50% of the isocenter dose. The guidelines were as follows: if <25% of the nontumorous liver received >50% of the isocenter dose, the total dose was increased to 60 Gy with 7.5 Gy each time; if 25-50%, the dose was 54 Gy with 6 Gy each time; if 50-75%, the dose was 48 Gy with 4 Gy each time; and if >75%, no treatment was given. This guideline was more strictly followed after the application of three-dimensional planning. The total radiation dose ranged from 48 to 60 Gy, and the median tumor dose was 56 Gy. During treatment, patients were monitored weekly with complete blood counts and liver function tests and AFP test.

Evaluation

The evaluation of tumor response was based on the change in mean tumor size (calculated according to the mean of three orthogonal diameters) on serial CT scans which are first started 4-6 wk after treatment completion and then performed at 1-, 3-mo interval. The evaluation of the change in tumor size was done at 3 mo after the treatment. Complete disappearance of the tumor was considered a complete response (CR), a decrease of >50% in tumor size was defined as a partial response (PR), a decrease of <50% in tumor size or no change was defined as stable disease (SD), and progression was defined as progressive disease (PD). CR and PR were considered to be responsible, whereas SD or PD not to be responsible. Acute toxicity was that occurred during treatment and 1 mo after the treatment. Subacute or chronic toxicity was defined as that occurring from 1 mo after radiotherapy.

Statistics

Statistical analysis was performed using SPSS 10.0. Overall survival was estimated from the date of diagnosis according to the Kaplan-Meier method. Log-rank statistics were used to identify the prognostic factors important for survival. Cox proportional models using enter stepwise regression were applied to all potentially significant variables for the multivariate analysis. $P < 0.05$ was considered statistically significant.

RESULTS

Tumor response

As shown in Table 2, tumor response (CR+PR) was evaluated by the change in mean tumor size on CT 3 mo after treatment completion.

Table 2 CT response of HCC to 3D-CRT combined with TACE

Response	No of patients (%)
Complete	12(12.8)
Partial	73(77.7)
Stable disease	6(6.4)
Progressive disease	3(3.1)

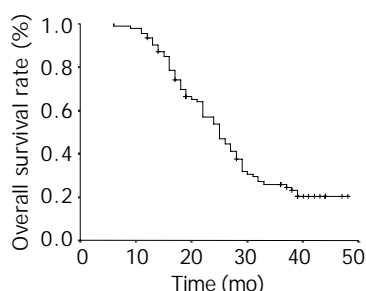


Figure 1 Actuarial survival of 94 patients treated with 3D-CRT combined with TACE.

Overall survival

The median follow-up was 37 mo (range 10-48 mo) after diagnosis. The overall survival rates of 1-, 2-, and 3-year were 93.6%, 53.8%, and 25.9%, respectively (median survival 25 mo, Figure 1).

Factors affecting overall survival

The results of univariate and multivariate analyses of prognosis factors for overall survival are shown in Table 3. On univariate analysis, age ($P=0.026$, Figure 2), Child-Pugh classification for cirrhosis of liver ($P=0.01$, Figure 3), Okuda stage ($P=0.008$, Figure 4), tumor size ($P=0.000$, Figure 5), tumor type ($P=0.029$, Figure 6), albuminemia ($P=0.035$, Figure 7), and radiation dose ($P=0.000$, Figure 8) were shown as significant factors. Multivariate regression identified the following independent favorable prognostic factors: younger age ($P=0.024$), high radiation dose ($P=0.001$), and small tumor size ($P=0.000$).

Table 3 Univariate and multivariate analyses of prognosis factors for overall survival

Univariate analysis	Multivariate analysis		
	<i>P</i>	R (95% CI)	<i>P</i>
Age (yr)	0.026	2.377	0.024
Tumor size	0.000	6.183	0.000
Radiation dose	0.000	0.491	0.001
Child-Pugh classification for cirrhosis of liver	0.010		
Karnofsky performance status	0.913		
Okuda stage	0.008		
Gender	0.202		
Tumor type	0.029		
PVT	0.235		
Albuminemia	0.035		
Bilirubinemia	0.305		
Chronic hepatitis in serum virology	0.060		
Alpha-fetoprotein	0.861		
TACE	0.892		

HR: Hazard ratio; 95% CI: Confidence interval.

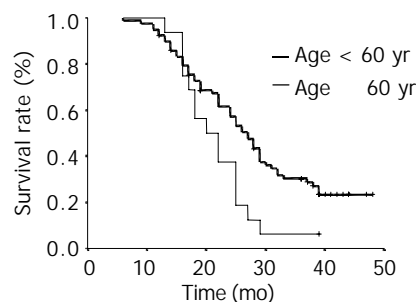


Figure 2 Univariate analysis of age on survival of patients treated with 3D-CRT combined with TACE.

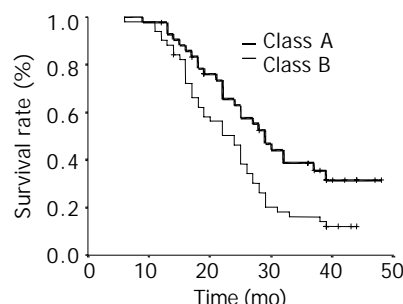


Figure 3 Univariate analysis of Child-Pugh classification on survival of patients treated with 3D-CRT combined with TACE.

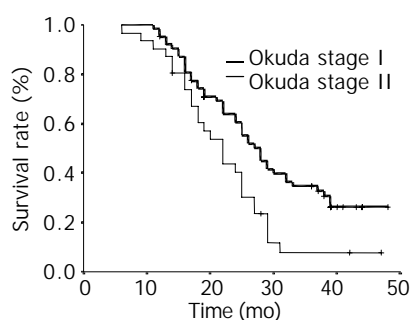


Figure 4 Univariate analysis of Okuda stage on survival of patients treated with 3D-CRT combined with TACE.

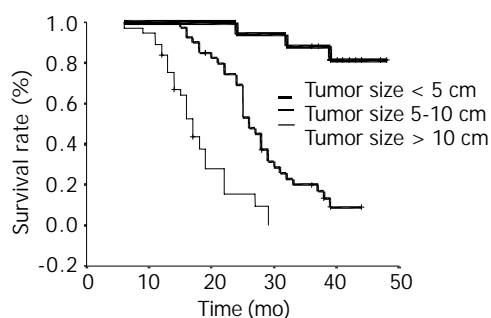


Figure 5 Univariate analysis of tumor size on survival of patients treated with 3D-CRT combined with TACE.

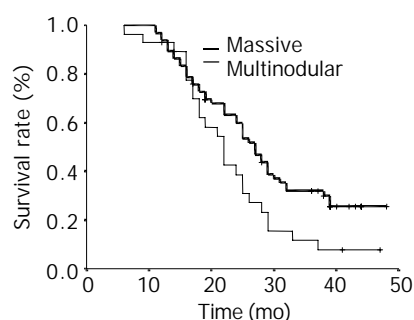


Figure 6 Univariate analysis of tumor type on survival of patients treated with 3D-CRT combined with TACE.

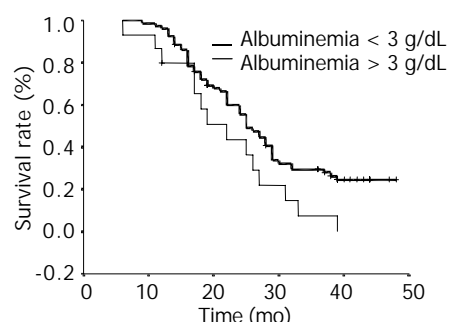


Figure 7 Univariate analysis of albuminemia on survival of patients treated with 3D-CRT combined with TACE.

Toxicity

In terms of acute toxicity, alterations in the liver function test (23 patients, 24.5%) and fever (51 patients, 54.3%) were frequently found in patients during the early time after TACE. These effects were transient and most patients recovered within 1-2 wk. Hematologic toxicity involved thrombocytopenia (platelets $<50\,000/\text{mm}^3$) in 13 patients and leucopenia (white blood cells $<2\,000/\text{mm}^3$) in 2 patients. Subacute and chronic toxicity involved radiation-induced liver disease (RILD) in

12 patients, 4 of whom died from RILD, and gastroduodenal ulcer in 5 patients. The patients other than the 4 victims of RILD were treated conservatively, and no death was found related to the treatment.

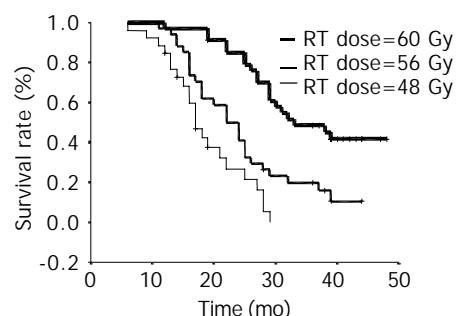


Figure 8 Univariate analysis of radiation dose on survival of patients treated with 3D-CRT combined with TACE.

DISCUSSION

Although TACE has been proved to be effective in treating HCC, and selectively and repeatedly used for patients with unresectable HCC, no survival benefits have been observed in at least two randomized trials of TACE^[22,23]. TACE is not a curative method and its limitation has also been well documented. After TACE, the tumor cells remain viable, especially in and around the capsule, and tumors may recur by the blood supply from the collateral circulation or portal vein or recanalization of the originally embolized artery^[6,24,25]. In advanced HCC, it is almost impossible to achieve a measurable response with TACE^[26].

Local radiotherapy can be an effective adjunct to the palliative treatment of HCC, even with portal vein thrombosis. Some studies of local radiotherapy, however, as either combination therapy with TACE or salvage therapy following TACE, have not shown a survival benefit, despite tumor response^[4-17]. This is because HCC eradication requires at least 50 Gy of radiation^[1,2]; but 33 Gy is a sufficient dose to induce RILD for whole liver radiation. With three-dimensional radiation planning, conformal radiotherapy can minimize scattering, limit unnecessary exposure of normal tissue, and deliver higher doses (40-80 Gy) to tumors^[27,28]. Therefore, it can be a feasible approach in the treatment of HCC with high dosage of radiation.

3D-CRT has been reported by a few studies to be effective in treatment of primary and metastatic tumors of lung and liver^[20, 21], but it has not been common to be applied in the treatment of HCC. The common therapy for HCC has been reported to be a daily dose of 1.8-2 Gy, 5 fractions per week, to a total delivered dose of 40-60 Gy^[4-17]. In our study of the 94 cases of HCC, we suggested that employing 3D-CRT could be beneficially combined with TACE with the following considerations.

Firstly, the combination of 3D-CRT with TACE may remedy the limitation of each alone and has synergistic effects. Secondly, tumor shrinkage after TACE allows the use of smaller irradiation fields, which permits higher tumor doses and improves the normal liver tolerance. Thirdly, combination therapy may also serve the purpose of eliminating residual cancer cells after TACE. Furthermore, the anticancer drug retained in the tumor may have a documented radiosensitizing effect^[6,29]. The anticancer drug, when mixed with lipiodol, has been reported to maintain relatively high concentrations in tumors as long as 27 d and decrease to a trace level after 47 d^[30]. Guo *et al.*^[6] reported that TACE followed by irradiation was a promising approach for large HCC and confirmed that TACE combined with radiotherapy was more effective than TACE alone.

In discussing the factors affecting the prognosis, we are not going to deal with the commonly known ones, which were also found in our study, such as age, Child-Pugh classification for cirrhosis of liver, Okuda stage, tumor size and type, and albuminemia. Only radiation dose is to be discussed, for it is of clinical importance in exploration of a better therapeutic method for HCC. In our present study, the radiation dose started at 60 Gy in 8 fractions within 17 d in cases with <25% of the nontumorous liver receiving >50% of the isocenter dose, at 56 Gy in 9 fractions within 19 d in cases with 25-50%, and 48 Gy in 12 fractions within 26 d in cases with 50-75%. Using the linear quadratic model, the biologic effective dose (BED) was here defined to be $nd(1+d/\alpha/\beta)$ in Gray, where n is the fractionation number, d is the daily dose, and α/β ratio is assumed to be 10 for tumors. The BEDs for our 3 different dose groups were equivalent respectively to those for 87.5 Gy total doses, 72 Gy total dose and 56 Gy total dose with a daily fraction of 2 Gy. The univariate and multivariate analyses of prognosis factors for overall survival showed that radiation dose is closely related to the prognosis. It seems clear that our virtually high total doses resulted in better response rates and overall survival. In our study, the radiologically documented response rates were 90.5%, our survival rates at 1-, 2-, and 3-year were 93.6%, 53.8%, and 25.9%, respectively, and our median survival rate was 25.0 mo. Besides better survival effect, hypofractionated 3D-CRT offers advantages of a shorter treatment course than a conventional radiotherapy and higher acceptance on the part of the patients without increasing side effects.

It has been reported that if less than 25% of the normal liver is treated with radiotherapy, then there may be no upper limit on dose associated with RILD; if 33%, 67%, or the whole liver is under uniform irradiation of 90 Gy, 47 Gy, or 31 Gy, respectively, there may be 5% risk of RILD associated with the treatment^[31]. In analyzing the correlation of RILD with patient-related and treatment-related dose-volume factors, Cheng *et al.*^[15] showed that after 3D-CRT, 12 of 68 patients developed RILD which was not found to be associated with their tumor volume. Compared with the documented ones, our results showed no increased toxicity in spite of the increased dose per fraction. This indicated that 3D-CRT played a critical role in the treatment of HCC.

In conclusion, 3D-CRT hypofractionated combined with TACE is a very safe and effective treatment method in higher tumor control and similar normal-tissue toxicity to conventional radiotherapy for HCC.

ACKNOWLEDGEMENTS

We thank Professor Liang Ping for his revision of the English version and An Sheng-li for his help in statistical analysis in the present study.

REFERENCES

- 1 **Oberfield RA**, Steele G Jr, Gollan JL, Sherman D. Liver cancer. *CA Cancer J Clin* 1989; **39**: 206-218
- 2 **Tang ZY**. Small hepatocellular carcinoma: current status and prospects. *HePatobiliary Pancreat Dis Int* 2002; **1**: 349-353
- 3 **Mok KT**, Wang BW, Lo GH, Liang HL, Liu SI, Chou NH, Tsai CC, Chen IS, Yeh MH, Chen YC. Multimodality management of hepatocellular carcinoma larger than 10 cm. *J Am Coll Surg* 2003; **197**: 730-738
- 4 **Qian J**, Feng GS, Vogl T. Combined interventional therapies of hepatocellular carcinoma. *World J Gastroenterol* 2003; **9**: 1885-1891
- 5 **Seong J**, Park HC, Han KH, Chon CY, Chu SS, Kim GE, Suh CO. Clinical results of 3-dimensional conformal radiotherapy combined with transarterial chemoembolization for hepatocellular carcinoma in the cirrhotic patients. *HePatol Res* 2003;

- 27: 30-35
- 6 **Guo WJ**, Yu EX, Liu LM, Li J, Chen Z, Lin JH, Meng ZQ, Feng Y. Comparison between chemoembolization combined with radiotherapy and chemoembolization alone for large hepatocellular carcinoma. *World J Gastroenterol* 2003; **9**: 1697-1701
- 7 **Stillwagon GB**, Order SE, Guse C, Klein JL, Lechner PK, Leibel SA, Fishman EK. 194 hepatocellular cancers treated by radiation and chemotherapy combinations: Toxicity and response: A Radiation Therapy Oncology Group Study. *Int J Radiat Oncol Biol Phys* 1989; **17**: 1223-1229
- 8 **Seong J**, Park HC, Han KH, Chon CY. Clinical results and prognostic factors in radiotherapy for unresectable hepatocellular carcinoma: a retrospective study of 158 patients. *Int J Radiat Oncol Biol Phys* 2003; **55**: 329-336
- 9 **Cheng JC**, Wu JK, Huang CM, Liu HS, Huang DY, Tsai SY, Cheng SH, Jian JJ, Huang AT. Dosimetric analysis and comparison of three-dimensional conformal radiotherapy and intensity-modulated radiation therapy for patients with hepatocellular carcinoma and radiation-induced liver disease. *Int J Radiat Oncol Biol Phys* 2003; **56**: 229-234
- 10 **Yamada K**, Izaki K, Sugimoto K, Mayahara H, Morita Y, Yoden E, Matsumoto S, Soejima T, Sugimura K. Prospective trial of combined transcatheter arterial chemoembolization and three-dimensional conformal radiotherapy for portal vein tumor thrombus in patients with unresectable hepatocellular carcinoma. *Int J Radiat Oncol Biol Phys* 2003; **57**: 113-119
- 11 **Li B**, Yu J, Wang L, Li C, Zhou T, Zhai L, Xing L. Study of local three-dimensional conformal radiotherapy combined with transcatheter arterial chemoembolization for patients with stage III hepatocellular carcinoma. *Am J Clin Oncol* 2003; **26**: E92-99
- 12 **Park HC**, Seong J, Han KH, Chon CY, Moon YM, Suh CO. Dose-response relationship in local radiotherapy for hepatocellular carcinoma. *Int J Radiat Oncol Biol Phys* 2002; **54**: 150-155
- 13 **Seong J**, Park HC, Han KH, Lee DY, Lee JT, Chon CY, Moon YM, Suh CO. Local radiotherapy for unresectable hepatocellular carcinoma patients who failed with transcatheter arterial chemoembolization. *Int J Radiat Oncol Biol Phys* 2000; **47**: 1331-1335
- 14 **Yamada K**, Soejima T, Minami T, Yoden E, Watanabe Y, Takenaka D, Imai M, Okayama T, Fujii M, Sugimura K. Three-dimensional treatment planning using electrocardiographically gated multi-detector row CT. *Int J Radiat Oncol Biol Phys* 2003; **56**: 235-239
- 15 **Cheng JC**, Wu JK, Huang CM, Liu HS, Huang DY, Cheng SH, Tsai SY, Jian JJ, Lin YM, Cheng TI, Horng CF, Huang AT. Radiation-induced liver disease after three-dimensional conformal radiotherapy for patients with hepatocellular carcinoma: dosimetric analysis and implication. *Int J Radiat Oncol Biol Phys* 2002; **54**: 156-162
- 16 **Chia-Hsien Cheng J**, Chuang VP, Cheng SH, Lin YM, Cheng TI, Yang PS, Jian JJ, You DL, Horng CF, Huang AT. Unresectable hepatocellular carcinoma treated with radiotherapy and/or chemoembolization. *Int J Cancer* 2001; **96**: 243-252
- 17 **Guo WJ**, Yu EX. Evaluation of combined therapy with chemoembolization and irradiation for large hepatocellular carcinoma. *Br J Radiol* 2000; **73**: 1091-1097
- 18 **Aoyama H**, Shirato H, Onimaru R, Kagei K, Ikeda J, Ishii N, Sawamura Y, Miyasaka K. Hypofractionated stereotactic radiotherapy alone without whole-brain irradiation for patients with solitary and oligo brain metastasis using noninvasive fixation of the skull. *Int J Radiat Oncol Biol Phys* 2003; **56**: 793-800
- 19 **Vesagas TS**, Aguilar JA, Mercado ER, Mariano MM. Gamma knife radiosurgery and brain metastases: local control, survival, and quality of life. *J Neurosurg* 2002; **97**(5 Suppl): 507-510
- 20 **Kelsey CR**, Schefter T, Nash R, Russ P, Baron AE, Zeng C, Gaspar LE. Retrospective clinicopathologic correlation of gross tumor size of hepatocellular carcinoma: implications for extracranial stereotactic radiosurgery. *Int J Radiat Oncol Biol Phys* 2003; **57**(2 Suppl): S283
- 21 **Onimaru R**, Shirato H, Shimizu S, Kitamura K, Xu B, Fukumoto S, Chang TC, Fujita K, Oita M, Miyasaka K,

- Nishimura M, Dosaka-Akita H. Tolerance of organs at risk in small-volume, hypofractionated, image-guided radiotherapy for primary and metastatic lung cancers. *Int J Radiat Oncol Biol Phys* 2003; **56**: 126-135
- 22 **Pelletier G**, Roche A, Ink O, Anciaux ML, Derhy S, Rougier P, Lenoir C, Attali P, Etienne JP. A randomized trial of hepatic arterial chemoembolization in patients with unresectable hepatocellular carcinoma. *J Hepatol* 1990; **11**: 181-184
- 23 Groupe d'Etude et de Traitement du Carcinome Hepatocellulaire. A comparison of lipiodol chemoembolization and conservative treatment for unresectable hepatocellular carcinoma. *N Engl J Med* 1995; **332**: 1256-1261
- 24 **Ernst O**, Sergent G, Mizrahi D, Delemazure O, Paris JC, L'Herminie C. Treatment of hepatocellular carcinoma by transcatheter arterial chemoembolization: comparison of planned periodic chemoembolization and chemoembolization based on tumor response. *Am J Roentgenol* 1999; **172**: 59-64
- 25 **Yu YQ**, Xu DB, Zhou XD, Lu JZ, Tang ZY, Mack P. Experience with liver resection after hepatic arterial chemoembolization for hepatocellular carcinoma. *Cancer* 1993; **71**: 62-65
- 26 **Seong J**, Keum KC, Han KH, Lee DY, Lee JT, Chon CY, Moon YM, Suh CO, Kim GE. Combined transcatheter arterial chemoembolization and local radiotherapy of unresectable hepatocellular carcinoma. *Int J Radiat Oncol Biol Phys* 1999; **43**: 393-397
- 27 **Aguayo A**, Patt YZ. Nonsurgical treatment of hepatocellular carcinoma. *Semin Oncol* 2001; **28**: 503-513
- 28 **McGinn CJ**, Ten Haken RK, Ensminger WD, Walker S, Wang S, Lawrence TS. Treatment of intrahepatic cancers with radiation doses based on a normal tissue complication probability model. *J Clin Oncol* 1998; **16**: 2246-2252
- 29 **Seong J**, Kim SH, Suh CO. Enhancement of tumor radioresponse by combined chemotherapy in murine hepatocarcinoma. *J Gastroenterol Hepatol* 2001; **16**: 883-889
- 30 **Raoul JL**, Heresbach D, Bretagne JF, Ferrer DB, Duvauferrier R, Bourguet P, Messner M, Gosselin M. Chemoembolization of hepatocellular carcinomas. A study of the biodistribution and pharmacokinetics of doxorubicin. *Cancer* 1992; **70**: 585-590
- 31 **Dawson LA**, Ten Haken RK, Lawrence TS. Partial irradiation of the liver. *Semin Radiat Oncol* 2001; **11**: 240-246

Edited by Kumar M and Chen WW **Proofread by** Xu FM

Transfection of IL-2 and/or IL-12 genes into spleen in treatment of rat liver cancer

Tian-Geng You, Hong-Shun Wang, Jia-He Yang, Qi-Jun Qian, Rui-Fang Fan, Meng-Chao Wu

Tian-Geng You, Hong-Shun Wang, Jia-He Yang, Qi-Jun Qian, Rui-Fang Fan, Meng-Chao Wu, Eastern Hepatobiliary Hospital, Second Military Medical University, 225 Changhai Road, Shanghai 200433, China

Supported by the National Natural Science Foundation of China, No. 30271476 and No. 39970838 and the Shanghai Science and technology Key Problem Foundation, No. 034119837

Correspondence to: Professor Jie-He Yang, Department of Comprehensive Treatment III, Eastern Hepatobiliary Hospital, Second Military Medical University, Changhai Road 225, Shanghai 200433, China. tgyou59@hotmail.com

Telephone: +86-21-25070769 **Fax:** +86-21-65562400

Received: 2004-02-02 **Accepted:** 2004-02-21

Abstract

AIM: To test the efficacy of gene therapy in rat liver tumor.

METHODS: A retroviral vector GCIL12EIL2PN encoding human IL-2 (hIL-2) and mouse IL-12 (mIL-12) fused gene and its packaging cell were constructed. The packaging cell lines contained of IL-2 and/or IL-12 genes were injected intrasplenically to transfect splenocyte at different time. The therapeutic effect, immune function and toxic effect were evaluated.

RESULTS: The average survival times of the 4 groups using IL genes at days 1, 3, 5 and 7 after tumor implantation were 53.3±3.7, 49.3±4.2, 31.0±2.1 and 24.3±1.4 d respectively in IL-2/IL-12 fused gene group, 25.0±2.5, 23.5±2.0, 18.3±2.4 and 12.0±1.8 d respectively in IL-2 gene treatment group, and 39.0±4.8, 32.0±3.9, 23.0±2.5 and 19.4±2.1 d respectively in IL-12 gene treatment group ($P < 0.01$, $n = 10$). In the IL-12/IL-2 fused gene treatment group, 30% of rats treated at days 1 and 3 survived more than 60 d and serum mIL-12 and hIL-2 levels were still high at day 3 after treatment. Compared with IL alone, NK cell activity was strongly stimulated by IL-2/IL-12 gene. Microscopy showed that livers were infiltrated by a number of lymphocytes.

CONCLUSION: IL-2 and/or IL-12 genes injected directly into spleen increase serum IL-2 and IL-12 levels and enhance the NK cell activity, which may inhibit the liver tumor growth. The therapy of fused gene IL-2/IL-12 is of low toxicity and relatively high NK cell activity. Our data suggest that IL-2/IL-12 fused gene may be a safe and efficient gene therapy for liver tumor. The gene therapy should be administrated as early as possible.

You TG, Wang HS, Yang JH, Qian QJ, Fan RF, Wu MC. Transfection of IL-2 and/or IL-12 genes into spleen in treatment of rat liver cancer. *World J Gastroenterol* 2004; 10(15): 2190-2194

<http://www.wjgnet.com/1007-9327/10/2190.asp>

INTRODUCTION

Gene therapy to liver cancer is limited by both number and

duration of died cancer cells being treated^[1,2]. Interleukin 2 (IL-2) and interleukin 12 (IL-12) were secreted mainly by mononuclear cell and B cell^[3], which play a prominent role in immune response to tumor. These cytokines are stimulated by antigens, for instance virus, bacteria and tumor cells. Others have shown that IL-2 and IL-12 were inhibited by colon cancer^[4] and both can up-regulated the T-cell and NK cell to kill tumor cell after administration of exogenous ILs.

The conditions under which the gene therapies of IL-2 and IL-12 are cytotoxic to liver tumor in an animal model have not been clear yet. Understanding the role and the mechanism of IL-2 and IL-12 in the induction of anti-tumor cytotoxic factors is relevant to both the long-term expression of IL and the safety of gene drug in liver tumor gene therapy.

IL-2, a glycoprotein consisted of 133 amino acids, through promotion of growth and proliferation of T cell, can induce either LAK cell or NK cell. IL-2 also induces immunocyte to produce interferon (INF) and tumor necrosis factor (TNF). Immunoreaction mediated by IL-2 increases therapeutic efficacy of colon cancer^[4,5]. Secretion of IL-2 and reaction to IL-2 are decreased in tumor patients by as yet unknown reasons. Previous report has demonstrated that metastases are related to the IL-2 level, and the tumor immune mediated by IL is decreased in favor of carcinogenesis, growth, diffusion and metastasis of tumor^[6-10].

IL-12 has p35 subunit and p40 subunit localized respectively on chromosome 3 and chromosome 5. The single subunit has no biological activity, and p35 gene and p40 gene are expressed simultaneously to have activity. IL-12 activates NK cell and LAK cell, promotes generation and differentiation of T cell and induces NK cell to express a small amount of TNF- β .

Primary liver cancer is common malignant tumors in China. The surgical treatment of the cancer is a main choice, but it is not ideal therapy because of high recurrence. Gene therapy is the new way for some diseases such as diabetes and tumors. Our previous work was to treat liver cancer with IL-12 gene alone, by which tumor growth was inhibited compared with control. Now we constructed the fused gene of IL-2/IL-12. However, little is known on liver cancer treatment with combination of IL-2/IL-12 gene therapy.

We hypothesized that the immunologic regulation to liver cancer following fused gene therapy of IL-2/IL-12 would be dependent upon the production and duration of the cytokines. The toxic effect of IL-2 and IL-12 would be dependent upon approach of drug delivery. In this study, using the model of implanted hepatoma of rats, we have shown that the liver tumors are reduced after IL-2 and/or IL-12 gene are injected into spleen and the cytokines are transferred into liver and blood circulation by porta vein.

MATERIALS AND METHODS

Construction of retrovirus vector of packaging mIL-12 gene and hIL-2 gene

Aprotinin, leupeptin, pepstatin, fetal calf serum and protein standard mixture were from Sigma. Plasmid pGCp35IRESp40 containing both p35 subunit and p40 subunit of mIL-12 gene was a gift from Professor Xin-Huan Liu. Plasmid pLIL2SN

containing hIL-2 gene was constructed by our laboratory. Cellular strains of hepatoma CBRH3 were provided kindly by Professor Hong Xie (Shanghai Institute of Biochemistry and Cell Biology, Chinese Academy of Sciences). Monotropic packaging cell PE501, amphiphilic packaging cell PA317 and cell NIH3T3 were provided by our laboratory. All other chemicals were of analytical grade and obtained from Merck or Sigma.

To amplify full length *p35* and *p40* genomes, PCR fragment was generated from downstream primer of mL-12 *p35* subunit and upstream primer of mL-12 *p40* subunit that templated with pGCp35IRESp-40SN. The products derived from PCR were harvested after 1% agarose gel electrophoresis. According to pLIL2PN templation, hIL-2 genome was then amplified and harvested. Fragments of mL-12 *p35* and *p40* derived from PCR were templated to amplify with downstream primer of *p35* and upstream primer of *p40* by PCR, which contain linker sequence. The mL-12 fused gene was harvested by electrophoresis^[11,12]. The mL-12 and hIL-2 gene fragments were connected respectively with pGEMTM-Teasy vector (Promega, USA) by T4 ligase (Boehringer Mannheim, Germany). The vector was transfected into *E. coli* TG1 competence cell and the positive clone was screened by PCR. Plasmid DNA was extracted from positive clone after partial exonuclease III digestion of PCR product, resulting in constructing GCILEXPn polyclonal sites after endonuclease (*Not I* and *Sal I*) (Promega, USA) that containing GCIL12EXPn of mL-12 gene, GCXEIL2PN of hIL-2 gene and GCIL12EIL2PN of mL-12 and hIL-2 fused gene.

Retrovirus packaging, identification, titer determination and expression

Reverse transcript virus was transfected into PE501 cell by electroporation. The clones were screened by G418 after 48 h. PA317 cell was infected by filtered supernatant 10-14 d late. G418 was screen after 3 d. Viral supernatants were harvested after amplifying 6 monoclonal from every groups for 2-3 wk. Stock cells were frozen at -80 °C.

Recombined reverse transcript viral vector was identified by RT-PCR. Titers of viral supernatants were determined with NIH3T3 cell. The packaging cells with highest viral titer that contain GCIL12EXPn, GCXEIL2PN and GCIL12EIL2PN were named as PA317-GCIL12EXPn, PA317-GCXEIL2PN and PA317-GCIL12EIL2PN, respectively. Protein expression of mL-12 and hIL-2 was determined by ELISA. ELISA kits (human IL-2 DuoSet and mouse IL-2 DuoSet) were from R&D Systems.

Implanted liver cancer in rats

Male Wister rats (200-250 g bm) were obtained from Animal Center of Chinese Academy of Sciences. Animals were maintained on a standard diet. Hepatoma CBRH3 cells were injected into abdominal cavity of rat. Rats were sacrificed and tumors were removed from abdominal cavity 7-9 d late. Tumors were cut into pieces of 0.05-0.75 cm and then were implanted into rat liver for one or more locations respectively. The tumors were grown up to 0.6-1 cm in diameter after 7-10 d of implantation.

Experimental procedure

Rats were anaesthetized with diethylether. The effects of IL-2 and/or IL-12 on liver cancer were studied in a total of 75 animals for 5 groups that contained 15 rats in every group: 1. Physiological saline control: 0.8 mL 9 g/L NaCl was injected into spleen following implanted liver cancer at day 1; 2. Blank vector control: 1×10^7 packaging cells of PA317-GCXEPN was injected into spleen of rat; 3. mL-12 gene group: 1×10^7 packaging cell PA317-GCIL12EXPn was injected into rat spleen after implanted rat liver cancer on days 1, 3, 5 and 7 thereafter; 4. hIL-12 gene group: 1×10^7 packing cell PA317-GCxeILPN was injected into

rat spleen after implanted rat liver cancer on days 1, 3, 5 and 7 respectively; 5. hIL-2 and mL-12 fused gene group: 1×10^7 packing cell PA317-GCIL12EIL2PN was injected into rat spleen after implanted rat liver cancer on days 1, 3, 5 and 7 thereafter. In addition, when rat survived over 2 mo, rats were named long term survivors and the liver cancer tissues were implanted into liver once more in order to observe cancer growth.

CT imaging and pathology

CT imaging was observed before and after treatment. The survival time and drug toxicity were observed. To observe the tumor cell and lymphocyte infiltration, the pathologic examination was performed following 5 and 7 d of treatment. The serum IL-2 and IL-12, according to the protocol of R&D Systems, were measured on d 1 before treatment and on d 3, 7, 30 and 60 thereafter.

Analysis of NK cytotoxic activity

NK target cell YAC-1 was obtained from the American Type Culture Collection (Bethesda, MD). The cytotoxicity of spleen NK cell was analyzed as follows^[13]. A single-cell suspension of spleen cells was centrifuged at 400 r/min for 30 min. The lymphocyte layers were harvested. For the preparation of targeted cells, YAC-1 was labeled with $^{51}\text{Cr}[\text{Na}_2\text{CrO}_4]$ and mixed with various numbers of spleen cell in a total volume of 200 μL of DMEM. The experimental radioactivity released (ER) in 100 μL samples of cell-free supernatants was determined. The amounts of radioactivity released in wells containing YAC-1 cells alone with and without 0.01% Triton X-100 were designated the total release (TR) and the spontaneous release (SR), respectively. The percentage of specific ^{51}Cr release was calculated by $[(\text{ER} - \text{SR}) / (\text{TR} - \text{SR})] \times 100$.

Statistical analysis

All results were expressed as the mean \pm SD of at least 10 individual measurements. A one-way analysis of variance (ANOVA) was first carried out to test for any differences in mean values between experimental and respective control group. If differences were established, the values were compared by two-tailed unpaired *t* test. The values were considered to significant difference if $P < 0.05$.

RESULTS

Identification of packing cell strain

The total RNA of packaging cell strains (PA317-GCIL12EXPn, PA317-GCXEIL2PN and PA317-GCIL12EIL2PN) was extracted. The RNA was amplified by RT-PCR and the product was harvested by electrophoresis. The sequence showed that PA317-GCXEIL2PN and PA317-GCIL12EIL2PN packaging cell strains contained the mL-12 sequence, and PA317-GCXEIL2PN and PA317-GCIL12EIL2PN packaging cell strains contained the hIL-2 sequence. The target genes were inserted into viral genomes and the packaging cell strains were transfected by IL gene.

Determination of titer of virus and protein expression

The highest virus titer of packaging cell was 2×10^6 CFU/mL of PA317-GCIL12EXPn, 2.4×10^6 CFU/mL of PA317-GCXEIL2PN and 1.4×10^6 CFU/mL of PA317-GCIL12EIL2PN respectively. Protein expression was measured by ELISA on these 3 packaging cell strains: 1. mL-12 fused protein: PA317-GCIL12EXPn expressed mL-12 fused protein 150 ng/ 10^6 /48 h and PA317-GCIL12EIL2PN expressed mL-2 fused protein 45.8 ng/ 10^6 /48 h; 2. hIL-2 protein: PA317-GCEXIL2PN expressed hIL-2 protein 7.5 ng/ 10^6 /48 h and PA317-GCIL12EIL2PN expressed hIL-2 protein 6.7 ng/ 10^6 /48 h.

Table 1 Average survival time (day) of rat ($n=0$, mean \pm SD)

Group	Injection on d 1	Injection on d 3	Injection on d 5	Injection on d 7
Physiologic saline control	10.7 \pm 1.5	-	-	-
Blank vector control	11.4 \pm 1.3	-	-	-
IL-2 gene therapy	25.0 \pm 2.5 ^b	23.5 \pm 2.0 ^b	18.3 \pm 2.4 ^b	12.0 \pm 1.8
IL-12 gene therapy	39.0 \pm 4.8 ^b	32.0 \pm 3.9 ^b	23.0 \pm 2.5 ^b	19.4 \pm 2.1 ^a
IL-12-IL-2 fused gene therapy	53.3 \pm 3.7 ^c	49.3 \pm 4.2 ^c	31.0 \pm 2.1 ^c	24.3 \pm 1.4 ^c

^a $P<0.05$ and ^b $P<0.01$ vs physiologic saline control and blank vector control; ^c $P<0.05$ vs IL-2 group or IL-12 group.

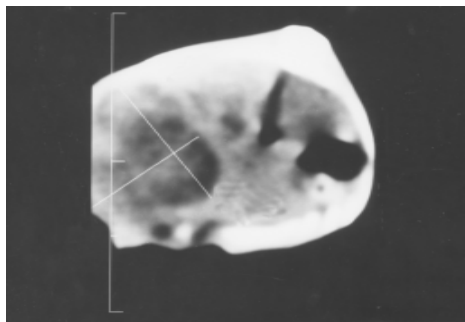
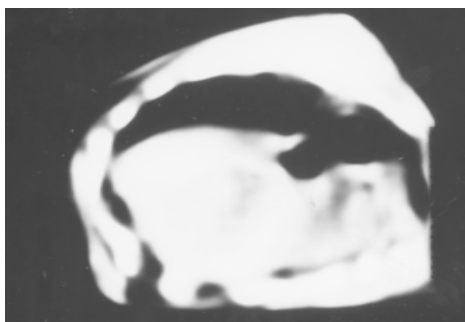
Average survival time by IL gene therapy

Table 1 shows the average survival time of rat. All rats were died within 15 d after implanting liver cancer in both physiologic saline control and blank vector control. Compared with control, the survival time of rat was prolonged significantly by treatment with IL-2 or IL-12 ($P<0.01$). The rat survival time of treatment with fused gene of IL-2/IL-12 was lengthened markedly compared with IL treatment alone ($P<0.05$). Moreover, the survival time of early treatment was much longer than that of later treatment with IL ($P<0.01$). In addition, 6 rats treated early with fused gene of IL-2/IL-12 were lived more than 60 d, but there were 3 rats treated with IL-12 that lived more than 60 d.

When the tumor was undetectable by abdominal pathologic biopsy in the rats that lived more than 60 d, the 4 rats were implanted tumor piece again. It was interested that there were no tumor growths in abdominal cavities 7 d late.

Imaging features

The liver tumor was detected by CT on day 7 after implantation in control (Figure 1). The 6 of 10 rats administrated early with IL-2/IL-12 fused gene showed that the liver tumors were reduced after 2 mo (Figure 2).

**Figure 1** CT scan of the liver cancer 7 d after implantation.**Figure 2** CT scan of the tumor treated with IL-2/IL-12 fused gene after 2 mo.

Pathologic features

A number of lymphocyte infiltrations in liver tumor were

observed significantly after 5 d of treatment with IL-2/IL-12 fused gene and 7 d of treatment with IL-2 gene or IL-12 gene (Figure 3).

**Figure 3** Pathological changes of implanted liver cancer (HE staining, original magnification: $\times 200$). There are numerous lymphocytes in tumor tissues.

Serum mIL-12 and hIL-2 levels

Compared with control, both IL-2 and IL-12 in serum were increased significantly in rats treated with IL gene on day 1 (Table 2). After the injection of IL-2/IL-12 fused gene, both IL-2 and IL-12 in serum reached the highest level on day 3, then decreased stepwise and maintained at a lower level for 2 mo (Table 3).

Table 2 Determination of serum hIL-2 or mIL-12 3 d after administration of IL gene (ng/mL)

Group	HIL-2	MIL-12
Physiologic saline control	<0.8	<0.8
Blank vector control	<0.8	<0.8
IL-2 gene therapy	19.4 \pm 1.8	<0.8
IL-12 gene therapy	<0.8	22 \pm 2.5
IL-12-IL-2fused gene therapy	18.5 \pm 2.4	20.5 \pm 2.5

Table 3 Determination of serum hIL-2 and mIL-12 on fused gene group (ng/mL)

Group	HIL-2	MIL-12
Control	<0.8	<0.8
On d 3 after therapy	18.5 \pm 2.4	20.5 \pm 2.5
On d 7 after therapy	10.2 \pm 2.5	11.5 \pm 2.5
One mo after therapy	5.3 \pm 1.2	6.2 \pm 1.4
Two mo after therapy	<0.8	<0.8

IL increases NK cell activity

IL-2 and IL-12 have been reported to increase NK cell activity. To determine if the IL-2/IL-12 fused gene could induce NK cell activation, rats were treated as described above with IL-2 and/or IL-12. The rats were sacrificed on day 7, and the spleen lymphocytes were assayed for the ability to kill ⁵¹Cr-labeled

YAC-1 target cells. There was a significant increase in NK activity after rats were injected with IL-2 or IL-12 alone ($P < 0.01$). Compared with IL alone, treatment with IL-2/IL-12 fused gene markedly enhanced NK cell activity ($P < 0.05$).

Toxicity of IL

Three rats (30%) in IL-2 group and 1 (10%) in IL-2/IL-12 group showed anorexia after administration of IL. The symptom was recovered 3-5 d late (Figure 4).

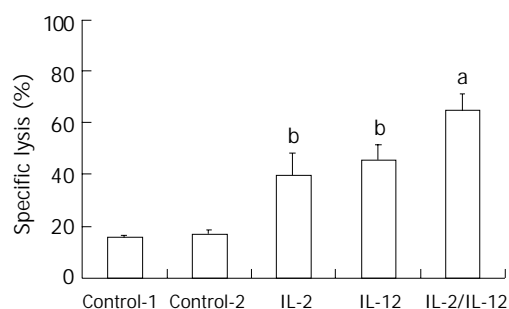


Figure 4 Activation of NK cell activity after administration of IL-2 and/or IL-12 ($n=5$). ^b $P < 0.01$ vs control; ^a $P < 0.05$ vs IL-2 group or IL-12 group.

DISCUSSION

The establishment of DNA recombination and transfection allowed us to utilize gene therapy for killing or inhibiting the tumor cells^[14]. The utility of recombinant adenoviral vectors for gene therapy is limited by the low transduction efficiency and lack of specificity for target cells^[15,16]. Spread of the virus throughout the cells maximizes the percent of cells within a cell expressing the gene of interest, and should improve the antitumor response. This may be significant for gene delivery expressing cytokines, tumor antigens or enzymes. One limitation of the transduction system is the inefficiency of the combined cytokines expression system. The initial work in this study was to construct the IL-2/IL-12 fused gene vector that was then injected into spleen, in which splenic cells, probably including liver cells, were transduced to express IL-2 and IL-12 simultaneously.

The active IL-12 is a heterogeneous dimer, which contains p35 subunit and p40 subunit, so that both subunits express simultaneously in cells if used to treat disease. Using PCR technique based on the subunit characterization of different gene sequences, we constructed the active IL-2/IL-12 fused gene and a linker sequence was incorporated into subunits of IL-12, so that the gene could correctly express protein. In present study, the IL-2 and IL-12 levels were not significantly different in serum.

The single gene therapy for the liver cancer is not ideal because it is resulted from multi-factors^[17]. Chen *et al.* suggested recently that TRAIL and chemotherapeutic agents or anticancer cytokines combination might be a novel strategy for the treatment of liver cancer. Combination of IL-2/IL-12 results in stable antitumor effect, which induces the cytotoxic T lymphocyte and NK cell^[18]. IL-2 and IL-12 have synergetic effect such as immunoregulatory^[19,20]. The antitumor immunologic effect from IL-2 and IL-12 depends on available concentration of IL-2 and IL-12. IL-2 and IL-12 also cause a long term antitumor immunologic memory^[21]. In present study, retrovirus vector containing IL-2/IL-12 genes was constructed, in which gene products of IL-2 and IL-12 were expressed simultaneously in the liver. We treated rat liver cancer with IL-2 and/or IL-12 gene. The liver cancer rats treated with IL-2 or IL-12 survived longer than those in control ($P < 0.01$). Compared with IL alone,

combination of IL-2/IL-12 gene showed a longer survival of 14-28 d in early treatment group and 5-12 d in late treatment group.

Spleen is the biggest immune organ that has a lot of immunocytes and produces antibodies and cytokines. Spleen is also the main organ of inducing immunoresponsiveness to heterologous antigen. The retrovirus packaging cell strain was injected into spleen, which expresses the high level of cytokine in order to activate immunocytes. In other hand, the retrovirus packaging cells would be transferred from spleen to liver by splenic veins and the liver cells would be infected by packaging cells resulting in enhanced anti-tumor immunity. In present study, the IL gene was injected into spleen and the blood concentration of IL was the highest on day 3. The IL concentration maintained at a level for 2 mo. Authors from Spain reported that gutless adenoviral vector encoding hIL-2 and mL-12 was injected into animals and IL was expressed by hepatocytes. The peak concentration of IL-12 was at 10 h and it completely disappeared by 72 h. If the vectors were administrated continually, the serum IL-12 would maintain at least for 48 wk^[22,23]. The rats received the splenic gene therapy survived longer than those in control. When combination of IL-2/IL-12 gene was injected into spleen, the high concentration of IL was determined from blood until day 3 and the rats survived a longer time compared with IL therapy alone.

Moreover, early gene treatment is better than late therapy. In this study, 6 rats (30%) with combined gene therapy on early stage survived a long term and the tumor nodes in liver was not detected by CT imaging and pathologic observation, in which the IL-2 and IL-12 kept a high concentration at least for 2 mo. As same as other therapy for cancer, the IL gene therapy should administrate as early as possible. In present study, the liver cancer rats treated with IL-2 or IL-12 on day 1 survived more than 8 d or 13 d respectively compared with that treated on d 7 (Table 1). The combined IL gene therapy has the similar result.

IL-2 or IL-12 produced significant toxic reaction if they were administrated enough dosage to maintain a high blood concentration. When IL-2 or IL-12 was injected into rat liver, some rats showed acute toxic reaction such as anorexia, convulsion and bleeding shock (unpublished data). In present study, when IL genes were injected into spleen, the severe acute toxic reaction was not observed in all groups.

A mechanism of IL gene treatment may be due to enhancement of NK cell activation and production of cytokines including IL^[24]. Several investigators have shown that NK cells are a relative smaller cell population in peripheral lymphoid organs but are abundant in the liver. An initial response to tumor cell may involve the innate arm of the immune response resulting in killing of mutant cell strain by NK cell^[25,26]. The findings in this study are novel since IL-2/IL-12 fused gene expresses IL-2 and IL-12 simultaneously that result in further stimulation of NK cells. We propose that liver tumor is inhibited because of IL production, such as IL-2 and IL-12, which is stimulated by IL gene therapy.

It is interesting that serum IL-2 and IL-12 levels do not change in IL-2/IL-12 gene therapy compared with IL alone, but NK cell activity is enhanced significantly compared with IL alone. We propose that the NK cell activity is strongly stimulated by both IL-2 and IL-12 at the same time, which was caused by IL-2/IL-12 fused gene expression^[27-30].

In summary, treatment with IL-2 and/or IL-12 gene increases serum IL-2 and IL-12 levels and enhances the NK cell activity, which may inhibit the liver tumor growth. The fused gene therapy of IL-2/IL-12 is of low toxicity and relatively high NK cell activity. We suggest that IL-2/IL-12 fused gene therapy may be a safe and efficient method for the treatment of liver cancer. For IL gene therapy, early intervention is better than late one.

REFERENCES

- 1 **Yang Y**, Wilson JM. Clearance of adenovirus-infected hepatocytes by MHC class I-restricted CD4⁺ CTLs *in vivo*. *J Immunol* 1995; **155**: 2564-2570
- 2 **Shi M**, Wang FS, Wu ZZ. Synergetic anticancer effect of combined quercetin and recombinant adenoviral vector expressing human wild-type p53, GM-CSF and B7-1 genes on hepatocellular carcinoma cells *in vitro*. *World J Gastroenterol* 2003; **9**: 73-78
- 3 **Rissoan MC**, Soumelis V, Kadowaki N, Grouard G, Briere F, Waal Malefyt R, Liu YJ. Reciprocal control of T helper cell and dendritic cell differentiation. *Science* 1999; **283**: 1083-1086
- 4 **Nakamori M**, Iwahashi M, Nakamura M, Ueda K, Zhang X, Yamaue H. Intensification of antitumor effect by T helper 1-dominant adoptive immunogene therapy for advanced orthotopic colon cancer. *Clin Cancer Res* 2003; **9**: 2357-2365
- 5 **Chi CH**, Wang YS, Lai YS, Chi KH. Anti-tumor effect of *in vivo* IL-2 and GM-CSF electrogene therapy in murine hepatoma model. *Anticancer Res* 2003; **23**: 315-321
- 6 **Taketo MM**. Cyclooxygenase-2 inhibitors in tumorigenesis. *J Natl Cancer Inst* 1998; **90**: 1529-1536
- 7 **Milanovich MR**, Snyderman CH, Wagner R, Johnson JT. Prognostic significance of prostaglandin E2 production by mononuclear cells and tumor cells in squamous cell carcinomas of the head and neck. *Laryngoscope* 1995; **105**: 61-65
- 8 **Arvind P**, Papavassiliou ED, Tsioulis GJ, Qiao L, Lovelace CI, Ducean B, Rigas B. Prostaglandin E2 down-regulates the expression of HLA-DA antigen in human colon adenocarcinoma cell lines. *Biochemistry* 1995; **34**: 5604-5609
- 9 **Pavlidis N**, Nicolaidis C, Bairaktari E, Kalef-Ezra J, Athanassiadis A, Seferiadis C, Fountzilias G. Soluble interleukin-2 receptors in patients with advanced colorectal carcinoma. *Int J Bio Markers* 1996; **11**: 6-11
- 10 **Satomi A**, Murakami S, Ishida K, Mastuki M, Hashimoto T, Sonoda M. Significance of increased neutrophils in patients with advanced colorectal cancer. *Acta Oncol* 1995; **34**: 69-73
- 11 **Merchinsky M**, Moss B. Resolution of vaccinia virus DNA concatemer junctions requires late-gene expression. *J Virol* 1989; **63**: 1595-1603
- 12 **Gnant MF**, Noll LA, Irvine KR, Puhlmann M, Terrill RE, Alexander HR Jr, Bartlett DL. Tumor-specific gene delivery using recombinant vaccinia virus in a rabbit model of liver metastases. *J Natl Cancer Inst* 1999; **91**: 1744-1750
- 13 **Zhang HG**, Xie J, Xu L, Yang P, Xu X, Sun S, Wang Y, Curiel DT, Hsu HC, Mountz JD. Hepatic DR5 induces apoptosis and limits adenovirus gene therapy product expression in the liver. *J Virol* 2002; **76**: 5692-5700
- 14 **Abo T**, Kawamura T, Watanabe H. Physiological responses of extrathymic T cells in the liver. *Immunol Rev* 2000; **174**: 135-149
- 15 **Khuri FR**, Nemunaitis J, Ganly I, Arseneau J, Tannock IF, Romei L, Gore M, Ironside J, MacDougall RH, Heise C, Randlev B, Gillenwater AM, Brusio P, Kaye SB, Hong WK, Kirn DH. A controlled trial of intratumoral ONYX-015, a selectively 3-replicating adenovirus, in combination with cisplatin and 5-fluorouracil in patients with recurrent head and neck cancer. *Nat Med* 2000; **6**: 879-885
- 16 **Walker JR**, McGeagh KG, Sundaresan P, Jorgensen TJ, Rabkin SD, Martuza RL. Local and systemic therapy of human prostate adenocarcinoma with the conditionally replicating herpes simplex virus vector G207. *Hum Gene Ther* 1999; **10**: 2237-2243
- 17 **Salazar-Mather TP**, Hamilton TA, Biron CA. A chemokine-to-cytokine-to-chemokine cascade critical in antiviral defense. *J Clin Invest* 2000; **105**: 985-993
- 18 **Gillies SD**, Lan Y, Brunkhorst B, Wong WK, Li Y, Lo KM. Bi-functional cytokine fusion proteins for gene therapy and antibody-targeted treatment of cancer. *Cancer Immunol Immunother* 2002; **51**: 449-460
- 19 **Dietrich A**, Kraus K, Brinckmann U, Friedrich T, Muller A, Liebert UG, Schonfelder M. Complex cancer gene therapy in mice melanoma. *Langenbecks Arch Surg* 2002; **387**: 177-182
- 20 **Li D**, Shugert E, Guo M, Bishop JS, O'Malley BW Jr. Combination nonviral interleukin 2 and interleukin 12 gene therapy for head and neck squamous cell carcinoma. *Arch Otolaryngol Head Neck Surg* 2001; **127**: 1319-1324
- 21 **Wigginton JM**, Wiltout RH. IL-12/IL-2 combination cytokine therapy for solid tumours: translation from bench to bedside. *Expert Opin Biol Ther* 2002; **2**: 513-524
- 22 **Wang L**, Hernandez-Alcoceba R, Shankar V, Zabala M, Kochanek S, Sangro B, Kramer MG, Prieto J, Qian C. Prolonged and inducible transgene expression in the liver using gutless adenovirus: a potential therapy for liver cancer. *Gastroenterology* 2004; **126**: 278-289
- 23 **Sobota V**, Bubenik J, Simova J, Jandlova T. Intratumoral IL-12 gene transfer improves the therapeutic efficacy of IL-12 but not IL-19. *Folia Biol* 2000; **46**: 191-193
- 24 **Tanaka M**, Saijo Y, Sato G, Suzuki T, Tazawa R, Satoh K, Nukiwa T. Induction of antitumor immunity by combined immunogene therapy using IL-2 and IL-12 in low antigenic Lewis lung carcinoma. *Cancer Gene Ther* 2000; **7**: 1481-1490
- 25 **Chen B**, Timiryasova TM, Haghighat P, Andres ML, Kajioka EH, Dutta-Roy R, Gridley DS, Fodor I. Low-dose vaccinia virus-mediated cytokine gene therapy of glioma. *J Immunother* 2001; **24**: 46-57
- 26 **Satoh Y**, Esche C, Gambotto A, Shurin GV, Yurkovetsky ZR, Robbins PD, Watkins SC, Todo S, Herberman RB, Lotze MT, Shurin MR. Local administration of IL-12-transfected dendritic cells induces antitumor immune responses to colon adenocarcinoma in the liver in mice. *J Exp Ther Oncol* 2002; **2**: 337-349
- 27 **Sangro B**, Qian C, Schmitz V, Prieto J. Gene therapy of hepatocellular carcinoma and gastrointestinal tumors. *Ann N Y Acad Sci* 2002; **963**: 6-12
- 28 **Sato T**. Locoregional immuno(bio)therapy for liver metastases. *Semin Oncol* 2002; **29**: 160-167
- 29 **Martinet O**, Divino CM, Zang Y, Gan Y, Mandeli J, Thung S, Pan PY, Chen SH. T cell activation with systemic agonistic antibody versus local 4-1BB ligand gene delivery combined with interleukin-12 eradicate liver metastases of breast cancer. *Gene Ther* 2002; **9**: 786-792
- 30 **Yoshida H**, Katayose Y, Unno M, Suzuki M, Kodama H, Takemura S, Asano R, Hayashi H, Yamamoto K, Matsuno S, Kudo T. A novel adenovirus expressing human 4-1BB ligand enhances antitumor immunity. *Cancer Immunol Immunother* 2003; **52**: 97-106

Edited by Zhang JZ and Chen WW Proofread by Xu FM

Combined gene therapy of endostatin and interleukin 12 with polyvinylpyrrolidone induces a potent antitumor effect on hepatoma

Pei-Yuan Li, Ju-Sheng Lin, Zuo-Hua Feng, Yu-Fei He, He-Jun Zhou, Xin Ma, Xiao-Kun Cai, De-An Tian

Pei-Yuan Li, Ju-Sheng Lin, He-Jun Zhou, Xin Ma, Xiao-Kun Cai, De-An Tian, Institute of Liver Diseases, Tongji Hospital, Tongji Medical College, Huazhong University of Science and Technology, Wuhan 430030, Hubei Province, China

Zuo-Hua Feng, Yu-Fei He, Department of Biochemistry and Molecular Biology, Tongji Medical College, Huazhong University of Science and Technology, Wuhan 430030, Hubei Province, China

Supported by the Major State Basic Research Development Program of China 973 Program, No. 2002CB513100

Correspondence to: Ju-Sheng Lin, Institute of Liver Diseases, Tongji Hospital, Tongji Medical College, Huazhong University of Science and Technology, Wuhan 430030, Hubei Province, China. linjusheng2001@163.com

Telephone: +86-27-83662578 **Fax:** +86-27-83662578

Received: 2003-10-20 **Accepted:** 2003-12-16

Abstract

AIM: To study the antitumor effect of combined gene therapy of endostatin and interleukin 12 (IL-12) with polyvinylpyrrolidone (PVP) on mouse transplanted hepatoma.

METHODS: Mouse endostatin eukaryotic plasmid (pSecES) with a mouse Igk signal sequence inside and mouse IL-12 eukaryotic plasmid (pmIL-12) were transfected into BHK-21 cells respectively. Endostatin and IL-12 were assayed by ELISA from the supernatant and used to culture endothelial cells and spleen lymphocytes individually. Proliferation of the latter was evaluated by MTT. H22 cells were inoculated into the leg muscle of mouse, which was injected intratumorally with pSecES/PVP, pmIL-12/PVP or pSecES+pmIL-12/PVP repeatedly. Tumor weight, serum endostatin and serum IL-12 were assayed. Tumor infiltrating lymphocytes, tumor microvessel density and apoptosis of tumor cells were also displayed by HE staining, CD31 staining and TUNEL.

RESULTS: Endostatin and IL-12 were secreted after transfection, which could inhibit the proliferation of endothelial cells or promote the proliferation of spleen lymphocytes. Tumor growth was highly inhibited by 91.8% after injection of pSecES+pmIL-12/PVP accompanied by higher serum endostatin and IL-12, more infiltrating lymphocytes, fewer tumor vessels and more apoptosis cells compared with injection of pSecES/PVP, pmIL-12/PVP or vector/PVP.

CONCLUSION: Mouse endostatin gene and IL-12 gene can be expressed after intratumoral injection with PVP. Angiogenesis of hepatoma can be inhibited synergistically, lymphocytes can be activated to infiltrate, and tumor cells are induced to apoptosis. Hepatoma can be highly inhibited or eradicated.

Li PY, Lin JS, Feng ZH, He YF, Zhou HJ, Ma X, Cai XK, Tian DA. Combined gene therapy of endostatin and interleukin 12 with polyvinylpyrrolidone induces a potent antitumor effect on hepatoma. *World J Gastroenterol* 2004; 10(15): 2195-2200 <http://www.wjgnet.com/1007-9327/10/2195.asp>

INTRODUCTION

Liver cancer is one of the most common neoplasms worldwide. In some parts of Asia and Africa the prevalence is more than 100/100 000 population^[1]. Treatments often come to failure because of its high resistance to chemotherapy or radiotherapy and the severe side-effects induced^[1]. At present the only curative options are partial hepatectomy or total hepatectomy with liver transplantation. But the chance for surgery is very limited. The effects of some other treatments such as intratumoral injection of ethanol or acetic acid, transarterial catheter embolization, and thermal destruction or microwave coagulation were also very poor due to the high incidence of tumor recurrence and hepatic failure^[1-3]. Now combined treatments including biotherapy have been regarded as the most promising methods to cure liver cancer^[4,5].

Among the biotherapies, antiangiogenic therapies have recently attracted an intense interest for their broad-spectrum action, low toxicity, and in direct endothelial targeting, the absence of drug resistance^[6]. Antiangiogenic therapy induced by endostatin could specifically inhibit endothelial proliferation and potently inhibit angiogenesis and tumor growth accompanied by apoptosis in tumor cells^[7-9]. Repeated cycles of antiangiogenic therapy were even followed by prolonged tumor dormancy without further therapy^[10].

More and more learners have begun to realize that the occurrence of tumors is a complex course induced by multiple genes and multiple steps. Interference of single factor on tumor often can not get satisfactory results. Although primary tumors were regressed to dormant microscopic lesions after endostatin therapy, tumor cells were not eradicated at all^[7,10]. Conventional chemotherapy or radiotherapy can do little on residual tumor cells, accurate recognition and clearance of which depends on the immune system of host^[11]. IL-12 is among the most potent cytokines in stimulating antitumor immunity^[12-14], which also showed significant inhibitory activity on angiogenesis^[15].

So antiangiogenesis therapy by endostatin in combination with antitumor immunotherapy by IL-12 has become an attractive approach. On one hand synergistically antiangiogenic effect may be achieved to induce tumor dormancy. On the other hand, residual tumor cells may be also eradicated by antitumor immunotherapy induced by IL-12. Due to the problems such as bioactive protein production in large quantities, high costs and daily administration of endostatin^[10,16], and the severe side-effects of system administration of IL-12^[17,18], local gene therapy has proved to be very effective and nontoxic at the same time^[19-24]. In this study combined intratumoral gene therapy of endostatin and IL-12 was observed in treatment of mouse hepatoma.

MATERIALS AND METHODS

Plasmid and host

Mouse endostatin eukaryote expression plasmid pSecES was constructed in our laboratory (data not shown). The expression of endostatin was under the control of *cytomegalovirus* (CMV) promoter. A mouse Igk signal peptide sequence was located upstream of endostatin sequence to lead endostatin to secrete out. Mouse IL-12 eukaryote expression plasmid (pmIL-12) was

a gift from Professor David M. Mahvi in Wisconsin University, USA. Both *M*, 35 000 light chain gene and *M*, 40 000 heavy chain gene linked by an internal ribosome entrance site were put downstream of CMV promoter^[25]. Empty plasmid pcDNA3.1, pcDNA3.1-lacZ and *E. coli* DH5 α were from the collection of our laboratory. DH5 α bacteria containing the plasmids were grown in LB medium to mid-log phase. The plasmids were then purified with Qiagen columns (Qiagen). An analytical gel of each plasmid (cut and uncut) was done to ensure that there was no contamination with other nucleic acids. The A_{260}/A_{280} ratios ranged from 1.8 to 2.0. Also each plasmid was confirmed to be free of endotoxin. For gene therapy, concentrated plasmid stock solution was made by lyophilizing and rehydrating with water. Then it was formulated into a solution containing 1 g/L plasmid, 50 g/L polyvinylpyrrolidone (PVP, K30, *M*, 40 000, from Sigma), 150 mmol/L NaCl before use.

Cell culture and animals

BHK-21, human umbilical vein endothelial cell line (HUVEC) ECV304 and mouse hepatoma cell line H22 were purchased from China Center for Type Culture Collection. All the cell lines were maintained in RPMI 1640 medium (GibcoBRL) supplemented with 100 mL/L fetal bovine serum (FBS), 10^5 U/L penicillin and 100 mg/L streptomycin. Cells were cultured at 37 with 50 mL/L CO₂. Six to 8-wk-old male BALB/c mice of specific-pathogen-free (SPF) grade (purchased from Hubei Experimental Animals Center, China) were maintained in a standard SPF animal's room. All animal studies were performed in accordance with acceptable animal use guidelines.

Secretion and activity of endostatin plasmid and IL-12 plasmid

In 6-well plate, 5×10^5 BHK-21 cells per well were transfected with 1 μ g pSecES or 1 μ g pmIL-12, 3 μ L LipoGen (InvivoGen) in accordance with directions of the manufacturer. Forty-eight hours after transfection, 0.1 mL ECV304 cells (2×10^7 /L) cultured in RPMI 1640 additionally supplemented with 2 μ g/L recombinant human basic fibro growth factor (rhbFGF) (PeproTech, UK) was inoculated to a 96-well plate. 0.1 mL supernant of BHK-21 cells transfected with pSecES was added to ECV304 cells per well. Seventy-two hours later, 20 μ L 5 g/L MTT was added per well. After 4 h, the supernant was discarded and 150 μ L DMSO was added. Absorbency at 570 nm was assayed. Forty-eight hours after transfection, mouse spleen cells were also produced by routine protocols and cultured in RPMI 1640 medium supplemented with 100 mL/L FBS for 2 h. Then the suspending lymphocytes were adjusted to 1×10^8 /L and seeded to a 24-well plate (0.5 mL per well). Also 0.5 mL supernant of BHK-21 cells transfected with pmIL-12 was added per well. Forty-eight hours later, the proliferation was evaluated by MTT assay as above. The supernant of BHK-21 transfected with pcDNA3.1-lacZ was used as control. Also transfection rate was evaluated by X-gal staining of BHK-21 transfected with pcDNA3.1-lacZ 48 h later. All the three kinds of supernant was stored at -20°C for further assay.

Combined gene therapy of endostatin and IL-12 for H22 hepatoma in vivo

In 0.1 mL PBS, 10^5 H22 cells were inoculated i.m. into the hind limb of BALB/c mice. Then the mice were randomly divided into five groups (6 per group): PVP/NaCl (untreated), pcDNA3.1 (empty vector), pSecES, pmIL-12, pSecES+pmIL-12. Another 6 mice were not inoculated for further assay of basic serum endostatin. From the next day after inoculation, 100 μ g pSecES/PVP and/or pmIL-12/PVP, 100 μ g pcDNA3.1/PVP or 100 μ L PVP/NaCl solution was injected into the inoculation site respectively with a 26 G needle every three days. After inoculation for 21 days, tumors were removed and weighed.

Before tumor dissection, mouse blood was collected and stored at 4°C overnight. Then the serum was stored at -20°C for further assay after centrifugation. The data were analyzed statistically by SPSS 10.0 procedure.

Assay of mouse endostatin and IL-12 (p70) in supernant or serum

The frozen supernant of BHK-21 transfected with pSecES, pmIL-12 or pcDNA3.1-lacZ and the frozen serum were thawed to room temperature. Then mouse endostatin and IL-12 (p70) were assayed according to the directions of CytELISA mouse endostatin kit (CytImmune, USA) and mouse IL-12 (p70) ELISA kit (Shengzhen Jingmei Biotech, China).

Detection of MVD, TILs and apoptosis of H22 hepatoma

Paraffin sections (5 μ m) of tumor tissues were stained with rat anti-mouse CD31 antibody (eBioscience). Then the primary antibody was detected by biotinylated secondary rabbit anti-rat IgG and SABC immunohistochemistry kit (Wuhan Boster Biotech, China) according to directions of its manufacturer. Paraffin sections were also stained with HE to reveal tumor infiltrating lymphocytes (TILs). Apoptosis of tumors was displayed by TdT-mediated dUTP nick end labeling (TUNEL) staining with an *in situ* cell death detection kit (Boehringer Mannheim, Germany) in accordance with the guideline of its manufacturer.

Tumor microvessel density (MVD) was counted as previously described^[26,27]. The CD31 staining sections were scanned in 40 \times microscope and "hot spots" (area with greatest vascula) were found, from which 3 random fields of 200 \times microscope were selected. The average vascular number of the three fields was looked as MVD. For HE and TUNEL staining sections, 5 random nonnecrotic tissue fields in 400 \times microscope was selected. The average number of TILs or apoptotic cells was counted. The data were analyzed statistically by SPSS 10.0 procedure.

RESULTS

Secretion and activity of endostatin plasmid and IL-12 plasmid

β -galactosidase expression was assessed by X-gal staining 48 h post-transfection. The transfection efficiency was about 30%. No endostatin or IL-12 was detected in the supernant of BHK-21 transfected with pcDNA3.1-lacZ. Endostatin secreted by BHK-21 transfected with pSecES was 65.5 ± 10.9 ng/ 10^6 cells. When this supernant was added to ECV304 stimulated by rhbFGF, the proliferation of the latter was inhibited by 29.2% 72 h later (inhibitory efficiency=1 - A of endostatin group/A of control group, $P < 0.01$). Also 221.8 ± 44.4 ng/ 10^6 cells IL-12 (p70) was detected in the supernant of BHK-21 transfected with pmIL-12. It could promote mouse spleen lymphocytes to proliferate by 15.2% (proliferation efficiency=A of IL-12 group/A of control group - 1, $P < 0.05$). The results are displayed in Figure 1.

Antitumor effect of combined gene therapy of endostatin and IL-12 for H22 hepatoma in vivo

On the next day after inoculation, the mice received gene therapy. No skin lesions were found in the injection sites. On d 21 after inoculation, tumors were dissected and weighed. Big tumors could be found in all mice of PVP/NS group and pcDNA3.1 group. In pSecES group, all mice formed tumors, some of which were much smaller. Four mice formed tumors in pmIL-12 group and only two mice formed small tumors in pSecES+pmIL-12 group. The average tumor weight of pSecES group was much lower than that of PVP/NS group or pcDNA3.1 group ($P < 0.01$) (Figure 2). The inhibitory rate was 56.4% (inhibitory efficiency=1 - tumor weight of pSecES group/tumor

weight of pcDNA3.1 group). For pmIL-12 group, the inhibitory rate was 85.7%. When pSecES gene therapy and pmIL-12 gene therapy were used in combination, tumor growth was inhibited by 91.8% ($P<0.01$).

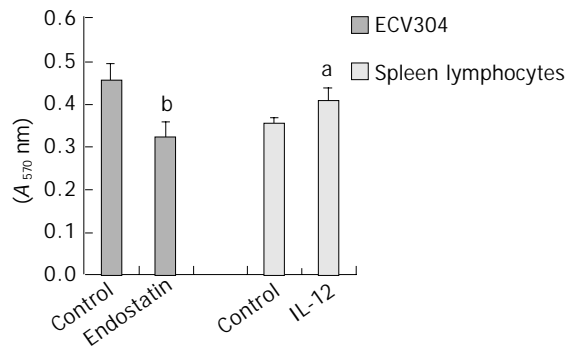


Figure 1 Proliferation of ECV304 inhibited by the supernant of BHK-21 transfected with pSecES and proliferation of spleen lymphocytes stimulated by the supernant of BHK-21 transfected with pmIL-12. Each bar represents A value of ECV304 or spleen lymphocytes, and mean \pm SD for 5 wells. ^a $P<0.05$ vs control, ^b $P<0.01$ vs control.

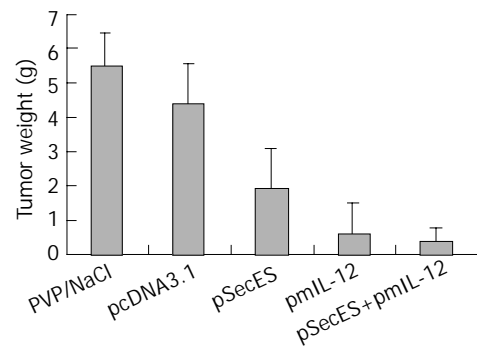


Figure 2 Hepatoma formation and growth inhibited by gene therapy of endostatin and IL-12. Each bar represents tumor weight of mice treated with PVP/NaCl, pcDNA3.1/PVP, pSecES/PVP, pmIL-12/PVP or pSecES+pmIL-12/PVP, and mean \pm SD for six mice. $P<0.01$ by ANOVA analysis.

Serum endostatin and IL-12 levels after gene therapy

When gene therapy was finished, the serum endostatin and IL-12 levels were evaluated by ELISA. The serum endostatin level in pSecES group was 117.1 ± 12.8 $\mu\text{g/L}$, which was much higher than that in pcDNA3.1 group (87.7 ± 6.1 $\mu\text{g/L}$) or the basic level

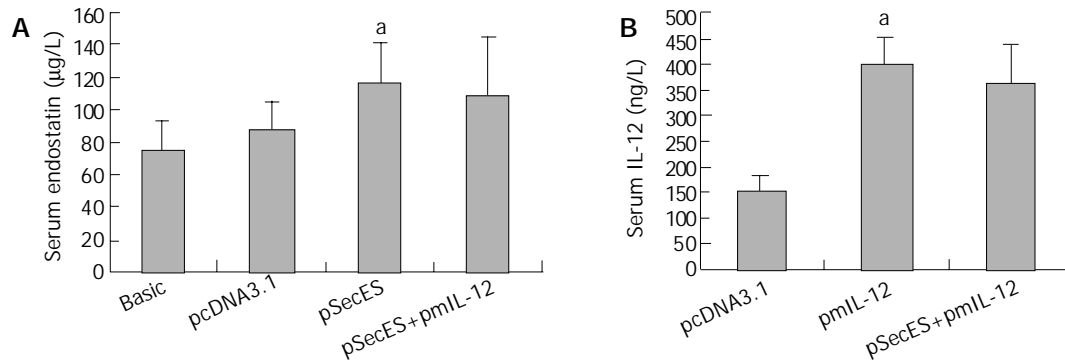


Figure 3 Increase of mice serum endostatin levels or IL-12 levels after gene therapy. A: Serum endostatin levels of mice treated with pcDNA3.1/PVP, pSecES/PVP, pSecES+pmIL-12/PVP or not inoculated with H22 cells (basic levels). Each bar represents mean \pm SD for six mice. ^a $P<0.05$ vs pcDNA3.1 group. B: Serum IL-12 levels of mice treated with pcDNA3.1/PVP, pmIL-12/PVP, pSecES+pmIL-12/PVP. Each bar represents mean \pm SD for six mice. ^a $P<0.05$ vs pcDNA3.1 group.

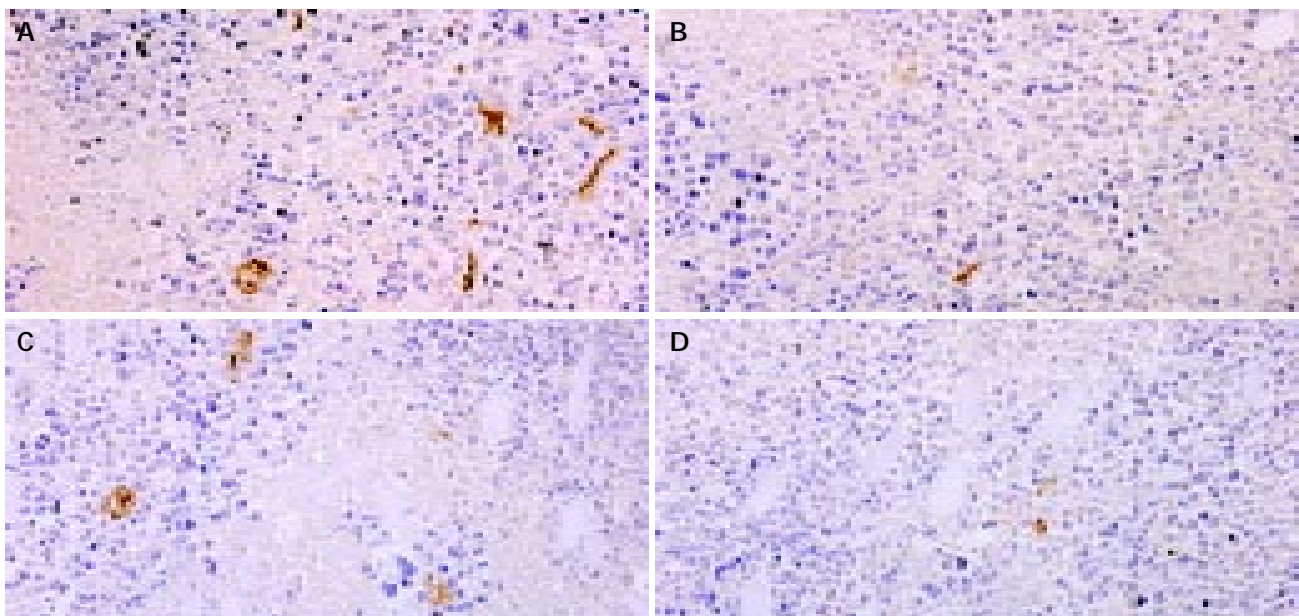


Figure 4 Hepatoma angiogenesis inhibited by gene therapy of endostatin and IL-12. MVD (CD31staining, 200 \times) of hepatoma treated with pSecES/PVP (7.3 ± 1.2) (B), pmIL-12/PVP (10.0 ± 1.7) (C) or pSecES+pmIL-12/PVP (3.7 ± 1.2) (D) was less than that treated with pcDNA3.1/PVP (22.7 ± 3.1 , $P<0.05$) (A).

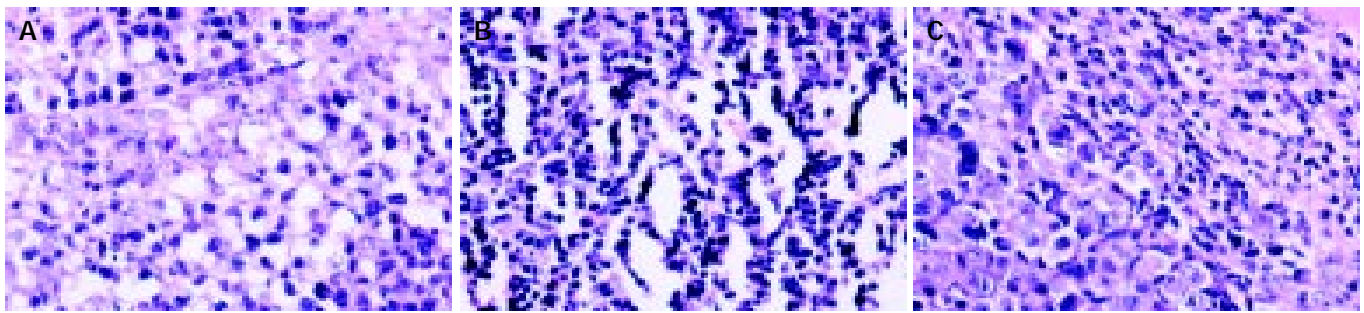


Figure 5 Lymphocytes infiltration into hepatoma promoted by gene therapy of IL-12. TILs (HE staining, 400 \times) of hepatoma treated with pmIL-12/PVP (146.2 \pm 24.6) (B) and pSecES+pmIL-12/PVP (123.2 \pm 21.4) (C) were more than that treated with pcDNA3.1/PVP (45.2 \pm 11.8, P <0.01) (A).

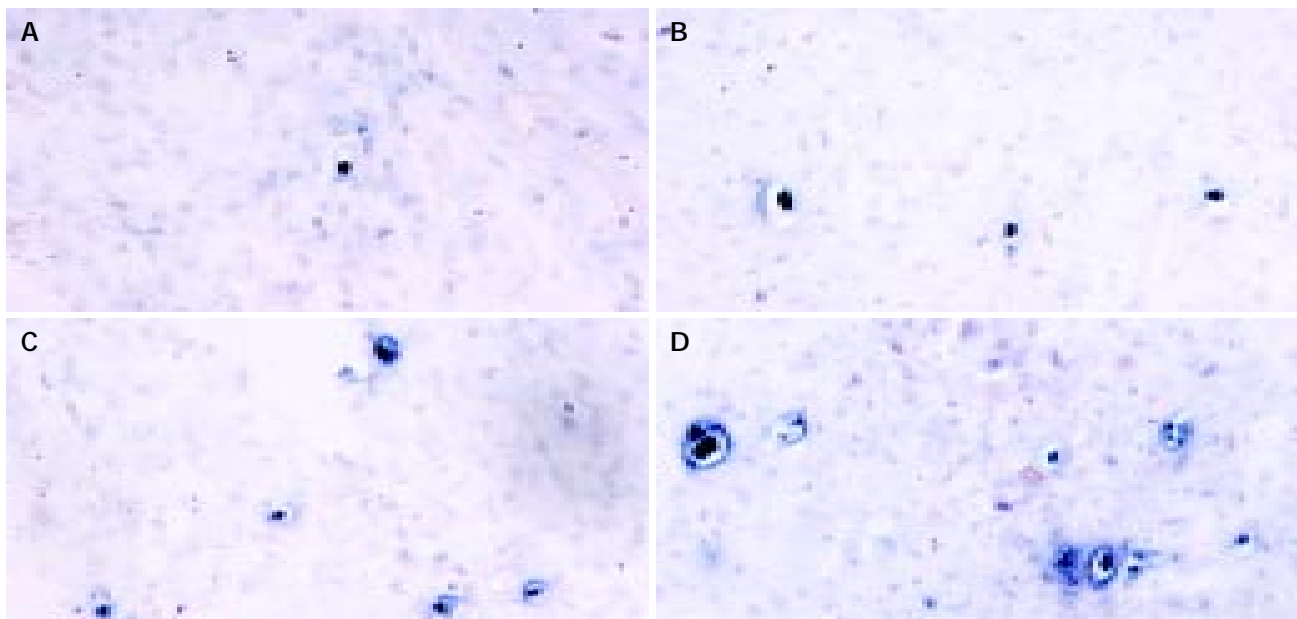


Figure 6 Apoptosis of hepatoma cells induced by gene therapy of endostatin and IL-12. Apoptotic tumor cells (TUNEL, 400 \times) treated with pSecES/PVP (11.2 \pm 2.3) (B), pmIL-12/PVP (14.4 \pm 3.5) (C) or pSecES+pmIL-12/PVP (24.8 \pm 4.8) (D) were more than those treated with pcDNA3.1/PVP (1.4 \pm 1.7, P <0.05) (A).

(75.8 \pm 6.6 μ g/L) (P <0.05). Also, after pmIL-12 gene therapy, the serum IL-12 level was higher in pmIL-12 group (401.0 \pm 51.6 ng/L) than in pcDNA3.1 group (154.8 \pm 25.8 ng/L) (P <0.05) (Figure 3).

MVD, TILs and apoptosis of H22 hepatoma after gene therapy

MVD were counted after CD31 staining in tumor sections. Compared with pcDNA3.1 group, MVD of hepatoma treated with pSecES/PVP or pmIL-12/PVP were much less. And in pSecES+pmIL-12 group, MVD were less than any single gene therapy group (P <0.05) (Figure 4).

Tumor sections were stained by HE, then TILs were evaluated. After pmIL-12/PVP or pSecES+pmIL-12/PVP gene therapy, TILs in hepatoma were more than that treated with pcDNA3.1/PVP (P <0.01). The results are displayed in Figure 5.

Also, tumor apoptosis was displayed by TUNEL staining. Figure 6 shows that there were only a few apoptotic tumor cells dispersed in 400 \times random scopes in pcDNA3.1 group. But in pSecES group or pmIL-12 group, apoptotic tumor cells increased. In pSecES+pmIL-12 group, apoptotic tumor cells were much more than any group (P <0.05).

DISCUSSION

Despite the progress in early diagnosis of liver cancer, its prognosis remains poor. In average, the mean life span was less than a year after diagnosis^[1]. How to prevent or cure the recurrence of remained tumor cells after partial hepatectomy

and how to inhibit tumor infiltrating in liver cancer patients in advanced stage are urgent challenges for liver cancer therapy. Now antiangiogenic therapy and immunotherapy have been paid more and more attention and many promising conclusions have been drawn^[28-31]. But in clinical trails, few satisfactory results were obtained by single biotherapy^[17,18,32]. Whether synergistic effects of antiangiogenesis therapy in combination with immunotherapy could be achieved is worthy to be researched.

Studies showed that angiogenesis played a very important role in the course of growth and metastasis of solid tumors including liver cancer. When the tumor size was beyond 2-3 mm³, oxygen and nutrition were not enough by simple diffusion. Then new vessels must be formed for further growth^[33]. However, angiogenesis was dependent on the cooperation of pro-angiogenesis factors and anti-angiogenesis factors^[34]. Among many inhibitors, endostatin, the C terminal of collagen X VIII, which is a M_r 20 000 protein with 184 amino acids in primary structure, has the strongest antiangiogenesis and antitumor effect. It was identified from the medium of a murine hemangioendothelioma (EOMA) cell line in 1997^[7]. Researchers indicated that both natural and recombinant endostatin could markedly inhibit endothelial cell proliferation *in vitro* and angiogenesis in chick chorioallantoic membrane, but had no effect on non-endothelial cells. When endostatin was administrated subcutaneously, primary tumors were regressed to dormant microscopic lesions and metastasis was inhibited. Repeated cycles of endostatin therapy showed prolonged tumor dormancy without further therapy^[7,10]. In our previous study, subcutaneous

injection of 10 mg/(kg.d) endostatin produced by gene engineering showed a potent inhibitory effect on the formation and growth of mouse H22 hepatoma^[35]. Also the clinical trial of endostatin has been carried out^[32]. But to obtain both high quantity and high quality of endostatin was necessary for optimal therapeutic benefit^[36]. It was indicated that the activity of endostatin expressed in mammalian cells was 1 000 times than recombinant protein extracted from *E.coli*^[37]. So gene therapy of endostatin has become a very good solution and many studies suggested that gene therapy of endostatin showed a powerful inhibition on liver cancer^[21,22].

When H22 hepatoma cells, derived from Balb/c mouse liver cancer in 1940 s, were inoculated into the leg muscle of mice, solid tumors formed quickly, which were easy to touch and easy for injection. Compared with viral vectors, non-viral vectors bore some advantages such as easy to handle, high capacity for DNA sequences, low toxicity, and non-immunogenic thus permitting repeated vector administrations^[38]. So we constructed endostatin eukaryotic plasmid pSecES, inside which a mouse Igk signal peptide sequence was put upstream endostatin sequence to let endostatin secrete out. *In vitro* high-levels endostatin with inhibitory activity on the proliferation of endothelial cells could be detected from the supernatant after transfection. And *in vivo*, for lower degradation of input DNA by endosomes and/or lysosomes and higher transfection efficiency, non-toxic PVP was used to enhance gene expression according to previous reports^[39,40]. Plasmid/PVP was injected intratumorally and repeatedly for a higher local concentration. After endostatin gene therapy, mice serum endostatin levels were consistently 2-3-fold higher than basic levels. Compared with controls, tumors formed slowly with less MVD and more apoptosis cells. The average tumor weight inhibitory rate was 56.4%. It was indicated that pro-angiogenic factors such as VEGF were induced when tumor vessels formed gradually, and antiangiogenic factors such as endostatin increased for a negative regulation^[41,42]. This opinion was also confirmed by our study that serum endostatin levels in mice burdened with big tumors after vector injection were increased compared with basic levels. When more endostatin were added by gene therapy, the balance would be broken and angiogenesis was inhibited.

Immunocytokines which were important in the regulation of the immune system could overcome immune tolerance against tumor antigens, thus tumor rejection was facilitated. It was benefic for prevention of recurrence of micro tumor cells and advanced tumors which could not accept operation or chemotherapy^[11,13]. Different cytokines (IL-2, IL-4, IL-12, INF- γ , TNF- α , GM-CSF) have been used to modulate the host's immune response either *in vitro* or *in vivo*. The activation and proliferation of immunocytes and antitumor immunity were induced more or less^[13]. IL-12 is among the most potent cytokines in stimulating antitumor immunity. It is a disulfide-linked heterodimeric cytokine. IL-12 acts by inducing a TH1 type of response, activating natural killer cells and cytotoxic T lymphocytes, enhancing expression of adhesion molecules on endothelial cells, thus facilitating the traffic of lymphocytes to the tumor, and inducing a potent antiangiogenic effect. In previous researches, the antitumor effect of IL-12 was established in various *in vivo* systems^[12-14]. However, the latter was reported to cause fatal toxicity in a clinical trial^[17], which led investigators to local administration of this cytokine by gene therapy or gene gun, that proved to be very effective and nontoxic at the same time^[23,24]. In our study, active IL-12 (p70) was expressed *in vitro* and *in vivo*. Tumors did not formed in 30% mice that received IL-12 gene therapy. The formed tumors were also highly inhibited with more TILs, less MVD and more apoptotic tumor cells. Moreover, the inhibitory effect of IL-12 gene therapy on H22 hepatoma was much better than that of endostatin plasmid ($P < 0.05$).

When combined gene therapy of endostatin and IL-12 was used, its antitumor effect was much better than others. Tumor formation was not observed in 66.7% mice. The average tumor weight inhibitory rate was 91.8%. But in mice that received endostatin gene therapy, no tumor regressed. The average tumor weight inhibitory rate was 56.4%. No tumor was formed in 33.3% mice after they received IL-12 gene therapy. The average tumor weight inhibitory rate was 85.7%. It was suggested that synergistic antitumor effect was achieved after combined gene therapy of endostatin and IL-12. The proposed mechanism of the combined gene therapy maybe a synergistic cooperation of an antiangiogenesis effect induced by endostatin and IL-12 in combination with an immune rejection induced by IL-12. On one hand, endostatin and IL-12, which were expressed locally in combination with increased serum levels after gene delivery mediated by plasmid with PVP, could inhibit angiogenesis of hepatoma synergistically. This was convinced by that MVD in pSecES+pmIL-12 group was much less than any single gene therapy group. But now the antiangiogenesis mechanism of endostatin and IL-12 was still not very clear. Through this way, H22 hepatoma cells came to apoptosis or necrosis due to lack of blood supply. On the other hand, more TILs (including activated CTL, NK, TH1 etc.) were observed in tumors that received IL-12 gene therapy or combined gene therapy, which maybe an indication of activated immune response on H22 hepatoma cells. Antitumor immune rejection induced by IL-12 through immunocytes or cytokines also promoted apoptosis of tumor cells. So there were much more apoptotic tumor cells in combined gene therapy group than any single one. Due to these factors, formation and growth of transplanted H22 hepatoma was prevented synergistically.

Combined gene therapies for liver cancer were also reported previously. Learners have focused on combined genes of two or three immunocytokines, or on suicide gene therapy in combination with genetic immunotherapy^[25,30,31,43]. Biotherapy in combination with chemotherapy for lymphoma was also studied^[44]. Before our reports, combined treatment with type 5 adenovirus vectors expressing murine angiostatin and IL-12 showed an antitumor effect on a murine breast cancer^[45]. Our report is the first to demonstrate the potent antitumor effect of combined gene therapy of endostatin and interleukin 12 with polyvinylpyrrolidone on hepatoma.

In conclusion, active target protein can be expressed by repeated local injections of plasmid with PVP. Through this way, a short-term course of combined gene therapy of endostatin and IL-12 can effectively prevent the formation and development of transplanted H22 hepatoma in mice. Antiangiogenic therapy in combination with immunotherapy may be used to regress or to eradicate other solid tumors.

ACKNOWLEDGEMENT

We thank Xiao-Yan Yang and Dong-Po Song for their expert technical assistance in animal experiments and Peng-Cheng Zhu for his help in histopathological analysis in this study.

REFERENCES

- 1 **Badvie S.** Hepatocellular carcinoma. *Postgrad Med J* 2000; **76**: 4-11
- 2 **Zibari GB,** Riche A, Zizzi HC, McMillan RW, Aultman DF, Boykin KN, Gonzalez E, Nandy I, Dies DF, Gholson CF, Holcombe RF, McDonald JC. Surgical and nonsurgical management of primary and metastatic liver tumors. *Am Surg* 1998; **64**: 211-220
- 3 **Okuda K.** Hepatocellular carcinoma. *J Hepatol* 2000; **32**(1 Suppl): 225-237
- 4 **Kamohara Y,** Kanematsu T. Treatment of liver cancer: current status and future prospectives. *Ganto Kagaku Ryoho* 2000; **27**: 987-992
- 5 **Sorokin P.** New agents and future directions in biotherapy. *Clin J Oncol Nurs* 2002; **6**: 19-24

- 6 **Zogakis TG**, Libutti SK. General aspects of anti-angiogenesis and cancer therapy. *Expert Opin Biol Ther* 2001; **1**: 253-275
- 7 **O'Reilly MS**, Boehm T, Shing Y, Fukai N, Vasios G, Lane WS, Flynn E, Birkhead JR, Olsen BR, Folkman J. Endostatin: an endogenous inhibitor of angiogenesis and tumor growth. *Cell* 1997; **88**: 277-285
- 8 **Huang X**, Wong MKK, Zhao Q, Zhu Z, Wang KZQ, Huang N, Ye C, Gorelik E, Li M. Soluble recombinant endostatin purified from *Escherichia coli*: antiangiogenic activity and antitumor effect. *Cancer Res* 2001; **61**: 478-481
- 9 **Sorensen DR**, Read TA, Porwol T, Olsen BR, Timpl R, Sasaki T, Iversen PO, Benestad HB, Sim BK, Bjerkvig R. Endostatin reduces vascularization, blood flow, and growth in a rat gliosarcoma. *Neuro Oncol* 2002; **4**: 1-8
- 10 **Boehm T**, Folkman J, Browder T, O'Reilly MS. Antiangiogenic therapy of experimental cancer does not induce acquired drug resistance. *Nature* 1997; **390**: 404-407
- 11 **Musiani P**, Modesti A, Giovarelli M, Cavallo F, Colombo MP, Lollini PL, Forni G. Cytokine, tumor-cell death and immunogenicity: a question of choice. *Immunol Today* 1997; **18**: 32-36
- 12 **Pham-Nguyen KB**, Yang W, Saxena R, Thung SN, Woo SL, Chen SH. Role of NK and T cells in IL-12-induced anti-tumor response against hepatic colon carcinoma. *Int J Cancer* 1999; **81**: 813-819
- 13 **Ruiz J**, Qian C, Drozdzik M, Prieto J. Gene therapy of viral hepatitis and hepatocellular carcinoma. *J Viral Hepat* 1999; **6**: 17-34
- 14 **Schmitz V**, Qian C, Ruiz J, Sangro B, Melero I, Mazzolini G, Narvaiza I, Prieto J. Gene therapy for liver diseases: recent strategies for treatment of viral hepatitis and liver malignancies. *Gut* 2002; **50**: 130-135
- 15 **Yao L**, Sgadari C, Furuke K, Bloom ET, Teruya-Feldstein J, Tosato G. Contribution of natural killer cells to inhibition of angiogenesis by interleukin-12. *Blood* 1999; **93**: 1612-1621
- 16 **Dhanabal M**, Ramchandran R, Volk R, Stillman IE, Lombardo M, Iruela-Arispe ML, Simons M, Sukhatme VP. Endostatin: yeast production, mutants, and antitumor effect in renal cell carcinoma. *Cancer Res* 1999; **59**: 189-197
- 17 **Leonard JP**, Sherman ML, Fisger GL, Buchanan LJ, Larsen G, Atkins MB, Sosman JA, Dutcher JP, Vogelzang NJ, Ryan JL. Effects of single-dose interleukin-12 exposure on interleukin-12-associated toxicity and interferon- γ production. *Blood* 1997; **90**: 2541-2548
- 18 **Lotze MT**, Zitvogel L, Campbell R, Robbins PD, Elder E, Haluszczak C, Martin D, Whiteside TL, Storkus WJ, Tahara H. Cytokine gene therapy of cancer using interleukin-12: murine and clinical trials. *Ann N Y Acad Sci* 1996; **795**: 440-454
- 19 **Peroulis I**, Jonas N, Saleh M. Antiangiogenic activity of endostatin inhibits c6 glioma growth. *Int J Cancer* 2002; **97**: 839-845
- 20 **Jin X**, Bookstein R, Wills K, Avanzini J, Tsai V, LaFace D, Terracina G, Shi B, Nielsen LL. Evaluation of endostatin antiangiogenesis gene therapy *in vitro* and *in vivo*. *Cancer Gene Ther* 2001; **8**: 982-989
- 21 **Li X**, Fu GF, Fan YR, Shi CF, Liu XJ, Xu GX, Wang JJ. Potent inhibition of angiogenesis and liver tumor growth by administration of an aerosol containing a transferrin-liposome-endostatin complex. *World J Gastroenterol* 2003; **9**: 262-266
- 22 **Wang X**, Liu FK, Li X, Li JS, Xu GX. Retrovirus-mediated gene transfer of human endostatin inhibits growth of human liver carcinoma cells SMMC7721 in nude mice. *World J Gastroenterol* 2002; **8**: 1045-1049
- 23 **Barajas M**, Mazzolini G, Genove G, Bilbao R, Narvaiza I, Schmitz V, Sangro B, Melero I, Qian C, Prieto J. Gene therapy of orthotopic hepatocellular carcinoma in rats using adenovirus coding for interleukin-12 (IL-12). *Hepatology* 2001; **33**: 52-61
- 24 **Zheng S**, Xiao ZX, Pan YL, Han MY, Dong Q. Continuous release of interleukin 12 from microencapsulated engineered cells for colon cancer therapy. *World J Gastroenterol* 2003; **9**: 951-955
- 25 **Oshikawa K**, Shi F, Rakhmievich AL, Sondel PM, Mahvi DM, Yang NS. Synergistic inhibition of tumor growth in a murine mammary adenocarcinoma model by combinational gene therapy using IL-12, pro-IL-18, and IL-1 β converting enzyme cDNA. *Proc Natl Acad Sci U S A* 1999; **96**: 13351-13356
- 26 **Weidner N**. Current pathologic methods for measuring intratumoral microvessel density within breast carcinoma and other solid tumors. *Breast Cancer Res Treat* 1995; **16**: 169-180
- 27 **Yamashita YI**, Shimada M, Hasegawa H, Minagawa R, Rikimaru T, Hamatsu T, Tanaka S, Shirabe K, Miyazaki JJ, Sugimachi K. Electroporation-mediated interleukin-12 gene therapy for hepatocellular carcinoma in the mice model. *Cancer Res* 2001; **61**: 1005-1012
- 28 **Cao Y**. Endogenous angiogenesis inhibitors and their therapeutic implications. *Int J Biochem Cell Biol* 2001; **33**: 357-369
- 29 **Ryan CJ**, Wilding G. Angiogenesis inhibitors. New agents in cancer therapy. *Drugs Aging* 2000; **17**: 249-255
- 30 **Wang Z**, Qiu SJ, Ye SL, Tang ZY, Xiao X. Combined IL-12 and GM-CSF gene therapy for murine hepatocellular carcinoma. *Cancer Gene Ther* 2001; **8**: 751-758
- 31 **Putzer BM**, Stiewe T, Rodicker F, Schildgen O, Ruhm S, Dirsch O, Fiedler M, Damen U, Tennant B, Scherer C, Graham FL, Roggendorf M. Large nontransplanted hepatocellular carcinoma in woodchucks: treatment with adenovirus-mediated delivery of interleukin 12/B7.1 genes. *J Natl Cancer Inst* 2001; **93**: 472-479
- 32 **Mundhenke C**, Thomas JP, Wilding G, Lee FT, Kelzc F, Chappell R, Neider R, Sebree LA, Friedl A. Tissue examination to monitor antiangiogenic therapy: a phase I clinical trial with endostatin. *Clin Cancer Res* 2001; **7**: 3366-3374
- 33 **Folkman J**, Watson K, Ingber D, Hanahan D. Induction of angiogenesis during the transition from hyperplasia to neoplasia. *Nature* 1989; **339**: 58-62
- 34 **Cavallaro U**, Christofori G. Molecular mechanisms of tumor angiogenesis and tumor progression. *J Neurooncol* 2000; **50**: 63-70
- 35 **Li PY**, Feng ZH, Zhang GM, Zhang H, Xue SL, Huang B, Lin JS. Inhibitory effect of recombinant endostatin on angiogenesis and tumor growth of hepatoma. *J Huazhong Univ Sci Tech [Med Sci]* 2003; **23**: 223-226
- 36 **Chen CT**, Lin J, Li Q, Phipps SS, Jakubczak JL, Stewart DA, Skripchenko Y, Forry-Schaudies S, Wood J, Schnell C, Hallenbeck PL. Antiangiogenic gene therapy for cancer via systemic administration of adenoviral vectors expressing secreted endostatin. *Hum Gene Ther* 2000; **11**: 1983-1996
- 37 **Yamaguchi N**, Anand-Apte B, Lee M, Sasaki T, Fukai N, Shapiro R, Que I, Lowik C, Timpl R, Olsen BR. Endostatin inhibits VEGF-induced endothelial cell migration and tumor growth independently of zinc binding. *EMBO J* 1999; **18**: 4414-4423
- 38 **Prince HM**. Gene transfer: A review of methods and applications. *Pathology* 1998; **30**: 335-347
- 39 **Mumper RJ**, Duguid JG, Anwer K, Barron MK, Nitta H, Rolland AP. Polyvinyl derivatives as novel interactive polymers for controlled gene delivery to muscle. *Pharm Res* 1996; **13**: 701-709
- 40 **Quezada A**, Horner MJ, Loera D, French M, Pericle F, Johnson R, Perrard J, Jenkins M, Coleman M. Safety toxicity study of plasmid-based IL-12 therapy in Cynomolgus monkeys. *J Pharm Pharmacol* 2002; **54**: 241-248
- 41 **Lai R**, Estey E, Shen Y, Despa S, Kantarjian H, Beran M, Maushouri T, Quackenbush RC, Keating M, Albitar M. Clinical significance of plasma endostatin in acute myeloid leukemia/myelodysplastic syndrome. *Cancer* 2002; **94**: 14-17
- 42 **Suzuki M**, Iizasa T, Ko E, Baba M, Saitoh Y, Shibuya K, Sekine Y, Yoshida S, Hiroshima K, Fujisawa T. Serum endostatin correlates with progression and prognosis of non-small cell lung cancer. *Lung Cancer* 2002; **35**: 29-34
- 43 **Sakai Y**, Kaneko S, Nakamoto Y, Kagaya T, Mukaida N, Kobayashi K. Enhanced anti-tumor effects of herpes simplex virus thymidine kinase/ganciclovir system by codelivering monocyte chemoattractant protein-1 in hepatocellular carcinoma. *Cancer Gene Ther* 2001; **8**: 695-704
- 44 **Bertolini F**, Fusetti L, Mancuso P, Gobbi A, Corsini C, Ferrucci PF, Martinelli G, Pruneri G. Endostatin, an antiangiogenic drug, induces tumor stabilization after chemotherapy or anti-CD20 therapy in a NOD/SCID mouse model of human high-grade non-Hodgkin lymphoma. *Blood* 2000; **96**: 282-287
- 45 **Gyorffy S**, Palmer K, Podor TJ, Hitt M, Gaudie J. Combined treatment of a murine breast cancer model with type 5 adenovirus vectors expressing murine angiostatin and IL-12: a role for combined anti-angiogenesis and immunotherapy. *J Immunol* 2001; **166**: 6212-6217

Analysis of clinical effect of high-intensity focused ultrasound on liver cancer

Chuan-Xing Li, Guo-Liang Xu, Zhen-You Jiang, Jian-Jun Li, Guang-Yu Luo, Hong-Bo Shan, Rong Zhang, Yin Li

Chuan-Xing Li, Guo-Liang Xu, Jian-Jun Li, Guang-Yu Luo, Hong-Bo Shan, Rong Zhang, Yin Li, Department of HIFU, Cancer Center, Sun Yat-sen University, Guangzhou 510060, Guangdong Province, China

Zhen-You Jiang, Medical College, Jinan University, Guangzhou 510632, Guangdong Province, China

Correspondence to: Chuan-Xing Li, Department of HIFU, Cancer Center, Sun Yat-sen University, Guangzhou 510060, Guangdong Province, China. lichx@163.net

Telephone: +86-20-87343381 **Fax:** +86-20-87342737

Received: 2003-12-10 **Accepted:** 2004-01-15

Abstract

AIM: To evaluate the clinical effect of high-intensity focused ultrasound (HIFU) in the treatment of patients with liver cancer.

METHODS: HIFU treatment was performed in 100 patients with liver cancer under general anesthesia and by a targeted ultrasound. Evaluation of efficacy was made on the basis of clinical symptoms, liver function tests, AFP, MRI or CT before and after the treatment.

RESULTS: After HIFU treatment, clinical symptoms were relieved in 86.6%(71/82) of patients. The ascites disappeared in 6 patients. ALT (95±44) U/L and AST (114±58) U/L before HIFU treatment were reduced to normal in 83.3%(30/36) and 72.9%(35/48) patients, respectively, after the treatment. AFP was lowered by more than 50% in 65.3%(32/49) patients. After HIFU treatment, MRI or CT findings indicated coagulation necrosis and blood supply reduction or disappearance of tumor in the target region.

CONCLUSION: HIFU can efficiently treat the patients with liver cancer. It will offer a significant noninvasive therapy for local treatment of liver tumor.

Li CX, Xu GL, Jiang ZY, Li JJ, Luo GY, Shan HB, Zhang R, Li Y. Analysis of clinical effect of high-intensity focused ultrasound on liver cancer. *World J Gastroenterol* 2004; 10(15): 2201-2204

<http://www.wjgnet.com/1007-9327/10/2201.asp>

INTRODUCTION

Since 1942, Lynn *et al.*^[1] firstly brought forward the conception of HIFU, i.e. high intensity focused ultrasound. Fry^[2] applied HIFU technology to experimentally treat nervous system diseases, and suggested the potential of HIFU in surgical operations. As a result, he found that ultrasound beam could form a preferable focal field at a special depth inside body, and destroy target tissue through focus pointing without damaging neighboring tissues. In 1956, Burov proposed that effect of short-time high-intensity ultrasound irradiation was better than low-intensity ultrasound. With research progress on HIFU technology, this technology has been used in clinic over the

years^[3-6]. The present study makes an assessment on clinic effect of HIFU in treating liver cancer.

MATERIALS AND METHODS

Materials

We performed HIFU treatments in 100 patients (80 male, 20 female, ranging 30-74 years with mean age of 56 years) with liver cancer from July 2001 to July 2003, totally 130 HIFU treatments, 1.30 times per patient. Patients included 62 primary liver cancers and 38 metastatic liver cancers. Sixty-eight patients were with single nodule, 22 with two nodules, 10 with three nodules. Totally 36 tumor nodules with a diameter less than 5 cm, 76 with a diameter between 5-10 cm, 30 with a diameter more than 10 cm were involved. All cases were investigated and verified by pathohistology or an obvious increase of serum AFP and positive imaging, and conformed to diagnostic standard of National Cooperation Conference and Hepatic Carcinoma Prevention and Treatment in 1997. Eighteen patients were in stage I, 48 patients in stage II, and 34 patients in stage III.

Instrument

JC type focused ultrasound tumor therapeutic system was designed by Chongqing HIFU Technology Co, Ltd. Chongqing, China. It includes two main parts, i.e. ultrasound real-time orientation monitor device and HIFU three-dimensional combination scanning therapeutic device. Under the control of a computer, it can orient to preassigned tumor target zone automatically, determine range of therapy.

The main parameters included therapy frequency 0.8 MHz, mean diameter of focal field 1.1 mm, length of focal field 9.8 mm, focus distance 135 mm, therapy power 140-240 W.

Methods

Routine examinations and preoperative preparation were conducted according to the principle of surgery. Based on the result of image and ultrasound examination, the therapeutic scheme of HIFU was constituted. HIFU treatment was performed with patient fixed properly. The tumor position and size, therapeutic layers and therapeutic range of every layer were determined by ultrasound diagnostic probe. Then the therapeutic probe treated tumor tissue of every layer from outside body, and in terms of order of layer, from spot to line, and from line to area, leading whole tumor to coagulation necrosis. During the therapeutic process, through changes of graphics of target field and echo of tissue between before and after therapy at every layer, real-time estimate of HIFU therapeutic effect by computer processing image system was carried out, and with feedback, ultrasound therapeutic dosage estimated in the therapy scheme was controlled according to changes of ultrasound photograph. The therapeutic method was divided into complete coverage and local coverage. Twenty-eight cases used complete coverage, including whole tumor focus and normal liver tissue within 2 cm away from edge of tumor, the other cases used local coverage due to reasons, such as large tumor volume, rib overlap or close-by, or involvement of liver tube or cholecyst, *etc.*

Observatory parameters

The following aspects were observed: Improvement of clinic symptoms; changes of liver function 2 d and 2 wk before and after therapy; changes of AFP 2 wk before and after therapy; changes in range and blood supply of coagulation necrosis of tumor focus, also shrink of tumor through re-examination of MRI or CT before and after therapy.

RESULTS

One hundred liver cancer patients were treated by using HIFU in this group, of which 82 exhibited clinic symptoms. Seventy-one patients were improved obviously after HIFU treatment: appetite increased, weight gained, discomfort or pain on liver region relieved. Remission rate for symptoms was 86.6% (71/82). For 6 patients who had had mild ascites, ascites disappeared after HIFU treatment. For patients with abnormal liver function

(ALT 95 ± 44 U/L, AST 114 ± 58 U/L), 2 d after HIFU treatment, liver enzymes rose slightly, but no obvious statistic difference was found compared with pre-treatment. The patients' liver enzymes fell to normal level after 2 wk, respectively, ALT 83.3% (30/36), AST 72.9% (35/48). For the patients whose AFP was increased, AFP was 50% less than original level 2 wk after HIFU treatment, in 65.3% (32/49), only one patient's AFP rose continuously after HIFU treatment, and multi-bone metastases were found by ECT examination. Self-comparison of MRI showed that T₁-weighted images and T₂-weighted images of tumor therapeutic region were high signal and low signal respectively after HIFU treatment. Enhanced MRI did not show enhanced signal, indicating that coagulation necrosis had occurred in the tumor therapeutic region, blood supply of tumor was diminished or eliminated, tumor of some patients had shrunk obviously after countercheck MRI (Figures 1-3).

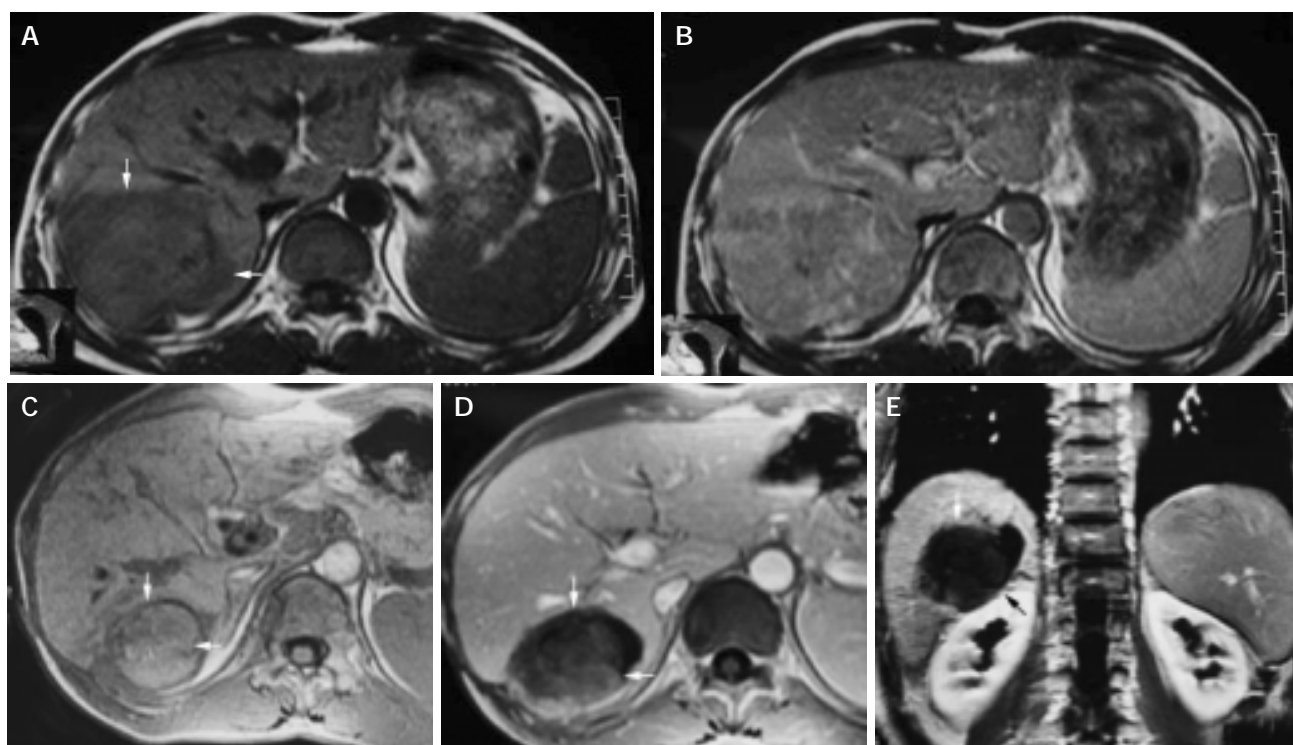


Figure 1 A 42-year-old male with hepatocellular carcinoma. A: MRI T₁-weighted images before HIFU treatment showed that liver tumor of right-posterior lobe was 115 mm×100 mm×66 mm; B: MRI enhanced imaging before HIFU revealed that enhancement of mass in liver right-posterior lobe was higher than that of surrounding normal liver tissues; C: MRI T₁-weighted imaging 11 mo after HIFU revealed that liver tumor of right-posterior lobe obviously decreased in size (50 mm×55 mm×60 mm); D, E: MRI enhanced imaging (cross section and coronal section) 11 mo after HIFU revealed that liver tumor had shrunk obviously, blood supply of tumor was eliminated, the tumor therapeutic region had coagulation necrosis.

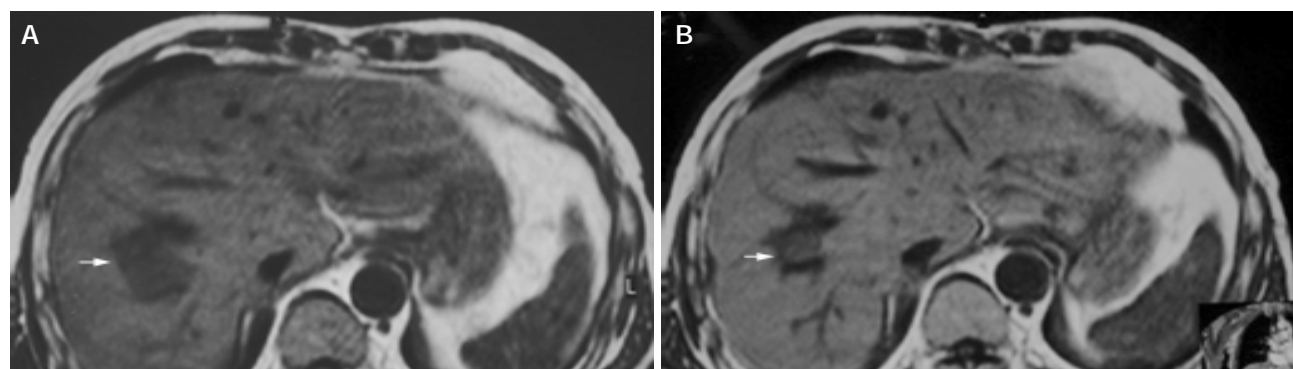


Figure 2 A 55-year-old man with metastatic hepatocarcinoma in sigmoid cancer postoperation. A: MRI images before HIFU treatment showed that liver tumor of right-posterior lobe was 40 mm×30 mm×30 mm; B: MRI images 2 wk after HIFU revealed that liver tumor of right-posterior lobe obviously decreased in size (20 mm×20 mm×15 mm).

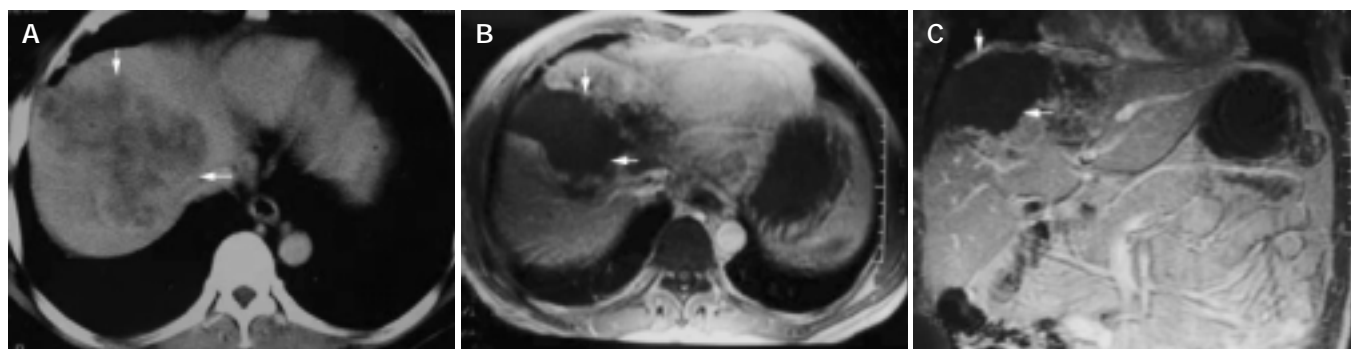


Figure 3 A 54-year-old man with primary carcinoma of liver in right lobe. A: CT enhanced imaging before HIFU treatment revealed that enhancement of mass in liver right-posterior lobe was higher than that of surrounding normal liver tissues (AFP: 5516 $\mu\text{g/L}$); B, C: MRI enhanced imaging (cross section and coronal section) 2 mo after HIFU revealed that necrotic tissue in the therapeutic region of the tumor was not enhanced (AFP: 183 $\mu\text{g/L}$).

DISCUSSION

HIFU is a high-tech developed successfully in the 1990's, a local way of treating tumor without any damages. It utilizes the physics characteristics of ultrasound beam with assemble and penetration, to focus low energy outside body on inner tumor target field, through instantaneous high temperature effect, cavitate effect, making tumor target tissue of focal zone coagulation necrosis, without destroying surrounding tissues^[7-14].

HIFU has the following characteristics in therapy of malignant tumors. Firstly, noninvasiveness. HIFU treats inner tumor without damaging outside body. Previous research on animal angiography indicated that after treating liver tumor of Morris rat using HIFU, nourishing blood vessels which diameter was less than 200 μm of irradiation zone closed, but they were normal for blood vessels which diameter was more than 200 μm ^[15]. Secondly, accuracy. HIFU can pass through tissues and accurately damage target tissues inside organisms. The boundary between therapy zone and un-therapy zone is clear, tissue beyond target zone is hardly destroyed or without damage^[16,17]. Ultrasound Therapy Section of London Emperor Hospital, Britain found that only six cells existed between cells killed completely and cells without damage^[18]. Thirdly, real-time therapy. For whole process of therapy, it is a real-time targeting and monitoring process, real-time estimating therapeutic effect and adjusting dosage^[19]. Fourthly, suitable therapy. According to the size and shape of tumor, it determines therapy range of tumor target zone, overlays tumor target zone. Therefore, treatment of malignant tumor using HIFU has many advantages such as less pain, no damage, fewer influences on splanchnic function, faster recovery for body and no increase of tumor metastasis chance^[20], *etc.*

It is shown that in this research, 100 liver cancer patients had obvious improvement in symptoms and signs after being treated by using HIFU. Short-term effect of HIFU therapy was obvious and affirmative in liver cancer. But for liver cancer patients who had huge block or multifocal big nodules, to make tumor completely occur coagulation necrosis, to gain the purpose of "ablation" tumor integrity, we performed treatment for two or three times. Firstly, we treated deeper tumor parts, to induce coagulation necrosis of the tumor, so as to make it easy to treat remaining superficial parts next time. Conversely, if at first, it makes superficial parts occur coagulation necrosis, and then treats deep tumor tissue, because of change of the impedance dispersion and absorb coefficient of sound, the attenuation of penetrating tissue with ultrasound will aggravate. Meanwhile, focus energy in focal field can not reach ideal degree, as a result it takes more time to make tumor tissue coagulation necrosis.

If tumor locates on the edge of liver with poor blood supply, during therapy of HIFU, We estimate every therapeutic effect by using real-time ultrasound imaging to monitor the change of

gray value. If gray value is changed, it indicates that tumor tissue must occur coagulation necrosis. However, tissues with coagulation necrosis do not always exhibit changes of gray value. For tumor in deep part, during real-time monitor, most changes of gray value are not distinct or lightly increased with suffusion. Through quantitative analysis and comparison of gray value of ultrasound imaging before and after therapy, we can find that the difference of gray rank before and after therapy is obvious. This indicates that local tumor tissues have no reversible coagulation necrosis.

For liver cancer patients with abundant blood supply relatively, we should first perform transcatheter arterial chemoembolization before using HIFU, so as to make inner tumor tissue have more iodised oil deposition, which not only is convenient to ultrasound orientation, but also changes the impedance dispersion and absorb coefficient of sound of tumor zone. Accordingly, it is convenient to energy sediment of focal zone, exerts cooperative function of raising temperature, excites high temperature to get to purpose of destruct therapy at local and makes tumor tissue coagulation necrosis^[21,22].

Yang *et al.*^[15] used HIFU to treat Morris rat hepatoma implanted in the liver. Treatment was administered with a lens-focused 4-MHz transducer that created a focused beam of 550 W/cm^2 at peak intensity. One hundred and twelve rats with liver tumors were divided into two groups of 56 each. Group 1 received HIFU therapy while group 2 (the control group) did not. All rats were killed immediately or 1, 3, 7, 14, 21, 28 d after treatment. Eight rats in each group were killed at each interval for pathologic and biochemical studies. Significant inhibition of the tumor growth was seen in the HIFU-treated group, with tumor growth inhibition rates of 65.4-93.1% from on d 3 to 28 after treatment. Ultrasound-treated tumors showed direct thermal cytotoxic necrosis and fibrosis. An additional 56 ACl rats with liver tumors were divided into 4 groups of 14 each. Group 1 received doxorubicin hydrochloride intraperitoneally and HIFU therapy; group 2, HIFU therapy; group 3, doxorubicin hydrochloride; and group 4 (the control group), neither HIFU nor doxorubicin hydrochloride. Significantly improved survival rates were noted in HIFU-treated animals (groups 1 and 2) compared with those of groups 3 and 4.

Research results of home and abroad using animals showed that HIFU can safely and effectively destroy inner liver tissue or liver transplant tumor^[23-30]. Clinic results showed that HIFU can also treat liver cancer securely and effectively^[11,31,32].

HIFU is a new method with definite therapeutic effect on tumor without damage and poisonous to normal tissues. With improvement of HIFU technology, accumulation of clinic application experience and further research on mechanism of HIFU, HIFU, as a new local therapy, would be applied more extensively to treat liver cancer.

REFERENCES

- 1 **Lynn JG**, Putnam TJ. Histological and cerebral lesions produced by focused ultrasound. *Am J Pathol* 1944; **20**: 637-649
- 2 **Fry WJ**, Fry FJ. Fundamental neurological research and human neurosurgery using intense ultrasound. *IRE Trans Med Electron* 1960; **7**: 166-181
- 3 **Chen W**, Wang Z, Wu F, Bai J, Zhu H, Zou J, Li K, Xie F, Wang Z. High intensity focused ultrasound alone for malignant solid tumors. *Zhonghua Zhongliu Zazhi* 2002; **24**: 278-281
- 4 **Wu F**, Chen WZ, Bai J, Zou JZ, Wang ZL, Zhu H, Wang ZB. Tumor vessel destruction resulting from high-intensity focused ultrasound in patients with solid malignancies. *Ultrasound Med Biol* 2002; **28**: 535-542
- 5 **Yang R**, Sanghvi NT, Rescorla FJ, Kopecky KK, Grosfeld JL. Liver cancer ablation with extracorporeal high-intensity focused ultrasound. *Eur Urol* 1993; **23**: 17-22
- 6 **Kennedy JE**, Ter Haar GR, Cranston D. High intensity focused ultrasound: surgery of the future? *Br J Radiol* 2003; **76**: 590-599
- 7 **Ter Haar GR**. High intensity focused ultrasound for the treatment of tumors. *Echocardiography* 2001; **18**: 317-322
- 8 **Paek BW**, Vaezy S, Fujimoto V, Bailey M, Albanese CT, Harrison MR, Farmer DL. Tissue ablation using high-intensity focused ultrasound in the fetal sheep model: potential for fetal treatment. *American J Obstetrics Gynecol* 2003; **189**: 702-705
- 9 **Wang Z**, Bai J, Li F, Du Y, Wen S, Hu K, Xu G, Ma P, Yin N, Chen W, Wu F, Feng R. Study of a "biological focal region" of high-intensity focused ultrasound. *Ultrasound Med Biol* 2003; **29**: 749-754
- 10 **Ter Haar G**. High intensity ultrasound. *Semin Laparosc Surg* 2001; **8**: 77-89
- 11 **Wu F**, Chen WZ, Bai J, Zou JZ, Wang ZL, Zhu H, Wang ZB. Pathological changes in human malignant carcinoma treated with high-intensity focused ultrasound. *Ultrasound Med Biol* 2001; **27**: 1099-1106
- 12 **Bailey MR**, Couret LN, Sapozhnikov OA, Khokhlova VA, Ter Haar G, Vaezy S, Shi X, Martin R, Crum LA. Use of overpressure to assess the role of bubbles in focused ultrasound lesion shape *in vitro*. *Ultrasound Med Biol* 2001; **27**: 695-708
- 13 **Prat F**, Ponchon T, Berger F, Chapelon JY, Gagnon P, Cathignol D. Hepatic lesions in the rabbit induced by acoustic cavitation. *Gastroenterology* 1991; **100**(5 Pt 1): 1345-1350
- 14 **Huo YM**, Chen YZ. Comparative study of ultrasound transducers in HIFU. *Zhongguo Yaoli Xuebao* 2000; **24**: 97-101
- 15 **Yang R**, Reilly CR, Rescorla FJ, Fauht PR, Sanahvi NT, Frv FJ, Franklin TD Jr, Lumena L, Grosfeld JL. High-intensity focused ultrasound in the treatment of experimental liver cancer. *Arch Surg* 1991; **126**: 1002-1009
- 16 **Wang ZB**, Wu F, Wang ZL, Zhang Z, Zou JZ, Liu C, Liu YG, Cheng G, Du YH, He ZC, Gu ML, Wang ZG, Feng R. Targeted damage effects of high intensity focused ultrasound (HIFU) on liver tissues of Guizhou Province miniswine. *Ultrason Sonochem* 1997; **4**: 181-182
- 17 **Yang R**, Sanghvi NT, Rescorla FJ, Galliani CA, Fry FJ, Griffith SL, Grosfeld JL. Extracorporeal liver ablation using sonography-guided high-intensity focused ultrasound. *Invest Radiol* 1992; **27**: 796-803
- 18 **Dorr LN**, Hynynen K. The effects of tissue heterogeneities and large blood vessels on the thermal exposure induced by short high-power ultrasound pulses. *Int J Hyperthermia* 1992; **8**: 45-59
- 19 **Vaezy S**, Shi X, Martin RW, Chi E, Nelson PI, Bailey MR, Crum LA. Real-time visualization of high-intensity focused ultrasound treatment using ultrasound imaging. *Ultrasound Med Biol* 2001; **27**: 33-42
- 20 **Oosterhof GO**, Conel EB, Smits GA, Debryne FM, Schalken JA. Influence of high-intensity focused ultrasound on the development of metastases. *Eur Urol* 1997; **32**: 91-95
- 21 **Jin CB**, Wu F, Wang ZB, Chen WZ, Zhu H. High intensity focused ultrasound therapy combined with transcatheter arterial chemoembolization for advanced hepatocellular carcinoma. *Zhonghua Zhongliu Zazhi* 2003; **25**: 401-403
- 22 **Zhao J**, Wang Z, Guo D, Yu C, Xie W, Li G. CT appearance and its diagnosis value in liver cancer after transcatheter oily chemoembolization combining with high intensity focused ultrasound therapy. *Zhonghua Ganzangbing Zazhi* 2001; **9**: 61-63
- 23 **Sibille A**, Prat F, Chapelon JY, abou el Fadil F, Henry L, Theilliere Y, Ponchon T, Cathignol D. Characterization of extracorporeal ablation of normal and tumor-bearing liver tissue by high intensity focused ultrasound. *Ultrasound Med Biol* 1993; **19**: 803-813
- 24 **Adams JB**, Moore RG, Anderson JH, Strandberg JD, Marshall FF, Davoussi LR. High-intensity focused ultrasound ablation of rabbit kidney tumors. *J Endourol* 1996; **10**: 71-75
- 25 **Sibille A**, Prat F, Chapelon JY, Abou-el-Fadil F, Henry L, Theilliere Y, Ponchon T, Cathignol D. Extracorporeal ablation of liver tissue by high-intensity focused ultrasound. *Oncology* 1993; **50**: 375-379
- 26 **Righetti R**, Kallel F, Stafford RJ, Price RE, Krouskop TA, Hazle JD, Ophir J. Elastographic characterization of HIFU-induced lesions in canine livers. *Ultrasound Med Biol* 1999; **25**: 1099-1113
- 27 **Gignoux BM**, Scoazec JY, Curiel L, Beziat C, Chapelon JY. High intensity focused ultrasonic destruction of hepatic parenchyma. *Ann Chir* 2003; **128**: 18-25
- 28 **Yang R**, Kopecky KK, Rescorla FJ, Galliani CA, Wu EX, Grosfeld JL. Sonographic and computed tomography characteristics of liver ablation lesions induced by high-intensity focussed ultrasound. *Invest Radiol* 1993; **28**: 796-801
- 29 **Cheng SQ**, Zhou XD, Tang ZY, Yu Y, Wang HZ, Bao SS, Qian DC. High-intensity focused ultrasound in the treatment of experimental liver tumour. *J Cancer Res Clinical Oncol* 1997; **123**: 219-223
- 30 **Ishikawa T**, Okai T, Sasaki K, Umemura S, Fujiwara R, Kushima M, Ichihara M, Ichizuka K. Functional and histological changes in rat femoral arteries by HIFU exposure. *Ultrasound Med Biol* 2003; **29**: 1471-1477
- 31 **Li CX**, Xu GL, Li JJ, Luo GY. High intensity focused ultrasound for liver cancer. *Zhonghua Zhongliu Zazhi* 2003; **25**: 94-96
- 32 **Wu F**, Wang Z, Chen W. Pathological study of extracorporeally ablated hepatocellular carcinoma with high-intensity focused ultrasound. *Zhonghua Zhongliu Zazhi* 2001; **23**: 237-239

Edited by Zhu LH and Chen WW Proofread by Xu FM

Honokiol induces apoptosis through p53-independent pathway in human colorectal cell line RKO

Tao Wang, Fei Chen, Zhe Chen, Yi-Feng Wu, Xiao-Li Xu, Shu Zheng, Xun Hu

Tao Wang, Fei Chen, Zhe Chen, Xiao-Li Xu, Shu Zheng, Xun Hu, Cancer Institute, Second Hospital of Medicine College of Zhejiang University, Hangzhou 310009, Zhejiang Province, China

Yi-Feng Wu, Life Science College of Zhejiang University, Hangzhou 310009, Zhejiang Province, China

Supported by the Cheung Kong Scholars Program, National Ministry of Education of China, and Li Ka Shing Foundation, Hong Kong

Co-first-authors: Tao Wang and Fei Chen

Correspondence to: Professor Xun Hu, Cancer Institute Second Hospital of Medicine College of Zhejiang University, Hangzhou 310009, Zhejiang Province, China. huxun@zju.edu.cn

Telephone: +86-571-87783868 **Fax:** +86-571-87214404

Received: 2004-02-21 **Accepted:** 2004-03-12

Abstract

AIM: To investigate the signal pathway of honokiol-induced apoptosis on human colorectal carcinoma RKO cells and to evaluate whether p53 and p53-related genes were involved in honokiol-treated RKO cells.

METHODS: Cell cycle distribution and subdiploid peak were analyzed with a flow cytometer and DNA fragment with electrophoresis on agarose gels. Transcriptional level of Bax, Bcl-2, Bid and Bcl-xl was accessed by RT-PCR. Western blotting was used to measure p53 protein expression and other factors related to apoptosis. Proliferation inhibition of two cell lines (RKO, SW480) with high expression of p53 and one cell line with p53 negative expression (LS180) was monitored by MTT assay.

RESULTS: Honokiol induced RKO cell apoptosis in a dose-dependent manner. The mRNA expression level and protein level of Bid were up-regulated while that of Bcl-xl was down-regulated, but no changes in Bax and Bcl-2 were observed. Western blotting showed p53 expression had no remarkable changes in honokiol-induced RKO cell apoptosis. LS180 cells treated with honokiol exhibited apparent growth inhibition like RKO cells and Sw480 cells.

CONCLUSION: Honokiol can induce RKO cells apoptosis through activating caspase cascade by p53-independent pathway.

Wang T, Chen F, Chen Z, Wu YF, Xu XL, Zheng S, Hu X. Honokiol induces apoptosis through p53-independent pathway in human colorectal cell line RKO. *World J Gastroenterol* 2004; 10(15): 2205-2208

<http://www.wjgnet.com/1007-9327/10/2205.asp>

INTRODUCTION

Honokiol is a major active constituent extracted from the bark of *Magnolia officianlis* (Chinese name for *Houpu*) (Figure 1). It has a variety of pharmacological effects, such as anti-inflammatory^[1], antithrombosis^[2], anti-arrhythmic^[3], antioxidant^[4] and anxiolytic effects^[5]. Recently, honokiol has been reported to exhibit a

potent cytotoxic activity by inducing cell apoptosis in some cell lines^[6-8]. Honokiol-triggered apoptotic process is accompanied with down-modulation of Bcl-XL, release of mitochondrial cytochrome C in CH27 cells^[9].

Cells undergoing apoptosis are characterized by distinct biochemical and morphological changes. Many of the biochemical and morphological events of apoptosis are a direct result of caspase-mediated cleavage of specific substrates^[10,11]. Together with caspase, Bcl-2 family is involved in inducing cell apoptosis and identified as essential components of the intracellular apoptotic signaling pathways. Cell viability versus death is determined by the relative abundance of various members of the Bcl-2 family, acting in concert with other proteins in the death pathway^[12,13].

In many tumor cells, wild-type p53 is considered to participate in apoptosis in response to DNA damage^[14]. P53 may transactivate apoptotic regulators, such as Bcl-2^[15-17] and Bax^[18,19]. Recent studies have shown that p53 plays a role in apoptosis by the mitochondrial-mediated apoptotic pathway^[20]. Activation of p53 upregulates Bax^[19] and increases the ratio of Bax:Bcl-2, releases cytochrome C and other polypeptides from the intermembrane space of mitochondria into cytoplasm. Cytochrome C activates caspase cascade^[12,13].

It is well known that a broad range of agents can induce tumor cell apoptosis through p53-regulated manner by Bax/mitochondria/caspase-9 pathway. But up to now, it is not clear that whether wild-type p53 takes part in honokiol-induced apoptosis. In this present study we examined whether wild-type p53 and p53-related gene were involved in honokiol-treated RKO cells.

MATERIALS AND METHODS

Materials

RPMI 1640 medium was obtained from Gibco BRL. Newborn bovine serum was supplied by Sijiqing Biotechnology Co. (Hangzhou, China). Monoclonal antibodies to Bax, Bcl-xl, Bid, Bcl-2, β -actin and p53 were purchased from NeoMarkers, Fremont, CA, USA. Honokiol was got from the National Institute for Pharmaceutical and Biological Products, Beijing, China. The drug was dissolved in DMSO with the stock concentration of 10 mg/mL. It was further diluted in culture medium with the final DMSO concentration <1%. 3-(4, 5-dimethylthiazol-2-yl)-2, 5-diphenyltetrazolium bromide (MTT) and propidium iodide (PI) were purchased from Sigma Chemical Corporation, USA.

Cell culture

Human colorectal cell lines RKO, SW480 and LS180 were provided by Cancer Institute of Zhejiang University. Three cells were maintained in RPMI 1640 medium (Gibco BRL) supplemented with 100 mL/L heat-inactivated fetal bovine serum (Si-Ji-Qing Biotechnology Co, Hangzhou, China), 100 U/mL penicillin and 100 μ g/mL streptomycin at 37 °C in a 50 mL/L CO₂ atmosphere.

Detection of DNA fragmentation

To detect DNA fragments, RKO cells were collected and lysed with lysis buffer containing 50 mmol/L Tris-HCl (pH 7.5),

20 mmol/L EDTA, and 10 g/L NP-40. Then 10 g/L SDS and RNase (5 µg/mL) were added to the supernatants, and incubated at 56 °C for 2 h, followed by incubation with proteinase K (2.5 µg/mL) at 37 °C for 2 h. After DNA was precipitated by addition of both ammonium acetate (3.3 mol/L) and ethanol (995 mL/L) dissolved in a loading buffer, DNA fragmentation was detected by electrophoresis on 15 g/L agarose gels and visualized with ethidium bromide staining.

Cell cycle analysis by FCM

Honokiol-treated RKO cells (5, 10, 15 µg/mL) and vehicle were fixed with 700 mL/L alcohol for 15 min at 4 °C, then stained with 1.0 µg/mL propidium iodide (PI, Sigma, USA). The red fluorescence of DNA-bound PI in individual cells was measured at 488 nm with a FACSCalibur (Becton Dickinson, USA) and the results were analyzed using ModFit 3.0 software. Ten thousand events were analyzed for each sample.

RT-PCR assay

RKO cells 1×10^5 were seeded on 24-well plate. After 24-h culture, cells were treated with 5, 10 µg/mL honokiol and vehicle for 48 h. Total RNA from RKO cells was extracted using Trizol (Invitrogen, USA). In RT-PCR, cDNA synthesis was performed using a RNA PCR kit (TaKaRa Biomedicals, Osaka, Japan) with the supplied oligo dT primer (Table 1). Reverse transcription was performed using a thermal program of 92 °C for 2 min, then 38 cycles of annealing for 30 s at 55 °C, extension for 90 s at 72 °C. As an internal control, semiquantitative analysis of β-actin was also amplified. This primer pair of β-actin had an optimal annealing temperature of 55 °C with 20 cycles and yielded a 350-bp PCR product. Samples were separated on 20 g/L agarose gel and visualized with ethidium bromide staining under UV light.

Western blotting

RKO cells (5×10^6) treated with 5, 10 µg/mL honokiol and vehicle respectively for 24 h were lysed by 4 g/L trypsin containing 0.2 g/L EDTA, then collected after washed twice with phosphate-buffered saline (PBS, pH 7.4). Total protein extract from RKO cells was prepared using cell lysis buffer [150 mmol/L NaCl, 0.5 mol/L Tris-HCl (pH 7.2), 0.25 mol/L EDTA (pH 8.0), 10 g/L Triton X-100, 50 mL/L glycerol, 12.5 g/L SDS]. The extract (30 µg) was electrophoresed on 12 g/L SDS-PAGE and electroblotted onto polyvinylidene difluoride membrane (PVDF, Millipore Corp., Bedford, MA) for 2 h in a buffer containing 25 mmol/L Tris-HCl (pH 8.3), 192 mmol/L glycine and 200 mL/L methanol. The blots were blocked with 50 g/L nonfat milk in TBST washing buffer for 2 h at room temperature and then incubated at 4 °C overnight with antibodies. All antibodies were diluted in TBST according to the manufacturer's instructions. After washed at room temperature with washing buffer, the blots were labeled with peroxidase-conjugated secondary antibodies.

Cell proliferation assay

RKO cells, SW480 and LS180 cells (1×10^4 in 100 µL) were seeded on 96-well plates in triplicate respectively. Following a 24-h culture at 37 °C, the medium was replaced with fresh medium containing vehicle control or various concentrations of honokiol

in a final volume of 200 µL. Cells were incubated at 37 °C for 68 h. Then 50 µL of MTT (2 mg/mL in PBS) was added to each well, incubated for an additional 4 h, the plate was centrifuged at 1 000 r/min for 10 min, then the medium was removed. The MTT formazan precipitate was dissolved in 100 µL DMSO, shaken mechanically for 10 min and then read immediately at 570 nm by a plate reader (Opsys MR, Denex Technology, USA).

Statistics

Statistical significance was determined by Student's *t*-test. A *P* value of 0.05 or less was considered significant.

RESULTS

DNA fragmentation detection in RKO cells

In honokiol-treated RKO cells, a degradation of chromosomal DNA into small internucleosomal fragments was evidenced by the formation of 180-200 bp DNA ladder on agarose gels (Figure 2), hallmark of cells undergoing apoptosis. No DNA ladders were detected in the samples isolated from control cultures. These results indicated that honokiol induced an apoptotic cell death in RKO cells

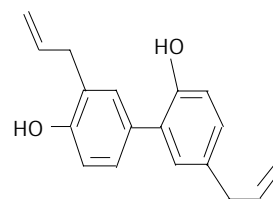


Figure 1 Chemical structure of honokiol (C₁₈H₁₈O₂, M_r 266.33).

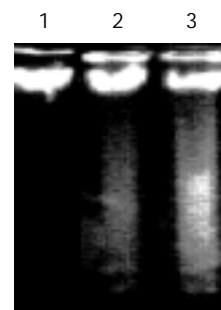


Figure 2 Differences in vehicle and honokiol induced apoptotic DNA laddering of RKO cells. Lane 1: Vehicle; Lane 2: 5 µg/mL; Lane 3: 10 µg/mL.

Effect of honokiol on cell cycle phase distribution

RKO cells were exposed to the increased concentrations of honokiol (5-15 µg/mL) for 48 h, and the cell growth was analyzed using flow cytometry. In the absence of honokiol, the cell populations were at G₁, S, and G₂/M phases (Figure 3), accompanied with increased concentrations of honokiol by a concomitant increase of the G₁ phase (Table 2). From Figure 3, we considered the peak areas of subdiploid were up at the

Table 1 Expected size of PCR amplification product with each apoptosis modulator primer pair

Apoptosis modulator	Upstream primer (5'-3')	Downstream primer (5'-3')	Size (bp)
Bax	ACCAAGAAGCTGAGCGAGTGT	ACAAACATGGTCACGGTCTGC	332
Bcl-xl	GGAGCTGGTGGTTGACTTTCT	CCGGAAGAGTTCATTCACTAC	379
Bid	GAC CCG GTG CCT CAG GA	ATG GTC ACG GTC TGC CA	586
Bcl-2	TTGTGGCCTTCTTTGAGTTCG	TACTGCTTAGTGAACCTTTT	332
β-actin	AGGCCAACC GCGAGAAGATGACC	GAAGTCCAGGGCGACGTAGCAC	350

increased concentrations of honokiol. This observation led to a suggestion of G1 arrest. When the cells were exposed to honokiol at 10 $\mu\text{g}/\text{mL}$ and above, subdiploid peak was significantly increased and the percentage of apoptotic cells in 10 000 cells was 14.1% and 20.31% respectively (Table 2).

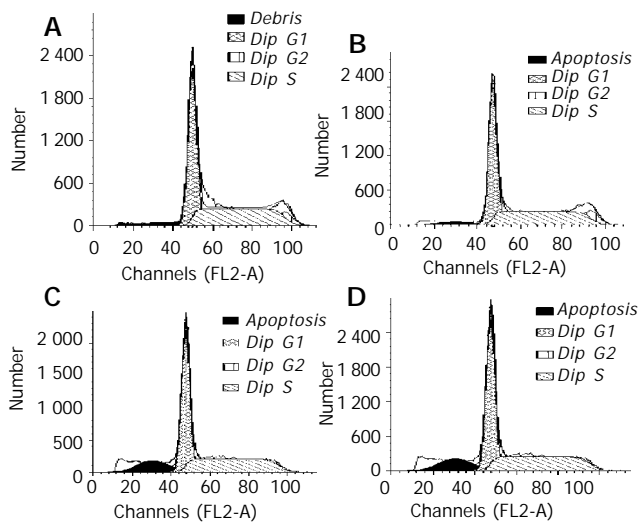


Figure 3 Apoptosis of RKO cells detected by FCM. A: Vehicle; B: 5 $\mu\text{g}/\text{mL}$ honokiol; C: 10 $\mu\text{g}/\text{mL}$ honokiol; D: 15 $\mu\text{g}/\text{mL}$ honokiol.

Table 2 Effect of honokiol on cell cycle distribution and apoptosis in RKO cells

Treatment ($\mu\text{g}/\text{mL}$)	Cell cycle distribution (%)			Apoptosis (%)
	G0/G1	S	G2/M	
Control	44.76	45.09	10.14	0.21
5	48.03	42.37	9.60	4.51
10	54.04	40.30	5.66	14.10 ^b
15	58.94	39.36	1.70	20.31 ^d

Cell cycle distribution was determined after 48 h of treatment in each group. The tabulated percentages were an average calculated on the results of three separate experiments. ^b $P < 0.01$, ^d $P < 0.01$ vs corresponding control group.

Semi-quantification of Bid, Bax, Bcl-2 and Bcl-xl mRNA expression

mRNA expression of apoptosis-related genes in response to different levels of honokiol was assessed. The Bcl-xl mRNA expression was significantly reduced in RKO cells exposed to honokiol, while Bid mRNA expression was remarkably up-regulated. No apparent changes of Bax and Bcl-2 were observed (Figure 4).

Effect of honokiol on expression of p53-related gene and p53

p53 and p53-related gene were found to be importantly involved in apoptosis induced by many agents. To study their role in honokiol-treated RKO, we monitored Bax, Bcl-2, Bcl-xl, Bid and p53 protein levels. Results in Figure 5 shows that no significant changes of Bax, Bcl-2 and p53 were found compared with vehicle. The level of Bcl-xl was decreased to vehicle level, while the level of Bid was increased remarkably after treated with 5 and 10 $\mu\text{g}/\text{mL}$ honokiol respectively. The protein levels were measured by quantitative Western blot analysis after normalized with β -actin content.

Inhibition of proliferation in RKO, Sw480 and LS180 cells

RKO cells had positively expressed of high wild-type p53 and SW480 cells had positive expression of high mutant p53, while LS180 had negative p53 antigen expression^[20-22]. Cells treated with various concentrations of honokiol resulted in a dose-

dependent cytotoxicity in three cells. As shown in Figure 6, honokiol-treated LS180 exhibited apparent growth inhibition like RKO cells and Sw480. Honokiol-mediated cytotoxicity occurred at the concentration of 5 $\mu\text{g}/\text{mL}$ and above. A significant decrease in cell number was seen at 10 $\mu\text{g}/\text{mL}$. The concentration leading to a 50% decrease in cell number (IC₅₀) was approximate 10.33, 12.98, 11.16 $\mu\text{g}/\text{mL}$ in RKO, SW480 and LS180 cells respectively.

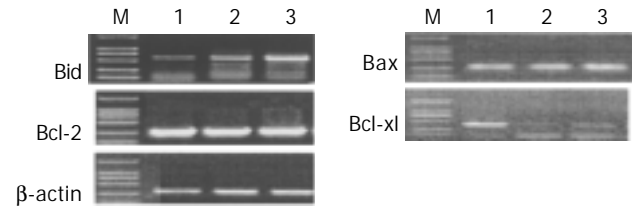


Figure 4 Analysis of Bcl-2, Bax, Bid and Bcl-xl mRNA by RT-PCR. M: DNA mark; Lane 1: Vehicle; Lane 2: 5 $\mu\text{g}/\text{mL}$ honokiol; Lane 3: 10 $\mu\text{g}/\text{mL}$ honokiol.

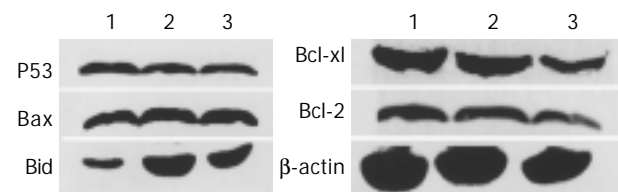


Figure 5 Western blotting of honokiol- and vehicle-induced Bax, Bcl-2, Bcl-xl, Bid and p53 protein levels in RKO cell line. Lane 1: Vehicle; Lane 2: 5 $\mu\text{g}/\text{mL}$; Lane 3: 10 $\mu\text{g}/\text{mL}$.

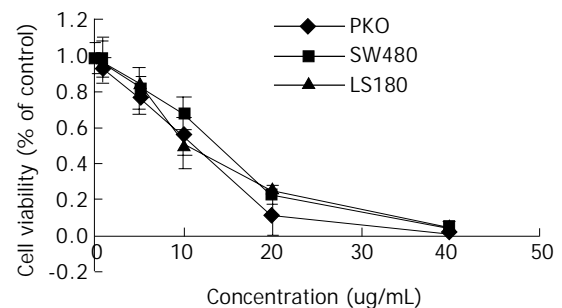


Figure 6 Concentration-dependent inhibition of RKO, SW480 and LS180 cells exposed to the various concentrations of honokiol shown by MTT assay.

DISCUSSION

p53 is a crucial protein in cellular stress response. p53-dependent arrest of cells in the G1 phase of the cell cycle was an important component of the cellular response to stress^[23]. Wild-type p53 was considered to participate in apoptosis in response to DNA damage in many tumor cells^[14,24]. When cells received UV or ionizing radiation and were exposed to anticancer drugs, p53 protein was accumulated^[25,26]. The increased p53 could transactivate its downstream target genes to induce cell cycle arrest, DNA repair, and apoptosis^[27,28]. p53-dependent apoptosis was also observed *in vivo*^[29]. However, p53-independent apoptotic cascades after administration of anticancer drugs or r-irradiation have been described.

In the present study, honokiol-treated RKO cells could induce apoptosis in a concentration-dependent manner, with the ratio of G1 phase increased. The agent also caused an increase of the expression of caspase-3 and caspase-7 in a dose-dependent manner, did not cause the significant increase

of caspase-9 (data not shown). In CH27 cells it promoted to release cytochrome C and activate caspase 3^[9].

p53-dependent apoptosis was activated by the Bax/mitochondrial/caspase-9 pathway. Bcl-2 and Bax expression were regulated by p53 both *in vitro* and *in vivo*, and Bax was a direct target of p53 transcriptional activation^[30]. Bax, a proapoptotic member of the Bcl-2 family, was located in the outer membrane of mitochondria^[25]. Increased in the ratio of Bax/Bcl-2 could cause changes in the membrane potential of mitochondria, consequently, cytochrome C and other polypeptides were released from the intermembrane space of mitochondria into cytoplasm. Once released, cytochrome C could activate procaspase-9 by self-cleavage^[12,13] and then other caspases^[12].

According to previous data, honokiol led to cell G1 arrest and cytochrome C release like p53. Thus it is necessary to evaluate the mRNA and protein expression of Bax and Bcl-2. Our results showed that honokiol-induced apoptosis of RKO cells was accompanied with up-regulation of Bid and down-modulation of Bcl-xl, but did not involve the regulation of Bcl-2 or Bax protein expression. Since pro-apoptotic Bax is a p53 downstream target, the lack of change of Bax and Bcl-xl supports the view that honokiol probably does not trigger the p53/Bax-mediated apoptosis pathway. Next we examined the expression of p53 in honokiol-treated RKO cells. We found that no significant change of p53 was observed (Figure 5). Finally we analyzed honokiol-induced apoptosis of the three cells with different p53 expression. Our data showed that honokiol-treated LS180 and SW480 cells exhibited apparent growth inhibition like RKO cells.

These results suggest that honokiol-induced caspase activation and cell apoptosis are entirely controlled by the p53-independent pathway.

REFERENCES

- 1 **Liou KT**, Shen YC, Chen CF, Tsao CM, Tsai SK. The anti-inflammatory effect of honokiol on neutrophils: mechanisms in the inhibition of reactive oxygen species production. *Eur J Pharmacol* 2003; **475**: 19-27
- 2 **Teng CM**, Chen CC, Ko FN, Lee LG, Huang TF, Chen YP, Hsu HY. Two antiplatelet agents from *Magnolia officinalis*. *Thromb Res* 1988; **50**: 757-765
- 3 **Liou KT**, Lin SM, Huang SS, Chih CL, Tsai SK. Honokiol ameliorates cerebral infarction from ischemia-reperfusion injury in rats. *Planta Med* 2003; **69**: 130-134
- 4 **Lo YC**, Teng CM, Chen CF, Chen CC, Hong CY. Magnolol and honokiol isolated from *Magnolia officinalis* protect rat heart mitochondria against lipid peroxidation. *Biochem Pharmacol* 1994; **47**: 549-553
- 5 **Watanabe K**, Watanabe H, Goto Y, Yamaguchi M, Yamamoto N, Hagino K. Pharmacological properties of magnolol and honokiol extracted from *Magnolia officinalis*: central depressant effects. *Planta Med* 1983; **49**: 103-108
- 6 **Hirano T**, Gotoh M, Oka K. Natural flavonoids and lignans are potent cytostatic agents against human leukemic HL-60 cells. *Life Sci* 1994; **55**: 1061-1069
- 7 **Hibasami H**, Achiwa Y, Katsuzaki H, Imai K, Yoshioka K, Nakanishi K, Ishii Y, Hasegawa M, Komiya T. Honokiol induces apoptosis in human lymphoid leukemia Molt 4B cells. *Int J Mol Med* 1998; **2**: 671-673
- 8 **Nagase H**, Ikeda K, Sakai Y. Inhibitory effect of magnolol and honokiol from *Magnolia obovata* on human fibrosarcoma HT-1080. Invasiveness *in vitro*. *Planta Med* 2001; **67**: 705-708
- 9 **Yang SE**, Hsieh MT, Tsai TH, Hsu SL. Down-modulation of BCL-XL, release of cytochrome c and sequential activation of caspases during honokiol-induced apoptosis in human squamous lung cancer CH27 cells. *Biochem Pharmacol* 2002; **63**: 1641-1651
- 10 **Miyashita T**, Krajewski S, Krajewska M, Wang HG, Lin HK, Liebermann DA, Hoffman B, Reed JC. Tumor suppressor p53 is a regulator of bcl-2 and bax gene expression *in vitro* and *in vivo*. *Oncogene* 1994; **9**: 1799-1805
- 11 **Miyashita T**, Harigai M, Hanada M, Reed JC. Identification of a p53-dependent negative response element in the bcl-2 gene. *Cancer Res* 1994; **54**: 3131-3135
- 12 **Li P**, Nijhawan D, Budihardjo I, Srinivasula SM, Ahmad M, Alnemri ES, Wang X. Cytochrome c and dATP-dependent formation of Apaf-1/caspase-9 complex initiates an apoptotic protease cascade. *Cell* 1997; **91**: 479-489
- 13 **Stennicke HR**, Deveraux QL, Humke EW, Reed JC, Dixit VM, Salvesen GS. Caspase-9 can be activated without proteolytic processing. *J Biol Chem* 1999; **274**: 8359-8362
- 14 **Lowe SW**, Bodis S, McClatchey A, Remington L, Ruley HE, Fisher DE, Housman DE, Housman DE, Jacks T. p53 status and the efficacy of cancer therapy *in vivo*. *Science* 1994; **266**: 807-810
- 15 **Haldar S**, Negrini M, Monne W, Sabbioni S, Croce CM. Down-regulation of bcl-2 by p53 in breast cancer cells. *Cancer Res* 1994; **54**: 2095-2097
- 16 **Beham A**, Marin MC, Fernandez A, Herrmann J, Brisbay S, Tari AM, Lopez-Berestein G, Lozano G, Sarkiss M, McDonnell TJ. Bcl-2 inhibits p53 nuclear import following DNA damage. *Oncogene* 1997; **15**: 2767-2772
- 17 **Marin MC**, Hsu B, Meyn RE, Donehower LA, el-Naggar AK, McDonnell TJ. Evidence that p53 and bcl-2 are regulators of a common cell death pathway important for *in vivo* lymphomagenesis. *Oncogene* 1994; **9**: 3107-3112
- 18 **Miyashita T**, Krajewski S, Krajewska M, Wang HG, Lin HK, Liebermann DA, Hoffman B, Reed JC. Tumor suppressor p53 is a regulator of bcl-2 and bax gene expression *in vitro* and *in vivo*. *Oncogene* 1994; **9**: 1799-1805
- 19 **Selvakumaran M**, Lin HK, Miyashita T, Wang HG, Krajewski S, Reed JC, Hoffman B, Liebermann D. Immediate early up-regulation of bax expression by p53 but not TGF-beta1: a paradigm for distinct apoptotic pathways. *Oncogene* 1994; **9**: 1791-1798
- 20 **Smith ML**, Chen IT, Zhan Q, O'Connor PM, Fornace AJ Jr. Involvement of the p53 tumor suppressor in repair of u.v.-type DNA damage. *Oncogene* 1995; **10**: 1053-1059
- 21 **Rodrigues NR**, Rowan A, Smith ME, Kerr IB, Bodmer WF, Gannon JV, Lane DP. p53 mutations in colorectal cancer. *Proc Natl Acad Sci U S A* 1990; **87**: 7555-7559
- 22 **Xu LH**, Deng CS, Zhu YQ, Liu SQ, Liu DZ. Synergistic antitumor effect of TRAIL and doxorubicin on colon cancer cell line SW480. *World J Gastroenterol* 2003; **9**: 1241-1245
- 23 **Luu Y**, Bush J, Cheung KJ Jr, Li G. The p53 Stabilizing Compound CP-31398 induces apoptosis by activating the intrinsic Bax/mitochondrial/caspase-9 pathway. *Exp Cell Res* 2002; **276**: 214-222
- 24 **Schuler M**, Bossy-Wetzel E, Goldstein JC, Fitzgerald P, Green DR. p53 induces apoptosis by caspase activation through mitochondrial cytochrome c release. *J Biol Chem* 2000; **275**: 7337-7342
- 25 **Li G**, Bush JA, Ho VC. p53-dependent apoptosis in melanoma cells after treatment with camptothecin. *J Invest Dermatol* 2000; **114**: 514-519
- 26 **Li G**, Ho VC, Mitchell DL, Trotter MJ, Tron VA. Differentiation-dependent p53 regulation of nucleotide excision repair in keratinocytes. *Am J Pathol* 1997; **150**: 1457-1464
- 27 **Green DR**, Reed JC. Mitochondria and apoptosis. *Science* 1998; **281**: 1309-1312
- 28 **Li G**, Ho VC. p53-dependent DNA repair and apoptosis respond differently to high- and low-dose ultraviolet radiation. *Br J Dermatol* 1998; **139**: 3-10
- 29 **Tron VA**, Trotter MJ, Tang L, Krajewska M, Reed JC, Ho VC, Li G. P53-regulated apoptosis is differentiation dependent in ultraviolet B-irradiated mouse keratinocytes. *Am J Pathol* 1998; **153**: 579-585
- 30 **Liebermann DA**, Hoffman B, Steinman RA. Molecular controls of growth arrest and apoptosis: p53-dependent and independent pathways. *Oncogene* 1995; **11**: 199-210

Natural history of chronic hepatitis C in patients on hemodialysis: Case control study with 4-23 years of follow-up

Kunio Okuda, Osamu Yokosuka

Kunio Okuda, Osamu Yokosuka, Department Medicine and Clinical Oncology, Graduate School of Medicine, Chiba University, Chiba 260-8670, Japan

Correspondence to: Osamu Yokosuka, M.D., Department of Medicine and Clinical Oncology, Graduate School of Medicine, Chiba University, Chiba 260-8670, Japan. yokosukao@faculty.chiba-u.jp

Telephone: +81-43-226-2083 **Fax:** +81-43-226-2088

Received: 2004-03-05 **Accepted:** 2004-04-09

Abstract

AIM: Hepatitis C virus (HCV) infection is very common among end-stage kidney disease patients on hemodialysis, but its natural history is not known.

METHODS: In this study, 189 dialysis patients (case) positive for HCV antibodies who were followed up for more than 4 years were compared with twice as many sex/age matched controls with chronic hepatitis C who were diagnosed in the same month as the case and followed up for comparable periods. The longest follow-up was 23 years in dialysis cases. The disease activities were graded into "asymptomatic" if ALT was less than 40 (35 in cases) IU/L, "low activities" if ALT was 40 (35)-79 IU/L, and "high activities" if ALT was above 80 IU/L during the last or latest 4 year period.

RESULTS: All 25 dialysis cases who were followed up for more than 15 years were asymptomatic and 15 of them were negative for HCV RNA. Of the 50 controls followed up for more than 15 years, 34 had high activities, and none cleared HCV RNA. There were 60 controls who were asymptomatic, but they were all positive for HCV RNA, while 22.3% of asymptomatic dialysis cases were RNA negative. No dialysis patients with chronic hepatitis C progressed to cirrhosis, whereas the disease progressed to cirrhosis in more than one quarter of the controls. These differences were highly significant ($P < 0.0001$).

CONCLUSION: Chronic hepatitis C among hemodialysis patients is mild in disease activity, and is not progressive, perhaps due to immunological abnormalities in these patients. Hepatic C virus is frequently cleared in asymptomatic dialysis patients during a long course. A possible mechanism for viral clearance is viral particle destruction on the surface of the dialyzer membrane.

Okuda K, Yokosuka O. Natural history of chronic hepatitis C in patients on hemodialysis: Case control study with 4-23 years of follow-up. *World J Gastroenterol* 2004; 10(15): 2209-2212
<http://www.wjgnet.com/1007-9327/10/2209.asp>

INTRODUCTION

Hepatitis C virus (HCV) infection is very common among patients on hemodialysis for chronic renal failure with global anti-HCV prevalence of up to 91%^[1], because of the frequent past blood transfusions and nosocomial infections^[2,3]. Although

at the clinical setting, dialysis patients with HCV infection seem to have a mild disease, reports on the natural history of hepatitis C in hemodialysis patients vary^[4]. Sterling *et al.*^[5] compared 50 consecutive patients with end-stage renal disease and HCV infection to HCV-positive controls. Ninety-six percent of patients on dialysis had normal alanine-aminotransferase (ALT) and low necroinflammatory score on biopsy. Despite minimal biochemical evidence of disease, some dialysis patients were more likely to have bridging hepatic fibrosis. Another cohort study^[6] showed that the crude relative risk of death comparing HCV positive to negative dialysis patients was not significant. However, adjustment for age, transplantation, and other factors raised the relative risk somewhat. Akpolat *et al.*^[7] compared liver histology between 9 dialysis patients and 37 patients with normal renal function, and found less active and progressive chronic hepatitis C in the former. They admitted that the number of patients was too small for conclusion. Thus, more information is required on the natural history of chronic HCV infection in hemodialysis patients. This study was designed to compare end-stage kidney disease patients who were positive for HCV antibodies and control patients infected with HCV but not on dialysis.

MATERIALS AND METHODS

At the end of 2001, 603 patients with renal failure were dialyzed with 221 consoles at Sanai Amalgamated Dialysis Center, Chiba, which consists of Sanai Memorial Hospital, Sanai Soga Hospital and Ichihara Dialysis Clinic. Of these 603 patients, 142 were tested positive for HCV antibodies. Many of these patients had chronic non-A, non-B hepatitis and were subsequently found to have HCV antibody positive. Dialysis patients commonly had cardiovascular, intracranial and other complications, and they died while on dialysis. At this center, about 55 patients on average died per year. As yet, none of these anti-HCV positive patients turned antibody negative during the observation period after 1991 when C100-3 antibody kit became available at the hospital. The antibody kit was subsequently changed to the 2nd and 3rd generation test. All dialysis patients underwent periodic blood tests that included ALT and aspartate-aminotransferase (AST) every 4 wk. In this study, 189 patients who were anti-HCV positive and followed up for more than 4 years to the end of 2001 constituted the study (case) subjects. Twenty-five patients were followed for more than 15 years (longest 23 years), 94 patients were followed for 10-15 years and 70 for 4-10 years (Table 1). Ten patients were treated with interferon^[8] and they were excluded. Currently 3 patients had cirrhosis, they were positive for both HBV and HCV. They were not included. The three patients had cirrhosis when dialysis was started at this hospital.

One patient with renal failure started on dialysis in 1978, 11 in 1983, 5 in 1984, 4 in 1985, 8 in 1986, 13 in 1987, 18 in 1988, 14 in 1989, 21 in 1990, 24 in 1991, 22 in 1992, 14 in 1993, 18 in 1994, 10 in 1995, and 6 in 1996. There were 137 male dialysis patients whose age ranged from 21 to 75 years, averaged 48.6±11.8 years, and 52 females whose age ranged 24 to 83 years, averaged 51.7±11.1 years.

The control group consisted of anti-HCV positive patients with chronic hepatitis who were diagnosed and followed up at the Liver Center of the Chiba University Hospital. The patients who were treated with interferon and had sustained virological response were excluded. At this center, approximately 1 200 HCV positive patients were followed up at an interval of 1 to 3 mo, and about 20-30 new patients were found per month. Out of these patients, two control patients for each dialysis case were chosen who were age (± 5 years) and sex matched, and found to be HCV positive in the same month and subsequently followed up for a similar period of time. All these patients were followed up for more than 4 years, and the disease activities were recorded in the last 4 years before death or in the latest 4 year period.

Diagnosis of cirrhosis was made on the basis of liver biopsy, imaging, blood chemistry and physical signs. Imaging findings suggestive of cirrhosis included ascites, liver surface irregularity, splenomegaly, enlarged left gastric vein, enlarged paraumbilical vein, obtuse liver edge, enlarged caudate lobe, excessively large left lobe compared to the right lobe, splenorenal or gastrosplenic shunt by ultrasound and CT, and esophago-gastric varices by endoscopy. The patients with past or currently elevated ALT in the absence of these features were diagnosed as having chronic hepatitis C.

Serum HCV RNA was measured using the branch DNA method and subsequently by Amplicor test (Nippon Roche, Tokyo). Viral load was measured twice at an interval of 2 or more years in dialysis patients to see the change in viral load. Beside the routine liver tests, 7S domain type IV collagen was measured as an indirect indicator of hepatic fibrosis in dialysis cases^[9,10].

The disease activities were graded into three categories: "asymptomatic" if ALT levels remained below 40 IU/L for the control group and below 35 IU/L for dialysis cases, the difference in the upper normal limit was due to normally low ALT and AST in dialysis patients^[11,12]; "low activities" if ALT fluctuated between 35 (40 in control) and 79 IU/L; and "high activities" if ALT levels exceeded 80 IU/L during the last 4 year period.

Statistical analyses were made by the χ^2 test and ANOVA.

RESULTS

The disease activities in these dialysis cases who were divided into three groups according to the length of dialysis (more than 15 years, 10-15 years and 4-10 years) are given in Table 1. All the 25 patients on dialysis for more than 15 years were asymptomatic, and only 3 of 50 controls were asymptomatic. The remainder of the controls all had disease activities. Of the 94 patients on dialysis for 10-15 years, 81 (85%) were asymptomatic and 6 (6.4%) had high activities. Whereas in the controls, only 26 (13.8%) of 188 were asymptomatic and 109 (58.0%) had high activities. Of the 70 patients on dialysis for 4-10 years, 58 (83%) were asymptomatic and 5 (7.1%) had high activities. The corresponding figures were 22.1% and 52.1%, respectively, in the controls. These differences were highly significant ($P < 0.001$). Table 1 also lists the number of patients in parentheses in whose serum HCV RNA levels were PCR negative or below the quantifiable level by Amplicor. Of the 25 long (more than 15 years) follow-up dialysis cases, RNA was negative or below the quantifiable level in 15 (60%). However, RNA was negative in only one of 14 dialysis cases with low disease activities, the remaining 13 cases were positive. All high activities cases were positive, while none of the control patients was negative for HCV RNA.

The clinical course of these 189 patients was uneventful from the point of view of liver disease. Many of these patients died from liver unrelated diseases, but the liver disease progressed to cirrhosis in none of them. The three cases of HCV positive

cirrhosis who were followed up had already had cirrhosis when they came to our hospital. All cases who were followed up for more than 15 years were asymptomatic by the end of the follow-up (Table 1). More dialysis cases who were follow-up for a shorter period of time had disease activities. Thus, chronic hepatitis C among dialysis patients seemed to slowly improve and seldom worsen. In contrast, the disease was progressive in most control patients. In the 50 control patients who were followed up for more than 15 years, the disease progressed to cirrhosis in 18 during the follow-up. In the 228 controls who were followed up for 10-15 years, cirrhosis developed in 62. In the 140 controls who were followed up for 4-10 years, 29 developed cirrhosis.

Table 1 Clinical evaluation of dialysis (case) and control patients in recent 4 years or last 4 years before liver unrelated death

Group	Number	Disease activities			
		Asymptomatic	Low	High	
Follow-up: <15 yr					
Case	Male	14(5)	14(5)	0	0 ^b
	Female	11(10)	11(10)	0	0 ^d
Control	Male	28(0)	0	8(0)	20 ^b (0)
	Female	22(0)	3(0)	5(0)	14 ^d (0)
Follow-up: 10-15 yr					
Case	Male	70(15)	58(14)	7(1)	5 ^b (0)
	Female	24(0)	23(10)	0	1 ^d (0)
Control	Male	140(0)	16(0)	29(0)	95 ^b (0)
	Female	48(0)	10(0)	24(0)	14 ^d (0)
Follow-up: 4-10 yr					
Case	Male	53(5)	41(5)	7(0)	5 ^b (0)
	Female	17(9)	17(9)	0	0 ^d
Control	Male	106(0)	24(0)	23(0)	59 ^b (0)
	Female	34(0)	7(0)	13(0)	14 ^d (0)

(): HCV RNA, PCR negative or below quantifiable level by Amplicor ^b $P < 0.001$, ^d $P < 0.001$ by χ^2 test.

Table 2 Serum HCV RNA in dialysis patients in the study

Range (KIU/mL)	Group		
	Asymptomatic	Low activities	High activities
<0.5	53	2	0
0.6-100	32	2	1
101-400	48	4	1
401->850 ¹	21	6	9
Total	154	14	11

¹Includes values above 1 000 by Amplicor Version I. Values by branched DNA method were converted to Amplicor values. $P < 0.001$ by χ^2 test.

Table 3 Comparison of the first and second measurements of HCV RNA at intervals longer than 2 years in dialysis patients

Change	Group		
	Asymptomatic	Low activities	High activities
Unchanged (change <50%)	44	1	2
Increased (+ >50%)	25	3	2
Decreased (- >50%)	36	5	2
Total	105	9	6

The initial serum levels of HCV RNA in 179 dialysis patients are given in Table 2. Of the 154 asymptomatic cases, the RNA

level was negative or below the quantifiable level in 53 (34.4%) and below 100 KIU/mL in 32 (20.8%), but the remaining 69 patients had RNA levels greater than 101 KIU/mL. All the 11 dialysis patients with high activities had high levels of RNA. Thus, differences among the three activity groups were significant by the χ^2 test ($P < 0.001$). Serum RNA could be measured twice at an interval of 2 years or longer in 120 patients. The change was less than 50% of the initial level (unchanged) in 44 (41.9%), increased by more than 50% in 25 (23.8%) and decreased by more than 50% in 36 (41.0%) (Table 3). Serum RNA clearly reflected the absence or presence of disease activities. Serum 7S fragment of type IV collagen was measured in 143 dialysis patients (Table 4). The values ranged from 1.8 to 12.0 $\mu\text{g/mL}$ with a mean of 5.59 ng/mL. The mean \pm SD for the asymptomatic group was 5.05 \pm 1.59 ng/mL, 6.21 \pm 1.94 ng/mL for the low activities group and 6.92 \pm 2.63 ng/mL for the high activity group. The differences were significant ($P < 0.05$) by ANOVA.

Table 4 Serum 7S fragment of type IV collagen in dialysis patients

Group	Number of patients	7S IV collagen (ng/mL)
Asymptomatic	118	5.05 \pm 1.59 ^{a,c}
Low activities	14	6.21 \pm 1.94 ^a
High activities	11	6.92 \pm 2.63 ^c
Total	143	5.59

^a $P < 0.05$, ^c $P < 0.05$ by ANOVA.

DISCUSSION

In this study, 189 dialysis patients with HCV infection were followed up for more than 4 years in comparison with 378 sex/age matched nondialysis control patients who were diagnosed as chronic hepatitis C. Disease activities were divided into three grades: asymptomatic, low activities (ALT not exceeding 80 IU/L) and high activities (ALT exceeding 80 IU/L) during the last or latest 4 year period. Of the 189 dialysis patients, 25 were followed up for more than 15 years. They all became asymptomatic after a varying period of elevated and fluctuating ALT, and 15 were HCV RNA negative. In a distinct contrast, the majority of controls who were followed up for a comparable period remained to have high activities (Table 1), and none lost HCV RNA, one quarter to one third of them progressed to cirrhosis. Serum type IV collagen 7S domain was measured in dialysis patients, and the results suggested that fibrogenetic activities increased with high disease activities. These results clearly showed that patients on hemodialysis became much better than nondialysis patients with chronic hepatitis C. No dialysis patients progressed to cirrhosis in this series.

The question is why there is such a distinct difference in the natural history of chronic hepatitis C between dialysis and nonuremic patients. It has been suggested that liver injury caused by HCV infection is mainly through immunologic processes^[13] rather than the virus that is directly cytopathic^[14]. It has been well established that patients with end-stage renal disease and on maintenance hemodialysis have severe immunologic abnormalities with reduced immune responsiveness^[15].

Some of our dialysis patients had a high viral load. RNA levels did not show direct correlation with disease activities, but more asymptomatic cases were RNA negative, and RNA levels tended to decrease in more patients when studied at an interval of 2 years or longer. There have been several studies on viral load in hemodialysis patients, but the results were not consistent. According to Umlauf *et al.*^[16], HCV viremia fluctuated with the time of undetectable RNA. Whereas in the

study of Fabrizi *et al.*^[17], HCV load was low and relatively stable. HCV RNA levels decreased in dialysis patients in another report^[18].

In 1996, we first described the phenomenon in which the number of HCV viral particles decreased after each dialysis procedure and restored to the previous level at the next dialysis^[19]. Subsequently it was found that viral particles were adsorbed onto the dialyzer membrane and destroyed^[20]. Our observations have since been confirmed. According to Furusyo *et al.*^[18], HCV RNA levels were significantly lower in 98 dialysis patients (0.4 mEq/mL) compared with 228 nonuremic patients (2.0 mEq/mL). The dialysis procedure itself might contribute to the reduction of viral load in the long run. Another possible explanation for viral load reduction in dialysis patients was coinfection with another hepatotropic virus^[21]. However, our earlier study in this dialysis center, the rates of infection with hepatitis G virus^[22] and TT virus^[23] were very low. Yokosuka *et al.*^[24] followed up 320 patients with chronic type C liver disease and found that no chronic hepatitis patients were seroconverted, seronegative conversion occurred in 2%, only in end stage cirrhotic patients with or without hepatocellular carcinoma. The difference in the temporal virus load between dialysis and non-dialysis patients was so remarkable that it required biological explanation. It is not known whether C-viruses are able to replicate in liver cells of immunologically compromised dialysis patients as in immunologically competent individuals. Hepatocytes of the dialysis patients might not have normal metabolic and synthetic capabilities under the influence of uremic state, as exemplified by very low AST and ALT levels in serum^[11,12]. Replication of viral particles within hepatocytes might be reduced for the same reason. It seems that the most plausible explanation would be the negative balance between mechanical destruction of viral particles by membrane dialysis procedure and viral replication.

ACKNOWLEDGMENT

The authors express sincere thanks to Dr. Irie Y for his help and support in preparing this manuscript.

REFERENCES

- 1 **Wasley A**, Alter MJ. Epidemiology of hepatitis C: geographic differences and temporal trends. *Semin Liver Dis* 2000; **20**: 1-16
- 2 **Zeldis JB**, Depner TA, Kuramoto IK, Gish RG, Holland OV. The prevalence of hepatitis C virus antibodies among hemodialysis patients. *Ann Intern Med* 1990; **112**: 958-960
- 3 **Okuda K**, Hayashi H, Kobayashi S, Irie Y. Mode of hepatitis C infection not associated with blood transfusion among chronic hemodialysis patients. *J Hepatol* 1995; **23**: 28-31
- 4 **Zacks SL**, Fried MW. Hepatitis B and C and renal failure. *Infect Dis Clin North Am* 2001; **15**: 877-899
- 5 **Sterling RK**, Sanyal AJ, Luketic VA, Stravitz RT, King AL, Post AB, Mills AS, Contos MJ, Shiffman ML. Chronic hepatitis C infection in patients with end stage renal disease. Characterization of liver histology and viral load in patients awaiting renal transplantation. *Am J Gastroenterol* 1999; **94**: 3576-3582
- 6 **Stehman-Breen CO**, Emerson S, Gretch D, Johnson RJ. Risk of death among chronic dialysis patients infected with hepatitis C virus. *Am J Kidney Dis* 1998; **32**: 629-534
- 7 **Akopolat I**, Ozyilkan E, Karagoz F, Akpolat T, Kandemir B. Hepatitis C in haemodialysis and nonuraemic patients: a histopathological study. *Int Urol Nephrol* 1998; **30**: 349-355
- 8 **Okuda K**, Hayashi H, Yokozeki K, Kondo T, Kashima T, Irie Y. Interferon treatment for chronic hepatitis C in haemodialysis patients: suggestions based on a small series. *J Gastroenterol Hepatol* 1995; **10**: 616-620
- 9 **Murawaki Y**, Ikuta Y, Koda M, Kawasaki H. Serum type III procollagen peptide, type IV collagen 7S domain, central triple-

- helix of type IV collagen and tissue inhibitor of metalloproteinase in patients with chronic viral liver disease: relation to liver histology. *Hepatology* 1994; **20**: 780-787
- 10 **Ishibashi K**, Kashiwagi T, Ito A, Tanaka Y, Nagasawa M, Toyama T, Ozaki S, Naito M, Azuma M. Changes in serum fibrogenesis markers during interferon therapy for chronic hepatitis type C. *Hepatology* 1996; **24**: 27-31
- 11 **Wolf PL**, Williams D, Coplon N, Coulson AS. Low aspartate transaminase activity in serum of patients undergoing hemodialysis. *Clin Chim* 1972; **18**: 567-568
- 12 **Yasuda K**, Okuda K, Endo N, Ishiwatari Y, Ikeda R, Hayashi H, Yokozeki K, Kobayashi S, Irie Y. Hypoaminotransferasemia in patients undergoing long-term hemodialysis; clinical and biochemical appraisal. *Gastroenterology* 1995; **109**: 1295-1300
- 13 **Rehermann B**. Interaction between the hepatitis C virus and the immune system. *Semin Liver Dis* 2000; **20**: 127-141
- 14 **Ballardini G**, Groff P, Pontisso P, Giostra F, Francesconi R, Lenzi M, Zauli D, Alberti A, Bianchi FB. Hepatitis C virus (HCV) genotype, tissue HCV antigens hepatocellular expression of HLA-A,B,C, and intercellular adhesion-1 molecules. Clues to pathogenesis of hepatocellular damage, and response to interferon treatment in patients with chronic hepatitis C. *J Clin Invest* 1995; **95**: 2067-2075
- 15 **Decamps-Latscha B**, Herbelin A. Long-term dialysis and cellular immunity: a critical survey. *Kidney Int* 1993; **43**: S135-S142
- 16 **Umlauf F**, Gruenewald K, Weiss G, Kessler H, Urbanek M, Haun M, Santner B, Koenig P, Keeffe EB. Patterns of hepatitis C viremia in patients receiving hemodialysis. *Am J Gastroenterol* 1997; **92**: 73-78
- 17 **Fabrizi F**, Martin P, Dixit V, Brezina M, Cole MJ, Vinson S, Mousa M, Gitnick G. Biological dynamics of viral load in hemodialysis patients with hepatitis C virus. *Am J Kidney Dis* 2000; **35**: 122-129
- 18 **Furusyo N**, Hayashi J, Ariyama I, Sawayama Y, Etoh Y, Shigematsu M, Kashiwagi S. Maintenance hemodialysis decreases serum hepatitis C virus (HCV) RNA levels in hemodialysis patients with chronic HCV infection. *Am J Gastroenterol* 2000; **95**: 490-496
- 19 **Okuda K**, Hayashi H, Yokozeki K, Irie Y. Destruction of hepatitis C virus particles by hemodialysis. *Lancet* 1996; **347**: 909-910
- 20 **Hayashi H**, Okuda K, Yokosuka O, Kobayashi S, Yokozeki K, Ohtake Y, Irie Y. Adsorption of hepatitis C virus particles onto the dialyzer membrane. *Artif Organs* 1997; **21**: 1056-1059
- 21 **Janusz Kiewicz-Lewandowska D**, Wysocki J, Rembowska J, Lewandowski K, Nowak T, Pernak M, Nowak J. Hepatitis G virus co-infection may affect the elimination of hepatitis C virus RNA from the peripheral blood of hemodialysis patients. *Acta Virol* 2001; **45**: 261-263
- 22 **Okuda K**, Kanda T, Yokosuka O, Hayashi H, Yokozeki K, Ohtake Y, Irie Y. GB virus-C infection among chronic haemodialysis patients: clinical implications. *J Gastroenterol Hepatol* 1997; **12**: 766-770
- 23 **Ikeuchi T**, Okuda K, Yokosuka O, Kanda T, Kobayashi S, Murata M, Hayashi H, Yokozeki K, Ohtake Y, Kashima T, Irie Y. Superinfection of TT virus and hepatitis C virus among chronic haemodialysis patients. *J Gastroenterol Hepatol* 1999; **14**: 796-800
- 24 **Yokosuka O**, Kojima H, Imazeki F, Tagawa M, Saisho H, Tamatsukuri S, Omata M. Spontaneous negativation of serum hepatitis C virus RNA is a rare event in type C chronic liver diseases: analysis of HCV RNA in 320 patients who were followed for more than 3 years. *J Hepatol* 1999; **31**: 394-399

Edited by Wang XL and Xu FM

Initial steroid-free immunosuppression after liver transplantation in recipients with hepatitis c virus related cirrhosis

Perdita Wietzke-Braun, Felix Braun, Burckhart Sattler, Giuliano Ramadori, Burckhardt Ringe

Perdita Wietzke-Braun, Giuliano Ramadori, Abteilung für Gastroenterologie und Endokrinologie, Georg-August-Universität, 37075 Göttingen, Germany

Felix Braun, Burckhardt Ringe, Georg-August-Universität, 37075 Göttingen, Germany

Burckhart Sattler, Zentrum Pathologie, Georg-August-Universität, 37075 Göttingen, Germany

Correspondence to: Dr. Perdita Wietzke-Braun, Abteilung für Gastroenterologie und Endokrinologie, Georg-August Universität, Robert-Koch-Str. 40, 37075 Göttingen, Germany. gramado@med.uni-goettingen.de

Telephone: +49-551-39-6301 **Fax:** +49-551-39-8596

Received: 2003-12-09 **Accepted:** 2004-02-24

Abstract

AIM: Steroids can increase hepatitis C virus (HCV) replication. After liver transplantation (LTx), steroids are commonly used for immunosuppression and acute rejection is usually treated by high steroid dosages. Steroids can worsen the outcome of recurrent HCV infection. Therefore, we evaluated the outcome of HCV infected liver recipients receiving initial steroid-free immunosuppression.

METHODS: Thirty patients undergoing LTx received initial steroid-free immunosuppression. Indication for LTx included 7 patients with HCV related cirrhosis. Initial immunosuppression consisted of tacrolimus 2×0.05 mg/kg·d po and mycophenolate mofetil (MMF) 2×15 mg/kg·d po. The tacrolimus dosage was adjusted to trough levels in the target range of 10-15 µg/L during the first 3 mo and 5-10 µg/L thereafter. Manifestations of acute rejection were verified histologically.

RESULTS: Patient and graft survival of 30 patients receiving initial steroid-free immunosuppression was 86% and 83% at 1 and 2 years. Acute rejection occurred in 8/30 patients, including 1 HCV infected recipient. All HCV-infected patients had HCV genotype II (1b). HCV seropositivity occurred within the first 4 mo after LTx. The virus load was not remarkably increased during the first year after LTx. Histologically, grafts had no severe recurrent hepatitis.

CONCLUSION: From our experience, initial steroid-free immunosuppression does not increase the risk of acute rejection in HCV infected liver recipients. Furthermore, none of the HCV infected patients developed serious chronic liver diseases. It suggests that it may be beneficial to avoid steroids in this particular group of patients after LTx.

Wietzke-Braun P, Braun F, Sattler B, Ramadori G, Ringe B. Initial steroid-free immunosuppression after liver transplantation in recipients with hepatitis c virus related cirrhosis. *World J Gastroenterol* 2004; 10(15): 2213-2217

<http://www.wjgnet.com/1007-9327/10/2213.asp>

INTRODUCTION

Liver diseases related to chronic viral hepatitis are the leading

indication for liver transplantation (LTx) worldwide^[1]. Hepatitis B virus and hepatitis C virus (HCV) infection account for the majority of liver diseases related to chronic viral hepatitis. In Europe, 8 422 patients received a liver graft for virus related cirrhosis between January 1988 to December 2000^[2]. Posttransplantation HCV infection is a relatively benign condition during the short-term follow-up and liver recipients reach survival rates similar to other indications. However, the natural history of posttransplantation HCV reinfection is variable. Almost all recipients became HCV seropositive during the first year after LTx. At 5 years posttransplantation, up to 30% of the recipients developed cirrhosis^[3,12]. The patients' immune status seems to be an important factor regarding the progression of fibrosis. The immunosuppressed liver recipients had a higher rate of fibrosis progression per year compared to patients without immunosuppression^[4].

The role of immunosuppressive treatment in the occurrence and severity of HCV reinfection has been discussed controversially^[5]. Since the first liver transplantation performed by Starzl in 1963, corticosteroids have been used traditionally for immunosuppression after organ transplantation due to the lack of other available immunosuppressive drugs^[6]. Nowadays, a variety of potent and selective immunosuppressive drugs are available, thus allowing avoidance of immunosuppressive drugs with unselective mode of action or unfavorable side effects^[7]. Corticosteroids have a well described spectrum of adverse effects including metabolic changes and an increased risk of cardio-vascular diseases. Also, corticosteroids have an unselective immunosuppressive mode of action. Furthermore, corticosteroids increased HCV replication *in vitro* and *in vivo*^[8-10]. After liver transplantation, high early HCV-RNA levels could be associated with more severe recurrence of hepatitis^[11]. Prieto *et al.* reported positive relationships between the number of rejection episodes, methylprednisolone (MP) boluses, treatment of rejection, cumulative dose of steroids and the development of HCV cirrhosis^[12]. These findings implicated that prevention of acute cellular rejection and avoidance of high-dose or maintenance steroids could be beneficial^[5], however, the experience with completely steroid-free immunosuppression after LTx is still limited.

Recently, we published a series of 30 patients receiving steroid-free immunosuppression that consisted of tacrolimus and mycophenolate mofetil (MMF)^[13]. Since the hypothesis that steroid-free immunosuppression might be particularly beneficial in HCV infected liver recipients, we analyzed this subgroup of liver recipients with regard to the risk of acute rejection, and development of serious HCV related liver disease in the graft.

MATERIALS AND METHODS

Patients

Thirty adult patients underwent LTx between June 1996 and January 1999. The detailed characteristics have been previously described^[13]. The indications for LTx included hepatitis C virus related cirrhosis in seven recipients. The HCV patients included 4 females and 3 males with a median (range) age of 58(43-62) years. HCV-RNA was seropositive prior to transplantation with a

median (range) viral load of $10^4(10^3-10^5)$ genome equivalent/mL. The serum HCV-specific RNA was detected by reverse transcription (RT)/polymerase chain reaction (PCR) as previously described by Mihm *et al.*^[14]. HCV genotype was classified as II (1b) in all seven patients according to Okamoto *et al.* and Simmonds *et al.*^[15,16]. Child-Turcotte-Pugh Score prior to LTx was Child A in 2, Child B in 2 and Child C in 3 patients. Four of the patients had a coexisting hepatocellular carcinoma.

Methods

Apart from an intravenous (IV) bolus of 500 mg MP before reperfusion of the graft, recipients received no further steroids. Tacrolimus (Prograf, Fujisawa GmbH, München, Germany) was started 6 h after reperfusion at an oral dosage of 2×0.05 mg/kg-d. Thereafter, tacrolimus dosages were adjusted to a target range of 10-15 μ g/L during the first three months and 5-10 μ g/L after the third month after LTx. Tacrolimus trough levels were measured by a microparticle enzyme immunoassay (Prograf-MEIA II, Abbott Laboratories, Chicago, IL, USA). MMF (Cell Cept, Hoffmann-La Roche, Grenzach-Wyhlen, Germany) was given orally starting from the first postoperative day (pod) at a body mass adjusted dosage of 2×15 mg/kg-d. Liver biopsies were performed routinely on d 7, after 6 mo, every year, and whenever clinically indicated. Acute rejection was defined as abnormal liver function tests, histological changes as graded by the Banff classification, and the necessity for therapy^[12]. Treatment of acute rejection consisted of IV-MP boluses of 500 mg over a period of 3-5 d with or without additional prednisolone tapering. Combined antiviral therapy consisting of interferon alfa and "low-dose" ribavirin was used in patients with HCV reinfection accompanied by chronic active hepatitis as described previously by Wietzke *et al.*^[17,18].

Statistical analysis

Actual survival was calculated by the Kaplan-Meier method.

RESULTS

Patient and graft survival

Twenty-two of the 30 patients receiving initial steroid-free immunosuppression have been alive after a median (range) follow-up of 1 386(44-2 037) d. Actual patient survival was 86.7% at 2 years and 73.3% at 5 years (Figure 1A). The actual patient survival of HCV-infected recipients was 85.7% at 2 years and 57.1% at 5 years, the difference was not statistically significant (Log-rank test (Cox-Mantel): $P=0.33$) (Figure 1B).

At present, four of the seven HCV infected liver recipients have been alive with a median (range) follow-up of 47(46-60)

mo after LTx. None of the deaths in the HCV patients was related to HCV reinfection. The causes of the 3 deaths were chronic graft dysfunction (CDF) on pod 164, heart failure due to preexisting toxic cardiomyopathy on pod 774, and a *de-novo* ovarian carcinoma on pod 950. One of the seven patients with HCV-related cirrhosis underwent successful retransplantation for primary nonfunction (PNF) on day 5 (Table 1).

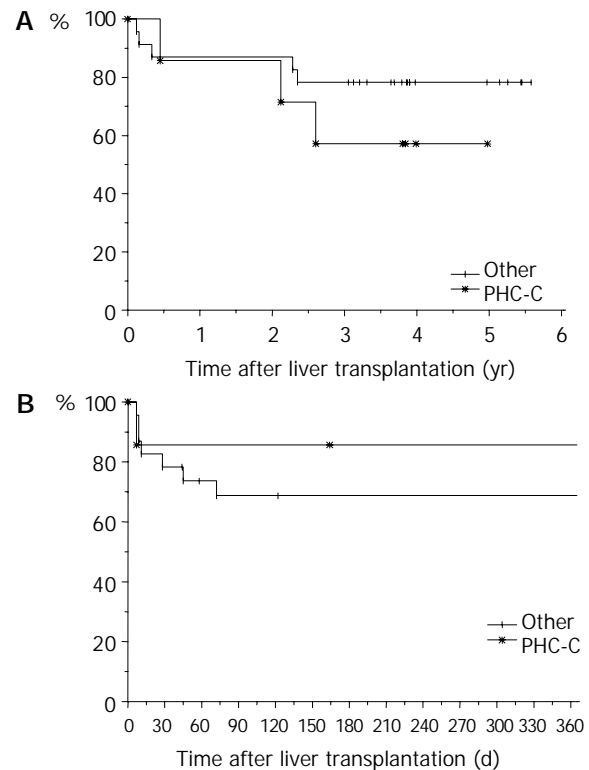


Figure 1 A: Actual patient survival according to primary indication (HCV related cirrhosis vs others) of liver recipients receiving steroid-free immunosuppression. B: Actual rejection free interval according to primary indication (HCV related cirrhosis vs others) during the first year after LTx in liver recipients receiving steroid-free initial immunosuppression.

Acute rejection episodes and immunosuppression

In total, 8 of the 30 liver recipients (26.2%) had an episode of acute rejection. The onset of acute rejection was between pod 7 and 72. The median (range) grade of acute rejection was 5.5(3-8) according to Banff classification. Low tacrolimus trough levels associated with diarrhea were observed in five of the eight recipients with acute rejection. Also, diarrhea was

Table 1 Characteristics of liver recipients with HCV-infection receiving initial steroid-free immunosuppression

#	Gender (M/F)	Rge (yr)	Child Class	HCC	HCV genotype	HCV viral load				Liver histology	Outcome (pod)
						prior	1 mo	4 mo	1 yr		
5	f	60	C	no	II (1b)	10^4	10^5	10^4	10^5		died (950), ovarian-ca
9	f	62	B	no	II (1b)	10^5	10^5	10^6	10^5	AR, hepatitis (+/-)	alive (1817), reLTx (5)
12	m	57	A	yes	II (1b)	10^5	10^5	10^4			died (774), heart failure
13	f	59	C	yes	II (1b)	10^5	10^5	10^5		hepatitis (+/-), fibrosis (+)	alive (1456)
19	m	58	B	yes	II (1b)	10^4	10^3		10^4	hepatitis (+)	alive (1402)
20	m	46	A	yes	II (1b)	10^3		10^4	10^4		alive (1389)
25	f	43	C	no	II (1b)	10^4	10^4	10^5			died, CDF (164)

Abbreviations: # (patient number), HCC (hepatocellular carcinoma), HCV (hepatitic C virus), pod (postoperative day), yr (year), mo (mo), prior (prior to LTx), AR (acute rejection), +/-/+/-/+/-/+/- (minimal/moderate/severe/reversed), reLTx (liver retransplantation), CDF (chronic graft dysfunction).

the predominant adverse effect when tacrolimus and MMF were given simultaneously. All acute rejection episodes completely resolved after IV-MP boluses and four of the patients with rejection episodes received additional steroid taper. In the further postoperative course, there was no graft loss due to rejection and all of these patients have been alive. Only one of the eight patients with acute rejection had HCV-related cirrhosis. This patient underwent retransplantation on pod 5 for PNF. Until retransplantation, immunosuppression was temporarily discontinued and the patient suffered from diarrhea, thus tacrolimus trough levels were low.

Only 3 of the 7 HCV patients received steroids after LTx, two in conjugation with tacrolimus first and then cyclosporine (CyA), and one for acute rejection. One patient was reconverted to tacrolimus after suspicion of CDF. MMF was intermittently discontinued in all 7 patients and withdrawn in 5 patients. The cause of MMF withdrawal was diarrhea in 3 patients and conversion to CyA in 2 patients. Maintenance immunosuppression in the HCV infected recipients consisted of tacrolimus monotherapy in 3 patients, tacrolimus/MMF in 2 patients, tacrolimus/prednisolone in 1 patient, and CyA/prednisolone in 1 patient.

HCV reinfection

All 7 HCV infected patients had HCV genotype II (1b). Recurrence of HCV-RNA in serum occurred within 4 mo after LTx in all seven liver recipients with HCV-related cirrhosis. Prior to LTx the median viral load was 10^4 (10^3 - 10^5) genome equivalent/mL. During the first four months, the viral load ranged from 10^3 to 6.5×10^5 genome equivalent/mL. The virus load was not markedly increased during the first year after LTx (Figure 2). Histologically, only 1 HCV patient had suspicion of minimal portal hepatitis in the most recent biopsy that occurred 15 mo after LTx and transaminases were within normal values (Table 1). Five months after LTx, another recipient had elevated transaminases (AST 55, ALT 109 U/L), suspicion of portal hepatitis and mild fibrosis in the graft. Combination therapy with subcutaneous interferon alfa-2a 3 MU three times per week and oral ribavirin 10 mg/kg body mass in three divided doses per day was given for 6 mo. At the end of treatment, the patient had transaminases within normal values (AST 9, ALT 12 U/L), and histological improvement without fibrosis, but positive serum HCV-RNA. A third recipient developed suspicion of minimal portal hepatitis and fibrosis associated with a reduction of small bile ducts. Liver histology improved after reintroduction of MMF. Initially, this patient underwent retransplantation for PNF and acute rejection was resolved.

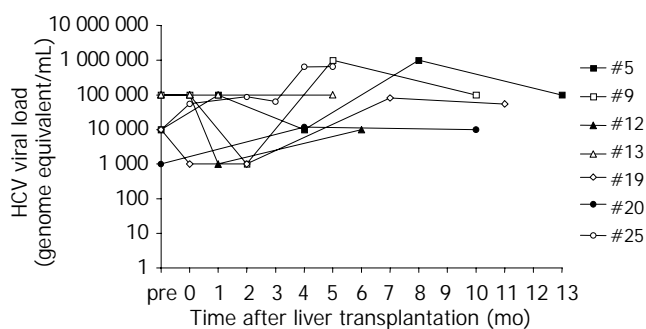


Figure 2 Serum virus concentration in seven HCV infected recipients during the first year after LTx. All patients received initial steroid-free immunosuppression.

DISCUSSION

Although steroids are known to increase HCV replication^[8],

they are given routinely for prophylaxis and treatment of rejection after solid organ transplantation. The potential risk of acute rejection must be faced against the benefit of steroid withdrawal. After LTx, HCV infection has been clearly identified as a risk factor for the development of early acute rejection^[19]. On the other hand, the presence, number, and treatment of acute rejections were found to be associated with the histologic recurrence of HCV infection after LTx^[20,21]. In 96 liver recipients, histologic recurrence of HCV infection occurred in 18% without acute rejection, 42% with one acute rejection episode, and 70% with more than one episode of acute rejection^[21]. In liver recipients, MP treatment for acute rejection was found to increase serum HCV RNA between 4 to 100 fold^[8]. OKT3, used for treatment of steroid-resistant rejection after LTx, was associated with more severe recurrences^[20]. The mutual relation between treatment of acute rejection and recurrence of HCV-infection after LTx sets the stage for a completely steroid-free immunosuppressive protocol.

Recently, it was clearly demonstrated that steroid-free immunosuppression after LTx was feasible and safe^[13,22-24]. The different immunosuppressive regimens consisted of CyA/azathioprine (Aza)^[23], CyA or tacrolimus monotherapy^[22], CyA/rapamycin, rapamycin monotherapy^[24], and tacrolimus/MMF^[13]. The reported rates of acute rejection were 65% for CyA and 66% for tacrolimus monotherapy^[22]. The combination of CyA/Aza resulted in 80% of acute rejection, but only 9% of acute rejections required treatment. Compared to patients receiving CyA/Aza/prednisone, the incidence and severity of rejection were similar in both groups but the dynamics of virus replication of HCV-RNA was faster among those treated with prednisone. The 2 year survival rate was 70.2% with prednisone and 78.3% without prednisone^[23]. The rate of acute rejection using rapamycin/CyA was 28% and with sirolimus monotherapy 75%^[24].

We reported that complete avoidance of corticosteroids after LTx could be performed without an increased risk of mortality, morbidity, and severe acute rejection. The rate of acute rejection with the use of tacrolimus in combination with MMF was only 26.2%^[13]. This rate of acute rejections might even be reduced, if underimmunosuppression were avoided. Low tacrolimus trough levels were observed in patients with diarrhea when tacrolimus and MMF were given simultaneously. Diarrhea could be avoided after introduction of a two hour dosing interval between tacrolimus and MMF administration^[13,25]. Therefore, the rate of acute rejections might be lower if tacrolimus and MMF are administered with a dosing interval.

In our present study, only 1 HCV patient developed acute rejection. This patient had a complicated clinical course with PNF, retransplantation, temporary discontinuation of immunosuppression, acute rejection, and received MP boluses as well as intermittent steroids until pod 255. Reinfection with HCV was noticed in all seven patients. Within 4 mo after LTx, all seven patients were HCV seropositive. Compared to the pretransplant HCV load, there was no significant increase during the first year after LTx. Also, liver histology was completely unsuspecting in 4 HCV patients. Three patients had suspicion of minimal portal hepatitis which was followed up by frequent biopsies in one patient. Another patient with supposed minimal portal hepatitis and additional mild fibrosis received combination therapy which improved transaminases and histology^[17]. Also, one patient with previous retransplantation developed portal hepatitis and fibrosis. MMF was reintroduced for reduction of small bile ducts, minimal portal hepatitis and fibrosis and resulted in histological improvement. None of the HCV infected patients developed serious chronic liver disease. However, one patient died of CDF which was related to underimmunosuppression after conversion to CyA for

suspicion of tacrolimus induced neurotoxicity. From our limited experience with the small number of patients, the avoidance of steroids did not alter the posttransplant HCV reinfection in serum and the histological alterations were mild despite all patients had HCV genotype II (1b). Feray *et al.* reported that HCV genotype II (1b) was a risk factor for recurrent hepatitis^[26,27]. However, the influence of HCV genotype II (1b) has been controversial. Gordon *et al.* reported a similar frequency of recurrent hepatitis with all HCV genotypes, but HCV genotype II (1b) was associated with a higher rate of cirrhosis^[28]. Thus, the avoidance of steroids seems to be beneficial for liver recipients with HCV genotype II (1b).

Hitherto, it remains unclear which immunosuppressive regimen is best for HCV liver recipients. MMF was discussed controversially in liver transplant recipients with HCV^[29]. In a recent prospective randomized trial comparing tacrolimus/prednisolone with tacrolimus/MMF/prednisolone in liver recipients with HCV, MMF had no impact on patient and graft survival, rejection or rate of HCV recurrence^[30]. However, MMF might reduce the frequency of acute rejection and therefore exposure to steroids^[31]. Our intention was to use a safe steroid-free immunosuppressive regimen. Tacrolimus is a potent immunosuppressive drug, but impairment of renal function might limit the use of tacrolimus especially during the early phase after LTx. Thus, we used a combination of tacrolimus and MMF which resulted in a low frequency of acute rejection^[13]. However, the combination of tacrolimus and MMF could cause diarrhea or other side effects that often required discontinuation or withdrawal of MMF. Thus, therapeutic drug monitoring of tacrolimus is an essential requirement for the combination of tacrolimus and MMF. Alternatively, anti-IL-2 receptor antibodies might have potential in steroid-free regimens. The use of anti-IL-2 receptor antibodies reduces the frequency of acute rejection after LTx, but there has been limited experience with HCV infection when anti-IL-2 receptor antibodies are given for induction of immunosuppression. Most recently, two immunosuppressive protocols using daclizumab have been reported with controversial results regarding HCV infection. Tacrolimus/MMF was compared with daclizumab/tacrolimus/MMF in a randomized open-label study and corticosteroids were eliminated 24 h after LTx in both arms. Steroids could be avoided safely after pod 1 and HCV recurrence was documented in 2 patients who did not receive daclizumab^[32]. In a group of 21 HCV infected liver recipients receiving daclizumab, MMF, and steroids for induction of immunosuppression, patients with HCV infection administered daclizumab were more likely to have an earlier onset of hepatitis, jaundice and greater histological activity compared with a well-matched HCV control group. Also, recurrent hepatitis progressed more rapidly in the daclizumab group. Nelson *et al.* concluded that daclizumab in combination with MMF might be associated with early recurrence of HCV and more rapid histological progression of disease in the early period after LTx^[33]. Also, triple and double immunosuppressive regimens had a higher rate of fibrosis and cirrhosis in HCV infected patients compared to monotherapy^[34,35]. These findings implicate that strenuous induction protocols should be avoided in HCV infected liver recipients.

As proposed by some centers, early withdrawal or avoidance of steroids in HCV infected patients could be beneficial. From our experience with the limited number of HCV infected liver recipients, initial steroid-free immunosuppression is safe, has a low risk of acute rejection without a need for high-dose steroids and high cumulative steroid dosages, which are likely to induce less severe HCV reinfection. Furthermore, none of the HCV infected patients developed serious chronic liver diseases. Therefore, it is high time to seriously reconsider the use of any steroids in liver transplantation especially for HCV-

infection patients and to prove this approach in a large randomized controlled trial.

REFERENCES

- Rosen HR. Hepatitis B and C in the liver transplant recipient: current understanding and treatment. *Liver Transplant* 2001; **7** (11 Suppl 1): S87-98
- European Liver Transplant Registry. <http://www.eltr.org>
- Gane EJ, Naoumov NV, Qian KP. A longitudinal analysis of hepatitis C virus replication following liver transplantation. *Gastroenterology* 1996; **110**: 167-177
- Berenguer M, Ferrell L, Watson J. HCV-related fibrosis progression following liver transplantation: increase in recent years. *J Hepatol* 2000; **32**: 673-684
- Samuel D, Feray C. Recurrence of hepatitis C virus infection after liver transplantation. *J Hepatol* 1999; **31**(Suppl 1): 217-221
- Starzl TE, Waddell WR, Marchioro TL. Reversal of rejection in human renal homografts with subsequent development of homograft tolerance. *Surg Gyn Obst* 1963; **117**: 385
- Braun F, Lorf T, Ringe B. Update of current immunosuppressive drugs used in clinical organ transplantation. *Transplant Int* 1998; **11**: 77-81
- Gane EJ, Portmann BC, Naoumov NV. Long-term outcome of hepatitis C infection after liver transplantation. *N Engl J Med* 1996; **334**: 815-820
- Magy N, Cribier B, Schmitt C. Effects of corticosteroids on HCV infection. *Int J Immunopharmacol* 1999; **21**: 253-261
- McHutchinson JG, Ponnudurai R, Bylund DL. Prednisone withdrawal followed by interferon alpha for treatment of chronic hepatitis C infection. *J Clin Gastroenterol* 2001; **32**: 133-137
- Sreekumar R, Gonzalez-Koch A, Maor-Kendler Y. Early identification of recipients with progressive histologic recurrence of hepatitis C after liver transplantation. *Hepatology* 2000; **32**: 1125-1130
- Prieto M, Berenguer M, Rayón JM. High incidence of allograft cirrhosis in hepatitis C virus genotype 1b following transplantation: relationship with rejection episodes. *Hepatology* 1999; **29**: 250-256
- Ringe B, Braun F, Schütz E. A novel management strategy of steroid-free immunosuppression after liver transplantation: efficacy and safety of tacrolimus and mycophenolate mofetil. *Transplantation* 2001; **71**: 508-515
- Mihm S, Hartmann H, Ramadori G. A reevaluation of the association of hepatitis C virus replication intermediates with peripheral blood cells including granulocytes by a tagged reverse transcription/polymerase chain reaction technique. *J Hepatol* 1996; **24**: 491-497
- Okamoto H, Tokita H, Sakamoto M, Horikita M, Kojima M, Iizuka H. Characterization of the genomic sequence of type V (or 3a) hepatitis C virus isolates and PCR primer for specific detection. *J Gen Virol* 1993; **74**: 2385-2390
- Simmonds P, Mc Omish F, Yap PL, Chan SW, Lin CK, Duscheiko G. Sequence variability in the 5'-noncoding region of hepatitis C virus: identification of a new virus type and restrictions on sequence diversity. *J Gen Virol* 1993; **74**: 661-668
- Wietzke P, Braun F, Ringe B, Ramadori G. Interferon alpha-2a and ribavirin therapy for hepatitis C recurrence after liver transplantation. *Transplant Proc* 2000; **32**: 2539-2542
- Wietzke-Braun P, Meier V, Braun F, Ramadori G. Combination of "low-does" ribavirin and interferon alpha-2a therapy followed by interferon alpha-2a monotherapy in chronic HCV-infected non-responders and relapsers after interferon alpha-2a monotherapy. *World J Gastroenterol* 2001; **7**: 222-227
- Gómez-Manero N, Herrero JI, Quiroga J, Sangro B, Pardo F, Cienfuegos JA, Prieto J. Prognostic model for early acute rejection after liver transplantation. *Liver Transplantation* 2001; **7**: 246-254
- Rosen HR, Shackleton CR, Higa L. Use of OKT3 is associated with early and severe recurrence of hepatitis C after liver transplantation. *Am J Gastroenterol* 1997; **92**: 1453
- Sheiner PA, Schwartz ME, Mor E. Severe or multiple rejection episodes are associated with early recurrence of hepatitis C after orthotopic liver transplantation. *Hepatology* 1995; **21**: 30

- 22 **Rolles K**, Davidson BR, Burroughs AK. A pilot study of immunosuppressive monotherapy in liver transplantation: tacrolimus versus microemulsified cyclosporin. *Transplantation* 1999; **68**: 1195
- 23 **Tisone G**, Angelico M, Palmieri G. A pilot study on the safety and effectiveness of immunosuppression without prednisone after liver transplantation. *Transplantation* 1999; **67**: 1308-1313
- 24 **Watson CJE**, Friend PJ, Jamieson NV, Frick TW, Alexander G, Gimson AE, Calne R. Sirolimus: A potent new immunosuppressant for liver transplantation. *Transplantation* 1999; **67**: 505-509
- 25 **Braun F**, Canelo R, Schütz E. How to handle Mycophenolate Mofetil in combination with Tacrolimus? *Transplant Proc* 1998; **30**: 4094-4095
- 26 **Feray C**, Caccamo L, Graeme J. European collaborative study on factors influencing outcome after liver transplantation for hepatitis C. *Gastroenterology* 1999; **117**: 619
- 27 **Feray C**, Gigou M, Samuel D. Influence of the genotypes of hepatitis C virus on the severity of recurrent liver disease after liver transplantation. *Gastroenterology* 1995; **108**: 1088
- 28 **Gordon FD**, Poterucha JJ, Germer J. Relationship between hepatitis C genotype and severity of recurrent hepatitis C after liver transplantation. *Transplantation* 1997; **63**: 1419
- 29 **Charlton MR**. Mycophenolate and hepatitis C: salve on a wound or gasoline on a fire? *Liver Transplant* 2002; **8**: 47-49
- 30 **Jain A**, Kashyap R, Demetris AJ, Eghstesad B, Pokharna R, Fung JJ. A prospective randomized trial of mycophenolate mofetil in liver transplant recipients with hepatitis C. *Liver Transplant* 2002; **8**: 40-46
- 31 **Wiesner RH**, Rabkin J, Klintmalm G. A randomized double-blind comparative study of mycophenolate mofetil and azathioprine in combination with cyclosporine and corticosteroids in primary liver transplant recipients. *Liver Transplant* 2001; **7**: 442-450
- 32 **Washburn K**, Speeg KV, Esterl R. Steroid elimination 24 hours after liver transplantation using daclizumab, tacrolimus, and mycophenolate mofetil. *Transplantation* 2001; **72**: 1675-1679
- 33 **Nelson DR**, Soldevila-Pico C, Reed A. Anti-Interleukin-2 receptor therapy in combination with mycophenolate mofetil is associated with more severe hepatitis C recurrence after liver transplantation. *Liver Transpl* 2001; **7**: 1064-1070
- 34 **Papatheodoridis GV**, Davies S, Dhillon AP. The role of different immunosuppression in the long-term histological outcome of HCV reinfection after liver transplantation for HCV cirrhosis. *Transplantation* 2001; **72**: 412-418
- 35 **International Panel**. Banff schema for grading liver allograft rejection. *Hepatology* 1997; **25**: 658-63

Edited by Zhu LH Proofread by Xu FM

Genotype and phylogenetic characterization of hepatitis B virus among multi-ethnic cohort in Hawaii

Mayumi Sakurai, Fuminaka Sugauchi, Naoky Tsai, Seiji Suzuki, Izumi Hasegawa, Kei Fujiwara, Etsuro Orito, Ryuzo Ueda, Masashi Mizokami

Mayumi Sakurai, Fuminaka Sugauchi, Seiji Suzuki, Izumi Hasegawa, Kei Fujiwara, Masashi Mizokami, Department of Clinical Molecular Informative Medicine, Nagoya City University Graduate School of Medical Sciences, Nagoya 467-8601, Japan
Etsuro Orito, Ryuzo Ueda, Department of Clinical Internal Medicine and Molecular Science, Nagoya City University Graduate School of Medical Sciences, Nagoya 467-8601, Japan
Naoky Tsai, Division of Gastroenterology, John A. Burns School of Medicine, University of Hawaii, USA
Correspondence to: Dr. Masashi Mizokami, Department of Clinical Molecular Informative Medicine, Nagoya City University Graduate School of Medical Sciences, Kawasumi, Mizuho, Nagoya 467-8601, Japan. mizokami@med.nagoya-cu.ac.jp
Telephone: +81-52-853-8292 **Fax:** +81-52-842-0021
Received: 2003-10-08 **Accepted:** 2004-04-15

Abstract

AIM: Hepatitis B virus (HBV) genomes in carriers from Hawaii have not been evaluated previously. The aim of the present study was to evaluate the distribution of HBV genotypes and their clinical relevance in Hawaii.

METHODS: Genotyping of HBV among 61 multi-ethnic carriers in Hawaii was performed by genetic methods. Three complete genomes and 61 core promoter/precore regions of HBV were sequenced directly.

RESULTS: HBV genotype distribution among the 61 carriers was 23.0% for genotype A, 14.7% for genotype B and 62.3% for genotype C. Genotypes A, B and C were obtained from the carriers whose ethnicities were Filipino and Caucasian, Southeast Asian, and various Asian and Micronesian, respectively. All cases of genotype B were composed of recombinant strains with genotype C in the precore plus core region named genotype Ba. HBeAg was detected more frequently in genotype C than in genotype B (68.4% vs 33.3%, $P < 0.05$) and basal core promoter (BCP) mutation (T1762/A1764) was more frequently found in genotype C than in genotype B. Twelve of the 38 genotype C strains possessed C at nucleotide (nt) position 1858 (C-1858). However there was no significant difference in clinical characteristics between C-1858 and T-1858 variants. Based on complete genome sequences, phylogenetic analysis revealed one patient of Micronesian ethnicity as having C-1858 clustered with two isolates from Polynesia with T-1858. In addition, two strains from Asian ethnicities were clustered with known isolates in carriers from Southeast Asia.

CONCLUSION: Genotypes A, B and C are predominant types among multi-ethnic HBV carriers in Hawaii, and distribution of HBV genotypes is dependent on the ethnic background of the carriers in Hawaii.

Sakurai M, Sugauchi F, Tsai N, Suzuki S, Hasegawa I, Fujiwara K, Orito E, Ueda R, Mizokami M. Genotype and phylogenetic characterization of hepatitis B virus among multi-ethnic cohort

in Hawaii. *World J Gastroenterol* 2004; 10(15): 2218-2222
<http://www.wjgnet.com/1007-9327/10/2218.asp>

INTRODUCTION

Hepatitis B virus (HBV) is one of the major causes of chronic liver diseases including chronic hepatitis, liver cirrhosis (LC) and hepatocellular carcinoma (HCC)^[1]. HBV has been classified into 7 genotypes from A to G based on a sequence divergence of 8% or greater of the entire genome sequences^[2-5]. The genotypes of HBV have distinct geographical distributions, which have been associated with anthropologic history^[6,7].

Recently, genotypes of HBV have been reported to be an influential factor in the clinical manifestation of chronic liver disease in the host. Genotype A is associated with chronic liver disease more frequently than genotype D in Europe^[8]. Genotype C induces more severe liver disease than genotype B found in Asia^[9,10]. Furthermore, it was reported that genotype B had two subgroups^[11], and these subgroups influence the clinical manifestations of liver disease in these patients^[12].

Hawaii has a large Asian American and Pacific Islander population. Many people have emigrated from various countries in Asia and the Pacific Basin, where HBV infection is endemic. Indeed, the estimated rate of HBV carriers in Hawaii ranges from 1.7% to 3%^[13,14], higher than 0.5% of the mainland of United States. However, there has been no information on genotype distribution and sequences of HBV in multi-ethnic carriers in Hawaii.

The aim of this study was to evaluate the HBV genotypes among 61 multi-ethnic carriers in Hawaii by genetic method, and to determine the influences of HBV genotypes on the clinical characteristics.

MATERIALS AND METHODS

Patients

A total of 61 serum samples with HBsAg-positive were collected from patients with HBV infection who admitted St. Francis Medical Center in Honolulu, Hawaii between 1995 and 2000. All the patients were classified into 4 clinical groups: a symptomatic carriers (ASC) ($n=14$) who had no subjective symptoms and had consistently normal serum alanine aminotransferase (ALT) levels for at least 1 year, patients ($n=39$) with chronic liver disease and persistently elevated serum ALT levels, such as those with chronic hepatitis (CH); patients with liver cirrhosis (LC) ($n=4$), and patients with hepatocellular carcinoma (HCC) ($n=4$). A clinical diagnosis was made on the basis of serum biochemical examination, ultrasonography, computerized tomography and liver biopsy performed as required. Patients coinfecting with hepatitis C virus or human immunodeficiency virus were excluded. No patients received antiviral treatment during the follow-up period. The study protocol was approved by the Ethics Committees of the participating institutions in accordance with the 1975 Declaration in Helsinki. Informed consent was obtained from each patient prior to any study related procedures.

Genotyping of HBV

The serum samples were stored at -20 °C until assay was performed. Serum DNA was extracted from 100 µL of serum using a DNA extractor kit (Genome Science Laboratory, Fukushima, Japan). The genotypes of HBV were determined by enzyme-linked immunosorbent assay (ELISA) (HBV GENOTYPE EIA, Institute of Immunology Co., Ltd., Tokyo, Japan) with monoclonal antibodies that are type-specific to epitope in the preS2-region product^[15]. If the result of ELISA was indeterminate, the genotypes were detected by restriction fragment length polymorphism (RFLP), as previously described^[16]. Genotype B was classified into 2 subgroups, "Ba" which has a recombinant sequence of genotype C in the precore/core region, or "Bj" which does not have it, by the method reported previously^[12]. Genotype G of HBV was detected by PCR with hemi-nested primers deduced from the unique insertion of 36 nucleotides (nt) in the core gene that is specific to this genotype^[17].

Sequencing of HBV genome

Three complete genomes and 61 core promoter/precore regions of HBV were amplified by polymerase chain reaction with several primer sets, as previously described^[18]. Amplified HBV DNA fragments were sequenced directly by dideoxy sequencing using a Taq Dye Deoxy Terminator cycle sequencing kit with a fluorescent 3100 DNA sequencer (Applied Biosystems, Foster City, CA, USA). These nucleotide sequences were deposited in the DDBJ/EMBL/GenBank databases under the accession numbers AB105172- AB105174.

Molecular evolutionary analysis of HBV

The pairwise nucleotide sequences were aligned using the CLUSTAL W program^[19]. The genetic distances were calculated with the 6-parameter method, and the phylogenetic tree was constructed by the neighbor-joining method^[20] using

ODEN program (version 1.1.1)^[21]. To confirm the reliability of the phylogenetic tree, bootstrap resampling tests were performed 1 000 times. Reference sequences of HBV, shown as accession numbers, were obtained from the DDBJ/EMBL/GenBank database.

Statistical analyses

Statistical differences were evaluated using the Mann-Whitney nonparametric test, the Fisher's exact probability test and the Student's *t*-test where appropriate. Differences were considered significant for a *P*-value less than 0.05.

RESULTS

Genotypes of HBV

The distribution of HBV genotypes among 61 multi-ethnic carriers in Hawaii was 14(23.0%) for genotype A, 9(14.7%) for genotype B and 38(62.3%) for genotype C. All the 9 genotype B strains were found to be Ba that has a recombinant sequence of genotype C in precore/core region. Genotypes D, E, F and G were not found in this study.

Comparison with clinical characteristics among HBV genotypes

Clinical and serological characteristics were compared among the patients infected with genotypes A, B and C (Table 1). Patients with HBV genotype A were of Filipino (*n*=10), Caucasian (*n*=3) and Polynesian (*n*=1) ethnicities. Genotype B was found in patients of Chinese (*n*=4), Taiwanese (*n*=2), Vietnamese (*n*=2), and Hawaiian/Chinese (*n*=1) ethnicities. Genotype C was found in the patients whose ethnic backgrounds were various Asian (*n*=33), Micronesian (*n*=3), and Caucasian (*n*=2). There were no significant differences in terms of the age, gender, serum AST, ALT, ALP, γ -GTP and the clinical stages of liver disease among them. The proportion of HBeAg positive-phenotype in patients with genotypes A, B

Table 1 Comparison of clinical backgrounds in carriers with HBV genotypes A, B and C

Features	Genotype <i>n</i> (%)				
	A (<i>n</i> =14)	B (<i>n</i> =9)	C (<i>n</i> =38)		
Age (mean±SD, yr)	49.1±14.5	46.9±13.0	43.0±11.9		
Gender (male:female)	10:4	4:5	21:17		
Race	Asian	Mainland Chinese	0(0)	5(33)	10(67)
		Philippine	10(83)	0(0)	2(17)
		Taiwanese	0(0)	2(50)	2(50)
		Hong Kong	0(0)	0(0)	8(100)
		Vietnamese	0(0)	2(40)	3(60)
		Korean	0(0)	0(0)	7(100)
		Japanese	0(0)	0(0)	1(100)
		Micronesian	0(0)	0(0)	3(100)
		Polynesian	1(100)	0(0)	0(0)
		Caucasian	3(60)	0(0)	2(40)
Liver disease		ASC	2(14)	3(33)	9(24)
		CH	10(71)	5(56)	24(63)
		LC	2(14)	1(11)	1(3)
		HCC	0(0)	0(0)	4(11)
		HBeAg (+)	8(57)	3(33) ^a	26(68) ^a
Laboratory finding		AST (U/L)	63.3±42.2	56.6±58.7	54.7±81.9
		ALT (U/L)	41.4±31.6	34.8±27.0	37.3±59.7
		ALP (U/L)	359.9±139.4	287.3±140.2	328.0±166.2
		γ -GTP (U/L)	121.0±121.3	55.9±37.2	66.8±103.0

^a*P*<0.05 between genotypes B and C. ASC: Asymptomatic carrier; CH: Chronic hepatitis; LC: Liver cirrhosis; HCC: Hepatocellular carcinoma; ALT: Alanine aminotransferase; AST: Aspartate aminotransferase; ALP: Alkaline phosphatase; γ -GTP: γ -glutamyl transpeptidase.

and C was 57.1%, 33.3% and 68.4% respectively, with a significant difference observed between genotypes B and C ($P < 0.05$). HCC was found in 10.5% of patients with genotype C.

Comparison with core promoter/precure sequences

The frequency of mutation in core promoter (nt 1762/1764) and precure (nt 1858 and nt 1896) region was compared among genotypes A, B and C (Table 2). No significant differences in the frequency of the core promoter mutants were found among genotypes A, B and C (21.4%, 44.4%, and 57.9% respectively). Precure stop mutation (A-1896) was detected in genotypes B and C (33.3% and 21.1%) but not detected in genotype A. Sequence analysis of the mutation at nt 1858 in the precure region showed that all genotype B strains and 68% of genotype C strains possessed a T nucleotide (T-1858). In contrast, all genotype A strains had a C nucleotide in this region (C-1858).

HBV genotype C with C-1858 or T-1858

In order to clarify the significance of nucleotide variety (C or T) at nt 1858 in clinical and virological characteristics, 12 genotype C strains with C-1858 were compared to that of 26 strains of

genotype C with T-1858 (Table 3). All strains of both groups were obtained only from carriers whose ethnic background is Asian. HBeAg positive-phenotype was more frequent in genotype C patients with C-1858 than in those with T-1858 (83.3% vs 61.5%). The precure stop mutation (A-1896) was found in 30.8% (8/26) of those with genotype C with nucleotide T-1858, but not in those subjects with the C-1858 nucleotide. There were no significant differences in frequencies in terms of the age, gender, serum AST, ALT, ALP, γ -GTP and the clinical stages of liver disease and BCP mutation between them.

Phylogenetic analysis

To clarify the phylogenetic characterization of genotype C with C-1858, the complete genome of three HBV strains in carriers was sequenced. These subjects were from Micronesia (HI-1), Hong Kong (HI-2) and Vietnam (HI-3). Molecular evolutionary analysis was also conducted (Figure 1). Of them, one strain (HI-1) was clustered into a subgroup of genotype C with T-1858 from Polynesian with significant bootstrap values. The HI-2 and HI-3 strains were clustered into a subgroup of genotype C from Thailand and Vietnam, and separated from

Table 2 Comparison of core promoter/precure sequences between genotypes A, B and C

Mutation		Genotype <i>n</i> (%)		
		A (<i>n</i> =14)	B (<i>n</i> =9)	C (<i>n</i> =38)
CP mutation	Double mutation	3(21)	4(44)	22(58%)
PC mutation	nt 1858	Cytosine (C)	14(100)	0(0)
		Thymine (T)	0(0)	9(100)
	nt 1896	Guanine (G)	14(100)	6(67)
		Adenine (A)	0(0)	3(33)

CP: Core promoter; PC: Precure; nt: Nucleotide.

Table 3 Clinical and virological characteristics in carriers of genotype C with C-1858 or T-1858

		Mutation <i>n</i> (%)	
		C-1858 (<i>n</i> =12)	T-1858 (<i>n</i> =26)
Age (mean±SD, yr)		41.7±13.0	43.5±11.6
Gender (male:female)		9:3	12:14
Race	Asian		
	Mainland Chinese	3(30)	7(70)
	Filipino	0(0)	2(100)
	Taiwanese	0(0)	2(100)
	Hong Kong	3(38)	5(63)
	Vietnamese	2(67)	1(33)
	Korean	1(14)	6(86)
	Japanese	0(0)	1(100)
	Micronesian	2(100)	0(0)
	Polynesian	0(0)	0(0)
	Caucasian	1(50)	1(50)
	Liver disease	ASC	2(17)
CH		8(67)	21(60)
LC		1(8)	1(3)
HCC		1(8)	3(9)
Laboratory finding		HBeAg (+)	10(83)
	AST (U/L)	34.9±17.0	63.8±97.6
	ALT (U/L)	23.2±11.2	43.8±71.3
	ALP (U/L)	334.6±186.3	324.9±157.0
	γ -GTP (U/L)	87.8±167.3	57.2±48.4
CP mutation	Double mutation	6(50)	16(62)
PC mutation	A-1896	0(0)	8(31)

ASC: Asymptomatic carrier; CH: Chronic hepatitis; LC: Liver cirrhosis; HCC: Hepatocellular carcinoma; ALT: Alanine aminotransferase; AST: Aspartate aminotransferase; ALP: Alkaline phosphatase; γ -GTP: γ -glutamyl transpeptidase; CP: Core promoter; PC: Precure.

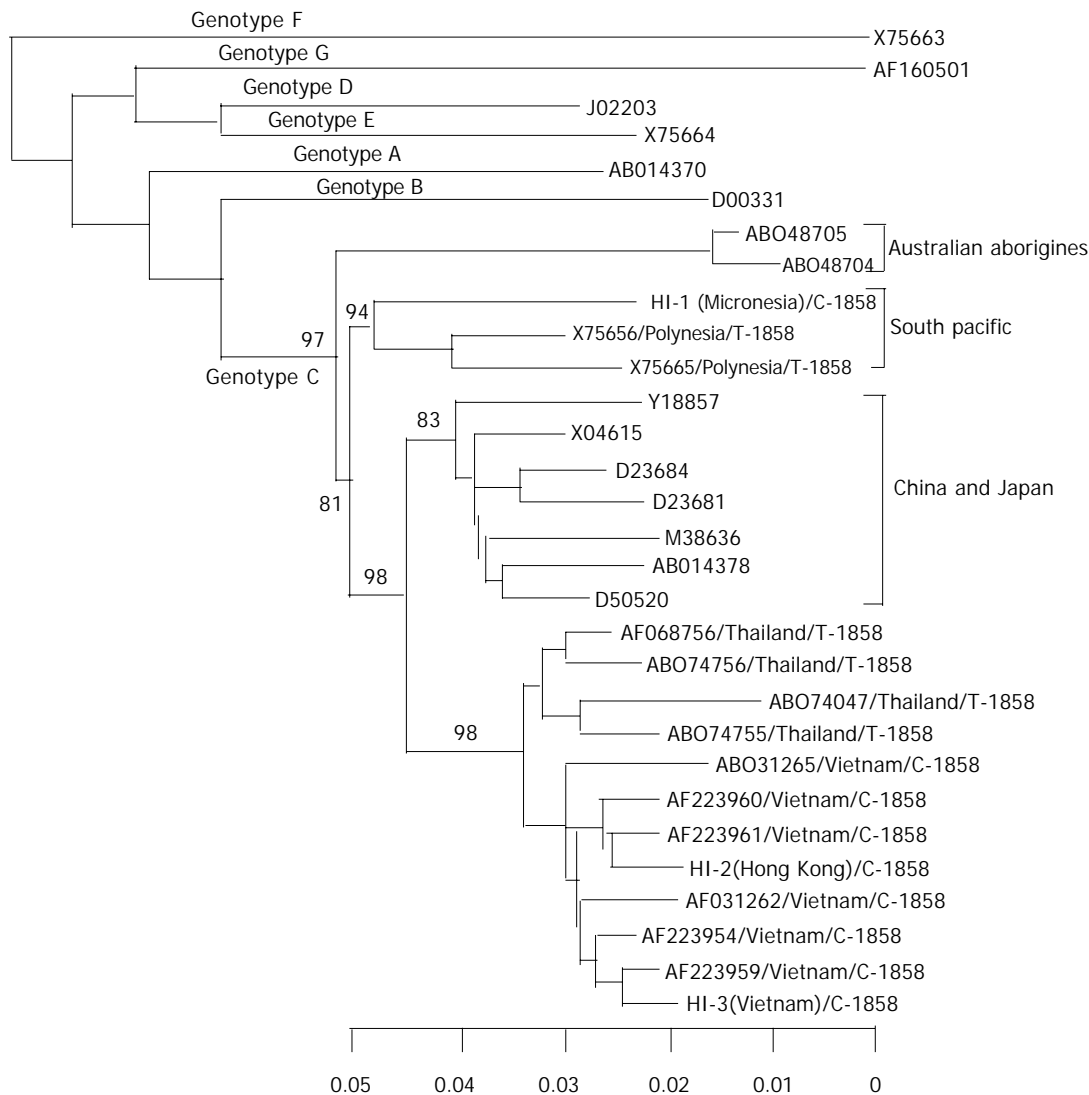


Figure 1 A phylogenetic tree based on the complete genome sequences of hepatitis B virus with 27 reference strains. Isolate names of HI-1, HI-2 and HI-3 were sequenced in this study. The length of the horizontal bar indicates the number of nucleotide substitutions per site. Numbers beside the main roots are the results of bootstrap analysis.

those strains of China and Japan. Moreover, the strains from Thailand and Vietnam had separate branches, and Hawaiian strains were clustered into the branch with Vietnam strains. Interestingly, all strains from Vietnam had C-1858, and those from Thailand had T-1858.

DISCUSSION

The findings of the present study indicate that HBV genotypes A, B and C are prevalent in Hawaii, and genotype C is the major genotype. Most cases of genotype A were found in immigrants from the Philippines and countries known to be prevalent regions for genotype A^[6]. Genotype B was found only in immigrants from Asian regions where genotype B was endemic. In addition, genotype C was obtained from immigrant who came from various Asian countries, where genotype C was prevalent^[22]. These results indicate that the distribution of HBV genotypes in Hawaii is associated with their respective ethnic background.

Recently, it was reported that genotype B could be classified into the Bj (j standing for Japan) and Ba (a standing for Asia) subgroups. Ba shared a genomic sequence with genotype C in the precore/core region, which was prevalent in Asian countries. Bj was restricted to Japan, and did not have this recombination^[11]. It was shown that Ba induces more severe liver disease than Bj

due to delayed seroconversion of HBeAg^[12]. In this study, we found that genotype B, prevalent in Hawaii, was classified as Ba because they were all obtained from carriers with Asian ethnicity (excluding Japanese). In addition, the rate of positive HBeAg (33.3%) and basal core promoter (BCP) mutation (44.4%) in patients of Hawaii infected with genotype B were higher than those in Japanese patients with genotype B^[9]. This result is also consistent with a previous report.

The double mutation in the core promoter, A-to-T mutation at nt 1762 and G-to-A mutation at nt 1764, was associated with reduced synthesis of precore mRNA^[23,24]. In addition, it has been reported that the BCP mutation was associated with the progression of liver disease^[25]. In this study, although it was not significant, BCP mutation was detected more frequently in genotype C than in genotype B. This result supports our previous observation that the BCP mutation was significantly more frequent in genotype C patients than in genotype B patients^[9]. In addition, the present study demonstrated that the proportion of HBeAg positivity in genotype C was significantly higher than that in genotype B (68.4% vs 33.3%). However, our study could not show the clinical difference between genotypes B and C most likely due to the small number of patients studied. In the future, a case-controlled study in multi-ethnic carriers with larger samples is required to confirm

if genotype C could induce more severe liver disease than genotype B^[9,10].

Interestingly, we detected 12 strains of genotype C possessing C-1858 in Hawaii. HBV strain with C-1858 could prevent the A-1896 precore mutation from shutting off the synthesis of HBeAg^[26]. This C-1858 variant was frequently found in genotypes A and F^[26]. In genotype C, the C-1858 variant was observed in Southeast Asian patients, and the phylogenetic origin of genotype C with C-1858 variant has been reported from Vietnam recently. In this study, the complete genomes of 3 genotype C strains with C-1858 were sequenced. One strain obtained from a Micronesian patient with C-1858 was clustered with previously reported Polynesian strains with T-1858. This indicates that both the C-1858 and T-1858 strains of genotype C are endemic to South Pacific countries. Two other strains obtained from patients with Hong Kong and Vietnamese ethnicities were clustered with the strains of genotype C from Southeast Asian countries. This result is consistent with geographic distribution of HBV genotype^[18]. Interestingly, in this subgroup, there were 2 variants of strains, one had C-1858, prevalent in Vietnam, and the other had T-1858, prevalent in Thailand.

The clinical significance of C-1858 or T-1858 among genotype C is not well known. In this study, we compared the clinical and laboratory characteristics between C-1858 and T-1858 variant, but there were no significant differences between them. The number of patients was not enough to clarify the importance of this variation, and its significance for clinical characteristics remains unknown. Further studies would be required using larger numbers of samples.

In conclusion, genotypes A, B and C are the predominant types among multi-ethnic HBV carriers in Hawaii, and the distribution of these genotypes is dependent on the ethnic origin of the carriers in Hawaii. The influence of these genotypes on the clinical manifestations of these HBV carriers in Hawaii is not well defined due to the current small sample size. Case-controlled study with larger cohorts from our unique community is needed.

REFERENCES

- 1 Lee WM. Hepatitis B virus infection. *N Engl J Med* 1997; **337**: 1733-1745
- 2 Okamoto H, Tsuda F, Sakugawa H, Sastrosowignjo RI, Imai M, Miyakawa Y, Mayumi M. Typing hepatitis B virus by homology in nucleotide sequence: comparison of surface antigen subtypes. *J Gen Virol* 1998; **69**: 2575-2583
- 3 Nordor H, Hammas B, Lofdahl S, Courouce AM, Magnus LO. Comparison of the amino acid sequences of nine different serotypes of hepatitis B surface antigen and genomic classification of the corresponding hepatitis B virus. *J Gen Virol* 1992; **73**: 1201-1208
- 4 Nordor H, Courouce AM, Magnus LO. Complete genome, phylogenetic relatedness, and structural protein of six strains of the hepatitis B virus, four of which represent two new genotypes. *Virology* 1994; **198**: 489-503
- 5 Stuyver L, De Gendt S, Van Geyt C, Zoulim F, Fried M, Schinazi RF, Rossau R. A new genotype of hepatitis B virus: Complete genome and phylogenetic relatedness. *J Gen Virol* 2000; **81**: 67-74
- 6 Nordor H, Hammas B, Lee SD, Bile K, Courouce AM, Mushahwar IK, Magnus LO. Genetic relatedness of hepatitis B viral strains of diverse geographical origin and natural variations in the primary structure of the surface antigen. *J Gen Virol* 1993; **74**: 1341-1348
- 7 Orito E, Ichida T, Sakugawa H, Sata M, Horiike N, Hino K, Okita K, Okanoue T, Iino S, Tanaka E, Suzuki K, Watanabe H, Hige S, Mizokami M. Geographic distribution of hepatitis B virus (HBV) genotype in patients with chronic HBV infection in Japan. *Hepatology* 2001; **34**: 590-594
- 8 Mayerat C, Mantegani A, Frei PC. Does hepatitis B virus (HBV) genotype influence the clinical outcome of HBV infection. *J Viral Hepat* 1999; **6**: 299-304
- 9 Orito E, Mizokami M, Sakugawa H, Michitaka K, Ishikawa K, Ichida T, Okanoue T, Yotsuyanagi H, Iino S. A case-control study for clinical and molecular biological differences between hepatitis B viruses of genotypes B and C. *Hepatology* 2001; **33**: 218-223
- 10 Kao JH, Chen PJ, Lai MY, Chen DS. Hepatitis B genotypes correlate with clinical outcomes in patients with chronic hepatitis B. *Gastroenterology* 2000; **118**: 554-559
- 11 Sugauchi F, Orito E, Ichida T, Kato H, Sakugawa H, Kakumu S, Ishida T, Chutaputti A, Lai CL, Ueda R, Miyakawa Y, Mizokami M. Hepatitis B virus of genotype B with or without recombination with genotype C over the precore region plus the core gene. *J Virol* 2002; **76**: 5985-5992
- 12 Sugauchi F, Orito E, Ichida T, Kato H, Sakugawa H, Kakumu S, Ishida T, Chutaputti A, Lai CL, Gish RG, Ueda R, Miyakawa Y, Mizokami M. Epidemiological and virological characteristics of hepatitis B virus genotype B having the recombination with genotype C. *Gastroenterology* 2003; **124**: 925-932
- 13 Ching N, Lumeng J, Pang R, Pang G, Or FW, Ching N, Ching C. Long term low dose interferon alpha-2b in multi-ethnic patients in Hawaii. *Hawaii Med J* 1996; **55**: 201-203
- 14 Pon EW, Ren H, Margolis H, Zhao Z, Schatz GC, Diwan A. Hepatitis B virus infection in Honolulu students. *Pediatrics* 1993; **92**: 574-578
- 15 Usuda S, Okamoto H, Iwanari H, Baba K, Tsuda F, Miyakawa Y, Mayumi M. Serological detection of hepatitis B virus genotypes by ELISA with monoclonal antibodies to type-specific epitopes in the preS2-region product. *J Virol Methods* 1999; **80**: 97-112
- 16 Mizokami M, Nakano T, Orito E, Tanaka Y, Sakagawa H, Mukaide M, Robertson BH. Hepatitis B virus genotype assignment using restriction fragment length polymorphism patterns. *FEBS Lett* 1999; **450**: 66-71
- 17 Kato H, Orito E, Sugauchi F, Ueda R, Gish RG, Usuda S, Miyakawa Y, Mizokami M. Determination of hepatitis B virus genotype G by polymerase chain reaction with hemi-nested primers. *J Virol Methods* 2001; **98**: 153-159
- 18 Sugauchi F, Mizokami M, Orito E, Ohno T, Kato H, Suzuki S, Kimura Y, Ueda R, Butterworth LA, Cooksley WG. A novel variant genotype C of hepatitis B virus identified in isolates from Australian Aborigines: Complete genome sequence and phylogenetic relatedness. *J Gen Virol* 2001; **82**: 883-892
- 19 Thompson JD, Higgins DG, Gibson TJ. CLUSTAL W: improving the sensitivity of progressive multiple sequence alignment through sequence weighting, position-specific gap penalties and weight matrix choice. *Nucleic Acids Res* 1994; **22**: 4673-4680
- 20 Saitou N, Nei M. The neighbor-joining method: a new method for reconstructing phylogenetic trees. *Mol Biol Evol* 1987; **4**: 406-425
- 21 Ina Y. ODEN: a program package for molecular evolutionary analysis and database search of DNA and amino acid sequences. *Comput Appl Biosci* 1994; **10**: 11-12
- 22 Kao JH. Hepatitis B viral genotypes: clinical relevance and molecular characteristics. *J Gastroenterol Hepatol* 2002; **17**: 643-650
- 23 Okamoto H, Tsuda F, Akahane Y, Sugai Y, Yoshihara M, Moriyama K, Tanaka T, Miyakawa Y, Mayumi M. Hepatitis B virus with mutations in the core promoter for an e antigen-negative phenotype in carriers with antibody to e antigen. *J Virol* 1994; **68**: 8102-8110
- 24 Buckwold VE, Xu Z, Chen M, Yen TS, Ou JH. Effects of a naturally occurring mutation in the hepatitis B virus basal core promoter on precore gene expression and viral replication. *J Virol* 1996; **70**: 5845-5851
- 25 Takahashi K, Aoyama K, Ohno N, Iwata K, Akahane Y, Baba K, Yoshizawa H, Mishiro S. The precore/core promoter mutant (T1762A1764) of hepatitis B virus: clinical significance and an easy method for detection. *J Gen Virol* 1995; **76**: 3159-3164
- 26 Li JS, Tong SP, Wen YM, Vitvitski L, Zhang Q, Trepo C. Hepatitis B virus genotype A rarely circulates as an HBe-minus mutant: possible contribution of a single nucleotide in the precore region. *J Virol* 1993; **67**: 5402-5410

HCV NS5A abrogates p53 protein function by interfering with p53-DNA binding

Guo-Zhong Gong, Yong-Fang Jiang, Yan He, Li-Ying Lai, Ying-Hua Zhu, Xian-Shi Su

Guo-Zhong Gong, Yong-Fang Jiang, Yan He, Li-Ying Lai, Ying-Hua Zhu, Xian-Shi Su, Center for Liver Diseases, Second Xiangya Hospital, Central South University, Changsha 410011, Hunan Province, China

Supported by the National Natural Science Foundation of China, No. 3967067

Correspondence to: Dr. Guo-Zhong Gong, Center for Liver Diseases, Second Xiangya Hospital, Central South University, 86 Renmin Zhong Road, Changsha 410011, Hunan Province, China. guozhong_gong@hotmail.com

Telephone: +86-731-5524222 **Fax:** +86-731-5533525

Received: 2003-12-12 **Accepted:** 2004-01-08

Abstract

AIM: To evaluate the inhibition effect of HCV NS5A on p53 transactivation on p21 promoter and explore its possible mechanism for influencing p53 function.

METHODS: p53 function of transactivation on p21 promoter was studied with a luciferase reporter system in which the luciferase gene is driven by p21 promoter, and the p53-DNA binding ability was observed with the use of electrophoretic mobility-shift assay (EMSA). Lipofectin mediated p53 or HCV NS5A expression vectors were used to transfect hepatoma cell lines to observe whether HCV NS5A could abrogate the binding ability of p53 to its specific DNA sequence and p53 transactivation on p21 promoter. Western blot experiment was used for detection of HCV NS5A and p53 proteins expression.

RESULTS: Relative luciferase activity driven by p21 promoter increased significantly in the presence of endogenous p53 protein. Compared to the control group, exogenous p53 protein also stimulated p21 promoter driven luciferase gene expression in a dose-dependent way. HCV NS5A protein gradually inhibited both endogenous and exogenous p53 transactivation on p21 promoter with increase of the dose of HCV NS5A expression plasmid. By the experiment of EMSA, we could find p53 binding to its specific DNA sequence and, when co-transfected with increased dose of HCV NS5A expression vector, the p53 binding affinity to its DNA gradually decreased and finally disappeared. Between the Huh 7 cells transfected with p53 expression vector alone or co-transfected with HCV NS5A expression vector, there was no difference in the p53 protein expression.

CONCLUSION: HCV NS5A inhibits p53 transactivation on p21 promoter through abrogating p53 binding affinity to its specific DNA sequence. It does not affect p53 protein expression.

Gong GZ, Jiang YF, He Y, Lai LY, Zhu YH, Su XS. HCV NS5A abrogates p53 protein function by interfering with p53-DNA binding. *World J Gastroenterol* 2004; 10(15): 2223-2227
<http://www.wjgnet.com/1007-9327/10/2223.asp>

INTRODUCTION

Hepatitis C virus (HCV) is recognized as a major causative agent leading to chronic hepatitis and cirrhosis^[1-3], which have a close relationship with the development of hepatocellular carcinoma (HCC)^[4,5]. HCV is a positive single-stranded RNA virus belonging to the Flaviridae family, and its genome only contains a single long open reading frame encoding a large polyprotein precursor that is thereafter processed by a combination of cellular and viral proteases into several mature proteins, including three or four structural proteins (core, E1, E2/P7) and at least 6 nonstructural proteins (NS): NS2, NS3, NS4A, NS4B, NS5A, NS5B^[6]. HCV NS5A as a nonstructural protein does not assemble into the HCV particles, but still has a lot of functions in the HCV replication and the development of chronic liver disease and hepatocellular carcinoma. Recent studies showed that HCV NS5A could interact with a number of cellular proteins including PKR, p53, Grb2 and Cdk1^[7-10], and enhance expression of some genes related to cell proliferation such as PCNA, NF- κ B, Stat-3, SRCAP and IL-8^[11-14], indicating that HCV NS5A has a critical role in promoting cell proliferation and malignant transformation. HCV NS5A prevents p53 and TNF- α mediated apoptosis^[15-17], and possibly perturbs the DNA repair when cells are treated with DNA damage agents including viruses, toxins or physical damage. HCV NS5A is important for the HCV replication. It can form a complex with an SNARE-like protein, hVAP-33 and HCV NS5B^[18] and can associate with ER and Golgi complex, and the amphipathic helix (AH) of the HCV NS5A is necessary for this membrane localization and for HCV RNA replication^[19,20]. Interaction of HCV NS5A with La protein can also maintain and benefit HCV RNA replication and HCV protein translation^[21,22]. Sequence mutation in HCV NS5A might be a reason for the responsiveness in the patient who received IFN treatment^[23-25]. The patients with wild type of interferon sensitive-determining region (ISDR) in HCV NS5A usually have a lower responsive rate to the IFN therapy, and the mechanism is that the wild type ISDR can bind PKR, which is induced by IFN and has an anti-viral activity, and can disrupt PKR function^[7,26,27]. The tumor suppressor p53 protein has been reported to possess a number of important functions. Activated p53 can transactivate a lot of target genes, maintain normal cell cycle through inducing apoptosis and repairing damaged DNA, and suppressing oncogenic transformation. In this study we explored the interaction between HCV NS5A and p53 and the mechanism by which the HCV NS5A abrogated the p53 transactivation.

MATERIALS AND METHODS

Cell lines and plasmids

P^{C53-NS3}, P^{wwp-luc} and P^{wwp-mut-luc} were kind gifts from Professor Vogelstein (The Johns Hopkins University). P^{C53-NS3} is an eukaryotic expression vector that is constructed by cloning normal human p53 cDNA into p^{CMV} plasmid. P^{wwp-luc} carries luciferase reporter gene driven by p21 promoter that contains the specific consensus DNA sequence binding to p53 protein. P^{wwp-mut-luc} is approximately the same vector as P^{wwp-luc} except for deletion mutation introduced in the p53 binding sequence

of p21 promoter. P^{CNS5A} is made in Dr. Siddiqui's laboratory (University of Colorado, USA) through inserting of HCV NS5A cDNA into P^{CMV} plasmid^[12]. The liver carcinoma cell lines Huh7 with p53 gene mutation and HepG2 with wild-type p53 gene were from ATCC(USA) and maintained in Dulbecco's Modified Eagle Medium (Life Technologies, USA) complemented with 100 mL/L fetal calf serum. The cells were transfected by the individual plasmids with Lipofectin reagent (Life Technologies, USA) when they became 60-70% confluent. Forty-eight hours after transfection, the cells were harvested for the analysis of relative luciferase activity and electrophoretic mobility shift assay (EMSA).

Relative luciferase activity assay

After 48 h of transfection, cells in the plates were washed two times with PBS, and then 750 μ L lysis buffer (0.1 mmol/L K₂HPO₄, pH 7.8, 10 mmol/L DTT, 5 g/L NP-40) was added onto plates. The plates were then placed on ice for 15 min and then cells were transferred into a clean 1.5-mL Eppendorf tube. After centrifugation at 15 000 g for 10 min, the supernatants were collected for further experiment. For relative luciferase activity assay, 0.4 mL determination buffer (0.1 mmol/L K₂HPO₄, pH 7.8, 0.15 mmol/L MgSO₄, 10 mmol/L DTT, 0.5 mmol/L ATP) and the different volumes of supernatant containing equivalent protein were put into 5-mL glass tube to observe the times of luminescence within 10 s using a luminometer (Optocomp II, MGM, USA). The experiment was repeated three times and each in triplicate.

Electrophoretic mobility-shift assay (EMSA)

In this experiment, we investigated the ability of p53 binding to the specific consensus DNA sequence, and studied if the binding could be influenced by HCV NS5A. Briefly, this experiment was done as following: (1) Labeling of DNA probe: 50 pmol chemically synthesized oligonucleotide 5' - GGACATGCCCGG GCATGTCC -3' which is the specific consensus DNA sequence to bind p53, 2 μ L γ -P³² ATP (74 000 GBq/mmol), 20 U T₄ polynucleotide kinase, 2 μ L reaction buffer and incubated for 30 min at 37 °C, then 60 μ L dH₂O was added to the mixture and the labeled oligonucleotides were purified from the free γ -P³² ATP by use of Sephadex-G25. The purified P³²-labeled DNA probe was stored at -20 °C until use. (2) Nuclear protein isolation: After transfection with different plasmids for 48 h, cells were washed 3 times with PBS and scrapped down from the plates and then transferred into 1.5-mL Eppendorf tubes and washed 3 times again with PBS. Lysis buffer 30 μ L (20 mmol/L Hepes, pH 7.9, 10 mmol/L KCl, 10 mmol/L Na₃VO₄, 1 mmol/L ETDA, 100 mL/L glycerol, 1 mmol/L PMSF, 3 g/L aprotinin, 1 g/L leupeptin, 1 mmol/L DTT, 2 g/L NP-40, 20 mmol/L NaF) was added to suspend the cells. After 15 min on ice, and centrifugation at 15 000 \times g for 1 min, the supernatant was discarded and the pellet resuspended in 20 μ L nuclear extract buffer (20 mmol/L Hepes, pH 7.9, 10 mmol/L KCl, 420 mmol/L NaCl, 10 mmol/L Na₃VO₄, 1 mmol/L ETDA, 200 mL/L glycerol, 1 mmol/L PMSF, 3 g/L aprotinin, 1 g/L leupeptin, 1 mmol/L DTT, 20 mmol/L NaF). After incubation at 4 °C for 30 min. with mild agitation, and centrifugation at 15 000 g for 5 min, aliquot supernatants were collected and stored at -70 °C until use. (3) Assessment of p53 binding to DNA probe: For each reaction tube, the followings were added: 2 μ g nuclear extraction protein, 2 μ L labeled probe containing p53 binding sequence, 1.5 μ L EMSA reaction buffer (50 mmol/L NaCl, 0.5 mmol/L ETDA, 40 mL/L glycerol, 1 mmol/L MgCl₂, 1 mmol/L DTT, 10 mmol/L Tris-Cl, pH 7.5, 0.05 g/L poly (dI-dC)) and dH₂O to a total volume of 15 μ L. After incubation for 30 min on ice, 20 μ L of samples was loaded onto 60 g/L undenatured PAGE and run at 160 V for approximately 6 h. The gel was dried and autoradiographed at -70 °C for about 16 h.

Western blotting to detect p53 and HCV NS5A protein expression

Cell lysates of Huh7 cells transfected with P^{C53-NS3} or co-transfected with P^{CNS5A} were made by routine method. The same amount of total protein from the cell lysate was used to load onto 120 g/L PAGE, and then transferred onto PV (polyvinylidene difluoride) membrane. After blocked in block solution (20 mmol/L Tris-HCl, pH 7.5, 150 mmol/L NaCl, 3 g/L PVP, 5 g/L Tween 20) for 2 h, the membrane was probed by anti-HCV NS5A or anti-p53, washed and incubated with the second enzyme-labeled antibody, and then observed by using an ECL kit (Boehringer Mannheim Co., Germany).

Statistical analysis

Statistical significance of differences between the 2 groups was determined by applying Student's *t* test or two-sample *t* test. Statistical significance of differences in more than 3 groups was determined by applying one-way ANOVA. A *P* value less than 0.05 was considered significant.

RESULTS

HCV NS5A protein inhibited the transactivation of endogenous p53 on p21 promoter

Relative luciferase activities in P^{wpp-luc}-transfected HepG2 cells (3.95×10^5) were significantly higher than that in P^{wpp-mut-luc} group (0.60×10^5 , $t=5.92$, $P<0.01$). Compared to P^{wpp-luc}-transfected HepG2 cells, the relative luciferase activities in the HepG2 cells co-transfected with P^{wpp-luc} and P^{CNS5A} decreased in a P^{CNS5A} dose- dependent manner ($F=20.71$, $P<0.01$), suggesting that HCV NS5A protein can inhibit the transactivation of endogenous p53 on p21 promoter. In contrast, the relative luciferase activities of the HepG2 cells co-transfected with P^{wpp-mut-luc} and P^{CNS5A} had little change ($F=0.76$, $P>0.05$) in comparison with P^{wpp-mut-luc}-transfected HepG2 cells. Those results indicated that endogenous p53 has a transactivation on p21 promoter, and HCV NS5A down-regulated p21 promoter activity through inhibiting endogenous p53 activity (Table 1).

Table 1 HCV NS5A inhibits the transactivation of endogenous p53 on p21 promoter

Group	Relative luciferase activity	<i>F</i>	<i>P</i>
P ^{wpp-luc} (1 μ g)			
+ P ^{CNS5A} (0 μ g)	3.49×10^{5b}	20.71	<0.01
+ P ^{CNS5A} (0.5 μ g)	2.69×10^5		
+ P ^{CNS5A} (1.0 μ g)	1.62×10^5		
+ P ^{CNS5A} (2.0 μ g)	0.58×10^5		
P ^{wpp-mut-luc} (1.0 μ g)			
+ P ^{CNS5A} (0 μ g)	0.60×10^5	0.76	>0.05
+ P ^{CNS5A} (0.5 μ g)	0.65×10^5		
+ P ^{CNS5A} (1.0 μ g)	0.62×10^5		
+ P ^{CNS5A} (2.0 μ g)	0.64×10^5		

^b $t=5.92$, $P<0.01$.

HCV NS5A protein abrogated exogenous p53 transactivation on p21 promoter

The mean of relative luciferase activity in the Huh7 cells individually transfected with P^{wpp-luc} and P^{wpp-mut-luc} was 0.47×10^5 and 0.45×10^5 respectively and there were no statistically differences between these two groups ($t=1.16$, $P>0.05$). This might be because p53 gene in Huh7 cells has been mutated and p53 protein has lost its normal transactivation function, therefore, no matter what happened to p21 promoter (wild type or mutated), the expression of p21 promoter driven luciferase gene was not affected. When P^{wpp-luc} or P^{wpp-mut-luc} was co-

transfected with $P^{C53-NS3}$ into Huh7 cells, respectively, the relative luciferase activities in the $P^{wpp-luc} + P^{C53-NS3}$ group greatly increased ($\chi=5.63 \times 10^5$), but the relative luciferase activities in the $P^{wpp-mut-luc} + P^{C53-NS3}$ group only mild increased ($\chi=0.50 \times 10^5$), and a remarkable variance between the two groups existed ($t=10.12$, $P<0.01$). These results indicated that exogenous p53 should have a strong transactivation on p21 promoter. In order to see if HCV NS5A protein has any effect on the exogenous p53 transactivation, we used P^{CNS5A} , $P^{C53-NS3}$ and $P^{wpp-luc}$ to co-transfect Huh7 cells, and the result showed that the relative luciferase activities in the $P^{CNS5A}+P^{C53-NS3}+P^{wpp-luc}$ group cells decreased in a P^{CNS5A} dose-dependent way ($F=24.23$, $P<0.01$). P^{CNS5A} and $P^{wpp-luc}$ were also used to transfect Huh7 cells to find out if HCV NS5A had a direct effect on p21 promoter. The result showed that HCV NS5A did not increase or decrease the relative luciferase activity. From those experiments we proposed that HCV NS5A down-regulated p21 promoter activity by inhibiting exogenous p53 activity, and not by HCV NS5A's direct effect on p21 promoter (Tables 2, 3).

Table 2 HCV NS5A inhibits exogenous p53 transactivation on p21 promoter

Group	Relative luciferase activity	F	P
$P^{wpp-luc}$ (1 μ g)	0.47×10^{5ab}	24.23	<0.01
+ $P^{C53-NS3}$ (1 μ g)	5.63×10^{5b}		
+ P^{CNS5A} (0.5 μ g)	1.61×10^5		
+ P^{CNS5A} (1.0 μ g)	0.69×10^5	0.69	>0.05
$P^{wpp-mut-luc}$ (1 μ g)	0.45×10^{5a}		
+ $P^{C53-NS3}$ (1 μ g)	0.50×10^5		
+ P^{CNS5A} (0.5 μ g)	0.43×10^5		
+ P^{CNS5A} (1.0 μ g)	0.48×10^5		

^a $t=1.16$, $P>0.05$; ^b $t=10.12$, $P<0.01$.

Table 3 HCV NS5A and p21 promoter activity

Group	Relative luciferase activity	F	P
$P^{wpp-luc}$ (1.0 μ g)	0.44×10^5	0.52	>0.05
+ P^{CNS5A} (0.5 μ g)	0.46×10^5		
+ P^{CNS5A} (1.0 μ g)	0.43×10^5		
$P^{wpp-luc}$ (1.0 μ g)	0.56×10^5	28.16	<0.01
+ P^{C53-NS} (0.5 μ g)	2.68×10^5		
+ P^{C53-NS} (1.0 μ g)	4.84×10^5		

HCV NS5A inhibited p53 protein transactivation through abrogation of p53 binding to the specific DNA

Through EMSA, the band of specific p53 and DNA probe complex was found in the nuclear lysates prepared from Huh7 cells transfected with $P^{C53-NS3}$, and verified by the appearance of the supershift after addition of the monoclonal anti-p53 (a generous gift of Dr. Harris, USA) or polyclonal anti-HCV NS5A antibody (a generous gift of Professor Rice, USA) in the EMSA mixtures. This p53-probe complex band did not occur in the nuclear lysates prepared from Huh7 cells untransfected with plasmids or only transfected with P^{CNS5A} , suggesting there is wild-type p53 protein expressed in these cells. In the next experiment, we used different doses of P^{CNS5A} and constant amount (1 μ g) of $P^{C53-NS3}$ to co-transfect Huh7 cells. The p53-probe band became gradually weakened and finally disappeared with increasing doses of P^{CNS5A} , suggesting that HCV NS5A could inhibit p53 transactivation through disruption of the binding of p53 to its specific consensus DNA (Figure 1).

HCV NS5A had no effect on p53 protein expression

p53 protein was expressed at about the same level between the Huh7 cells transfected with p53 expression vector and the Huh7

cells co-transfected with P^{CNS5A} and p53 expression vectors (Figure 2). This result indicates that HCV NS5A does not affect p53 protein expression.

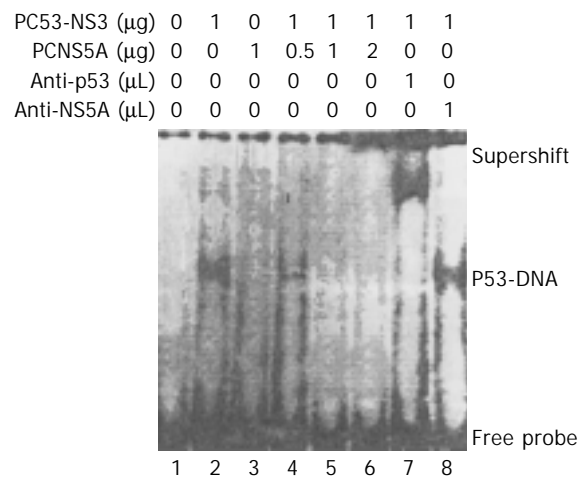


Figure 1 HCVNS5A inhibits p53 binding to its specific DNA probe. Lane 1: Negative control; Lane 2: Transfected with pC53-NS3 only; Lane 3: Transfected with pCNS5A only; Lanes 4-6: Co-transfected with pC53-NS3 (1 μ g) and different dose of pCNS5A; Lanes 7-8: Transfected with pC53-NS3, and anti-p53, antiNS5A anti-bodies were added to the reaction mixture individually.

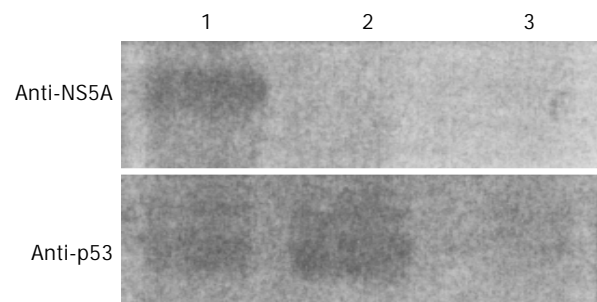


Figure 2 Western blotting for the expression of NCV NS5A and p53 proteins. Lane 1: Huh 7 cells co-transfected with $P^{C53-NS3}$ and P^{CNS5A} ; Lane 2: Huh 7 cells transfected with $P^{C53-NS3}$; Lane 3: Huh 7 cells untransfected.

DISCUSSION

HCV NS5A is a phosphoprotein that exists in two different forms of M_r 56 000 and 58 000 with modifications of serine residues, and M_r 58 000 form is produced by additional phosphorylation of the M_r 56 000 form^[28-30]. Initial studies found that HCV NS5A contains acidic and proline-rich amino acids in its carboxyl-terminal, and this structure feature resembles eukaryotic transcription activator^[31,32]. Later studies showed that the HCV NS5A with amino-terminal deleted (1-146) mutant did have a strong transcriptional activation, but the whole length HCV NS5A showed no apparent transcriptional activity^[33]. The potential transactivation of HCV NS5A has attracted great attention and become the research focus of the nonstructural proteins of HCV due to its important role in the pathogenesis of chronic liver disease and even hepatocellular carcinoma. Clinical observations suggested the responsiveness of patients to IFN treatment might be related to HCV NS5A ISDR sequence mutations^[23-25]. Several experiments from Katze's laboratory and others confirmed that HCV NS5A could repress RNA dependent protein kinase (PKR) function, by which HCV can escape the effect of IFN, and also inhibit apoptosis and promote cell proliferation^[7,26,27]. When PKR is dysfunctional, sustained

expression of eIF-2 α in cells results in cell growth and differentiation, and induces malignant transformation and the development of tumors in nude mice. ISDR of HCV NS5A can bind the domain of PKR and prevent the PKR dimerizing which is the critical process to activate PKR function. Mapping studies found that ISDR and the adjacent C-terminal 26 amino acids can form a heterodimer with PKR. The effect of HCV NS5A on the protection of apoptosis induced by TNF- α and p53 was further identified^[16,17]. In the present study, we explored the possible effect of HCV NS5A on the transactivation of p53. Luciferase reporter gene driven by p21 promoter was used in this experiment, which showed that both endogenous and exogenous p53 protein could transactivate p21 promoter as expected. But, when HCV NS5A protein was introduced, by transfection or co-transfection with HCV NS5A expressing vector, the p21 promoter function activated by p53 was greatly depressed. This finding is in agreement with previous reports^[8,11]. To further understand the mechanism of interaction between HCV NS5A and p53, we did an EMSA experiment for p53 binding to its consensus DNA probe, to see if HCV NS5A could disturb the binding reaction. The result showed that HCV NS5A disrupted p53 binding to its DNA probe, and with the increase of dosage of HCV NS5A expressing vector transfected, inhibition of the binding seemed more remarkable. All the above results suggested HCV NS5A depressed the p53 transactivation by interrupting the binding between p53 and its specific DNA. Recent studies also evidenced that HCV NS5A could physically associate with p53 and form a complex, which might be the reason why p53 binding to its DNA was disrupted^[8,34]. Further, we wanted to know whether p53 protein expression was affected by the presence of HCV NS5A. Through western blot, we found that after co-transfection of HCV NS5A expressing vector, the level of p53 protein expression in the cells did not show any change compared to empty vector transfected cells. This result was also similarly found in another report^[11]. In summary, according to our experiments and previous reports by others, HCV NS5A represses p53 transactivation function by disrupting p53 binding to its specific DNA through HCV NS5A and p53 complex formation, not by the disturbance of the p53 protein expression. HCV NS5A can interact with many cellular factors in the host cells such as PKR, p53, Bcl2 and disrupt their functions^[7,8,26,27,34,35], which are related to the processes of apoptosis. HCV NS5A can also interact with unknown cellular factors and induce the expression of genes such as SRCAP, NF- κ B and PCNA^[11-13], which are related to the promotion of cell proliferation. HCV NS5A seems to be a very active protein interacting with host cellular proteins and taking a major part in modulating cell growth and death, as well as in the development of hepatocellular carcinoma.

ACKNOWLEDGEMENTS

We would like to thank Dr. A Siddiqui and G Waris from University of Colorado School of Medicine for their help in this study.

REFERENCES

- 1 **Choo QL**, Kuo G, Weiner AJ, Overby LR, Bradley DW, Houghton M. Isolation of a cDNA clone derived from a blood-borne non-A, non-B viral hepatitis genome. *Science* 1989; **244**: 359-362
- 2 **Kuo G**, Choo QL, Alter HJ, Gitnick GL, Redeker AG, Purcell RH, Miyamura T, Dienstag JL, Alter MJ, Stevens CE. An assay for circulating antibodies to a major etiologic virus of human non-A, non-B hepatitis. *Science* 1989; **244**(3 Suppl): 362-364
- 3 **Seeff LB**. Natural history of hepatitis C. *Hepatology* 1997; **26**: 21S-28S
- 4 **Saito I**, Miyamura T, Ohbayashi A, Harada H, Katayama T, Kikuchi S, Watanabe Y, Koi S, Onji M, Ohta Y, Choo QL, Houghton M, Kuo G. Hepatitis C virus infection is associated with the development of hepatocellular carcinoma. *Proc Natl Acad Sci U S A* 1990; **87**: 6547-6549
- 5 **Di Bisceglie AM**, Lyra AC, Schwartz M, Reddy RK, Martin P, Gores G, Lok AS, Hussain KB, Gish R, Van Thiel DH, Younossi Z, Tong M, Hassanein T, Balart L, Fleckenstein J, Flamm S, Blei A, Befeler AS. Hepatitis C virus-related hepatocellular carcinoma in the United States: influence of ethnic status. *Am J Gastroenterol* 2003; **98**: 2060-2063
- 6 **Clarke B**. Molecular virology of hepatitis C virus. *J Gen Virol* 1997; **78**(Pt 10): 2397-2410
- 7 **Gale M Jr**, Blakely CM, Kwieciszewski B, Tan SL, Dossett M, Tang NM, Korth MJ, Polyak SJ, Katze MG. Control of PKR protein kinase by hepatitis C virus nonstructural 5A protein: molecular mechanisms of kinase. *Mol Cell Biol* 1998; **18**: 5308-5319
- 8 **Majumder M**, Ghosh AK, Steele R, Ray R. Hepatitis C virus NS5A physically associates with p53 and regulates p21/waf1 gene expression in a p53-dependent manner. *J Virol* 2001; **75**: 1401-1407
- 9 **Tan SL**, Nakao H, He Y, Vijaysri S, Neddermann P, Jacobs BL, Mayer BJ, Katze MG. NS5A, a nonstructural protein of hepatitis C virus, binds growth factor receptor-bound protein 2 adaptor protein in a Src homology3 domain/ligand-dependent manner and perturbs mitogenic signaling. *Proc Natl Acad Sci U S A* 1999; **96**: 5533-5538
- 10 **Arima N**, Kao CY, Licht T, Padmanabhan R, Sasaguri Y, Padmanabhan R. Modulation of cell growth by the hepatitis C virus nonstructural protein NS5A. *J Biol Chem* 2001; **276**: 12675-12684
- 11 **Ghosh AK**, Steele R, Meyer K, Ray R, Ray RB. Hepatitis C virus NS5A protein modulates cell cycle regulatory genes and promotes cell growth. *J Gen Virol* 1999; **80**(Pt 5): 1179-1183
- 12 **Gong G**, Waris G, Tanveer R, Siddiqui A. Human hepatitis C virus NS5A protein alters intracellular calcium level, induces oxidative stress, and activates STAT-3 and NF- κ B. *Proc Natl Acad Sci U S A* 2001; **98**: 9599-9604
- 13 **Ghosh AK**, Majumder M, Steele R, Yaciuk P, Chrivia J, Ray R, Ray RB. Hepatitis C virus NS5A protein modulates transcription through a novel cellular transcription factor SRCAP. *J Biol Chem* 2000; **275**: 7184-7188
- 14 **Polyak SJ**, Khabar KS, Paschal DM, Ezelle HJ, Duverlie G, Barber GN, Levy DE, Mukaida N, Gretch DR. Hepatitis C virus nonstructural 5a protein induces interleukin-8 leading to partial inhibition of the interferon-induced antiviral response. *J Virol* 2001; **75**: 6095-6106
- 15 **Lan KH**, Sheu MI, Hwang SJ, Yen SH, Chen SY, Wu JC, Wang YJ, Kato N, Omata M, Chang FY, Lee SD. HCV NS5A interacts with p53 and inhibits p53-mediated apoptosis. *Oncogene* 2002; **21**: 4801-4811
- 16 **Majumder M**, Ghosh AK, Steele R, Zhou XY, Phillips NJ, Ray R, Ray RB. Hepatitis C virus NS5A protein impairs TNF-mediated hepatic apoptosis, but not by an anti-fas antibody, in transgenic mice. *Virology* 2002; **294**: 94-105
- 17 **Ghosh AK**, Majumder M, Steele R, Meyer K, Ray R, Ray RB. Hepatitis C virus NS5A protein protects against TNF-alpha mediated apoptotic cell death. *Virus Res* 2000; **67**: 173-178
- 18 **Tu H**, Gao L, Shi ST, Taylor DR, Yang T, Mircheff AK, Wen Y, Gorbalenya AE, Hwang SB, Lai MM. Hepatitis C virus RNA polymerase and NS5A complex with a SNARE-like protein. *Virology* 1999; **263**: 30-41
- 19 **Elazar M**, Cheong KH, Liu P, Greenberg HB, Rice CM, Glenn JS. Amphipathic helix-dependent localization of NS5A mediates hepatitis C virus RNA replication. *J Virol* 2003; **77**: 6055-6061
- 20 **Brass V**, Bieck E, Montserret R, Wolk B, Hellings JA, Blum HE, Penin F, Moradpour D. An amino-terminal amphipathic alpha-helix mediates membrane association of hepatitis C virus nonstructural protein 5A. *J Biol Chem* 2002; **277**: 8130-8139
- 21 **Houshmand H**, Bergqvist A. Interction of hepatitis C virus NS5A with la protein revealed by T7 phage display. *Biochem Biophys Res Commun* 2003; **309**: 695-701
- 22 **He Y**, Tan SL, Tareen SU, Vijaysri S, Langland JO, Jacobs BL, Katze MG. Regulation of mRNA translation and cellular sig-

- naling by hepatitis C virus nonstructural protein NS5A. *J Virol* 2001; **75**: 5090-5098
- 23 **Schiappa DA**, Mittal C, Brown JA, Mika BP. Relationship of hepatitis C genotype 1 NS5A sequence mutations to early phase viral kinetics and interferon effectiveness. *J Infect Dis* 2002; **185**: 868-877
- 24 **Hung CH**, Lee CM, Lu SN, Wang JH, Tung HD, Chen TM, Hu TH, Chen WJ, Changchien CS. Mutations in the NS5A and E2-PePHD region of hepatitis C virus type 1b and correlation with the response to combination therapy with interferon and ribavirin. *J Viral Hepat* 2003; **10**: 87-94
- 25 **Watanabe H**, Enomoto N, Nagayama K, Izumi N, Marumo F, Sato C, Watanabe M. Number and position of mutations in the interferon (IFN) sensitivity-determining region of the gene for nonstructural protein 5A correlate with IFN efficacy in hepatitis C virus genotype 1b infection. *J Infect Dis* 2001; **183**: 1195-1203
- 26 **Tan SL**, Katze MG. How hepatitis C virus counteracts the interferon response: the jury is still out on NS5A. *Virology* 2001; **284**: 1-12
- 27 **Gale M Jr**, Kwieciszewski B, Dossett M, Nakao H, Katze M. Antiapoptotic and oncogenic potentials of hepatitis C virus are linked to interferon resistance by viral repression of the PKR protein kinase. *J Virol* 1999; **73**: 6506-6516
- 28 **Kaneko T**, Tanji Y, Satoh S, Hijikata M, Asabe S, Kimura K, Shimotohno K. Production of two phosphoproteins from the NS5A region of the hepatitis C viral genome. *Biochem Biophys Res Commun* 1994; **205**: 320-326
- 29 **Hirota M**, Satoh S, Asabe S, Kohara M, Tsukiyama-Kohara K, Kato N, Hijikata M, Shimotohno K. Phosphorylation of nonstructural 5A protein of hepatitis C virus: HCV group-specific hyperphosphorylation. *Virology* 1999; **257**: 130-137
- 30 **Tanji Y**, Kaneko T, Satoh S, Shimotohno K. Phosphorylation of hepatitis C virus-encoded nonstructural protein NS5A. *J Virol* 1995; **69**: 3980-3986
- 31 **Chung KM**, Song OK, Jang SK. Hepatitis C virus nonstructural protein 5A contains potential transcriptional activator domain. *Mol Cells* 1997; **7**: 661-667
- 32 **Tanimoto A**, Ide Y, Arima N, Sasaguri Y, Padmanabhan R. The amino terminal deletion mutants of Hepatitis C virus nonstructural protein NS5A function as transcriptional activators in yeast. *Biochem Biophys Res Commun* 1997; **236**: 360-364
- 33 **Kato N**, Lan KH, One-Nia SK, Shiratori Y, Omata M. Hepatitis C virus nonstructural region 5A protein is a potent transcriptional activator. *J Virol* 1997; **71**: 8856-8859
- 34 **Qadri I**, Iwahashi M, Simon F. Hepatitis C virus NS5A protein binds TBP and p53, inhibiting their DNA binding and p53 interactions with TBP and ERCC3. *Biochim Biophys Acta* 2002; **1592**: 193-204
- 35 **Chung YL**, Sheu ML, Yen SH. Hepatitis C virus NS5A as a potential viral Bcl-2 homologue interacts with Bax and inhibits apoptosis in hepatocellular carcinoma. *Int J Cancer* 2003; **107**: 65-73

Edited by Zhu LH and Chen WW Proofread by Xu FM

Early diagnosis of bacterial and fungal infection in chronic cholestatic hepatitis B

Xiong-Zhi Wu, Dan Chen, Lian-San Zhao, Xiao-Hui Yu, Mei Wei, Yan Zhao, Qing Fang, Qian Xu

Xiong-Zhi Wu, Lian-San Zhao, Xiao-Hui Yu, Yan Zhao, Qing Fang, Qian Xu, Infectious Disease Center, West China Hospital of Sichuan University, Chengdu 610041, Sichuan Province, China
Dan Chen, Mei Wei, Luzhou Medical College, Luzhou 646000, Sichuan Province, China

Correspondence to: Xiong-Zhi Wu, Infectious Disease Center, West China Hospital of Sichuan University, Chengdu 610041, Sichuan Province, China. ilwxz@163.com

Telephone: +86-28-85422650 **Fax:** +86-28-85423783

Received: 2004-01-02 **Accepted:** 2004-01-12

Abstract

AIM: To investigate the early diagnostic methods of bacterial and fungal infection in patients with chronic cholestatic hepatitis B.

METHODS: One hundred and one adult in-patients with chronic hepatitis B were studied and divided into 3 groups: direct bilirubin (DBil)/total bilirubin (TBil) ≥ 0.5 , without bacterial and fungal infection (group A, $n=38$); DBil/TBil < 0.5 , without bacterial and fungal infection (group B, $n=23$); DBil/TBil ≥ 0.5 , with bacterial or fungal infection (group C, $n=40$). The serum biochemical index and pulse rate were analyzed.

RESULTS: Level of TBil, DBil, alkaline phosphatase (ALP) and DBil/ALP in group A increased compared with that in group B. The level of ALP in group C decreased compared with that in group A, whereas the level of TBil, DBil and DBil/ALP increased (ALP: 156 ± 43 , 199 ± 68 , respectively, $P < 0.05$; TBil: 370 ± 227 , 220 ± 206 , respectively, $P < 0.01$; DBil: 214 ± 143 , 146 ± 136 , respectively, $P < 0.01$; DBil/ALP: 1.65 ± 1.05 , 0.78 ± 0.70 , respectively, $P < 0.001$). The level of DBil and infection affected DBil/ALP. Independent of the effect of DBil, infection caused DBil/ALP to rise ($P < 0.05$). The pulse rate in group A decreased compared with that in group B (63.7 ± 6.4 , 77.7 ± 11.4 , respectively, $P < 0.001$), and the pulse rate in group C increased compared with that in group A (81.2 ± 12.2 , 63.7 ± 6.4 , respectively, $P < 0.001$). The equation (infection = 0.218 pulse rate + 1.064 DBil/ALP - 16.361), with total accuracy of 85.5%, was obtained from stepwise logistic regression. Pulse rate (< 80 /min) and DBil/ALP (< 1.0) were used to screen infection. The sensitivity was 62.5% and 64.7% respectively, and the specificity was 100% and 82.8% respectively.

CONCLUSION: Bacterial and fungal infection deteriorate jaundice and increase pulse rate, decrease serum ALP and increase DBil/ALP. Pulse rate, DBil/ALP and the equation (infection = 0.218 pulse rate + 1.064 DBil/ALP - 16.361) are helpful to early diagnosis of bacterial and fungal infection in patients with chronic cholestatic hepatitis B.

Wu XZ, Chen D, Zhao LS, Yu XH, Wei M, Zhao Y, Fang Q, Xu Q. Early diagnosis of bacterial and fungal infection in chronic cholestatic hepatitis B. *World J Gastroenterol* 2004; 10(15): 2228-2231 <http://www.wjgnet.com/1007-9327/10/2228.asp>

INTRODUCTION

Patients with chronic hepatitis are known to be abnormally susceptible to infection as a result of multiple immunologic defects^[1-6]. The incidence of bacteremia in chronic liver disease is 5- to 7- fold higher than that found in other hospitalized patients^[7]. Infection is often associated with systemic inflammatory response syndrome and multiple organ dysfunction syndrome that is easy to develop into liver failure^[8,9]. Infection can prove fatal either directly or by precipitation of encephalopathy, gastrointestinal hemorrhage, hepatic hemodynamic derangement, portal hypertension, or renal failure^[9-17]. About 33% mortality in bacteremic patients with chronic liver disease has been noted^[18]. Considering the low positivity rate and lengthy bacterial culture, severe chronic liver disease patients with clinical diagnosis of infection should get the antibiotic treatment immediately to improve the survival opportunity before pathogen diagnosis^[19-24]. However, clinical diagnosis is made more difficult by the absence of the typical clinical feature of infection - that is, fever, leucocytosis, and localized symptoms^[9,21]. Clinically apparent focus of infection could not be found in 20% to 60% of bacteremic patients with chronic liver disease^[9,25,26]. No specific site is identified in one third to one half of the infections, in which case the only clue may be deterioration of hepatic precoma or coma or renal function. The preventive antibiotic treatment is often applied to serious patients who have the liability to infection (such as the protein in ascites < 10 g/L, gastrointestinal hemorrhage, and previous spontaneous bacterial peritonitis), and in the meantime it might increase the risk of drug resistance^[19,27-30]. The early diagnostic methods of secondary bacterial and fungal infection in patients with chronic hepatitis B have not been studied. To reduce infection related mortality, the development of new methods for early diagnosis is of great significance.

MATERIALS AND METHODS

Patients

One hundred and one adult in-patients with chronic icteric hepatitis B in West China Hospital from October 2002 to March 2003 were studied and divided into three groups: direct bilirubin (DBil)/total bilirubin (TBil) ≥ 0.5 , without bacterial or fungal infection (group A, $n=38$); DBil/TBil < 0.5 , without bacterial or fungal infection (group B, $n=23$); DBil/TBil ≥ 0.5 , with bacterial and fungal infection (group C, $n=40$).

Inclusion criteria

All patients in the study met with the following criteria: positive HBsAg or HBVDNA; TBil > 17.1 mmol/L; age between 14 to 65 years. In addition, the patients in group C had the following features: leukocytes $\geq 10 \times 10^9/L$ or neutrophils $\geq 7 \times 10^9/L$ or the ratio of neutrophil $\geq 70\%$ in blood; leukocytes in urine ≥ 5 per visual field under high power microscope; leukocytes $\geq 0.5 \times 10^9/L$ or neutrophils $\geq 0.25 \times 10^9/L$ in ascites; bacterial culture of blood, urine, phlegm or ascites was positive.

Exclusion criteria

The patient who had one of the followings was excluded from

group A and group B: infected with other pathogens rather than HBV; complicated with other diseases which had not relation with hepatitis B; recently occurring gastrointestinal hemorrhage. The patient who had one of the followings was excluded from group C: infected with other virus; complicated with other liver diseases which had not relation with hepatitis B; recently occurring gastrointestinal hemorrhage; leukocytes in urine ≥ 5 per visual field under high power microscope but normal in routine blood test in female patients who were in menstruation or in patient who had non-inflammatory nephrosis.

Investigation indexes

Blind tests for TBil, DBil, indirect bilirubin (IBil), DBil/IBil, alanine aminotransferase (ALT), aspartate aminotransferase (AST), AST/ALT, serum total protein (TP), albumin (ALB), globulin (GLOB), ALB/GLOB, γ -glutamyltransferase (GGT), alkaline phosphatase (ALP), DBil/ALP, lactate dehydrogenase (LDH), cholinesterase (ChE), serum total bile acid (TBA) and pulse rate were performed. The first liver biochemical test of group A and B after hospitalization and the first liver biochemical test of group C after confirmation of infection were done, and pulse rate of all patients were measured after 15-min bed rest.

Statistical analysis

All data were presented as mean \pm SE. Analysis of variance and covariance was used to determine whether there were significant differences among the three groups. Data with significant difference were entered into a stepwise logistic regression analysis. Statistical calculations were performed by SPSS (Version: 11.0, Chicago, USA).

RESULTS

Clinical features of infection

Fifteen percent of patients in group C showed a rise in leukocyte or neutrophil in blood, 55% of patients showed a rise in the ratio of neutrophil in blood lightly, and 12.5% of patients showed an increase in leukocyte or neutrophil in ascites. Eleven patients showed a leukocyte rise in urine (in these cases, 5 patients showed an increase in leukocyte or neutrophil in blood or in the ratio of neutrophil, 5 patients had a history of fever, 2 patients showed spontaneous bacterial peritonitis). Fifteen patients presented with the localized symptoms of infection. Sixteen patients had a history of fever (the fever was light and persisted shortly in most patients). Positivity rate of bacterial culture was 25% (3/12).

Table 1 Comparison of serum bilirubin

Group	Case	Tbil ($\mu\text{mol/L}$)	DBil ($\mu\text{mol/L}$)	IBil ($\mu\text{mol/L}$)	DBil/TBil
A	38	220 \pm 206	146 \pm 136	73 \pm 72	0.660 \pm 0.078
B	23	59 \pm 33 ^b	22 \pm 12 ^d	38 \pm 23	0.361 \pm 0.105 ^d
C	40	370 \pm 227 ^{bf}	214 \pm 143 ^{bf}	136 \pm 92 ^{df}	0.631 \pm 0.840 ^f

^b P <0.01 *vs* group A; ^d P <0.001 *vs* group A; ^f P <0.001 *vs* group B.

Table 2 Comparison of TBA, ALP, DBil/ALP and pulse rate (mean \pm SE)

Group	<i>n</i>	TBA($\mu\text{mol/L}$)	<i>n</i>	ALP(U/L)	<i>n</i>	DBil/ALP	<i>n</i>	Pulse rate(times/min)
A	22	148 \pm 89	29	199 \pm 68	29	0.78 \pm 0.70	38	63.7 \pm 6.4
B	16	31 \pm 17 ^d	18	149 \pm 50 ^a	18	0.14 \pm 0.06 ^b	23	78 \pm 11 ^d
C	22	140 \pm 60 ^f	34	156 \pm 43 ^{ac}	34	1.65 \pm 1.05 ^{df}	40	81 \pm 12 ^d

^a P <0.05 *vs* group A; ^c P <0.05 *vs* group B; ^b P <0.01 *vs* group A; ^d P <0.001 *vs* group A; ^f P <0.001 *vs* group B.

Analysis of variance

Level of TBil, DBil, ALP and DBil/ALP in group A increased significantly compared with that in group B (P <0.01, P <0.01, P <0.05, P <0.01, respectively). The level of ALP in group C decreased compared with that in group A (156 \pm 43, 199 \pm 68, respectively, P <0.05), whereas the level of TBil, DBil and DBil/ALP increased significantly (TBil: 370 \pm 227, 220 \pm 206, respectively, P <0.01; DBil: 214 \pm 143, 146 \pm 136, respectively, P <0.01; DBil/ALP: 1.65 \pm 1.05, 0.78 \pm 0.70, respectively, P <0.001). The level of IBil in group C decreased compared with that in group A (P <0.001) (Tables 1, 2).

The pulse rate in group A decreased significantly compared with that in group B (63.7 \pm 6.4, 77.7 \pm 11.4, P <0.001). The pulse rate in group C increased compared with that in group A and normal adults (81.2 \pm 12.2, 63.7 \pm 6.4, 72, P <0.001), but decreased compared with that in infectious patients without hepatitis (81.2 \pm 12.2, 90, P <0.001) (Table 2, Figure 1).

The level of ALT, AST, AST/ALT, TP, ALB, GLOB, ALB/GLOB, GGT, LDH, and ChE showed no significant difference among the three groups (data not shown).

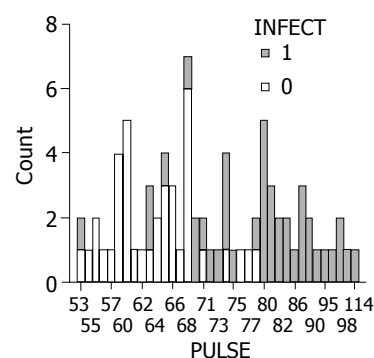


Figure 1 Pulse rate in cholestatic patients. 1: With bacterial or fungal infection; 0: Without bacterial and fungal infection.

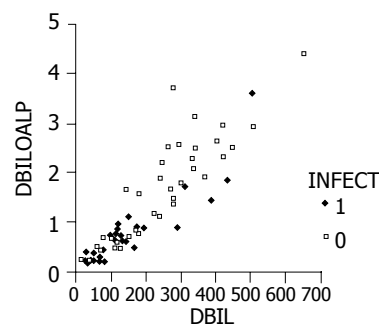


Figure 2 DBil/ALP and DBil in cholestatic patients. 1: With bacterial or fungal infection, 0: Without bacterial and fungal infection.

Analysis of covariance

There was linear correlation between DBil and DBil/ALP in groups A and C, and the distribution of DBil between the two groups was closely similar (Figure 2). The level of DBil and infection affected DBil/ALP (P <0.05, P <0.001, respectively)

(Table 3). Independent of the effect of DBil, infection caused DBil/ALP to rise ($P<0.05$) (Table 4).

Table 3 Tests of between-subjects effects (dependent variable: DBil/ALP)

Source	Type III sum of squares	Df	Mean square	F	P
Corrected model	50.025	2	25.012	129.672	<0.001
Infection	1.172	1	1.172	6.074	0.017
DBil	38.709	1	38.709	200.682	<0.001

Table 4 Pairwise comparisons (dependent variable: DBil/ALP)

Infection I	Infection J	Mean difference(I-J)	SE	P	95% CI
1	2	-0.293 ¹	0.119	0.017	-0.531 -0.055
2	1	0.293 ¹	0.119	0.017	0.0551 0.531

¹The mean difference is significant at the 0.05 level.

Logistic regression

The stepwise logistic regression was used to establish the best statistical model to early diagnose infection, and the equation (infection=0.218 pulse rate+1.064 DBil/ALP -16.361, $P<0.001$) was obtained. Its overall accuracy was 85.5%, and accuracy for diagnosing infection and noninfection were 85.7% and 85.3%, respectively (Table 5).

Table 5 Logistic analysis of bacterial and fungal infection

	B	SE	Wald	Df	P	Exp (B)
Pulse rate	0.218	0.059	13.468	1	<0.001	1.244
DBil/ALP	1.064	0.447	5.657	1	0.017	2.899
Constant	-16.361	4.251	14.815	1	<0.001	<0.001

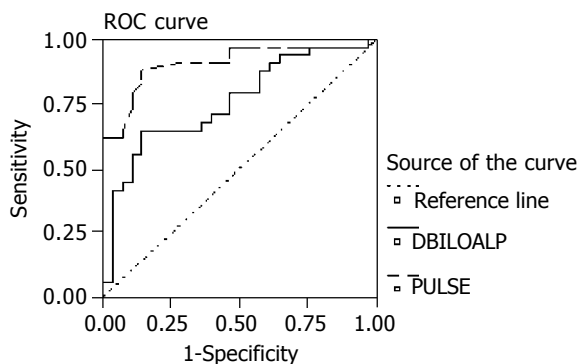


Figure 3 Receiver operator characteristic curve of pulse rate and DBil/ALP.

Screening test

Because the diagnostic index of pulse rate at 80/min to screen infection was the greatest, the cut off point was selected at 80/min (Figure 3). The sensitivity (Sen), specificity (Spe), diagnostic index (DI), false positive rate (α), false negative rate (β), Youden's index (γ), crude accuracy (CA), adjusted agreement (AA), positive predictive value (PV+) and negative predictive value (PV-) were 62.5%, 100%, 1.625, 100%, 71.7%,

62.5%, 80.8%, 83.6%, 0% and 37.5%, respectively. Area under the curve (A_z)=0.889 ($P<0.001$) (Table 6). Because the diagnostic index of DBil/ALP at 1.0 was the greatest, the cut off point was selected at 1.0 (Figure 3). Sen, Spe, DI, α , β , γ , CA, AA, PV+ and PV- were 64.7%, 82.8%, 1.475, 81.5%, 66.7%, 47.5%, 73.0%, 73.9%, 17.8% and 35.3%, respectively. A_z =0.7373 ($P<0.001$) (Table 6). Pulse rate was a better index than DBil/ALP ($P<0.001$).

DISCUSSION

Bacterial and fungal infections are the common complications of chronic hepatitis, frequently aggravating hepatitis. Since the bacterium culture in chronic hepatitis patients is often negative, clinical diagnosis plays a major role. However, a large number of patients do not often present with the typical clinical features of infection. In a prospective study, fever was initially absent in 45% of cases, and leukocytosis was absent in 25% of cases^[10]. Urinary tract infection is the common type of infection and the source of bacteremia in up to 50% of patients with cirrhosis, and 20% of episodes of spontaneous bacterial peritonitis^[10-30]. However, patients with urinary tract infection often do not have localized symptoms or physical findings^[10,11]. Careful urinalysis is important to exclude infection in patients with chronic liver disease^[10]. In our study, the leukocyte or neutrophil in blood rose in 15% of infected patients, and the ratio of neutrophil rose lightly in 55% of patients. Leukocyte or neutrophil in ascites increased in 5 patients, and leukocyte in urine rose in 11 patients. Sixteen patients had a history of fever (the fever was mild and short-lasting in most patients). Only 37.5% of patients presented localized symptoms of infection. The positivity rate of bacterial culture was 25%(3/12). Therefore, early diagnosis of bacterial and fungal infection is difficult in chronic hepatitis.

The level of ALP frequently rises in cholestatic patients. However, in serious liver disease, along with the increase of serum TBil and DBil, sometimes ALP decreased. Hadjis discovered that the synthesis of ALP decreased in the case of widespread hepatocyte necrosis. As well as ALT and AST, it is a marker of disease aggravation. In our study, the level of TBil and DBil in cholestatic patients with infection increased compared with that without infection, but ALP in infection patients decreased compared with that without infection.

In order to characterize the contrary alteration of DBil and ALP in infection patients, we introduced a new index -that is the ratio of DBil to ALP. The level of DBil/ALP showed significant difference between the three groups (0.7829±0.7002, 0.1377±0.0652, 1.6468±1.0500, respectively, $P<0.01$). Analysis of covariance showed that the level of DBil and infection affected DBil/ALP, and independent of the effect of DBil, infection led to DBil/ALP increase ($P<0.05$).

To test whether DBil/ALP could be used to screen infection, a screening test was performed. Its sensitivity, specificity, positive predictive value and negative predictive value were 64.7%, 82.8%, 81.5% and 66.7%, respectively (the cut off point at 1.0). Therefore, we hypothesize that DBil/ALP can be used as an "infection index" to diagnose infection early in chronic cholestatic hepatitis B. If DBil/ALP is greater than 1.0, the probability of infection is 82.8%.

The mean pulse rate in normal adults is 72/min, but it frequently increases in infection, often above 90/min. Because the vagus's excitement increased in cholestatic patient, the

Table 6 Screening test of bacterial and fungal infection

Diagnosis		Sensitivity	Specificity	Diagnostic Index	A_z	Z	P
Pulse rat	80/min	0.625	1.000	1.625	0.889	20.372	<0.001
DBil/ALP	1.0	0.647	0.828	1.475	0.7373	4.022	<0.001

pulse rate decreased compared with that in normal adults (63.7 ± 6.4 , 72 , $P < 0.001$). Although the pulse rate in cholestatic patient increased after infection (81.2 ± 12.2 , 63.7 ± 6.4 , $P < 0.001$), it was slower compared with that in infection patients without cholestasis (81.2 ± 12.2 , 90 , $P < 0.001$). That is why alteration of pulse rate in those patients is likely to be neglected in clinic.

To test whether pulse rate could be used to screen infection, a screening test was done. Its sensitivity, specificity, positive predictive value and negative predictive value were 62.5%, 100%, 100% and 71.7%, respectively (the cut off point at 80/min). Pulse rate was better for screening infection than DBil/ALP ($P < 0.001$).

In order to establish the best statistical model to diagnose infection early, the equation (infection = 0.218 pulse rate + 1.064 DBil/ALP - 16.361 , $P < 0.001$) was obtained from the stepwise logistic regression. Its total accuracy, the accuracy of diagnosing infection and noninfection was 85.5%, 85.7% and 85.3%, respectively.

It is interesting that there is notable relationship between the logistic equation and screening test. Among the 18 indexes that we studied, only pulse rate and DBil/ALP could affect the logistic equation. The equation can be described approximately as "infection = 0.2 pulse rate + DBil/ALP - 16 ". As 0.2 multiplied by 80 is 16 , if pulse rate = 80 /min, the equation = 0 obviously. But if pulse rate < 80 /min, DBil/ALP significantly affects the equation. For severe chronic cholestatic hepatitis B, if pulse rate = 80 /min, perhaps the antibiotic treatment should be applied immediately before pathogen diagnosis to improve the survival opportunity. If DBil/ALP = 1.0 but pulse rate < 80 /min, the equation is helpful to estimate the probability of infection. If DBil/ALP < 1.0 and pulse rate < 80 /min, the equation is useful to exclude infection. It is a sensitive, quick, simple and economical method to diagnose infection early and possibly improve the survival opportunity of severe chronic cholestatic hepatitis B.

REFERENCES

- Rimola A, Soto R, Bory F, Arroyo V, Perra C, Rodes J. Reticuloendothelial system phagocytic activity in cirrhosis and its relation to bacterial infections and prognosis. *Hepatology* 1984; **4**: 53-58
- Larcher VF, Wyke RJ, Mowat AP, Williams R. Bacterial and fungal infection in children with fulminant hepatic failure: possible role of opsonisation and complement deficiency. *Gut* 1982; **23**: 1037-1043
- Wyke RJ, Yousif-Kadaru AG, Rajkovic IA, Eddleston AL, Williams R. Serum stimulatory activity and polymorphonuclear leucocyte movement in patients with fulminant hepatic failure. *Clin Exp Immunol* 1982; **50**: 442-449
- Wyke RJ, Rajkovic IA, Williams R. Impaired opsonization by serum from patients with chronic liver disease. *Clin Exp Immunol* 1983; **51**: 91-98
- Wyke RJ, Rajkovic IA, Eddleston AL, Williams R. Defective opsonisation and complement deficiency in serum from patients with fulminant hepatic failure. *Gut* 1980; **21**: 643-649
- Inamura T, Miura S, Tsuzuki Y, Hara Y, Hokari R, Ogawa T, Teramoto K, Watanabe C, Kobayashi H, Nagata H, Ishii H. Alteration of intestinal intraepithelial lymphocytes and increased bacterial translocation in a murine model of cirrhosis. *Immunol Lett* 2003; **90**: 3-11
- Graudal N, Milman N, Kirkegaard E, Korner B, Thomsen AC. Bacteremia in cirrhosis of the liver. *Liver* 1986; **6**: 297-301
- Iber FL. Patients with cirrhosis and liver failure are at risk for bacterial and fungus infection. *Am J Gastroenterol* 1999; **94**: 2001-2003
- Rolando N, Wade J, Davalos M, Wendon J, Philpott-Howard J, Williams R. The systemic inflammatory response syndrome in acute liver failure. *Hepatology* 2000; **32**(4 Pt 1): 734-739
- Wyke RJ, Canalese JC, Gimson AE, Williams R. Bacteraemia in patients with fulminant hepatic failure. *Liver* 1982; **2**: 45-52
- Ruiz-del-Arbol L, Urman J, Fernandez J, Gonzalez M, Navasa M, Monescillo A, Albillos A, Jimenez W, Arroyo V. Systemic, renal, and hepatic hemodynamic derangement in cirrhotic patients with spontaneous bacterial peritonitis. *Hepatology* 2003; **38**: 1210-1218
- Navasa M, Follo A, Filella X, Jimenez W, Francitorra A, Planas R, Rimola A, Arroyo V, Rodes J. Tumor necrosis factor and interleukin-6 in spontaneous bacterial peritonitis in cirrhosis: relationship with the development of renal impairment and mortality. *Hepatology* 1998; **27**: 1227-1232
- Poddar U, Thapa BR, Prasad A, Sharma AK, Singh K. Natural history and risk factors in fulminant hepatic failure. *Arch Dis Child* 2002; **87**: 54-56
- Zhao C, Chen SB, Zhou JP, Xiao W, Fan HG, Wu XW, Feng GX, He WX. Prognosis of hepatic cirrhosis patients with esophageal or gastric variceal hemorrhage: multivariate analysis. *Hepatobiliary Pancreat Dis Int* 2002; **1**: 416-419
- De Mattos AA, Coral GP, Menti E, Valiatti F, Kramer C. Bacterial infection in cirrhotic patients. *Arq Gastroenterol* 2003; **40**: 11-15
- De las Heras D, Fernandez J, Gines P, Cardenas A, Ortega R, Navasa M, Barbera JA, Calahorra B, Guevara M, Bataller R, Jimenez W, Arroyo V, Rodes J. Increased carbon monoxide production in patients with cirrhosis with and without spontaneous bacterial peritonitis. *Hepatology* 2003; **38**: 452-459
- Perdomo Coral G, Alves de Mattos A. Renal impairment after spontaneous bacterial peritonitis: incidence and prognosis. *Can J Gastroenterol* 2003; **17**: 187-190
- Barnes PF, Arevalo C, Chan LS, Wong SF, Reynolds TB. A prospective evaluation of bacteremic patients with chronic liver disease. *Hepatology* 1988; **8**: 1099-1103
- Chu CM, Chang KY, Liaw YF. Prevalence and prognostic significance of bacterascites in cirrhosis with ascites. *Dig Dis Sci* 1995; **40**: 561-565
- Runyon BA, Hoefs JC. Culture-negative neutrocytic ascites: a variant of spontaneous bacterial peritonitis. *Hepatology* 1984; **4**: 1209-1211
- Rimola A, Garcia-Tsao G, Navasa M, Piddock LJ, Planas R, Bernard B, Inadomi JM. Diagnosis, treatment and prophylaxis of spontaneous bacterial peritonitis: a consensus document. International Ascites Club. *J Hepatol* 2000; **32**: 142-153
- Navasa M, Rimola A, Rodes J. Bacterial infections in liver disease. *Semin Liver Dis* 1997; **17**: 323-333
- Fernandez J, Bauer TM, Navasa M, Rodes J. Diagnosis, treatment and prevention of spontaneous bacterial peritonitis. *Baillieres Best Pract Res Clin Gastroenterol* 2000; **14**: 975-990
- Evans LT, Kim WR, Poterucha JJ, Kamath PS. Spontaneous bacterial peritonitis in asymptomatic outpatients with cirrhotic ascites. *Hepatology* 2003; **37**: 897-901
- Javaloyas de Morlius M, Ariza Cardenal J, Gudiol Munte F. Bacteremia in patients with hepatic cirrhosis. Etiopathogenic analysis and prognosis of 92 cases. *Med Clin* 1984; **82**: 612-616
- Jones EA, Sherlock S, Crowley N. Bacteraemia in association with hepatocellular and hepatobiliary disease. *Postgrad Med J* 1967; **43**: 7-11
- Sort P, Gines P, Navasa M, Arroyo V. Current treatment of ascites and spontaneous bacterial peritonitis in Spain: analysis of a survey of gastroenterologists and hepatologists. *Gastroenterol Hepatol* 1997; **20**: 437-441
- Navasa M, Follo A, Llovet JM, Clemente G, Vargas V, Rimola A, Marco F, Guarner C, Forne M, Planas R, Banares R, Castells L, Jimenez De Anta MT, Arroyo V, Rodes J. Randomized, comparative study of oral ofloxacin versus intravenous cefotaxime in spontaneous bacterial peritonitis. *Gastroenterology* 1996; **111**: 1011-1017
- Salmeron JM, Tito L, Rimola A, Mas A, Navasa MA, Llach J, Gines A, Gines P, Arroyo V, Rodes J. Selective intestinal decontamination in the prevention of bacterial infection in patients with acute liver failure. *J Hepatol* 1992; **14**: 280-285
- Rolando N DRA. Treatment and prevention of bacterial and mycotic infection in acute liver failure. *Rev Gastroenterol Peru* 1997; **17**(Suppl 1): 100-106

Increased oxidative DNA damage, inducible nitric oxide synthase, nuclear factor κ B expression and enhanced antiapoptosis-related proteins in *Helicobacter pylori*-infected non-cardiac gastric adenocarcinoma

Chi-Sen Chang, Wei-Na Chen, Hui-Hsuan Lin, Cheng-Chung Wu, Chau-Jong Wang

Chi-Sen Chang, Wei-Na Chen, Division of Gastroenterology, Chung Shan Medical University, Taichung, Taiwan, china

Chi-Sen Chang, Wei-Na Chen, Division of Gastroenterology, Taichung Veterans General Hospital, Taichung, Taiwan, china

Cheng-Chung Wu, Division of General Surgery, Taichung Veterans General Hospital, Taichung, Taiwan, china

Chi-Sen Chang, Wei-Na Chen, Hui-Hsuan Lin, Chau-Jong Wang, Institute of Biochemistry, Chung Shan Medical University, Taichung, Taiwan, china

Cheng-Chung Wu, National Young-Min Medical University, Taipei, Taiwan, china

Correspondence to: Chau-Jong Wang, Institute of Biochemistry, College of Medicine, Chung Shan Medical University, No. 110, Sec. 1, Chien Kuo North Road, 402, Taichung, Taiwan, china. wjg@csmu.edu.tw

Telephone: +886-4-24730022 **Fax:** +886-4-23248167

Received: 2004-03-15 **Accepted:** 2004-04-09

Abstract

AIM: Several epidemiological studies have demonstrated a close association between *Helicobacter pylori* (*H Pylori*) infection and non-cardiac carcinoma of the stomach. *H pylori* infection induces active inflammation with neutrophilic infiltrations as well as production of oxygen free radicals that can cause DNA damage. The DNA damage induced by oxygen free radicals could have very harmful consequences, leading to gene modifications that are potentially mutagenic and/or carcinogenic. The aims of the present study were to assess the effect of *H pylori* infection on the expression of inducible nitric oxidative synthase (iNOS) and the production of 8-hydroxy-deoxyguanosine (8-OHdG), a sensitive marker of oxidative DNA injury in human gastric mucosa with and without tumor lesions, and to assess the possible factors affecting cell death signaling due to oxidative DNA damage.

METHODS: In this study, 40 gastric carcinoma specimens and adjacent specimens were obtained from surgical resection. We determined the level of 8-OHdG formation by HPLC-ECD, and the expression of iNOS and mechanism of cell death signaling [including nuclear factor- κ B (NF κ B), MEKK-1, Caspase 3, B Cell lymphoma leukemia-2 (Bcl-2), inhibitor of apoptosis protein (IAP) and myeloid cell leukemia-1 (Mcl-1)] by Western-blot assay.

RESULTS: The concentrations of 8-OHdG, iNOS, NF κ B, Mcl-1 and IAP were significantly higher in cancer tissues than in adjacent non-cancer tissues. In addition, significantly higher concentrations of 8-OHdG, iNOS, NF κ B, Mcl-1 and IAP were detected in patients infected with *H pylori* compared with patients who were not infected with *H pylori*. Furthermore, 8-OHdG, iNOS, NF κ B, Mcl-1 and IAP concentrations were significantly higher in stage 3 and 4 patients than in stage 1 and 2 patients.

CONCLUSION: Chronic *H pylori* infection induces iNOS expression and subsequent DNA damage as well as enhances anti-apoptosis signal transduction. This sequence of events supports the hypothesis that oxygen-free radical-mediated damage due to *H pylori* plays a pivotal role in the development of gastric carcinoma in patients with chronic gastritis.

Chang CS, Chen WN, Lin HH, Wu CC, Wang CJ. Increased oxidative DNA damage, inducible nitric oxide synthase, nuclear factor κ B expression and enhanced antiapoptosis-related proteins in *Helicobacter pylori*-infected non-cardiac gastric adenocarcinoma. *World J Gastroenterol* 2004; 10 (15): 2232-2240

<http://www.wjgnet.com/1007-9327/10/2232.asp>

INTRODUCTION

Helicobacter pylori (*H pylori*) infection is associated with an increased risk of both peptic ulcer and gastric cancer^[1] Chronic gastritis induced by *H pylori* significantly increases the risk for non-cardiac gastric cancer^[2,3], and host responses that may affect the threshold for carcinogenesis include alteration of epithelial cell proliferation and apoptosis. Although the linkage between *H pylori* infection and gastric cancer is convincing, the molecular mechanism or mechanisms responsible are unclear, and both bacterial and host factors are implicated. One possible factor is that increased inflammation generates reactive oxygen and nitrogen intermediates that have been shown to damage DNA directly^[4].

Mucosal hyperproliferation has been reproducibly demonstrated in *H pylori*-infected human^[5-7] and rodent gastric tissue^[8-10], and proliferation scores normalize following successful eradication in humans^[5-7]. However, maintenance of tissue integrity requires that enhanced cell production is accompanied with increased rates of cell loss consequently, studies have also examined the effect of *H pylori* on apoptosis. In contrast to hyperproliferation, *H pylori* has been associated with increased^[11-14], unchanged^[15], or even decreased^[16] levels of apoptosis *in vivo*, and within a particular population, substantial heterogeneity exists among apoptosis scores^[11-14]. These observations suggest that increases in proliferation that are not balanced by concordant increases in apoptosis over years of colonization may heighten the retention of mutated cells, ultimately enhancing the risk for gastric malignancy in certain populations. Alteration of epithelial cell proliferation and apoptosis is a manifestation of *H pylori*-induced gastritis. However, the precise mechanisms underlying these effects remain incompletely clarified. In this study, we aimed to assess the effect *H pylori* infection on the expression of iNOS and the production of 8-OHdG, a sensitive marker of oxidative DNA injury in human gastric mucosa with and without tumor lesions, as well as the possible factors affecting cell death signaling due to oxidative DNA damage.

MATERIALS AND METHODS

Patients

In this study, 40 patients (aged 68.3±11.4 years, range 39–84 years, M/F: 26/14) with non-cardiac gastric adenocarcinoma were included. Specimens from tumor site and adjacent non-tumor site were obtained from surgical resection. By TNM staging according to the criteria described by the International Union Against Cancer^[17], there were 2 cases in stage 1, 6 cases in stage 2, 8 cases in stage 3 and 24 cases in stage 4 (Table 1). *H. pylori* infection was assessed by the following three methods: histology (haematoxylin and eosin staining or Giemsa staining, rapid urease test (CLO test, Delta West Pty Ltd, Perth, Australia) and serum *H. pylori* ELISA IgG assays (Trinity Biotech USA, Jamestown, NY). A patient was considered *H. pylori* positive if one or more of the diagnostic methods applied were positive, and *H. pylori* negative if all methods were negative. There were 29 patients (72.5%) with *H. pylori* infection and 11 patients (27.5%) without *H. pylori* infection. We determined the level of 8-OHdG formation by HPLC-ECD, and the expression of iNOS and cell death signaling, including NFκB, MEKK1, Caspase 3, Bcl-2, Mcl-1 and IAP by Western-blot assay.

Table 1 Characteristics of all patients

Case No	Stage	<i>H. pylori</i> infection	Case No	Stage	<i>H. pylori</i> infection
1	II	+	21	III	+
2	IV	+	22	IV	+
3	IV	+	23	IV	+
4	III	+	24	IV	+
5	IV	+	25	IV	-
6	IV	+	26	IV	+
7	IV	+	27	I	+
8	III	-	28	I	-
9	III	+	29	IV	-
10	III	+	30	II	+
11	IV	+	31	IV	+
12	IV	-	32	IV	+
13	IV	-	33	IV	+
14	IV	+	34	III	+
15	IV	+	35	II	+
16	II	+	36	III	+
17	III	-	37	IV	-
18	IV	+	38	IV	+
19	IV	+	39	IV	+
20	II	-	40	II	-

DNA extraction and digestion

DNA was extracted with Dneasy tissue kit (QIAGEN) according to the protocol of Dahlhaus and Apple^[18] with minor modifications as described previously^[19]. Briefly, one volume of nuclear fraction obtained from surgical tissue was mixed with ten volumes of extraction buffer (1 mol/L NaCl, 10 mmol/L Tris-HCl, 1 mmol/L EDTA, 5 g/L SDS, pH 7.4) and one volume of chloroform:isoamylalcohol (12:1 v/v). After vigorous shaking, the aqueous phase was separated by centrifugation. This step was repeated three times before DNA was precipitated with absolute ethanol (-70 °C). DNA pellet was dissolved in TE buffer (10 mmol/L Tris-HCl, 1 mmol/L EDTA, pH 7.4), and then incubated with RNase A to remove RNA. After incubation, DNA was extracted with chloroform:isoamylalcohol, and precipitated with absolute ethanol again. The DNA pellet was dissolved in 10 mmol/L Tris-HCl (pH 7.0) and hydrolyzed according to the previous procedure^[20]. Briefly, 200 µg DNA in 200 µL 10 mmol/L Tris-HCl (pH 7.0) was first denatured at 95 °C for 3 min. The digestion was carried out at 37 °C for 1 h with 100 units DNase I (from bovine pancreas, Sigma) in a buffer containing 10 mmol/L MgCl₂, followed by incubation with 5 units nuclease P₁ (from penicillium citrinum, Sigma) in

100 µmol/L ZnCl₂ for an additional hour. The mixture was incubated finally with 3 units alkaline phosphatase (from *Escherichia coli*, Sigma) at 37 °C for 1 h. The incubation was terminated with acetone (HPLC grade, Merck, Germany) to precipitate proteins. After 12 000 g centrifugation for 15 min, the supernatant was dried under vacuum in a rotary evaporator (Eyela, Tokyo, Japan) and DNA was dissolved in distilled H₂O.

8-OHdG assay

8-OHdG levels were determined by HPLC/ECD consisting of a BAS PM-80 pump (Bioanalytical Systems, West Lafayette, IN, USA), a CMA-200 microautosampler (CAM/Microdialysis, Stockholm, Sweden), a BAS-4C amperometric detector (Bioanalytical Systems, West Lafayette, IN, USA), a microbore reversed-phase column (Inertsil-2, 5-µm ODS, 1.0×150 mm I.D. G.L. Sciences, Tokyo, Japan) Beckman I/O 406 interface, and Beckman system gold data analysis software (Beckman Instruments). A potential of +0.6 V was selected for the glassy carbon working electrode which corresponded to a silver/silver chloride reference electrode. The mobile phase consisted of 12.5 mmol/L citric acid, 30 mmol/L NaOH, 25 mmol/L sodium acetate, 10 mmol/L acetic acid glacial and 50 mL/L methanol (pH 5.3). The flow rate was set at 1 mL/min. Under these conditions, the retention time of 8-OHdG was 8.49 min with a significantly higher signal than background noise.

Immunoblot analysis

Cancerous and non-cancerous tissue samples were homogenized with ten volumes of homogenization buffer (50 mmol/L Tris, 5 mmol/L EDTA, 150 mmol/L sodium chloride, 10 g/L Nonidet P-401 g/L SDS, 5 g/L deoxycholic acid, 1 mmol/L sodium orthovanadate, 170 µg/mL leupeptin, 100 µg/mL phenylsulfonyl fluoride; pH 7.5). After 30 min of mixing at 4 °C, the mixture was centrifuged at 800 r/min for 10 min, and the supernatant was collected. The protein content of the samples was determined with the Bio-Rad protein assay reagent using BSA as a standard. For Western blotting analysis, 50 µg protein from both cancerous and non-cancerous tissue samples was resolved on 100 g/L SDS-PAGE gels along with prestained protein molecular weight standards (Bio-Rad). The separated proteins were then blotted onto NC membrane (0.45 µm, Bio-Rad) and reacted with primary antibodies (against iNOS, NFκB, MEKK1, Caspase 3, Bcl-2, Mcl-1 and IAP). After washed, the blots were incubated with peroxidase-conjugated goat anti-mouse antibody. Immunodetection was carried out using the enhanced chemiluminescence (ECL) Western blotting detection kit (Amersham Corp., UK). Relative protein expression levels were quantified by densitometric measurement of ECL reaction bands and normalized with values of tubulin. Finally, enhanced chemiluminescence (ECL) was used to detect the membrane, and then the membrane was exposed to X-ray film to observe results. All the immunoblot results were determined by Alpha Imager 2000 documentation & analysis system (Alpha Innotech Corporation).

Statistical analysis

Each parameter expressed by fold of increase of the data from cancer tissue was compared to the adjacent non-cancer tissue. The results were reported as mean±SE from individual magnitudes. Data were analyzed with Student's *t*-test. Statistical differences were considered significant when *P*<0.05.

RESULTS

To assess the effect of *H. pylori* infection on each determined parameter, the results were expressed by fold of increase comparing the data of cancer tissue with those of the adjacent non-cancer tissue. The concentrations of 8-OHdG were analyzed by HPLC/ECD. There were significantly higher concentrations

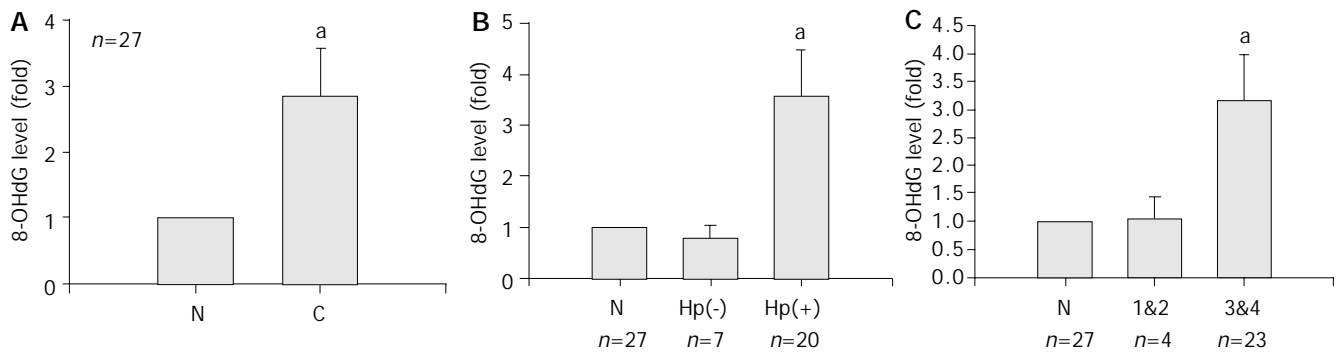


Figure 1 Concentrations of 8-OHdG. A: Higher concentration of 8-OHdG in cancer tissues compared with adjacent non-cancer tissues. B: Higher concentration of 8-OHdG in cancer tissues of patients with and without *H pylori* infection. C: Significantly higher 8-OHdG concentrations in stage 3 and 4 patients ^a $P < 0.05$, N: non-cancer tissue, Hp(-): without *H pylori* infection, Hp(+): with *H pylori* infection, 1&2: gastric cancer stages 1 and 2, 3&4: gastric cancer stages 3 and 4.

of 8-OHdG in cancer tissues than in adjacent non-cancer tissues (Figure 1). In addition, significantly higher concentrations of 8-OHdG were detected in patients infected with *H pylori* than in those without *H pylori* infection. 8-OHdG levels were also significantly higher in stage 3 and 4 patients than in stage 1 and 2 patients.

Immunoblot analysis of several factors affecting cell death signaling related to oxidative DNA damage showed increased concentrations of iNOS and NFκB in patients infected with *H pylori* compared to patients who were tested negative for *H pylori* (Figure 2A-B). Furthermore, iNOS and NFκB concentrations were significantly higher in stage 3 and 4 patients than in stage 1 and 2 patients.

Although there were some increases in the concentrations of MEKK1 and Caspase-3 in the cancer tissue (Figure 2C-D), these changes were not statistically significant. In addition, no significant increases of MEKK1 and Caspase-3 in patients infected with *H pylori* were noted. The concentrations of Caspase-3 in stage 1 and 2 patients were significantly lower than those in stage 3 and 4 patients.

Among the anti-apoptosis-related proteins, there were some increases in the concentrations of Bcl-2 in the cancer tissue (Figure 2E). However, the changes were not statistically significant. In addition, no significant increase of Bcl-2 in patients infected with *H pylori* was noted. The concentrations of Bcl-2 in stage 1 and 2 patients were significantly lower than those in stage 3 and 4 patients. Mcl-1 and IAP concentrations were significantly higher in the cancer tissues than in the adjacent non-cancer tissues (Figure 2F-G). In addition, Mcl-1 and IAP concentrations were significantly higher in *H pylori*-positive patients than in *H pylori*-negative patients. Stage 3 and 4 patients had significantly higher concentrations of Mcl-1 and IAP than stage 1 and 2 patients.

Table 2 8-oHdG, iNOS, NFκB, Mel-1 and IAP Concentrations in cancer and adjacent non-cancer tissues

	Cancer tissue	<i>H pylori</i> (+)	Stages I & II	Stages III & IV
8-OHdG	a	a	-	a
iNOS	b	b	-	b
NF-κB	a	a	-	a
MEKK1	-	-	-	-
Caspase 3	-	-	b	-
Bcl-2	-	-	b	-
Mcl-1	a	a	-	a
IAP	a	a	-	a

: increase, : decrease, -: no significant change, ^a $P < 0.05$, ^b $P < 0.01$ compared with control, by one sample *t*-test and independent *t*-test, respectively.

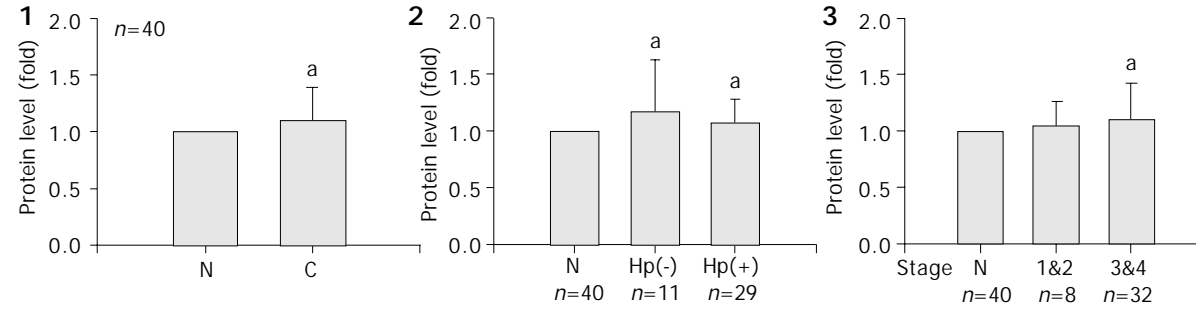
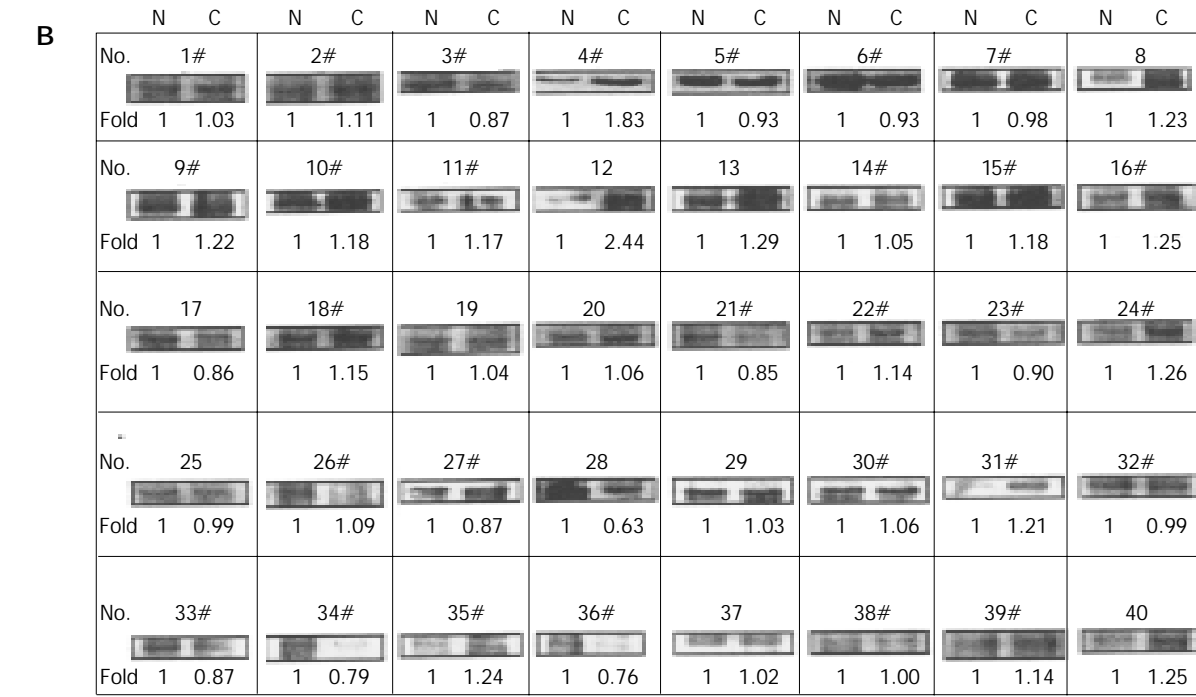
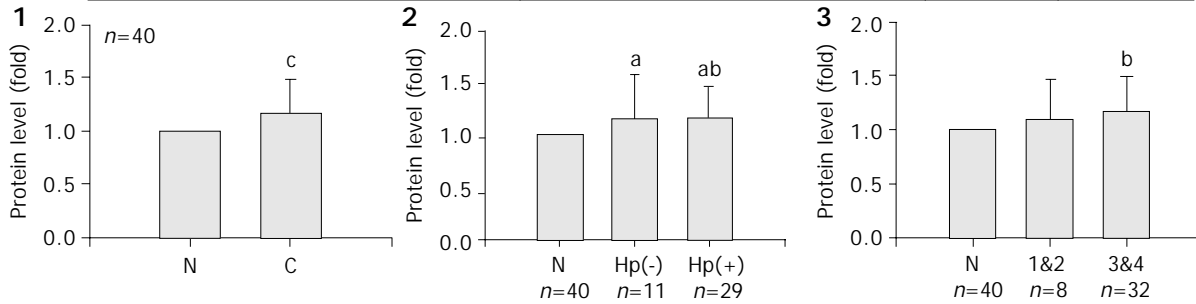
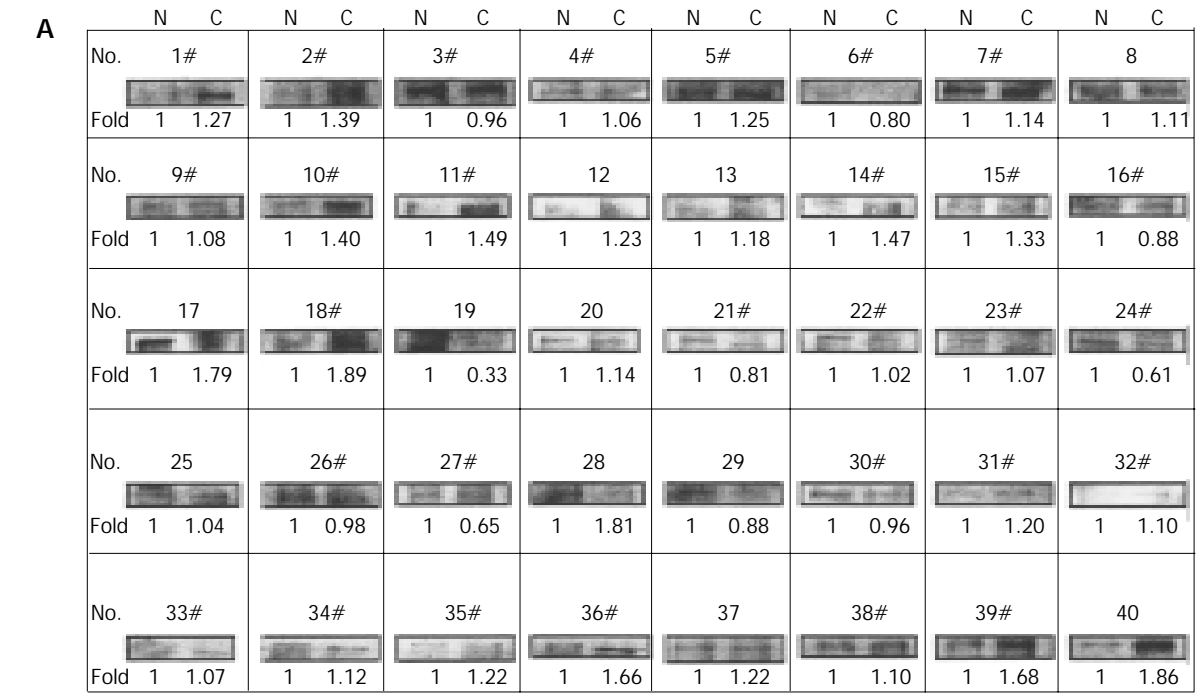
In summary, 8-OHdG, iNOS, NFκB, Mcl-1 and IAP concentrations were significantly higher in cancer tissues than in adjacent non-cancer tissues (Table 2). In addition, significantly higher concentrations of 8-OHdG, iNOS, NFκB, Mcl-1 and IAP were detected in patients infected with *H pylori* compared to patients who were not infected with *H pylori*.

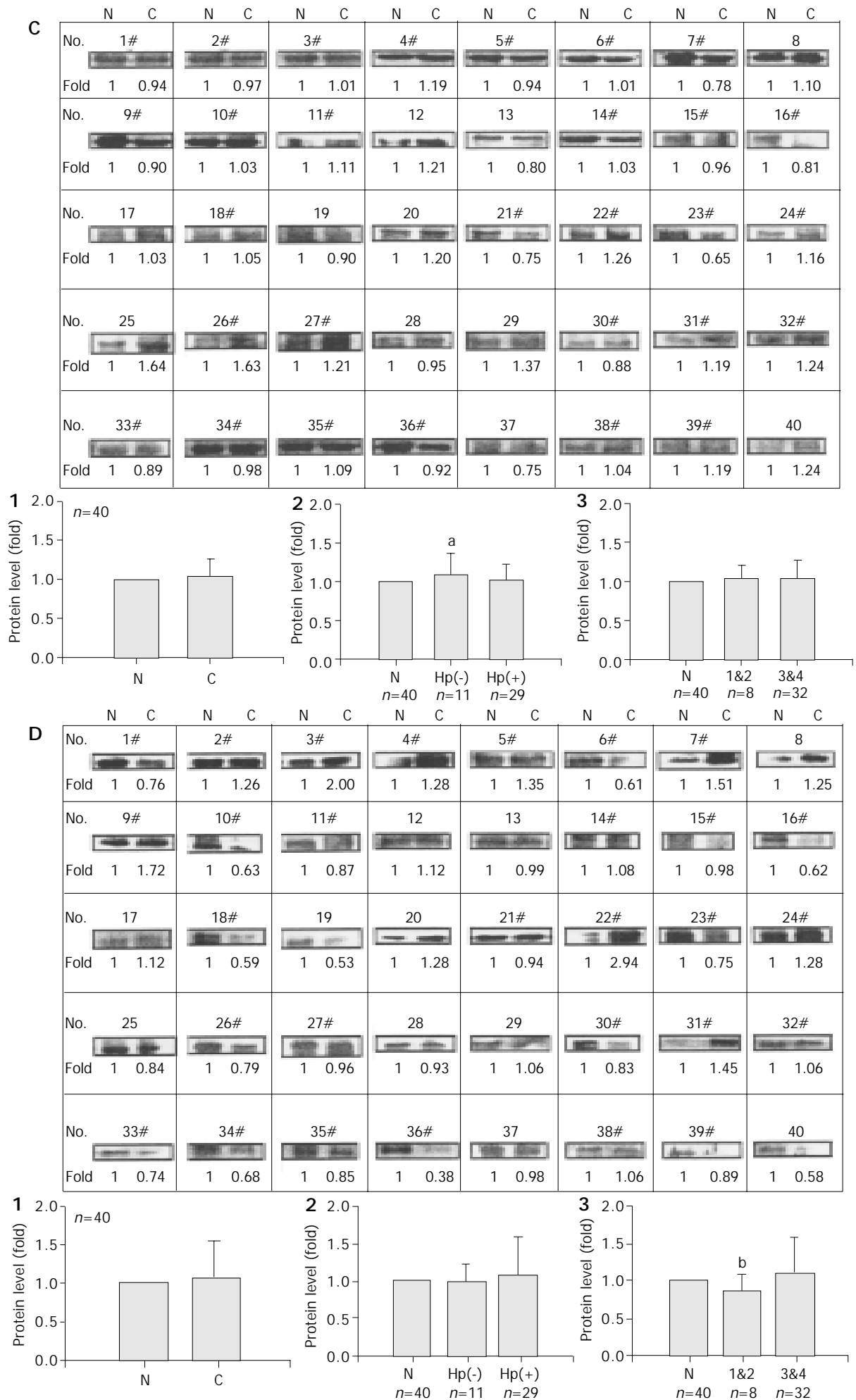
Furthermore, 8-OHdG, iNOS, NFκB, Mcl-1 and IAP concentrations were significantly higher in stage 3 and 4 patients than in stage 1 and 2 patients.

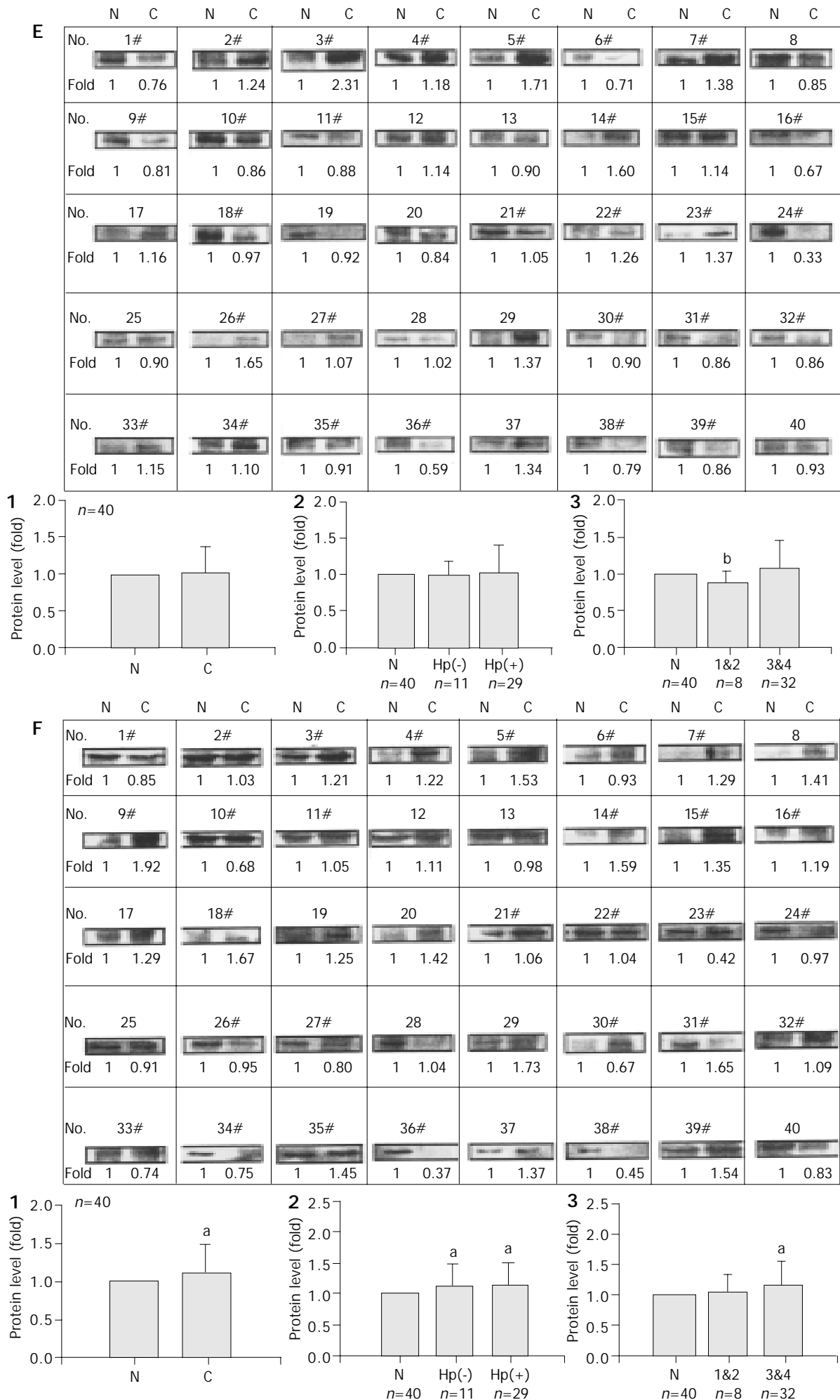
DISCUSSION

H pylori infection may influence the progression from chronic gastritis to adenocarcinoma of the distal stomach by a multifactorial, multistep process, in which chronic inflammation plays a major role. Free radical mediated oxidative DNA damage was involved in this process^[21-23]. The DNA damage provoked by oxygen free radicals can have very harmful consequences, leading to gene modifications that are potentially mutagenic and/or carcinogenic. Recently, 8-OHdG has been accepted as a sensitive marker for oxidative DNA damage in affected organs. Chronic gastritis due to *H pylori* infection is characterized by the accumulation of oxidative DNA damage measured by concentrations of 8-OHdG, indicating mutagenic and carcinogenic potential^[24]. In this study, we demonstrated an increase in the concentrations of 8-OHdG in cancer tissues. Furthermore, the increase was significantly higher in patients infected with *H pylori* as well as in patients with advanced gastric cancer. The increased level of oxidative DNA damage suggested a mechanistic link between *H pylori* infection and gastric carcinoma^[25,26].

H pylori-associated inflammation related to DNA damage is indicated by increased levels of oxidative DNA damage, increased occurrence of apoptosis, as well as increased expression of iNOS, which seemed to provide the mechanistic links between *H pylori* infection and gastric carcinogenesis^[27,28]. Upregulation of iNOS expression might contribute to the oxidative DNA damage observed during *H pylori* infection^[25]. Recent studies have shown that nitric oxide (production of iNOS) reacts rapidly with superoxide anions produced by *H pylori*-infected gastric tissues to form peroxynitrate, which could induce oxidative damage^[29]. This may increase the mutation rate in infected hyperproliferative gastric mucosa. In addition, the expressions of iNOS are closely related to tumor angiogenesis, and involved in progression of the disease as well as lymph node metastasis. Thus the expressions of iNOS might serve as indexes for evaluating staging of gastric carcinoma. In this study, we observed significantly higher increases in the concentrations of iNOS in patients infected with *H pylori* and in patients with advanced gastric cancer, compared with *H pylori*-negative patients and low stage gastric cancer patients, respectively.







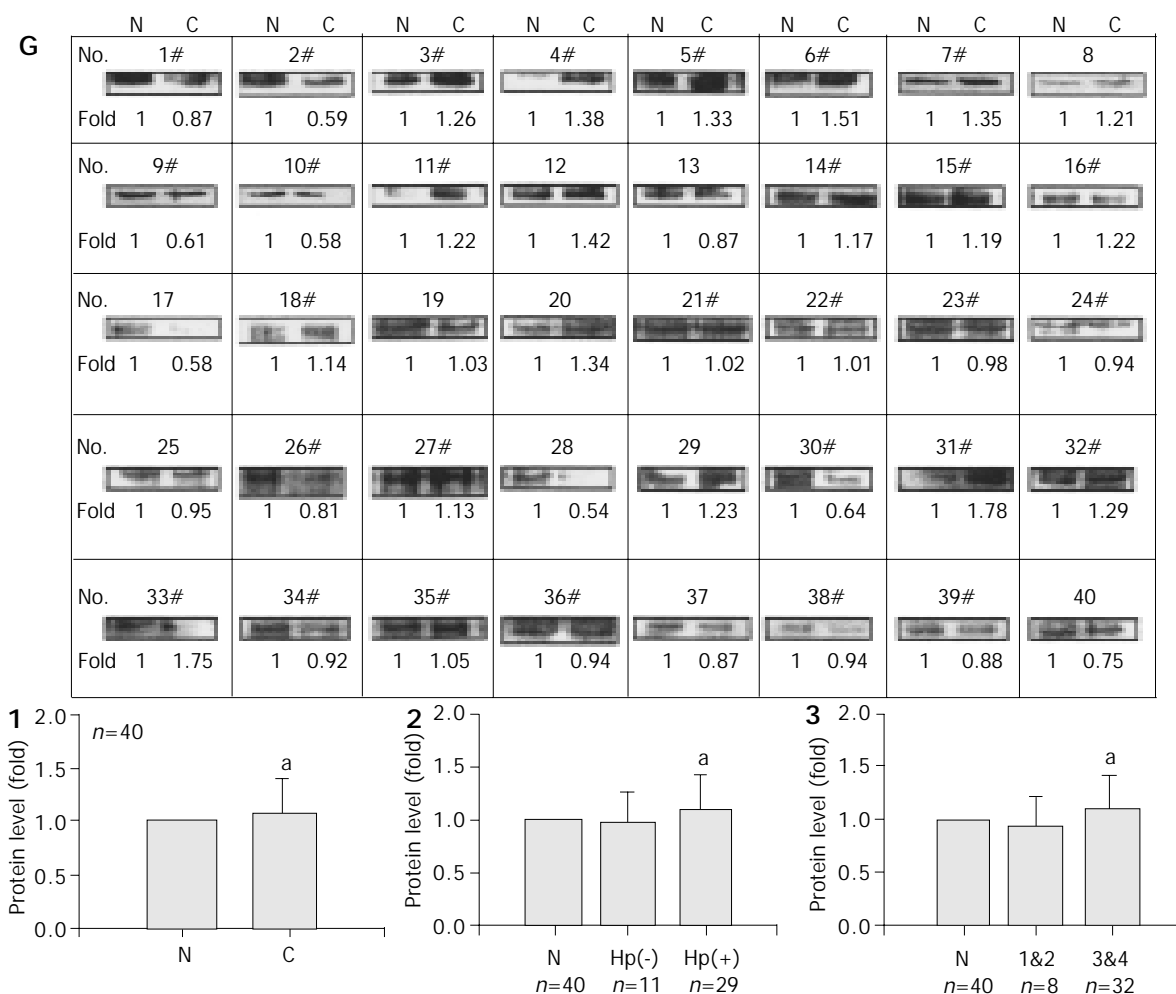


Figure 2 Immunoblot analysis of factors affecting cell death. A: Immunoblot analysis of iNOS. 1: Significantly higher concentrations of iNOS in cancer tissues compared with adjacent non-cancer tissues. 2: Significantly higher concentrations of iNOS in cancer tissues of patients with and without *H pylori* infection. 3: Significantly higher iNOS concentrations in stage 3 and 4 patients. #=*H pylori* infected, ^a*P*<0.05, ^b*P*<0.01, N: non-cancer tissue, C: cancer tissue, Hp(-): without *H pylori* infection, Hp(+): with *H pylori* infection, 1&2: gastric cancer stages 1 and 2, 3&4: gastric cancer stages 3 and 4. B: Immunoblot analysis of NFκB. 1: Significantly higher concentrations of NFκB in cancer tissues in comparison with adjacent non-cancer tissues. 2: Significantly higher concentrations of NFκB in cancer tissues of patients with and without *H pylori* infection. 3: Significantly higher NFκB concentrations in stage 3 and 4 patients #=*H pylori* infected, *P*<0.05, N: non-cancer tissue, C: cancer tissue, Hp(-): without *H pylori* infection, Hp(+): with *H pylori* infection, 1&2: gastric cancer stages 1 and 2, 3&4: gastric cancer stages 3 and 4. C: Immunoblot analysis of MEKK1. 1: Concentrations of MEKK1 in cancer tissues and adjacent non-cancer tissues. 2: Significantly higher concentrations of MEKK1 in cancer tissues of patients without *H pylori* infection. 3. No differences in MEKK1 concentrations in cancer tissues with different stages. #=*H pylori* infected, ^a*P*<0.05, N: non-cancer tissue, C: cancer tissue, Hp(-): without *H pylori* infection, Hp(+): with *H pylori* infection, 1&2: gastric cancer stages 1 and 2, 3&4: gastric cancer stages 3 and 4. D: Immunoblot analysis of Caspase 3. 1: Similar concentrations of Caspase 3 in cancer tissues and adjacent non-cancer tissues. 2: Similar concentrations of Caspase 3 in cancer tissues of patients with and without *H pylori* infection. 3: Significantly lower Caspase 3 concentrations in stage 1 and 2 patients. #=*H pylori* infected, ^b*P*<0.01, N: non-cancer tissue, C: cancer tissue, Hp(-): without *H pylori* infection, Hp(+): with *H pylori* infection, 1&2: gastric cancer stages 1 and 2, 3&4: gastric cancer stages 3 and 4. E: Immunoblot analysis of Bcl-2. 1: Similar concentrations of Bcl-2 in cancer tissues and adjacent non-cancer tissues. 2: No differences in concentrations of Bcl-2 in cancer tissues of patients with and without *H pylori* infection. 3: Significantly higher Bcl-2 concentrations in stage 1 and 2 patients. #=*H pylori* infected, ^b*P*<0.01, N: non-cancer tissue, C: cancer tissue, Hp(-): without *H pylori* infection, Hp(+): with *H pylori* infection, 1&2: gastric cancer stages 1 and 2, 3&4: gastric cancer stages 3 and 4. F: Immunoblot analysis of Mcl-1. 1: Significantly higher concentrations of Mcl-1 in cancer tissues in comparison with adjacent non-cancer tissues. 2: Significantly higher concentration of Mcl-1 in cancer tissues of patients with and without *H pylori* infection. 3: Significant higher Mcl-1 concentrations in stage 3 and 4 patients than #=*H pylori* infected, ^a*P*<0.05, N: non-cancer tissue, C: cancer tissue, Hp(-): without *H pylori* infection, Hp(+): with *H pylori* infection, 1&2: gastric cancer stages 1 and 2, 3&4: gastric cancer stages 3 and 4. G: Immunoblot analysis of IAP. 1: Significantly higher concentrations of IAP in cancer tissues compared with adjacent non-cancer tissues, 2: Significantly higher concentrations of IAP in cancer tissues with *H pylori* infection, 3: Significantly higher IAP concentrations in stage 3 and 4 patients #=*H pylori* infected, ^a*P*<0.05, N: non-cancer tissue, C: cancer tissue, Hp(-): without *H pylori* infection, Hp(+): with *H pylori* infection, 1&2: gastric cancer stages 1 and 2, 3&4: gastric cancer stages 3 and 4.

NFκB has been found to be a critical regulator of genes involved in inflammation, cell proliferation, and apoptosis^[30]. Recent studies suggested that NFκB might play a critical role in protecting cells against apoptosis^[31,32]. The magnitude of the stimulus and the cell type involved may determine whether

NFκB leads to cell survival or cell death. Maeda *et al.* reported cag PAI positive *H pylori* was capable of inducing apoptotic effects mainly through the mitochondrial pathway. Antiapoptotic effects mediated by NFκB activation were also observed by Maeda *et al.*^[33]. In this study, we revealed an

increase in the concentrations of NF κ B in cancer tissues. In addition, the increase was significantly higher in patients infected with *H pylori* as well as in patients with advanced gastric cancer compared with *H pylori*-negative patients and low stage gastric cancer patients, respectively.

Recent investigations implicated mitogen-activated protein kinases (MAPK) as additional mediators of *H pylori*-dependent NF κ B activation and IL-8 expression. Studies have demonstrated the presence of cross-talk between the MAPK and NF κ B pathways^[21-34]. MAPK cascades are signal transduction networks that target transcription factors and thus participate in a diverse array of cellular functions including cytokine production. In this study, there was an increase in the concentrations of MEKK1, a member of the MAPK signaling cascade in cancer tissues. However, the increase was not significant in all the studied patient groups.

Kanai *et al.* noted that transforming growth factor- α played an anti-apoptotic role in gastric mucosal cells by enhancing the expression of Bcl-2 family proteins via an NF κ B-dependent pathway^[35]. NF κ B is now known to upregulate transcription of several anti-apoptotic genes, including a cellular inhibitor of apoptosis, a Bcl-2 homolog, and cyclooxygenase-2, as well as pro-apoptotic genes, such as bax and p53. Tumor cells can have abnormal expression levels of factors such as Bcl-2 family proteins that slow the progression of apoptosis and elevate NF κ B-regulated transcription, which can inhibit TNF- α -induced apoptosis. However, in this study, no significant changes in the concentrations of Bcl-2 in cancer tissues or patients infected with *H pylori* were noted. Furthermore, upregulation of anti-apoptotic gene mcl-1 might play a role in interleukin-6-mediated protection of gastric cancer cells from the apoptosis induced by hydrogen peroxide^[36]. The anti-apoptotic role played by NF κ B also involves the ability of this transcriptional factor to induce expression of genes that promote cell survival, such as the genes coding for TRAF1, TRAF2, and the cellular inhibitors of apoptosis 1 and 2 (c-IAP1, c-IAP2)^[37]. In this study, we demonstrated an increase in the concentrations of IAP and Mcl-1, anti-apoptosis related proteins in cancer tissues. Furthermore, the increase was significantly higher in patients infected with *H pylori* as well as in patients with advanced gastric cancer, compared with *H pylori*-negative and non-advanced gastric patients, respectively. Therefore, enhanced antiapoptosis-related protein expression may contribute to disease progression.

Caspase3 is a member of the cell death effector (CED)-3 family, which is involved in the induction of apoptosis. Hoshi *et al.* reported Caspase 3 was involved in the development or regulation of apoptotic cell death in cell turnover of normal and neoplastic mucosa of the human stomach^[38]. These results indicate that gastric adenocarcinoma is associated with an inhibition of apoptosis and the augmentation of proliferative activity of tumor cells when compared to non-neoplastic gastric mucosa. However, in this study, there was no difference of increase in Caspase 3 between patients with or without *H pylori* infection or patients with or without advanced gastric cancer.

In conclusion, chronic *H pylori*-induced iNOS expression and subsequent DNA damage as well as signal transduction appear to make an important contribution to *H pylori*-related gastric carcinogenesis. This sequence of events found in this study supports the hypothesis that oxygen-free radical-mediated damage induced by *H pylori* plays a vital role in the development of gastric carcinoma in patients with chronic gastritis.

ACKNOWLEDGEMENT

The authors would like to thank the Biostatistics Task Force of Taichung Veterans General Hospital for their help with the statistical analyses performed in this study.

REFERENCES

- 1 **Wang KX**, Wang XF, Peng JL, Cui YB, Wang J, Li CP. Detection of serum anti-*Helicobacter pylori* immunoglobulin G in patients with different digestive malignant tumors. *World J Gastroenterol* 2003; **9**: 2501-2504
- 2 **Nomura A**, Stemmermann GN, Chyou PH, Kato I, Perez-Perez GI, Blaser MJ. *Helicobacter pylori* infection and gastric carcinoma among Japanese Americans in Hawaii. *N Engl J Med* 1991; **325**: 1132-1136
- 3 **Parsonnet J**, Friedman GD, Vandersteen DP, Chang Y, Vogelman JH, Orentreich N, Sibley RK. *Helicobacter pylori* infection and the risk of gastric carcinoma. *N Engl J Med* 1991; **325**: 1127-1131
- 4 **Van Antwerp DJ**, Martin SJ, Kafri T, Green DR, Verma IM. Suppression of TNF- α induced apoptosis by NF- κ B. *Science* 1996; **274**: 787-789
- 5 **Correa P**, Ruiz B, Shi TY, Janney A, Sobhan M, Torrado J, Hunter F. *Helicobacter pylori* and nucleolar organizer regions in the gastric antral mucosa. *Am J Clin Pathol* 1994; **101**: 656-660
- 6 **Fraser AG**, Sim R, Sankey EA. Effect of eradication of *Helicobacter pylori* on gastric epithelial cell proliferation. *Aliment Pharmacol Ther* 1994; **8**: 167-173
- 7 **Lynch DA**, Mapstone NP, Clarke AM, Sobala GM, Jackson P, Morrison L, Dixon MF, Quirke P, Axon AT. Cell proliferation in *Helicobacter pylori* associated gastritis and the effect of eradication therapy. *Gut* 1995; **36**: 346-350
- 8 **Fox JG**, Dangler CA, Taylor NS, King A, Koh TJ, Wang TC. High-salt diet induces gastric epithelial hyperplasia and parietal cell loss, and enhances *Helicobacter pylori* colonization in C57BL/6 mice. *Cancer Res* 1999; **59**: 4823-4828
- 9 **Peek R**, Wirth HP, Moss SF, Yang M, Abdalla AM, Tham KT, Zhang T, Tang LH, Modlin IM, Blaser MJ. *Helicobacter pylori* alters gastric epithelial cell cycle events and gastrin secretion in Mongolian gerbils. *Gastroenterology* 2000; **118**: 48-59
- 10 **Israel DA**, Salama N, Arnold CN, Moss SF, Ando T, Wirth HP, Tham KT, Camorlinga M, Blaser MJ, Falkow S, Peek RM Jr. *Helicobacter pylori* strain-specific differences in genetic content, identified by microarray, influence host inflammatory responses. *J Clin Invest* 2001; **107**: 611-620
- 11 **Moss SF**, Calam J, Agarwal B, Wang S, Holt PR. Induction of gastric epithelial apoptosis by *Helicobacter pylori*. *Gut* 1996; **38**: 498-501
- 12 **Mannick EE**, Bravo LE, Zarama G, Realpe JL, Zhang XJ, Ruiz B, Fonham ET, Mera R, Miller MJ, Correa P. Inducible nitric oxide synthase, nitrotyrosine and apoptosis in *Helicobacter pylori* gastritis: effects of antibiotics and antioxidants. *Cancer Res* 1996; **56**: 3238-3243
- 13 **Jones NL**, Shannon PT, Cutz E, Yeager H, Sherman PM. Increase in proliferation and apoptosis of gastric epithelial cells early in the natural history of *Helicobacter pylori* infection. *Am J Pathol* 1997; **151**: 1695-1703
- 14 **Rudi J**, Kuck D, Strand S, von Herbay A, Mariani SM, Krammer PH, Galle PR, Stremmel W. Involvement of the CD95 (APO-1/Fas) Receptor and Ligand System in *Helicobacter pylori*-induced Gastric Epithelial Apoptosis. *J Clin Invest* 1998; **102**: 1506-1514
- 15 **Anti M**, Armuzzi A, Iascone E, Valenti A, Lippi ME, Covino M, Vecchio FM, Pierconti F, Buzzi A, Pignataro G, Bonvicini F, Gasbarrini G. Epithelial-cell apoptosis and proliferation in *Helicobacter pylori*-related chronic gastritis. *Ita J Gastroenterol Hepatol* 1998; **30**: 153-159
- 16 **Hirasawa R**, Tatsuta M, Iishi H, Yano H, Baba M, Uedo N, Sakai N. Increase in apoptosis and decrease in ornithine decarboxylase activity of the gastric mucosa in patients with atrophic gastritis and gastric ulcer after successful eradication of *Helicobacter pylori*. *Am J Gastroenterol* 1999; **94**: 2398-2402
- 17 International Union Against Cancer; Sobin L and Wittekind C, eds. TNM Classification of Malignant Tumors. 6th ed. New York, USA: Wiley-Liss 2002: 65-68
- 18 **Dahlhaus M**, Appel KE. N-Nitrosodimethylamine, N-nitrosodiethylamine, and N-nitrosomorpholine fail to generate 8-hydroxy-2'-deoxyguanosine in liver DNA of male F344 rats. *Mutat Res* 1993; **285**: 295-302
- 19 **Shen HM**, Ong CN, Lee BL, Shi CY. Aflatoxin B1-induced 8-hydroxydeoxyguanosine formation in rat hepatic DNA. *Car-*

- cinogenesis* 1995; **16**: 419-422
- 20 **Yermilov V**, Rubio J, Becchi M, Friesen MD, Pignatelli B, Ohshima H. Formation of 8-nitroguanine by the reaction of guanine with peroxyxynitrite *in vitro*. *Carcinogenesis* 1995; **16**: 2045-2050
- 21 **Mercurio F**, Zhu H, Murray BW, Shevchenko A, Bennett BL, Li J, Young DB, Barbosa M, Mann M, Manning A, Rao A. IKK-1 and IKK-2: cytokine-activated I κ B kinases essential for NF κ B activation. *Science* 1997; **278**: 860-866
- 22 **Yu J**, Russell RM, Salomon RN, Murphy JC, Palley LS, Fox JG. Effect of *Helicobacter mustelae* infection on ferret gastric epithelial cell proliferation. *Carcinogenesis* 1995; **16**: 1927-1931
- 23 **Peek RM Jr**, Moss SF, Tham KT, Perez-Perez GI, Wang S, Miller GG, Atherton JC, Holt PR, Blaser MJ. *Helicobacter pylori* cagA⁺ strains and dissociation of gastric epithelial cells proliferation from apoptosis. *J Natl Cancer Inst* 1997; **89**: 863-868
- 24 **Farinati F**, Cardin R, Degan P, Rugge M, Mario FD, Bonvicini P, Naccarato R. Oxidative DNA damage accumulation in gastric carcinogenesis. *Gut* 1998; **42**: 351-356
- 25 **Baik SC**, Youn HS, Chung MH, Lee WK, Cho MJ, Ko GH, Park CK, Kasai H, Rhee KH. Increased oxidative DNA damage in *Helicobacter pylori*-infected human gastric mucosa. *Cancer Res* 1996; **56**: 1279-1282
- 26 **Papa A**, Danese S, Sgambato A, Ardito R, Zannoni G, Rinelli A, Vecchio FM, Gentiloni-Silveri N, Cittadini A, Gasbarrini G, Gasbarrini A. Role of *Helicobacter pylori* CagA⁺ infection in determining oxidative DNA damage in gastric mucosa. *Scand J Gastroenterol* 2002; **37**: 409-413
- 27 **Hahm KB**, Lee KJ, Kim JH, Cho SW, Chung MH. *Helicobacter pylori* infection, oxidative DNA damage, gastric carcinogenesis, and reversibility by rebamipide. *Dig Dis Sci* 1998; **43**(Suppl 9): 72S-77S
- 28 **Koh E**, Noh SH, Lee YD, Lee HY, Han JW, Lee HW, Hong S. Differential expression of nitric oxide synthase in human stomach cancer. *Cancer Lett* 1999; **146**: 173-180
- 29 **Tamir S**, Tannenbaum S. The role of nitric oxide in the carcinogenic process. *Biochim Biophys Acta* 1996; **1288**: F31-36
- 30 **Baldwin AS Jr**. The NF- κ B and I κ B proteins: new discoveries and insights. *Annu Rev Immunol* 1996; **14**: 649-683
- 31 **Wang CY**, Mayo MW, Baldwin AS Jr. TNF- and cancer therapy-induced apoptosis: potentiation by inhibition of NF- κ B. *Science* 1996; **274**: 784-787
- 32 **Beg AA**, Baltimore D. An essential role for NF- κ B in preventing TNF α -induced cell death. *Science* 1996; **274**: 782-784
- 33 **Maeda S**, Yoshida H, Mitsuno Y, Hirata Y, Ogura K, Shiratori Y, Omata M. Analysis of apoptotic and antiapoptotic signaling pathways induced by *Helicobacter pylori*. *Gut* 2002; **50**: 771-778
- 34 **Malinin NL**, Boldin MP, Kovalenko AV, Wallach D. MAP3K-related kinase involved in NF- κ B induction by TNF, CD95 and IL-1. *Nature* 1997; **385**: 540-544
- 35 **Dumont A**, Hehner SP, Hofmann TG, Ueffing M, Droge W, Schmitz ML. Hydrogen peroxide-induced apoptosis is CD95-independent, requires the release of mitochondria-derived reactive oxygen species and the activation of NF- κ B. *Oncogene* 1999; **18**: 747-757
- 36 **Lin MT**, Juan CY, Chang KJ, Chen WJ, Kuo ML. IL-6 inhibits apoptosis and retains oxidative DNA lesions in human gastric cancer AGS cells through up-regulation of anti-apoptotic gene mcl-1. *Carcinogenesis* 2001; **22**: 1947-1953
- 37 **Wang CY**, Mayo MW, Korneluk RG, Goeddel DV, Baldwin AS Jr. NF- κ B antiapoptosis: induction of TRAF1 and TRAF2 and c-IAP1 and c-IAP2 to suppress caspase-8 activation. *Science* 1998; **281**: 1680-1683
- 38 **Hoshi T**, Sasano H, Kato K, Yabuki N, Ohara S, Konno R, Asaki S, Toyota T, Tateno H, Nagura H. Immunohistochemistry of Caspase3/ CPP32 in human stomach and its correlation with cell proliferation and apoptosis. *Anticancer Res* 1998; **18**: 4347-4353

Edited by Wang XL Proofread by Xu FM

Japanese herbal medicine, *Saiko-keishi-to*, prevents gut ischemia/reperfusion-induced liver injury in rats via nitric oxide

Yoshinori Horie, Mikio Kajihara, Shuka Mori, Yoshiyuki Yamagishi, Hiroyuki Kimura, Hironao Tamai, Shinzo Kato, Hiromasa Ishii

Yoshinori Horie, Mikio Kajihara, Shuka Mori, Yoshiyuki Yamagishi, Hiroyuki Kimura, Hironao Tamai, Shinzo Kato, Hiromasa Ishii, Department of Internal Medicine, School of Medicine, Keio University, Tokyo 160-8582, Japan

Supported by the Grants from Tsumura Co. Ltd

Correspondence to: Yoshinori Horie, M.D., Department of Internal Medicine, School of Medicine, Keio University, 35 Shinanomachi Shinjuku-ku, Tokyo 160-8582, Japan. yhorie@sc.itc.keio.ac.jp

Telephone: +81-3-5363-3789 **Fax:** +81-3-3356-9654

Received: 2004-02-06 **Accepted:** 2004-03-16

Abstract

AIM: To determine whether *Saiko-keishi-to* (TJ-10), a Japanese herbal medicine, could protect liver injury induced by gut ischemia/reperfusion (I/R), and to investigate the role of NO.

METHODS: Male Wistar rats were exposed to 30-min gut ischemia followed by 60 min of reperfusion. Intravital microscopy was used to monitor leukocyte recruitment. Plasma tumor necrosis factor (TNF) levels and alanine aminotransferase (ALT) activities were measured. TJ-10 1 g/(kg·d) was intragastrically administered to rats for 7 d. A NO synthase inhibitor was administered.

RESULTS: In control rats, gut I/R elicited increases in the number of stationary leukocytes, and plasma TNF levels and ALT activities were mitigated by pretreatment with TJ-10. Pretreatment with the NO synthase inhibitor diminished the protective effects of TJ-10 on leukostasis in the liver, and the increase of plasma TNF levels and ALT activities. Pretreatment with TJ-10 increased plasma nitrite/nitrate levels.

CONCLUSION: TJ-10 attenuates the gut I/R-induced hepatic microvascular dysfunction and sequential hepatocellular injury via enhancement of NO production.

Horie Y, Kajihara M, Mori S, Yamagishi Y, Kimura H, Tamai H, Kato S, Ishii H. Japanese herbal medicine, *Saiko-keishi-to*, prevents gut ischemia/reperfusion-induced liver injury in rats via nitric oxide. *World J Gastroenterol* 2004; 10(15): 2241-2244
<http://www.wjgnet.com/1007-9327/10/2241.asp>

INTRODUCTION

Herbal medicines that have been used in China for thousands of years are now being manufactured in Japan as drugs containing ingredients of standardized quality and quantity. The clinical efficacy of these medicines has been utilized by Japanese Western-medicine practitioners for more than 20 years and is well recognized. One of the herbal medicines, *Saiko-keishi-to* (TJ-10) (Chinese name; *Chai-Hu-Gui-Zhi-Tang*), is a common drug to treat duodenal ulcer, pancreatitis, and chronic liver disease in Japan. It is an oral medicine and consists of 9 herb components: *Bupleurum* root, *Pinellia tuber*, *Scutellaria*

root, *Jujube* fruit, *Ginger rhizome*, ginseng root, cinnamon bark, peony root and *Glycyrrhiza* root. Another common herbal medicine, Sho-saiko-to (TJ-9), consists of 7 components of them: *Bupleurum* root, *Pinellia tuber*, *Scutellaria* root, jujube fruit, ginger rhizome, ginseng root, and *Glycyrrhiza* root. In a double-blind multicenter clinical trial, TJ-9 was reported to reduce the elevated serum activities of aspartate transaminase, alanine transaminase (ALT), and glutamyl transpeptidase in chronic active hepatitis patients^[1]. TJ-9 has been shown to improve liver function as well as the symptoms associated with chronic liver disease including digestive discomfort^[2]. Although TJ-10 has been often administered to patients with chronic liver disease as well as TJ-9, there are few epidemiological reports^[3], and little is known about mechanisms of its cytoprotective effects on liver damage. Recently, because of its major pharmaceutical effects, TJ-10 is presumed to gradually improve biological defense mechanisms. One of the components of TJ-10, *Saikosaponin*, has been reported to inhibit hepatocyte necrosis induced by galactosamine^[4], and *Saikosaponin-d* has been shown to reduce microsomal lipid peroxidation induced by NADPH and CCl₄^[5]. However, its mode of action has not been fully elucidated.

Nitric oxide (NO) has been found to be a modulator of the adhesive interactions between leukocytes, platelets, and endothelial cells^[6-9] as well as an important modulator of tissue blood flow, arterial pressure, and neurotransmission^[8], and NO-dependent cell-cell interactions have been demonstrated in tissues exposed to ischemia and reperfusion (I/R), an injury process in which leukocyte-endothelial cell adhesion plays a critical role. A role of NO in the pathobiology of I/R injury has been supported by observations that inhibition of NO biosynthesis could elicit most of the microvascular alterations observed in tissues exposed to I/R^[7,10], and NO-donating compounds have been shown to provide significant protection against the microvascular dysfunction that is normally associated with I/R^[7]. We developed a murine model of leukocyte-dependent hepatocellular dysfunction that was elicited by gut I/R^[11-13]. The model allows *in vivo* assessment of the effects of I/R on leukocyte sequestration in sinusoids of different regions of the liver lobule, leukocyte adherence in postsinusoidal venules, and the number of perfused sinusoids. Using this model, we have recently demonstrated that inhibition of both NO synthase and supplementation with exogenous NO could affect the leukocyte rolling, leukocyte adhesion, and sinusoidal perfusion elicited in the liver by gut I/R^[14-16].

Some herbal medicines have been reported to have an inducing effect on NO production by non-stimulated macrophages^[17]. We have recently reported that TJ-9 could attenuate the gut I/R-induced hepatic microvascular dysfunction and sequential hepatocellular injury via NO^[18]. However, little is known about the effect of TJ-10 on plasma NO levels and I/R injury *in vivo*. TJ-9 is contraindicated for liver cirrhosis, because of its side-effect, causing lung fibrosis. Since TJ-10 has 30% less *Saikosaponin* compared to TJ-9, it seems to be safer. Therefore, frequency and importance of TJ-10 are expected to increase in Japan. In the present study, we investigated whether TJ-10 modulated the gut I/R-induced microvascular dysfunction in the liver, and the role of NO in the responses by inhibiting NO synthase.

MATERIALS AND METHODS

Animals and surgical procedure

Male Wistar rats (200-250 g) were fed a standard rat chow for 2 wk, and TJ-10 (1 g/kg in saline) or saline alone was then administered for 7 d intragastrically through a tube. Experiments below were performed 18 h after the final dose of TJ-10 or saline. The rats were fasted for 18 h prior to each experiment, and then intraperitoneally anesthetized with pentobarbital sodium (35 mg/kg). The left carotid artery was cannulated, and a catheter was positioned in aortic arch to monitor blood pressure. The left jugular vein was cannulated for drug administration. All experiments were performed according to the criteria outlined in the National Research Council Guide.

Intravital microscopy

After laparotomy, one lobe of the liver was examined through an inverted intravital microscope (TMD-2S, Diaphoto, Nikon, Tokyo, Japan) and images were recorded with a silicon intensified target (SIT) camera (C-2400-08, Hamamatsu photonicus, Shizuoka, Japan). The liver was placed on an adjustable Plexiglas microscope stage and covered with a nonfluorescent coverslip that allowed observation of a 2 cm² segment of tissue. The liver was carefully positioned to minimize the influence of respiratory movements, and its surface was moistened and covered with cotton gauze soaked with saline. Images of microcirculation at the surface of the liver were observed through consecutive microfluorographs of hepatic microcirculation, that is, those of rhodamine-6G-labeled leukocytes in the sinusoids, were observed at 90 min after the onset of SMA occlusion and recorded on a digital video recorder. The number of stationary leukocytes was determined off-line during playback of videotape images. A leukocyte was considered to be stationary within the microcirculation (sinusoids) if it remained stationary for more than 10 s. The lobule, which had the fewest stationary leukocytes, was selected for observation at the basal condition. Stationary leukocytes were quantified in both the midzonal and pericentral regions of the liver lobule and expressed as the number per field of view (2.1×10⁵ μm²). The percentage of non-perfused sinusoids was calculated as the ratio of the number of non-perfused sinusoids to the total number of sinusoids per microscopic field.

Experimental protocols

We observed the surface of liver for 10 min before ligating the superior mesenteric artery to ensure that all parameters measured on-line were in a steady state. The superior mesenteric artery was then ligated for 0 (sham) or 30 min with a snare created from a polyethylene tube. At the end of the ischemic period, the ligation was gently removed. Leukocyte accumulation and the number of non-perfused sinusoids (NPS) were measured before ischemia, immediately following reperfusion, and every 15 min for 1 h thereafter. In one set of experiments, 7 untreated animals, and 5 TJ-10-treated animals in the control groups (sham gut I/R) and gut I/R groups were used. In another set of experiments in which TJ-10 was administered, the rats were given a NO synthase (NOS) inhibitor, N^G-monomethyl-L-arginine (L-NMMA; Sigma, St. Louis, MO) (0.5 mg/kg, i.v.) 30 min before the onset of ischemia. These experiments were performed with 5 animals in each group. In some experiments, the rats were given dexamethasone (2 mg/kg, Sigma, St. Louis, MO) with or without L-NMMA (0.5 mg/kg, i.v.) 30 min before the onset of ischemia. These experiments were performed with 5 animals in each group.

Tumor necrosis factor and endotoxin assay

Sixty min after the onset of reperfusion, blood plasma samples

for tumor necrosis factor (TNF) detection were collected from the inferior vena cava at a point proximal to the hepatic vein. Plasma TNF concentration was determined in a microtiter plate using a TNF immunoassay kit (BioSource International, Camarillo, CA) based on enzyme-linked immunosorbent assay (ELISA) as described in our previous study^[19]. Plasma endotoxin levels were measured by endospecy (an endotoxin-specific chromogen. Seikagaku Co., Tokyo, Japan) according to our previous report^[20].

Enzyme and nitrite/nitrate assay

Blood samples for enzyme activities were collected from the carotid artery 6 h after the onset of reperfusion. Serum ALT activity was determined by conventional UV methods as previously described^[21]. Blood samples for nitrite/nitrate assay were collected from the inferior vena cava 16 h after the last administration of TJ-10 (saline as control). The combined levels of nitrite and nitrate in plasma were determined by a previously reported method^[22]. Five separate experiments were performed.

Statistical analysis

The data were analyzed by standard statistical methods, i.e., ANOVA and Scheffe's (post hoc) test. All values were reported as mean±SD. *P*<0.05 was considered statistically significant.

RESULTS

Figure 1A shows the effects of TJ-10 and/or L-NMMA on the gut I/R induced leukostasis in sinusoids of the midzonal and pericentral (including the terminal hepatic venule [THV]) regions of the liver lobule (panel A), and the entire liver lobule (sinusoids + THV, panel B). In control rats, gut I/R elicited significant increases in the number of stationary leukocytes compared to basal values. Pretreatment with TJ-10 blunted the gut I/R-induced leukostasis in the midzonal (untreated+I/R: 9.6±0.6, TJ-10+I/R: 3.6±0.6, per field) and the pericentral regions (untreated+I/R: 6.0±0.7, TJ-10+I/R: 3.6±0.5, per field). L-NMMA diminished the protective effect of TJ-10 in the pericentral region (5.6±0.2, per field), but did not significantly affect the gut I/R-induced leukostasis in the midzonal region or the entire liver lobule.

Figure 1B shows the effect of TJ-10 and/or L-NMMA on the gut I/R-induced elevation of plasma TNF levels. In the control rats, gut I/R elevated the plasma TNF-α levels. Pretreatment with TJ-10, however, blunted the gut I/R-induced elevation of plasma TNF-α levels (untreated+I/R: 140.8±12.6, TJ-10+I/R: 61.7±22.5 ng/L). L-NMMA diminished the protective effects of TJ-10 (113.2±13.7 ng/L).

Figure 1C shows the effect of TJ-10 and/or L-NMMA on the gut I/R-induced elevation of serum endotoxin levels. In the control rats, gut I/R elevated the serum endotoxin levels. Pretreatment with TJ-10, however, blunted the gut I/R-induced elevation of serum endotoxin levels (untreated+I/R: 39.2±8.1, TJ-10+I/R: 11.1±3.3 ng/L). L-NMMA diminished the protective effects of TJ-10 (34.7±5.3 ng/L).

Figure 1D illustrates the effect of TJ-10 and/or L-NMMA on the gut I/R-induced elevation of plasma ALT activities. In the control rats, gut I/R elevated the plasma ALT activities. Pretreatment with TJ-10, however, blunted the gut I/R-induced elevation of plasma ALT levels (untreated+I/R: 146.6±13.0, TJ-9+I/R: 76.0±7.0 IU/L). L-NMMA diminished the protective effects of TJ-10 (123.2±11.9 IU/L).

Table 1 shows the effects of TJ-9 and TJ-10 on plasma nitrite/nitrate levels. Pretreatment with TJ-10 increased the plasma nitrite/nitrate levels as well as TJ-9.

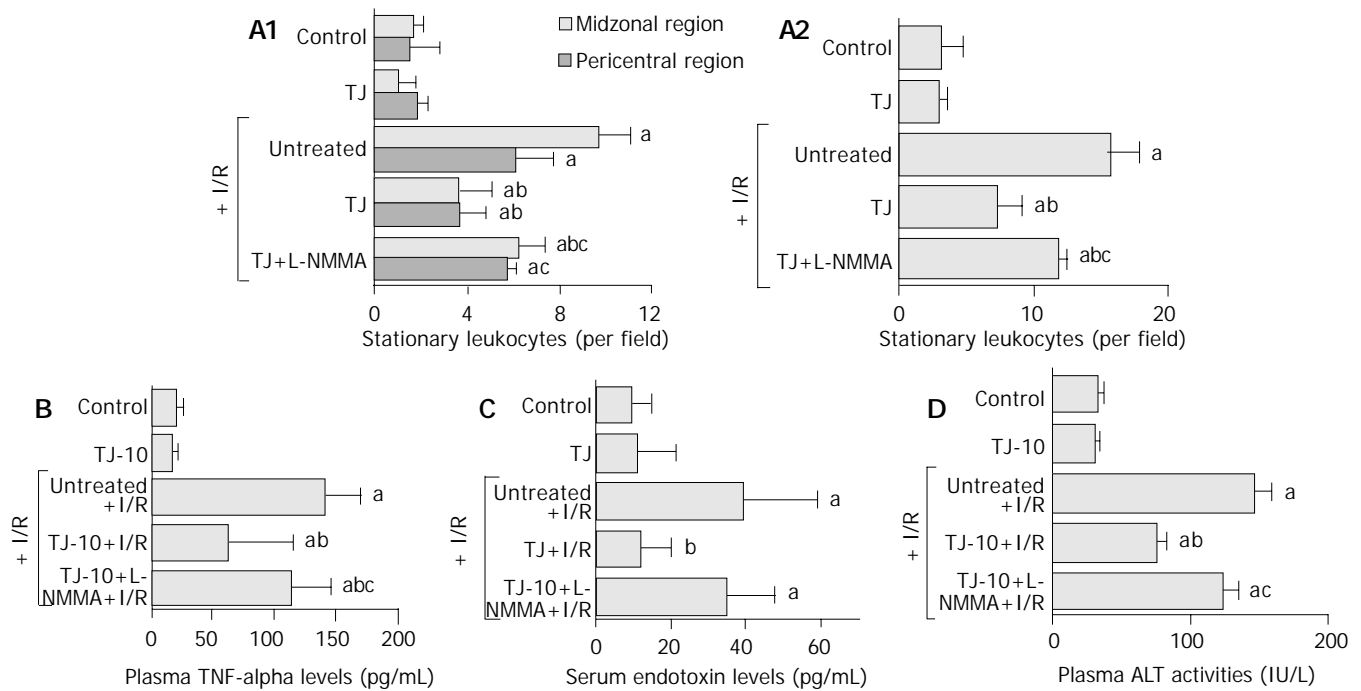


Figure 1 Effects of Saiko-keishi-to (TJ-10) and/or an NO synthase inhibitor (N^G-monomethyl-L-arginine, L-NMMA) on the number of stationary leukocytes, plasma TNF- α levels, serum endotoxin levels, and plasma ALT activities. A: In each region (the midzonal and pericentral regions) (panel A) and the entire (combined) liver lobule (panel B) after 30 min of gut ischemia and 60 min of reperfusion; B: Plasma TNF- α levels at 60 min after gut I/R; C: Serum endotoxin levels at 60 min after gut I/R; D: Plasma ALT activities at 6 h after gut I/R.

Table 1 Effects of Sho-saiko-to (TJ-9) and Saiko-keishi-to (TJ-10) on plasma nitrite/nitrate levels ($n = 5$)

Group	Plasma nitrite/nitrate levels
Control	17.1 \pm 2.9
TJ-9	35.8 \pm 4.3 ^a
TJ-10	39.0 \pm 4.0 ^a

^a $P < 0.05$ vs control.

DISCUSSION

Herbal medicines are widely used in Japan. The clinical efficacy of these medicines has been utilized by Japanese Western-medicine practitioners for more than 20 years and is well recognized. In cases of gastroenterological and hepatological diseases, they are often used for patients with chronic liver disease as well as gastrointestinal functional disorder. Although TJ-9 has been the most famous herbal medicine for chronic liver disease in Japan, TJ-10 is another common drug to treat duodenal ulcer, pancreatitis, and chronic liver disease. TJ-10 has effectiveness for more kinds of diseases rather than TJ-9. Indeed, the components of TJ-10 include all of the 7 components of TJ-9. Although TJ-10 has been often administered to patients with chronic liver disease as well as TJ-9, there were few epidemiological reports^[3], and little is known about mechanisms of the cytoprotective effects on liver damage.

Previously published work has demonstrated that reperfusion of the ischemic small intestine could elicit an acute inflammatory response both in the intestine and in distant organs, such as the liver^[11,12,23] and lung^[23,24]. In the liver, the response was characterized by leukocyte plugging of sinusoids, leukocyte adherence in postcapillary venules, a reduction in the number of perfused sinusoids, hepatocellular hypoxia, and leakage of enzymes (ALT) from hepatocytes^[11,12,23,25]. Recently, we have reported that TJ-9 could attenuate the gut I/R-induced responses in the liver^[18]. In the present study, it was demonstrated that TJ-10 had a similar effect to TJ-9 on the gut

I/R-induced responses in the liver. NO has been found to be a modulator of the adhesive interactions between leukocytes, platelets, and endothelial cells^[6-9], and NO-dependent cell-cell interactions have been demonstrated in tissues exposed to ischemia and reperfusion (I/R), an injury process in which leukocyte-endothelial cell adhesion plays a critical role. Depletion and/or inactivation of NO has been implicated as a key event in the recruitment of leukocytes in tissues exposed to I/R^[26-28]. We previously demonstrated that treatment with L-NMMA resulted in exaggerated leukostasis and cellular injury in the murine liver after gut I/R and that increased delivery/generation of NO in the liver via a NO donor attenuated the inflammatory responses and microvascular dysfunction elicited in the liver by gut I/R^[13]. These results suggest a protective effect of NO on the gut I/R-induced responses in the rat liver. The finding in the present study that L-NMMA diminished the protective effect of TJ-10 on the increase in plasma TNF- α and serum endotoxin levels, leukostasis in the liver, and plasma ALT activities, suggested that TJ-10 could prevent the gut I/R-induced cytokine production and microvascular dysfunction in the liver by elevating sinusoidal NO level. NO could modulate leukocyte- and/or platelet-endothelial cell interactions^[6,9,13,14]. Since pretreatment with TJ-10 actually increased plasma nitrite/nitrate levels in the present study, the increase in NO production by hepatocytes and macrophages after treatment with TJ-10 appeared to be involved in the cytoprotective effects of TJ-10.

In the present study, L-NMMA diminished the protective effect of TJ-10 on the increase in plasma TNF- α and serum endotoxin levels, leukostasis in the liver, and plasma ALT activities. While, in the previous study^[18], L-NMMA did not affect the protective effect of TJ-9 on the increase in leukostasis in the midzonal region, the total number of stationary leukocytes, or the plasma ALT activity. One likely interpretation is that a mechanism other than the increase in NO production mediates the protective effects of TJ-9. Steroids have been known to prevent reperfusion injury^[29]. The evidence in our previous study^[18] that L-NMMA did not affect either TJ-9- or dexamethasone-induced decrease in the gut I/R-elevated plasma

ALT activities, raises a possibility that TJ-9-increased blood corticosterone level may prevent the gut I/R-induced microvascular and hepatocellular injury. Since L-NMMA diminished the protective effect of TJ-10 on the gut I/R-induced increase in plasma ALT activities, corticosteroid effect was not involved in the prevention of gut I/R-induced hepatocellular injury by TJ-10. *Kampo* (herbal medicines) prescriptions affect as the complex. For example, though one of the components in TJ-10, cinnamon bark, which is not included in TJ-9, had a very strong anti-oxidant effect, there was no significant difference between TJ-9 and 10 in the potential for anti-oxidation^[30]. Thus, our results suggest that TJ-10 has different characteristics from TJ-9, even including all components of TJ-9.

Recently, the importance of the way of traditional diagnosis "Sho" in the use of *Kampo* prescriptions has come to be widely described even in package insert drug information pamphlets of *Kampo* prescriptions. "Sho" is judged comprehensively by a complex of subjective and objective symptoms at a certain point of illness. The process is generally complicated, but we sometimes diagnose by tonus felt on the abdomen. Namely, hypertonus is "Jitsu Sho", and hypotonus is "Kyo Sho". General fatigue, sleepiness, sleepless, appetite loss, tiredness of eyes, easily catching cold, dizziness, looking pale, and so on are symptoms of "Kyo Sho". TJ-10 suits for "Kyo Sho" rather than TJ-9. Moreover, most patients with chronic hepatitis have "Kyo Sho". TJ-10 prevents microvascular dysfunction in the liver increase in NO production. Symptoms of "Kyo Sho" described above seem to be caused by microvascular dysfunction. Taken together, TJ-10 is recommended for chronic hepatitis patients with "Kyo Sho".

Although further studies are required to clarify the mechanisms of the protective effects of TJ-10 on reperfusion injury, this study has demonstrated the protective effect of TJ-10 on reperfusion injury via NO.

REFERENCES

- Hirayama C, Okumura M, Tanikawa K, Yano M, Mizuta M, Ogawa N. A multicenter randomized controlled clinical trial of *Shosaiko-to* in chronic active hepatitis. *Gastroenterol Jpn* 1989; **24**: 715-719
- Fujiwara K, Ohta Y, Ogata I, Oka Y, Hayashi S, Oka H. Treatment trial of traditional oriental medicine in chronic viral hepatitis. In: Ohta Y ed. *New Trends in Peptic Ulcer and Chronic Hepatitis: Part II chronic hepatitis*. Tokyo: *Excerpta Medica* 1987: 141-146
- Itoh T, Shibahara N, Mantani N, Tahara E, Shimada Y, Terasawa K. Effect of *kampo* treatment on chronic viral hepatitis. *J Trad Med* 1997; **14**: 204-210
- Abe H, Sakaguchi M, Yamada M, Arichi S. Pharmacological actions of saikosaponins isolated from *Bupleurum falcatum*. I. Effects of *Saikosaponin* on liver function. *Planta Medica* 1980; **40**: 366-372
- Abe H, Orita M, Konishi H, Arichi S, Odashima S. Effects of *Saikosaponin*-d on enhanced CCl₄-hepatotoxicity by phenobarbitone. *J Pharm Pharmacol* 1985; **37**: 555-559
- Kurose I, Kubes P, Suzuki M, Wolf R, Anderson DC, Paulson J, Miyasaka M, Granger DN. Inhibition of nitric oxide production mechanisms of vascular albumin leakage. *Circ Res* 1993; **73**: 164-171
- Kurose I, Wolf R, Grisham MB, Granger DN. Modulation of ischemia/reperfusion-induced microvascular dysfunction by nitric oxide. *Circ Res* 1994; **74**: 376-382
- Moncada S, Palmer RM, Higgs EA. Nitric oxide: Physiology, pathophysiology, and pharmacology. *Pharmacol Rev* 1991; **43**: 109-142
- Radomski MW, Palmer RM, Moncada S. Endogenous nitric oxide inhibits human platelet adhesion to vascular endothelium. *Lancet* 1987; **2**: 1057-1058
- Granger DN, Kurose I, Kubes P. Nitric oxide: A modulator of cell-cell adhesion and protein exchange in postcapillary venules. In: Shock, Sepsis, and Organ Failure-Nitric Oxide. G. Schlang, H. Redl, eds. *Springer, Heidelberg, Germany* 1994: 121-136
- Horie Y, Wolf R, Miyasaka M, Anderson DC, Granger DN. Leukocyte adhesion and the hepatic microvascular responses to intestinal ischemia-reperfusion. *Gastroenterology* 1996; **111**: 666-673
- Horie Y, Wolf R, Anderson DC, Granger DN. Hepatic leukostasis and hypoxic stress in adhesion molecule-deficient mice after gut ischemia-reperfusion. *J Clin Invest* 1997; **99**: 781-788
- Horie Y, Ishii H. Liver dysfunction elicited by gut ischemia-reperfusion. *Pathophysiology* 2001; **8**: 11-20
- Horie Y, Wolf R, Granger DN. Role of nitric oxide in gut ischemia reperfusion-induced hepatic microvascular dysfunction. *Am J Physiol* 1997; **273**: G1007-G1013
- Horie Y, Wolf R, Anderson DC, Granger DN. Nitric oxide modulates gut ischemia/reperfusion-induced P-selectin expression in murine liver. *Am J Physiol* 1998; **275**: H520-H526
- Horie Y, Yamagishi Y, Kato S, Kajihara M, Kimura H, Ishii H. Low-dose ethanol attenuates gut ischemia/reperfusion-induced liver injury in rats via nitric oxide production. *J Gastroenterol Hepatol* 2003; **18**: 211-217
- Fukuda K. Modulation of nitric oxide production by crude drugs and *Kampo* medicines. *J Traditional Med* 1998; **15**: 22-32
- Horie Y, Kajihara M, Yamagishi Y, Kimura H, Tamai H, Kato S, Ishii H. A Japanese herbal medicine, *Sho-Saiko-To*, prevents Ischemia/reperfusion-induced hepatic microvascular dysfunction in rats. *J Gastroenterol Hepatol* 2001; **16**: 1260-1266
- Horie Y, Wolf R, Russell J, Shanley TP, Granger DN. Role of Kupffer cells in gut ischemia-reperfusion-induced hepatic microvascular dysfunction in mice. *Hepatology* 1997; **26**: 1499-1505
- Tamai H, Kato S, Horie Y, Ohki E, Yokoyama H, Ishii H. Effect of acute ethanol administration on the intestinal absorption of endotoxin in rats. *Alcohol Clin Exp Res* 2000; **24**: 390-394
- Horie Y, Kato S, Ohki E, Hamamatsu H, Fukumura D, Kurose I, Suzuki H, Suematsu M, Miura S, Ishii H. Effect of lipopolysaccharides on erythrocyte flow velocity in rat liver. *J Gastroenterol* 1997; **32**: 783-790
- Horie Y, Kimura H, Kato S, Ohki E, Tamai H, Yamagishi Y, Ishii H. Role of nitric oxide in endotoxin-induced hepatic microvascular dysfunction in rats chronically fed ethanol. *Alcohol Clin Exp Res* 2000; **24**: 845-851
- Hill J, Lindsay T, Rusche J, Valeri CR, Shepro D, Hechman HB. A Mac-1 antibody reduces liver and lung injury but not neutrophil sequestration after intestinal ischemia-reperfusion. *Surgery* 1992; **112**: 166-172
- Carden DL, Young JA, Granger DN. Pulmonary microvascular injury after intestinal ischemia-reperfusion: role of P-selectin. *J Appl Physiol* 1993; **75**: 2529-2534
- Simpson R, Alon R, Kobzik L, Valeri CR, Shepro D, Hechtman HB. Neutrophil and nonneutrophil-mediated injury in intestinal ischemia reperfusion. *Ann Surg* 1993; **218**: 444-454
- Kubes P, Suzuki M, Granger DN. Nitric oxide: an endogenous modulator of leukocyte adhesion. *Proc Natl Acad Sci U S A* 1991; **88**: 4651-4655
- Ma XL, Weyrich AS, Lefer DJ, Lefer AM. Diminished basal nitric oxide release after myocardial ischemia and reperfusion promotes neutrophil adherence to coronary endothelium. *Circ Res* 1993; **72**: 403-412
- Siegrfried MR, Erhardt J, Rider T, Ma XL, Lefer AM. Cardioprotection and attenuation of endothelial dysfunction by organic nitric oxide donors in myocardial ischemia-reperfusion. *J Pharmacol Exp Ther* 1991; **260**: 668-675
- Valen G, Kawakami T, Tahepold P, Starkopf J, Kairane C, Dumitrescu A, Lowbeer C, Zilmer M, Vaage J. Pretreatment with methylprednisolone protects the isolated rat heart against ischemic and oxidative damage. *Free Radic Res* 2000; **33**: 31-43
- Yoshikawa T. Free radical and *Kampo* medicines. *Kyoto University Kampo Seminar* 1995; **4**: 24-37

KAI1 gene expression in colonic carcinoma and its clinical significances

De-Hua Wu, Li Liu, Long-Hua Chen, Yan-Qing Ding

De-Hua Wu, Long-Hua Chen, Department of Radiation Oncology, Nanfang Hospital, First Military Medical University, Guangzhou 510515, Guangdong Province, China

Li Liu, Yan-Qing Ding, Department of Pathology, First Military Medical University, Guangzhou 510515, Guangdong Province, China
Supported by the National Natural Science Foundation, No. 30370649

Correspondence to: Dr. Yang-Qing Ding, Department of Pathology, First Military Medical University, Guangzhou 510515, Guangdong Province, China. dyq@fimmu.com

Telephone: +86-20-61642148 **Fax:** +86-20-61642148

Received: 2003-12-12 **Accepted:** 2004-02-01

Abstract

AIM: To investigate *KAI1* gene expression in the progression of human colonic carcinoma and its clinical significances.

METHODS: *KAI1* expression was detected by *in situ* hybridization and immunohistochemistry in the 4 established cell lines of colorectal carcinoma with different metastatic potentials, and in 80 specimens of colonic carcinoma, 21 colonic carcinoma specimens with lymphatic metastasis and 20 controls of normal colonic mucosa.

RESULTS: The expressions of *KAI1* in HT29 and SW480 cell lines were higher than those in LoVo and SW620. The expression of *KAI1* gene was significantly higher in colorectal carcinoma compared with normal colonic mucosa and lymphatic metastasis ($\chi^2=46.838$, $P<0.01$). The expression of *KAI1* gene had no relationship with histological grade. The *KAI1* expressions in Dukes A and B carcinoma were higher at both mRNA and protein levels compared to Dukes C carcinoma ($\chi^2=16.061$, $P<0.05$). The expression of *KAI1* in colonic carcinoma specimens with lymphatic metastasis was almost lost. The results of *in situ* hybridization were in concordance with immunohistochemistry.

CONCLUSION: *KAI1* is highly related to the metastasis of colonic carcinoma and may be a useful indicator of metastasis in colonic carcinoma.

Wu DH, Liu L, Chen LH, Ding YQ. *KAI1* gene expression in colonic carcinoma and its clinical significances. *World J Gastroenterol* 2004; 10(15): 2245-2249

<http://www.wjgnet.com/1007-9327/10/2245.asp>

INTRODUCTION

Colorectal carcinoma is one of the most common forms of malignancy, and metastasis is the major cause of mortality in human population. Timely and precise identification of the occurrence of metastasis and its contributive factors are very important in the enhancement of prognosis and effects of treatment. *KAI1* gene was first identified in human prostate carcinoma and mapped to human chromosome 11p11.2^[1]. It encodes 267 amino acids belonging to plasma membrane glycoprotein, which consists of 4 transmembrane domains and

1 large and 1 small extracellular domains. The extracellular domains have 3 potential N-glycosylation sites. According to its special structure, it may be predicted that the function of *KAI1* gene may come down to cell-cell adherence and cell-matrix connection^[2]. The role of *KAI1* in tumor progression may not be limited to prostatic cancer. It was reported to be important in preventing the development of metastases in a wide variety of human tumor types, including cervical^[3], breast^[4], pancreatic^[5], esophageal^[6], bladder^[7], and ovarian cancers^[8]. In the present study, the expression of *KAI1* was detected by *in situ* hybridization in 4 cell lines of colorectal carcinoma, and in paraffin-embedded normal colonic epithelium, carcinoma, and lymphatic metastasis. The purpose was to explore the relationship between *KAI1* expression and colonic carcinoma metastasis and its clinical significances.

MATERIALS AND METHODS

Cell lines and culture conditions

LoVo and HT29 cell lines were cultured in RPMI 1640 supplemented with 100 mL/L heat-inactivated fetal bovine serum (FBS) and 100 U/mL penicillin/streptomycin. SW480 and SW620 were cultured in DMEM medium supplemented with the 100 mL/L FBS. All cells were grown in 50 mL/L CO₂ humidified atmosphere at 37 °C.

Tissue specimens

A total of 80 colonic carcinoma specimens, 20 normal colonic mucosa samples and 20 lymphatic metastasis samples were obtained from Nanfang Hospital. All the samples were routinely fixed in 40 g/L formaldehyde solution, embedded in paraffin, and cut into 4 μm thick sections. Samples were selected according to the pathological diagnosis and reviewed by a pathologist to confirm the diagnosis.

In situ hybridization (ISH) assays

The digoxigenin-labeled *KAI1*-cDNA probe for *in situ* hybridization was prepared as described in one of our previous papers^[9]. The ISH was performed according to the instruction of the enhanced sensitive ISH detection kit (purchased from Boster Biotechnology Company). Briefly, the sections were deparaffinized with xylene, dehydrated with graded ethanol and incubated in 30 mL/L H₂O₂ to block endogenous peroxidases for 30 min at room temperature. After being treated for 10 min with Triton X-100 and for 40 s with 3% pepsin, the sections were prehybridized for 3 h and hybridized overnight at 37 °C. The final concentrations of the labeled probes were 0.15 ng/μL. After hybridization, excess probes were removed through rinsing in 2×SSC (1×SSC is 0.15 mol/L NaCl plus 0.015 mol/L sodium citrate pH 7.0), 0.5×SSC, 0.2×SSC, respectively. The sections were incubated with an antidigoxigenin antibody conjugated biotin for 120 min at room temperature and then added strept-avidin biotin complex for 30 min. For color reaction, diaminobenzidine (DAB) was used. If the ISH signals were present, the cytoplasm would be full of brown granules. For ISH of the four colorectal carcinoma cell lines, the cells were incubated and grown on cover slip for 24 h, fixed with 950 mL/L

ethanol and washed with PBS (phosphate-buffered saline pH 7.2) 3 times, and then carried out ISH as described above. For negative controls, the digoxigenin-labeled KAI1-cDNA probe was replaced by prehybridized solution.

Immunohistochemical assays

To confirm the results of *KAI1* gene expression on *in situ* hybridization, immunohistochemical studies were performed as described previously^[9,10]. Briefly, the fixed cells and sections were subjected to immunostaining by using an ultrasensitive streptavidin-peroxidase technique (Maixin Biotechnology Company). Endogenous peroxidases were blocked by incubating with 5 mL/L H₂O₂ for 30 min at room temperature. The cells and sections were subsequently treated for 10 min with Triton X-100 and for 40 s with 30 g/L pepsin. The cells and sections were incubated for 30 min at 37 °C with normal nonimmune serum before overnight incubation at 4 °C with specific monoclonal KAI1-antibody (BD pharmingen technical company) at a dilution of 1:100. The cells and sections were then treated with biotin-conjugated second antibody before adding streptavidin-peroxidase. For color reaction, diaminobenzidine was used. If the positive signals were present, the cytoplasm and membrane were stained brown. For negative controls, the monoclonal KAI1 antibody was replaced by PBS.

Review and scoring of the section

The stained sections were reviewed and scored independently by two pathologists under Olympus microscope. The different degrees of intensity of staining were graded on a scale of 0 to 3 as follows: 0 indicated that the number of positive cells was less than 10%; 1 indicated weak positive and the number of positive cells more than 10%, but less than 30%; 2 indicated positive and the number of positive cells more than 30% but less than 50%; 3 indicated strong positive and the number of positive cells more than 50%.

Statistical analysis

Fisher's exact probability test was adopted to examine the relationship between the variables. A *P* value <0.05 was considered statistically significant.

RESULTS

KAI1 gene expression in colorectal carcinoma cell lines

HT29 and SW480 cell lines were derived from primary colorectal adenocarcinoma. SW620 and LoVo cell lines were established from metastatic colorectal carcinoma. Especially, SW620 cell line was isolated from the same case as was SW480 cell line. The expressions of KAI1 mRNA and protein in HT29 and SW480 cells were positive, whereas those in SW620 and LoVo cells were negative (Figures 1, 2).

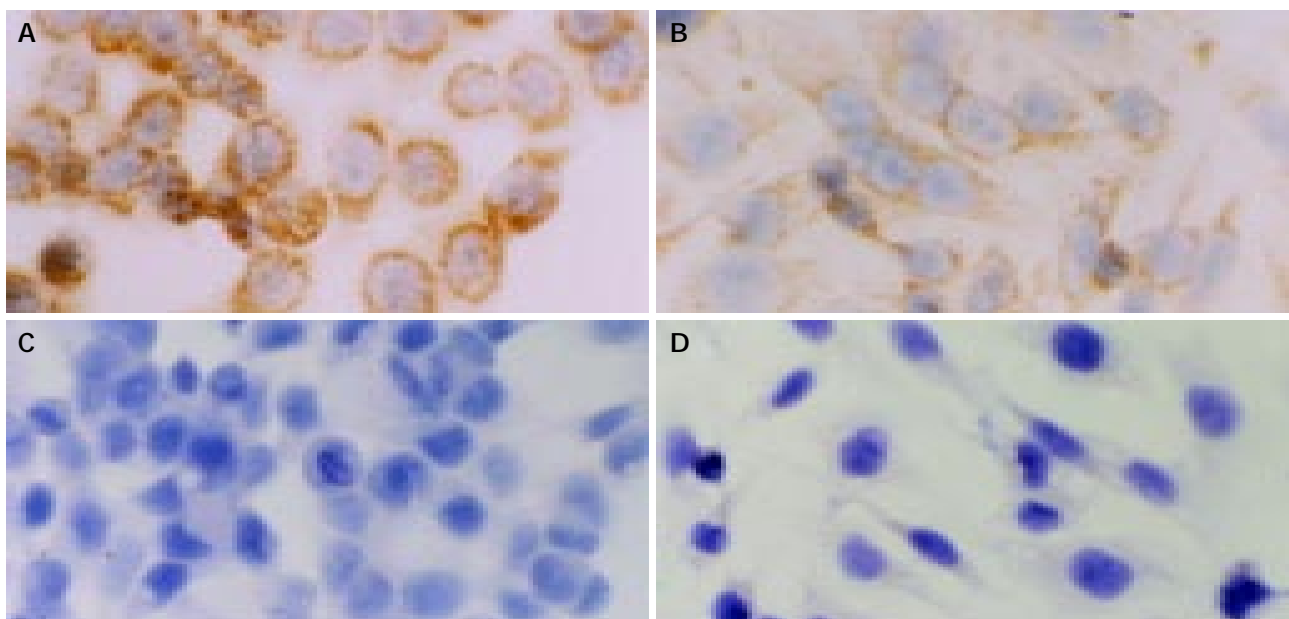


Figure 1 *In situ* hybridization detection of expression of KAI1 mRNA in colorectal carcinoma cell lines (Original magnification: ×400). A: In HT29 cells, the positive expression (brown granule) was located in cytoplasm; B: In SW480 cells, the positive expression was located in cytoplasm; C: In SW620 cells, the expression of KAI1 mRNA was negative; D: In LoVo cells, the expression of KAI1 mRNA was negative.

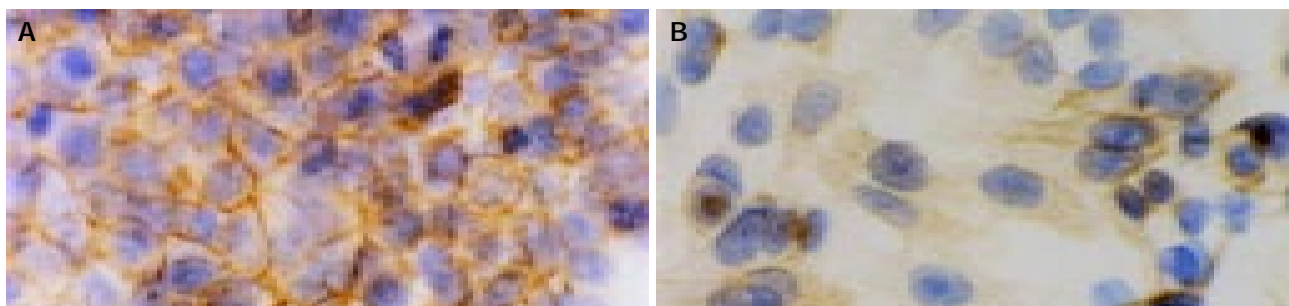


Figure 2 Expression of KAI1 protein detected by immunohistochemistry in colorectal carcinoma cell lines (Original magnification: ×400). A: In HT29 cells, the positive expression located in cytoplasm and membrane; B: In SW480 cells, the positive expression located in cytoplasm and membrane.

Heterogeneous expression of *KAI1* mRNA in colonic carcinoma tissue

Of the 80 colonic carcinoma specimens, 56(70%) were classified as *KAI1* positive (Figure 3). There were 4 cases (20%) with positive *KAI1* mRNA expression in normal colonic mucosa and 2 cases (10%) in lymphatic metastasis. The results are shown in Table 1. The positivity ratio was significantly higher in colonic carcinoma than that in normal colonic mucosa and in lymphatic metastasis ($\chi^2=46.838$, $P<0.01$). The expression in lymphatic metastasis was almost lost.

To further investigate the relationship between the expression of *KAI1* and the clinical pathology, we sorted the colonic carcinomas based on histological grades and Dukes stages. Histological grade I means well differentiated adenocarcinoma, II means moderately differentiated and III means poorly differentiated. The results indicated that *KAI1* expression had no relationship with histological grades ($\chi^2=3.887$, $P>0.05$). The expression in Dukes A and B carcinoma was markedly higher in comparison with Dukes C carcinoma ($\chi^2=16.061$, $P<0.01$).

KAI1 protein expression analyzed by immunohistochemistry

There were 52(65%) cases with positive *KAI1* protein expressions in the colonic carcinomas (Figure 3). The positive ratios of normal colonic mucosa and lymphatic metastasis were 25% and 10%, respectively. The *KAI1* expressions in 3 groups were significantly different ($\chi^2=28.298$, $P<0.01$). Overall, the immunohistochemical results agreed well with those from the *in situ* hybridization assays.

DISCUSSION

Loss of the function of metastasis suppressor genes is an important step in the progression of a tumor type. Several candidate antimetastasis or anti-invasion genes have been studied in colorectal carcinoma, including nm23^[11], E-cadherin^[12], and CD44^[13], but inconsistent findings have been reported. For example, in separate studies, nm23 expression has been found to be directly correlated, not to be correlated, or inversely correlated with metastatic potential in colorectal cancer^[14-16]. *KAI1* has been thought to be one of such metastasis suppressor genes, because it was shown to suppress the ability of human prostatic cancer cells to metastasize when the tumor was transplanted into nude mice^[1] and because *KAI1* mRNA expression was reduced in advanced pancreatic cancer^[17] so that the pancreatic cancer cells spread to lymph nodes and distant organs. Furthermore, the transfer of the *KAI1* gene into mammary cancer cells has been shown to lead to suppression of their metastatic potential, whereas their primary tumor growth has not been affected^[18-20].

KAI1 is a member of the transmembrane-4 superfamily (TM4SF), many of which, including *KAI1*, are CD antigens present on the surface of leukocytes^[21,22]. At least three TM4SF members are implicated in metastasis, including CD9/MRP-1, CD63/ME491, and CD82/*KAI1*^[23]. *KAI1* and other TM4SF members, such as integrins and E-cadherin, have been demonstrated to bind to each other and relay extracellular signals to signal transduction pathways that are important in cellular adhesion, invasive motility, and metastasis^[24-27].

In our previous studies, we transfected the *KAI1* cDNA

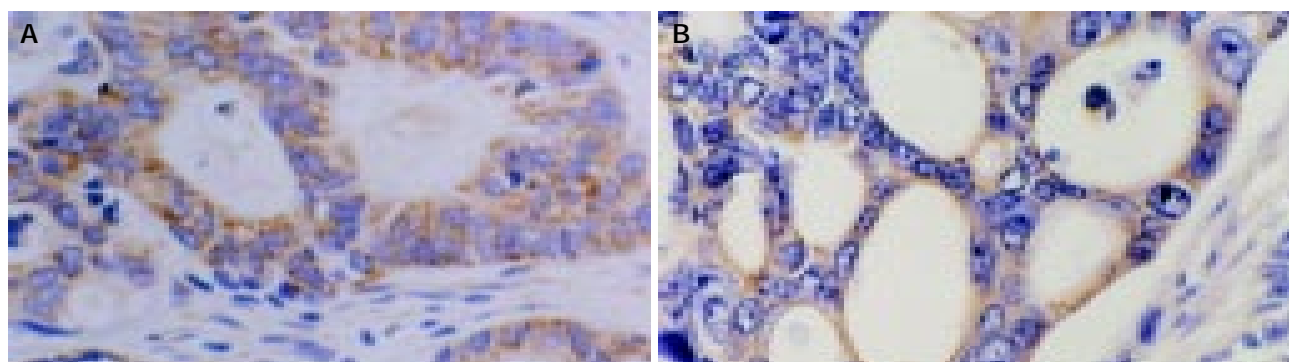


Figure 3 *In situ* hybridization and immunohistochemical detection of *KAI1* mRNA and protein in colonic carcinoma (Original magnification: $\times 400$). A: *In situ* hybridization detection found that strong *KAI1* mRNA staining was located in cytoplasm (brown granule); B: Detection by immunohistochemistry showed strong *KAI1* protein staining was in cytoplasm and membrane.

Table 1 *KAI1* gene expression in normal colonic mucosa, colonic carcinoma and lymphatic metastasis *n* (%)

Tissue	KAI1/CD82 expression				Total
	0	1	2	3	
Normal colonic mucosa	16(80.0)	3(15.0)	1(5.0)	0	20
Colonic carcinoma					
Histological grade					
I	6(23.1)	2(7.7)	12(46.2)	6(23.1)	26
II	10(26.3)	12(31.6)	14(36.8)	2(5.3)	38
III	8(50.0)	6(37.5)	2(12.5)	0	16
Dukes stage					
Dukes A	1(4.3)	6(26.1)	9(39.1)	7(30.4)	23
Dukes B	3(17.6)	6(35.3)	5(29.4)	3(17.6)	17
Dukes C	20(50.0)	10(25.0)	8(20.0)	2(5.0)	40
Lymphatic metastasis	18(90.0)	2(10.0)	0	0	20

into a colorectal carcinoma cell line, LoVo, and found that the KAI1 transfectant exhibited significantly increased homotypic cell adhesion and suppressed invasion and metastasis^[9]. Our findings were consistent with those in the studies of prostatic cancer^[2] and breast cancer^[18] cells.

In this study, we first investigated KAI1 mRNA expression in 4 colorectal carcinoma cell lines and found *KAI1* gene expression was much higher in HT29 and SW480 cell lines than in SW620 and LoVo cell lines. SW480 was isolated from a high-grade primary colonic tumor, and SW620 was isolated from a metastatic lymph node from the same patient 1 year later at the time of clinical relapse. KAI1 protein expression was high in SW480 but reduced in SW620. The colonic cancer cell line derived from metastatic lesions, LoVo, hardly exhibited any expression. In our observation we found that *KAI1* gene expressions both at mRNA and protein level, were inversely correlated with the metastatic potential of some established colorectal carcinoma cell lines.

We next examined KAI1 expression in normal colonic mucosa, carcinoma and lymphatic metastasis by *in situ* hybridization. The results indicated that KAI1 gene was highly expressed in colonic carcinoma compared with normal colonic epithelium and lymphatic metastasis. We found that although the expression had no relationship with histological grades, it was significantly correlated with Dukes stages. This indicates that the KAI1 mRNA expression may be positively related with the Dukes stages. The data shown in Table 1 demonstrate that KAI1 expression increases at an earlier tumor stage of colonic carcinoma, while decreases at advanced stages, and is possibly lost in metastases. That is to say, the expression of KAI1 has a reverse correlation with metastasis in colorectal carcinoma.

How does reduced TM4SF expression cause changes of invasive ability of tumor cells? It was hypothesized that tetraspanins might be implicated in the assembly of integrin-contained signaling complexes, thus modulating the function of integrin receptors in cell migration^[24]. Some results indicated that integrin-tetraspanin protein complexes played an important role in regulating protrusive activity of the tumor cells and contributed to extracellular matrix-induced production of matrix metalloproteinase 2 (MMP-2), and as a consequence, the invasive ability of cells^[28].

KAI1 has been extensively studied for its involvement in the progression of different human cancers. The mechanism of down-regulation of KAI1 has also been analyzed, however, much debate still exists. Recent study found a putative p53 consensus-binding site within the promoter region of KAI1 and demonstrated that the loss of p53 function, which was commonly observed in many types of cancer, led to the down-regulation of the *KAI1* gene, which might result in the progression of metastasis^[29]. But other data suggested that the down-regulation of KAI1 was not associated with either mutation, allelic loss, methylation of the promoter, or p53 regulation^[30]. Our previous study also demonstrated that mutation of the KAI1 gene, methylation of CpG islands and the abnormality of p53 were not related to low expression of KAI1.

In conclusion, KAI1 expression increases in an earlier tumor stage of colonic carcinoma, decreases in advanced stages, and is possibly lost in lymphatic metastases. The loss of KAI1 expression is correlated with higher stage, a surrogate marker for metastatic potential. The down-regulation of KAI1 in Dukes C and loss in metastasis demonstrate that loss of KAI1 expression occurs in cancer progression. The selection of cells that have the ability to spread from the primary tumor to the metastasis may favor those cells that have lost KAI1 expression. Those cells would be expected to be less adhesive, more invasive, and more motile^[31], and these characteristics are necessary for metastasis.

REFERENCES

- Dong JT**, Lamb PW, Rinker-Schaeffer CW, Vukanovic J, Ichikawa T, Isaacs JT, Barrett JC. KAI1, a metastasis suppressor gene for prostate cancer on human chromosome 11p11.2. *Science* 1995; **268**: 884-886
- Dong JT**, Isaacs WB, Barrett JC, Isaacs JT. Genomic organization of the human KAI1 metastasis-suppressor gene. *Genomics* 1997; **41**: 25-32
- Liu FS**, Chen JT, Dong JT, Hsieh YT, Lin AJ, Ho ES, Hung MJ, Lu CH. KAI1 metastasis suppressor gene is frequently down-regulated in cervical carcinoma. *Am J Pathol* 2001; **159**: 1629-1634
- Debies MT**, Welch DR. Genetic basis of human breast cancer metastasis. *J Mammary Gland Biol Neoplasia* 2001; **6**: 441-451
- Friess H**, Guo XZ, Tempia Caliera AA, Fukuda A, Martignoni ME, Zimmermann A, Korc M, Buchler MW. Differential expression of metastasis-associated genes in papilla of Vater and pancreatic cancer correlates with disease stage. *J Clin Oncol* 2001; **19**: 2422-2432
- Miyazaki T**, Kato H, Shitara Y, Yoshikawa M, Tajima K, Masuda N, Shouji H, Tsukada K, Nakajima T, Kuwano H. Mutation and expression of the metastasis suppressor gene KAI1 in esophageal squamous cell carcinoma. *Cancer* 2000; **89**: 955-962
- Jackson P**, Kingsley EA, Russell PJ. Inverse correlation between KAI1 mRNA levels and invasive behaviour in bladder cancer cell lines. *Cancer Lett* 2000; **156**: 9-17
- Liu FS**, Dong JT, Chen JT, Hsieh YT, Ho ES, Hung MJ. Frequent down-regulation and lack of mutation of the KAI1 metastasis suppressor gene in epithelial ovarian carcinoma. *Gynecol Oncol* 2000; **78**: 10-15
- Liu L**, Wu DH, Li ZG, Yang GZ, Ding YQ. Effects of KAI1/CD82 on biological behavior of human colorectal carcinoma cell line. *World J Gastroenterol* 2003; **9**: 1231-1236
- Wu DH**, Liu L, Chen LH, Ding YQ. Expression of KAI1/CD82 in human colorectal tumor. *Diyi Junyi Daxue Xuebao* 2003; **23**: 714-715
- Dursun A**, Akyurek N, Gunel N, Yamac D. Prognostic implication of nm23-H1 expression in colorectal carcinomas. *Pathology* 2002; **34**: 427-432
- El-Bahrawy MA**, Poulson R, Jeffery R, Talbot I, Alison MR. The expression of E-cadherin and catenins in sporadic colorectal carcinoma. *Hum Pathol* 2001; **32**: 1216-1224
- Wong K**, Rubenthiran U, Jothy S. Motility of colon cancer cells: modulation by CD44 isoform expression. *Exp Mol Pathol* 2003; **75**: 124-130
- Forte A**, D'Urso A, Gallinaro LS, Lo Storto G, Soda G, Bosco D, Bezzi M, Vietri F, Beltrami V. NM23 expression as prognostic factor in colorectal carcinoma. *G Chir* 2002; **23**: 61-63
- Heys SD**, Langlois N, Smith IC, Walker LG, Eremin O. NM23 gene product expression does not predict lymph node metastases or survival in young patients with colorectal cancer. *Oncol Rep* 1998; **5**: 735-739
- Cheah PY**, Cao X, Eu KW, Seow-Choen F. NM23-H1 immunostaining is inversely associated with tumour staging but not overall survival or disease recurrence in colorectal carcinomas. *Br J Cancer* 1998; **77**: 1164-1168
- Guo X**, Friess H, Graber HU, Kashiwagi M, Zimmermann A, Korc M, Buchler MW. KAI1 expression is up-regulated in early pancreatic cancer and decreased in the presence of metastases. *Cancer Res* 1996; **56**: 4876-4880
- Yang X**, Wei LL, Tang C, Slack R, Mueller S, Lippman ME. Overexpression of KAI1 suppresses *in vitro* invasiveness and *in vivo* metastasis in breast cancer cells. *Cancer Res* 2001; **61**: 5284-5288
- Ono M**, Handa K, Withers DA, Hakomori S. Motility inhibition and apoptosis are induced by metastasis-suppressing gene product CD82 and its analogue CD9, with concurrent glycosylation. *Cancer Res* 1999; **59**: 2335-2339
- Takaoka A**, Hinoda Y, Sato S, Itoh F, Adachi M, Hareyama M, Imai K. Reduced invasive and metastatic potentials of KAI1-transfected melanoma cells. *Jpn J Cancer Res* 1998; **89**: 397-404
- White A**, Lamb PW, Barrett JC. Frequent downregulation of

- the KAI1(CD82) metastasis suppressor protein in human cancer cell lines. *Oncogene* 1998; **16**: 3143-3149
- 22 **Okochi H**, Mine T, Nashiro K, Suzuki J, Fujita T, Furue M. Expression of tetraspans transmembrane family in the epithelium of the gastrointestinal tract. *J Clin Gastroenterol* 1999; **29**: 63-67
- 23 **Adachi M**, Taki T, Konishi T, Huang CI, Higashiyama M, Miyake M. Novel staging protocol for non-small-cell lung cancers according to MRP-1/CD9 and KAI1/CD82 gene expression. *J Clin Oncol* 1998; **16**: 1397-1406
- 24 **Rubinstein E**, Le Naour F, Lagaudriere Gesbert C, Billard M, Conjeaud H, Boucheix C. CD9, CD63, CD81, and CD82 are components of a surface tetraspan network connected to HLA-DR and VLA integrins. *Eur J Immunol* 1996; **26**: 2657-2665
- 25 **Bienstock RJ**, Barrett JC. KAI1, a prostate metastasis suppressor: prediction of solvated structure and interactions with binding partners; integrins, cadherins, and cell-surface receptor proteins. *Mol Carcinog* 2001; **32**: 139-153
- 26 **Hiroki H**, Arimichi T, Takahiro T, Toshihiko T, Toshihiko T, Keiichi K, Nobuoki K, Yoshio Y, Masayuki M. Integrin alpha3 expression as a prognostic factor in colon cancer: association with MRP-1/CD9 and KAI1/CD82. *Int J Cancer* 2002; **97**: 518-525
- 27 **Hemler ME**, Mannion BA, Berditchevski F. Association of TM4SF proteins with integrins: relevance to cancer. *Biochim Biophys Acta* 1996; **1287**: 67-71
- 28 **Muneyuki T**, Watanabe M, Yamanaka M, Shiraishi T, Isaji S. KAIL/CD82 expression as a prognostic factor in sporadic colorectal cancer. *Anticancer Res* 2001; **21**: 3581-3587
- 29 **Mashimo T**, Watabe M, Hirota S, Hosobe S, Miura K, Tegtmeyer PJ, Rinker-Shaeffer CW, Watabe K. The expression of the KAI1 gene, a tumor metastasis suppressor, is directly activated by p53. *Proc Natl Acad Sci* 1998; **95**: 11307-11311
- 30 **Uzawa K**, Ono K, Suzuki H, Tanaka C, Yakushiji T, Yamamoto N, Yokoe H, Tanzawa H. High prevalence of decreased expression of KAI1 metastasis suppressor in human oral carcinogenesis. *Clin Cancer Res* 2002; **8**: 828-835
- 31 **Geradts J**, Maynard R, Birrer MJ, Hendricks D, Abbondanzo SL, Fong KM, Barrett JC, Lombardi DP. Frequent loss of KAI1 expression in squamous and lymphoid neoplasms. An immunohistochemical study of archival tissues. *Am J Pathol* 1999; **154**: 1665-1671

Edited by Kumar M Proofread by Chen WW and Xu FM

Influence of serum from liver-damaged rats on differentiation tendency of bone marrow-derived stem cells

Hai Hong, Jian-Zhi Chen, Feng Zhou, Ling Xue, Guo-Qiang Zhao

Hai Hong, Jian-Zhi Chen, Feng Zhou, Ling Xue, Guo-Qiang Zhao, Department of Pathology, Medical School of Sun Yat-Sen University, Guangzhou 510080, Guangdong Province, China
Supported by the National Natural Science Foundation of China, No. 30170473

Correspondence to: Professor Guo-Qiang Zhao, Department of Pathology, Medical School of Sun Yat-Sen University, 74 Zhongshan 2nd Rd., Guangzhou 510080, Guangdong Province, China. gqzhao@gzsums.edu.cn

Telephone: +86-20-87331075 **Fax:** +86-20-87331236

Received: 2003-12-10 **Accepted:** 2004-01-07

Abstract

AIM: Recent studies in both rodents and humans indicated that bone marrow (BM)-derived stem cells were able to home to the liver after they were damaged and demonstrated plasticity in becoming hepatocytes. However, the question remains as to how these stem cells are activated and led to the liver and where the signals initiating the mechanisms of activation and differentiation of stem cells originate. The aim of this study was to investigate the influence of serum from liver-damaged rats on differentiation tendency of bone marrow-derived stem cells.

METHODS: Serum samples were collected from rats treated with a 2-acetylaminofluorene (2-AAF)/carbon tetrachloride (CCl₄) program for varying time points and then used as stimulators of cultured BM stem cells. Expression of M₂- and L-type isozymes of rat pyruvate kinase, albumin as well as integrin-β1 were then examined by reverse transcription polymerase chain reaction (RT-PCR) to estimate the differentiation state of BM stem cells.

RESULTS: Expression of M₂-type isozyme of pyruvate kinase (M₂-PK), a marker of immature hepatocytes, was detected in each group stimulated with experimental serum, but not in controls including mature hepatocytes, BM stem cells without serum stimulation, and BM stem cells stimulated with normal control serum. As a marker expressed in the development of liver, the expression signal of integrin-β1 was also detectable in each group stimulated with experimental serum. However, expression of L-type isozyme of pyruvate kinase (L-PK) and albumin, marker molecules of mature hepatocytes, was not detected in groups stimulated with experimental serum.

CONCLUSION: Under the influence of serum from rats with liver failure, BM stem cells begin to differentiate along a direction to hepatocyte lineage and to possess some features of immature hepatocytes.

Hong H, Chen JZ, Zhou F, Xue L, Zhao GQ. Influence of serum from liver-damaged rats on differentiation tendency of bone marrow-derived stem cells. *World J Gastroenterol* 2004; 10 (15): 2250-2253

<http://www.wjgnet.com/1007-9327/10/2250.asp>

INTRODUCTION

Recent studies in both rodents and humans indicated that bone marrow (BM) stem cells were able to home to the liver after they were damaged, and demonstrated plasticity in becoming hepatocytes^[1-4]. Questions remain as to how BM stem cells are activated and led to the liver and where the signals initiating the mechanisms of activation and differentiation of stem cells originate. Transfused oval cells (hepatic stem cells) that had a selective tropism for the liver in an animal model of liver-damage suggested that "signal molecules" were present in serum of this animal model and played an important role in mediating both hepatic and non-hepatic stem cell activation^[5]. However, the influence of these putative signal molecules in serum on the differentiation state of bone marrow-derived stem cells is yet unclear. The purposes of the present work were to confirm the existence of signaling molecules in serum of liver-damaged rats and to observe its effects on the differentiation of BM stem cells into hepatocytes.

MATERIALS AND METHODS

Establishment of animal model of liver-damage

Male Sprague-Dawley (SD) rats, 6-week-old, were used for the establishment of an animal model of liver-damage. The model was made by means of a 2-AAF/CCl₄ program according to Petersen^[1]. In experimental group, 2-acetylaminofluorene (2-AAF, Sigma), 2.5 g/L in earthenut oil, was administered to stomach of rats everyday for 7 d. On the 7th d of 2-AAF administration, an Ld50 dose of CCl₄ was given by intraperitoneal injection. Animal blood was taken at the time points of 2, 4, 8, 12, and 24 h after CCl₄ injection. Experimental serum was prepared on standby. The serum from normal animals was used as control.

Isolation and culture of bone marrow stromal cells

The SD rats were sacrificed by means of ether asphyxia. Bone marrow was collected from tibiae and BM cells were suspended in Dulbecco's modified Eagle's medium (DMEM) with fetal bovine serum. After centrifugation and re-suspension, the cells were seeded in a culture flask and cultured under a routine condition (37 °C, 50 mL/L CO₂). The solution of medium was changed every 4 d while the cells floating on the medium were discarded. The cells adhering to bottom of the flask (so-called BM stromal cells) were cultured sequentially for 12-14 d. After 3 population doublings, the purified cells were harvested and used in the following stimulating culture with experimental serum.

Stimulating culture of BM stromal cells with experimental serum

BM stromal cells were cultured sequentially in a specialized medium (DMEM-F12) containing 3 ml/L experimental rat serum. In the control group, the culture medium contained 3 mL/L normal rat serum instead of experimental rat serum. Cultures were grown and submerged for 12 d. The cells were harvested on the 13th culture day for ribonucleic acid (RNA) isolation.

Table 1 Primer pairs for RT-PCR

Marker genes	Primer pairs	PCR fragments
M ₂ -PK	5'ccatctaccacttgagttatcga3' / 5'tcatggtacaggcactacacgc3'	431 bp
L-PK	5'acctctgccttctggatactgact3' / 5'tgcaagactccggttcgtatct3'	322 bp
Albumin	5'gagccccgaaagaacgagtggt3' / 5'ggggaatctctggctcatcacg3'	389 bp
INT-β1	5'tacttcagactccgcattgg3' / 5'cagtgactgcaaaaatcgctcg3'	488 bp
GAPDH	5'ccatggagaaggctggg3' / 5'caaagttgcatggtgacc3'	180 bp

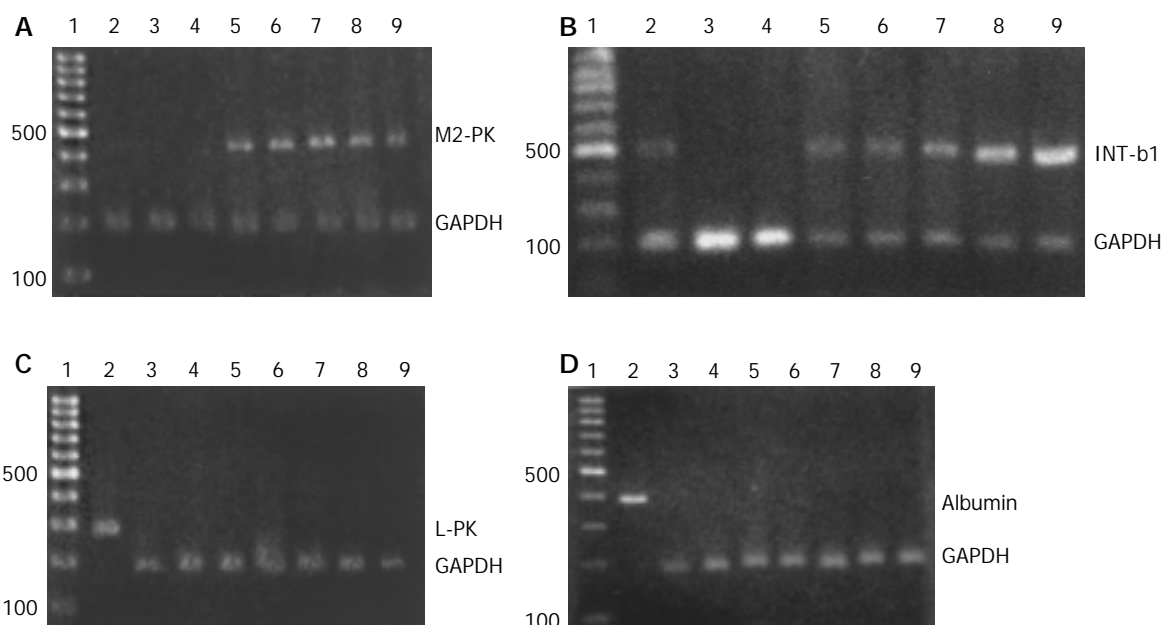


Figure 1 Expressions of M₂-PK, Integrin-β1, L-PK and albumin in BM stem cells. A: Expression of M₂-PK in BM stem cells. Lane 1, 100 bp DNA marker; Lane 2, Hepatocytes; Lane 3, BM stem cells without stimulation; Lane 4, BM stem cells stimulated with control serum; Lane 5, BM stem cells stimulated with experimental serum for 2 h; Lane 6, BM stem cells stimulated with experimental serum for 4 h; Lane 7, BM stem cells stimulated with experimental serum for 8 h; Lane 8, BM stem cells stimulated with experimental serum for 12 h; Lane 9, BM stem cells stimulated with experimental serum for 24 h. B: Expression of Integrin-β1 in BM stem cells. Lane 1, 100 bp DNA marker; Lane 2, Hepatocytes; Lane 3, BM stem cells without stimulation; Lane 4, BM stem cells stimulated with control serum; Lane 5, BM stem cells stimulated with experimental serum for 2 h; Lane 6, BM stem cells stimulated with experimental serum for 4 h; Lane 7, BM stem cells stimulated with experimental serum for 8 h; Lane 8, BM stem cells stimulated with experimental serum for 12 h; Lane 9, BM stem cells stimulated with experimental serum for 24 h. C: Expression of L-PK in BM stem cells. Lane 1, 100 bp DNA marker; Lane 2, Hepatocytes; Lane 3, BM stem cells without stimulation; Lane 4, BM stem cells stimulated with control serum; Lane 5, BM stem cells stimulated with experimental serum for 2 h; Lane 6, BM stem cells stimulated with experimental serum for 4 h; Lane 7, BM stem cells stimulated with experimental serum for 8 h; Lane 8, BM stem cells stimulated with experimental serum for 12 h; Lane 9, BM stem cells stimulated with experimental serum for 24 h. D: Expression of albumin in BM stem cells. Lane 1, 100 bp DNA marker; Lane 2, Hepatocytes; Lane 3, BM stem cells without stimulation; Lane 4, BM stem cells stimulated with control serum; Lane 5, BM stem cells stimulated with experimental serum for 2 h; Lane 6, BM stem cells stimulated with experimental serum for 4 h; Lane 7, BM stem cells stimulated with experimental serum for 8 h; Lane 8, BM stem cells stimulated with experimental serum for 12 h; Lane 9, BM stem cells stimulated with experimental serum for 24 h.

Isolation of RNA

RNA was extracted from the cells collected from the cultures described above, according to the protocol of QIAGEN RNA easy mini kit. RNA samples were then stored at -80 °C.

Primers selection

Genes of M₂-type and L-type isozymes of rat pyruvate kinase (M₂-PK, L-PK), albumin and integrin-β1 (INT-β1) were selected as the markers representing different differentiation stages of hepatocyte lineage. The gene of glyceraldehyde-3-phosphate-dydrogenase (GAPDH) was used as an internal control for RT-PCR reactions. Primer pairs used for RT-PCR are shown in Table 1.

RT-PCR reactions

RNA samples were first reversely transcribed into cDNA, and then used as templates in the following PCR reactions. The

reaction cocktails (containing 1 μg template cDNA, 50 μmol/L dNTPs, 400 μmol/L primers, 1×PCR buffer, 2.5 mmol/L MgCl₂, 1 U Taq-polymerase, add H₂O to 50 μL of total volume) were run on GeneAmp® PCR System 9600 (AB) with a combined program of program 1 (at 94 °C for 5 min), program 2 (at 95 °C for 1 min, at 60 °C for 1 min, at 72 °C for 1 min; 30 cycles), and program 3 (at 95 °C for 1 min, at 60 °C for 1 min, at 72 °C for 5 min). The PCR products were electrophoresed in 12 g/L agarose gel, stained with ethidium bromide, and photographed.

RESULTS

M₂-PK, as a marker of immature hepatocytes, was used to estimate the differentiation state of BM stem cells stimulated by the experimental serum. The results showed that the expression signals of M₂-PK were detected in each group

stimulated with experimental serum, but not in the control group of normal BM stem cells that had no stimulation, BM stem cells stimulated with control serum, and normal mature hepatocytes (Figure 1A). Integrin- β 1 is a marker expressed during the development of liver. In this study, its expression signals were also detectable in each group stimulated with experimental serum as those observed in the positive control of hepatocytes (Figure 1B). L-PK and albumin, as marker molecules of mature hepatocytes, were used to estimate the terminal differentiation state of BM stem cells under the influence of experimental serum. However, no signals were detected in the experimental groups, except for the positive control of hepatocytes (Figure 1C, D).

DISCUSSION

The existence of liver stem cells had been widely proved in both rodents and humans^[1-4,6-9]. By extension, liver stem cells could be divided into three groups: (1) mature hepatocytes that proliferate during normal liver tissue renewal and after less severe liver damage, (2) oval cells that are activated to proliferate when the liver damage is extensive and chronic, and (3) exogenous liver stem cells that may derived from bone marrow cells and respond to severe liver damage^[10]. However, in a narrow sense, the concept of liver stem cells is usually limited to hepatic oval cells and non-hepatic bone marrow stem cells.

A phenomenon that was often observed both in experimental animal models and in clinics was that the proliferation of liver stem cells occurred most often in conditions of severe liver damages or chronic liver diseases^[11-15]. Maybe it is the reason that stem cells were seldom detected in healthy livers. Thus it can be understood that liver-damage is an important prerequisite for activation of liver stem cells. This suggests that the signals initiating activation of hepatic or non-hepatic stem cells might originate from damaged livers. This hypothesis had been partially proved by our previous experimental work^[5]. In our previous experiments, oval cells isolated from male SD rats were transfused, through caudal vein into the circulatory system of a female rat with liver damage. Sex-determining gene *sry* that was located on Y chromosome was then examined respectively by PCR and *in situ* hybridization technique in the liver, kidney and spleen of experimental animals. The results of cell-transplant experiments showed that *sry* gene was detectable only in the liver but not in the spleen and kidney of rats with liver damages and that no signals could be detected in control animals, neither in the liver, spleen nor in the kidney. It could be also morphologically observed that some exogenous cells with *sry* marker migrated into the parenchyma of liver and settled there, suggesting that transfused oval cells had a selective tropism for damaged liver. These results also suggested that signaling molecules existed in the serum of animals with liver damage and might play a role in mediating stem cell activation.

In the present study, an animal model of liver-damage was established with a 2-AAF/CCl₄ program. In this model, the capacity of hepatocyte self-regeneration was first impaired by 2-AAF and then the liver was damaged severely by CCl₄. In this status, the damaged liver would likely produce a signal to initiate the activation of stem cells in the bone marrow. The results of the present study showed that the expression of M₂-PK, a marker of immature hepatocyte^[16-22], could be detected in each group stimulated with experimental serum, but not in any of the control groups. Integrin- β 1 is a marker expressed during the development of liver. Its expression could be detected in fetal hepatocyte as early as at 8th wk of gestation^[30]. In the present results, the expression signal of integrin- β 1 was also detectable in each group stimulated with experimental

serum. Thus, the functional state of BM-derived stem cells was changed under the influence of experimental serum, thus differentiating toward the direction of a hepatocyte lineage. Although the markers of a mature hepatocyte, L-PK and albumin were not detectable in stimulated BM stem cells, the leap from an undetermined state to a determined state was a marker of entry into the process of programmed differentiation. A variety of possibilities could account for the lack of detectable signals for L-PK and albumin in stimulated BM stem cells. Among the possibilities, one could be the deficiency in intensity and time of stimulation, while another could, by reasoning, be that the postulated "signal molecules" existing in the experimental serum were involved only in the early activation and determination of BM stem cells, while the terminal differentiation of the cells into hepatocytes might still need other signals.

The results in the present study indicated that the driving force promoting differentiation of BM stem cells to hepatocytes was certainly generated from the serum of rats treated by 2-AAF/CCl₄. It has been further testified that some "signal molecules" were existed in the circulation of rats treated by 2-AAF/CCl₄ and that they might play an important role in the initiation of activation of stem cell. It would be helpful for understanding the mechanisms of stem cell differentiation if the "signal molecules" could be further identified and isolated.

Recent studies have convincingly demonstrated that adult bone marrow contains cells capable of differentiating into hepatocyte-like cells. Nevertheless, what type of cell population are the ancestor cells for hepatocytes still remains a question. In the vast majority of reports, hematopoietic cells were considered to be capable of "transdifferentiating" into hepatocytes^[2,4,23-28]. However, Wagers (2002) deemed that there was little evidence for transdifferentiation of adult hematopoietic stem cells^[29]. The present study showed that bone marrow stromal cells demonstrated the plasticity in changing into hepatocytes. By this token, the debate about origin of liver stem cells will keep on.

REFERENCES

- 1 **Petersen BE**, Bowen WC, Patrene KD, Mars WM, Sullivan AK, Murase N, Boggs SS, Greenberger JS, Goff JP. Bone marrow as a potential source of hepatic oval cells. *Science* 1999; **284**: 1168-1170
- 2 **Lagasse E**, Connors H, Al Dhalimy M, Reitsma M, Dohse M, Osborne L, Wang X, Finegold M, Weissman IL, Grompe M. Purified hematopoietic stem cells can differentiate into hepatocytes *in vivo*. *Nat Med* 2000; **6**: 1229-1234
- 3 **Theise ND**, Nimmakayalu M, Gardner R, Illei PB, Morgan G, Teperman L, Henegariu O, Krause DS. Liver from bone marrow in humans. *Hepatology* 2000; **32**: 11-16
- 4 **Alison M**, Poulsom R, Jeffery R, Dhillon AP, Quaglia A, Jacob J, Novelli M, Prentice G, Williamson J, Wright NA. Hepatocytes from non-hepatic adult stem cells. *Nature* 2000; **406**: 257
- 5 **Chen JZ**, Hong H, Xiang J, Xue L, Zhao GQ. A selective tropism of transfused oval cells for liver. *World J Gastroenterol* 2003; **9**: 544-546
- 6 **Crosby HA**, Hubscher S, Fabris L, Joplin R, Sell S, Kelly D, Strain AJ. Immunolocalization of putative human liver progenitor cells in livers from patients with end-stage primary biliary cirrhosis and sclerosing cholangitis using the monoclonal antibody OV-6. *Am J Pathol* 1998; **152**: 771-779
- 7 **Lowes KN**, Brennan BA, Yeoh GC, Olynyk JK. Oval cell numbers in human chronic liver diseases are directly related to disease severity. *Am J Pathol* 1999; **154**: 537-541
- 8 **Theise ND**, Saxena R, Portmann BC, Thung SN, Yee H, Chiriboga L, Kumar A, Crawford JM. The canals of Hering and hepatic stem cells in humans. *Hepatology* 1999; **30**: 1425-1433
- 9 **Malhi H**, Irani AN, Gagandeep S, Gupta S. Isolation of human progenitor liver epithelial cells with extensive replication capacity and differentiation into mature hepatocytes. *J Cell Sci* 2002; **115**: 2679-2688

- 10 **Sell S.** The role of progenitor cells in repair of liver injury and in liver transplantation. *Wound Repair Regen* 2001; **9**: 467-482
- 11 **Roskams T,** Yang SQ, Koteish A, Durnez A, DeVos R, Huang X, Achten R, Verslype C, Diehl AM. Oxidative stress and oval cell accumulation in mice and humans with alcoholic and nonalcoholic fatty liver disease. *Am J Pathol* 2003; **163**: 1301-1311
- 12 **Lowes KN,** Croager EJ, Olynyk JK, Abraham LJ, Yeoh GC. Oval cell-mediated liver regeneration: Role of cytokines and growth factors. *J Gastroenterol Hepatol* 2003; **18**: 4-12
- 13 **Fausto N,** Campbell JS. The role of hepatocytes and oval cells in liver regeneration and repopulation. *Mech Dev* 2003; **120**: 117-130
- 14 **Oh SH,** Hatch HM, Petersen BE. Hepatic oval 'stem' cell in liver regeneration. *Semin Cell Dev Biol* 2002; **13**: 405-409
- 15 **Faris RA,** Konkin T, Halpert G. Liver stem cells: a potential source of hepatocytes for the treatment of human liver disease. *Artif Organs* 2001; **25**: 513-521
- 16 **Tian YW,** Smith PG, Yeoh GC. The oval-shaped cell as a candidate for a liver stem cell in embryonic, neonatal and precancerous liver: identification based on morphology and immunohistochemical staining for albumin and pyruvate kinase isoenzyme expression. *Histochem Cell Biol* 1997; **107**: 243-250
- 17 **Tee LB,** Kirilak Y, Huang WH, Smith PG, Morgan RH, Yeoh GC. Dual phenotypic expression of hepatocytes and bile ductular markers in developing and preneoplastic rat liver. *Carcinogenesis* 1996; **17**: 251-259
- 18 **Steinberg P,** Klingelhoffer A, Schafer A, Wust G, Weisse G, Oesch F, Eigenbrodt E. Expression of pyruvate kinase M2 in preneoplastic hepatic foci of N-nitrosomorpholine-treated rats. *Virchows Arch* 1999; **434**: 213-220
- 19 **Hacker HJ,** Steinberg P, Bannasch P. Pyruvate kinase isoenzyme shift from L-type to M2-type is a late event in hepatocarcinogenesis induced in rats by a choline-deficient/DL-ethionine-supplemented diet. *Carcinogenesis* 1998; **19**: 99-107
- 20 **Tee LB,** Kirilak Y, Huang WH, Morgan RH, Yeoh GC. Differentiation of oval cells into duct-like cells in preneoplastic liver of rats placed on a choline-deficient diet supplemented with ethionine. *Carcinogenesis* 1994; **15**: 2747-2756
- 21 **Scott RJ,** English V, Noguchi T, Tanaka T, Yeoh GC. Pyruvate kinase isoenzyme transitions in cultures of fetal rat hepatocytes. *Cell Differ Dev* 1988; **25**: 109-118
- 22 **Vessey CJ,** de la Hall PM. Hepatic stem cells: a review. *Pathology* 2001; **33**: 130-141
- 23 **Wang X,** Ge S, McNamara G, Hao QL, Crooks GM, Nolte JA. Albumin-expressing hepatocyte-like cells develop in the livers of immune-deficient mice that received transplants of highly purified human hematopoietic stem cells. *Blood* 2003; **101**: 4201-4208
- 24 **Fiegel HC,** Lioznov MV, Cortes-Dericks L, Lange C, Kluth D, Fehse B, Zander AR. Liver-specific gene expression in cultured human hematopoietic stem cells. *Stem Cells* 2003; **21**: 98-104
- 25 **Austin TW,** Lagasse E. Hepatic regeneration from hematopoietic stem cells. *Mech Dev* 2003; **120**: 131-135
- 26 **Mallet VO,** Mitchell C, Mezey E, Fabre M, Guidotti JE, Renia L, Coulombel L, Kahn A, Gilgenkrantz H. Bone marrow transplantation in mice leads to a minor population of hepatocytes that can be selectively amplified *in vivo*. *Hepatology* 2002; **35**: 799-804
- 27 **Avital I,** Inderbitzin D, Aoki T, Tyan DB, Cohen AH, Ferrarasso C, Rozga J, Arnaout WS, Demetriou AA. Isolation, characterization, and transplantation of bone marrow-derived hepatocyte stem cells. *Biochem Biophys Res Commun* 2001; **288**: 156-164
- 28 **Mitaka T.** Hepatic stem cells: from bone marrow cells to hepatocytes. *Biochem Biophys Res Commun* 2001; **281**: 1-5
- 29 **Wagers AJ,** Sherwood RI, Christensen JL, Weissman IL. Little evidence for developmental plasticity of adult hematopoietic stem cells. *Science* 2002; **297**: 2256-2259
- 30 **Couvelard A,** Bringuier AF, Dauge MC, Nejjari M, Darai E, Benifla JL, Feldmann G, Henin D, Scoazec JY. Expression of integrins during liver organogenesis in humans. *Hepatology* 1998; **27**: 839-847

Edited by Wang XL and Qin D Proofread by Xu FM

Pathophysiological significance of a reaction in mouse gastrointestinal tract associated with delayed-type hypersensitivity

Wan-Gui Yu, Ping Lin, Hui Pan, Lan Xiao, En-Cong Gong, Lin Mei

Wan-Gui Yu, Department of Physiology, Medical College of Yangtze University, Jingzhou 434000, Hubei Province, China

Ping Lin, Department of Physiology, Medical School of Hubei Institute for Nationalities, Enshi, 445000, Hubei Province, China

Hui Pan, Lan Xiao, Lin Mei, Department of Physiology and Pathophysiology, Peking University Health Science Center, Beijing, 100083, China

En-Cong Gong, Department of Pathology, Peking University Health Science Center, Beijing, 100083, China

Supported by the National Natural Science Foundation of China, No. 30170419

Correspondence to: Dr. Lin Mei, Department of Physiology and Pathophysiology, Peking University Health Science Center, Beijing, 100083, China. linmei@bjmu.edu.cn

Telephone: +86-10-82801477 **Fax:** +86-10-82801746

Received: 2003-12-17 **Accepted:** 2004-01-08

Abstract

AIM: To explore the pathophysiological significance of delayed type hypersensitivity (DTH) reaction in mouse gastrointestinal tract induced by an allergen 2,4-dinitrochlorobenzene (DNCB).

METHODS: BALB/c mice were randomly divided into control and DTH₁₋₆ groups. After sensitized by DNCB smeared on the abdominal skin, the mice were challenged with DNCB by gavage or enema. The weight, stool viscosity and hematochezia were observed and accumulated as disease active index (DAI) score; the gastrointestinal motility was represented by active charcoal propulsion rate; the colon pathological score was achieved by macropathology and HE staining of section prepared for microscopy; and the leukocyte migration inhibitory factor (LMIF) activity was determined by indirect capillary assay of the absorbance (A) of migrated leukocytes.

RESULTS: Active charcoal propulsion rates of small intestine in the DNCB gavages groups were significantly higher than that in the control group ($P < 0.01$). The DAI scores and pathological score in DNCB enema groups were also higher than that in the control group ($P < 0.05$), and there were significant rises in LMIF activity in DNCB enema groups as compared with control groups ($P < 0.01$).

CONCLUSION: Mouse gastrointestinal DTH reaction could be induced by DNCB, which might facilitate the mechanism underlying the ulcerative colitis.

Yu WG, Lin P, Pan H, Xiao L, Gong EC, Mei L. Pathophysiological significance of a reaction in mouse gastrointestinal tract associated with delayed-type hypersensitivity. *World J Gastroenterol* 2004; 10(15): 2254-2258
<http://www.wjgnet.com/1007-9327/10/2254.asp>

INTRODUCTION

The gastrointestinal tract (GI) is not only an important organ in digestion and endocrine, but also the largest peripheral

immunological organ in the body^[1]. The secretory immunoglobulin A (s-IgA) and T cell are responsible for developing mucosa vaccines and producing oral tolerance^[2,3]. Furthermore, the manifestation of T cell mediated reaction in GI tract was most often in the way of delayed-type hypersensitivity (DTH), thereby resulting in ulcerative colitis^[4,5]. 2,4-dinitrochlorobenzene (DNCB), a chemical compound of low molecular weight, could combine with tissue protein to function as a full antigen in activating T cell mediated DTH reaction, such as skin DTH^[6] and colon inflammation/ulcer^[5,7,8]. Gastrointestinal DTH (or colitis) induced by DNCB in rabbit, guinea pig and rat has been reported^[5,7,8], but that in mice has not been reported. In this study, DNCB-induced DTH in mice GI tract were found, and its pathophysiological significance was discussed.

MATERIALS AND METHODS

Animals

Healthy male BALB/c mice weighing 18-21 g (supplied by the Department of Experimental Animals, Peking University Health Science Center) were used. Animals were fed with a standard diet and allowed free access to water.

Preparation of major chemicals

DNCB solution For DNCB sensitization, 330 mg DNCB (Beijing Chemical Reagent Company, Beijing, P.R. China) was dissolved in 10 mL of acetone-olive oil (1:1) vehicle. For DNCB gavage, 300 mg DNCB was first mixed with a minimum volume of polysorbate 80, and a minimum volume of ethanol was added until the mixture was completely dissolved, followed by the addition of olive oil to achieve a final DNCB concentration of 6.6 g/L. The ratios of polysorbate 80-ethanol-olive oil in this vehicle were 6.6%, 8.8% and 84.6%, respectively. Then the 6.6% solution was diluted to 1.3 g/L and 0.3 g/L DNCB solution. For DNCB enema, DNCB was dissolved in 600 mL/L ethanol to achieve 4 g/L, 2 g/L, and 1 g/L DNCB solution, separately. All these DNCB solutions were stored at 4 °C.

Activated charcoal suspension The suspension was made according to Qi *et al.*^[9] with a little modification. A total of 6 g activated charcoal (Tianjin 6th Chemical Reagent Company, Tianjin, China) and 2 g astragalum (Beijing Chemical Reagent Company, China) were dissolved in 50 mL of normal saline (NS) just before intragastric use.

RPMI 1640 One milliliter of RPMI 1640 culture medium contained 100 IU penicillin and 100 µg streptomycin, and then the pH was adjusted to 6.8-7.2.

Phytohemagglutinin (PHA) A 100 mg PHA was dissolved in 10 mL incomplete RPMI1640, and then sterilized and preserved at -20 °C.

Ammonium chloride solution (erythrocyte lytic fluid) A total of 1.03 g Tris and 3.735 g NH₄Cl were dissolved in 500 mL distilled water.

Induction of DTH response in GI tract

Grouping Ninety-six BALB/c mice were randomly divided into 10 groups, including DTH₁₋₆, DTH negative (DTH₋) group and control group.

Sensitization On the first day of experiment, mouse fur on abdomen (2.5 cm diameter) was shaved. A total of 50 μ L of 33 g/L DNCB was smeared on the shaved skin once a day for 1 or 4 d. Mice in the DTH₍₋₎ and control groups were smeared with acetone-olive oil vehicle.

Gavage All the mice were fasted for 6 h before gavage. On the second day of experiment the mice in DTH₁, DTH₂ and DTH₃ groups were gavaged with 0.8 mL of 0.3 g/L, 1.3/L and 6.6 g/L DNCB, respectively. The DTH₍₋₎ group was gavaged 1.3 g/L DNCB and the control group was gavaged polysorbate 80-ethanol-olive oil vehicle. On the third day, 0.8 mL of activated charcoal was gavaged to each mouse. Twenty minutes later, the mice were killed by decapitation for determination of gastrointestinal motility.

Enema On the 5 th day, a silica-gel tube with 10 mm diameter was inserted into the colons of the mice, its tip being 3-3.5 cm far from the anus. The mice in DTH₄, DTH₅ and DTH₆ groups were intracolonicly administered 1 g/L, 2 g/L and 4 g/L DNCB (2 μ L/g) once a day for 4 d. DTH₍₋₎ group was administered 2 g/L DNCB and the control group was administered 600 mL/L ethanol vehicle.

Evaluation of the animals

Gastrointestinal motility After each mouse was killed, the whole small intestine was taken out, rinsed with NS quickly, and the intestinal wall was cut open longitudinally, laid and unfolded on a flat plate for estimation of the active charcoal migration distance (cm). The gastrointestinal motility was expressed by charcoal propulsion rate by using the formula: charcoal propulsion rate = migration distance of active charcoal / the distance from pylorus-duodenum junction to ileocecum $\times 100\%$.

Body mass and stool By using disease activity index (DAI) score^[10], the body mass and stool were scored as follows: Body mass: score 0-normal; score 1-1-5% lower than normal; score 2-6-10% lower than normal; score 3-11-15% lower than normal; and score 4-above 15% lower than normal. Stool viscosity: score 0-normal; score 2-fluffy; and score 4-diarrhea. Stool hemorrhage: score 0-normal; and score 2-apparent hemorrhage.

Pathological score On the 9 th d, all the mice received enema were killed by cervical dislocation. The colon was cut open longitudinally along the attachments of mesenteries and was first macropathologically observed. Then specimens were taken from inflammatory/ulcerative colon and were fixed in 40 g/L formaldehyde. Paraffin-embedded 5- μ m thick section was made for HE staining. The macropathological score and microscopy score were obtained by adopting Dr. Murano's method^[10] with slight modification as follows: Macropathological score: score 0-no cementation (colon was easily detached from other tissues) and no inflammation in colon; score 1-moderate cementation or local congestion; score 2-severe cementation with one ulcer (<1 cm); score 3- more than one ulcer (<1 cm) with inflammation; and score 4-more than one ulcer (>1 cm) with inflammation.

Microscopy: score 0-normal colon mucosa or slight congestion; score 1-mucosa hyperemia, infiltration of chronic inflammatory cells and decrease of the number of goblet cell in colon mucosa; score 2-mucosa hyperemia, infiltration of chronic inflammatory cells and local superficial erosion; and score 3-atrophic change with ulcer and serious infiltration of chronic inflammatory cells in colon mucosa.

Measurement of leukocyte migration inhibitory factor (LMIF) activity

LMIF preparation By following our previous method^[11], the spleen lymphocytes (2×10^6 /mL) of mice received enema were cultured in PHA (60 μ g/mL) for 72 h. Then the supernatant containing LMIF component was collected by centrifugation

(1 500 r/min, 15 min), followed by lyophilization. The lyophilized powder was stored at -20 . Working solution (LMIF solution) was prepared by dissolving the lyophilized powder in RPMI-1640 to one third of its original volume before using.

Preparation of peripheral leukocytes A suspension of indicator cells (migrated leukocytes) was prepared from the anti-coagulated whole blood of guinea pigs. Three percent gelatin of 1/3 volume of the blood was added to the blood before culturing the sample at 37 for 30 min. The upper layer rich in leukocytes was taken out and centrifuged (1 000 r/min) for 10 min. Then the sediment was washed twice with Hanks' solution free of Mg²⁺ and Ca²⁺, and again centrifuged (1 000 r/min) for 10 min. Finally, the sediment was used as the indicator cell and was adjusted to a concentration of $(1.6-1.8) \times 10^7$ cells/mL RPMI 1640.

Detection of leukocyte absorbance By following our previous work^[11] with a little improvement, the leukocyte was injected into a capillary tube of 80 μ L volume. After heat-sealing one end of the tube and spinning at 1 000 r/min for 10 min, the tubes were cut at the liquid-cell interface. The portion containing the cells was placed inside each chamber of a 24-well plate filled with 210 μ L LMIF solution for culture. Twelve hours later, 200 μ L solution was taken out from each chamber and was put in an well of a 96-well plate, followed by an addition of 20 μ L methylthiazolotetrazolium, MTT) was added into each well before the plate was incubated at 37 for 4 h. Then the supernatant was removed, 200 μ L of DMSO was added into each well and the plate was shaken for 10 min. The absorbance (A value) of the migration cells was determined in Micro plate Reader at a wavelength of 570 nm. The average of A values of 3 wells was regarded as a mean A value. The above processes were repeated for 9 times.

Statistical analysis

Data were expressed as mean \pm SE. Analysis of variance (ANOVA) and student's *t* test were used for comparison among the groups and between paired data. $P < 0.05$ was considered to be statistically significant.

RESULTS

Gastrointestinal motility

Active charcoal propulsion rates of small intestine in the DTH₁ (0.3 g/L DNCB) and DTH₂ (1.3 g/L DNCB) groups were significantly higher than that in the control group ($P < 0.01$) and DTH₍₋₎ groups ($P < 0.05$ or $P < 0.01$), whereas there was no significant difference between the control group and DTH₍₋₎ group (Figure 1). All the mice in DTH₃ group died after the 0.66% DNCB gavage.

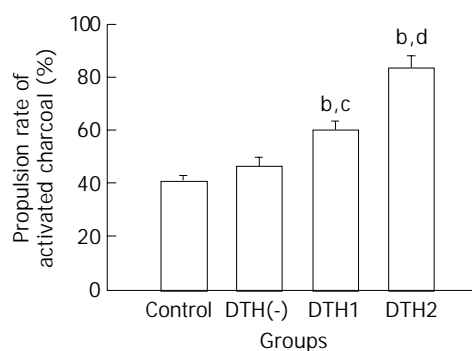


Figure 1 Effect of DNCB gavage on gastrointestinal motility in sensitized mice. ^b $P < 0.01$ vs control, ^c $P < 0.05$ vs DTH₍₋₎, ^d $P < 0.01$ vs DTH₍₋₎ and DTH₁, $n = 8$ in control; $n = 7$ in DTH₍₋₎, DTH₁ and DTH₂ groups.

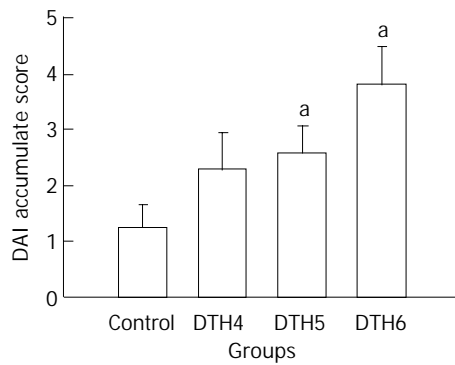


Figure 2 Effect of DNCB enema on DAI score in sensitized mice. ^a $P < 0.05$ vs control. $n = 16$ in control group and DTH₄ group; $n = 11$ in DTH₅ group; $n = 17$ in DTH₆ group.

DAI score and pathological score

Diarrhea was first found in the mice 24 h after DNCB enema, and weight loss was found 3 d later. Serious weight loss and obvious diarrhea were seen in the 4 g/L DNCB group, 24% of whom died. DAI scores are shown in Figure 2.

Pathologically, the control and DTH₍₋₎ groups had normal histological structures and glands, no ulcer was found except

for occasional slight mucosa congestion (Figure 3A). In DTH₄ (1 g/L DNCB) group, there was slight colic edema, mucosa congestion, infiltration of lymphocytes and a decrease in the number of glands and goblet cells (Figure 3B). In DTH₅ (2 g/L DNCB) group, intestinal adhesion and flatulence were found. A more disturbing array of glands, local erosion, dramatic decrease in goblet cells and diffuse inflammatory cellular infiltration were found (Figure 3C). In DTH₆ (4 g/L DNCB) group, more extensive colic cementation, expansion of the proximal intestinal cavity, some white exudates, mucosa congestion, necrosis and multiple ulcers were found. Under the microscope, mucosa atrophy, decrease of glands and disturbance of tissue structure were observed (Figure 3D), moreover, erosion, hemorrhage, necrosis as well as deeper/extensive ulcers were easily seen (Figure 3E). The pathological score in each group is shown in Figure 4.

The LMIF activities and its relationship with colitis

With the increased DNCB doses in enema, which exacerbated colonic tissue damage, we could see an increase of the LMIF activity (A value decreased). The LMIF activity was significantly increased in the DTH₅ and DTH₆ groups as compared with the control group ($P < 0.01$, student's t -test) (Table 1). There were also significant differences in LMIF activity ($P < 0.01$) among DTH₄, DTH₅ and DTH₆ groups (ANOVA).

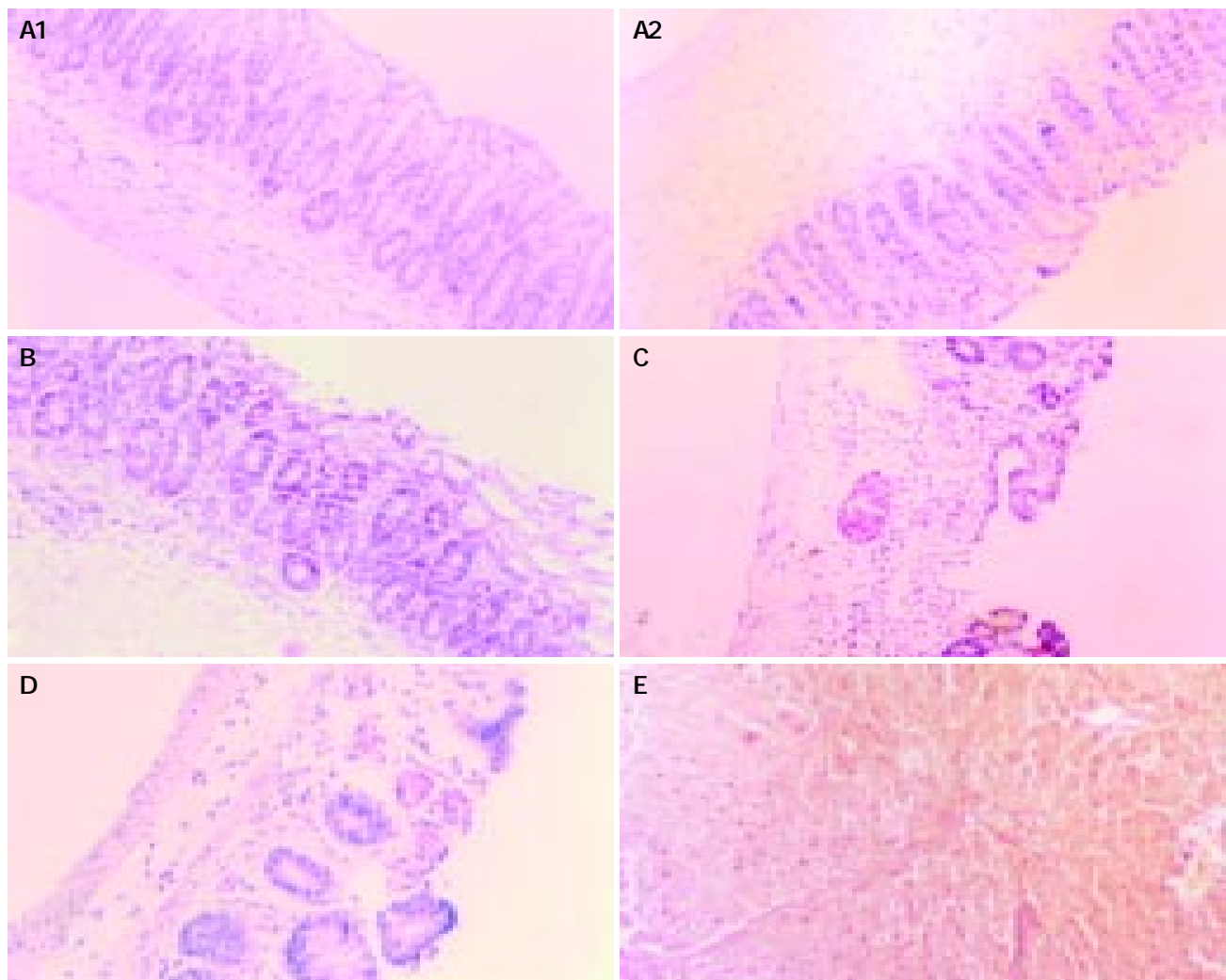


Figure 3 The pathological change of colon by DNCB enema in sensitized mice. A1: control 600 mL/L ethanol, normal histological structures. A2: DTH₍₋₎, only slight mucosa congestion. B: 1 g/L DNCB, hyperemia, infiltration of chronic inflammatory cells, decrease of the number of goblet cell in colon mucosa. C: 2 g/L DNCB, superficial erosion, chronic inflammation of colon mucosa. D: 4 g/L DNCB, atrophic changes of colon mucosa with chronic inflammation. E: 4 g/L DNCB, ulcer and hemorrhage in colon mucosa (HE, $\times 200$).

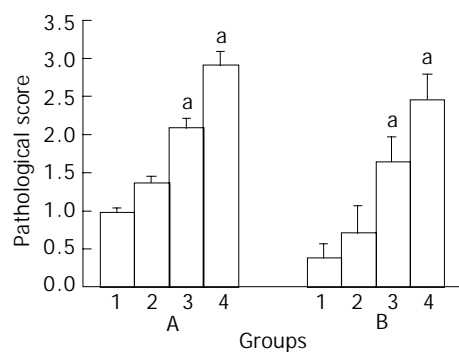


Figure 4 Pathological score in the mice received DNCB enema after sensitization. 4A: macropathology; 4B: microscopically observation. group 1: control (600 mL/L ethanol, $n=16$); group 2: DTH₄ (1 g/L DNCB, $n=17$); group 3: DTH₅ (2 g/L DNCB, $n=17$); and group 4: DTH₆ (4 g/L DNCB, $n=17$)^a $P<0.05$ vs group 4A1 and 4B1, respectively.

Table 1 Effect of DNCB enema on LMIF activity in sensitized mice

Group	Skin smearing (50 μ L/mouse)	Enema (2 μ L/g bm)	A value (mean \pm SE)
Control	Acetone-olive oil	600 mL/L ethanol	0.426 \pm 0.009
DTH _(c)	Acetone-olive oil	2 g/L DNCB	0.401 \pm 0.007
DTH ₄	33 g/L DNCB	1 g/L DNCB	0.383 \pm 0.038
DTH ₅	33 g/L DNCB	2 g/L DNCB	0.220 \pm 0.012 ^b
DTH ₆	33 g/L DNCB	4 g/L DNCB	0.139 \pm 0.019 ^d

^b $P<0.01$ when compared with the control and DTH_(c) (student's t -test). ^d $P<0.01$ between DTH₄, DTH₅ and DTH₆ groups (ANOVA); $n=9$ in each group. A, the absorbance of migration leukocytes. The skin smearing and enema were completed daily for 4 d.

DISCUSSION

For the first time, here, we reported DTH response of mice GI tract by intra-gastrointestinal administration of DNCB. The evidence of gastrointestinal DTH response were as follows: DNCB-sensitized mouse showed increased GI motility, diarrhea, hematochezia and colitis after DNCB challenge; and the activity of LMIF released from sensitized T-lymphocyte was significantly increased after DNCB enema. The mechanism of the DTH phenomenon might be the same as that of the ear skin DTH reaction in our previous study^[6].

What is the pathophysiological significance of GI DTH reaction? Early in the 1960's, Bicks *et al.* found that inflammation and ulcer could be induced by DNCB enema in guinea pigs^[4], which he thought as being a cellular immune induced by DNCB that resulted in a DTH reaction in GI tract. Later, several other researchers explored the relations between DNCB-activated cellular immune and GI disorder, but they either indirectly inferred the possibility of GI being influenced by DTH skin tests^[12] or only focused on the pathological relation of DNCB-colitis with human ulcerative colitis (UC)^[5,7,8]. Comparing with previous DNCB-colitis in rat, guinea pig and rabbit by other researchers, our work here not only successfully created DNCB-colitis model in mouse, but also found a more convenient and more sensitive animal model for DTH study^[13]. In our study, we proved, using the specific DTH index of LMIF^[14,15], that DNCB could induce DTH in mouse GI tract, and this kind of DTH might be the essence of UC.

MIF is one of the cytokines released from sensitized T cell after subjecting the allergen again^[14,15]. According to the target cell, LMIF can be classified as LMIF and MMIF^[16]. There was a dramatic positive correlation between LMIF activity and the

gravity of DTH response^[17]. We found that the ConA-stimulated lymphocytes from mesenteric lymph node of DNCB-treated mouse showed higher LMIF activity than the control, and LMIF activity increased as DNCB concentration increased (Table 1), whereas in DTH_(c) group, neither higher LMIF activity nor colon inflammation/ulcer was found, indicating a possible relations among GI DTH response, LMIF activity and UC. Secondly, we know that the main clinical manifestations of UC are diarrhea and pus hematochezia, which result from an irritated intestinal peristaltic and inflectional ulcer^[18,19]. Our results were in accordance with the clinical manifestations of UC (Figures 1-4), indicating that colitis in mouse caused by DNCB was basically similar to human UC in pathology. Finally, two representatives but separate works by Bartnik *et al.*^[20] and Murakami *et al.*^[21] support the hypothesis that the essence of UC is gastrointestinal DTH response. Bartnik *et al.* reported that patients with severe or moderate ulcerative colitis showed LMIF release, which was significantly greater than that observed in patients with other large bowel diseases^[20]; and Murakami *et al.* reported that the number of MIF expressing cells increased at the colonic mucosa in patients with ulcerative colitis, and MIF induced significant levels of IL-1 and IL-8 in monocytes and dendrite cells in UC patients, indicating a role of MIF in the induction and/or perpetuation of the inflammatory environment in UC^[21]. Comparing with all the other cytokines reported in UC^[22], we think that the distinctive (unique) significance of LMIF in UC and its pivotal role in connecting DTH with UC have been showed by Bartnik and Murakami.

To sum up, we have enough reasons to conclude that the GI DTH in mouse may provide not only experimental models of human UC, but also insight into pathogenic mechanisms of the UC, an inflammatory bowel disease (IBD) of unknown etiology.

REFERENCES

- 1 Takahashi I, Kiyono H. Gut as the largest immunologic tissue. *J Parenter Enteral Nutr* 1999; **23**(5 Suppl): S7-12
- 2 Czerkinsky C, Anjuere F, McGhee JR, George-Chandy A, Holmgren J, Kieny MP, Fujiyoshi K, Mestecky JF, Pierrefite-Carle V, Rask C, Sun JB. Mucosal immunity and tolerance: relevance to vaccine development. *Immunol Rev* 1999; **170**: 197-222
- 3 Galliaerde V, Desvignes C, Peyron E, Kaiserlian D. Oral tolerance to haptens: intestinal epithelial cells from 2,4-dinitrochlorobenzene-fed mice inhibit hapten-specific T cell activation *in vitro*. *Eur J Immunol* 1995; **25**: 1385-1390
- 4 Bicks RO, Rosenberg EW. A chronic delayed hypersensitivity reaction in the guinea pig colon. *Gastroenterology* 1964; **46**: 543-549
- 5 Rabin BS, Rogers SJ. A cell-mediated immune model of inflammatory bowel disease in the rabbit. *Gastroenterology* 1978; **75**: 29-33
- 6 Mei L, Li LQ, Li YF, Deng YL, Sun CW, Ding GF, Fan SG. Conditioned immunosuppressive effect of cyclophosphamide on delayed-type hypersensitivity response and a preliminary analysis of its mechanism. *Neuroimmunomodulation* 2000; **8**: 45-50
- 7 Glick ME, Falchuk ZM. Dinitrochlorobenzene-induced colitis in the guinea-pig: studies of colonic lamina propria lymphocytes. *Gut* 1981; **22**: 120-125
- 8 Zhang YB, Zou YH, Lian ZC, Chen WQ. Experimental model of ulcerative colitis in rat and its abnormality of colonic electricity. *Laboratory Animal Science Administration* 2002; **19**: 5-7
- 9 Qi HB, Luo JY, Liu X. Effect of enterokinetic prucalopride on intestinal motility in fast rats. *World J Gastroenterol* 2003; **9**: 2065-2067
- 10 Murano M, Maemura K, Hirata I, Toshina K, Nishikawa T, Hamamoto N, Sasaki S, Saitoh O, Katsu K. Therapeutic effect of intracolonic administered nuclear factor kappa B (p65) antisense oligonucleotide on mouse dextran sulphate sodium

- (DSS)-induced colitis. *Clin Exp Immunol* 2000; **120**: 51-58
- 11 **Mei L**, Li LQ, Fan SG, Ding GF. An assay of leukocyte migration inhibitory factor (LMIF) and the conditioned suppression effect on LMIF. *Chin J Microbiol Immunol* 1998; **18**: 474-478
- 12 **Shell-Duncan B**, Wood JW. The evaluation of delayed-type hypersensitivity responsiveness and nutritional status as predictors of gastro-intestinal and acute respiratory infection: a prospective field study among traditional nomadic Kenyan children. *J Trop Pediatr* 1997; **43**: 25-32
- 13 **Gold D**. Delayed-type hypersensitivity to *Entamoeba histolytica* in mice and hamsters: a comparison. *Parasitol Res* 1989; **75**: 335-342
- 14 **Bloom BR**, Bennett B. Mechanism of a reaction *in vitro* associated with delayed-type hypersensitivity. *Science* 1966; **153**: 80-82
- 15 **Wolberg WH**, Goelzer ML. *In vitro* assay of cell mediated immunity in human cancer: Definition of leukocyte migration inhibitory factor. *Nature* 1971; **229**: 632-634
- 16 **Matsui Y**, Oshima S. Migration inhibition and stimulation factors produced from peripheral blood lymphocyte cultures of sensitized guinea pigs. *Asian Pac J Allergy Immunol* 1985; **3**: 151-155
- 17 **Malorny U**, Goebeler M, Gutwald J, Roth J, Sorg C. Difference in migration inhibitory factor production by C57Bl/6 and BALB/c mice in allergic and irritant contact dermatitis. *Int Arch Allergy Appl Immunol* 1990; **92**: 356-360
- 18 **Soffer EE**. Diarrhea and malabsorption In: Stoller JK, Ahmad M, Longworth DL, eds. The Cleveland clinic intensive review of internal medicine. *New York Lippincott Williams Wilkins* 2000: 730-732
- 19 **Stenson WF**. Inflammatory bowel disease In: Yamada T, Apers DH, Laine L, Owyang C, Powell DW, eds. Textbook of gastroenterology. *New York Lippincott Williams Wilkins* 1999: 1782-1783
- 20 **Bartnik W**, ReMine SG, Shorter RG. Leukocyte migration inhibitory factor (LMIF) release by human colonic lymphocytes. *Arch Immunol Ther Exp* 1981; **29**: 397-405
- 21 **Murakami H**, Akbar SM, Matsui H, Horiike N, Onji M. Macrophage migration inhibitory factor activates antigen-presenting dendritic cells and induces inflammatory cytokines in ulcerative colitis. *Clin Exp Immunol* 2002; **128**: 504-510
- 22 **Zhou T**, Lin P, Pan H, Mei L. Ulcerative colitis: a review in its pathogenesis and immune mechanisms. *Shijie Huaren Xiaohua Zazhi* 2003; **11**: 1782-1786

Edited by kumar M and Xu FM

Hepatitis B virus X gene induces human telomerase reverse transcriptase mRNA expression in cultured normal human cholangiocytes

Sheng-Quan Zou, Zhen-Liang Qu, Zhan-Fei Li, Xin Wang

Sheng-Quan Zou, Zhan-Fei Li, Xin Wang, Department of Surgery, Tongji Hospital of Tongji Medical College, Huazhong University of Science and Technology, Wuhan 430030, Hubei Province, China
Zhen-Liang Qu, Department of General Surgery, the 254th Military Hospital, Tianjin 300142, China

Supported by the National High Technology Research and Development Program of China, 863 Program, No. 2002AA214061

Correspondence to: Dr. Sheng-Quan Zou, Department of Surgery, Tongji Hospital of Tongji Medical College, Huazhong University of Science and Technology, Wuhan 430030, Hubei Province, China. sqzou@tjh.tjmu.edu.cn

Telephone: +86-27-83662398

Received: 2003-10-20 **Accepted:** 2003-12-29

Abstract

AIM: To study the transcriptional regulation of human telomerase reverse transcriptase (hTERT) mRNA in normal human cholangiocytes (HBECs) after hepatitis B virus X (HBx) gene transfection and to elucidate the possible mechanism of HBV infection underlying cholangiocarcinoma.

METHODS: HBECs were cultured *in vitro* and co-transfected with a eukaryotic expression vector containing the HBx coding region and a cloning vector containing coding sequences of enhanced green fluorescent protein (EGFP) using lipid-mediated gene transfer. The transfection efficiency was determined by the expression of EGFP. The expressions of hTERT mRNA and HBx protein in HBECs were detected by RT-PCR and immunocytochemical stain, respectively.

RESULTS: The transfection efficiencies were about 15% for both HBx gene expression plasmid and empty vector. No hTERT mRNA was expressed in HBECs when transfected with OPTI-MEM medium and empty vector, but a dramatic increase was observed for hTERT mRNA expression in HBECs when transfected with HBx expression vector. HBx protein was only expressed in HBECs when transfected with HBx expression vector.

CONCLUSION: HBx transfection can activate the transcriptional expression of hTERT mRNA. Cis-activation of hTERT mRNA by HBx gene is the primary mechanism underlying the proliferation, differentiation and tumorigenesis of biliary epithelia.

Zou SQ, Qu ZL, Li ZF, Wang X. Hepatitis B virus X gene induces human telomerase reverse transcriptase mRNA expression in cultured normal human cholangiocytes. *World J Gastroenterol* 2004; 10(15): 2259-2262

<http://www.wjgnet.com/1007-9327/10/2259.asp>

INTRODUCTION

Telomeres make up the ends of chromosomes of eukaryote and progressively shorten with each cell cycle. Critically short

telomeres induce cellular senescence and death^[1]. Telomere lengths become stabilized by the activation of telomerase in most tumor cells, highly proliferative cells and human somatic cells. The activation of telomerase is a crucial step in tumorigenesis and cellular senescence^[2]. The most important catalytic protein subunit of telomerase ribonucleoprotein is hTERT whose expression parallels telomerase activity^[3]. It is known that hTERT expression is regulated mainly at the transcriptional level and that the core promoter of hTERT encompasses numerous transcription factor binding sites. All these factors, which regulate hTERT promoter region individually or coordinately, comprise a complex regulation system^[4]. A recent study has shown that HBV DNA integration locates upstream to the hTERT promoter and that HBV enhancer can cis-activate the transcriptional expression of hTERT gene in hepatocarcinoma cell lines^[5]. HBx gene also activates the expression of telomerase^[6]. All these findings provide a new mechanism of HBV in liver carcinogenesis. There is a prominent expression of HBx protein in tissues of both intrahepatic^[7,8] and extrahepatic cholangiocarcinomas^[9]. So far, it is not clear whether HBV infection involves in the tumorigenesis of cholangiocarcinoma and if HBx gene can regulate the expression of telomerase gene. In order to determine the possible correlation of HBV infection and cholangiocarcinogenesis, we transferred HBx gene into human normal cholangiocytes (HBECs) and assayed the expression of hTERT mRNA by RT-PCR.

MATERIALS AND METHODS

Cell and culture

HBECs, isolated from normal human bile ducts^[10], were kindly provided by Dr. Ludwik K. Trejdosiewicz (ICRF Cancer Medical Research Unit, St James's University Hospital, Leeds, UK). HBECs were maintained as adherent monolayers in "HBEC medium" comprising a 1:1 mixture of Ham's F12 and DMEM (Gibco BRL[®]), supplemented with 50 g/L fetal bovine serum (Gibco BRL[®]), 5 ng/mL epidermal growth factor (Intergen Company), 0.4 µg/mL hydrocortisone hemisuccinate, 2 nmol/L triiodothyronine and 5 µg/mL insulin (all from Sigma) and 10 ng/mL human recombinant hepatocyte growth factor (R&D Systems,). Cells were seeded in 25 cm² tissue culture flasks and propagated at 37 °C in a humidified atmosphere of 550 mL/L CO₂ in air and monolayers passaged approximately once a week at or before confluence by incubation in trypsin-versene for approximately 5 min until the cells were shrunken. Trypsin activity was quenched by addition of fresh medium containing FBS and cells were seeded at 1/2 split ratio.

Plasmids and transfection

The plasmids pcDNA3, pCMV-X and pEGFP were the gifts from Professor Xiao-Dong Zhang (Institute for Molecular Biology, Nankai University, China). The empty pcDNA3 vector, a eukaryotic expression vector, was used as negative control. pCMV-X was constructed by inserting the entire HBx

coding region (HBV nucleotides 1 372-1 833 465 bp) into the *EcoRI/EcoRV* sites of the pCDNA3 vector^[11]. Cloning vector pEGFP carried an enhanced green fluorescent protein (EGFP) gene that was cloned between the two MCS of the pPD16.43. EGFP encoded by pEGFP could emit bright green fluorescence in eukaryotic cells. All the plasmids contained ampicillin resistance genes for propagation and selection in *E. coli*.

Transient transfection of plasmids into HBECs was performed using Lipofectamine (Gibco BRL[®]) according to the protocol recommended by the manufacturer. The day before transfection, cells were trypsinized and seeded in 6-well plates. On the day of transfection, cells reached 60% confluence. 2.9 μ g pCDNA3 DNA or pCMV-X DNA and 0.1 μ g pEGFP DNA were diluted with OPTI-MEM medium (Invitrogen) and then mixed with Lipofectamine. A total of 1 mL transfection medium was added to the cells after the cells were washed one time by OPTI-MEM medium. The cells were incubated at 37 $^{\circ}$ C in a humidified atmosphere of 50 mL/LCO₂ in air for 3 h. After 3 h incubation, the transfection medium was replaced with fresh complete medium containing serum and the cells were incubated for another 36 h. Then the cells were harvested and extracted. The expression of transfected gene was examined by immunocytochemistry. The cells transfected with OPTI-MEM medium were used as blank control and transfected with pCDNA3 vector as empty vector control, co-transfected pEGFP as a marker for transfection efficiency^[12].

RT-PCR of hTERT mRNA

Total cellular RNAs were extracted from different groups by TRIzol reagent (Gibco BRL[®]). A 2 μ g of extracted RNA was reverse transcribed into cDNA first-strand with 200 units of Moloney murine leukemia virus reverse transcriptase (Promega) and 1 μ g of oligo (dT)₁₅ primer (Promega) in a final volume of 25 μ L of enzyme buffer for 60 min at 42 $^{\circ}$ C. hTERT cDNA analysis was performed by PCR amplification of a 145 bp fragment using primer pairs 5'-CGGAAGAGTGTCTG GAGCAA-3' (sense) and 5'-GGATGAAGCGGAGTCTGGA-3' (antisense) as described previously^[13]. A 320 bp fragment of GAPDH gene was amplified as an internal control. The primers for GAPDH were 5'GGAAGCTTGTCATCAATGG 3' (sense) and 5'CTGTGGTCATGAGTCCTTC 3' (antisense). PCR was performed with 5 μ L of cDNA first-strand in a 50 μ L reaction mixture containing 2 mmol/L MgCl₂, 1 mmol/L dNTPs, 0.4 μ mol/L of each primer, and 2.5 units of *Taq* DNA polymerase (Promega). The reaction mixture was heated at 94 $^{\circ}$ C for 5 min, then 33 cycles of PCR were performed. Each cycle included denaturation at 94 $^{\circ}$ C for 40 s, annealing at 60 $^{\circ}$ C for 40 s and extension at 72 $^{\circ}$ C for 90 s. A 10 μ L PCR products was assessed by 15 g/L agarose electrophoresis and ethidium bromide staining (0.5 μ g/mL), visualized under ultraviolet light and analyzed by NIH Image software.

Immunocytochemistry

Cells in different groups were cultured on coverslips and fixed with acetone and methanol. Detection of HBx protein expression in the transfected cells was performed by the ultrasensitive immunocytochemistry kit (Maixin Company, Fuzhou, China) according to the manufacturer's instructions. Rabbit anti-human HBx polyclonal antibody (1:800) was provided by Dr. Wen-Liang Wang (The 4th Military Medical University, Xi'an, China).

RESULTS

Transfection efficiency

Under fluorescence microscope, EGFP can only be observed in the HBx gene transfected cell cultures and the cells of empty

vector control (Figure 1). There was no such green fluorescence in the cells of the blank control. Transfection efficiency was estimated by counting the percentage of EGFP-expressing cells in at least 3 fields of vision under fluorescence microscope. For the HBx gene transfected cell cultures and empty vector control, the transfection efficiency was about 15%.

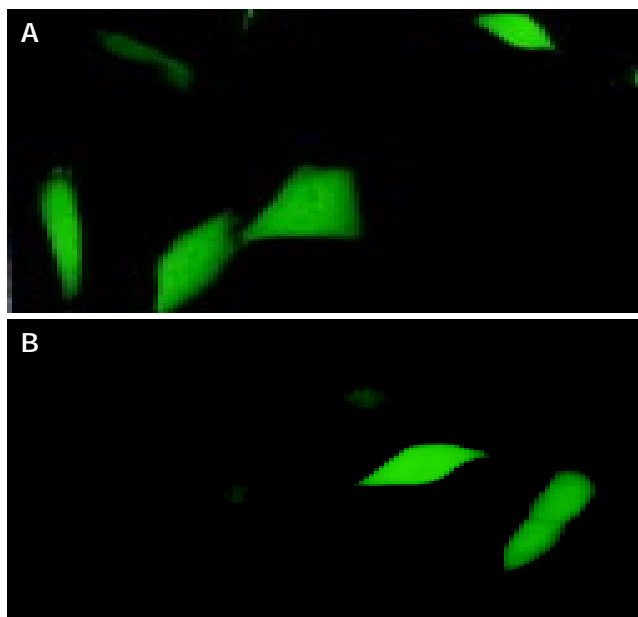


Figure 1 Transfection efficiency evaluated by EGFP-expressing cells in the HBx gene transfected cell cultures and empty vector control. pEGFP 0.1 μ g and pCMV-X (or pCDNA3) 2.9 μ g were co-transfected into HBECs by Lipofectamine. Thirty-eight hours after transfection. EGFP-expressing cells were visible under fluorescence microscope in the HBx gene transfected cell cultures (A) and empty vector control (B), but not in the blank control (Under fluorescence microscope $\times 200$).

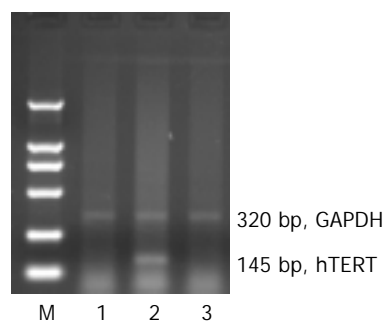


Figure 2 Analysis of hTERT mRNA expression by RT-PCR. RT-PCR was performed on total RNA extracted from HBECs transfected with OPTI-MEN medium (1), pCMV-X (2) and pCDNA3 (3), respectively. M: DL2000 Marker.

hTERT mRNA expression

To examine the effects of HBx gene on hTERT transcription, pCMV-X expression vector was co-transfected with pEGFP into HBECs. The expression of human GAPDH RNA in all of the samples was quantitatively measured and used as an internal control. After RT-PCR analysis, a prominent level of hTERT transcript was detected in the HBx gene transfected cell cultures. In contrast, as shown in Figure 2, hTERT mRNA of HBECs in the blank control and empty vector control were undetectable. The relative expression level of hTERT mRNA was determined by measuring band intensities of both hTERT transcript and GAPDH transcript and calculating the ratio of hTERT to GAPDH. As shown in Figure 3, after transferred with HBx

gene, the HBECs exhibit more distinct hTERT mRNA expression in contrast to those transfected with blank control and empty vector.

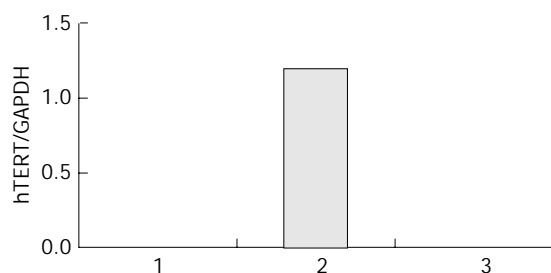


Figure 3 Quantitative and relative changes of hTERT mRNA expression analyzed by NIH Image software. Dramatic expression of hTERT mRNA was observed in HBECs when transferred with pCMV-X vector (lane 2), but there was no hTERT mRNA expression in HBECs when transferred with OPTI-MEM medium (lane 1) and empty vector (lane 3).

HBx protein expression in HBECs

HBx protein expression in transferred HBECs was identified by immunocytochemistry. Positive signals could be observed sporadically in the HBx gene transfected cell cultures (Figure 4B). As for the HBECs in the blank control and empty vector control, there are no such observable positive signals (Figures 4A, C).

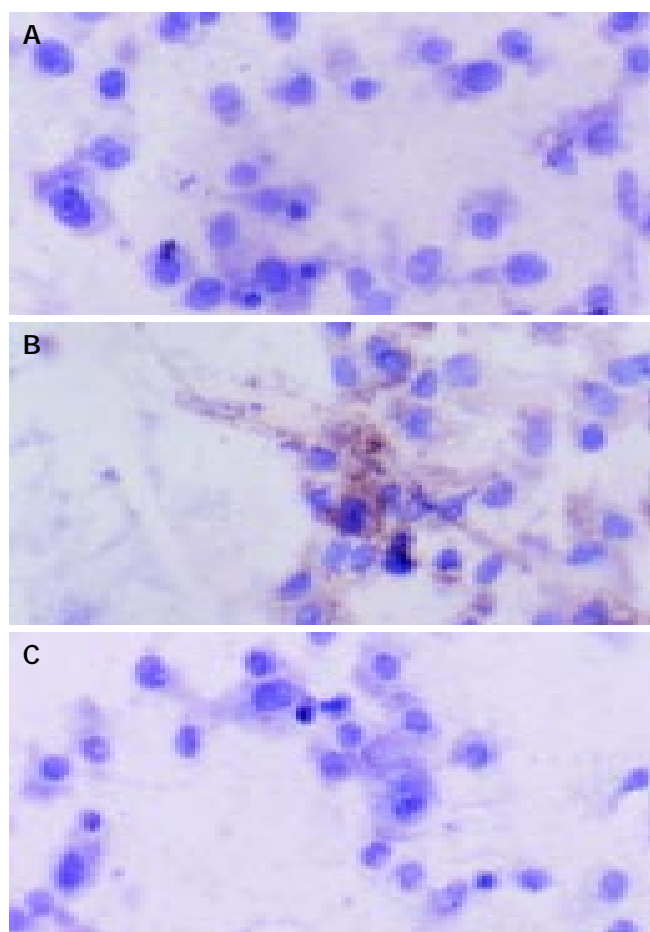


Figure 4 HBx protein expression in transferred HBECs assayed by ultrasensitive immunocytochemistry. The blank vector and OPTI-MEM transfected HBECs showed no expression of HBx protein (A, C), but pale brown positive signals scattered in pCMV-X vector transfected HBECs (B). Immunocytochemistry (S-P methods, $\times 200$).

DISCUSSION

HBECs were isolated from normal human bile duct epithelia and cultured *in vitro*. As no retroviral transduction with SV-40 large T antigen cDNA was performed, the cells were not immortalized. They were really primary culture cells and would only grow for a few passages before becoming senescent, the cells simply stopped dividing and died eventually. Though there was expression of telomerase endogenous genes (such as the telomerase RNA component gene) in this kind of finite cell lines, telomerase was inactivated as the expression of hTERT was repressed. The inhibition of hTERT expression originated from the presence of numerous transcription factors in the core promoter of hTERT. Transcriptional repressors such as p53^[14,15], Mad1^[16,17] and myeloid-specific zinc finger protein 2^[18], could specifically inhibit the transcriptional expression of hTERT mRNA in normal human somatic cells. Our results confirmed this hypothesis. When we transferred the empty vector and OPTI-MEM medium into the HBECs, we could not assay the expression of hTERT mRNA. Dramatic hTERT mRNA expression in HBECs transfected with HBx gene showed that HBx gene could cis-activate transcriptional expression of hTERT gene. An early study also showed that normal human cells could restore the telomerase activity in the presence of other oncogenic viruses^[19]. It has been reported that HBV genome was integrated into the promoter region of hTERT both in HuH-4 human hepatocellular carcinoma-derived cell line^[5] and in liver tumor tissues^[20]. The integration of HBV enhancer upstream of the hTERT promoter cis-activated hTERT gene transcription in HuH-4 cells^[5]. It is known that the up-regulation of telomerase activity could be observed in hepatocellular carcinoma cell line HepG2 after transferred with X gene^[6]. Together with our results, this was a most important demonstration of transcriptional regulation of telomerase gene through HBx gene in carcinogenesis of both human hepatocarcinomas and cholangiocarcinomas. The precise mechanism of such an action is still unknown.

It has been well known that HBx protein encoded by HBx gene, is a potential oncogenic factor and mainly acts as a transcriptional co-activator involving in multiple gene regulation and signaling pathway^[21]. Up-regulation of telomerase gene expression may be another major role of HBx at the stage of carcinogenesis^[22]. Our early study found that higher expression levels of HBx protein and mRNA could be assayed in the tissues of cholangiocarcinomas^[9,23]. Based on our present finding that HBx protein expression could be detected in HBECs transfected with HBx gene, we could suggest that HBV infection and its genome integration might involve in the pathogenesis of cholangiocarcinomas^[24]. HBx protein, which has long been studied as the major causative factor for hepatocarcinogenesis^[25,26], might still play more important role in the carcinogenesis of cholangiocarcinomas than other proteins encoded by other genes of HBV^[27]. As for the mechanism for HBx protein' carcinogenic action, we deduced there should be a binding site for HBx protein in the core promoter region of hTERT gene although this motif has not been identified. Another notion derived from our study is that HBx protein may recruit some cis-action elements (such as c-Myc^[28], AP-2^[29]) or repress other factors (like p53^[30], E2F1^[31]) in mediating the transcriptional regulation of hTERT gene. When exogenous HBx gene was transferred into HBECs, HBx protein translation was achieved in some of HBECs. It is the expression of HBx protein in the transfected cells that be responsible for cis-activation of hTERT mRNA directly or indirectly.

In summary, HBECs do not show the expression of hTERT mRNA and a dramatic high expression of hTERT mRNA can be observed in HBECs transfected with HBx gene. The cis-activation of hTERT gene by HBx is the primary mechanism

underlying proliferation, differentiation and tumorigenesis of biliary epithelia.

ACKNOWLEDGMENTS

We thank Dr. Ludwik K. Trejdosiewicz for kindly providing us HBECs and Professor Xiao-Dong Zhang for providing us three kinds of plasmids.

REFERENCES

- Aragona M**, Maisano R, Panetta S, Giudice A, Morelli M, La Torre I, La Torre F. Telomere length maintenance in aging and carcinogenesis. *Int J Oncol* 2000; **17**: 981-989
- Kim NW**, Piatyszek MA, Prowse KR, Harley CB, West MD, Ho PL, Coviello GM, Wright WE, Weinrich SL, Shay JW. Specific association of human telomerase activity with immortal cells and cancer. *Science* 1994; **266**: 2011-2015
- Dhaene K**, Van Marck E, Parwaresch R. Telomeres, telomerase and cancer: an up-date. *Virchows Arch* 2000; **437**: 1-16
- Poole JC**, Andrews LG, Tollefsbol TO. Activity, function, and gene regulation of the catalytic subunit of telomerase (hTERT). *Gene* 2001; **269**: 1-12
- Horikawa I**, Barrett JC. Cis-Activation of the human telomerase gene (hTERT) by the hepatitis B virus genome. *J Natl Cancer Inst* 2001; **93**: 1171-1173
- Zhou WP**, Shen QH, Gu BY, Ren H, Zhang DH. Effects of hepatitis B virus X gene on apoptosis and the activity of telomerase in HepG2 cells. *Zhonghua Ganzhangbing Zazhi* 2000; **8**: 212-214
- Wang WL**, Gu GY, Hu M. Expression and significance of HBV genes and their antigens in human primary intrahepatic cholangiocarcinoma. *World J Gastroenterol* 1998; **4**: 392-396
- Wang W**, Gu G, Hu M. Expression and significance of hepatitis B virus genes in human primary intrahepatic cholangiocarcinoma and its surrounding tissue. *Zhonghua Zhongliu Zazhi* 1996; **18**: 127-130
- Qu ZL**, Zou SQ, Zhen SL, Wu XZ, Cui NQ. The expression and significance of hepatitis B virus X protein in extrahepatic bile duct carcinomas and the surrounding noncancerous tissues. *Zhonghua Shiyan Waike Zazhi* 2002; **19**: 401-402
- Cruickshank SM**, Southgate J, Selby PJ, Trejdosiewicz LK. Inhibition of T cell activation by normal human biliary epithelial cells. *J Hepatol* 1999; **31**: 1026-1033
- Gottlob K**, Fulco M, Levrero M, Graessmann A. The hepatitis B virus HBx protein inhibits caspase 3 activity. *J Biol Chem* 1998; **273**: 33347-33353
- Jaiswal M**, LaRusso NF, Shapiro RA, Billiar TR, Gores GJ. Nitric oxide-mediated inhibition of DNA repair potentiates oxidative DNA damage in cholangiocytes. *Gastroenterology* 2001; **120**: 190-199
- Nakamura TM**, Morin GB, Chapman KB, Weinrich SL, Andrews WH, Lingner J, Harley CB, Cech TR. Telomerase catalytic subunit homologs from fission yeast and human. *Science* 1997; **277**: 955-959
- Kanaya T**, Kyo S, Hamada K, Takakura M, Kitagawa Y, Harada H, Inoue M. Adenoviral expression of p53 represses telomerase activity through down-regulation of human telomerase reverse transcriptase transcription. *Clin Cancer Res* 2000; **6**: 1239-1247
- Xu D**, Wang Q, Gruber A, Bjorkholm M, Chen Z, Zaid A, Selivanova G, Peterson C, Wiman KG, Pisa P. Downregulation of telomerase reverse transcriptase mRNA expression by wild type p53 in human tumor cells. *Oncogene* 2000; **19**: 5123-5133
- Oh S**, Song YH, Yim J, Kim TK. Identification of Mad as a repressor of the human telomerase (hTERT) gene. *Oncogene* 2000; **19**: 1485-1490
- Gunes C**, Lichtsteiner S, Vasserot AP, Englert C. Expression of the hTERT gene is regulated at the level of transcriptional initiation and repressed by Mad1. *Cancer Res* 2000; **60**: 2116-2121
- Fujimoto K**, Kyo S, Takakura M, Kanaya T, Kitagawa Y, Itoh H, Takahashi M, Inoue M. Identification and characterization of negative regulatory elements of the human telomerase catalytic subunit (hTERT) gene promoter: possible role of MZF-2 in transcriptional repression of hTERT. *Nucleic Acids Res* 2000; **28**: 2557-2562
- Baega AC**, Berger A, Schlegel R, Veldman T, Schlegel R. Cervical epithelial cells transduced with the papillomavirus E6/E7 oncogenes maintain stable levels of oncoprotein expression but exhibit progressive, major increases in hTERT gene expression and telomerase activity. *Am J Pathol* 2002; **160**: 1251-1257
- Gozuacik D**, Murakami Y, Saigo K, Chami M, Mugnier C, Lagorce D, Okanoue T, Urashima T, Brechot C, Paterlini-Brechot P. Identification of human cancer-related genes by naturally occurring hepatitis B virus DNA tagging. *Oncogene* 2001; **20**: 6233-6240
- Murakami S**. Hepatitis B virus X protein: a multifunctional viral regulator. *J Gastroenterol* 2001; **36**: 651-660
- Horikawa I**, Barrett JC. Transcriptional regulation of the telomerase hTERT gene as a target for cellular and viral oncogenic mechanisms. *Carcinogenesis* 2003; **24**: 1167-1176
- Qu ZL**, Zou SQ, Wei GH, Sun ZC, Wu XZ. *In situ* nucleic acid detection of HBV X gene in extrahepatic biliary tract carcinomas and its clinicopathological significance. *Zhonghua Waike Zazhi* 2004; **42**: 88-91
- Liu X**, Zou S, Qiu F. Pathogenesis of hilar cholangiocarcinoma and infection of hepatitis virus. *Zhonghua Waike Zazhi* 2002; **40**: 420-422
- Diao J**, Garces R, Richardson CD. X protein of hepatitis B virus modulates cytokine and growth factor related signal transduction pathways during the course of viral infections and hepatocarcinogenesis. *Cytokine Growth Factor Rev* 2001; **12**: 189-205
- Guo SP**, Wang WL, Zhai YQ, Zhao YL. Expression of nuclear factor-kappa B in hepatocellular carcinoma and its relation with the X protein of hepatitis B virus. *World J Gastroenterol* 2001; **7**: 340-344
- Wang WL**. Expression of five different antigens of HBV in human intrahepatic cholangiocarcinoma and cholangiohepatocarcinoma. *Zhonghua Zhongliu Zazhi* 1993; **15**: 252-255
- Su F**, Theodosis CN, Schneider RJ. Role of NF-kappaB and myc proteins in apoptosis induced by hepatitis B virus HBx protein. *J Virol* 2001; **75**: 215-225
- Kekule AS**, Lauer U, Weiss L, Lubber B, Hofschneider PH. Hepatitis B virus transactivator HBx uses a tumour promoter signalling pathway. *Nature* 1993; **361**: 742-745
- Kwon JA**, Rho HM. Transcriptional repression of the human p53 gene by hepatitis B viral core protein (HBc) in human liver cells. *Biol Chem* 2003; **384**: 203-212
- Choi M**, Lee H, Rho HM. E2F1 activates the human p53 promoter and overcomes the repressive effect of hepatitis B viral X protein (Hbx) on the p53 promoter. *IUBMB Life* 2002; **53**: 309-317

Edited by Chen WW and Wang XL Proofread by Xu FM

In vitro anti-coxsackievirus B₃ effect of ethyl acetate extract of Tian-hua-fen

Zhen-Hong Li, Bao-Ming Nie, Hong Chen, Shu-Yun Chen, Ping He, Yang Lu, Xiao-Kui Guo, Jing-Xing Liu

Zhen-Hong Li, Bao-Ming Nie, Hong Chen, Shu-Yun Chen, Ping He, Yang Lu, Xiao-Kui Guo, Jing-Xing Liu, Department of Microbiology and Parasitology, Shanghai Second Medical University, Shanghai 200025, China

Supported by Project of National Nature Science Foundation of China, No. 39970691 and Project from Education Commission of Shanghai, China, No. 2000B04

Correspondence to: Jing-Xing Liu, Department of Microbiology and Parasitology, Shanghai Second Medical University, Shanghai 200025, China. lee1217@citiz.net

Telephone: +86-21-64453285 **Fax:** +86-21-64453285

Received: 2003-11-12 **Accepted:** 2004-02-01

Abstract

AIM: To investigate the anti-coxsackievirus B₃ (CVB_{3m}) effect of the ethyl acetate extract of Tian-hua-fen on HeLa cells infected with CVB_{3m}.

METHODS: HeLa cells were infected with CVB_{3m} and the cytopathic effects (CPE) were observed through light microscope and crystal violet staining on 96-well plate and A₆₀₀ was detected using spectrophotometer. The protective effect of the extract to HeLa cells and the mechanism of the effect were also evaluated through the change of CPE and value of A₆₀₀.

RESULTS: The extract had some toxicity to HeLa cells at a higher concentration while had a marked inhibitory effect on cell pathological changes at a lower concentration. Consistent results were got through these two methods. We also investigated the mechanism of its anti-CVB_{3m} effect and the results indicated that the extract represented an inhibitory effect through all the processes of CVB_{3m} attachment, entry, biosynthesis and assemble in cells.

CONCLUSION: The results demonstrate that the ethyl acetate extract of Tian-hua-fen has a significant protective effect on HeLa cells infected with CVB_{3m} in a dose-dependent manner and this effect exists through the process of CVB_{3m} attachment, entry, biosynthesis and assemble in cells, suggesting that the ethyl acetate extract of Tian-hua-fen can be developed as an anti-virus agent.

Li ZH, Nie BM, Chen H, Chen SY, He P, Lu Y, Guo XK, Liu JX. *In vitro* anti-coxsackievirus B₃ effect of ethyl acetate extract of Tian-hua-fen. *World J Gastroenterol* 2004; 10(15): 2263-2266 <http://www.wjgnet.com/1007-9327/10/2263.asp>

INTRODUCTION

Tian-hua-fen is the dried root of *Trichosanthes kirilowii Maxim* or *Trichosanthes japonica Regel*. The major component of it is mass starch, various amino acids, phytohemagglutinin, saccharide, saponin and some other things^[1]. Tian-hua-fen was mentioned in Compendium of Materia Medica written by Li Shizhen in the late 14th Century as a drug to reset menstruation

and facilitating the expulsion of retained placenta. For a long time, Tian-hua-fen had been used in the powdered form in conjunction with other Chinese herbal medicines to induce abortion^[2]. Clinical applications over the years proved that Tian-hua-fen had multiple pharmacological effects, such as termination of pregnancy, anti-tumor, anti-inflammation, anti-virus and immunoregulation and so on^[3-5]. The anti-virus, especially anti-HIV-1, effect of trichosanthin (TCS) has been known to us. But to the author's knowledge research about the non-protein parts of Tian-hua-fen is rare. Coxsackievirus B is the major pathogen of viral myocarditis and now there is no effective therapeutic drug. In the process of screening anti-virus agents from Chinese medicinal herb we found that the nonprotein parts of Tian-hua-fen had a notable anti-virus effect *in vitro* and *in vivo*.

MATERIALS AND METHODS

Preparation of the ethyl acetate extract of Tian-hua-fen

A total amount of 200 g Tian-hua-fen powder (Shanghai drug store) was macerated with 2 L 750 mL/L ethanol overnight, then was boiled in water under reflux for 3 h and the boiled fluid was filtered. The filtrate was evaporated under reduced pressure to gain a residue. The residue was suspended in water and partitioned with petroleum ether, ethyl acetate and n-BuOH (Analytical pure, Shanghai chemical company Ltd) successively. The four fractions were evaporated under reduced pressure to give petroleum ether fraction (0.56 g), ethyl acetate fraction (0.82 g), n-BuOH fraction (0.85 g) and aqueous fraction (12.7 g), respectively.

Preparation of HeLa cells and titration of virus titer

HeLa cells were stored in liquid nitrogen with 100 g/L dimethyl sulphoxide (DMSO) and 900 mL/L fetal calf serum (FCS) and maintained in culture flasks in complete RPMI 1640 medium (Gibcol, BRL America). Subculture was carried out every 2-3 d after it had formed a confluent monolayer. CVB_{3m} (Stored by our laboratory) was serially diluted to 10⁻¹⁰ with non-FCS RPMI1640 culture medium. On 40-well plate, 0.025 mL CVB_{3m} with variable dilution and 0.025 mL non-FCS RPMI1640 culture medium were added to each well. Finally, 0.05 mL viable HeLa cells (3×10⁵/mL) were added. Each dilution was quadrupled and normal HeLa cells co-cultured only with RPMI1640 containing 10 mL/L FCS were prepared as negative control at the same time. Then the cells were incubated at 37 °C with 50 mL/L CO₂ for 72 h. The cytopathic effects (CPE) were observed under light microscope. The titer at which cells appeared 50% CPE was designated 1 TCID₅₀ (50% tissue culture infectious doses). A 100 TCID₅₀ was used as the infectious titer in the following experiment.

Assay of the toxicity of the extract to HeLa cells

A total of 5 mg extract was dissolved in 5 μL DMSO, then 2.5 mL deionized water was added and the liquid was sterilized at 115 °C for 20 min. After cooling to 55 °C, 2.5 mL 2×RPMI 1640 culture medium (without FCS) was added to make the end concentration of the extract (1 mg/mL). The original liquid

was diluted with non-FCS RPMI 1640 culture medium serially from 1:2 to 1:1 024. A total of the 0.025 mL sample with various concentration and 0.025 mL of the same culture medium were added to each well on 96-well plate. Finally 0.05 mL viable HeLa cells (3×10^5 /mL) were added. Each concentration of the sample was quadrupled. Two controls, HeLa cells co-cultured only with RPMI1640 (containing 100 mL/L FCS) and 1 g/L DMSO respectively were prepared synchronously. Cells were incubated at 37 °C with 50 mL/L CO₂ for 72 h. CPE was observed under light microscope and the concentration at which cells appeared <50% CPE (compared with that of extract-free cultures) was regarded as the lowest toxic concentration. In addition, cells were stained with 5 g/L crystal violet (Ameresco) and A_{600} was detected using spectrophotometer.

Assay of the anti-CVB_{3m} effect of the extract

The extract was diluted serially from 1:256 at which it had no toxicity to HeLa cells to 1:8 192 with non-FCS RPMI 1640 culture medium. Then 0.025 mL extract with variable concentration was added to each well of 96-well plate. Then 0.025 mL 100 TCID₅₀CVB_{3m} was overlaid. After incubation at 37 °C with 50 mL/L CO₂ for 1 h, 0.05 mL viable HeLa cells (3×10^5 /mL) were added. Each concentration was quadrupled and three controls, normal HeLa cells co-cultured only with RPMI1640 (containing 100 mL/L FCS), 100 TCID₅₀CVB_{3m} and the extract (1:256 mg/mL), respectively were prepared synchronously. Cells were grown for 3 days and then CPE was observed under light microscope. Later, the cells were stained with 5 g/L crystal violet and A_{600} was measured using spectrophotometer.

Primary study on the mechanism of anti-CVB_{3m} effect of the extract^[6]

The extract was diluted with non-FCS RPMI1640 culture medium from 1:256 to 1:8 192. HeLa cells (1.5×10^4 /well) were seeded onto three 96-well plates and allowed to attach to the well bottom. When the cells were confluent the culture medium was discarded and the cells were rinsed twice with the same culture medium. The cells on three plates were treated respectively as follows: The first plate: 0.025 mL 100TCID₅₀CVB_{3m} and 0.025 mL extract of variable concentration were added to each well. After incubation at 37 °C with 50 mL/L CO₂ for 1 h, the mixture was substituted with 0.1 mL non-FCS RPMI1640 culture medium; the second plate: 0.025 mL 100TCID₅₀CVB_{3m} and 0.025 mL extract of variable concentration were added. The plate was incubated at 37 °C with 50 mL/L CO₂ for 1 h. Then the mixture was substituted with 0.025 mL extract of

variable concentration and 0.075 mL non-FCS RPMI1640 culture medium; the third plate: 0.025 mL 100TCID₅₀CVB_{3m} and 0.025 mL non-FCS RPMI1640 culture medium were added first. After incubation at 37 °C with 50 mL/L CO₂ for 1 h the mixture was discarded and 0.025 mL extract of variable concentration and 0.075 mL non-FCS RPMI1640 culture medium were overlaid. Three controls, HeLa cells co-cultured only with RPMI1640 containing 100 mL/L FCS, 100TCID₅₀CVB_{3m} and extract (1:256 mg/mL) respectively were prepared synchronously and each extract concentration was quadrupled. At last all plates were incubated at 37 °C with 50 mL/L CO₂. When the cells treated with CVB_{3m} appeared 100% CPE, the cells were stained with 5 g/L crystal violet and A_{600} was detected using spectrophotometer.

RESULTS

Titration of CVB_{3m} titers

The incubation was terminated after 72 h and CPE was observed under light microscope. The results showed the cells in all quadrupled wells treated with CVB_{3m} at titer of 10^{-1} - 10^{-6} appeared 100% CPE. About the cells treated with CVB_{3m} at titer of 10^{-7} , the cells in two wells appeared 100% CPE while the others appeared 50% CPE. In regards to the cells co-cultured with CVB_{3m} at titer of 10^{-8} - 10^{-10} , the cells in four wells appeared no CPE completely. Then TCID₅₀ was calculated as 10^{-7} according to Reed-Muench method^[7].

Assay of toxicity of ethyl acetate extract to HeLa cells

After incubation for 72 h, CPE induced by the extract was observed under light microscope. The results showed the cells co-cultured with extract at concentration from 1:2-1:128 mg/mL appeared CPE of different degrees, while the cells co-cultured with extract at concentration from 1:256 to 1:8 192 mg/mL appeared no CPE. The 50% toxic concentration was 1:128 mg/mL according to Reed-Muench method. The value of A_{600} also indicated that the extract had no toxicity to HeLa cells from 1:256 mg/mL. The cells co-cultured with 1 g/L DMSO appeared no CPE, which showed that DMSO at this concentration had no toxicity to HeLa cells (Table 1).

Assay of the anti-CVB_{3m} effect of the extract

From 1:256 to 1:8 192 mg/mL the extract showed various protective effects to HeLa cells and the effect was decreased with the increased dilution. The protective effect was best at concentration from 1:256 to 1:1 024 mg/mL. The minimal effective inhibitory concentration (EIC) was 1:8 192. The value

Table 1 Cytotoxicity of ethyl acetate extract to HeLa cells shown in the value of A_{600}

Dilution	1:2	1:4	1:8	1:16	1:32	1:64	1:128	1:256	1:512	1:1 024
Value of A_{600}	0.20±0.029	0.22±0.030	0.32±0.022	0.29±0.069	0.38±0.043	0.59±0.035	0.69±0.075	1.30±0.069	1.23±0.061	1.29±0.056

The A_{600} value of the cells co-cultured with the extract at concentration from 1:2 to 1:128 mg/mL was lower than that of normal HeLa cells (1.32±0.034), which showed that the extract had some toxicity to HeLa cells at these concentrations. From 1:256 mg/mL the A_{600} value became close to that of normal HeLa cells, which indicated that from 1:256 mg/mL the extract had no toxicity to HeLa cells again.

Table 2 Protective effect of ethyl acetate extract on HeLa cells shown in the value of A_{600}

Dilution	1:256	1:512	1:1 024	1:2 048	1:4 096	1:8 192
Value of A_{600}	1.09±0.017	1.02±0.122	0.89±0.060	0.91±0.039	0.83±0.048	0.77±0.028

The A_{600} value of the cells co-cultured only with RPMI1640 was 1.32±0.02; the A_{600} value of the cells co-cultured only with 10^{-5} CVB_{3m} was 0.22±0.026; and the A_{600} value of the cells co-cultured only with extract at concentration of 1:256 mg/mL was 1.21±0.042. As shown in the table the value of A_{600} of the cells treated with extract is higher than that of the cells infected with CVB_{3m} while not treated with the extract ($^bP < 0.01$), indicating the protective effect of the extract on HeLa cells from CVB_{3m} infection.

Table 3 Protective effect of ethyl acetate extract on HeLa cells shown in percentage (A_{600} value of cells protected with the extract/ A_{600} value of normal HeLa cells)

Dilution	1:256	1:512	1:1 024	1:2 048	1:4 096	1:8 192	10 ⁻⁵ CVB _{3m}
The ratio of A_{600}	88.56±0.032	79.46±0.008	73.07±0.057	65.57±0.023	61.83±0.038	56.1±0.015	16.7±0.027

The percentage of vital cells protected with the extract accounted for compared with normal HeLa cells decreased with the increased extract dilution, and it was preferable from concentration 1:256 mg/mL to 1:1 024 mg/mL. ^b $P < 0.01$ vs group of 10⁻⁵ CVB_{3m}.

Table 4 The value of A_{600} obtained from various infective phase

Dilution/ A_{600}	1:256	1:512	1:1 024	1:2 048	1:4 096	1:8 192
First group	0.45±0.041	0.56±0.011	0.63±0.036	0.65±0.043	0.37±0.076	0.38±0.029
Second group	0.72±0.022	0.96±0.013	0.69±0.009	65.00±0.025	0.78±0.056	0.73±0.054
Third group	0.53±0.030	0.48±0.036	0.40±0.049	0.39±0.066	0.39±0.077	0.32±0.015

The A_{600} value of the cells co-cultured only with RPMI1640, cells co-cultured only with 10⁻⁵ CVB_{3m} and cells co-cultured only with extract (1:256 mg/mL) was 1.29±0.011, 0.24±0.023 and 1.20±0.029, respectively. The value of A_{600} of the cells treated with extract of variable concentration at different time of CVB_{3m} infection was higher than that of the cells infected with CVB_{3m} and not treated with the extract, which indicated the protective effect of the extract existed through all the processes of CVB_{3m} attachment, entry, biosynthesis and assemble in cells.

of A_{600} obtained using crystal violet staining showed that starting from 1:256 mg/mL, the value of A_{600} decreased with the increased dilution. There was a negative correlation between them ($r=0.8525$, $P < 0.01$, Tables 2-3, Figure 1).

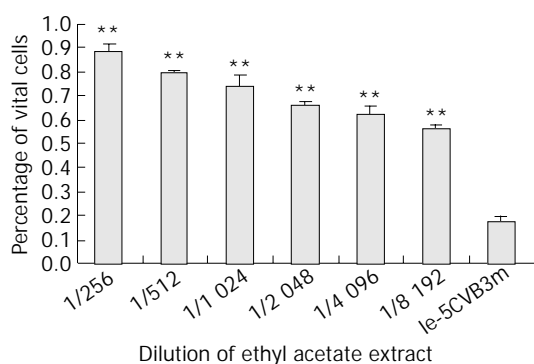


Figure 1 The protective effect of the extract on HeLa cells expressed in column figure. The value of A_{600} obtained using crystal violet staining decreased with the increased dilution of the extract. From 1:256 to 1:8 192 mg/mL the extract showed various protective effects on HeLa cells and the effect was decreased with the increased dilution of the extract. The protective effect was best at concentration of 1:256 to 1:1 024 mg/mL.

Primary study on the mechanism of anti-CVB_{3m} effect of the extract in vitro

In the first group, the extract was added in the process of virus adsorption. In second group, the extract was added in the process of virus adsorption and also after adsorption while in the third one, the extract was added after virus adsorption. The value of A_{600} of the three groups were obtained. Among all three groups, A_{600} obtained from the cells treated with extract from 1:256 to 1:8 192 mg/mL was higher than that treated with 100TCID₅₀ CVB_{3m}, and that of the second group was the highest. This suggested the extract exerted anti-CVB_{3m} effect through all the processes of the virus infection (Table 4).

DISCUSSION

Proliferation of virus primarily depends on the biosynthesis system of host cells because virus deficit the enzymes needed for their proliferation. Virus proliferation was similar to nucleotide replication of host cells and there is also great similarity between its products such as nucleotide and proteins

and that of host cells. So the demand for killing virus while not infecting the normal physiological function of host cells brings us great difficulty to design and synthesize effective anti-virus drug. The development of anti-virus drugs is very slow compared with that of anti-bacteria drugs in the last one hundred years since the discovery of virus. Though it is an important way to synthesize anti-virus drugs using chemical methods, it is very slow and time-consuming. In recent years, many countries are paying more and more attention to look for anti-virus agents from Chinese medicinal herbs. Tian-hua-fen is a traditional Chinese medicinal herb. It has been used in Chinese for centuries to induce mid-term abortion. And there were many records about its biological efficacy. In the 70 s, the active ingredient of Tian-hua-fen, TCS, a protein from the root tuber of the Chinese medicinal herb *Trichosanthes kirilowii Maxim* was found and purified. It is a monomeric protein with a pI (isoelectric point) of 9.4 and an apparent molecular weight of 24 kDa. There are no cysteine residues in the molecule^[8]. TCS is a member of type 1 ribosome-inactivating protein (RIP) family^[7-9]. RIP is a group of cytotoxic proteins acting on eukaryotic ribosomes. They can inactivate 60S ribosomal subunits by only hydrolyzing a single phosphodiester bond between the guanosine residue at position 4 325(G4 325) and the adenosine residue at position 4 326(A4 326) in 28S rRNA. TCS can inactivate eukaryotic ribosomes through its N-glycosidase activity by hydrolyzing the N-C glycosidic bond of adenylic acid at 4 324 site in 28S rRNA of rat liver^[10]. Thus cell protein synthesis was inhibited. Clinical application over the years showed TCS had multiple pharmacological effects. The research about TCS was once popular since McGrath *et al.*^[11,12] reported it could inhibit HIV-1 for the first time. But the sever side effect prevented its more extensive clinical application^[13]. There are some other components such as polysaccharide, phytohemagglutinin, sterol and palmitic acid and so on in Tian-hua-fen besides TCS^[14]. Polysaccharide in Tian-hua-fen had marked immunoregulation effect^[1]. The galactose-binding lectin from Tian-hua-fen stimulated the incorporation of D-[3-3H]glucose into lipids in isolated rat epididymal adipocytes^[15]. In the process of screening anti-virus agents, we found the ethyl acetate extract of Tian-hua-fen had obvious preventive effect on HeLa cells from CVB_{3m} infection. This showed the potential anti-virus effect of the ethyl acetate extract of Tian-hua-fen. In this study, Tian-hua-fen was treated with chemical reagents and then was extracted with organic reagents. Finally, four kinds of extract were obtained. The anti-CVB_{3m} effect of the four fractions was tested and the results showed

ethyl acetate fraction had the best preventive effect on HeLa cells from CVB_{3m} infection. The preventive effect decreased as the extract dilution increased. There was an obvious correlation between them. The ethyl acetate fraction was further chromatographed on silica gel column and their anti-virus effect was also tested. The results suggested that toxicity of the further extract to HeLa cells was decreased compared with the former one and there also existed a negative correlation between the preventive effect and the dilution.

Many methods have been developed for determining the antiviral activities of compounds in cell culture. For viruses that cause discernable cytopathic effects (CPE) microscopically in cells, visual scoring of CPE inhibition is performed most frequently because it is rapid, and allows a number of compounds to be evaluated using 96-well microplates^[16]. Since solely relying on visual scoring was inaccurate for assessing the cytotoxicities, the use of a dye or stain is very important. The results indicated that methods using bisbenzimidazole, crystal violet, fluorescein diacetate, MTT, neutral red, or rhodamine 6G were similar to visual scoring for determining anti-influenza virus activity in cell culture. Rapid staining (15 min) methods could be done with crystal violet and rhodamine 6G, and rhodamine 6G gave a high background in microwells containing only water (no cells or virus) which had to be subtracted^[17], whereas other methods for determining antiviral activity of test substances may be much more tedious, requiring more microplates, compound, and/or time than the above methods. These include the plaque reduction assay^[18], virus yield reduction assay^[19], determining drug effect by counting the number of infected cells stained by fluorescent antibody^[20] and [³H]TdR incorporation^[21]. For this reason, we preferred crystal violet staining in our study in order to quantitatively screen anti-virus agents.

We also did some primary study on the anti-CVB_{3m} mechanism of the extract. The extract was added before virus adsorption, during adsorption and after adsorption and then the cells were stained with crystal violet and A₆₀₀ was measured. The value of A₆₀₀ of the three groups was higher than that of the cells infected with virus. This indicated the three kinds of treatment had preventive effect on HeLa cells from CVB_{3m} infection at different levels and suggested that the extract could act through virus adsorption, penetration and synthesis in cells.

Our results showed that the ethyl acetate extract of Tian-hua-fen had marked anti-CVB_{3m} effect *in vitro*. Some questions still remained to be answered. Which component play key role in the process of anti-virus? Which has the better anti-virus effect between the crude extract and the further extract? What is the anti-virus mechanism of it? To answer these questions needs more and further research. Anyway it is sure that the ethyl acetate extract of Tian-hua-fen has marked anti-virus effect. The answers to the above questions will help to wide the range of virus that Tian-hua-fen resists and also help to make Tian-hua-fen a clinical-used drug.

REFERENCES

- 1 Wang Y. Trichosanthin. Second Edition, Beijing. *China Science Press* 2000; **18**: 81
- 2 Shaw PC, Chan WL, Yeung HW, Ng TB. Minireview: trichosanthin-a protein with multiple pharmacological properties. *Life Sci* 1994; **55**: 253-262
- 3 Wu L, LaRosa G, Kassam N, Gordon CJ, Heath H, Ruffing N, Chen H, Humblías J, Samson M, Parmentier M, Moore JP, Mackay CR. Interaction of chemokine receptor CCR5 with its ligands: multiple domains for HIV-1 gp120 binding and a single domain for chemokine binding. *J Exp Med* 1997; **186**: 1373-1381
- 4 Zheng YT, Chan WL, Chan P, Huang H, Tam SC. Enhancement of the anti-herpetic effect of trichosanthin by acyclovir and interferon. *FEBS Lett* 2001; **496**: 139-142
- 5 Fan ZS, Ma BL. IL-10 and trichosanthin inhibited surface molecule expression of antigen processing cells and T-cell proliferation. *Zhongguo Yaoli Xuebao* 1999; **20**: 353-357
- 6 Carlucci MJ, Sclaro LA, Errea MI, Matulewicz MC, Damonte EB. Antiviral activity of natural sulphated galactans on herpes virus multiplication in cell culture. *Planta Med* 1997; **63**: 429-432
- 7 Krah DL. Receptors for binding measles virus on host cells and erythrocytes. *Biologicals* 1991; **19**: 223-227
- 8 Maraganore JM, Joseph M, Bailey MC. Purification and characterization of trichosanthin. Homology to the ricin A chain and implications as to mechanism of abortifacient activity. *J Biol Chem* 1987; **262**: 11628-11633
- 9 Barbieri L, Battelli MG, Stirpe F. Ribosome-inactivating proteins from plants. *Biochim Biophys Acta* 1993; **1154**: 237-282
- 10 Zhang C, Gong Y, Ma H, An C, Chen D, Chen ZL. Reactive oxygen species involved in trichosanthin-induced apoptosis of human choriocarcinoma cells. *Biochem J* 2001; **355**(Pt 3): 653-661
- 11 McGrath MS, Hwang KM, Caldwell SE, Gaston I, Luk KC, Wu P, Ng VL, Crowe S, Daniels J, Marsh J. GLQ223: an inhibitor of human immunodeficiency virus replication in acutely and chronically infected cells of lymphocyte and mononuclear phagocyte lineage. *Proc Natl Acad Sci U S A* 1989; **86**: 2844-2848
- 12 McGrath MS, Santulli S, Gaston I. Effects of GLQ223 on HIV replication in human monocyte/macrophages chronically infected *in vitro* with HIV. *AIDS Res Hum Retroviruses* 1990; **6**: 1039-1043
- 13 Byers VS, Levin AS, Malvino A, Waites L, Robins RA, Baldwin RW. A phase II study of effect of addition of trichosanthin to zidovudine in patients with HIV disease and failing antiretroviral agents. *AIDS Res Hum Retroviruses* 1994; **10**: 413-420
- 14 Wu AM, Wu JH, Tsai MS, Herp A. Carbohydrate specificity of an agglutinin isolated from the root of *Trichosanthes kirilowii*. *Life Sci* 2000; **66**: 2571-2581
- 15 Ng TB, Wong CM, Li WW, Yeung HW. Effect of *Trichosanthes kirilowii* lectin on lipolysis and lipogenesis in isolated rat and hamster adipocytes. *Ethnopharmacol* 1985; **14**: 93-98
- 16 Sidwell RW, Huffman JH. Use of disposable micro tissue culture plates for antiviral and interferon induction studies. *Appl Microbiol* 1971; **22**: 797-801
- 17 Smee DF, Morrison AC, Barnard DL, Sidwell RW. Comparison of colorimetric, fluorometric, and visual methods for determining anti-influenza (H1N1 and H3N2) virus activities and toxicities of compounds. *J Virol Methods* 2002; **106**: 71-79
- 18 Desideri N, Conti C, Mastromarino P, Mastropaolo F. Synthesis and anti-rhinovirus activity of 2-styrylchromones. *Antivir Chem Chemother* 2000; **11**: 373-381
- 19 Semple SJ, Pyke SM, Reynolds GD, Flower RL. *In vitro* antiviral activity of the anthraquinone chrysophanic acid against poliovirus. *Antiviral Res* 2001; **49**: 169-178
- 20 Smee DF, Sidwell RW, Barnett BB, Spendlove RS. Bioassay system for determining ribavirin levels in human serum and urine. *Chemotherapy* 1981; **27**: 1-11
- 21 Baba M, Pauwels R, Balzarini J, Arnout J, Desmyter J, De Clercq E. Mechanism of inhibitory effect of dextran sulfate and heparin on replication of human immunodeficiency virus *in vitro*. *Proc Nat Acad Sci U S A* 1998; **85**: 6132-6136

FR167653 attenuates murine immunological liver injury

Hong-Wei Yao, Jun Li, Ji-Qiang Chen

Hong-Wei Yao, Ji-Qiang Chen, Zhejiang Respiratory Drugs Research Laboratory of State Food and Drug Administration of China, School of Medicine, Zhejiang University, Hangzhou 310031, Zhejiang Province, China

Jun Li, Institute of Clinical Pharmacology, Anhui Medical University, Hefei 230032, Anhui Province, China

Correspondence to: Dr. Hong-Wei Yao, Zhejiang Respiratory Drugs Research Laboratory of State Food and Drug Administration of China, School of Medicine, Zhejiang University, Hangzhou 310031, Zhejiang Province, China. yhgwei@hotmail.com

Telephone: +86-571-87217150

Received: 2003-12-19 **Accepted:** 2004-01-13

Abstract

AIM: To study the effect of FR167653 on immunological liver injury (ILI) in mice.

METHODS: ILI was established by tail vein injection of 2.5 mg *Bacillus Calmette-Guerin* (BCG), and 10 d later with 10 mg lipopolysaccharide (LPS) in 0.2 mL saline (BCG plus LPS). Alanine aminotransferase (ALT), aspartate aminotransferase (AST) in sera and malondialdehyde (MDA), glutathione peroxidase (GSHpx) contents in liver homogenates were assayed by spectrophotometry. The levels of tumor necrosis factor- α (TNF- α) and nitric oxide (NO) levels in sera were determined using ELISA. Interleukin-1 (IL-1) produced by peritoneal macrophages was determined by the method of ^3H -infiltrated cell proliferation. The nuclear factor-kappa B (NF- κB) p65 in liver tissue was analyzed with reverse transcription polymerase chain reaction (RT-PCR). Liver samples collected were stained with hematoxylin and eosin.

RESULTS: FR167653 (50, 100, 150 mg/kg) could significantly decrease the serum transaminase (ALT, AST) activity and MDA content in liver homogenate, and improve reduced GSHpx level of liver homogenate. Liver histopathological examination showed FR167653 (100, 150 mg/kg) significantly reduced inflammatory cells infiltration and liver cells necrosis. FR167653 (50, 100, 150 mg/kg) significantly lowered TNF- α and NO levels in serum, and IL-1 produced by peritoneal macrophages. Moreover, expression of NF- κB mRNA in liver tissue of ILI induced by BCG plus LPS was significantly reduced by FR167653.

CONCLUSION: All results showed that FR167653 had significant inhibitory action on ILI in mice.

Yao HW, Li J, Chen JQ. FR167653 attenuates murine immunological liver injury. *World J Gastroenterol* 2004; 10(15): 2267-2271
<http://www.wjgnet.com/1007-9327/10/2267.asp>

INTRODUCTION

It has been demonstrated that tissue inflammation plays a critical role in liver pathology via induction of cellular injury. The infiltration of mononuclear phagocytes into the liver has been shown to correlate with the severity of liver injury. Kupffer

cells (KCs) are among the first cells that respond to endotoxins, including lipopolysaccharides (LPS), and are considered to be the primary macrophages involved in the clearance of gut-derived bacteria or bacterial toxins. High portal level of LPS can lead to a pronounced secretion of proinflammatory mediators by KCs and ultimately to endotoxin-induced liver injury^[1,2]. Moreover, proinflammatory cytokines such as tumor necrosis factor- α (TNF- α) and interleukin-1 (IL-1) β have been linked to liver injury^[3-5], and shown to be early and important mediators of liver injury^[6-8]. Thus, inhibition of KCs activity and proinflammatory cytokines production would be beneficial to alleviate liver injury.

FR167653, 1-[7-(4-fluorophenyl)-1,2,3,4-tetrahydro-8-(4-pyridyl)pyrazolo[5,1-c][1,2,4]triazin-2-yl]-2-phenylethanedione sulfate monohydrate, was first discovered to be a potent dual inhibitor of IL-1 and TNF- α production in LPS-stimulated human monocytes and phytohemagglutinin-stimulated human lymphocytes^[9]. Takahashi *et al.*^[10] and Kawano *et al.*^[11] also confirmed the inhibitory effect of FR167653 on cytokine production. FR167653 ameliorated endotoxin shock in rabbits and intravascular coagulation in rats^[9,12], and also ameliorated cardiac dysfunction caused by chronic infusion of LPS in rats^[13]. Furthermore, FR167653 protected lung, liver, and heart against ischemia-reperfusion injury in dogs^[14-17], and the protection against liver ischemia-reperfusion injury was associated with inhibition of proinflammatory cytokines from KCs^[18, 19]. Recent studies suggest that FR167653 inhibits IL-1 β and TNF- α production via specific inhibition of p38 MAPK activity^[12,17,20-22]. Because effective therapy has not been established for liver injury, development of an anti-inflammatory compound is urgently needed. From this viewpoint, it is worthwhile to assess the anti-inflammatory and immunomodulatory effect of FR167653. In the current study, we administered FR167653 to a murine model of *Bacillus Calmette Guerin* (BCG) and LPS-induced liver injury and assessed histopathological changes and its effects on cytokine production.

MATERIALS AND METHODS

Animals and reagents

Male Kunming strain mice weighing 18-22 g were purchased from Animal Center of Anhui Medical University. Mice were allowed to access to food and tap water *ad libitum*, and acclimated to facilities for at least 1 wk before any treatments. 1, 1, 3, 1-tetraethoxypropane (TEP) and 5, 5'-dithiobis-(2-nitrobenzoic acid) (DTNB) were purchased from FLUKA Co., Switzerland. BCG was purchased from Institute of Shanghai Biological Products. ConA, LPS from *Escherichia coli*, and TNF- α ELISA kit were purchased from Sigma Co., St. Louis, USA. The primers of NF- κB and β -actin were synthesized by BIOASIA Biotech Co. Shanghai. FR167653 supplied by the Fujisawa Pharmaceutical Co. Ltd. (Tokyo, Japan), was dissolved to 20 mL/L with 5 g/L methylcellulose solution. To obtain the dose of 50, 100, or 150 mg/kg body mass (BM), 2.5, 5, or 7.5 $\mu\text{L/g}\cdot\text{bm}$. of 20 mL/L FR167653 solution was injected subcutaneously.

Model of BCG and LPS-induced immunological liver injury (ILI) and treatment^[23]

Each mouse was injected with 2.5 mg BCG (viable bacilli) in 0.2 mL saline via tail vein, and 10 d later with 10 mg LPS in 0.2 mL

saline. At 4, 8, and 12 h post-injection of LPS, animals received FR167653 at 50, 100, and 150 mg/kg, s.c., respectively. The control group was subcutaneously administered the same volume of 5 g/L methylcellulose solution. The mice were anesthetized with ether, then sacrificed by cervical dislocation 16 h after LPS injection and blood was collected, and centrifuged at 1 500 r/min for 10 min at room temperature. Serum was aspirated and stored at -70 °C until assayed as described below. The liver was also removed and stored at -70 °C until required.

Measurement of ALT, AST

Serum ALT, and AST were determined using commercial kits purchased from Institute of Shanghai Biological Products affiliated to the Ministry of Health.

Measurement of MDA and GSHpx in liver homogenate

Livers were thawed, weighed and homogenized with Tris-HCl buffer (5 mmol/L, containing 2 mmol/L EDTA, pH 7.4). Homogenates were centrifuged at 1 000 r/min for 10 min at room temperature and the supernatant was used immediately for the assays of MDA and GSHpx. MDA was measured by the thiobarbituric acid method according to standard techniques. The content of MDA was expressed as nmol per gram liver tissue. GSHpx was measured by the DTNB method, and its content was expressed as U per milligram protein.

Measurement of TNF- α , IL-1, and nitric oxide (NO)

Serum TNF- α and NO were measured using commercial kits produced by Sigma Co. and Beijing Biotinge-Tech Co. Ltd, and their levels were expressed as pg/mL and μ mol/L respectively. IL-1 produced by peritoneal macrophages was measured according to the method of 3 H-infiltrated cell proliferation.

RT-PCR assay for NF- κ B p65 mRNA in liver tissue

Liver tissue RNA was extracted using RNA easy kit (Invitrogen, USA). To test the efficacy of reverse transcriptase, RT-PCR was performed for β -actin mRNA. Briefly, the first strand of cDNA was synthesized by reverse transcriptase and pooled. The resulting cDNA samples were adjusted to PCR buffer conditions and run for PCR simultaneously. The primers for NF- κ B p65 were 5'-GCG GCC AAG CTT AAG ATC TGC CGA GTA AAC-3', and 5'-CGC TGC TCT AGA GAA CAC AAT GGC CAC TTG CCG-3'. The primers for β -actin were 5'-TGG AAT CCT GTG GCA TCC ATG AA-3', and 5'-TAA AAC GCA GCT CAG TAA CAG TC-3'. The amplifications of NF- κ B p65 and β -actin genes are expected to generate 198 bp and 348 bp fragments, respectively. Amplification was performed for 30 cycles, each of which consisted of 1 min of denaturation at 94 °C, 1 min of annealing at 58 °C, and 3 min of primer extension at 72 °C. Ten μ L of reaction mixture was loaded to 10 g/L agarose gel containing 0.5 μ g/mL ethidium bromide for electrophoresis, the gel was then placed under ultraviolet light for semi-quantitative detection.

Histological examination of liver specimens

Formalin-fixed liver specimens were embedded in paraffin and

stained with hematoxylin and eosin for conventional morphological evaluation.

Statistical analysis

All values were expressed as mean \pm SD. The significance of differences between groups was determined by ANOVA followed by Student's *t* test. *P* value of less than 0.05 was considered significant.

RESULTS

Effects of FR167653 on ILI induced by BCG plus LPS in mice

The levels of ALT and AST in plasma and MDA content in liver homogenate were significantly increased after the sequential injection of BCG and LPS. Meanwhile, the GSHpx level in liver homogenate was sharply decreased (Figures 1, 2). FR167653 (50, 100, 150 mg/kg, s.c.) could not only significantly decrease ALT, AST, and MDA levels, but also evidently increase GSHpx level in mice with ILI (Figures 1, 2). Liver histopathologic examination showed extensive inflammatory cells infiltration and liver cells necrosis. FR167653 (100, 150 mg/kg) significantly reduced inflammatory cells infiltration and liver cells necrosis (Figure 3).

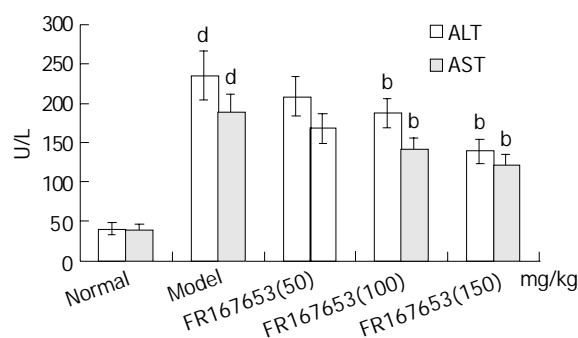


Figure 1 Effect of FR167653 on serum ALT and AST activities in ILI mice. *n*=8, mean \pm SD, ^b*P*<0.01 vs model group; ^d*P*<0.01 vs normal group.

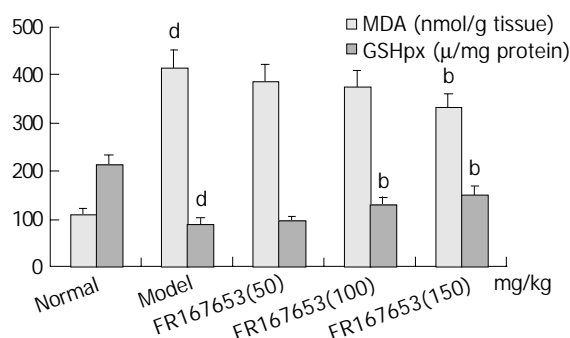


Figure 2 Effect of FR167653 on MDA and GSHpx contents in liver homogenates of ILI mice. *n*=8, mean \pm SD, ^b*P*<0.01 vs model group; ^d*P*<0.01 vs normal group.

Table 1 Effect of FR167653 on serum TNF- α , NO and IL-1 from peritoneal macrophages in ILI mice

Group	Dose (mg/kg)	TNF- α (pg/mL)	NO (μ mol/L)	IL-1 (10^3 /min)
Normal	-	Under detection limit	15.7 \pm 4.3	6.4 \pm 1.42
Model	-	523.1 \pm 28.6 ^d	117.8 \pm 10.7 ^d	21.5 \pm 5.04 ^d
FR167653	50	491.8 \pm 20.5 ^a	109.3 \pm 10.5	17.4 \pm 3.81
	100	404.9 \pm 18.5 ^b	95.4 \pm 8.9 ^b	14.7 \pm 3.05 ^b
	150	341.8 \pm 19.1 ^b	84.3 \pm 8.7 ^b	11.9 \pm 2.85 ^b

n=8, mean \pm SD, ^a*P*<0.05, ^b*P*<0.01 vs model group; ^d*P*<0.01 vs normal group.

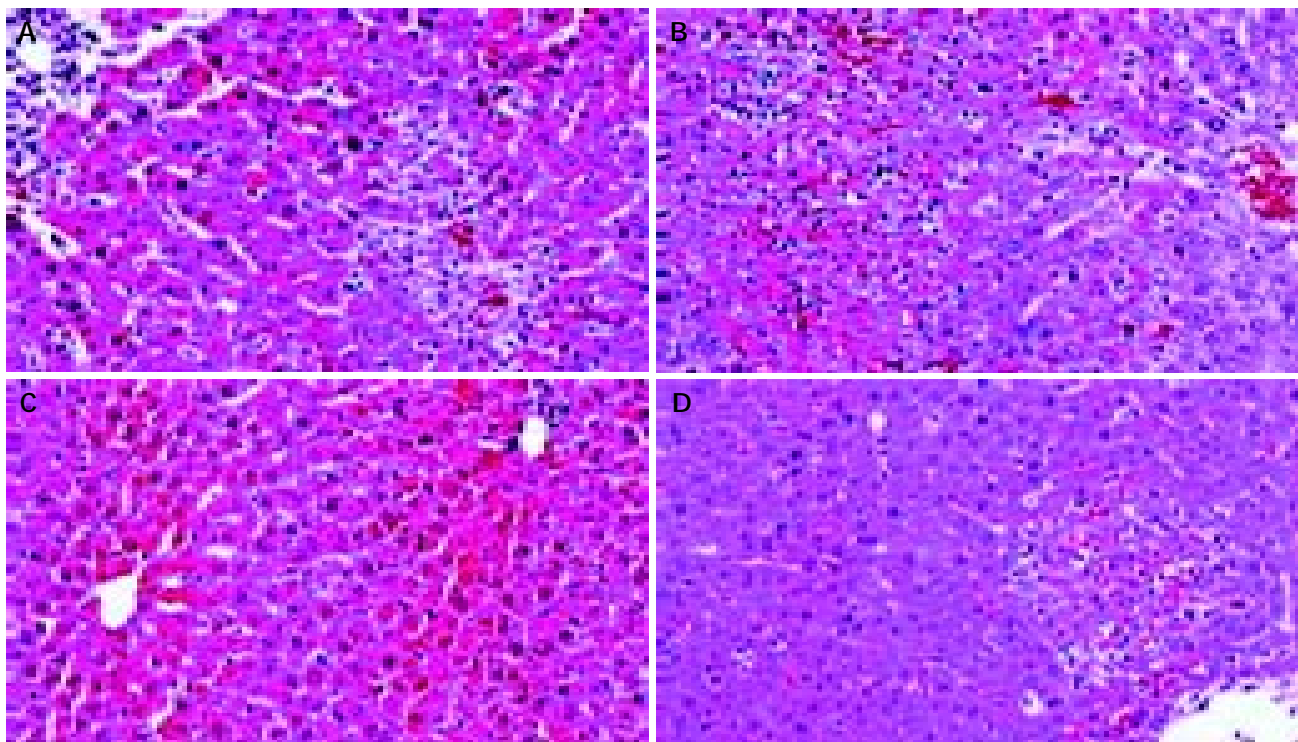


Figure 3 Effect of FR167653 on liver histopathology of ILI mice. A: Normal group; B: Model group; C: Model plus FR167653 (100 mg/kg); D: Model plus FR167653 (150 mg/kg). All sections were stained with hematoxylin and eosin (200 \times).

Effects of FR167653 on TNF- α , IL-1, and NO

The levels of TNF- α and NO were elevated significantly in mice injected with BCG and then challenged with LPS. Likewise, IL-1 excreted by peritoneal macrophages was also significantly increased in the model group (Table 1). FR167653 (50, 100, 150 mg/kg) obviously counteracted the increase of TNF- α and NO levels in sera. IL-1 produced by peritoneal macrophages was also significantly inhibited by FR167653 (Table 1).

Effects of FR167653 on NF- κ B p65 expression in liver tissue

Gel electrophoresis and semi-quantitative analysis showed that FR167653 significantly reduced expression of NF- κ B mRNA in liver tissue of ILI induced by BCG plus LPS compared with model group (Figure 4).

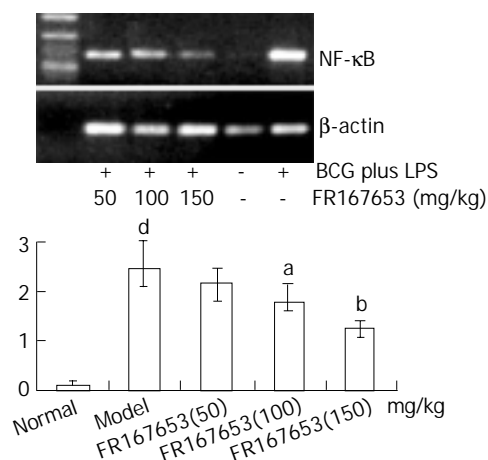


Figure 4 Effect of FR167653 on NF- κ B mRNA in liver tissue of ILI mice. $n=3$, mean \pm SD. ^a $P<0.05$. ^b $P<0.01$ vs model group; ^d $P<0.01$ vs normal group.

DISCUSSION

It has been demonstrated that severe hepatitis could be induced

by injecting a small dose of bacterial LPS into BCG-pretreated mice^[23]. In the present study, ILI was successfully induced by BCG plus LPS. On this basis, FR167653 (50, 100, 150 mg/kg) could significantly lower the increased plasma transaminase levels and MDA contents in liver homogenate. Meanwhile, GSHpx levels were increased significantly. Histopathologic examination showed FR167653 significantly reduced inflammatory cells infiltration and liver cells necrosis.

Although several parameters of the inflammatory response contribute to liver injury^[24], one well-studied pathway is the production of TNF- α . In a number of liver injury models, elevated TNF- α levels were present and correlated with liver injury^[23,25,26]. Inhibition of TNF- α activity can decrease liver injury. The addition of soluble TNF receptors that diminished the biological effect of TNF- α could significantly decrease liver enzyme levels, improve liver histology, and reduce mortality immediately after acute carbon tetrachloride administration. Similar results were seen in chronic alcohol-induced liver disease in rats. In humans, elevated levels of TNF- α are seen in hepatitis and are associated with increased mortality^[27]. Furthermore, TNF- α might act as the first mediator of liver injury, its elevation would result in release of a number of proinflammatory mediators including IL-1, NO, IL-6, IL-8^[3,28], further deteriorating the liver injury. In the present study, TNF- α in the sera and IL-1 produced by peritoneal macrophages were significantly increased in mice with ILI compared with control. FR167653, a potent inhibitor of TNF- α and IL-1, suppressed elevated TNF- α and IL-1 levels, which was consistent with previous observations^[29]. As potent producers of inflammatory cytokines such as TNF- α and IL-1, KCs have been implicated in the pathway leading to liver injury^[30]. Whether inhibition of FR167653 on TNF- α production was associated with diminished KCs proliferation, and decreased inflammatory cells infiltration needs to be further clarified.

A growing body of evidence suggests that sustained production of NO resulting from up-regulation of inducible NOS (iNOS) after LPS challenge may cause hepatocellular injury, either directly^[31,32], or indirectly, by forming reactive nitrogen

intermediates^[33]. Menezes *et al.*^[34,35] demonstrated that a NO scavenger, NOX, decreased hepatocellular injury and improved survival after hemorrhagic shock. As reported previously, the synthesis of NO was regulated by various factors including TNF- α , IL-1, and NF- κ B. The inhibition of NF- κ B led to a decrease in the inducible isoform of NO and the transcription of TNF- α in KCs^[36-38]. Moreover, synthetic double-stranded oligodeoxynucleotides (ODN) transfer with a high affinity to NF- κ B (NF- κ B/decoy/ODN) *in vivo* effectively suppressed endotoxin-induced fatal liver injury in mice^[39]. In our study, we observed significant suppression of NF- κ B p65 mRNA in liver tissue and NO in sera of BCG plus LPS - induced ILI by FR167653. It indicated that inhibition of FR167653 on liver injury might be related with decreased NO production through inhibiting NF- κ B transcription. Recent studies suggested that p38 MAPK inhibitor, SB203580, diminished phosphorylation of the transactivation domain of the p65 subunit of NF- κ B^[40]. Moreover, the pharmacological characteristics and chemical structure of FR167653 resemble SB203580^[41,42]. Therefore, inhibition of FR167653 on liver injury was associated with reduced expression of NF- κ B via p38 MAPK, and led to down-regulation of TNF- α , IL-1, and NO.

REFERENCES

- 1 Enomoto N, Ikejima K, Yamashina S, Hirose M, Shimizu H, Kitamura T, Takei Y, Sato And N, Thurman RG. Kupffer cell sensitization by alcohol involves increased permeability to gut-derived endotoxin. *Alcohol Clin Exp Res* 2001; **25**(6 Suppl): 51S-54S
- 2 Lukkari TA, Jarvelainen HA, Oinonen T, Kettunen E, Lindros KO. Short-term ethanol exposure increases the expression of Kupffer cell CD14 receptor and lipopolysaccharide binding protein in rat liver. *Alcohol Alcohol* 1999; **34**: 311-319
- 3 Shito M, Balis UJ, Tompkins RG, Yarmush ML, Toner M. A fulminant hepatic failure model in the rat: involvement of interleukin-1beta and tumor necrosis factor-alpha. *Dig Dis Sci* 2001; **46**: 1700-1708
- 4 Nishioji K, Okanou T, Mori T, Sakamoto S, Itoh Y. Experimental liver injury induced by *Propionibacterium acnes* and lipopolysaccharide in macrophage colony stimulating factor-deficient osteopetrotic (*op/op*) mice. *Dig Dis Sci* 1999; **44**: 1975-1984
- 5 Bradham CA, Plumpe J, Manns MP, Brenner DA, Trautwein C. Mechanisms of hepatic toxicity I. TNF-induced liver injury. *Am J Physiol* 1998; **275**: G387-392
- 6 Spitzer JA, Zheng M, Kolls JK, Vande Stouwe C, Spitzer JJ. Ethanol and LPS modulate NF-kappaB activation, inducible NO synthase and COX-2 gene expression in rat liver cells *in vivo*. *Front Biosci* 2002; **7**: a99-108
- 7 Wang JH, Redmond HP, Wu QD, Bouchier-Hayes D. Nitric oxide mediates hepatocyte injury. *Am J Physiol* 1998; **275**: G1117-1126
- 8 Hoek JB, Pastorino JG. Ethanol, oxidative stress, and cytokine-induced liver cell injury. *Alcohol* 2002; **27**: 63-68
- 9 Yamamoto N, Sakai F, Yamazaki H, Nakahara K, Okuhara M. Effect of FR167653, a cytokine suppressive agent, on endotoxin-induced disseminated intravascular coagulation. *Eur J Pharmacol* 1996; **314**: 137-142
- 10 Takahashi S, Shigeta J, Inoue H, Tanabe T, Okabe S. Localization of cyclooxygenase-2 and regulation of its mRNA expression in gastric ulcers in rats. *Am J Physiol* 1998; **275**: G1137-1145
- 11 Kawano T, Ogushi F, Tani K, Endo T, Ohmoto Y, Hayashi Y, Sone S. Comparison of suppressive effects of a new anti-inflammatory compound, FR167653, on production of PGE₂ and inflammatory cytokines, human monocytes, and alveolar macrophages in response to endotoxin. *J Leukoc Biol* 1999; **65**: 80-86
- 12 Yamamoto N, Sakai F, Yamazaki H, Sato N, Nakahara K, Okuhara M. FR167653, a dual inhibitor of interleukin-1 and tumor necrosis factor-alpha, ameliorates endotoxin-induced shock. *Eur J Pharmacol* 1997; **327**: 169-174
- 13 Gardiner SM, Kemp PA, March JE, Bennett T. Influence of FR167653, an inhibitor of TNF-alpha and IL-1, on the cardiovascular responses to chronic infusion of lipopolysaccharide in conscious rats. *J Cardiovasc Pharmacol* 1999; **34**: 64-69
- 14 Kamoshita N, Takeyoshi I, Ohwada S, Iino Y, Morishita Y. The effects of FR167653 on pulmonary ischemia-reperfusion injury in dogs. *J Heart Lung Transplant* 1997; **16**: 1062-1072
- 15 Kobayashi J, Takeyoshi I, Ohwada S, Iwanami K, Matsumoto K, Muramoto M, Morishita Y. The effects of FR167653 in extended liver resection with ischemia in dogs. *Hepatology* 1998; **28**: 459-465
- 16 Koyano T, Takeyoshi I, Takahashi T, Hasegawa Y, Sato Y, Ishikawa S, Matsumoto K, Morishita Y. Effect of FR167653 on ischemia-reperfusion injury of the canine heart: ultrastructural study. *Transplant Proc* 1998; **30**: 3370-3371
- 17 Kobayashi M, Takeyoshi I, Yoshinari D, Matsumoto K, Morishita Y. P38 mitogen-activated protein kinase inhibition attenuates ischemia-reperfusion injury of the rat liver. *Surgery* 2002; **131**: 344-349
- 18 Hashimoto K, Nishizaki T, Yoshizumi T, Uchiyama H, Okano S, Ikegami T, Yanaga K, Sugimachi K. Beneficial effect of FR167653 on cold ischemia/reperfusion injury in rat liver transplantation. *Transplantation* 2000; **70**: 1318-1322
- 19 Minami S, Furui J, Kanematsu T. Role of carcinoembryonic antigen in the progression of colon cancer cells that express carbohydrate antigen. *Cancer Res* 2001; **61**: 2732-2735
- 20 Kobayashi M, Takeyoshi I, Yoshinari D, Koibuchi Y, Koyama T, Kawashima Y, Ohwada S, Matsumoto K, Morishita Y. FR167653 ameliorates ischemia-reperfusion injury of the rat liver through P38 mitogen-activated protein kinase pathway. *Transplant Proc* 2001; **33**: 865
- 21 Takahashi S, Keto Y, Fujita T, Uchiyama T, Yamamoto A. FR167653, a p38 mitogen-activated protein kinase inhibitor, prevents *Helicobacter pylori*-induced gastritis in Mongolian gerbils. *J Pharmacol Exp Ther* 2001; **296**: 48-56
- 22 Lasky JA, Ortiz LA, Tonthat B, Hoyle GW, Corti M, Athas G, Lungarella G, Brody A, Friedman M. Connective tissue growth factor mRNA expression is upregulated in bleomycin-induced lung fibrosis. *Am J Physiol* 1998; **275**: L365-371
- 23 Wang GS, Liu GT. Influences of Kupffer cell stimulation and suppression on immunological liver injury in mice. *Zhongguo Yaoli Xuebao* 1997; **18**: 173-176
- 24 Moulin F, Copple BL, Ganey PE, Roth RA. Hepatic and extrahepatic factors critical for liver injury during lipopolysaccharide exposure. *Am J Physiol Gastrointest Liver Physiol* 2001; **281**: G1423-1431
- 25 Zhang XL, Quan QZ, Sun ZQ, Wang YJ, Jiang XL, Wang D, Li WB. Protective effects of cyclosporine A on T-cell dependent ConA-induced liver injury in Kunming mice. *World J Gastroenterol* 2001; **7**: 569-571
- 26 Zang GQ, Zhou XQ, Yu H, Xie Q, Zhao GM, Wang B, Guo Q, Xiang YQ, Liao D. Effect of hepatocyte apoptosis induced by TNF-alpha on acute severe hepatitis in mouse models. *World J Gastroenterol* 2000; **6**: 688-692
- 27 Madhotra R, Gilmore IT. Recent developments in the treatment of alcoholic hepatitis. *Q J Med* 2003; **96**: 391-400
- 28 Muntane J, Rodriguez FJ, Segado O, Quintero A, Lozano JM, Siendones E, Pedraza CA, Delgado M, O'Valle F, Garcia R, Montero JL, De La Mata M, Mino G. TNF-alpha dependent production of inducible nitric oxide is involved in PGE₁ protection against acute liver injury. *Gut* 2000; **47**: 553-562
- 29 Hou Z, Yanaga K, Kamohara Y, Eguchi S, Tsutsumi R, Furui J, Kanematsu T. A new suppressive agent against interleukin-1beta and tumor necrosis factor-alpha enhances liver regeneration after partial hepatectomy in rats. *Hepatology* 2003; **26**: 40-46
- 30 Luckey SW, Petersen DR. Activation of Kupffer cells during the course of carbon tetrachloride-induced liver injury and fibrosis in rats. *Exp Mol Pathol* 2001; **71**: 226-240
- 31 Engin A, Bozkurt BS, Altan N, Memi L, Bukan N. Nitric oxide-mediated liver injury in the presence of experimental bile duct obstruction. *World J Surg* 2003; **27**: 253-255
- 32 Nadler EP, Dickinson EC, Beer-Stolz D, Alber SM, Watkins SC, Pratt DW, Ford HR. Scavenging nitric oxide reduces hepatocellular injury after endotoxin challenge. *Am J Physiol*

- Gastrointest Liver Physiol* 2001; **281**: G173-181
- 33 **Fintelmann S**, Jung M, Weidenbach H, Steinle AU, Beger HG, Nussler AK. Effect of cellular growth factors on hepatocytes in experimental infection—regulation of NF-kappa B and glutathione homeostasis. *Langenbecks Arch Chir Suppl Kongressbd* 1998; **115**(Suppl 1): 405-408
- 34 **Menezes J**, Hierholzer C, Watkins SC, Lyons V, Peitzman AB, Billiar TR, Twardy DJ, Harbrecht BG. A novel nitric oxide scavenger decreases liver injury and improves survival after hemorrhagic shock. *Am J Physiol* 1999; **277**: G144-151
- 35 **Hierholzer C**, Billiar TR, Twardy DJ, Harbrecht B. Reduced hepatic transcription factor activation and expression of IL-6 and ICAM-1 after hemorrhage by NO scavenging. *Arch Orthop Trauma Surg* 2003; **123**: 55-59
- 36 **Shimohashi N**, Nakamuta M, Uchimura K, Sugimoto R, Iwamoto H, Enjoji M, Nawata H. Selenoorganic compound, ebselen, inhibits nitric oxide and tumor necrosis factor-alpha production by the modulation of jun-N-terminal kinase and the NF-kappaB signaling pathway in rat Kupffer cells. *J Cell Biochem* 2000; **78**: 595-606
- 37 **Cao Q**, Mak KM, Lieber CS. Dilinoleoylphosphatidylcholine decreases acetaldehyde-induced TNF-alpha generation in Kupffer cells of ethanol-fed rats. *Biochem Biophys Res Commun* 2002; **299**: 459-464
- 38 **Lin M**, Rippe RA, Niemela O, Brittenham G, Tsukamoto H. Role of iron in NF-kappa B activation and cytokine gene expression by rat hepatic macrophages. *Am J Physiol* 1997; **272** (6 Pt 1): G1355-1364
- 39 **Ogushi I**, Iimuro Y, Seki E, Son G, Hirano T, Hada T, Tsutsui H, Nakanishi K, Morishita R, Kaneda Y, Fujimoto J. Nuclear factor kappa B decoy oligodeoxynucleotides prevent endotoxin-induced fatal liver failure in a murine model. *Hepatology* 2003; **38**: 335-344
- 40 **Wilms H**, Rosenstiel P, Sievers J, Deuschl G, Zecca L, Lucius R. Activation of microglia by human neuromelanin is NF-kappaB dependent and involves p38 mitogen-activated protein kinase: implications for Parkinson's disease. *FASEB J* 2003; **17**: 500-502
- 41 **Cuenda A**, Rouse J, Doza YN, Meier R, Cohen P, Gallagher TF, Young PR, Lee JC. SB 203580 is a specific inhibitor of a MAP kinase homologue which is stimulated by cellular stresses and interleukin-1. *FEBS Lett* 1995; **364**: 229-233
- 42 **Lee JC**, Laydon JT, McDonnell PC, Gallagher TF, Kumar S, Green D, McNulty D, Blumenthal MJ, Heys JR, Landvatter SW. A protein kinase involved in the regulation of inflammatory cytokine biosynthesis. *Nature* 1994; **372**: 739-746

Edited by Zhu LH Proofread by Chen WW and Xu FM

Therapeutic plasma exchange in patients with hyperlipidemic pancreatitis

Jui-Hao Chen, Jiann-Horng Yeh, Hsin-Wen Lai, Chao-Sheng Liao

Jui-Hao Chen, Hsin-Wen Lai, Chao-Sheng Liao, Department of Gastroenterology, Shin kong Wu-Ho-Su Memorial Hospital, Taipei, Taiwan, china

Jiann-Horng Yeh, Department of Neurology, Shin kong Wu-Ho-Su Memorial Hospital, Taipei, Taiwan, china

Correspondence to: Jui-Hao Chen, Department of Gastroenterology, Shin kong Wu-Ho-Su Memorial Hospital, 95 Wenchang Road, Shih-Lin District, Taipei, Taiwan, china. m000723@ms.skh.org.tw

Telephone: +886-2-28332211 **Fax:** +886-2-28389335

Received: 2004-02-20 **Accepted:** 2004-04-09

Abstract

AIM: To clarify the effectiveness of plasma exchange by comparing the mortality and morbidity before and after the intervention of plasma exchange.

METHODS: Plasma exchange has been available as an optional therapy for hyperlipidemic pancreatitis since August 1999 in our hospital. The patients were assorted into 2 groups (group I: before August 1999 and group II: after August 1999). Group I consisted of 34 patients (before the availability of plasma exchange). Group II consisted of 60 patients (after the availability of plasma exchange). Twenty patients in group II received plasma exchange after giving their consent. The mortality and morbidity were compared between group I and group II. Furthermore, the patients with severe hyperlipidemic pancreatitis (Ranson's score = 3) were analyzed separately. The mortality and morbidity were also compared between those receiving plasma exchange (group A) and those who did not receive plasma exchange (group B).

RESULTS: There was no statistical difference in the mortality, systemic and local complications between group I and group II. When the patients with severe hyperlipidemic pancreatitis were analyzed separately, there was no statistical difference between group A and group B.

CONCLUSION: Plasma exchange can not ameliorate the overall mortality or morbidity of hyperlipidemic pancreatitis. The time of plasma exchange might be the critical point. If patients with hyperlipidemic pancreatitis can receive plasma exchange as soon as possible, better result may be predicted. Further study with more cases is needed to clarify the role of plasma exchange in the treatment of hyperlipidemic pancreatitis.

Chen JH, Yeh JH, Lai HW, Liao CS. Therapeutic plasma exchange in patients with hyperlipidemic pancreatitis. *World J Gastroenterol* 2004; 10(15): 2272-2274
<http://www.wjgnet.com/1007-9327/10/2272.asp>

INTRODUCTION

Hypertriglyceridemia (HTG) is a rare cause of pancreatitis. Hyperlipidemic pancreatitis (HLP) secondary to HTG presents

typically as an episode of acute pancreatitis or recurrent acute pancreatitis or rarely as chronic pancreatitis^[1]. The typical clinical profile of HLP is a patient with preexisting lipid abnormality along with the presence of secondary factors (such as poorly controlled diabetes mellitus, alcohol abuse, pregnancy, or a medication) that can induce HTG^[1]. It is generally accepted that a TG level more than 1 000 mg/dL is needed to precipitate an episode of acute pancreatitis^[2]. It is postulated that hydrolysis of TG by pancreatic lipase into free fatty acid is toxic to pancreatic endothelium and acinar cells^[3]. In an animal study, hyperlipidemia could intensify the course of acute edematous pancreatitis and necrotizing pancreatitis^[3].

Plasmapheresis has been claimed to reduce triglyceride level rapidly in HLP^[4-11] and is believed to halt the progression of HLP^[8-10]. Actually, experiences of plasmapheresis in HLP are limited and only sporadic cases were reported^[5-11]. There was no control study in the past concerning whether plasmapheresis could improve the mortality or morbidity of HLP. Our aim was to analyze the benefits of plasma exchange by comparing the mortality and morbidity of HLP patients with those without receiving such an intervention.

MATERIALS AND METHODS

Patient characteristics

From September 1992 to June 2003, a total of 862 patients with acute pancreatitis were reviewed and 94 patients were consistent with hyperlipidemic pancreatitis (HLP). As plasma exchange has been available as an optional therapy of HLP since August 1999 in our hospital, the patients were assorted into 2 groups (group I: before August 1999 and group II: after August 1999). Group I consisted of 34 patients (before the availability of plasmapheresis) and group II consisted of 60 patients (after the availability of plasmapheresis). Twenty of 60 patients in group II received plasma exchange after giving their consents. The Ranson's score was used for assessment of the severity of pancreatitis. Half of the patients receiving plasma exchange were severe cases (Ranson's score = 3). The anatomical change of acute pancreatitis was assessed according to the Balthazar's grading. The enrolled criteria of plasma exchange in HLP were as followings: (1) overt symptoms of acute pancreatitis, (2) pancreatitis proved by CT, ultrasound or elevation of pancreatic enzymes, (3) triglyceride (TG) >1 000 mg/dL and lactescent serum, (4) exclusion of other causative conditions, such as gall stone, trauma or neoplasm, (5) patient's agreement. The mortality and morbidity between group I and group II were compared.

Furthermore, the patients with severe HLP (Ranson's score = 3) were analyzed separately. We divided the patients with severe HLP (a total of 29 patients) into 2 groups. Group A received plasma exchange, while group B did not receive the intervention. The mortality and morbidity between group A and group B were also compared.

The secondary factors inducing HTG in our patients included diabetes mellitus (46 patients), alcoholic consumption (32 patients) and oral contraceptive (one patient). The median time for starting plasma exchange was 3 d after symptom onset (range, 2-6 d).

Apheresis

Plasma exchange was carried out using membrane filtration in a KM 8800 membrane plasmapheresis monitor (Kuraray, Osaka, Japan) with a Plasmacure plasma separator (Kuraray, Osaka, Japan) to separate plasma from blood. One calculated plasma volume was processed during each session of plasma exchange. One course of plasma exchange treatment consisted of one or two daily sessions based on the doctor's decision, single session in 13 patients and two sessions in 7. Heparin was used as the anticoagulant. Either a double lumen catheter in a central vein (fifteen patients) or a dialysis catheter in an antecubital vein (five patients) was used for vascular access. Replacement fluid was given with fresh frozen plasma (FFP) in 8 patients and isovolumetric 5% albumin solution in 12 patients.

Statistical analysis

t-test and chi-square test were used for statistical analysis. $P < 0.05$ was considered statistically significant.

RESULTS

The demographic characteristics of all the patients are summarized in Table 1. The mean age and sex distribution were similar in both groups. The initial mean TG level was around 1900 in both groups. The severity of pancreatitis was predicted by the Ranson's criteria. Severe pancreatitis (Ranson's score ≥ 3) was 20.6% in group I and 36.7% in group II ($P = 0.105$). The anatomical change of pancreatitis was assessed according to the Balthazar's grading system and 54.2% of group I and 41.3% of group II were belonged to Balthazar grade D or E ($P = 0.305$).

The mortality rate, systemic and local complications of both groups are demonstrated in the Table 2. The systemic complication was defined by the Atlanta definition^[12]: (1) pulmonary insufficiency, $\text{PaO}_2 < 8$ kPa, (2) renal insufficiency, $\text{Cr} > 2$ mg/dL, (3) shock, $\text{SBP} < 12$ kPa, (4) UGI bleeding > 500 mL/24 h. The local complications included abscess and pseudocyst formation. There was no significant difference between group I and group II in mortality and complications. Further comparison of individual items of systemic and local complications between the two groups revealed no statistical differences (Tables 3, 4).

Table 1 Demographic characteristics

	Group I (<i>n</i> =34)	Group II (<i>n</i> =60)	<i>P</i> value
Age (yr)	40.8±6.8	42.3±8.9	0.394
Initial TG	1922±1287	1913±612	0.966
DM (%)	38(13/34)	55(33/60)	0.118
Alcohol (%)	44(15/34)	28.3 (17/60)	0.121
Ranson > 3 (%)	20.6(7/34)	36.7(22/60)	0.105
Balthazar D, E (%)	54.2(13/24)	41.3(19/46)	0.305

Table 2 Comparison of mortality and morbidity between patients before and after availability of plasma exchange

	Group I (%, <i>n</i> =34)	Group II (%, <i>n</i> =60)	<i>P</i> value
Mortality (%)	5.9(2/34)	6.7(4/60)	0.881
Systemic complications (%)	17.6(6/34)	18.3(11/60)	0.934
Local complications (%)	11.8(4/34)	6.7(4/60)	0.395

When severe hyperlipidemic pancreatitis (Ranson's score ≥ 3) was analyzed separately (Table 5), the mortality rate, systemic and local complications of group A (with plasmapheresis) and group B (without plasmapheresis) were not statistically different ($P = 0.369, 0.153, 0.454$, respectively).

The mean serum concentration of TG and lipase fell significantly after plasma exchange. The serum TG level declined

from 2019 ± 780 mg/dL to 691 ± 331 mg/dL (65.8% reduction) and the serum lipase level declined from 4007 ± 355 U/L to 447 ± 35 U/L (88.8% reduction).

Table 3 Comparison of systemic complications between patients before and after the availability of plasma exchange

	Group I (%, <i>n</i> =34)	Group II (%, <i>n</i> =60)	<i>P</i> value
ARF	17.6(6/34)	10(6/60)	0.286
UGI bleeding	0(0/34)	8.3(5/60)	0.084
Shock	8.8(3/34)	10(6/60)	0.852
ARDS	11.8(4/34)	10(6/60)	0.790

ARF: Acute renal failure; ARDS: Acute respiratory distress syndrome.

Table 4 Comparison of local complications between patients before and after availability of plasma exchange

	Group I (%, <i>n</i> =34)	Group II (%, <i>n</i> =60)	<i>P</i> value
Abscess	17.6(6/34)	10(6/60)	0.286
Pseudocyst	0(0/34)	8.3(5/60)	0.084

Table 5 Comparison of patients with severe hyperlipidemic pancreatitis receiving plasma exchange and not receiving plasma exchange

	Group A: PE(+) (%, <i>n</i> =10)	Group B: PE(-) (%, <i>n</i> =19)	<i>P</i> value
Ranson > 3			
Mortality	30(3)	15.8(3)	0.369
Systemic complications	70(7)	42.1(8)	0.153
Local complications	10(1)	21.1(4)	0.454

PE (+): With plasma exchange; PE (-): Without plasma exchange.

DISCUSSION

The association between hyperlipidemia and acute pancreatitis was first described by Speck in 1865^[1]. Studies on patients with familial HTG and their longterm follow-up have shown that extreme elevation of TG occurred during episode of acute pancreatitis^[13]. It has been generally believed that a TG level of more than 1000 mg/dL was needed to precipitate an acute pancreatitis^[2]. The hypothesis of hyperlipidemic pancreatitis is that pancreatic damage was resulted from toxic injury to the capillary endothelium and the damage of pancreatic acinar cells was caused by free fatty acids liberated by pancreatic lipase^[3]. Conservative treatment (fasting, lipid lowering drugs, insulin or fluid restoration) might decrease TG level slowly in a time span of days to weeks^[14]. In contrast, plasmapheresis might remove excessive lipid from serum in about 2 h^[4,6]. Sporadic reports about plasmapheresis used in hyperlipidemic pancreatitis were seen in the past^[4-10]. They all concluded that plasmapheresis was helpful for treating or preventing acute hyperlipidemic pancreatitis. However, no control study to assess the value of plasmapheresis in the treatment of hyperlipidemic pancreatitis is available.

Different methods have been used in plasmapheresis. Plasma exchange is superior to double filtration in the removal of excessive TG because the membrane of plasma separator was usually blocked by the larger particles of chylomicron^[6]. We used plasma exchange with replacement of albumin or fresh frozen plasma (FFP) in the treatment of HLP in this study. FFP could supply lipoprotein lipase and apolipoprotein from the healthy donor^[13]. Lipoprotein lipase and apolipoprotein were essential for the catabolism of TG^[13].

In our study, plasma exchange could remove TG effectively

from turbid plasma in a short time (about 2 h). TG declined from $2\,019\pm 780$ mg/dL to 691 ± 331 mg/dL (65.8% reduction). It was also postulated that plasmapheresis could remove circulating activated enzymes and inflammatory mediators^[15], but its beneficial effects in pancreatitis has not been proved^[10]. The serum lipase level declined from $4\,007\pm 355$ U/L to 447 ± 35 U/L (88.8% reduction) after plasma exchange in our patients.

Despite the marked reduction in TG and lipase after plasma exchange, we could not achieve statistically significant improvement in the mortality and morbidity after the intervention of plasma exchange. The mortality was 5.9% before the intervention (group I) and 6.7% after the intervention (group II). The rate of systemic complications (acute renal failure, UGI bleeding, shock, or pulmonary insufficiency) was 17.6% in group I and 18.3% in group II. The rate of local complications (abscess or pseudocyst) was 11.8% in group I and 6.7% in group II. While individual items of complications were considered, there were still no statistical differences between the two groups.

When the patients with severe HLP (Ranson's score ≥ 3) were analyzed separately, the mortality rate was 30% in group A (with plasma exchange) and 15.8% in group B (without plasma exchange). The mortality in severe HLP was not decreased by plasma exchange. The rate of systemic complication was 70% in group A and 42.1% in group B ($P=0.153$). The rate of local complication was 10% in group A and 21.1% in group B ($P=0.454$). Again, plasma exchange was not able to alter the complication rate significantly.

Why could plasma exchange not improve the mortality and morbidity in HLP? We proposed that the time of plasmapheresis might be the critical point. If patients with HLP could receive plasma exchange as soon as possible, better result might be expected^[5].

In conclusion, plasma exchange fails to improve the overall mortality and morbidity of HLP in our study. Further study with more cases is needed to clarify the role of plasmapheresis in the treatment of HLP.

REFERENCES

- 1 **Yadav D**, Pitchumoni CS. Issues in hyperlipidemic pancreatitis. *J Clin Gastroenterol* 2003; **36**: 54-62
- 2 **Toskes PP**. Hyperlipidemic pancreatitis. *Gastroenterol Clin North Am* 1990; **19**: 783-791
- 3 **Hofbauer B**, Friess H, Weber A, Baczako K, Kisling P, Schilling M, Uhl W, Dervenis C, Buchler MW. Hyperlipaemia intensifies the course of acute oedematous and acute necrotising pancreatitis in the rat. *Gut* 1996; **38**: 753-758
- 4 **Yeh JH**, Chen JH, Chiu HC. Plasmapheresis for hyperlipidemic pancreatitis. *J Clin Apheresis* 2003; **18**: 181-185
- 5 **Furuya T**, Komatsu M, Takahashi K, Hashimoto N, Hashizume T, Wajima N, Kubota M, Itoh S, Soeno T, Suzuki K, Enzan K, Matsuo S. Plasma exchange for hypertriglyceridemic acute necrotizing pancreatitis: report of two cases. *Ther Apher* 2002; **6**: 454-458
- 6 **Yeh JH**, Lee MF, Chiu HC. Plasmapheresis for severe lipidemia: comparison of serum-lipid clearance rates for the plasma-exchange and double-filtration variants. *J Clin Apheresis* 2003; **18**: 32-36
- 7 **Piolot A**, Nadler F, Cavallero E, Coquard JL, Jacotot B. Prevention of recurrent acute pancreatitis in patients with severe hypertriglyceridemia: value of regular plasmapheresis. *Pancreas* 1996; **13**: 96-99
- 8 **Valbonesi M**, Occhini D, Frisoni R, Malfanti L, Capra C, Gualandi F. Cyclosporin-induced hypertriglyceridemia with prompt response to plasma exchange therapy. *J Clin Apheresis* 1991; **6**: 158-160
- 9 **Lennertz A**, Parhofer KG, Samtleben W, Bosch T. Therapeutic plasma exchange in patients with chylomicronemia syndrome complicated by acute pancreatitis. *Ther Apher* 1999; **3**: 227-233
- 10 **Saravanan P**, Blumenthal S, Anderson C, Stein R, Berkelhammer C. Plasma exchange for dramatic gestational hyperlipidemic pancreatitis. *J Clin Gastroenterol* 1996; **22**: 295-298
- 11 **Bildirici I**, Esinler I, Deren O, Durukan T, Kabay B, Onderoglu L. Hyperlipidemic pancreatitis during pregnancy. *Acta Obstet Gynecol Scand* 2002; **81**: 468-470
- 12 **Bradley EL**. A clinically based classification system for acute pancreatitis. *Arch Surg* 1993; **128**: 586-590
- 13 **Athyros VG**, Giouleme OI, Nikolaidis NL, Vasiliadis TV, Bouloukos VI, Kontopoulos AG, Eugenidis NP. Long-term follow-up of patients with acute hypertriglyceridemia-induced pancreatitis. *Clin Gastroenterol* 2002; **34**: 472-475
- 14 **Fortson MR**, Freedman SN, Webster PD 3rd. Clinical assessment of hyperlipidemic pancreatitis. *Am J Gastroenterol* 1995; **90**: 2134-2139
- 15 **Heinisch A**, Balle C, Kadow R. Plasmapheresis in severe acute pancreatitis-a new therapeutic option? *Gastroenterology* 1995; **108**: 359

Edited by Wang XL Proofread by Chen WW and Xu FM

Insulin is necessary for the hypertrophic effect of cholecystokinin-octapeptide following acute necrotizing experimental pancreatitis

Péter Hegyi, Zoltán Rakonczay Jr, Réka Sári, László Czakó, Norbert Farkas, Csaba Góg, József Németh, János Lonovics, Tamás Takács

Péter Hegyi, Zoltán Rakonczay Jr, Réka Sári, László Czakó, Norbert Farkas, Csaba Góg, József Németh, János Lonovics, Tamás Takács, First Department of Medicine, Faculty of Medicine, University of Szeged Szeged H6722, Hungary

Péter Hegyi, Zoltán Rakonczay Jr, School of Cell and Molecular Biosciences, Medical School, University of Newcastle, Newcastle upon Tyne, NE2 4HH, United Kingdom

Supported by The Wellcome Trust Grant No. 022618, and by the Hungarian Scientific Research Fund D42188, T43066 and T042589

Correspondence to: Péter Hegyi, M.D., Ph.D., University of Szeged, Faculty of Medicine, First Department of Medicine, PO Box 469, H-6701, Szeged, Hungary. hep@in1st.szote.u-szeged.hu

Telephone: +36-62-545-200 **Fax:** +36-62-545-185

Received: 2003-08-26 **Accepted:** 2003-09-05

Abstract

AIM: In previous experiments we have demonstrated that by administering low doses of cholecystokinin-octapeptide (CCK-8), the process of regeneration following L-arginine (Arg)-induced pancreatitis is accelerated. In rats that were also diabetic (induced by streptozotocin, STZ), pancreatic regeneration was not observed. The aim of this study was to deduce whether the administration of exogenous insulin could in fact restore the hypertrophic effect of CCK-8 in diabetic-pancreatic rats.

METHODS: Male Wistar rats were used for the experiments. Diabetes mellitus was induced by administering 60 mg/kg body mass of STZ intraperitoneally (i.p.), then, on d 8, pancreatitis was induced by 200 mg/100 g body mass Arg i.p. twice at an interval of 1 h. The animals were injected subcutaneously twice daily (at 7 a.m. and 7 p.m.) with 1 µg/kg of CCK-8 and/or 2 IU mixed insulin (300 g/L short-action and 700 g/L intermediate-action insulin) for 14 d after pancreatitis induction. Following this the animals were killed and the serum amylase, glucose and insulin levels as well as the plasma glucagon levels, the pancreatic mass/body mass ratio (pm/bm), the pancreatic contents of DNA, protein, amylase, lipase and trypsinogen were measured. Pancreatic tissue samples were examined by light microscopy on paraffin-embedded sections.

RESULTS: In the diabetic-pancreatic rats treatment with insulin and CCK-8 significantly elevated pm/bm and the pancreatic contents of protein, amylase and lipase vs the rats receiving only CCK-8 treatment. CCK-8 administered in combination with insulin also elevated the number of acinar cells with mitotic activities, whereas CCK-8 alone had no effect on laboratory parameters or the mitotic activities in diabetic-pancreatic rats.

CONCLUSION: Despite the hypertrophic effect of CCK-8 being absent following acute pancreatitis in diabetic-rats, the simultaneous administration of exogenous insulin

restored this effect. Our results clearly demonstrate that insulin is necessary for the hypertrophic effect of low-doses of CCK-8 following acute pancreatitis.

Hegy P, Rakonczay Jr Z, Sári R, Czakó L, Farkas N, Góg C, Németh J, Lonovics J, Takács T. Insulin is necessary for the hypertrophic effect of cholecystokinin-octapeptide following acute necrotizing experimental pancreatitis. *World J Gastroenterol* 2004; 10(15): 2275-2277

<http://www.wjgnet.com/1007-9327/10/2275.asp>

INTRODUCTION

We have previously demonstrated that the administration of low doses of cholecystokinin-octapeptide (CCK-8) accelerated the processes of regeneration following L-arginine (Arg)-induced pancreatitis^[1] and this was not observed in rats that were also diabetic^[2]. The most significant difference in the regeneration was observed after two wk of CCK-8 treatment^[1]. In addition, the histologic examination revealed that the majority of hypertrophized pancreatic acinar cells were found surrounding the enlarged islets of Langerhans following CCK-8 administration. It appears that the close proximity of the islets of Langerhans functions to protect the acinar cells as well as accelerate the regenerative process during Arg-evoked pancreatic tissue damage. A reason for this may be due to the interaction of acinar and islet cells. The exocrine and endocrine pancreas possesses a multitude of complex anatomical and functional interrelations^[3]. It is well documented that intact islets of Langerhans are necessary for normal pancreatic exocrine function^[4], and so we set out to investigate whether the administration of exogenous insulin could restore the hypertrophic effect of CCK in diabetic-pancreatic rats.

MATERIALS AND METHODS

Male Wistar rats weighing 250-300 g were divided into five groups. The animals were kept at a constant room temperature of 25 °C with a 12-h light-dark cycle, and were allowed free access to water and standard laboratory chow (Biofarm, Zagyvaszántó, Hungary). Rats in group D (diabetic -control group) were injected with 60 mg/kg body mass of streptozotocin (Zanosar[®], The Upjohn Company, Kalamazoo, MI) intraperitoneally (i.p.). In group DP (diabetic and pancreatic) the rats received STZ as in group D, and on d 8, pancreatitis was induced by 200 mg/100 g body mass Arg (Sigma, St. Louis, MO) i.p. twice at an interval of 1h. In group DPC, apart from being given Arg and STZ, the rats were also administered 1 µg/kg of CCK-8 (synthesized by Botond Penke, Department of Medical Chemistry University of Szeged) subcutaneously (s.c.) twice daily (at 7 a.m. and 7 p.m.). In group DPI, besides being administered Arg and STZ, the rats received 2 IU mixed insulin (300 g/L short-action and 700 g/L intermediate-action insulin, HUMULIN M3[®], Lilly Hungária Kft, Hungary) s.c. twice

Table 1 Laboratory parameters changes in diabetic-pancreatic rats due to a 14 d administration of insulin and/or CCK-8

	Serum glucose	Serum insulin	pm/bm	Pancreatic DNA	Pancreatic protein	Pancreatic amylase	Pancreatic trypsinogen	pancreatic lipase
Insulin treatment				-	-		-	-
CCK-8 treatment	-	-	-	-	-	-	-	-
Insulin and CCK-8 treatment				-				-

CCK-8: cholecystokinin-octapeptide, pm/bm: pancreatic weight/body weight ratio. increased or decreased activity/ level, - no change, significantly larger increase of activity compared with the sign. All changes are given in comparison to the untreated diabetic-pancreatic rats (group DP).

daily (at 7 a.m. and 7 p.m.). In group DPCI, diabetes and pancreatitis were induced as in group DP and the rats were administered CCK-8 and mixed insulin as mentioned before. The animals were killed in the morning by exsanguination through the abdominal aorta 14 d after pancreatitis induction. The serum amylase, glucose, insulin and plasma glucagon levels, pancreatic mass/body mass ratio (pm/bm), the pancreatic contents of DNA, protein, amylase, lipase and trypsinogen were measured^[2]. Pancreatic tissue samples were examined by light microscopy on paraffin-embedded sections. Results were expressed as mean±SE. Statistical analysis was performed by using ANOVA. *P* values <0.05 were accepted as significant.

RESULTS

In diabetic groups D, DP, and DPC, the serum glucose levels (22.5±1.5 mmol/L, 29.5±0.8 mmol/L and 29.0±0.7 mmol/L respectively) were significantly elevated and the insulin levels (0.70±0.30 U/l, 0.35±0.09 U/l and 0.20±0.05 U/l, respectively) were significantly lower vs those in insulin-treated groups DPI and DPCI (14.5±2.3 mmol/L and 12.9±2.8 mmol/L; 401±38 U/L and 138±35 U/L, respectively). These results clearly indicated the presence of diabetes mellitus in the animals studied and the efficacy of insulin treatment. There were no significant differences in plasma glucagon and serum amylase levels in group D as compared with any of the other groups. In groups DPI and DPCI, pm/bm (2.98±0.21 mg/g, 3.58±0.11 mg/g, respectively) was significantly elevated vs group DP (2.09±0.26 mg/g). However, no significant differences were observed in pm/bm between group DPC and group DP (2.62±0.26 mg/g and 2.09±0.26 mg/g, respectively). In group DPCI (insulin- and CCK-8-treated diabetic-pancreatic rats), the pancreatic protein content (250±35 mg/p) was significantly elevated vs groups DP and DPC (147±10 mg/p and 148±10 mg/p, respectively). In groups DPI and DPCI (insulin-treated rats), the pancreatic amylase content (3 948±1 288 U/p, 10 502±2 935 U/p, respectively) was significantly elevated vs groups DP and DPC (158±5 U/p and 182±25 U/p, respectively). In group DPCI, pancreatic amylase content (10 502±2 935 U/p) was significantly elevated vs group DPI (3 948±1 288 U/p). No significant differences were found in the pancreatic DNA and lipase contents between group D and any other groups. In group DPCI, the pancreatic trypsinogen content was significantly elevated vs group DPI (976±132 IU/p and 592±63 IU/p, respectively). However, no significant differences were observed in the pancreatic trypsinogen content between group DPC (655±36 IU/p) and DP (776±48 IU/p). Histological examination revealed signs of chronic inflammation in diabetic-pancreatic rats, where acute inflammatory cells had been replaced by interstitial tissues, mononuclear cells and fibroblasts. Histological examination did not show any differences between groups DPC and DP. In group DPCI, a more intense mitotic activity was observed vs group DPC due to the effect of insulin (Table 1).

DISCUSSION

The intraperitoneal administration of high doses of Arg induces selective pancreatic acinar cell damage without any morphological change to the islets of Langerhans^[5]. STZ has been reported to be specifically toxic to the β-cells of the islets of Langerhans and to induce a dose-dependent and irreversible diabetes in rats without any morphological change to the exocrine pancreas^[6]. These models seemed to be suitable for studying the correlation between diabetes mellitus and pancreatitis. The role of insulin in the process of spontaneous and CCK-8-promoted pancreatic regeneration following acute pancreatitis has not yet been characterised in detail. The interesting finding which showed that periinsular acini remained intact during Arg-induced-pancreatitis as well as a lack of the hypertrophic effect of CCK in diabetic rats prompted us to continue studies on the effects of insulin in the process of pancreatic remodelling. Our hypothesis stated that insulin was necessary for the regenerative effect of CCK-8, therefore, we evoked diabetes and pancreatitis in rats as described earlier^[2] and then, in the diabetic rats insulin was administered by s.c. injections. The elevation of serum insulin level and the diminution of serum glucose level, clearly showed the efficacy of the insulin treatment. CCK-8 could only elevate pw/bw, the pancreatic contents of protein, amylase and lipase in the presence of insulin. Moreover, CCK-8 could also increase the number of acinar cells with mitotic activity when insulin was administered, but CCK-8 alone had no effect on the laboratory parameters or the mitotic activity in diabetic-pancreatic rats. Lines of evidence demonstrate that both pancreatic secretory and growth processes are (at least partially) under the control of pancreatic islet hormones. Hypoinsulinemia was known to cause pancreatic atrophy and fat infiltration of the exocrine pancreas in guinea pigs^[7]. In contrast to this, endogenous and exogenous insulin evoked an increase in pancreatic enzyme synthesis and growth^[8]. These direct (via acinar insulin receptors) and indirect (influence on CCK receptors) effects of insulin are well understood. It was also demonstrated that insulin binding to its receptors on the pancreatic acini could be correlated with the subsequent stimulation of protein synthesis^[9]. Another indirect observation was that anti-insulin serum completely blocked the CCK-8-stimulated pancreatic secretion in rats^[10]. It further suggests that endogenous insulin is necessary for the stimulatory action of CCK-8 on pancreatic exocrine secretion and growth^[10]. The present study proves our hypothesis that insulin is indeed necessary for the hypertrophic effect of CCK-8 following acute necrotizing experimental pancreatitis.

REFERENCES

- 1 Hegyi P, Takacs T, Jarmay K, Nagy I, Czako L, Lonovics J. Spontaneous and cholecystokinin-octapeptide-promoted regeneration of the pancreas following L-arginine-induced pancreatitis in rat. *Int J Pancreatol* 1997; **22**: 193-200

- 2 **Takacs T**, Hegyi P, Jarmai K, Czako L, Gog C, Rakonczay Z, Nemeth J, Lonovics J. CCK fails to promote pancreatic regeneration in diabetic rats following the induction of experimental pancreatitis. *Pharm Res* 2001; **44**: 363-372
- 3 **Williams JA**, Goldfine ID. The insulin-acinar relationship. In: Go VLW et al. eds. *The Exocrine Pancreas: Biology, Pathobiology and Diseases*. New York: *Raven Press* 1993: 789-802
- 4 **Moessner J**, Logsdon CD, Williams JA, Goldfine ID. Insulin, via its own receptor, regulates growth and amylase synthesis in pancreatic acinar AR42J cells. *Diabetes* 1985; **34**: 891-897
- 5 **Tani S**, Itoh H, Okabayashi Y, Nakamura T, Fujii M, Fujisawa T, Koide M, Otsuki M. New model of acute necrotizing pancreatitis induced by excessive doses of arginine in rats. *Dig Dis Sci* 1990; **35**: 367-374
- 6 **Junod A**, Lambert AE, Orci L, Pictet R, Gonet AE, Renold AE. Studies on the diabetogenic action of streptozotocin. *Proc Soc Exp Biol Med* 1967; **126**: 201
- 7 **Balk MW**, Lang CM, White WJ, Munger BL. Exocrine pancreatic dysfunction in guinea pigs with diabetes mellitus. *Lab Invest* 1975; **32**: 28-32
- 8 **Saito A**, Williams JA, Kanno T. Potentiation of cholecystokinin-induced exocrine secretion by both exogenous and endogenous insulin in isolated and perfused rat pancreata. *J Clin Invest* 1980; **65**: 777-782
- 9 **Sankaran H**, Iwamoto Y, Korc M, Williams JA, Goldfine ID. Insulin action in pancreatic acini from streptozotocin-treated rats. II. Binding of ¹²⁵I-insulin to receptors. *Am J Physiol* 1981; **240**: G63-G68
- 10 **Lee KY**, Zhou LU, Ren XS, Chang TM, Chey WY. An important role of endogenous insulin on exocrine pancreatic secretion in rats. *Am J Physiol* 1990; **258**(2 Pt 1): G268-G274

Edited by Zhu LH **Proofread by** Xu FM

Effects of terlipressin on systolic pulmonary artery pressure of patients with liver cirrhosis: An echocardiographic assessment

Engin Altintas, Necdet Akkus, Ramazan Gen, M. Rami Helvacı, Orhan Sezgin, Dilek Oguz

Engin Altintas, Orhan Sezgin, Division of Gastroenterology, Mersin University, School of Medicine, Mersin, Turkey

Necdet Akkus, Cardiology Department, Mersin University, School of Medicine, Mersin, Turkey

Ramazan Gen, M. Rami Helvacı, Internal Medicine Department, Mersin University, School of Medicine, Mersin, Turkey

Dilek Oguz, Gastroenterology Department, Türkiye Yüksek İhtisas Hospital, Ankara, Turkey

Correspondence to: Dr. Engin Altintas, Mersin Üniversitesi Tıp Fakültesi Hastanesi İç Hastalıkları A.D., 33079 Mersin, Türkiye. enginaltintas@mersin.edu.tr

Telephone: +90-324337 43 00 **Fax:** +90-324336 7117

Received: 2004-03-03 **Accepted:** 2004-04-09

Abstract

AIM: Portopulmonary hypertension is a serious complication of chronic liver disease. Our aim was to search into the effect of terlipressin on systolic pulmonary artery pressure among cirrhotic patients.

METHODS: Twelve patients (6 males and 6 females) with liver cirrhosis were recruited in the study. Arterial blood gas samples were obtained in sitting position at rest. Contrast enhanced echocardiography and measurements of systolic pulmonary artery pressure were performed before and after the intravenous injection of 2 mg terlipressin.

RESULTS: Of 12 patients studied, the contrast enhanced echocardiography was positive in 5, and the positive findings in contrast enhanced echocardiography were reversed to normal in two after terlipressin injection. The mean systolic pulmonary artery pressure was 25.5 ± 3.6 mmHg before terlipressin injection, and was 22.5 ± 2.5 mmHg after terlipressin ($P=0.003$). The systolic pulmonary artery pressure was above 25 mmHg in seven of these 12 patients. After the terlipressin injection, systolic pulmonary artery pressure was <25 mmHg in four of these cases (58.3% vs 25%, $P=0.04$).

CONCLUSION: Terlipressin can decrease the systolic pulmonary artery pressure in patients with liver cirrhosis.

Altintas E, Akkus N, Gen R, Helvacı MR, Sezgin O, Oguz D. Effects of terlipressin on systolic pulmonary artery pressure of patients with liver cirrhosis: An echocardiographic assessment. *World J Gastroenterol* 2004; 10(15): 2278-2280
<http://www.wjgnet.com/1007-9327/10/2278.asp>

INTRODUCTION

The spectrum of pulmonary vascular disorders in liver disease and portal hypertension ranges from hepatopulmonary syndrome characterized by intrapulmonary vascular dilatations (IPVD) to pulmonary hypertension (portopulmonary hypertension), in which pulmonary vascular resistance is elevated^[1].

Hepatopulmonary syndrome (HPS) is incurable but resolves over time after liver transplantation^[2]. In patients with cirrhosis, 1% pulmonary hypertension is developed^[2,3]. Portopulmonary hypertension (PPH) is irreversible and there is no effective treatment^[4]. Mortality of liver transplantation in patients with PPH ranges from 50% to 100%^[4]. The common causes of HPS and PPH are portal hypertension and portosystemic shunting, indicating that vasoactive and angiogenic factors originating from the liver can control pulmonary circulation^[4].

So far, observational studies have examined several drugs^[5-8]. No clearly effective medical therapies for PPH have been found. In the present study, we investigated the effects of terlipressin that was used in the treatment of variceal hemorrhage on systolic pulmonary artery pressure (SPAP) among cirrhotic patients.

MATERIALS AND METHODS

Patients

Twelve cirrhotic patients without any malignancy, heart failure, renal failure (serum creatinin >20 mg/L), chronic obstructive lung disease, pneumonia, and anemia (hemoglobin level <100 mg/L) were studied. All patients had portal hypertension. The presence of hepatic dysfunction or portal hypertension was assessed by the following: (1) clinical history of complications related to liver disease and portal hypertension (ascites, hepatic encephalopathy, esophagogastric varices, variceal bleeding and spontaneous bacterial peritonitis); (2) liver function tests (aspartate and alanine aminotransferase, alkaline phosphatase, total bilirubin, prothrombin time, and albumin); and (3) abdominal ultrasound evidences of cirrhosis and portal hypertension (small, nodular liver, hepatofugal portal venous flow, portosystemic collateral circulation, splenomegaly, and ascites). The severity of hepatic dysfunction was stratified according to the Pugh-Child's criteria.

Methods

Chest X-ray and electrocardiogram were performed for all patients. Blood samples were obtained to calculate the score of Pugh-Child in the morning of study day. Arterial blood gas samples were obtained from a single radial artery puncture while the patient was breathing room air in sitting position at rest.

Transthoracic contrast-enhanced echocardiography (CEE) was performed to investigate the intrapulmonary vascular dilatations. CEE was performed after the administration of 10 mL of hand-agitated normal saline solution in the supine position via an upper extremity peripheral vein. Positive results were qualitatively defined as any visual opacification of the left heart chamber more than three cardiac cycles after appearance of microbubbles in the right ventricle^[9]. These findings suggested intrapulmonary passage of microbubbles through either dilated precapillary and capillary vessels or direct arteriovenous communications. Echocardiographic assessments were carried out with Wingmed system five 1.7 MHz electronic probe by an experienced cardiologist. Left lateral position was used during measurements. Left atrium, left ventricular diastolic and systolic dimensions were calculated with standard M-mode echocardiographic pictures in parasternal long axis view. Wall motions and wall thickness were also evaluated. Fractional

shortening was studied at level of chordae tendinae (left ventricular end diastolic dimension-left ventricular end systolic dimension/left ventricular end diastolic dimension $\times 100$). Each parameter represented the mean value of three successive measurements. Maximum flow rates with continuous wave Doppler (CW) at level of tricuspid valves were used to calculate SPAP (modified Bernoulli equation: $\Delta p=4V^2$). SPAPs were computed by adding estimated right atrial pressure (5 mmHg) to pressure gradient calculated by modified Bernoulli equation.

CEE and measurements of SPAP were performed before and after the intravenous injection of 2 mg terlipressin (Glypressin® 1 mg flacon, ERKIM Ilac AS, Istanbul, Turkey).

All statistical calculations were done using the SPSS 11.0 software. The measurements were given as the mean values. The paired sample test, Cochran's Q test, and Friedman's test were used to determine the difference of SPAP, the frequency of CEE, and the frequency of patients whose SPAP ≥ 25 mmHg respectively before and after terlipressin injection. $P < 0.05$ was accepted as statistically significant.

RESULTS

The clinical and demographical characteristics of patients are shown in Table 1. A total of 12 patients, six males and six females were studied, with a mean age of 52 years. The mean score of Pugh-Child was 5.08, and the mean value of arterial pO_2 was 77.83 mmHg. Ascites was detected in two patients. Two patients suffered from dyspnea. In two patients, chest X ray films showed bilaterally reticulonodular densities at the basal areas.

Before the injection of terlipressin intravenously, a positive CEE was detected in 5 patients, and two of them were disappeared after the drug was injected. Three of the patients who had evident hypoxemia suffered dyspnea, and CEE was positive in these patients. After terlipressin injection, CEE was negative in two of the three patients. Arterial pO_2 was high in the rest two patients with CEE (+), after terlipressin injection CEE positivity was continued. There was not any difference before and after the drug injection according to the frequency of the positivity of CEE (5/12 vs 3/12, $P=0.15$ according to Cochran's Q test). This meaningless result might be due to the small number of patients. The SPAP value was ≥ 25 mmHg in four of five patients with positive CEE. Two patients with a negative CEE after the drug injection had the lowest SPAP value in this group, 24 mmHg and 27 mmHg respectively.

Although the value of SPAP was 25.5 ± 3.6 mmHg before the drug injection, it was decreased to 22.5 ± 2.5 mmHg after

terlipressin injection ($P=0.003$). The value of SPAP was above the level of 25 mmHg as the limit of pulmonary hypertension in seven patients. After the injection of terlipressin, it continued to be higher above this level in three patients [7/12 (58.3%) patients versus 3/12 (25%) patients]. This difference was statistically significant ($P=0.04$). CEE was positive in one of the three patients whose SPAP was >25 mmHg after terlipressin injection. The positivity of CEE disappeared after terlipressin injection in one patient who had a SPAP value lower than 25 mmHg.

DISCUSSION

The association of pulmonary hypertension with portal hypertension, also known as portopulmonary hypertension (PPH), is a complication of chronic liver disease that has been associated with high morbidity and mortality at the time of liver transplantation^[2-4]. PPH has been defined as mean pulmonary artery pressure >25 mmHg in the presence of a normal pulmonary capillary wedge pressure and portal hypertension^[2-4].

The presence of intrapulmonary vascular dilatations can be confirmed using one of the three imaging modalities: contrast-enhanced echocardiography, perfusion lung scan - technetium 99 m-labeled macroaggregated albumin scanning, and pulmonary arteriography^[9,10]. A Doppler echocardiogram is a highly sensitive and noninvasive diagnostic modality for both measuring PAP and determining IPVD. Therefore, it should be considered as the first screening method of choice^[11].

Heretofore, therapy for chronic management of PPH is lacking. Recently, continuous intravenous infusion of epoprostenol has been demonstrated to improve symptomatology and survival in the general population of patients with PPH^[5]. Anecdotal reports suggested that long-term epoprostenol therapy given by continuous infusion might be effective for patients with portopulmonary hypertension, but the efficacy of epoprostenol has not been rigorously studied in this subgroup of patients^[5-7]. Kuo *et al.*^[5] reported the use of epoprostenol in the more specific instance of PPH. Over a period of 6-14 mo, epoprostenol (10-28 ng/kg.min) therapy was associated with a 29-46% decrease in mean pulmonary artery pressure, a 22-71% decrease in pulmonary vascular resistance, and a 25-75% increase in cardiac output in a group of four patients^[5]. These results suggest that effective chronic therapy for PPH is available. In combination with inhaled nitric oxide as acute intraoperative therapy, epoprostenol infusion represented an additional therapeutic option for treatment of PPH in the liver transplant candidate^[5].

Table 1 Characteristics of patients. PBS: primary biliary cirrhosis, HBV: hepatitis B virus, HCV: hepatitis C virus, N: Normal, BB-Nod: bilateral basillary nodularity, (-): absent, (+): present, PAP: pulmonary artery pressure and, CEE: contrast enhanced echocardiography

Sex	Age (yr)	Etiology	Pugh-Child Score	pO_2 (mmHg)	Ascites	Dyspnea	Chest X-ray	PAP-0 (mmHg)	PAP-1 (mmHg)	CEE-0	CEE-1
F	60	PBS	5	89	(-)	(-)	N	28	26	(+)	(+)
F	55	HBV	4	85	(-)	(-)	N	24	24	(-)	(-)
M	54	Alcohol	4	65	(-)	(+)	BB-Nod	27	21	(+)	(-)
F	48	Cryptogenic	5	60	(-)	(+)	N	24	20	(+)	(-)
M	58	HCV	4	63	(-)	(+)	N	28	24	(+)	(+)
M	56	HBV	4	73	(-)	(-)	N	25	25	(-)	(-)
M	52	HBV	5	88	(-)	(-)	N	30	22	(+)	(+)
F	50	HBV	10	90	(+)	(+)	BB-Nod	31	26	(-)	(-)
M	48	HCV	5	85	(-)	(-)	N	21	22	(-)	(-)
M	60	HBV	7	80	(+)	(-)	N	20	19	(-)	(-)
F	55	HCV	4	71	(-)	(-)	N	27	22	(-)	(-)
F	39	HBV	4	85	(-)	(-)	N	21	19	(-)	(-)

There are no long-term studies or guidelines on the use of pharmacotherapy in PPH. In view of the rarity of this disease, much of the traditional treatment of this disease has been empirical. Inhaled NO could decrease the pulmonary artery pressures in some patients with PPH and might have some promise for long-term treatment of this disease^[12]. Other medications have been reported to cause amelioration of pulmonary hypertension in patients with portal hypertension including beta-blockers, nitrates, calcium-channel blockers, prostacyclin and prostacyclin analogs, phosphodiesterase inhibitors (sildenafil), L-arginine, and, endothelin antagonists^[3]. In view of the decreased incidence of variceal bleeding in patients taking beta-blockers and nitrates, we encourage the use of these medications in patients with PPH. Beta-blocking agents, which are used in the treatment for portal hypertension may have deleterious effects on the setting of pulmonary hypertension because they decrease cardiac output and increase pulmonary vascular resistance. Vasodilators are usually ineffective and poorly tolerated because these patients usually have a decreased systemic vascular resistance. Most patients with porto-pulmonary hypertension do not receive anticoagulants because the risk of bleeding is deemed to be elevated, especially when esophageal varices are present.

In patients with hepatopulmonary syndrome, supplemental oxygen and liver transplantation were the usual treatments of choice^[2]. Pharmacologic approaches were limited in improving hypoxemia^[2]. Outcome following liver transplantation was variable, increased cardiopulmonary mortality occurred in patients with moderate to severe pulmonary hypertension. Although a few reports have demonstrated improvement of pulmonary hypertension after liver transplantation, this procedure was a very risky one in patients with markedly increased pulmonary artery pressures^[13]. Report about combined liver-lung transplantation might open a perspective for selected patients with porto-pulmonary hypertension^[14].

Terlipressin is a long-acting vasopressin analogue that has been proved useful in the treatment of variceal hemorrhage. Terlipressin could reduce portal pressure in cirrhotic patients mainly through intense splanchnic vasoconstriction that decreases portal venous inflow^[15]. Hepatic blood flow might also be reduced by terlipressin^[15]. The systemic haemodynamic response to terlipressin was moreover associated with the decrease in portal pressure^[16]. After administration of terlipressin, the azygos blood flow decreased significantly^[17]. In patients with cirrhosis, a single injection of 2 mg terlipressin significantly and markedly reduced portal pressure and azygos blood flow for up to 4 h^[17]. The azygos blood flow (superior porto-systemic collateral circulation) correlated strongly with portal venous flow in patients with portal hypertension^[17]. It could be expected that terlipressin could reverse the vasodilatation of dilated intrapulmonary arteries with HPS and PPH. It can also decrease SPAP by reducing the increased blood flow that may facilitate pulmonary arterial hypertension. In our study, it reduced SPAP from 25.5±3.6 mmHg to 22.5±2.5 mmHg and, this result was statistically meaningful. CEE that showed intrapulmonary vascular dilatation was positive in 5 patients, and it was reversed to normal in 2 patients after terlipressin injection. However, more studies are needed to decide whether this result is meaningful or not.

Chronic terlipressin therapy in combination with a multidisciplinary, well-planned evaluation and treatment plan, may be the answer to a heretofore untreatable disease. This one is a prestudy, because more and detailed studies are

required to show its efficiency. In the context of persisting uncertainty about the cause and treatment of PPH, future studies must focus on the pathophysiology of PPH, predicting reversibility after liver transplantation, and identifying other treatment options.

REFERENCES

- 1 **Hervé P**, Lebrec D, Brenot F, Simonneau G, Humbert M, Sitbon O, Duroux P. Pulmonary vascular disorders in portal hypertension. *Eur Respir J* 1998; **11**: 1153-1166
- 2 **Krowka MJ**. Hepatopulmonary syndrome and portopulmonary Hypertension. *Curr Treat Options Cardiovasc Med* 2002; **4**: 267-273
- 3 **Budhiraja R**, Hassoun PM. Portopulmonary hypertension; A tale of two circulations. *Chest* 2003; **123**: 562-576
- 4 **Naaije R**. Hepatopulmonary syndrome and portopulmonary hypertension. *Swiss Med Wkly* 2003 Mar 22; **133**: 163-169
- 5 **Kuo PC**, Johnson LB, Plotkin JS, Howell CD, Bartlett ST, Rubin LJ. Continuous intravenous infusion of epoprostenol for the treatment of portopulmonary hypertension. *Transplantation* 1997; **63**: 604-606
- 6 **Rafanan AL**, Maurer J, Mehta AC, Schilz R. Progressive portopulmonary hypertension after liver transplantation treated with epoprostenol. *Chest* 2000; **118**: 1497-1500
- 7 **Schroeder RA**, Rafii AA, Plotkin JS, Johnson LB, Rustgi VK, Kuo PC. Use of aerosolized inhaled epoprostenol in the treatment of portopulmonary hypertension. *Transplantation* 2000; **70**: 548-550
- 8 **Krowka MJ**, Plevak DJ, Findlay JY, Rosen CB, Wiesner RH, Krom RA. Pulmonary hemodynamics and perioperative cardiopulmonary-related mortality in patients with portopulmonary hypertension undergoing liver transplantation. *Liver Transpl* 2000; **6**: 443-450
- 9 **Krowka MJ**, Tajik AJ, Dickson ER, Wiesner RH, Cortese DA. Intrapulmonary vascular dilatations in liver transplant candidates: screening by two-dimensional contrast enhanced echocardiography. *Chest* 1990; **97**: 1165-1170
- 10 **Lange PA**, Stoller JK. The hepatopulmonary syndrome. *Ann Intern Med* 1995; **22**: 521-529
- 11 **Torregrosa M**, Genesca J, Gonzalez A, Evangelista A, Mora A, Margarit C, Esteban R, Guardia J. Role of Doppler echocardiography in the assessment of portopulmonary hypertension in liver transplantation candidates. *Transplantation* 2001; **71**: 572-574
- 12 **Findlay JY**, Harrison BA, Plevak DJ, Krowka MJ. Inhaled nitric oxide reduces pulmonary artery pressures in portopulmonary hypertension. *Liver Transpl Surg* 1999; **5**: 381-387
- 13 **Krowka MJ**, Plevak DJ, Findlay JY, Rosen CB, Wiesner RH, Krom RA. Pulmonary hemodynamics and perioperative cardiopulmonary-related mortality in patients with portopulmonary hypertension undergoing liver transplantation. *Liver Transpl* 2000; **6**: 443-450
- 14 **Pirene J**, Verleden G, Nevens F, Delcroix M, Van Raemdonck D, Meyns B, Herijgers P, Daenen W, De Leyn P, Aerts R, Coosemans W, Decaluwe H, Koek G, Vanhaecke J, Schetz M, Verhaegen M, Cicalese L, Benedetti E. Combined liver and (heart-) lung transplantation in liver transplant candidates with refractory portopulmonary hypertension. *Transplantation* 2002; **73**: 140-142
- 15 **Oberti F**, Veal N, Kaassis M, Pilette C, Rifflet H, Trouve R, Cales P. Hemodynamic effects of terlipressin and octreotide administration alone or in combination in portal hypertensive rats. *J Hepatol* 1998; **29**: 103-111
- 16 **Moller S**, Hansen EF, Becker U, Brinch K, Henriksen JH, Bendtsen F. Central and systemic haemodynamic effects of terlipressin in portal hypertensive patients. *Liver* 2000; **20**: 51-59
- 17 **Escorsell A**, Bandi JC, Moitinho E, Feu F, Garcia-Pagan JC, Bosch J, Rodes J. Time profile of the haemodynamic effects of terlipressin in portal hypertension. *J Hepatol* 1997; **26**: 621-627

Empirical antibiotic treatment with piperacillin-tazobactam in patients with microbiologically-documented biliary tract infections

Gabrio Bassotti, Fabio Chistolini, Francis Sietchiping-Nzepa, Giuseppe de Roberto, Antonio Morelli

Gabrio Bassotti, Fabio Chistolini, Francis Sietchiping-Nzepa, Giuseppe de Roberto, Antonio Morelli, Gastrointestinal and Hepatology Section, Department of Clinical and Experimental Medicine, University of Perugia, Italy

Correspondence to: Dr. Gabrio Bassotti, Strada del Cimitero, 2/a, San Marco 06131 Perugia, Italy. gabassot@tin.it

Fax: +39-75-5847570

Received: 2003-11-26 **Accepted:** 2004-01-17

Abstract

AIM: To report our experience with empiric antimicrobial monotherapy (piperacillin/tazobactam, of which no data are available in such specific circumstances) in microbiologically-documented infections in patients with benign and malignant conditions of the biliary tract.

METHODS: Twenty-three patients, 10 with benign and 13 with malignant conditions affecting the biliary tree and microbiologically-documented infections were recruited and the efficacy of empirical antibiotic therapy was assessed.

RESULTS: The two groups featured similar demographic and clinical data. Overall, the infective episodes were most due to Gram negative agents, more than 60% of such episodes (mostly in malignant conditions) were preceded by invasive instrumental maneuvers. Empirical antibiotic therapy with a single agent (piperacillin/tazobactam) was effective in more than 80% of cases. No deaths were reported following infections.

CONCLUSION: An empiric therapeutic approach with piperacillin/tazobactam is highly effective in biliary tract infections due to benign or malignant conditions.

Bassotti G, Chistolini F, Sietchiping-Nzepa F, de Roberto G, Morelli A. Empirical antibiotic treatment with piperacillin-tazobactam in patients with microbiologically-documented biliary tract infections. *World J Gastroenterol* 2004; 10(15): 2281-2283
<http://www.wjgnet.com/1007-9327/10/2281.asp>

INTRODUCTION

The common causes of intra-abdominal infections are those related to the biliary tract^[1]. However, to obtain a microbiological diagnosis in biliary tract infections (BTI) is not easy, due to the difficulty of sampling bile and the low incidence of positive blood cultures. Therefore, antimicrobial therapy is often empirical^[2], and the choice of an appropriate regimen depends on the knowledge of the most common causative bacteria and the reported efficacy of antimicrobial drugs in BTI. Moreover, the paucity of randomized clinical trials for BTI treatment probably justifies the fact that there is no standardized approach to these infections^[2].

The present study was to report our experience with empirical single antibiotic treatment with piperacillin-tazobactam of BTI in patients with benign and malignant diseases of the biliary tract, since there are no specific data on this compound in the treatment of such infections.

MATERIALS AND METHODS

Twenty-three consecutive patients (15 men, 8 women, age range 22-88 years) with microbiologically documented BTI entered the study. Underlying disease and causative organisms were assessed. Empirical treatment (4.5 g t.i.d) was started immediately after obtaining samples (blood and/or bile) for microbiological cultures, and concordance with antibiogram and its efficacy were also evaluated. The treatment was judged effective when fever and clinical symptoms of infection resolved within 72 h, whereas the persistence of fever beyond 72 h from the start of treatment, the deterioration of clinical conditions or the death as a result of the primary infection was considered as failure.

RESULTS

Overall, records were obtained from 10 patients with benign and 13 patients with malignant conditions affecting the biliary tree. Table 1 shows the clinical characteristics of the two groups. In more than 60% of patients, BTI were preceded by an invasive procedure on the biliary tree, and this was less frequent in benign than in malignant conditions (50% vs 77%).

Table 1 Demographic and clinical variables of 23 patients with BTI

	Benign conditions	Malignant conditions
No (%)	10/23(43.5)	13/23(56.5)
Average duration of treatment (d)	7±1	10±1
Underlying condition (No.)	Cholelithiasis (7) Acute cholecystitis (2) Iatrogenic stenosis (1)	Cholangiocarcinoma (6) Pancreatic carcinoma (4) Gallbladder carcinoma (2) Infiltrating hepatoma (1)
Previous instrumental invasive maneuvers (No)	None (5) PTD (3) ERCP (2)	None (3) PTD (10)

Abbreviations: BTI=biliary tract infections; ERCP=endoscopic retrograde cholangio-pancreatography; PTD=percutaneous transhepatic drainage.

Table 2 Microbiological variables in 23 patients with BTI

	Benign conditions (10 patients)	Malignant conditions (13 patients)
Insulation medium (No.)	Blood (7) Bile (3)	Blood (6) Bile (7)
Polymicrobial infections	1 (4%)	7 (30%)
Isolated pathogens (No. cases)	<i>E.coli</i> (4) Enterococcus spp (3) Pseudomonas spp (3) Enterobacter spp (2) Streptococcus spp (2) Klebsiella spp (1) Candida spp (1)	Enterococcus spp (6) Staphylococcus spp (6) Candida spp (5) <i>E.coli</i> (2) Pseudomonas spp (2) Proteus spp (1) Enterobacter spp (1) Salmonella spp (1)

Table 2 shows the microbiological characteristics of the pathogens isolated in both groups. As expected, most infections were caused by Gram negative agents, and 30% of them (almost exclusively found in malignant conditions) were polymicrobial. *Candida spp* were always isolated from bile in polymicrobial infections. In 19(82.6%) patients there was no need of modifying the empiric therapeutic schedule, whereas in the remaining 4 the antibiotic regimen was modified according to the antibiogram showing resistance or insensitivity to piperacillin/tazobactam. In all patients with BTI due to benign conditions, decrease of fever and improvement of clinical conditions were observed within 3-18 h. A slower trend was observed in patients with BTI due to malignant conditions (improvement within 8-24 h), probably due to more polymicrobial infections and resistances to the empiric regimen. After the results from the antibiogram were obtained, these latter patients treated with more targeted antibiotic regimens, had the disappearance of fever and improvement of the clinical conditions. No deaths were reported attributable to BTI.

DISCUSSION

In this study, we reported our experience with an empiric antibiotic regimen in BTI, and showed that a monotherapy with piperacillin/tazobactam (that, to the best of our knowledge has still not been assessed in such circumstances) might be effective in more than 80% of cases. The organisms more commonly cultured in our patients, in both benign and malignant conditions, were Gram negative bacteria, the pathogens were more frequently associated with obstructive conditions of the biliary tree^[3,4]. Several infective episodes followed invasive instrumental procedures, especially percutaneous drainage (that also gave a discrete yield for bile culture, as previously shown for this procedure^[5]), and were mostly represented by polymicrobial infections.

A preferred therapeutic schedule for BTI, until recently, was usually a combination of a penicillin (usually ampicillin) and an aminoglycoside^[6-9]. This combination had limited anaerobic coverage, frequent resistance (to ampicillin) of Gram negative bacteria, and the risks of renal damage (aminoglycoside, significantly increased in patients with cholestasis)^[10]. However, other antibiotics (such as the ureidopenicillins) exhibited a broad spectrum of activity, that included many anaerobes, *enterococci* and *P.aeruginosa*, in addition to Gram negative bacilli^[11], so that they may result in appealing for use as single agents. Actually, it has been shown that monotherapy with a ureidopenicillin (mezlocillin, piperacillin) is equally or more effective than the traditional approach with ampicillin/aminoglycoside for treatment of BTI^[12-14], although in patients undergoing nonsurgical invasive procedure of the biliary tree and/or with suspected increased risk of *P.aeruginosa* the association of ureidopenicillin/aminoglycoside has been still

justifiable^[15,16]. On the other hand, the combination of piperacillin with the beta-lactamase inhibitor tazobactam (that displays a substantial elimination in bile^[17,18]) might be a reasonable alternative when the local resistance pattern featured a high incidence of ureidopenicillin-resistant *E.coli* or *Klebsiella spp*^[2,19], as also shown by its effectiveness as single empiric agent in high-risk, febrile neutropenic patients with cancer^[20].

Experience with quinolones for treatment of BTI was still limited^[2,21]. However, there is good evidence that monotherapy with these compounds might be as effective as combination therapy for treatment of BTI^[22-24].

To date, the combination of piperacillin/tazobactam has been demonstrated clinically- and cost-effective in both uncomplicated and complicated intraabdominal infections^[25-27], although no specific data on BTI are available. Therefore, we feel that our experience might be a useful adjunct to the therapeutic armamentarium.

In conclusion, empiric antibiotic treatment with piperacillin/tazobactam is frequently effective in BTI due to benign and malignant conditions. Of course, in such circumstances an early operative drainage of the biliary tree is always mandatory, regardless of the presence or absence of suppuration in the common bile duct^[28], to prevent relapses and septic complications.

REFERENCES

- 1 **Lea AS**, Feliciano DV, Gentry DO. Intra-abdominal infections -an update. *J Antimicrob Chemother* 1982; **9**(Suppl A): 107-113
- 2 **Westphal JF**, Brogard JM. Biliary tract infections. A guide to drug treatment. *Drugs* 1999; **57**: 81-91
- 3 **Leung JW**, Ling TK, Chan RC, Cheung SW, Lai CW, Sung JJ, Chung SC, Cheng AF. Antibiotics, biliary sepsis, and bile duct stones. *Gastrointest Endosc* 1994; **40**: 716-721
- 4 **Carpenter HA**. Bacterial and parasitic cholangitis. *Mayo Clin Proc* 1998; **73**: 473-478
- 5 **Brody LA**, Brown KT, Getrajdman GI, Kannegieter LS, Brown AE, Fong Y, Blumgart LH. Clinical factors associated with positive bile cultures during primary percutaneous biliary drainage. *J Vasc Interv Radiol* 1998; **9**: 572-578
- 6 **Boey JH**, Way LW. Acute cholangitis. *Ann Surg* 1980; **191**: 264-270
- 7 **Thompson JE**, Tomkins RK, Longmire WP. Factors in management of acute cholangitis. *Ann Surg* 1982; **195**: 137-145
- 8 **Munro R**, Sorrell TC. Biliary sepsis: reviewing treatment options. *Drugs* 1986; **31**: 449-454
- 9 **Chang WT**, Lee KT, Wang SR, Chuang SC, Kuo KK, Chen JS, Sheen PC. Bacteriology and antimicrobial susceptibility in biliary tract disease: an audit of 10-year's experience. *Kaohsiung J Med Sci* 2002; **18**: 221-228
- 10 Desai TK, Tsang TK. Aminoglycoside nephrotoxicity in obstructive jaundice. *Am J Med* 1988; **85**: 47-50
- 11 **Eliopoulos GM**, Moellering RC. Azlocillin, mezlocillin and piperacillin: new broad spectrum penicillins. *Ann Intern Med* 1982; **97**: 755-760

- 12 **Muller EL**, Pitt HA, Thompson JE, Doty JE, Mann LL, Manchester B. Antibiotics in infections of the biliary tract. *Surg Gynecol Obstet* 1987; **165**: 285-292
- 13 **Gerecht WB**, Henry NK, Hoffman WW, Muller SM, LaRusso NF, Rosenblatt JE, Wilson WR. Prospective randomized comparison of mezlocillin therapy alone with combined ampicillin and gentamicin therapy for patients with cholangitis. *Arch Intern Med* 1989; **149**: 1279-1284
- 14 **Thompson JE**, Pitt HA, Doty JE, Coleman J, Irving C. Broad spectrum penicillins as an adequate therapy for acute cholangitis. *Surg Gynecol Obstet* 1990; **171**: 275-282
- 15 **Levine JG**, Botet J, Kurtz RC. Microbiological analysis of sepsis complicating non-surgical biliary drainage in malignant obstruction. *Gastrointest Endosc* 1990; **36**: 364-368
- 16 **Demediuk B**, Speer AG, Hellyar A. Induced antibiotic resistant bacteria in cholangitis with biliary sepsis. *Aust N Z J Surg* 1996; **66**: 778-780
- 17 **Sörgel F**, Kinzig M. Pharmacokinetic characteristics of piperacillin/tazobactam. *Intensive Care Med* 1994; **20**: S14-S20
- 18 **Westphal JF**, Brogard JM, Caro-Sampara F, Adloff M, Blickle JF, Monteil H, Jehl F. Assessment of the biliary excretion of piperacillin-tazobactam in humans. *Antimicrob Agents Chemother* 1997; **41**: 1636-1640
- 19 **Chamberland S**, L'Ecuyer J, Lessard C, Bernier M, Provencher P, Bergeron MG. Antibiotic susceptibility profiles of 941 gram-negative bacteria isolated from septicemic patients throughout Canada. *Clin Infect Dis* 1992; **15**: 615-628
- 20 **Del Favero A**, Menichetti F, Martino P, Bucaneve G, Micozzi A, Gentile G, Furno P, Russo D, D'Antonio P, Ricci P, Martino B, Mandelli F. A multicenter, double-blind, placebo-controlled trial comparing piperacillin-tazobactam with and without amikacin as empiric therapy for febrile neutropenia. *Clin Infect Dis* 2001; **33**: 1295-1301
- 21 **Westphal JF**, Blicklé JF, Brogard JM. Management of biliary tract infections: potential role of quinolones. *J Antimicrob Chemother* 1991; **28**: 486-490
- 22 **Sung JJ**, Lyon DJ, Suen R, Chung SC, Co AL, Cheng AF, Leung JW, Li AK. Intravenous ciprofloxacin as treatment for patients with acute suppurative cholangitis: a randomized, controlled clinical trial. *J Antimicrob Chemother* 1995; **35**: 855-864
- 23 **Karachalios GN**, Nasiopoulou DD, Bourlinou PK, Reppa A. Treatment of acute biliary tract infections with ofloxacin: a randomized, controlled clinical trial. *Int J Clin Pharmacol Ther* 1996; **34**: 555-557
- 24 **Rekhnimitr R**, Fogel EL, Kalayci C, Esber E, Lehman GA, Sherman S. Microbiology of bile in patients with cholangitis or cholestasis with and without plastic biliary endoprosthesis. *Gastrointest Endosc* 2002; **56**: 885-889
- 25 **Cohn SM**, Lipsett PA, Buchman TG, Cheadle WG, Milsom JW, O'Marro S, Yellin AE, Jungerwirth S, Rochefort EV, Haverstock DC, Kowalsky SF. Comparison of intravenous/oral ciprofloxacin plus metronidazole versus piperacillin/tazobactam in the treatment of complicated intraabdominal infections. *Ann Surg* 2000; **232**: 254-262
- 26 **Dietrich ES**, Schubert B, Ebner W, Daschner F. Cost efficacy of tazobactam/piperacillin versus imipenem/cilastatin in the treatment of intra-abdominal infection. *Pharmacoeconomics* 2001; **19**: 79-94
- 27 **Holzheimer RG**, Dralle H. Antibiotic therapy in intra-abdominal infections - a review on randomised clinical trials. *Eur J Med Res* 2001; **30**: 277-291
- 28 **Connor MJ**, Schwartz ML, McQuarrie DG, Sumer HW. Acute bacterial cholangitis: an analysis of clinical manifestations. *Arch Surg* 1982; **117**: 437-444

Edited by Wang XL Proofread by Xu FM

Determination of glycosylated hemoglobin in patients with advanced liver disease

Theresa Lahousen, Karin Hegenbarth, Rottraut Ille, Rainer W. Lipp, Robert Krause, Randie R. Little, Wolfgang J. Schnedl

Karin Hegenbarth, Rainer W. Lipp, Robert Krause, Wolfgang J. Schnedl, Department of Internal Medicine, School of Medicine, Medical University Graz, Auenbruggerplatz 15, A-8063 Graz, Austria
Theresa Lahousen, Rottraut Ille, Department of Psychiatry, School of Medicine, Medical University Graz, Auenbruggerplatz 31, A-8063 Graz, Austria

Randie R. Little, University of Missouri School of Medicine, Department of Pathology and Child Health, One Hospital Drive, Columbia, MO 65212, USA

Correspondence to: Dr. Wolfgang J. Schnedl, Department of Internal Medicine, Medical University Graz, Auenbruggerplatz 15, A-8036 Graz, Austria. wolfgang.schnedl@meduni-graz.at

Telephone: +43-316-385-81801 **Fax:** +43-316-385-3062

Received: 2004-02-23 **Accepted:** 2004-04-09

Abstract

AIM: To evaluate the glycosylated hemoglobin (HbA_{1c}) determination methods and to determine fructosamine in patients with chronic hepatitis, compensated cirrhosis and in patients with chronic hepatitis treated with ribavirin.

METHODS: HbA_{1c} values were determined in 15 patients with compensated liver cirrhosis and in 20 patients with chronic hepatitis using the ion-exchange high performance liquid chromatography and the immunoassay methods. Fructosamine was determined using nitroblue tetrazolium.

RESULTS: Forty percent of patients with liver cirrhosis had HbA_{1c} results below the non-diabetic reference range by at least one HbA_{1c} method, while fructosamine results were either within the reference range or elevated. Twenty percent of patients with chronic hepatitis (hepatic fibrosis) had HbA_{1c} results below the non-diabetic reference range by at least one HbA_{1c} method. In patients with chronic hepatitis treated with ribavirin, 50% of HbA_{1c} results were below the non-diabetic reference using at least one of the HbA_{1c} methods.

CONCLUSION: Only evaluated in context with all liver function parameters as well as a red blood count including reticulocytes, HbA_{1c} results should be used in patients with advanced liver disease. HbA_{1c} and fructosamine measurements should be used with caution when evaluating long-term glucose control in patients with hepatic cirrhosis or in patients with chronic hepatitis and ribavirin treatment.

Lahousen T, Hegenbarth K, Ille R, Lipp RW, Krause R, Little RR, Schnedl WJ. Determination of glycosylated hemoglobin in patients with advanced liver disease. *World J Gastroenterol* 2004; 10(15): 2284-2286

<http://www.wjgnet.com/1007-9327/10/2284.asp>

INTRODUCTION

Measurement of glycosylated hemoglobin (HbA_{1c}) is used for routine evaluation and management of patients with diabetes mellitus. Concentrations of HbA_{1c} provide a means of assessing

long-term glycemic status and correlate well with development of complications related to diabetes mellitus^[1,2]. The liver plays a major role in regulating glucose metabolism because it is the main source of endogenous glucose and a major site involved in insulin metabolism. Because liver disease is associated with an increased prevalence of impaired glucose tolerance and diabetes mellitus, there is a need for tools to measure its long-term glycemic control^[3]. Previous studies indicated that both HbA_{1c} and fructosamine measurement should not be used in patients with liver cirrhosis, although the reason for this was unclear^[4-6]. Shortened erythrocyte life span as in hemolytic anemia is known to cause clinically and analytically low HbA_{1c} values independent of glycemia^[7], but measurement of fructosamine, which has been used to document glycemic status over a period of 2-4 wk, should not be affected by erythrocyte life span. This study described the determination of HbA_{1c} and fructosamine as well as parameters of liver disease and anemia in patients with advanced liver disease.

MATERIALS AND METHODS

Blood samples were collected, with and without EDTA, from 15 consecutive patients with compensated liver cirrhosis and 20 patients with chronic hepatitis and fibrosis of the liver. Diagnostic liver biopsies were performed routinely in all patients during the course of treatment in the Division of Gastroenterology and Hepatology, Department of Internal Medicine, Medical University in Graz. Liver cirrhosis was histologically defined as a diffuse process characterized by fibrosis and the conversion of normal liver architecture into structurally abnormal nodules^[8,9]. Of 15 patients with compensated liver cirrhosis Child-Pugh class A (total bilirubin <2 mg/dL, serum albumin >3.5 g/dL, prothrombin time 1-4 s prolonged, no hepatic encephalopathy and no ascites), 6 were tested positive for hepatitis C, 8 had alcoholic liver disease and 1 had primary biliary cirrhosis. Of the 20 patients with chronic hepatitis and fibrosis, 19 were tested positive for hepatitis C and 1 suffered from alcoholic liver disease. Ten of these patients with chronic hepatitis C were treated with interferon- α plus the antiviral drug ribavirin that can cause reversible hemolytic anemia^[10]. None of the patients included in the study had a history of impaired glucose tolerance or diabetes mellitus.

HbA_{1c} was measured within 3 d of collection using the Hi-Auto A_{1c} HA-8140 HPLC (Menarini Diagnostics, Florence, Italy), the DCA 2000 immunoassay method (Bayer, Vienna, Austria) and the Roche Cobas Integra immunoassay method (Roche, Vienna, Austria). Each of these HbA_{1c} methods was certified by the National Glycohemoglobin Standardization Program (NGSP)^[11]. Routine hematological data were determined with a Coulter counter (Beckman, Vienna, Austria). Blood glucose was determined with a hexokinase/glucose-6-phosphate dehydrogenase colorimetric method (Gluco-Quant; Roche, Vienna, Austria) and used as mean of 4-6 measurements on separate days during the preceding 1 mo. The relationship of blood glucose and HbA_{1c} was calculated according to MBG (mmol/L)=(1.98·HbA_{1c})-4.29^[12]. Fructosamine was determined with a colorimetric test that uses nitroblue tetrazolium in alkaline solution (Unimate FRA; Roche, Vienna, Austria). Reference

ranges were provided by each manufacturer and in most cases represented the mean \pm 2SD of a population without known diabetes. All determinations were analyzed blindly and the procedures were in accordance with the declaration of Helsinki and the local ethics committee recommendations.

RESULTS

Forty percent (6/15) of the patients with liver cirrhosis had HbA_{1c} levels below the non-diabetic reference range with at least one HbA_{1c} method, while fructosamine concentrations were either within the reference range ($n=10$) or elevated ($n=5$) (Figure 1). Twenty percent (2/10) of the patients with chronic hepatitis had HbA_{1c} levels below the non-diabetic reference range with at least one HbA_{1c} method. Fructosamine concentrations of all the 10 patients with chronic hepatitis were below the non-diabetic reference range. In patients with chronic hepatitis treated with ribavirin, 50% (5/10) of HbA_{1c} levels were below the non-diabetic reference range detected by at least one of the HbA_{1c} methods (Figure 1). One patient in this group demonstrated a fructosamine concentration within the diabetic range.

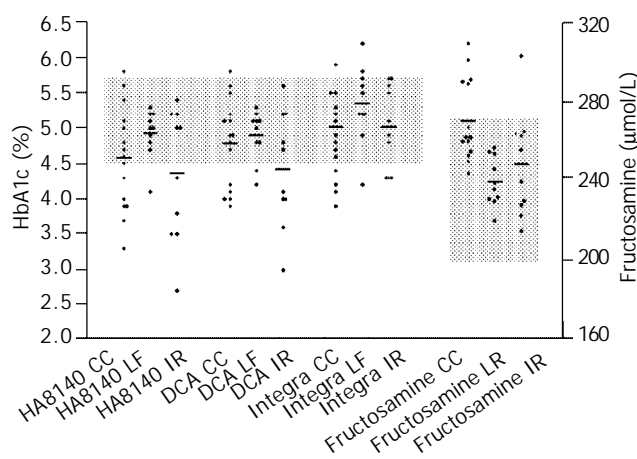


Figure 1 HbA_{1c} level and fructosamine concentration in patients with liver disease. CC: Compensated cirrhosis; LF: Chronic hepatitis (liver fibrosis); IR: Chronic hepatitis with interferon and ribavirin treatment. Shaded areas represent the mean \pm 2SD reference range for each test (HbA_{1c}: 4.5-5.7%; fructosamine: 200-272 μ mol/L).

Table 1 shows the percentage of patients in each group

(cirrhosis, chronic hepatitis, chronic hepatitis with interferon and ribavirin treatment) that the levels of erythrocyte, hematocrit and hemoglobin were below the normal range, and reticulocyte counts above the normal range. Although 30-53% of the patients with cirrhosis and chronic hepatitis demonstrated moderate anemia, none had a reticulocyte count within normal. All of those with low HbA_{1c} also demonstrated anemia but some patients with anemia did not have low HbA_{1c}. Seventy to eighty percent of the patients with chronic hepatitis treated with ribavirin demonstrated moderate anemia and 30% also had high reticulocyte counts (Table 1). All of those with high reticulocyte counts, as well as some of those with anemia and normal reticulocyte counts, had below-normal HbA_{1c}. This study showed elevated reticulocytes, which might be a sign of shortened erythrocyte life span, in only 3 patients with chronic hepatitis and ribavirin treatment. In these patients HbA_{1c} was below the non-diabetic reference range on all methods. We also found HbA_{1c} values below the non-diabetic reference range in up to 40% of the patients with liver cirrhosis and in 50% of the patients with chronic hepatitis treated with ribavirin as measured by at least one of the HbA_{1c} methods. In these groups of patients the HbA_{1c} levels were negatively correlated to the percentage of reticulocytes (Pearson correlation, $r=-0.55$ to -0.79 depending on method, $P<0.05$ for all methods). There was no significant relationship between HbA_{1c} and reticulocyte count in the patients with chronic hepatitis and no ribavirin therapy.

We performed an one-sample *t*-test comparing mean blood glucose calculated of HbA_{1c} results (MBG (mmol/L) = $(1.98 \cdot \text{HbA}_{1c}) - 4.29$) and measured blood glucose as the actual value. HbA_{1c} results of the HPLC Menarini HA-8140 and the immunoassay method DCA 2000 were used to calculate a desired blood glucose value because in Pearson correlation they did not correlate with blood glucose. In patients with chronic hepatitis treated with ribavirin the one sample *t*-test for measured blood glucose and calculated blood glucose resulted in a significant difference ($t_{9\text{Menarini}}=7.68$, $P<0.05$; $t_{9\text{DCA}}=6.67$, $P<0.05$). In patients with liver cirrhosis calculated blood glucose was up to 1 mmol/L lower than measured blood glucose but a high standard deviation (Table 2) caused no statistical difference.

No correlation was found for all 3 groups between HbA_{1c} results and hepatic serum parameters as -glutamyl transferase (GGT), glutamate-oxalate transaminase (GOT) and glutamyl-pyruvic transaminase (GPT). In all 3 patient groups total protein measured in serum was within normal and albumin was normal in all patients with chronic hepatitis. Three patients with compensated cirrhosis had serum albumin below normal. There was no correlation found in all 3 patient groups between

Table 1 Percentage of patients outside the reference range for parameters of anemia

Group	Patients below normal (%) (Reference range)			Patients above normal (%) Reticulocytes (5-20%)
	Erythrocytes (4.5-5.9 T/L)	Hct (40-50%)	Hb (13-17 g/dL)	
Cirrhosis ($n=15$)	46	53	40	0
Chronic hepatitis ($n=10$)	30	30	30	0
Chronic hepatitis /ribavirin ($n=10$)	80	80	70	30

Hct: Hematocrit; Hb: Hemoglobin.

Table 2 Values of measured blood glucose (mean \pm SD) and calculated mean blood glucose values [MBG (mmol/L) = $(1.98 \cdot \text{HbA}_{1c}) - 4.29$]

	Measured MBG (mmol/L)	Menarini HA-8140 Calculated MBG (mmol/L)	DCA 2000 Bayer Calculated MBG (mmol/L)
Cirrhosis ($n=15$)	5.8 \pm 1.9	4.8	5.1
Chronic hepatitis ($n=10$)	5.1 \pm 0.3	5.4	5.4
Chronic hepatitis /Ribavirin ($n=10$)	5.2 \pm 0.4	4.3	4.5

MBG: Mean blood glucose.

fructosamine results and total protein or albumin. In patients with hepatic cirrhosis, mean fructosamine was within the high non-diabetic reference range. In patients with chronic hepatitis, fructosamine was close to the middle of the non-diabetic reference range. Five patients with cirrhosis and one patient with chronic hepatitis treated with ribavirin had high fructosamine levels even though they had normal blood glucose values.

DISCUSSION

The liver plays a major role in regulating glucose metabolism because it is the main source of endogenous glucose and a major site involved in insulin metabolism. The most common pathogenic agents in liver disease are alcohol abuse and infectious hepatitis that may cause disturbed erythropoiesis and decreased red cell survival. Macrocytic anemia is a common feature in liver disease but is still incompletely understood^[13]. The antiviral drug ribavirin has been widely used in combination with interferon in the treatment of chronic hepatitis C and a major side effect of ribavirin is a reversible hemolytic anemia^[10].

Glycated hemoglobin (GHb) measured as HbA_{1c} in diabetic patients, is used for evaluating long-term control of diabetes mellitus. GHb is the result of irreversible non-enzymatic glycation at one or both NH₂-terminal valines of the hemoglobin's α -chain. The extent of glycation and the relative involvement of the hemoglobin's α - and β -chains still remain unclear. Depending on the determination method used the concentration of HbA_{1c} is approximately 4-6% in healthy non-diabetic patients. Glycated hemoglobin most accurately reflects the previous 2-3 mo of glycemic control. Diabetic patients could present with abnormal liver chemistries, representing findings from benign hepatic steatosis to severe cirrhosis of the liver. Some medications to treat diabetes mellitus have an effect on liver metabolism or could even cause hepatotoxic reactions. Liver cirrhosis promotes glucose intolerance and diabetes through various mechanisms including insulin resistance and impaired insulin secretion. Sixty to 80% of patients with liver disease have glucose intolerance and 10-15% eventually develop overt diabetes.

In this study we demonstrated HbA_{1c} values below the non-diabetic reference range in up to 40% of the patients with liver cirrhosis while fructosamine results were either within the reference range or elevated in the diabetic range. However, protein metabolism was normal in our patients and although fructosamine results depend on glycation of serum proteins the results might be altered by reduced hepatic protein synthesis due to impairment of liver function. In 50% of the patients with chronic hepatitis treated with ribavirin, HbA_{1c} values were below the non-diabetic reference range as measured by at least one of the HbA_{1c} methods. In these groups of patients the HbA_{1c} results were negatively correlated to the percentage of reticulocytes that might be caused by disturbed erythropoiesis and decreased red cell survival. In patients with liver cirrhosis and chronic hepatitis treated with ribavirin, the HbA_{1c} calculated value of mean blood glucose was up to 1 mmol/L (18 mg/dL) lower than measured mean blood glucose. This underlines that impairment of liver function has influence on results of HbA_{1c} determination. Fructosamine may be a more reasonable marker for long term glucose control in patients with liver disease, but based on our findings we recommend frequent blood glucose monitoring as a measure for glucose control in patients with advanced liver disease.

We conclude that only evaluated in context with all liver function parameters as well as a red blood count including reticulocytes, HbA_{1c} should be used in patients with liver disease. Although the pathophysiologic reasons have still not

been confirmed, our data demonstrate that HbA_{1c} and fructosamine measurements should be used with caution when evaluating long-term glucose control in patients with hepatic cirrhosis or in patients with chronic hepatitis with ribavirin treatment. This interference may be due to alterations in erythrocyte lifespan and altered protein metabolism, but further investigations are needed to elucidate the exact cause of the interference in patients with liver disease.

ACKNOWLEDGEMENTS

We kindly acknowledge the determination of HbA_{1c} by the following laboratories: Institute of Chemical and Laboratory Diagnostics, Medical University Graz and Laboratory of the County Hospital in Wagna, Austria. Determination of fructosamine was performed in the Laboratory of the Department of Gynecology, Medical University Graz, Austria.

REFERENCES

- 1 Diabetes Control and Complications Trial Research Group: The effect of intensive treatment of diabetes on the development and progression of long-term complications in insulin-dependent diabetes mellitus. *N Engl J Med* 1993; **329**: 977-986
- 2 Turner RC, Cull CA, Frighi V, Holman RR. Glycemic control with diet, sulfonylurea, metformin, or insulin in patients with type 2 diabetes mellitus: progressive requirement for multiple therapies (UKPDS 49). UK Prospective Diabetes Study (UKPDS) Group. *JAMA* 1999; **281**: 2005-2012
- 3 Shetty A, Wilson S, Kuo P, Laurin JL, Howell CD, Johnson L, Allen EM. Liver transplantation improves cirrhosis-associated impaired oral glucose tolerance. *Transplantation* 2000; **69**: 2451-2454
- 4 Trenti T, Cristani A, Cioni G, Pentore R, Mussini C, Ventura E. Fructosamine and glycated hemoglobin as indices of glycemic control in patients with liver cirrhosis. *Ric Clin Lab* 1990; **20**: 261-267
- 5 Cacciatore L, Cozzolino G, Giardina MG, De Marco F, Sacca L, Esposito P, Francica G, Lonardo A, Matarazzo M, Varriale A. Abnormalities of glucose metabolism induced by liver cirrhosis and glycosylated hemoglobin levels in chronic liver disease. *Diabetes Res* 1988; **7**: 185-188
- 6 Nomura Y, Nanjo K, Miyano M, Kikuoka H, Kuriyama S, Maeda M, Miyamura K. Hemoglobin A₁ in cirrhosis of the liver. *Diabetes Res* 1989; **11**: 177-180
- 7 Jiao Y, Okumiya T, Saibara T, Park K, Sasaki M. Abnormally decreased HbA_{1c} can be assessed with erythrocyte creatine in patients with shortened erythrocyte age. *Diabetes Care* 1998; **21**: 1732-1735
- 8 Bravo AA, Sheth SG, Chopra S. Current concepts: liver biopsy. *N Engl J Med* 2001; **344**: 495-500
- 9 Oberti F, Valsesia E, Pilette C, Rousselet MC, Bedossa P, Aube C, Gallois Y, Rifflet H, Maiga MY, Penneau-Fontbonne D, Cales P. Noninvasive diagnosis of hepatic fibrosis or cirrhosis. *Gastroenterology* 1997; **113**: 1609-1616
- 10 De Franceschi L, Fattovich G, Turrini F, Ayi K, Brugnara C, Manzato F, Noventa F, Stanzial AM, Solero P, Corrocher R. Hemolytic anemia induced by ribavirin therapy in patients with chronic hepatitis C infection: role of membrane oxidative damage. *Hepatology* 2000; **31**: 997-1004
- 11 Little RR, Rohlfing CL, Wiedmeyer HM, Myers GL, Sacks DB, Goldstein DE. The national glycohemoglobin standardization program: a five-year progress report. *Clin Chem* 2001; **47**: 1985-1992
- 12 Rohlfing C, Wiedmeyer HM, Little RR, England JD, Tennill A, Goldstein DE. Defining the relationship between plasma glucose and HbA_{1c}. *Diabetes Care* 2002; **25**: 275-278
- 13 Maruyama S, Hirayama C, Yamamoto S, Koda M, Udagawa A, Kadowaki Y, Inoue M, Sagayama A, Umeki K. Red blood cell status in alcoholic and non-alcoholic liver disease. *J Lab Clin Med* 2001; **138**: 332-337

Expression and localization of c-Fos and NOS in the central nerve system following esophageal acid stimulation in rats

Xiao-Wei Shuai, Peng-Yan Xie

Xiao-Wei Shuai, Peng-Yan Xie, Department of Gastroenterology, First Hospital of Peking University, Beijing 100034, China

Supported by the Beijing Natural Science Foundation, No.7042030

Correspondence to: Dr. Peng-Yan Xie, Department of Gastroenterology, First Hospital of Peking University, Beijing 100034, China. pengyanx2002@yahoo.com

Telephone: +86-10-66551122-2581

Received: 2004-01-02 **Accepted:** 2004-02-09

Abstract

AIM: To determine the distribution of neurons expressing c-Fos and nitric oxide synthase (NOS) in the central nerve system (CNS) following esophageal acid exposure, and to investigate the relationship between c-Fos and NOS.

METHODS: Twelve Wistar rats were randomly divided into two equal groups. Hydrochloric acid with pepsin was perfused in the lower part of the esophagus for 60 min. As a control, normal saline was used. Thirty minutes after the perfusion, the rats were killed and brains were removed and processed for c-Fos immunohistochemistry and NADPH-d histochemistry. Blood pressure (BP), heart rate (HR), and respiratory rate (RR) during the experimental procedures were recorded every 10 min.

RESULTS: There were no significant differences in BP, HR and RR between the two groups. c-Fos immunoreactivity was significantly increased in rats receiving acid plus pepsin perfusion in amygdala (AM), paraventricular nucleus (PVN), parabrachial nucleus (PBN), nucleus tractus solitarius and dorsal motor nucleus of vagus (NTS/DMV), nucleus ambiguus (NA), reticular nucleus of medulla (RNM) and area postrema (AP). NOS reactivity in this group was significantly increased in PVN, PBN, NTS/DMV, RNM and AP. c-Fos and NOS had significant correlation between PVN, PBN, NTS/DMV, RNM and AP.

CONCLUSION: Acid plus pepsin perfusion of the esophagus results in neural activation in areas of CNS, and NO is likely one of the neurotransmitters in some of these areas.

Shuai XW, Xie PY. Expression and localization of c-Fos and NOS in the central nerve system following esophageal acid stimulation in rats. *World J Gastroenterol* 2004; 10(15): 2287-2291
<http://www.wjgnet.com/1007-9327/10/2287.asp>

INTRODUCTION

Reflux esophagitis (RE) is a common gastrointestinal motility disorder. Esophageal reflux occurs when gastric contents move in a retrograde direction into the esophagus, and esophagitis develops by prolonged exposure to gastric contents. This happens when the lower esophageal sphincter fails to provide an adequate mechanical barrier, when the esophageal peristaltic

contractions fail to provide adequate clearance of the gastric contents, and/or when gastric contents exist for a prolonged time due to gastroparesis^[1]. Esophageal motility is controlled by a variety of factors of which the nerve system is the most important one. Locally, motility disorder caused by esophagitis is usually due to the decreased release of acetylcholine^[2,3], signal transduction failure^[4], and/or decreased intracellular Ca²⁺^[5]. In CNS, little has been known about the distribution of activated neurons after esophageal acid exposure^[6].

It is reported that *c-fos* is the most well characterized IEGs (immediate early genes) in neurons; the *c-fos* message is induced within minutes of stimuli and the protein is expressed within 1-3 h^[7-10]. The expression of *c-fos* in CNS is considered to be a marker of neuronal activity following an appropriate stimulus, and the site of central expression of c-Fos in response to a stimulus is used as a means of elucidating the course of the response^[11-16]. Nitric oxide (NO) acts as an intercellular messenger in CNS. As a highly diffusible and short-lived gas, NO is always studied by means of nitric oxide synthase (NOS)^[17]. Studies have shown that NOS-containing neurons are identical to those selectively stained for NADPH diaphorase^[18]. The present study was designed to determine the distribution of neurons expressing c-Fos and NOS in CNS following esophageal acid exposure, and to investigate the relationship between c-Fos and NOS.

MATERIALS AND METHODS

Animals

Twelve male Wistar rats weighing 220-260 g were housed in standard home cages under conditions of controlled illumination (12:12 h light/dark cycle), humidity, and temperature (18-26 °C) for at least 7 d prior to the experimental procedure. They were fed a standard rat diet and tap water. The animals were deprived of food but not water 12-16 h before each experiment. They were randomly divided into two equal groups. All procedures were approved by the Committee for Animal Care and Usage for Research and Education of the Peking University.

Methods

Rats were anaesthetized with an intraperitoneal injection of urethane (1.0 g/kg). After a rat reached a complete state of anesthesia, the abdominal wall and gastric wall were incised, and a drainage cannula was inserted in the gastric cardia to collect run-off solution from the esophagus. The anesthetized rat, strapped supine to an animal board, was then positioned with its head elevated at a slight angle (20-30°). A single lumen clear vinyl tube (ID 0.05 mm, A 0.8 mm) was passed by mouth into the esophagus. The tip of the cannula was located 3 cm above the esophagogastric junction. The cannula was then positioned and connected to a continuous perfusion pump (Medical Equipment Ltd. Zhejiang University, Hangzhou, China). A solution containing hydrochloric acid (HCl 0.1 mol/L) and pepsin (2 000-4 000 U/mL) (pH 1.5) was perfused continuously at a rate of 10 mL/h for 60 min. As a control, normal saline was used. Blood pressure (BP), heart rate (HR) and respiratory rate

(RR) during the experimental procedures were recorded every 10 min. After perfusion, the rat was left undisturbed for another 30 min before being deeply anesthetized with urethane (1.5 g/kg i.p.). The animal then was transcardially perfused with 9 g/L saline followed by 40 g/L paraformaldehyde in 0.1 mol/L phosphate buffer saline (PBS, pH 7.3). The brain was removed and postfixed in the same fixative overnight and cryoprotected by immersion in 200 g/L sucrose for 72 h. Coronal sections (40 μ m) of the brain were cut in a cryostat. Every fourth section was used to reveal c-Fos immunoreactivity and NADPH-diaphorase (NADPH-d) staining, and the second set of sections was used as a control for the immunohistochemical reaction.

The sections were collected and rinsed in 0.01 mol/L PBS containing 3 g/L Triton X-100 (PBST). Then they were incubated at 37 $^{\circ}$ C for 2 h in a solution containing 1 mmol/L NADPH (Biomol, London, UK), 0.5 mmol/L nitroblue tetrazolium (Biomol), Tris-HCl 50 mmol/L, and Triton X-100 2 g/L. After a rinse in PBST, sections were placed into a 50 g/L goat serum for 30 min at room temperature (RT), and incubated overnight at RT in primary antibody c-Fos (1:200, Santa Cruz Biotechnology, California, USA). After washing for 15 min with PBST, the sections were incubated in biotinylated anti-rabbit IgG (Zymed, South San Francisco, Canada) diluted 1:300 in PBST at RT for 2 h, and then incubated in peroxidase-conjugated streptavidin (1:300 dilution, Zymed) for 2 h at RT. The immunoreactivity was visualized by incubating with 0.05 mol/L Tris-HCl buffer containing 0.1 g/L 3,3'-diaminobenzidine, and 0.3 mL/L H₂O₂ for 10-20 min at RT. The stained sections were mounted on APES-coated glass slides, dehydrated and coverslipped.

Statistical analysis

BP, HR and RR recorded every 10 min during the 90-min experimental procedures were averaged per animal and then per experimental group, respectively. The distribution of c-Fos and NADPH-d positive cells was detected under a microscope (Olympus, Tokyo, Japan), and the cells were counted on LEICA Q550CW system (Leica Microsystems Imaging Solutions Ltd, Wetzlar, Germany). The numbers of cells containing c-Fos immunoreactivity and NADPH-d were counted unilaterally in specific nuclei in several sections; 5 sections for amygdala

(AM), nucleus tractus solitarius and dorsal motor nucleus of vagus (NTS/DMV), nucleus ambiguus (NA) and reticular nucleus of medulla (RNM) and 4 sections for paraventricular nucleus (PVN), supraoptic nucleus (SON), parabrachial nucleus (PBN) and area postrema (AP). The average number of c-Fos or NADPH-d positive neurons per section for each rat was calculated, respectively, by dividing the total number of c-Fos or NADPH-d positive cells obtained from all sections by the number of sections taken for each brain nucleus. Data were expressed as mean \pm SD of the respective brain areas. Statistical analyses were performed by SPSS 12.0 using the *t*-test, and a *P* value of less than 0.05 was considered statistically significant. The relationship between c-Fos and NADPH-d positive cells was performed by the correlation analysis.

RESULTS

BP, HR and RR to acid-pepsin perfusion

Esophageal acid perfusion did not change BP (18.03 \pm 1.07 vs 17.26 \pm 0.62 kPa, *F*=2.663, *P*=0.134), HR (275.30 \pm 14.43 vs 265.00 \pm 22.12 beats/min, *F*=1.343, *P*=0.273), and RR (92.00 \pm 10.41 vs 94.56 \pm 9.46 breathes/min, *F*=0.078, *P*=0.785) compared with control group.

c-Fos and NADPH-d staining in CNS

The c-Fos positive cell nuclei of activated cells showed the characteristic dark brown staining of oxidized DAB. In both groups of rats, c-Fos expression was observed in several brain regions. In telencephalon and diencephalon, c-Fos positive cells were mainly located in AM (Figure 1A, B), PVN (Figure 1C, D), SON and the numbers of the former two areas increased significantly in the acid-pepsin perfusion group (Table 1). Esophageal exposure to acid and pepsin also stimulated a significantly greater number of c-Fos-labeled neurons in areas of brain stem including PBN, NTS/DMV, NA (Figure 2A, D), RNM and AP (Table 1). NADPH-d activity was visualized as a vibrant blue color within perikarya, dendrites and axons. Acid-pepsin perfusion significantly increased the numbers of NADPH-d stained cells in PVN (Figure 1C, D), PBN, NTS/DMV, RNM and AP (Table 1). There were some coexistence of Fos

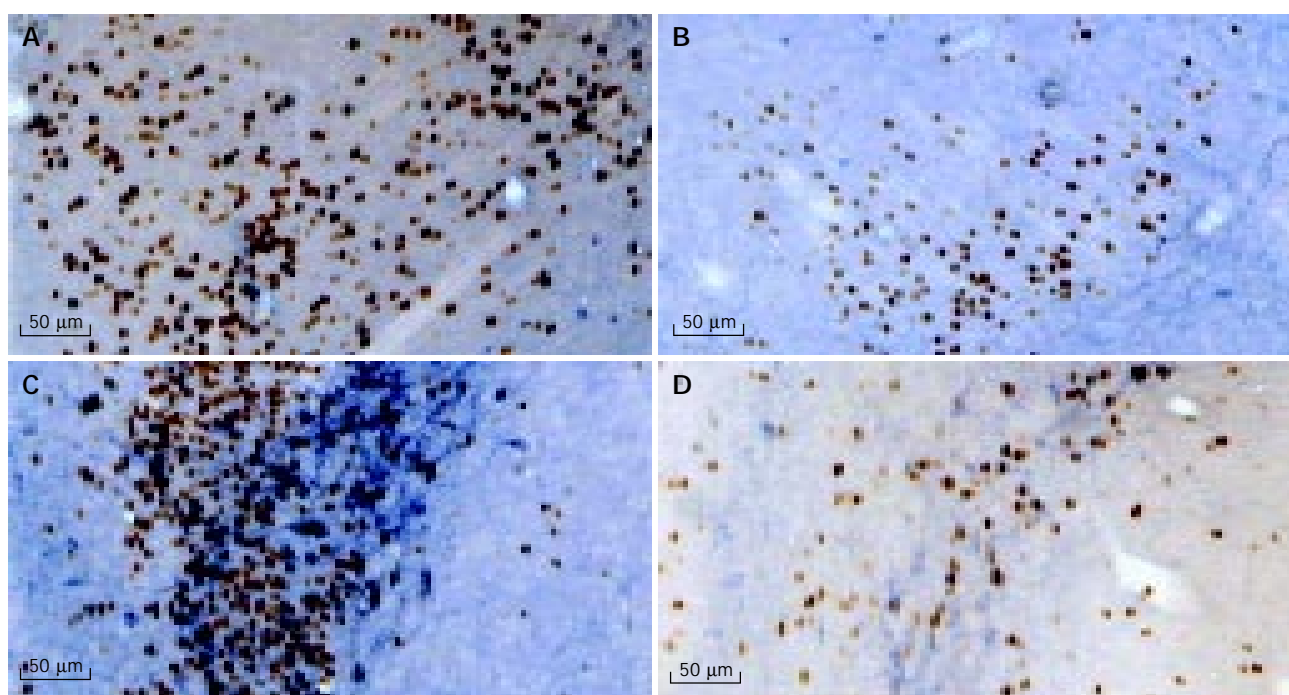


Figure 1 Photomicrographs showing c-Fos and NOS positive neurons in amygdala (A and B), paraventricular nucleus (C and D). A and C were taken from rats with acid-pepsin perfusion, while B and D were taken from rats with saline perfusion. (3V: the third ventricle).

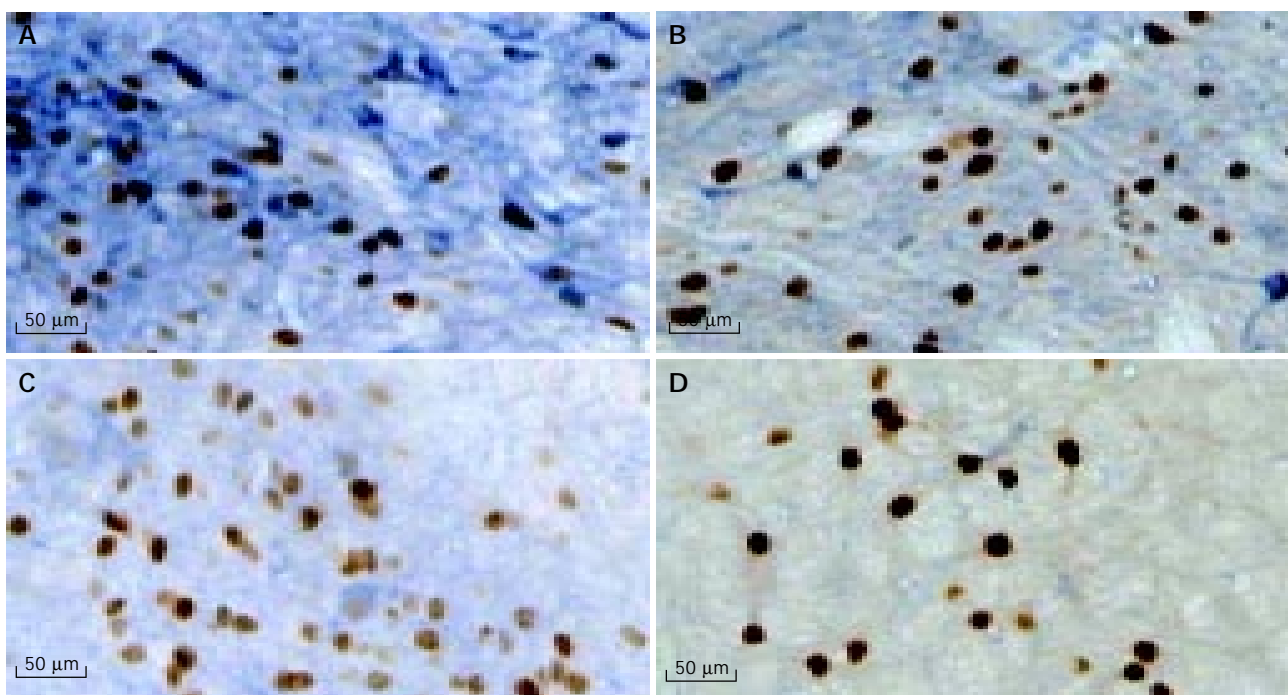


Figure 2 Photomicrographs showing c-Fos and NOS positive neurons in nucleus tractus solitarius (A and B), nucleus ambiguus (C and D). A and C were taken from rats with acid-pepsin perfusion, while B and D were taken from rats with saline perfusion.

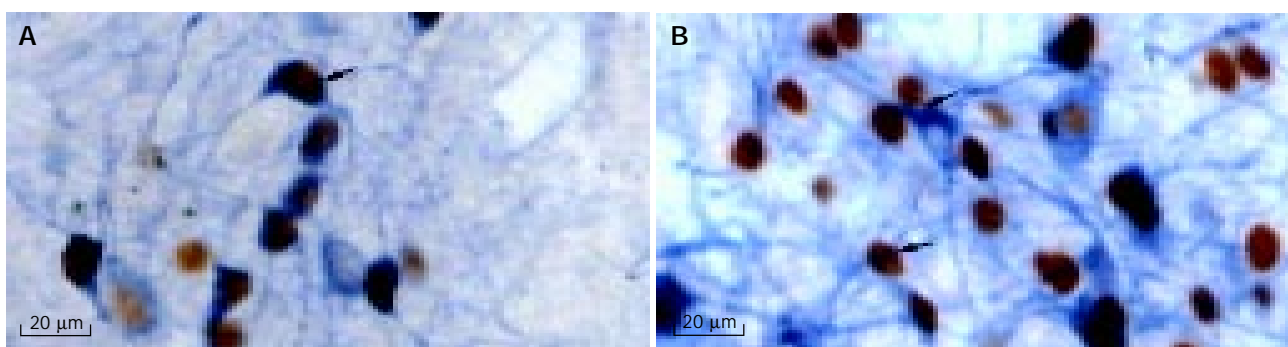


Figure 3 Photomicrographs showing the coexistence of c-Fos and NADPH-d positive staining, i.e. colocalization (left) and close proximity (right).

Table 1 Effects of esophageal acid-pepsin perfusion on c-Fos and NOS expression in brain nuclei, as determined by the average of number of c-Fos or NADPH-d positive neurons/section

Nuclei	Acid-pepsin perfusion			Saline perfusion		
	c-Fos	NOS	c-Fos&NOS	c-Fos	NOS	c-Fos&NOS
AM	341.3±13.7 ^b	8.0±2.0	1.7±0.7	166.2±2.7	6.5±0.5	1.9±0.4
PVN	551.1±11.6 ^b	151.8±48.5 ^b	127.6±34.1 ^b	232.2±12.9	66.9±1.5	64.1±4.4
SON	181.0±3.5	96.2±2.4	66.0±7.0	183.3±5.8	95.3±4.2	64.9±2.1
PBN	103.0±4.1 ^b	17.1±1.8 ^b	2.9±1.0 ^b	79.7±2.6	3.4±0.6	1.1±0.5
NTS/DMV	161.1±6.9 ^b	48.8±6.8 ^b	32.3±4.7 ^b	75.0±0.8	23.7±0.7	8.4±1.5
NA	42.7±0.8 ^b	2.1±0.4	1.0±0.2	25.0±1.5	2.0±0.6	1.0±0.2
RNM	77.4±7.6 ^b	15.1±1.5 ^b	7.6±1.1 ^b	32.9±0.4	5.1±0.5	1.9±0.3
AP	190.1±11.1 ^b	6.0±2.3 ^b	2.3±1.1 ^a	107.2±2.1	1.9±0.6	0.9±0.3

Data are expressed as mean±SD. ^a*P*<0.05, acid-pepsin perfusion vs saline perfusion. ^b*P*<0.01, acid-pepsin perfusion vs saline perfusion. c-Fos, c-Fos positive neurons; NOS, NADPH-d positive neurons.

and NADPH-d positive staining (Figure 3). The coexistence included colocalization that was visualized as blue-stained perikarya (NADPH-d activity) containing a clearly visible dark brown nucleus (c-Fos protein), and close proximity that was visualized as c-Fos positive nucleus being within

neuronal processes of NADPH-d, and that was the presence of NADPH-d positive staining within 3 μm from c-Fos-positive nucleus. Both of them have been adopted as a criterion of close proximity^[19,20]. The coexisting cells were mainly observed in PVN, SON and NTS/DMV.

Correlation between c-Fos and NADPH-d positive cells

There was a high correlation between c-Fos and NADPH-d positive cells in PVN, PBN, NTS/DMV, RNM and AP. The correlation coefficient (r) was 0.805, 0.943, 0.923, 0.947, 0.869 (all $P < 0.01$) respectively. There was no correlation between c-Fos and NADPH-d expression in AM, SON, and NA.

DISCUSSION

Acid, in combination with pepsin, was chosen to be the stimulant in this rat model of gastroesophageal reflux. This combination has been shown to cause esophagitis in experimental models^[21,22].

The nerve supply to esophagus is composed of extrinsic and intrinsic components. The extrinsic innervation is mainly through the autonomic nervous system, which is divided into sympathetic and parasympathetic components. The parasympathetic innervation of esophagus is supplied by the vagus nerves. Three types of vagal afferent fibers are classified on the basis of their sensitivity to mechanical stimulation: those responding to mucosal stroking (mucosal receptors), those responding to circular tension (tension receptors) and those responding to mucosal stroking and circular tension (tension/mucosal receptors)^[23]. Sensory afferents from the esophagus usually travel to NTS. DMV, which contains preganglionic motor neurons, has efferent fibers. The dorsal vagal complex (DVC) comprising NTS and DMV is the center of the integration of vagal control of esophagus^[24,25]. Exposing the subdiaphragmatic vagus nerves (SDV) to horseradish peroxidase (HRP), Norgren *et al.* found that retrogradely labeled neurons occurred within NA and the reticular formation caudal to NA, and DMV whereas anterograde HRP reaction product occurred in NTS and AP^[26]. Besides, connections of NTS with the medullary reticular formation and AP existed^[27]. They were reported to take part in some visceral reflexes. In the present study, c-Fos positive neurons were seen in NTS, DMV, NA, RNM, and AP. In comparison with the controls, the number was greater in the acid-pepsin group. In this context, the present results confirm those reports mentioned above. During the esophageal exposure to acid, a cascade of chemoreceptors that lie along the passage is stimulated. Some of these signals are carried by vagal afferents to NTS in brainstem. From there, visceral information is disseminated to various brain sites, where it affects regulatory functions by engaging endocrine, autonomic, and some other effector mechanisms. But how all these different pathways interconnect within subnuclei is still unknown. It has been reported that PBN is related to noxious information from the visceral organs^[14]. Esophageal acid exposure also induces high density of c-Fos expression in PBN.

A significantly increased number of c-Fos positive nuclei was observed in AM and PVN. Although many of c-Fos staining cells were seen in SON, there was no significant increase in this area in response to acid-pepsin perfusion. PVN is immediate beneath the ependyma of the third ventricle. The afferent connections of PVN are from hippocampal formation, septal nuclei, locus ceruleus, AM, and NTS. The efferent connections appear, in part, to be reciprocal to the afferent systems. The AM has reciprocal connections with locus ceruleus, substantia nigra, NTS, DMV, PBN, reticular formation, and nuclei of the hypothalamus. The present study showed that only some of those areas expressed c-Fos immunoreactivity, which suggests that those activated neurons are related to esophageal innervation. In order to exclude the potential contribution of the pressor response to the induction of c-Fos in NTS and other nuclei, BP, HR, and RR were recorded during the experimental procedures. There were no significant changes in BP, HR, and RR between the two groups.

It has been reported that NOS exists in neurons of DVC.

The premotoneurons in NTS express NOS, and NO acting in the NA takes part in the esophageal peristalsis^[28]. The present study showed that many NADPH-d positive neurons were seen in PBN, NTS/DMV, RNM, and that some were seen in NA and AP. This suggests that NO release may modulate characteristics of the activated neurons in these nuclei that are evoked by esophageal acid stimulus. It has been reported that NOS inhibitor, N-nitro-L-arginine methyl ester (L-NAME), reduces the spontaneous discharge rate of the NTS neurons *in vivo* and *in vitro*, which confirms that NO has the excitatory effect on NTS^[29]. L-NAME also reduces the c-Fos expression in DVC, suggesting that c-Fos expression is, in part, related to NO release in DVC. Little has been known about the neurotransmitters in telencephalon and diencephalon. In the present study, many NADPH-d positive cells were observed in PVN and SON, but only few were found in AM.

The present study observed the coexistence of c-Fos and NADPH-d positive staining. It is possible that the neuronal cells containing NOS are activated during esophageal acid exposure, which may cause NO release to themselves or to other brain regions in modulating the esophageal reflux.

In conclusion, acid-pepsin exposure to lower part of the esophagus stimulates the mucosal receptors, which in turn activates the neurons of NTS through vagal afferent fibers, and finally the neurons in DMV and NA to modulate the esophageal peristalsis. The possible nuclei involved in these procedures are AM, PVN, PBN, RNM, and AP. Double labeled staining of c-Fos and NADPH-d suggests that NO is one of the neurotransmitters in PVN, PBN, NTS/DMV, RNM and AP.

REFERENCES

- Zarling EJ. A review of reflux esophagitis around the world. *World J Gastroenterol* 1998; **4**: 280-284
- Biancani P, Sohn UD, Rich HG, Harnett KM, Behar J. Signal transduction pathways in esophageal and lower esophageal sphincter circular muscle. *Am J Med* 1997; **103**(5A): 23S-28S
- Cao Y, Xie P, Xing Y. Role of endogenous cholinergic nerve in esophageal dysmotility with reflux esophagitis. *Zhonghua Neike Zazhi* 2001; **40**: 670-672
- Kim N, Sohn UD, Mangannan V, Rich H, Jain MK, Behar J, Biancani P. Leukotrienes in acetylcholine-induced contraction of esophageal circular smooth muscle in experimental esophagitis. *Gastroenterology* 1997; **112**: 1548-1558
- Rich H, Sohn UD, Behar J, Kim N, Biancani P. Experimental esophagitis affects intracellular calcium stores in the cat lower esophageal sphincter. *Am J Physiol* 1997; **272**(6 Pt 1): G1523-G1529
- Suwanprathes P, Ngu M, Ing A, Hunt G, Seow F. c-Fos immunoreactivity in the brain after esophageal acid stimulation. *Am J Med* 2003; **115**(Suppl 3A): 31S-38S
- Hughes P, Dragunow M. Induction of immediate-early gene and the control of neurotransmitter-regulated gene expression within the nervous system. *Pharmacol Rev* 1995; **47**: 133-178
- Muller R, Bravo R, Burckhardt J, Curran T. Induction of c-fos gene and protein by growth factors precedes activation of c-myc. *Nature* 1984; **312**: 716-720
- Sonnenberg JL, Macgregor-Leon PF, Curran T, Morgan JJ. Dynamic alterations occur in the levels and composition of transcription factor AP-1 complexes after seizure. *Neuron* 1989; **3**: 359-365
- Sheng M, Greenberg ME. The regulation and function of c-fos and other immediate early genes in the nervous system. *Neuron* 1990; **4**: 477-485
- Yamamoto T, Sawa K. C-Fos-like immunoreactivity in the brainstem following gastric loads of various chemical solutions in rats. *Brain Res* 2000; **866**: 135-143
- Schicho R, Schemann M, Pabst MA, Holzer P, Lippe IT. Capsaicin-sensitive extrinsic afferents are involved in acid-induced activation of distinct myenteric neurons in the rat stomach. *Neurogastroenterol Motil* 2003; **15**: 33-44
- Tong C, Ma W, Shin SW, James RL, Eisenach JC. Uterine cervi-

- cal distension induces cFos expression in deep dorsal horn neurons of the rat spinal cord. *Anesthesiology* 2003; **99**: 205-211
- 14 **Monnikes H**, Ruter J, Konig M, Grote C, Kobelt P, Klapp BF, Arnold R, Wiedenmann B, Tebbe JJ. Differential induction of *c-fos* expression in brain nuclei by noxious and non-noxious colonic distension: role of afferent C-fibers and 5-HT₃ receptors. *Brain Res* 2003; **966**: 253-264
- 15 **Tada H**, Fujita M, Harris M, Tatewaki M, Nakagawa K, Yamamura T, Pappas TN, Takahashi T. Neural mechanism of acupuncture-induced gastric relaxations in rats. *Dig Dis Sci* 2003; **48**: 59-68
- 16 **de Medeiros MA**, Canteras NS, Suchecki D, Mello LE. Analgesia and c-Fos expression in the periaqueductal gray induced by electroacupuncture at the Zusanli point in rats. *Brain Res* 2003; **973**: 196-204
- 17 **Bredt DS**, Hwang PM, Snyder SH. Localization of nitric oxide synthase indicating a neural role for nitric oxide. *Nature* 1990; **347**: 768-770
- 18 **Dawson TM**, Bredt DS, Fotuhi M, Hwang PM, Snyder SH. Nitric oxide synthase and neuronal NADPH diaphorase are identical in brain and peripheral tissues. *Proc Natl Acad Sci USA* 1991; **88**: 7797-7801
- 19 **Li J**. Nitric oxide synthase (NOS) coexists with activated neurons by skeletal muscle contraction in the brainstem of cats. *Life Sci* 2002; **71**: 2833-2843
- 20 **Tassorelli C**, Joseph SA. NADPH-diaphorase activity and Fos expression in brain nuclei following nitroglycerin administration. *Brain Res* 1995; **695**: 37-44
- 21 **Lanas A**, Royo Y, Ortego J, Molina M, Sainz R. Experimental esophagitis induced by acid and pepsin in rabbits mimicking human reflux esophagitis. *Gastroenterology* 1999; **116**: 97-107
- 22 **Pursnani KG**, Mohiuddin MA, Geisinger KR, Weinbaum G, Katzka DA, Castell DO. Experimental study of acid burden and acute oesophagitis. *Br J Surg* 1998; **85**: 677-680
- 23 **Page AJ**, Blackshaw LA. An *in vitro* study of the properties of vagal afferent fibres innervating the ferret oesophagus and stomach. *J Physiol* 1998; **512**(Pt 3): 907-916
- 24 **Hornby PJ**, Abrahams TP. Central control of lower esophageal sphincter relaxation. *Am J Med* 2000; **108**(Suppl 4a): 90S-98S
- 25 **Sang Q**, Goyal RK. Swallowing reflex and brain stem neurons activated by superior laryngeal nerve stimulation in the mouse. *Am J Physiol Gastrointest Liver Physiol* 2001; **280**: G191-G200
- 26 **Norgren R**, Smith GP. Central distribution of subdiaphragmatic vagal branches in the rat. *J Comp Neurol* 1988; **273**: 207-223
- 27 **Herbert H**, Moga MM, Saper CB. Connections of the parabrachial nucleus with the nucleus of the solitary tract and the medullary reticular formation in the rat. *J Comp Neurol* 1990; **293**: 540-580
- 28 **Beyak MJ**, Xue S, Collman PI, Valdez DT, Diamant NE. Central nervous system nitric oxide induces oropharyngeal swallowing and esophageal peristalsis in cat. *Gastroenterology* 2000; **119**: 377-385
- 29 **Ma S**, Abboud FM, Felder RB. Effect of L-arginine-derived nitric oxide synthesis on neuronal activity in nucleus tractus solitarius. *Am J Physiol* 1995; **268**(2 Pt 2): R487-R491

Edited by Xia HHX and Chen WW Proofread by Xu FM

Effect of octreotide on human pancreatic cancer cells after transfected with somatostatin receptor type 2 gene

Zheng-Ren Liu, Ren-Yi Qin, Gao-Song Wu, Qing Chang, Da-Yu Wang, Sheng-Quan Zou, Fa-Zu Qiu

Zheng-Ren Liu, Ren-Yi Qin, Gao-Song Wu, Qing Chang, Da-Yu Wang, Sheng-Quan Zou, Fa-Zu Qiu, Department of General Surgery, Tongji Hospital, Tongji Medical College, Huazhong University of Science and Technology, Wuhan 430030, Hubei Province, China

Supported by the Natural Science Foundation of Hubei Province, No. 2000J068

Correspondence to: Professor Ren-Yi Qin, Department of General Surgery, Tongji Hospital, Tongji Medical College, Huazhong University of Science and Technology, Wuhan 430030, Hubei Province, China. ryqin@tjh.tjmu.edu.cn

Telephone: +86-27-83662389

Received: 2003-10-27 **Accepted:** 2003-12-16

Abstract

AIM: To observe the effect of octreotide on apoptosis rate of human pancreatic cancer cells PC-3 after transfected with somatostatin receptor type 2 (SST2) gene.

METHODS: SST2 plasmid was transfected into PC-3 cells by liposome. Result of transfection was detected by immunocytochemical staining and Western blotting. Apoptosis rates of PC-3 cells under different dosages of octreotide were measured by MTT assay and flow cytometry (FCM).

RESULTS: Apoptosis rate caused by octreotide of transfected PC-3 cells was $7.56 \pm 1.06\%$ at the dosage of $0.20 \mu\text{g/mL}$, $9.25 \pm 1.73\%$ at the dosage of $0.40 \mu\text{g/mL}$ and $14.18 \pm 2.71\%$ at the dosage of $0.80 \mu\text{g/mL}$. Apoptosis rate caused by octreotide of non-transfected PC-3 cells was $5.76 \pm 0.75\%$ at the dosage of $0.20 \mu\text{g/mL}$, $6.69 \pm 0.80\%$ at the dosage of $0.40 \mu\text{g/mL}$ and $7.26 \pm 1.28\%$ at the dosage of $0.80 \mu\text{g/mL}$. Transfected PC-3 cells growth inhibition rate caused by octreotide was $9.36 \pm 1.34\%$ at the dosage of $0.20 \mu\text{g/mL}$, $12.03 \pm 1.44\%$ at the dosage of $0.40 \mu\text{g/mL}$ and $20.23 \pm 4.21\%$ at the dosage of $0.80 \mu\text{g/mL}$. Non-transfected PC-3 cells growth inhibition rate caused by octreotide was $6.44 \pm 0.66\%$ at the dosage of $0.20 \mu\text{g/mL}$, $7.65 \pm 0.88\%$ at the dosage of $0.40 \mu\text{g/mL}$ and $9.29 \pm 1.32\%$ at the dosage of $0.80 \mu\text{g/mL}$. We found that octreotide caused higher apoptosis rate and inhibition rate in transfected groups than in non-transfected groups ($P < 0.05$) at the tested dosages (0.20 , 0.40 and $0.80 \mu\text{g/mL}$).

CONCLUSION: Deficiency of SST2 was probably the major reason why octreotide had little effect on PC-3 cells. Transfecting SST2 gene could strengthen the ability of octreotide of killing PC-3 cells. It provided an experimental evidence for using both octreotide and transfection with SST2 gene on clinical treatment of pancreatic cancer.

Liu ZR, Qin RY, Wu GS, Chang Q, Wang DY, Zou SQ, Qiu FZ. Effect of octreotide on human pancreatic cancer cells after transfected with somatostatin receptor type 2 gene. *World J Gastroenterol* 2004; 10(15): 2292-2294
<http://www.wjgnet.com/1007-9327/10/2292.asp>

INTRODUCTION

Octreotide, the artificial synthetic somatostatin analogue, which possesses the advantage of relative specificity, long lasting and small ill effect, has already been applied to clinical therapy extensively. Its anti-tumor mechanism mainly depends on the expression of somatostatin receptor, especially SST2^[1-3]. Most tumors highly express SST2, but some do not express or low express. For example, 90% human pancreatic cancer cells have lost the ability of expressing SST2, which leads to the unsatisfactory treatment effect in pancreatic cancer^[4]. We did the experiment to explore octreotide's effect on the apoptosis rate of pancreatic cancer (PC-3) cells after transfected with SST2 gene.

MATERIALS AND METHODS

Materials

PC-3 cells were a gift from China Medical University. RPMI 1640, fetal calf serum, Liposome 2000 Reagent were purchased from Gibco Co. USA. Octreotide was kindly presented by Novartis Co. Swiss. MTT, DMSO and G418 were purchased from Sigma Co. USA. Goat-anti-human SST2 monoclonal antibody was purchased from Santa Cruz Co. USA. Rabbit-anti-goat and DAB were purchased from Zhongshan Biotechnology Co. Beijing, China. ECL kit was purchased from Amersham Pharmacia Biotechnology Inc. ABC test kit was purchased from Huamei Co. China. Human SST2 plasmid was kindly presented by Junbo Hu of Maryland University, USA.

Methods

SST2 plasmid amplification and transfection We adopted colon bacillus (DH-5 α) to amplify and extract the human SST2 plasmid, which was identified by endonuclease. We cultured the PC-3 cells with RPMI 1640 supplemented with 100 mL/L fetal calf serum. When PC-3 cells were in exponential growth phase, the human SST2 plasmid was transfected into PC-3 cells mediated by Liposome 2000 reagent and screened with culture medium with 600 mg/L G418.

Immunocytochemical staining Transfective effect was detected by immunocytochemical staining. ABC test kit was adopted to stain the cells crawling on the slides with immunocytochemical staining. Goat-anti-human SST2 monoclonal antibody was diluted to 1:100. Blank groups used PBS instead of goat-anti-human antibody.

Western blotting Expression of SST2 was detected by western-blot. Transfected cells were collected and lysed with the cell-lysis to extract protein. Goat-anti-human SST2 monoclonal antibody (1:1 000) was used. The signals were developed with the ECL kit.

FCM Apoptosis rate was detected by flow cytometry. When the PC-3 cells were in exponential growth phase, octreotide at different dosages (0.05 , 0.10 , 0.20 , 0.40 , $0.80 \mu\text{g/mL}$) was added. After 24 h, culture medium was renewed and octreotide added according to the above dosages. Cells in the culture medium were collected and preserved in 700 mL/L alcohol at -20°C . Cells were collected after 48 h; the apoptosis rate was detected by flow cytometry.

MTT assay MTT assay was adopted to detect the sensitivity of PC-3 cells *in vitro* after using different dosages of octreotide. We divided them into three groups: blank groups (no cells), control groups (no drug) and octreotide groups. Octreotide treated cells were divided into five groups according to the dosages (0.05, 0.10, 0.20, 0.40, 0.80 $\mu\text{g}/\text{mL}$). Then the transfected PC-3 cells and non-transfected cells were inoculated into the 96-well culture panel, about $3 \times 10^6/\text{L}$ in each well. Each panel had 10 replicate wells. After 24-h culture, octreotide was added and then cultivated for another 48 h. The sensitivity of PC-3 cells was detected with MTT assay and inhibition rate was measured by detecting the value of the A ($\lambda=550 \text{ nm}$). Inhibition rate of PC-3 cells growth = $[(A_{\text{control group}} - A_{\text{blank group}}) - (A_{\text{experiment group}} - A_{\text{blank group}})] / (A_{\text{control group}} - A_{\text{blank group}}) \times 100\%$.

Statistical analysis

t-test and SPSS software were employed to analyze data. $P < 0.05$ indicates significant difference.

RESULTS

Expression of SST2 in transfected and non-transfected PC-3 cells

Cells crawling on the slides were stained by immunocytochemical staining. SST2 gene expressing PC-3 cells would present brown particles spreading mainly in the cytoplasm and cell membrane (Figure 1). PC-3 cells non-transfected were negative-expression (Figure 2). We proved that PC-3 cells did not express SST2. In contrast, they could express SST2 after transfected with SST2 gene. And it also proved that the transfection was effective and accorded with the requirement of our experiments.

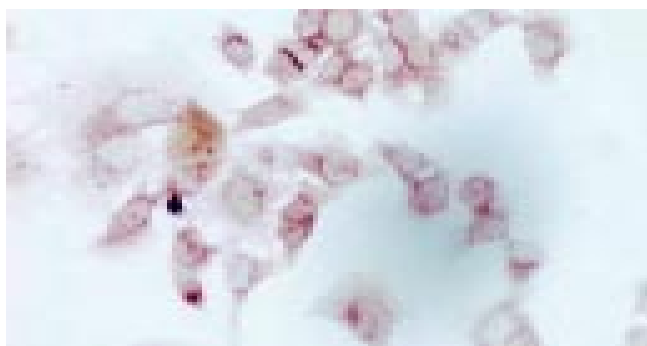


Figure 1 SST2 expressed in the transfected PC-3 cells (10 \times 40).

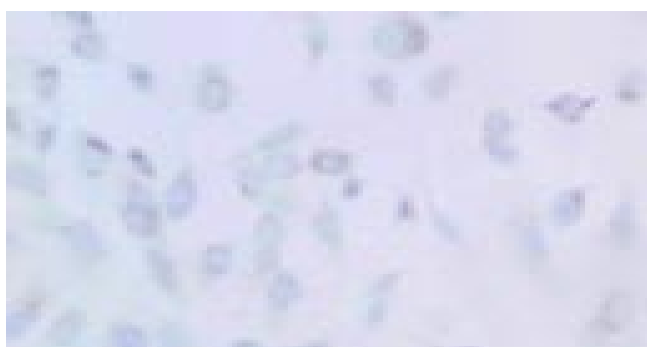


Figure 2 SST2 did not express in non-transfected PC-3 cells (10 \times 40).

Western blotting of SST2 expression

Protein of transfected PC-3 cells was extracted and the expression of SST2 was detected by Western blotting. SST2 in transfected PC-3 cells was detected (Figure 3), the M_r is about

40 000. It also proved that the transfection was effective at protein level. This was the base of our next experiments.

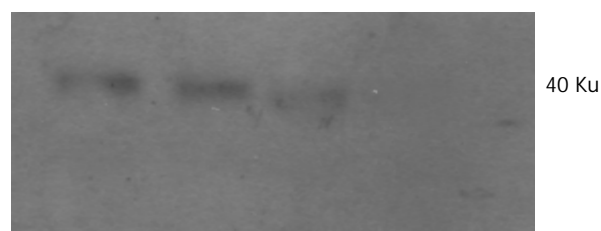


Figure 3 SST2 could be detected in the transfected PC-3 cells.

Analysis of PC-3 cell inhibition rate by MTT assay

Inhibition rate was detected by MTT assay. Growth inhibition rate of transfected PC-3 cells caused by octreotide was $3.45 \pm 0.91\%$ at the dosage of 0.05 $\mu\text{g}/\text{mL}$, $5.18 \pm 1.21\%$ at the dosage of 0.10 $\mu\text{g}/\text{mL}$, $9.36 \pm 1.34\%$ at the dosage of 0.20 $\mu\text{g}/\text{mL}$, $12.03 \pm 1.44\%$ at the dosage of 0.40 $\mu\text{g}/\text{mL}$ and $20.23 \pm 4.21\%$ at the dosage of 0.80 $\mu\text{g}/\text{mL}$. The inhibition rate caused by octreotide for non-transfected PC-3 cells was $3.28 \pm 0.54\%$ at the dosage of 0.05 $\mu\text{g}/\text{mL}$, $4.08 \pm 0.45\%$ at the dosage of 0.10 $\mu\text{g}/\text{mL}$, $6.44 \pm 0.66\%$ at the dosage of 0.20 $\mu\text{g}/\text{mL}$, $7.65 \pm 0.88\%$ at the dosage of 0.40 $\mu\text{g}/\text{mL}$ and $9.29 \pm 1.32\%$ at the dosage of 0.80 $\mu\text{g}/\text{mL}$. After using octreotide (0.05-0.80 $\mu\text{g}/\text{mL}$) for 48 h, we found that it caused a higher inhibition rate in transfected groups than in non-transfected groups ($P < 0.05$) at different dosages (0.20, 0.40 and 0.80 $\mu\text{g}/\text{mL}$). It proved that the expression of SST2 could enhance octreotide's effect on the inhibition of PC-3 cells (Figure 4).

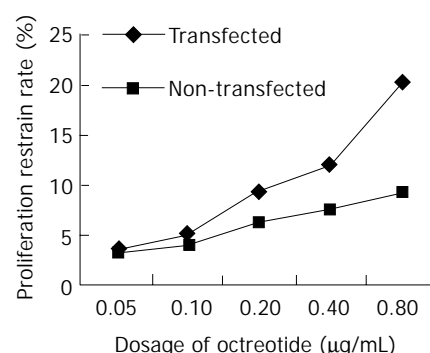


Figure 4 Transfected PC-3 cells growth inhibition rate under octreotide.

Flow cytometric analysis of PC-3 cell apoptosis rate

When 0.05-0.80 $\mu\text{g}/\text{mL}$ octreotide was added and incubated for 48 h, the PC-3 cells would show the typical apoptosis peak measured by flow cytometry. Moreover, the higher the drug dosage was, the higher the apoptosis rate was. Higher dosages (0.20, 0.40 and 0.80 $\mu\text{g}/\text{mL}$) of octreotide caused a greater increase of inhibition in PC-3 cells transfected groups than in non-transfected groups ($P < 0.05$) (Table 1).

Table 1 Apoptosis rate of PC-3 cells transfected and non-transfected with SST2 gene under different dosages of octreotide (mean \pm SD)

Dosage of octreotide ($\mu\text{g}/\text{mL}$)	Apoptosis rate of transfected PC-3 cells (%)	Apoptosis rate of non-transfected PC-3 cells (%)	<i>P</i>
0.05	3.65 \pm 0.66	2.77 \pm 0.33	>0.05
0.10	4.45 \pm 0.78	3.23 \pm 0.57	>0.05
0.20	7.56 \pm 1.06	5.76 \pm 0.75	<0.05
0.40	9.25 \pm 1.73	6.69 \pm 0.80	<0.05
0.80	14.18 \pm 2.71	7.26 \pm 1.28	<0.05

DISCUSSION

At present, somatostatin has been widely used in therapy of various tumors especially endocrine tumors. In a majority of cases, favorable effect has been noted. In combined treatment with classical chemotherapeutic drugs, such as 5-fluorouracil, somatostatin has synergistic action of killing tumor cells^[5]. The mechanism of somatostatin's anti-tumor effect *in vitro* lies in combining with its receptor. Somatostatin receptor belongs to a protein G coupled receptor family^[6]. According to the similarity of structure and difference in affinity to somatostatin, somatostatin receptors are classified into two categories: (1) having strong affinity to somatostatin, including SST2A, SST2B, SST3 and SST5; (2) having weak affinity to somatostatin, including SST1 and SST4^[7,8]. It is known that somatostatin receptors are extensively distributed in human central nervous system and other tissues. The category and amount of somatostatin receptor expression is different in various tumors. Somatostatin receptor, especially SST2 is usually highly expressed in many tumor tissues. SST2 may play a role in anti-tumor effect of somatostatin (It is considered as a tumor suppressing gene)^[9-11]. The mechanisms of somatostatin's anti-tumor action are as follows: (1) direct negative effect on tumor growth; (2) inhibiting the growth of tumors by interfering with synthesis of growth factors, which are produced via paracrine and autocrine of tumor cells; (3) anti-tumor effects by inhibiting excretion of somatotropin, insulin, gastrin and other hormones or depressing insulin-like growth factor-I (IGF-I), epidermal growth factor (EGF) and other growth factors; (4) interference with DNA synthesis of tumor cells; (5) suppression of angiogenesis of tumors^[12].

Substantial evidence has shown that loss or low expression of SST2 was observed in primary pancreatic cancer^[9,13-15]. Our previous research results have also shown that expression of SST2 was detected in 12.5 % of primary pancreatic cancers. These results suggest that expression of SST2 was deficient in a majority of pancreatic cancer tissues, which may be the main reason why somatostatin and somatostatin analogues were nearly inefficacious in the treatment of pancreatic cancer. But it is interesting that expression of SST2 was observed in the majority of adjacent histologically noncancerous pancreas, which was beneficial for somatostatin and somatostatin analogues to suppress fast invasion and growth of tumor cells. These results also suggest that if expression of SST2 in pancreatic cancer and adjacent histologically noncancerous pancreas was reduced; somatostatin and somatostatin analogues were nearly inefficacious in the treatment of pancreatic cancer. But if expression of SST2 in both pancreatic cancer and adjacent histologically noncancerous pancreas were observed, somatostatin and somatostatin analogues were efficacious^[11,1]. Therefore, different expression of SST2 in pancreatic cancer and adjacent histologically noncancerous pancreas is bound to result in different effects of treatment, which may be the main reason why reports of effects of somatostatin and somatostatin analogues treatment on pancreatic cancer are inconsistent at the present time. We believe that it is very important to make clear whether SST2 is expressed in pancreatic cancer and adjacent histologically noncancerous pancreas before somatostatin and somatostatin analogues are used in treatment of pancreatic cancer. We have demonstrated that transfecting SST2 gene into human pancreatic cancer cells which lack SST2 could markedly up-regulate SST2 expression, increase apoptosis rate of human pancreatic cancer cells and

enhance somatostatin analogue octreotide to inhibit growth of human pancreatic cancer cells and induce apoptosis. These results suggest that it may be an exciting molecular biological therapy for human pancreatic cancer deficiency of SST2 gene via transfection with SST2 gene and combination with somatostatin analogue.

REFERENCES

- 1 **Guillermet J**, Saint-Laurent N, Rochaix P, Cuvillier O, Levade T, Schally AV, Pradayrol L, Buscail L, Susini C, Bousquet C. Somatostatin receptor subtype 2 sensitizes human pancreatic cancer cells to death ligand-induced apoptosis. *Proc Natl Acad Sci U S A* 2003; **100**: 155-160
- 2 **Moneta D**, Richichi C, Aliprandi M, Dournaud P, Dutar P, Billard JM, Carlo AS, Viollet C, Hannon JP, Fehlmann D, Nunn C, Hoyer D, Epelbaum J, Vezzani A. Somatostatin receptor subtypes 2 and 4 affect seizure susceptibility and hippocampal excitatory neurotransmission in mice. *Eur J Neurosci* 2002; **16**: 843-849
- 3 **Hofland LJ**, Lamberts SW. Somatostatin receptor subtype expression in human tumors. *Ann Oncol* 2001; **12**(Suppl 2): S31-36
- 4 **Raderer M**, Hamilton G, Kurtaran A, Valencak J, Haberl I, Hoffmann O, Kornek GV, Vorbeck F, Hejna MH, Virgolini I, Scheithauer W. Treatment of advanced pancreatic cancer with the long-acting somatostatin analogue lanreotide: *in vitro* and *in vivo* results. *Br J Cancer* 1999; **79**: 535-537
- 5 **Weckbecker G**, Raulf F, Tolcsvai L, Bruns C. Potentiation of the anti-proliferative effects of anti-cancer drugs by octreotide *in vitro* and *in vivo*. *Digestion* 1996; **57**(Suppl 1): 22-28
- 6 **Burchett SA**, Flanary P, Aston C, Jiang L, Young KH, Uetz P, Fields S, Dohlman HG. Regulation of stress response signaling by the N-terminal dishevelled/EGL-10/pleckstrin domain of Sst2, a regulator of G protein signaling in *Saccharomyces cerevisiae*. *J Biol Chem* 2002; **277**: 22156-22167
- 7 **Prevost G**, Veber N, Viollet C, Roubert V, Roubert P, Benard J, Eden P. Somatostatin-14 mainly binds the somatostatin receptor subtype 2 in human neuroblastoma tumors. *Neuroendocrinology* 1996; **63**:188-197
- 8 **Hoyer D**, Bell GI, Berelowitz M, Epelbaum J, Feniuk W, Humphrey PP, O'Carroll AM, Patel YC, Schonbrunn A, Taylor JE. Classification and nomenclature of somatostatin receptors. *Trends Pharmacol Sci* 1995; **16**: 86-88
- 9 **Rochaix P**, Delesque N, Esteve JP, Saint-Laurent N, Voight JJ, Vaysse N, Susini C, Buscail L. Gene therapy for pancreatic carcinoma: local and distant antitumor effects after somatostatin receptor sst2 gene transfer. *Hum Gene Ther* 1999; **10**: 995-1008
- 10 **Hofland LJ**, Lamberts SW. Somatostatin analogs and receptors. Diagnostic and therapeutic applications. *Cancer Treat Res* 1997; **89**: 365-382
- 11 **Paillard F**. Somatostatin receptor gene transfer induces bystander effects. *Hum Gene Ther* 1999; **10**: 857-859
- 12 **Zaki M**, Harrington L, McCuen R, Coy DH, Arimura A, Schubert ML. Somatostatin receptor subtype 2 mediates inhibition of gastrin and histamine secretion from human, dog, and rat antrum. *Gastroenterology* 1996; **111**: 919-924
- 13 **Froidevaux S**, Hintermann E, Torok M, Macke HR, Beglinger C, Eberle AN. Differential regulation of somatostatin receptor type 2 (sst2) expression in AR4-2J tumor cells implanted into mice during octreotide treatment. *Cancer Res* 1999; **59**: 3652-3657
- 14 **Delesque N**, Buscail L, Esteve JP, Saint-Laurent N, Muller C, Weckbecker G, Bruns C, Vaysse N, Susini C. sst2 somatostatin receptor expression reverses tumorigenicity of human pancreatic cancer cells. *Cancer Res* 1997; **57**: 956-962
- 15 **Buscail L**, Saint-Laurent N, Chastre E, Vaillant JC, Gespach C, Capella G, Kalthoff H, Lluis F, Vaysse N, Susini C. Loss of sst2 somatostatin receptor gene expression in human pancreatic and colorectal cancer. *Cancer Res* 1996; **56**: 1823-1827

Inhibitory effect of *Huangqi Zhechong* decoction on liver fibrosis in rat

Shuang-Suo Dang, Xiao-Li Jia, Yan-An Cheng, Yun-Ru Chen, En-Qi Liu, Zong-Fang Li

Shuang-Suo Dang, Xiao-Li Jia, Yan-An Cheng, Yun-Ru Chen, Department of Infectious Diseases, Second Hospital of Xi'an Jiaotong University, Xi'an 710004, Shaanxi Province, China

En-Qi Liu, Center of Experimental Animal, Xi'an Jiaotong University, Xi'an 710004, Shaanxi Province, China

Zong-Fang Li, Department of Surgery, Second Hospital of Xi'an Jiaotong University, Xi'an 710004, Shaanxi Province, China

Supported by the Science and Technology Foundation of Shaanxi Province, No. 2002k11-G7

Correspondence to: Shuang-Suo Dang, Department of Infectious Disease, Second Hospital of Xi'an Jiaotong University, Xi'an 710004, Shaanxi Province, China. shuang suo640212@sohu.com

Telephone: +86-29-83036998

Received: 2003-12-19 **Accepted:** 2004-01-15

Abstract

AIM: To assess the inhibitory effect of *Huangqi Zhechong* decoction on hepatic fibrosis in rats induced by CCl₄ plus alcohol and high fat low protein diet.

METHODS: Male SD rats were randomly divided into hepatic fibrosis model group, control group and 3 treatment groups consisting of 12 rats in each group. Except for the normal control group, all the rats were subcutaneously injected with CCl₄ at a dosage of 3 mL/kg. In 3 treated groups, either high-dose group (9 mL/kg), or medium-dose group (6 mL/kg), or low-dose group (3 mL/kg) was daily gavaged with *Huangqi Zhechong* decoction, and saline vehicle was given to model and normal control rats. Enzyme-linked immunosorbent assay (ELISA) and biochemical examinations were used to determine the changes of alanine aminotransferase (ALT), aspartate aminotransferase (AST), hyaluronic acid (HA), laminin (LN), type-III-procollagen-N-peptide (PIIIP), and type IV collagen content in serum, and hydroxyproline (Hyp) content in liver after sacrificing the rats. Pathologic changes, particularly fibrosis were examined by hematoxylin and eosin (HE) and Van Gieson staining.

RESULTS: Compared with the model control group, serum ALT, AST, HA, LN, PIIIP and type IV collagen levels dropped markedly in *Huangqi Zhechong* decoction groups, especially in the medium-dose *Huangqi Zhechong* decoction group (1 954±576 U/L vs 759±380 U/L, 2 735±786 U/L vs 1 259±829 U/L, 42.74±7.04 ng/mL vs 20.68±5.85 ng/mL, 31.62±5.84 ng/mL vs 14.87±1.45 ng/mL, 3.26±0.69 ng/mL vs 1.47±0.46 ng/mL, 77.68±20.23 ng/mL vs 25.64±4.68 ng/mL, respectively) ($P<0.05$). The Hyp content in liver tissue was also markedly decreased (26.47±11.24 mg/mgprot vs 9.89±3.74 mg/mgprot) ($P<0.01$). Moreover, the stage of the rat liver fibrosis in *Huangqi Zhechong* decoction groups was lower than that in model group, and more dramatic drop was observed in medium-dose *Huangqi Zhechong* decoction group ($P<0.01$).

CONCLUSION: *Huangqi Zhechong* decoction can inhibit hepatic fibrosis resulted from chronic liver injure, retard the development of cirrhosis, and notably ameliorate the liver

function. It may be a safe and effective therapeutic drug for patients with fibrosis.

Dang SS, Jia XL, Cheng YA, Chen YR, Liu EQ, Li ZF. Inhibitory effect of *Huangqi Zhechong* decoction on liver fibrosis in rat. *World J Gastroenterol* 2004; 10(15): 2295-2298

<http://www.wjgnet.com/1007-9327/10/2295.asp>

INTRODUCTION

Liver fibrosis is common in most chronic liver diseases regardless of the etiology^[1-8]. Although new therapeutic approaches have recently been proposed, there is no established therapy for liver fibrosis^[9]. *Huangqi Zhechong* decoction is a traditional Chinese medicine. The aim of the present study was to investigate the protective effects of *Huangqi Zhechong* decoction on liver fibrosis in rats of CCl₄-induced cirrhosis.

MATERIALS AND METHODS

Reagents

CCl₄ (Xi'an Chemical Factory) was diluted into 400 g/L in olive oil (Xi'an Chemical Factory). *Huangqi Zhechong* decoction was self-made by the Pharmaceutical Department of the Second Hospital, Xi'an Jiaotong University. The kit for Hyp was bought from Nianjing Jiancheng Biological Institute. Kits for HA, LN, PIIIP and type IV collagen were bought from Senxiong Company, Shanghai.

Animals

Sixty adult male SD rats weighing 150-200 g were provided by the Laboratory Animal Center of the College of Medicine, Xi'an Jiaotong University. The rats were randomly divided into 5 groups of 12 each: control group; model group; and 3 treatment groups. Except for the control rats, all rats were subcutaneously injected with 400 g/L CCl₄ (CCl₄:Olive oil 2:3), 3 mL/kg·b.w., at every 3 d for 6 wk, and fed with high fat low protein diet (75% pure maize plus 20% lard and 0.5% cholesterol) and 300 mL/L alcohol as drinks. In the 3 treatment groups, *Huangqi Zhechong* decoction was administered daily via gastric tube to high-dose, medium-dose and low-dose groups at a dosage of 9 mL/kg, 6 mL/kg and 3 mL/kg for 6 wk, respectively. After 6 wk, except the dead, all the rats were anesthetized with 200 g/L urethane (5 mL/kg, abdominal injection). Blood was taken from abdominal aorta, centrifuged at 4 °C, and plasma were kept at -20 °C for assays.

Pathological observations

Hepatic tissues were fixed in 40 g/L solutions of formaldehyde in 0.1% mol/L phosphate-buffered saline (pH 7.4), and embedded in paraffin. Five-micrometer thick section slides were prepared. All the sections stained with HE and standard van Gieson staining (VG) were coded and scored by blind reading. Van Gieson's method was used to detect collagen fibers^[10]. Liver condition was classified according to the standard formulated by China Medical Association in 1995^[11],

and fibrosis was graded from 0 to 4 (0: no fibrosis; 1: portal area fibrosis; 2: fibrotic septa between portal tracts; 3: fibrosis septa and structure disturbance of hepatic lobule; and 4: cirrhosis).

Statistical analysis

Results were expressed as mean±SD. Quantitative data were analyzed by using ANOVA in statistical software SPSS 11.0. A value of $P<0.05$ was considered statistically significant. Redit test was used for statistical analysis of the qualitative data.

RESULTS

Hyp content in liver tissues

Liver Hyp level was significantly lower in rats treated with CCl_4 and *Huangqi Zhechong* decoction compared to the rats treated with CCl_4 alone ($P<0.01$). And the liver Hyp level of rat in 3 *Huangqi Zhechong* decoction treatment groups has no significant difference from control group (Table 1).

Plasma levels of ALT and AST

Plasma levels of ALT and AST in model group were higher than those in the controls ($P<0.01$), while the *Huangqi Zhechong* decoction treatment groups showed significant lower

ALT and AST levels than the model group. Furthermore, among the 3 treatment groups the medium-dose group showed the best effect and the levels of ALT and AST in serum showed no difference compared with the normal group (Table 1).

Table 1 Level of serum ALT, AST and liver Hyp

Group	<i>n</i>	ALT (U/L)	AST (U/L)	Liver Hyp (μg/mgprot)
Control	12	86.0±17.7	329±40	10.02±1.05
Model	11	1 954±576 ^d	2 735±786 ^d	26.47±11.24 ^d
High-dose group	9	989±576 ^{ad}	1 584±988 ^c	15.01±7.59 ^b
Medium-dose group	10	759±380 ^{bc}	1 259±829 ^a	9.89±3.74 ^b
Low-dose group	10	1 003±530 ^{ad}	1 650±928 ^c	10.06±2.58 ^b

^a $P<0.05$, ^b $P<0.01$ vs model group; ^c $P<0.05$, ^d $P<0.01$ vs control group.

HA, LN, PIIP and type IV collagen levels in serum

Serum levels of HA, LN, PIIP and type IV collagen in model group, compared with the controls, were all markedly increased ($P<0.01$). And compared with the model group, the serum levels of HA, LN, PIIP and type IV collagen were significant decreased in the 3 treatment groups ($P<0.01$) (Table 2).

Table 2 Serum levels of HA, LN, PIIP and type IV collagen

Group	<i>n</i>	PIIP (ng/mL)	Type IV collagen (ng/mL)	LN (ng/mL)	HA (ng/mL)
Control	12	0.34±0.67	18.47±3.43	10.07±1.74	17.96±5.86
Model	11	3.26±0.69 ^d	77.68±20.23 ^d	31.62±5.84 ^d	42.74±7.04 ^d
High-dose group	9	2.01±0.40 ^{bd}	39.14±4.97 ^{bd}	16.32±2.73 ^{bd}	21.71±5.69 ^b
Medium-dose group	10	1.47±0.46 ^{bd}	25.64±4.68 ^b	14.87±1.45 ^{bd}	20.68±5.85 ^b
Low-dose group	10	1.84±0.27 ^{bd}	29.09±2.78 ^b	17.02±2.74 ^{bd}	24.18±7.89 ^b

^a $P<0.05$, ^b $P<0.01$ vs model group; ^c $P<0.05$, ^d $P<0.01$ vs control group.

Table 3 Pathological observation of liver condition

Group	<i>n</i>	Liver condition					<i>U</i>
		0	I	II	III	IV	
Model	11	0	0	0	3	8	
High-dose group	9	0	2	3	3	1	2.98 ^a
Medium-dose group	10	0	4	4	2	0	4.01 ^b
Low-dose group	10	0	2	4	3	1	3.75 ^b

^a $P<0.05$, ^b $P<0.01$ vs model group; The value of *U* represents the Redit value of the two groups, $U>1.96$ means $P<0.05$, $U>2.58$ means $P<0.01$.

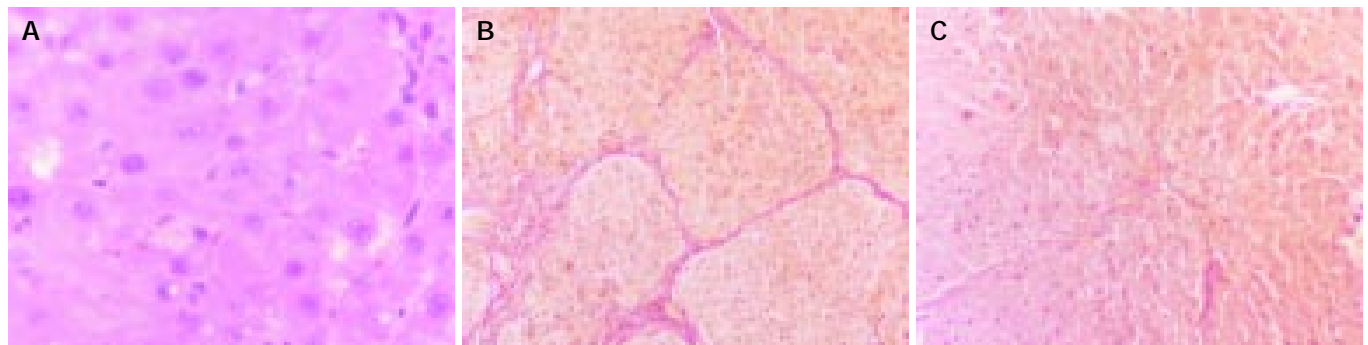


Figure 1 Liver tissue under light microscope. A: Normal liver tissue in control group (HE staining, original magnification: ×400); B: Liver fibrosis tissue in model group, more fibrous tissue was formed in liver. A large amount of inflammatory cells soaked into the intralobular and the interlobular (van Gieson staining, original magnification: ×200); C: Liver fibrosis tissue in *Huangqi Zhechong* decoction group. The pathological change of liver was rather lighter compared with the model (van Gieson staining, original magnification: ×200).

Pathological assay

At the end of the study, the liver of control rats had no appreciable alterations (Figure 1A). In the model group, the margin of liver was uneven; more fibrous tissues formed and extended into the hepatic lobules to separate them incompletely; a large amount of inflammatory cells infiltrated in the intralobular and the interlobular regions; the liver structure was disordered with some displacement of central veins, and there were more necrotic and degenerated liver cells compared with the control (Figure 1B). While in the 3 treatment groups, especially in the medium-dose group, the pathological changes of liver was rather milder, showing less fibrous tissue proliferation and inflammatory cell infiltration in the interlobular space; the hepatic cell cords arranged radially with less displacement of central veins and less degenerated or necrosis hepatic cells, without any pseudolobule observed (Figure 1C). Compared with the model group, the liver condition of the rats was significantly improved in *Huangqi Zhechong* decoction groups (Table 3).

DISCUSSION

The incidence rate of chronic hepatopathy in China is high, which afflicts the patients by progressively developing irreversible cirrhosis^[12,13]. Hepatic fibrosis is the intermediate and crucial stage of this process, characterized by reversibility. If treated properly in this stage, cirrhosis could be successfully prevented^[14]. But it remains a problem to prevent cirrhosis or to control its progression in patients with a chronic liver disease^[15]. Great efforts have been made to find safe and effective drugs. Recent clinical and experimental observations have demonstrated that Chinese medicines might be of some preventive and therapeutic values against fibrosis^[16-18].

Of *Huangqi Zhechong* decoction, the Chinese traditional medicine, the *Astragalus* has the effects of activating blood circulation to relieve stasis, strengthening “spleen”, supplementing and smoothening “qi” to eliminate fullness, reinforcement body’s immunological function. It also could preserve the integrity of hepatocytes, eliminate toxic free radicals, inhibit lipid peroxidation of cytomembrane, relieve necrosis of hepatocytes, and obviously antifibrosis^[19-23]. *Thoroughfare* is mainly used to activate blood circulation, remove stasis, and dredge the liver^[24].

Huangqi Zhechong decoction has been used in clinic for many years to prevent liver fibrosis and shown good effect. However, its effect and the associated mechanisms need further experimental evidence. CCl₄ is a super-hepatotoxin, with which the CCl₃ free radical is produced during metabolic processes and acts on liver cells to covalently conjugate with the membranous unsaturated lipid to cause lipid peroxidation and necrosis of hepatocytes^[25-27]. For this reason, CCl₄ was used to induce liver fibrosis.

We started to treat the rats with *Huangqi Zhechong* decoction at the same time of subcutaneous injection with CCl₄. After 6 wk, the histological features showed that there were no appreciable alterations in control group. But pathological evaluation showed that the rats in model group almost had integrity fibrosis septum, and pseudolobular could be seen in nearly every section. While the rats received *Huangqi Zhechong* decoction had less fibrosis, the reticular fibrosis in the interlobular septum was limited remarkably, and no pseudolobular could be seen. In addition, *Huangqi Zhechong* decoction, especially the medium-dose administration could decrease the scores of hepatic fibrosis grading.

ALT and AST are indexes to describe liver functions. Most part of ALT is presented in the cytoplasm of liver cell, discharged in blood when degeneration, hyper permeability and necrosis of liver cells occur. So the increase of ALT level in serum reflects the degree of liver cell injury. Our study

showed that the *Huangqi Zhechong* decoction could decrease serum levels of ALT and AST in rats with hepatic injury caused by CCl₄. It indicates that *Huangqi Zhechong* decoction may work through protecting the liver cells.

HA, LN, PIIIP and type IV collagen are good serum markers of hepatic fibrosis. In this study, the serum contents of these 4 markers in the model group were much higher than those of the controls ($P < 0.01$). And the *Huangqi Zhechong* decoction groups had significantly low HA, LN, PIIIP and type IV collagen levels in serum than those in the controls, which indicated that *Huangqi Zhechong* decoction could successfully prevent hepatic fibrosis.

Hyp content in liver is another important index to react the hepatic fibrosis. In fibrotic liver, collagen fibers increase, which induced the rise of Hyp content in liver^[28]. So Hyp level could provide the information about the degree and variant process of cirrhosis. In this study, we observed that the liver Hyp level in the model group was much higher than that of the controls and *Huangqi Zhechong* decoction groups.

In summary, *Huangqi Zhechong* decoction may play a role in antifibrotic therapy. It can protect the liver cells and inhibit the deposition of collagen fibers in liver. It may provide a safe and effective strategy for inhibition of cirrhosis in clinic use.

REFERENCES

- 1 Ma X, Qiu DK, Peng YS. Immunohistochemical study of hepatic oval cells in human chronic viral hepatitis. *World J Gastroenterol* 2001; **7**: 238-242
- 2 Reshetnyak VI, Sharafanova TI, Ilchenko LU, Golovanova EV, Poroshenko GG. Peripheral blood lymphocytes DNA in patients with chronic liver diseases. *World J Gastroenterol* 2001; **7**: 235-237
- 3 McCaughan GW, Gorrell MD, Bishop GA, Abbott CA, Shackel NA, McGuinness PH, Levy MT, Sharland AF, Bowen DG, Yu D, Slaitini L, Church WB, Napoli J. Molecular pathogenesis of liver disease: an approach to hepatic inflammation, cirrhosis and liver transplant tolerance. *Immunol Rev* 2000; **174**: 172-191
- 4 Okazaki I, Watanabe T, Hozawa S, Arai M, Maruyama K. Molecular mechanism of the reversibility of hepatic fibrosis: with special reference to the role of matrix metalloproteinases. *J Gastroenterol Hepatol* 2000; **15**(Suppl): D26-32
- 5 Jung SA, Chung YH, Park NH, Lee SS, Kim JA, Yang SH, Song IH, Lee YS, Suh DJ, Moon IH. Experimental model of hepatic fibrosis following repeated periportal necrosis induced by allyl alcohol. *Scand J Gastroenterol* 2000; **35**: 969-975
- 6 Plummer JL, Ossowicz CJ, Whibley C, Ilsley AH, Hall PD. Influence of intestinal flora on the development of fibrosis and cirrhosis in a rat model. *J Gastroenterol Hepatol* 2000; **15**: 1307-1311
- 7 Croquet V, Moal F, Veal N, Wang J, Oberti F, Roux J, Vuillemin E, Gallois Y, Douay O, Chappard D, Cales P. Hemodynamic and antifibrotic effects of losartan in rats with liver fibrosis and/or portal hypertension. *J Hepatol* 2002; **37**: 773-780
- 8 Marcellin P, Asselah T, Boyer N. Fibrosis and disease progression in hepatitis C. *Hepatology* 2002; **36**(5 Suppl 1): S47-56
- 9 Friedman SL. Molecular regulation of Hepatic fibrosis, an integrated cellular response to tissue injury. *J Biol Chem* 2000; **275**: 2247-2250
- 10 Zhu H, Zeng L, Zhu D, Yuan Y. The role of TGF-beta 1 in mice hepatic fibrosis by Schistosomiasis Japonica. *J Tongji Med Univ* 2000; **20**: 320-321
- 11 China Medical Association infectious branch. The standard of grading and staging of viral hepatitis. *Zhonghua Chuanranbing Zazhi* 1995; **13**: 241-247
- 12 Lamireau T, Desmouliere A, Bioulac-Sage P, Rosenbaum J. Mechanisms of hepatic fibrogenesis. *Arch Pediatr* 2002; **9**: 392-405
- 13 Brenner DA, Waterboer T, Choi SK, Lindquist JN, Stefanovic B, Burchard E, Yamauchi M, Gillan A, Rippe RA. New aspects of hepatic fibrosis. *J Hepatol* 2000; **32**(1 Suppl): 32-38
- 14 Riley TR 3rd, Bhatti AM. Preventive strategies in chronic liver disease: part II. Cirrhosis. *Am Fam Physician* 2001; **64**: 1735-1740
- 15 Murphy F, Arthur M, Iredale J. Developing strategies for liver

- fibrosis treatment. *Expert Opin Investig Drugs* 2002; **11**: 1575-1585
- 16 **Liu C**, Jiang CM, Liu CH, Liu P, Hu YY. Effect of Fuzhenghuayu decoction on vascular endothelial growth factor secretion in hepatic stellate cells. *Hepatobiliary Pancreat Dis Int* 2002; **1**: 207-210
- 17 **Liu P**, Liu CH, Wang HN, Hu YY, Liu C. Effect of salvianolic acid B on collagen production and mitogen-activated protein kinase activity in rat hepatic stellate cells. *Acta Pharmacol Sin* 2002; **23**: 733-738
- 18 **Kusunose M**, Qiu B, Cui T, Hamada A, Yoshioka S, Ono M, Miyamura M, Kyotani S, Nishioka Y. Effect of Sho-saiko-to extract on hepatic inflammation and fibrosis in dimethylnitrosamine induced liver injury rats. *Biol Pharm Bull* 2002; **25**: 1417-1421
- 19 **Wang RT**, Shan BE, Li QX. Extracorporeal experimental study on immuno-modulatory activity of Astragalus membranaceus extract. *Zhongguo Zhongxiyi Jiehe Zazhi* 2002; **22**: 453-456
- 20 **Chu DT**, Lin JR, Wong W. The *in vitro* potentiation of LAK cell cytotoxicity in cancer and aids patients induced by F3—a fractionated extract of Astragalus membranaceus. *Zhonghua Zhongliu Zazhi* 1994; **16**: 167-171
- 21 **Zhang YD**, Shen JP, Zhu SH, Huang DK, Ding Y, Zhang XL. Effects of astragalus (ASI, SK) on experimental liver injury. *Yaoxue Xuebao* 1992; **27**: 401-406
- 22 **Tan YW**, Yin YM, Yu XL. Influence of Salvia miltiorrhizae and Astragalus membranaceus on hemodynamics and liver fibrosis indexes in liver cirrhotic patients with portal hypertension. *Zhongguo Zhongxiyi Jiehe Zazhi* 2001; **21**: 351-353
- 23 **Fu QL**. Experimental study on yiqi-huoxue therapy of liver fibrosis. *Zhongguo Zhongxiyi Jiehe Zazhi* 1992; **12**: 228-229
- 24 **Chen H**, Weng L. Comparison on efficacy in treating liver fibrosis of chronic hepatitis B between Astragalus Polygonum anti-fibrosis decoction and jinshuibao capsule. *Zhongguo Zhongxiyi Jiehe Zazhi* 2000; **20**: 255-257
- 25 **Kanta J**, Dooley S, Delvoux B, Breuer S, D'Amico T, Gressner AM. Tropoelastin expression is up-regulated during activation of hepatic stellate cells and in the livers of CCl₄-cirrhotic rats. *Liver* 2002; **22**: 220-227
- 26 **Yan JC**, Ma Y, Chen WB, Xu CJ. Dynamic observation on vascular diseases of liver tissues of rats induced by CCl₄. *Shijie Huaren Xiaohua Zazhi* 2000; **8**: 42-45
- 27 **Yan JC**, Chen WB, Ma Y, Xu CJ. Immunohistochemical study on hepatic vascular forming factors in liver fibrosis induced by CCl₄ in rats. *Shijie Huaren Xiaohua Zazhi* 2000; **8**: 1238-1241
- 28 **Garcia L**, Hernandez I, Sandoval A, Salazar A, Garcia J, Vera J, Grijalva G, Muriel P, Margolin S, Armendariz-Borunda J. Pirfenidone effectively reverses experimental liver fibrosis. *J Hepatol* 2002; **37**: 797-805

Edited by Kumar M and Chen WW Proofread by Xu FM

Transanal approach in repairing acquired rectovestibular fistula in females

Ya-Jun Chen, Ting-Chong Zhang, Jin-Zhe Zhang

Ya-Jun Chen, Ting-Chong Zhang, Jin-Zhe Zhang, Beijing Children's Hospital, Capital University of Medical Sciences, Beijing 100045, China

Correspondence to: Dr. Ya-Jun Chen, Beijing Children's Hospital, Capital University of Medical Sciences, Beijing 100045, China. chen-yajun@hotmail.com

Telephone: +86-10-63296188 **Fax:** +86-10-68011503

Received: 2003-12-17 **Accepted:** 2004-01-13

Abstract

AIM: To summarize the operative experience of the transanal approach in acquired rectovestibular fistula repair.

METHODS: Ninety-six cases of acquired rectovestibular fistula in young females were analyzed retrospectively. The etiology and operative procedure were discussed. Operative essential points were, the patient was laid in prone frog position, with the knees and hips flexed at 90°; the perineum was elevated; and the anal opening was exposed. Four stay sutures were applied to the margin of the fistular orifice in the anal opening at points 3, 6, 9 and 12 o'clock. A circular incision of mucosa surrounding the stay sutures was made. The fistula was dissected from its anal opening to its vestibular opening. The wound of vestibule was sutured, and the rectoanal wound was then sutured transversely.

RESULTS: All the 96 patients recovered uneventfully from operation with a successful rate of 93.75%.

CONCLUSION: The transanal approach in the treatment of the acquired rectovestibular fistula is a simple and feasible technique.

Chen YJ, Zhang TC, Zhang JZ. Transanal approach in repairing acquired rectovestibular fistula in females. *World J Gastroenterol* 2004; 10(15): 2299-2300

<http://www.wjgnet.com/1007-9327/10/2299.asp>

INTRODUCTION

Acquired rectovestibular fistula in small girls is a common anorectal disease. Its etiology is still indefinite. Some of pediatric surgeons described it as a kind of congenital malformation. In China, most thought it as an acquired disease caused by the infection of crypts of *Morgagni*^[1-7]. There are two main surgical procedures that are commonly adopted, transanal and perineal approach^[8-13].

MATERIALS AND METHODS

Patients

Ninety-six patients with an average age of four years and two mo, ranging from 6 mo to 14 years, were admitted and operated. Most patients came with the complaint of passing stool or flatus through vagina. Half of them had a history of perineal inflammation at the early life of 2-3 mo. An external opening

was usually found in the vestibule, a little bit right or left to the vaginal opening, while the internal opening was always found at the mid-point of the dentate line on the anterior anorectal wall. The diameter of fistula orifice ranged from 2 to 8 mm.

Preoperative preparation

Metronidazole tablet (30 mg/kg per day, divided t.i.d) and oral garamycina (15 mg/kg per day, divided t.i.d) were given before operation for 3 d. Nothing but water by mouth was allowed for 1 d before operation day. Enema was performed at the night before operation day and on the morning of the operation day.

Operative methods

Under general anesthesia, patient was laid in prone frog position, with knees and hips flexed at 90° fixed at the caudal end of the operation table, with a soft pillow placed under the pubis. Almost half roll of sterile bandage was inserted into rectum to prevent rectal discharge. The tail of bandage might be soaked with iodophor before being sent deeply into the rectum, and it was tied by a long heavy silk, which was left outside the anal orifice in order to make the removal of the bandage easily after operation. The anal opening was widely stretched bilaterally to expose the inner opening of fistula, four stay sutures were applied to four points at 3, 6, 9 and 12 o'clock respectively. The stay sutures were pulled, and a circular incision of mucosa around the inner opening of fistula was made by Bovie. The fistula was dissected toward the outer opening in the vestibule and resected. The wound of vestibule was sutured interruptedly with 5-0 Dexon. Usually fistula was about 0.8 cm long. The levator ani muscle was approximated longitudinally to abolish the dead space anterior to the rectum. The anorectal wall was freed proximally for about 1.0 cm to make the wound closed without tension. The packing bandage in rectum was pulled out after operation.

Postoperative treatment

Nothing but water by mouth was provided for 3 d after operation, and intravenous antibiotics were given 3 to 5 d. Perianal area was kept clean and dry by warm ventilation 3 to 5 times every day for some 5 d.

RESULTS

Six cases, about 6.25% of all patients, had recurrence of fistula. However, three of them healed spontaneously 2 to 3 wk later without any specific treatment except sitz bath with 30 g/L boric acid.

DISCUSSION

Bryndorf and Madsen reported rectovestibular fistula, a fistulous tract between the bowel and the low female genital tract, in 1960^[14]. The disease is more common in Asian than in Europeans. There were two controversial opinions about its etiology, the congenital or the acquired. Chatterjee *et al.*^[1-5] described rectovestibular fistula with normal anus in females as a kind of congenital malformation, double terminal of the alimentary tract. The family history, coexisting anomalies as

anal stenosis or sacral vertebrae abnormality and the stratified squamous epithelium lining of fistular wall were the basis favouring the congenital consideration. The inflammatory changes of fistula might be secondary.

Most doctors in China believe that the development of rectovestibular fistula with normal anus in small girls was similar to the inflammatory fistula-in-ano in males^[6-8]. The inflammation started by the infection of crypts of Morgagni, perianal abscess formation followed, and finally it ruptured through the vestibule. On the other hand, some deep crypts or anal glands cystoid dilatation as well as infantile hypoergic immunity of the rectoanal mucosa make the rectum mucosa barrier imperfect^[15-17]. All these might play a role in anal fistula formation. Certainly it was not the congenital double termination of the alimentary tract. None of patients had a definite history of fistula at birth, and neither did a surgical specimen show normal histology of mucosa, submucosa and continuous smooth muscle in the fistula tract.

Ninety-six females with acquired rectovestibular fistula were treated by transanal approach in the last 10 years with a satisfactory result. The main experience may be concluded as: (1) Rectal bandage packing may prevent stool contamination during operation. (2) Fistula should be dissected completely by Bovie to make a bloodless operation field. (3) Rectum and vagina should be separated clearly. (4) Anterior rectal wall should be sutured perfectly without tension. (5) Dead space anterior to rectum should be eliminated by suturing the levator ani muscles and central body.

The favorite age for operation ought to be 3 to 5 years in order to wait for the improvement of the symptoms and also for better development of perianal structures of the child.

Recurrence of fistula, if happened, often occurred about 7 d after operation, and its symptoms included perineal inflammation, followed by passing of stool or flatus through the sutured incision. By sitz bath in 30 g/L boric acid and waiting for inflammation subsiding, half of the patients with early recurrent fistula healed spontaneously.

Diverting colostomy provides a clean operation area for anal fistula repair^[11,12], but it needs at least three operations. We believe that a careful preoperative, operative and postoperative treatment offers a satisfactory result without a diverting colostomy.

REFERENCES

- 1 **Chatterjee SK**. Double termination of the alimentary tract-a second look. *J Pediatr Surg* 1980; **15**: 623-627
- 2 **Bagga D**, Chadha R, Malhotra CJ, Dhar A. Congenital H-type vestibuloanorectal fistula. *Pediatr Surg Int* 1995; **10**: 481-484
- 3 **Rintala RJ**, Mildh L, Lindahl H. H-type anorectal malformations: incidence and clinical characteristics. *J Pediatr Surg* 1996; **31**: 559-562
- 4 **Bianchini MA**, Fava G, Cortese MG, Vinardi S, Costantino S, Canavese F. A rare anorectal malformation: a very large H-type fistula. *Pediatr Surg Int* 2001; **17**: 649-651
- 5 **Yazici M**, Etensel B, Gürsoy H, Özksaçk S. Congenital H-type anovestibular fistula. *World J Gastroenterol* 2003; **9**: 881-882
- 6 **Zhang JZ**. Etiological and pathological study of fistula-in-ano in children. *Zhonghua Xiaerwaike Zazhi* 1988; **9**: 111-112
- 7 **Sun L**, Wang YX, Liu Y. Histopathological study of fistula-in-ano in female. *Zhonghua Xiaerwaike Zazhi* 1995; **16**: 136-137
- 8 **Chen YJ**, Niu ZY, Zhang JZ, Liu YT, Li L, Wang DY. Transperineal approach to repair acquired rectovestibular fistula in female. *Shiyong Erkelinchuang Zazhi* 2001; **16**: 242-243
- 9 **Tsugawa C**, Nishijima E, Muraji T, Satoh S, Kimura K. Surgical repair of rectovestibular fistula with normal anus. *J Pediatr Surg* 1999; **34**: 1703-1705
- 10 **Kulshrestha S**, Kulshrestha M, Prakash G, Gangopadhyay AN, Sarkar B. Management of congenital and acquired H-type anorectal fistulae in girls by anterior sagittal anorectovaginoplasty. *J Pediatr Surg* 1998; **33**: 1224-1228
- 11 **Mirza I**, Zia-ul-Miraj M. Management of perineal canal anomaly. *Pediatr Surg Int* 1997; **12**: 611-612
- 12 **Ismail A**. Perineal canal: a simple method of repair. *Pediatr Surg Int* 1994; **9**: 603-604
- 13 **Rao KL**, Choudhury SR, Samujh R, Narasimhan KL. Perineal canal-repair by a new surgical technique. *Pediatr Surg Int* 1993; **8**: 449-450
- 14 **Bryndorf J**, Madsen CM. Ectopic anus in the female. *Acta Chir Scand* 1960; **118**: 466-478
- 15 **Watanabe Y**, Todani T, Yamamoto S. Conservative management of fistula in ano in infants. *Pediatr Surg Int* 1998; **13**: 274-276
- 16 **Festen C**, van Harten H. Perianal abscess and fistula-in-ano in infants. *J Pediatr Surg* 1998; **33**: 711-713
- 17 **Rosen NG**, Gibbs DL, Soffer SZ, Hong A, Sher M, Pena A. The nonoperative management of fistula-in-ano. *J Pediatr Surg* 2000; **35**: 938-939

Edited by Zhu LH and Chen WW Proofread by Xu FM

Hepatitis B virus reactivation in a patient undergoing steroid-free chemotherapy

Daisuke Shimizu, Kenichi Nomura, Yosuke Matsumoto, Kyoji Ueda, Kanji Yamaguchi, Masahito Minami, Yoshito Itoh, Shigeo Horiike, Masuji Morita, Masafumi Taniwaki, Takeshi Okanoue

Daisuke Shimizu, Kenichi Nomura, Yosuke Matsumoto, Kyoji Ueda, Shigeo Horiike, Masafumi Taniwaki, Molecular Hematology and Oncology, Kyoto Prefectural University of Medicine Graduate School of Medical Science, Kyoto 602-0841, Japan

Kanji Yamaguchi, Masahito Minami, Yoshito Itoh, Takeshi Okanoue, Molecular Gastroenterology and Hepatology, Kyoto Prefectural University of Medicine Graduate School of Medical Science, Kyoto 602-0841, Japan

Masuji Morita, School of Nursing, Kyoto Prefectural University of Medicine Graduate School of Medical Science, Kyoto 602-0841, Japan

Masafumi Taniwaki, Clinical Molecular Genetics and Laboratory Medicine, Kyoto Prefectural University of Medicine Graduate School of Medical Science, Kyoto 602-0841, Japan

Correspondence to: Dr. Kenichi Nomura, Molecular Hematology and Oncology, Kyoto Prefectural University of Medicine Graduate School of Medical Science, Kawaramachi-Hirokoji, Kamigyo-Ku, Kyoto 602-0841, Japan. nomuken@sun.kpu-m.ac.jp

Telephone: +81-75-251-5521 **Fax:** +81-75-251-0710

Received: 2004-03-15 **Accepted:** 2004-04-09

Abstract

A 62-year-old Japanese man who was positive for hepatitis B surface antigen (HBsAg) and anti-HBe antibody, underwent chemotherapy for non-Hodgkin's lymphoma (NHL). Mutations were detected in the precore region (nt1896) of HBV. Because steroid-containing regimen may cause reactivation of hepatitis B virus (HBV) and hepatitis may progress to be fulminant after its withdrawal, we administered CHO (CPA, DOX and VCR) therapy and the patient obtained complete response. However, he developed acute exacerbation of hepatitis due to HBV reactivation. Recovery was achieved with lamivudine (100 mg/d) and plasma exchange. The present case suggests that acute exacerbation of hepatitis can occur with steroid-free regimen. Because the efficacy of the prophylactic use of lamivudine has been reported and the steroid enhances curability of malignant lymphoma, the steroid containing regimen with prophylaxis of lamivudine should be evaluated further.

Shimizu D, Nomura K, Matsumoto Y, Ueda K, Yamaguchi K, Minami M, Itoh Y, Horiike S, Morita M, Taniwaki M, Okanoue T. Hepatitis B virus reactivation in a patient undergoing steroid-free chemotherapy. *World J Gastroenterol* 2004; 10(15): 2301-2302

<http://www.wjgnet.com/1007-9327/10/2301.asp>

INTRODUCTION

CHOP regimen consisting of cyclophosphamide (CPA), doxorubicin (DOX), vincristine (VCR), and prednisolone (PSL) is performed as the first line therapy for non-Hodgkin's lymphoma (NHL) because of its high response rate and less incidence of side effect. However, CHOP regimen for hepatitis B virus (HBV) carrier may cause reactivation of HBV due to prednisolone and hepatitis may progress to be fulminant after its withdrawal. On the other hand, it has already been proven

that steroid containing-regimens show higher complete response and survival rate than steroid free regimens^[1]. Thus, it is difficult to choose which chemotherapeutic regimen for NHL carrying HBV.

We described an asymptomatic HBV carrier patient with NHL who received CHO therapy. Although he achieved complete response, hepatitis acutely exacerbated. Lamivudine and plasma exchange improved hepatic failure.

CASE REPORT

A 62-year-old man complained of tonsil swelling, redness and sore throat. He was referred to our hospital in August 2003. Needle biopsy from tonsil revealed him as having NHL (diffuse large B-cell lymphoma). He was admitted to our hospital on August 21 because tonsil swelling developed rapidly. Two enlarged cervical lymph nodes were palpable and right tonsil swelled. Hematological studies showed WBC 5 600/mL, Hb 15.4 g/dL and platelet $7.2 \times 10^4/\text{mm}^3$, LDH 167 IU/L, GOT 25 IU/L, GPT 15 IU/L, ALP 392 IU/L, Ch-E 163 IU/L, T-bil 1.82 mg/dL, prothrombin time (PT) 14.7 s, IL-2 receptor 564 U/mL, indocyanine green test (ICG) 25%. Serological tests showed HBsAg (+), HBeAg (-), HBeAb (+). HBV-DNA level was 4.7 LGE/mL (TMA method). Mutant virus having mutation at precore and core promoter region was detected by enzyme-linked mini-sequence assay (Smitest HBV Pre-C ELMA, Roche Diagnostics, Tokyo, Japan) and enzyme-linked specific probe assay (Smitest HBV core promoter mutation detection kit, Genome Science Laboratory, Tokyo, Japan). Ultrasonography revealed cirrhotic pattern of liver and mild splenomegaly. Neck magnetic resonance imaging revealed swelling of right tonsil and two cervical lymph nodes. Computed tomography scanning revealed no lymph node swelling in chest and abdomen. Bone marrow aspiration revealed involvement of abnormal lymphocytes. Thus, we diagnosed he was at stage IV.

He received first course of CHO regimen on August 22. Although tonsil swelling improved, liver dysfunction gradually developed after the third course. After the fourth course, liver dysfunction got severe, as serum LDH level was 499 IU/L, GOT 650 IU/L, GPT 422 IU/L, T-bil 1.49 mg/dL, PT 25.9 s and HBV-DNA level increased 6.2 LGE/mL. We diagnosed it as acute exacerbation of HBV and started both lamivudine (100 mg/d) and plasma exchange. Liver dysfunction improved gradually. In January 2004, hematological data improved as LDH 328 IU/L, GOT 98 IU/L, GPT 54 IU/L, T-bil 3.66 mg/dL, PT 19.6 s, HBV DNA 2.8 LGE/mL. He was following good clinical course and remained complete response for NHL.

DISCUSSION

It has been reported that steroid may induce exacerbation of hepatitis after cessation of steroid therapy or during tapering of steroid. Cheng *et al.* reported that 50 NHL patients carrying HBV were randomized to receive either ACE (epirubicin, CPA and etoposide) or PACE (prednisolone+ACE). The cumulative incidence of HBV reactivation was 38% and 73%, respectively. On the other hand, it is clear that PACE chemotherapy was

more effective than ACE arm in the treatment of NHL, because CR rate was 46% and 35%, overall survival rate at 46 mo was 68% and 36%, respectively^[1]. Thus, there is no consensus regarding the best therapy for NHL with HBV.

Regarding to HBV-DNA, cases with a point mutation from G to A at nucleotide 1896 of the precore region of HBV tended to develop fulminant hepatitis with steroid containing treatment^[2-5]. Because we detected the mutant HBV in peripheral blood before chemotherapy, we performed CHO regimen and obtained CR for NHL. However, hepatitis acutely exacerbated.

Recently, several reports have shown promising results for the prophylactic use of lamivudine in cancer patients before chemotherapy^[6-8]. However, we did not administer prophylaxis of lamivudine in the present patient, because (1) he was an asymptomatic HBV-carrier, (2) lamivudine-resistant virus might appear after lamivudine treatment or acute exacerbation after discontinuation of lamivudine, and (3) in Japan, adefovir dipivoxil was not available. Theoretically, the steroid containing regimen with lamivudine prophylaxis for NHL patients carrying HBV may be the best therapy. To prove the efficacy of this therapy, further studies are required.

REFERENCES

- 1 **Cheng AL**, Hsiung CA, Su JJ, Chen PJ, Chang MC, Tsao CJ, Kao WY, Uen WC, Hsu CH, Tien HF, Chao TY, Chen LT, Whang-Peng J. Steroid-free chemotherapy decreases risk of hepatitis B virus (HBV) reactivation in HBV-carriers with lymphoma. *Hepatology* 2003; **37**: 1320-1328
- 2 **Carman WF**, Jacyna MR, Hadziyannis S, Karayiannis P, McGarvey MJ, Makris A, Thomas HC. Mutation preventing formation of hepatitis B e antigen in patients with chronic hepatitis B infection. *Lancet* 1989; **2**: 588-591
- 3 **Sato T**, Kato J, Kawanishi J, Kogawa K, Ohya M, Sakamaki S, Niitsu Y. Acute exacerbation of hepatitis due to reactivation of hepatitis B virus with mutations in the core region after chemotherapy for malignant lymphoma. *J Gastroenterol* 1997; **32**: 668-671
- 4 **Dai MS**, Lu JJ, Chen YC, Perng CL, Chao TY. Reactivation of precore mutant hepatitis B virus in chemotherapy-treated patients. *Cancer* 2001; **92**: 2927-2932
- 5 **Skrabs C**, Muller C, Agis H, Mannhalter C, Jager U. Treatment of HBV-carrying lymphoma patients with Rituximab and CHOP: a diagnostic and therapeutic challenge. *Leukemia* 2002; **16**: 1884-1886
- 6 **Persico M**, De Marino F, Russo GD, Morante A, Rotoli B, Torella R, De Renzo A. Efficacy of lamivudine to prevent hepatitis reactivation in hepatitis B virus-infected patients treated for non-Hodgkin lymphoma. *Blood* 2002; **99**: 724-725
- 7 **Silvestri F**, Ermacora A, Sperotto A, Patriarca F, Zaja F, Damiani D, Fanin R, Baccarani M. Lamivudine allows completion of chemotherapy in lymphoma patients with hepatitis B reactivation. *Br J Haematol* 2000; **108**: 394-396
- 8 **Rossi G**, Pelizzari A, Motta M, Puoti M. Primary prophylaxis with lamivudine of hepatitis B virus reactivation in chronic HBsAg carriers with lymphoid malignancies treated with chemotherapy. *Br J Haematol* 2001; **115**: 58-62

Edited by Wang XL Proofread by Chen WW and Xu FM

Alverine citrate induced acute hepatitis

Mehmet Arhan, Seyfettin Köklü, Aydın S Köksal, Ömer F Yolcu, Senem Koruk, Irfan Koruk, Ertugrul Kayacetin

Mehmet Arhan, Seyfettin Köklü, Aydın S Köksal, Ömer F Yolcu, Senem Koruk, Irfan Koruk, Ertugrul Kayacetin, Kavaklik mah, Ahmet Apaydin cad, Sultan Apartment, No 39/7, Sahinbey 27060, Gaziantep, Turkey

Correspondence to: Dr. Irfan Koruk, Kavaklik mah, Ahmet Apaydin cad, Sultan Apartment, No 39/7, Sahinbey 27060, Gaziantep, Turkey. irfan_koruk@yahoo.com

Telephone: +90-342-3397615 **Fax:** +90-312-3124120

Received: 2004-02-20 **Accepted:** 2004-03-13

Abstract

Alverine citrate is a commonly used smooth muscle relaxant agent. A MEDLINE search on January 2004 revealed only 1 report implicating the hepatotoxicity of this agent. A 34-year-old woman was investigated because of the finding of elevated liver function tests on biochemical screening. Other etiologies of hepatitis were appropriately ruled out and elevated enzymes were ascribed to alverine citrate treatment. Although alverine citrate hepatotoxicity was related to an immune mechanism in the first case, several features such as absence of predictable dose-dependent toxicity of alverine citrate in a previous study and absence of hypersensitivity manifestations in our patient are suggestive of a metabolic type of idiosyncratic toxicity.

Arhan M, Köklü S, Köksal AS, Yolcu ÖF, Koruk S, Koruk I, Kayacetin E. Alverine citrate induced acute hepatitis. *World J Gastroenterol* 2004; 10(15): 2303-2304

<http://www.wjgnet.com/1007-9327/10/2303.asp>

INTRODUCTION

Toxic hepatitis is a liver injury caused by drugs and chemicals. The severity varies from nonspecific changes in liver functions such as abnormalities in liver enzymes to fulminant hepatic failure and cirrhosis. Its incidence has been increased over the past several decades. Drugs have been estimated to be responsible for 15-20% of all cases of fulminant and subfulminant hepatitis in Western countries and 18% of acute liver failure in the United States^[1,2].

Alverine citrate is a smooth muscle relaxant agent, commonly used in patients with irritable bowel syndrome in association with simethicone. Hepatotoxicity of alverine citrate is extremely rare and has been reported only in 1 patient before^[3]. Herein we report a new case of alverine citrate-induced hepatotoxicity occurred in a middle-aged woman that resolved completely after discontinuation of the drug.

CASE REPORT

On July 24, 2003, a 34-year-old woman was admitted to the Outpatient Clinic of Gastroenterology Department of Yuksek Ihtisas Hospital with the chief complaint of dyspepsia lasting for 2 years. She described bloating after meals and sometimes had gastroesophageal reflux symptoms. She did not have any chronic disease states. Physical examination was completely normal. Her biochemical tests including liver enzymes (AST, ALT, ALP and GGT) were all within normal limits. Upper

gastrointestinal endoscopy was performed showing grade I esophagitis and pangastritis. On July 29, omeprazole PO 20 mg bid, liquid alginate acid (Gaviscon) PO 10 mL qid (30 min after meal and at bedtime) and meteospasmyl (a tablet containing 60 mg alverine citrate and 300 mg simethicone) PO tid (before meals) were prescribed. Till the 14th d after prescription she told that she used all of the drugs as recommended. At that time omeprazole was ceased and she continued to medical treatment with Gaviscon and meteospasmyl.

She was admitted to another hospital because of arthralgia lasting for years on August 18, 2003, but therapy was managed on an outpatient basis. Amitriptyline 25 mg PO bid was added to Gaviscon and Meteospasmyl and a gastroenterology consultation was requested because of the finding of abnormal liver function test values on biochemical screening. On August 18, serum liver enzymes were as follows: ALT: 319 IU/L, AST: 211 IU/L (N: 40 IU/L for both); ALP: 184 IU/L (N: 35-129), GGT: 116 IU/L (N: 5-40) and normal direct and indirect bilirubin levels. She began to take amitriptyline on August 23 and readmitted to our hospital on August 26. Her ALT and AST levels were 1119 IU/L and 853 IU/L, respectively. Other biochemical tests such as, hemoglobin level, white blood cell count, platelet count, and prothrombin time were within normal limits. Hepatobiliary imaging with ultrasonography was normal. Viral markers for hepatitis including hepatitis A, B and C viruses, cytomegalovirus, Epstein-Barr virus, and herpes simplex virus were all negative. Autoantibodies (antinuclear, antimitochondrial, anti-smooth-muscle, anti-liver-kidney microsomal enzymes and anti-soluble liver antigen) were also negative. She denied taking any other medications and using alcohol or any herbal and folk remedies anytime. There were no known environmental issues that could be contributing.

Liver enzyme elevations were thought to be drug induced. Amitriptyline, Gaviscon and Meteospasmyl were all immediately discontinued on August 26. The ALT and AST values decreased to 597 IU/L and 237 IU/L 8 d after withdrawal of all drugs and became completely normal 18 d after cessation. The time course of liver function tests is presented in Table 1. Liver biopsy was not performed, and rechallenge with Meteospasmyl was not attempted because of ethical reasons. Since she had continuing mild symptoms related to gastroesophageal reflux, she continued to take Gaviscon and omeprazole without any increase in biochemical parameters.

Table 1 Time course of liver function tests

Date	AST (IU/L)	ALT (IU/L)	GGT (IU/L)	ALP (IU/L)
7/24/2003	30	32	21	162
8/18	211	319	116	184
8/26	853	1119	-	-
9/3	237	597	-	229
10/2	22	21	35	75

Omeprazole, alginate acid, and alverine citrate were started on 7/30/2003. Omeprazole was ceased on 8/10/2003. Amitriptyline was added to alginate acid and alverine citrate on 8/23/2003 and all medications were discontinued on 8/26/2003. ALP: Alkaline phosphatase; ALT: Alanine aminotransferase; AST: Aspartate aminotransferase; GGT: γ -glutamyl transferase.

DISCUSSION

Meteospasmyl is a most widely used drug for irritable bowel syndrome. It contains 60 mg alverine citrate and 300 mg simethicone. Simethicone has been used as an antifoaming agent and considered as an inert one^[4]. It is excreted via feces without any metabolizing in the gastrointestinal system. It has been widely used in patients with gastrointestinal gas and for the improvement of visibility during radiologic examination^[5]. To our knowledge, no systemic side effect regarding simethicone was reported in the literature.

Alverine is one of the papaverine congeners. Its antispasmodic effects are mediated by processes involving smooth muscle cells, extrinsic nervous system, and calcium channels^[6]. In humans, the drug is completely absorbed by the gastrointestinal tract and mainly metabolised in the liver, with negligible amounts excreted in the urine^[3]. Side effects such as flushing on the face and neck, nausea, headache, dizziness, and allergic skin eruptions may be observed. To our knowledge, hepatotoxicity associated with alverine use was reported once in the literature. Hepatotoxicity was not reported for the other papaverine derivatives other than trimebutine^[7].

In our patient increase in liver enzymes was ascribed to alverine treatment due to several reasons. There was a temporal relationship between alverine treatment and hepatitis. Liver function tests were normal before treatment and increases appeared three weeks after the start of alverine treatment. The timeline of exposure to alverine and initial observation of increase in liver function tests were consistent with drug-induced liver disease^[8]. Liver function tests completely normalized three weeks after withdrawal of the drug. Furthermore other etiologies of hepatitis (alcohol, steatohepatitis, autoimmune hepatitis and viral hepatitis) were appropriately ruled out. Omeprazole was not thought to be responsible for our patient's hepatitis in view of her prior uses of this drug without adverse effects. Neither chemical nor clinical side effects were seen in her consequent follow-up after alginic acid and omeprazole were started again. We therefore classified our case as probable alverine-induced hepatotoxicity according to the Naranjo probability scale^[9].

Drugs cause liver injury either via intrinsic toxicity (dose-dependent or predictable) or host idiosyncrasy (dose-independent or unpredictable). Idiosyncratic hepatotoxicity may be in metabolic or immunoallergic form. Metabolic-type idiosyncratic injury develops as a result of the susceptibility of rare individuals to hepatotoxicity from a drug that is usually safe at conventional doses. In this pattern, reactions would occur among susceptible individuals who possess an isolated genetic enzymatic alteration not expressed under normal conditions, which would become clinically apparent following the

administration of certain drugs^[10]. The mechanism of alverine induced liver disease is unknown. In the first case described in the literature alverine hepatotoxicity was related to immune mechanisms due to the presence of transient hypereosinophilia, eosinophil polymorphonuclear cells in the liver inflammatory infiltrates, and antinuclear autoantibodies. In our patient autoantibodies were negative and there was no hypereosinophilia in the peripheral blood smear. Several features such as the absence of predictable dose-dependent toxicity of alverine and fever, rash, and arthralgia (hypersensitivity manifestations) in our patient were consistent with a metabolic type of idiosyncratic toxicity.

In conclusion, alverine is a smooth muscle relaxant drug. This report presents the second case of alverine-associated possible liver toxicity. Alverine citrate should be included in the list of drugs causing toxic hepatitis.

REFERENCES

- 1 **Bernuau J**, Benhamou JP. Fulminant and subfulminant liver failure. In: Bircher J, Benhamou JP, McIntyre N, Rizzetto M, Rodes J, eds. *Oxford Textbook of Clinical Hepatology*, 2nd ed. *Oxford: Oxford University Press* 1999: 1341-1372
- 2 **Ostapowicz G**, Fontana RJ, Schiodt FV, Larson A, Davern TJ, Han SH, McCashland TM, Shakil AO, Hay JE, Hynan L, Crippin JS, Blei AT, Samuel G, Reisch J, Lee WM. U.S. Acute Liver Failure Study Group. Results of a prospective study of acute liver failure at 17 tertiary care centers in the United States. *Ann Intern Med* 2002; **137**: 947-954
- 3 **Malka D**, Pham B, Courvalin JC, Corbic M, Pessayre D, Erlinger S. Acute hepatitis caused by alverine associated with anti-lamin A and C autoantibodies. *J Hepatol* 1997; **27**: 399-403
- 4 **Brecevic L**, Bosan KI, Strajnar F. Mechanism of antifoaming action of simethicone. *J Appl Toxicol* 1994; **14**: 207-211
- 5 **Sudduth RH**, DeAngelis S, Sherman KE, McNally PR. The effectiveness of simethicone in improving visibility during colonoscopy when given with a sodium phosphate solution: a double-blind randomized study. *Gastrointest Endosc* 1995; **42**: 413-415
- 6 **Lemann M**, Coffin B, Chollet R, Jian R. Gut sensitivity: methodology for study in man and pathophysiological implications. *Gastroenterol Clin Biol* 1995; **19**: 270-281
- 7 **Bacq Y**, Vaillant L, Moneqier du Sorbier C. Severe erythema multiforme and hepatitis during treatment with trimebutine. *Gastroenterol Clin Biol* 1989; **13**: 522-523
- 8 **Lewis JH**. Drug-induced liver disease. *Med Clin of North Am* 2000; **84**: 1275-1311
- 9 **Naranjo CA**, Busto U, Sellers EM, Sandor P, Ruiz I, Roberts EA. A method for estimating the probability of adverse drug reactions. *Clin Pharmacol Ther* 1981; **30**: 239-245
- 10 **Farrell GC**. Liver disease caused by drugs, anesthetics, and toxins. In: Feldman M, Scharschmidt BF, Sleisenger MH, eds. *Sleisenger and Fordtran's gastrointestinal and liver disease*. 6th ed. *Philadelphia: W.B. Saunders Company* 1998: 1221-1253

Edited by Wang XL Proofread by Chen WW and Xu FM

Pregnant woman with fulminant hepatic failure caused by hepatitis B virus infection: A case report

Yue-Bo Yang, Xiao-Mao Li, Zhong-Jie Shi, Lin Ma

Yue-Bo Yang, Xiao-Mao Li, Zhong-Jie Shi, Lin Ma, Department of Obstetrics and Gynecology, Third Affiliated Hospital, Sun Yat-sen University, Guangzhou 510630, Guangdong Province, China

Correspondence to: Professor Xiao-Mao Li, Department of Obstetrics and Gynecology, Third Affiliated Hospital, Sun Yat-sen University, Guangzhou 510630, Guangdong Province, China. tigerlee777@163.net

Telephone: +86-20-85515609 **Fax:** +86-20-87565575

Received: 2004-02-21 **Accepted:** 2004-03-04

Abstract

AIM: To report the experience in successfully treating pregnant women with severe hepatitis.

METHODS: Comprehensive medical treatments were performed under strict monitoring.

RESULTS: Pregnant woman with severe hepatitis was successfully rescued.

CONCLUSION: Vital measures taken in the treatment of pregnant women with severe hepatitis include termination of the pregnancy at a proper time and control of various complications, such as disseminated intravascular coagulation (DIC), hepatorenal syndrome, hepatic encephalopathy and infection.

Yang YB, Li XM, Shi ZJ, Ma L. Pregnant woman with fulminant hepatic failure caused by hepatitis B virus infection: A case report. *World J Gastroenterol* 2004; 10(15): 2305-2306
<http://www.wjgnet.com/1007-9327/10/2305.asp>

INTRODUCTION

Hepatitis B virus (HBV) infection is common in China^[1], and it is one of the most common causes of severe hepatitis in pregnancy, with a high mortality rate of 43-80%^[2]. In this paper, we reported a pregnant woman with severe hepatitis B infection complicated by postpartum massive hemorrhage, hepatorenal syndrome, hepatic encephalopathy, spontaneous bacterial peritonitis and infection of biliary tract. Under strict monitoring, we applied comprehensive medical treatments. Both the mother and the child were discharged in healthy condition.

CASE REPORT

A 33-year-old pregnant woman was admitted in our hospital on April 15, 2003, presenting with a 38-week pregnancy, 10-d puffiness and yellow urine, and 3-d deep jaundice. She had a history of HBsAg(+), HBeAg(+) and HBcAb(+) for about 10 years, but her liver function had been normal until she got pregnant. The last menstrual period (LMP) was 2002-7-22. The expected date of confinement (EDC) was 2003-4-29. Physical examination showed she had normal vital signs, an urgent and painful looking, clear mind, icteric sclera and xanthochromia, bulbar conjunctiva edema, normal heart and

lung on auscultation, absence of abdominal tenderness or rebound tenderness, no detection of liver or spleen and no shifting dullness on palpation, moderate edema of both legs. Obstetrical conditions were as follows: she had left occipitoanterior position (LOP) of fetus, the height of fundus was 36 cm, the abdomen circumference was 99 cm, fetal heart rate (FHR) was 120 beats/min. No dilatation of cervix was found. Laboratory findings were as follows: aspartate transaminase (AST) was 125.0 U/L, alanine transaminase (ALT) was 138.0 U/L, albumin (ALB) was 32.5 g/L; total bilirubin (TB) was 383.9 μmol/L, blood urea nitrogen (BUN) was 36.03 mmol/L, creatinine (CREAT) was 402.6 μmol/L, white blood cell count (WBC) was 21.60×10⁹/L, hemoglobin (Hb) was 82 g/L, prothrombin time (PT) was 24 s, uric protein was (+++). β-ultrasonography showed her liver was in a chronic hepatitis state, and moderate ascites and a little liquid in both sides of thoracic cavity were also found. Markers of series of hepatitis virus were negative for hepatitis A, C, D and E, but positive for HBsAg (+), HBeAg (+) and HBcAb (+). Therefore she was diagnosed as pregnancy associated with hepatitis B infection and fulminant hepatic failure of pregnancy (FHFP).

After admission, the pregnant woman received supportive treatments. Later, because of "fetal distress", she received a cesarean section plus hysterectomy under general anesthesia. During the operation, we found yellow ascites of about 1 500 mL, and the same color of amniotic fluid was also found. The newborn was a mature male baby with normal vital signs, and transmitted to pediatrics department and given hepatitis B virus (HBV) specific immunoglobulin (HBIG) and HBV vaccine. After the delivery of placenta and membrane, there was no sign of uterine contraction, and massive hemorrhage occurred (about 2 000 mL). So hysterectomy was performed. The liver was obviously small, which was about the palm size and a little harder than normal.

After operation, the patient developed a clinical course of exacerbation. She developed hepatic encephalopathy of degree III, hepatorenal syndrome, spontaneous bacterial peritonitis, infection of biliary tract, secondary fungal infection, septicemia and prolonged healing of the wound. The comprehensive and well-designed rescue measures were taken and her condition was under control on June 25. After a hospitalization of 104 d, the patient and her newborn were discharged in generally good conditions.

DISCUSSION

Generally, a pregnant woman with fulminant hepatic failure refers to failure of liver function caused by viral hepatitis. Often the complications included disseminated intravascular coagulation (DIC) that presents a hemorrhage trend^[3,4], hepatic encephalopathy, hepatorenal syndrome, toxic intestinal tympanites, cerebral edema and infection of biliary tract, and so on. A pregnant woman with severe hepatitis often had hypodynamia, deep jaundice, hypocoagulability, hypoproteinemia, coma and acute renal failure. It was reported that many viruses including hepatitis virus (HAV, HBV, HCV, HDV, HEV, HGV, and so forth^[5,6]), cytomegalovirus (CMV), TTV^[7] and herpes virus^[8], could cause severe hepatitis. But HEV and HBV

infections were most frequent^[9-12]. Clinically, about 0.2-0.5% of total patients with hepatitis would develop into severe hepatitis. The prognosis of severe hepatitis during late pregnancy was so poor that it could be listed among the causes of maternity and parity mortality. In this report, the patient with a 10-year history of hepatitis had a 38-wk pregnancy. She developed severe hepatic dysfunction with hypocoagulability, hepatic encephalopathy and hepatorenal syndrome. She was positive for HBsAg, HBeAg, and HBcAb. Therefore the diagnosis of pregnancy associated with severe hepatitis and HBV infection was confirmed^[13,14]. Under strict monitoring, we took comprehensive therapeutic measures and got a successful result. The key points of rescuing the patient were as follows.

The general treatment included: (1) The patient was asked to have an absolute rest in bed with a diet low in lipid and protein^[15] and rich in fiber and vitamins. The total energy should be controlled at 1 500 kcal. Intra-gastrointestinal food could not only neutralize gastric acid, promote gastro-intestinal movement, but also reduce the incidence of toxic intestinal tympanites, endotoxemia, infection of biliary tract, peritonitis or even septicemia. (2) Protecting liver function, gastric membrane and preventing gastrointestinal hemorrhage. (3) Using antibiotics to prevent and treat infections, gamma globulin to promote immune state and neutralize endotoxins. HBIG, which can neutralize HBV and is relatively safe for gestational period, should also be used. (4) Maintaining the balance of body fluid and electrolytes and using dexamethasone for a short period of time (3-5 d) to improve the toxic symptoms and the maturity of fetal lung, thus getting ready for planned delivery.

To terminate pregnancy at a proper time, internal carotid artery cesarean was performed and a tube placed to detect the central vein pressure and determine the amount of transfusion, thus preventing the incidence of cerebral edema or pulmonary edema. Before cesarean section, colocolysis and atropine were used. But sedatives such as luminal were not taken into consideration. General anesthesia instead of epidural anesthesia was to avoid epidural hematoma^[16], and during cesarean section^[17], we chose longitudinal incision. After cesarean section, we performed hysterectomy and placed an absorbable hemostatic gauze on the cervical stump to reduce hemorrhage during and after operation. We also detected the size of liver during operation to make a general evaluation of its condition of direct prognosis. We perfused the abdomen cavity with iodophors to reduce abdominal infection. We remained a gastric tube during operation to prevent intestinal tympanites and to put in medicines that could improve the movement of intestine. After operation, we remained a drainage tube in abdomen to facilitate the expulsion of ascites and to inspect whether there was continuous hemorrhage.

To prevent and cure complications, measures were taken to reduce possible motivations such as using none or as few as sedatives and narcotics, to avoid too much or too fast diuretics or relieving of ascites, to prevent constipation or mass hemorrhage or infection, to adjust intestinal environment by lactulose towards pH<7 to reduce absorption of NH₃ and endotoxin which would exacerbate the condition of hepatic encephalopathy, to take metronidazole and norfloxacin to compress intestinal bacteria which could produce NH₃, to use colocolysis to accelerate the expulsion of intestinal bacteria and endotoxin and NH₃-removing medicines, to keep normal neurotransmitter by applying L-dopa or aceglutamide, to inject hepat amine intravenously to keep amino-acid balance, to use Chinese formulated medicines such as *Angong niuhuang wan*. Heparin in low dose was used to prevent dissipation of large amount of plot and thrombin factors and to improve clotting mechanism. Thrombin factors such as fresh frozen plasma,

plot, cryoprecipitate, pro- thrombin complex, and fibrinogen were used in a great quantity. Hepatorenal syndrome was treated by restricting the infusion of fluid, correcting hypoproteinemia and hypovolemia in time. Diuretics such as furosemide, diuretics complex (furosemide + dopamine + phentolamine) or mannitol + furosemide were used.

To promote regeneration of hepatocytes, glucagon and insulin were used to trigger the synthesis of hepatocyte DNA, human albumin was used to neutralize indirect bilirubin, stimulate regeneration of hepatocytes and prevent further necrosis of hepatocytes.

Blood routine, clotting function, liver function and biochemical indices, especially ALT, AST, alkaline phosphatase (AKP), acetylcholine esterase (CHE), alpha fetoprotein (AFP) and glucose (GLU) were monitored. Intensive nursing and sterile operation were performed, regular mouth care and clean of incision and perineum were maintained. 50% glucose + insulin was used to promote wound healing.

Before labor, HBIG or anti-HBV medicines (safe for both maternity and fetus) were given to interrupt intrauterine HBV infection^[1]. The newborn was also given HBIG and HB vaccine^[18] to build up active and passive immunity.

REFERENCES

- 1 **Li XM**, Yang YB, Hou HY, Shi ZJ, Shen HM, Teng BQ, Li AM, Shi MF, Zou L. Interruption of HBV intrauterine transmission: a clinical study. *World J Gastroenterol* 2003; **9**: 1501-1503
- 2 **Liu LC**, Shi JF, Feng PQ. Treatment for digestive emergencies. Beijing: *China Med Sci Technol Publish House* 1996: 162
- 3 **Tank PD**, Nandanwar YS, Mayadeo NM. Outcome of pregnancy with severe liver disease. *Int J Gynaecol Obstet* 2002; **76**: 27-31
- 4 **Xu H**. Analysis of 18 cases of postpartum haemorrhagic shock in pregnancy with virus hepatitis. *Zhonghua Fuchanke Zazhi* 1992; **27**: 150-152
- 5 **Khuroo MS**, Kamili S. Aetiology, clinical course and outcome of sporadic acute viral hepatitis in pregnancy. *J Viral Hepat* 2003; **10**: 61-69
- 6 **Duff P**. Hepatitis in pregnancy. *Semin Perinatol* 1998; **22**: 277-283
- 7 **Yan J**, Chen LL, Luo YH, Mao YF, He M. High frequencies of HGV and TTV infections in blood donors in Hangzhou. *World J Gastroenterol* 2001; **7**: 637-641
- 8 **Fink CG**, Read SJ, Hopkin J, Peto T, Gould S, Kurtz JB. Acute herpes hepatitis in pregnancy. *J Clin Pathol* 1993; **46**: 968-971
- 9 **Smith JL**. A review of hepatitis E virus. *J Food Prot* 2001; **64**: 572-586
- 10 **Coursaget P**, Buisson Y, N'Gawara MN, Van Cuyck-Gandre H, Roue R. Role of hepatitis E virus in sporadic cases of acute and fulminant hepatitis in an endemic area (Chad). *Am J Trop Med Hyg* 1998; **58**: 330-334
- 11 **Hussaini SH**, Skidmore SJ, Richardson P, Sherratt LM, Cooper BT, O'Grady JG. Severe hepatitis E infection during pregnancy. *J Viral Hepat* 1997; **4**: 51-54
- 12 **Molinie C**, Desrame J. Viral hepatitis E. *Med Trop* 1996; **56**: 285-288
- 13 **Hamid SS**, Jafri SM, Khan H, Shah H, Abbas Z, Fields H. Fulminant hepatic failure in pregnant women: acute fatty liver or acute viral hepatitis? *J Hepatol* 1996; **25**: 20-27
- 14 **Ochs A**. Acute hepatopathies in pregnancy: diagnosis and therapy. *Schweiz Rundsch Med Prax* 1992; **81**: 980-982
- 15 **Wienbeck M**. The treatment of hepatic emergencies. *Fortschr Med* 1979; **97**: 189-193
- 16 **Sato T**, Hashiguchi A, Mitsuse T. Anesthesia for cesarean delivery in a pregnant woman with acute hepatic failure. *Anesth Analg* 2000; **91**: 1441-1442
- 17 **Zhang ZJ**. Cesarean section in pregnancy complicated by severe hepatitis and heart disease. *Zhonghua Fuchanke Zazhi* 1990; **25**: 12-14
- 18 **Murata R**, Isshiki G, Yoshioka H, Chiba Y, Tada H, Koike M, Kimura M. Prevention of vertical transmission of hepatitis B virus by yeast recombinant hepatitis B vaccine. *Acta Paediatr Jpn* 1989; **31**: 180-185

ISI journal citation reports 2003 – GASTROENTEROLOGY AND HEPATOLOGY

Rank	Abbreviated journal title	ISSN	2003 Total cites	Impact factor	Immediacy index	2003 Articles	Cited Half-life
1	GASTROENTEROLOGY	0016-5085	46 174	12.718	2.810	316	6.9
2	HEPATOLOGY	0270-9139	30 844	9.503	1.574	296	5.5
3	SEMIN LIVER DIS	0272-8087	2 524	6.524	0.810	42	4.7
4	GUT	0017-5749	20 612	5.883	1.147	307	6.5
5	J HEPATOL	0168-8278	11 111	5.283	0.879	281	5.0
6	LIVER TRANSPLANT	1527-6465	2 944	4.242	0.621	211	2.9
7	AM J GASTROENTEROL	0002-9270	17 923	4.172	0.678	391	5.1
8	ALIMENT PHARM THERAP	0269-2813	60 32	3.529	0.573	372	3.9
9	AM J PHYSIOL-GASTR L	0193-1857	11 047	3.421	0.634	268	5.9
10	GASTROINTEST ENDOSC	0016-5107	10 047	3.328	1.798	331	4.8
11	WORLD J GASTROENTERO	1007-9327	2 387	3.318	0.345	632	2.4
12	J VIRAL HEPATITIS	1352-0504	1 320	3.258	0.386	70	4.0
13	ENDOSCOPY	0013-726X	4 238	3.227	0.349	152	5.5
14	INFLAMM BOWEL DIS	1078-0998	1 278	3.023	0.625	40	3.8
15	HELICOBACTER	1083-4389	798	2.624	0.426	68	3.6
16	NEUROGASTROENT MOTIL	1350-1925	848	2.500	0.333	66	3.7
17	DIS COLON RECTUM	0012-3706	8 130	2.343	0.191	256	7.6
18	SCAND J GASTROENTERO	0036-5521	7 271	2.140	0.118	238	7.6
19	LIVER	0106-9543	1 337	2.076		0	5.4
20	J GASTROINTEST SURG	1091-255X	1 236	1.881	0.430	142	3.6
21	PANCREAS	0885-3177	2 271	1.855	0.364	140	5.8
22	INT J COLORECTAL DIS	0179-1958	1 167	1.848	0.373	83	6.4
23	GASTROENTEROL CLIN N	0889-8553	1 517	1.684	0.019	54	6.7
24	PANCREATOLOGY	1424-3903	240	1.596	0.115	52	2.2
25	EUR J GASTROEN HEPAT	0954-691X	3 163	1.578	0.367	177	4.6
26	J CLIN GASTROENTEROL	0192-0790	3 215	1.564	0.484	155	7.2
27	J GASTROEN HEPATOL	0815-9319	3 171	1.530	0.254	193	4.5
28	DIGEST LIVER DIS	1590-8658	637	1.463	0.151	159	2.5
29	J PEDIATR GASTR NUTR	0277-2116	3 963	1.402	0.257	183	6.1
30	DIGESTION	0012-2823	2 193	1.399	0.091	55	7.7
31	DIGEST DIS SCI	0163-2116	9 149	1.387	0.144	347	7.9
32	CAN J GASTROENTEROL	0835-7900	813	1.265	0.134	82	3.9
33	J GASTROENTEROL	0944-1174	1 625	1.179	0.319	191	4.5
34	DIGEST DIS	0257-2753	534	1.151	0.031	32	5.7
35	Z GASTROENTEROL	0044-2771	918	1.076	0.112	116	5.4
36	ABDOM IMAGING	0942-8925	1 190	0.996	0.194	124	5.0
37	BEST PRACT RES CL GA	1521-6918	342	0.992	0.000	66	3.4
38	HEPATOL RES	1386-6346	406	0.991	0.168	155	2.6
39	GASTROEN CLIN BIOL	0399-8320	1 497	0.884	0.235	153	6.3
40	HEPATO-GASTROENTEROL	0172-6390	3 886	0.837	0.044	544	5.0
41	DIS ESOPHAGUS	1120-8694	354	0.809	0.027	75	4.7
42	ACTA GASTRO-ENT BELG	0001-5644	345	0.670	0.065	31	5.2
43	DIGEST SURG	0253-4886	548	0.619	0.114	79	4.2
44	CURR OPIN GASTROEN	0267-1379	300	0.598	0.050	60	3.9
45	REV ESP ENFERM DIG	1130-0108	255	0.348	0.211	57	6.0
46	CHIR GASTROENTEROL	0177-9990	74	0.157	0.039	76	
47	LIVER INT	1478-3231	4		0.053	75	

Citation indexes of Chinese scientific journals in 2003 (ISI JCR 2004)

Rank	Abbreviated journal title	2003 total cites	Impact factor	Index immediacy	2003 articles	Cited half-life
1	WORLD J GASTROENTERO	2 387	3.318	0.345	632	2.4
2	CHINESE J ASTRON AST	229	1.768	0.065	62	2.2
3	CELL RES	354	1.729	0.192	52	3.2
4	FUNGAL DIVERS	207	1.437	0.189	53	2.5
5	CHINESE PHYS	855	1.347	0.193	233	2.3
6	ACTA PHYS SIN ¹	2 410	1.130	0.172	586	2.9
7	CHINESE PHYS LETT	1 955	1.095	0.173	664	2.4
8	ACTA PETROL SIN ¹	444	1.078	0.067	89	4.0
9	ASIAN J ANDROL	188	1.064	0.140	57	2.6
10	ACTA GEOL SIN	467	1.040	0.457	46	4.4
11	EPISODES	411	1.020	0.056	36	7.0
12	ACTA PHARMACOL SIN	1 586	0.884	0.120	208	4.8
13	SCI CHINA SER D	737	0.801	0.272	151	3.8
14	CHEM J CHINESE U ¹	2 391	0.796	0.093	569	3.7
15	COMMUN THEOR PHYS	727	0.666	0.242	310	2.3
16	ACTA CHIM SINICA	1 375	0.643	0.105	381	3.9
17	BIOMED ENVIRON SCI	387	0.609	0.043	47	6.7
18	CHINESE SCI BULL	2 302	0.593	0.136	544	4.7
19	CHINESE J CHEM	578	0.592	0.118	255	2.7
20	ACTA MECH SINICA	270	0.587	0.043	70	6.2
21	CHINESE J STRUC CHEM ¹	319	0.548	0.039	152	3.3
22	CHINESE J CATAL	396	0.542	0.083	180	3.6
23	SCI CHINA SER B	838	0.541	0.069	72	9.2
24	CHINESE J INORG CHEM ¹	481	0.535	0.075	281	3.0
25	ACTA BIOCH BIOPH SIN ¹	386	0.524	0.053	190	3.7
26	CHINESE J ORG CHEM ¹	430	0.497	0.069	246	3.3
27	J RARE EARTH	263	0.486	0.049	144	3.6
28	ACTA PHYS-CHIM SIN ¹	516	0.468	0.093	257	3.2
29	ADV ATMOS SCI	231	0.449	0.069	101	4.3
30	SCI CHINA SER C	228	0.440	0.029	68	4.3
31	J UNIV SCI TECHNOL B	145	0.437	0.087	104	2.7
32	CHINA OCEAN ENG	95	0.413	0.119	59	
33	CHINESE MED J	1 245	0.393	0.081	431	6.0
34	ACTA MECH SOLIDA SIN	115	0.389	0.021	47	4.0
35	CHINESE J GEOPHYS ¹	278	0.375	0.038	133	4.4
36	CHEM RES CHINESE U	175	0.370	0.054	112	3.6
37	CHINESE J CHEM	172	0.357	0.062	145	3.0
38	J WUHAN UNIV TECHNOL	139	0.356	0.037	81	3.1
39	SCI CHINA SER E	210	0.355	0.028	72	3.8
40	ACTA POLYM SIN ¹	410	0.351	0.055	146	4.4
41	CHINESE ANN MATH B	169	0.343	0.019	52	5.4
42	CHINESE CHEM LETT	717	0.342	0.028	394	3.8
43	PROG NAT SCI	360	0.335	0.136	154	3.6
44	RARE METAL MAT ¹	435	0.329	0.149	262	3.1
45	T NONFERR METAL SOC	413	0.322	0.026	348	3.6
46	ACTA BOT SIN	712	0.321	0.063	222	5.3
47	PROG CHEM	121	0.319	0.045	66	3.9
48	J CENT SOUTH UNIV T	80	0.299	0.000	75	
49	SPECTROSC SPECT ANAL ¹	427	0.298	0.020	352	3.4
50	ACTA MATH SIN	327	0.297	0.041	49	6.6
51	HIGH ENERG PHYS NUC ¹	293	0.285	0.105	238	3.0
52	J MATER SCI TECHNOL	318	0.275	0.026	190	3.7
53	ALGEBR COLLOQ	106	0.274	0.038	52	5.9
53	RARE METALS	98	0.274	0.033	61	
55	J ENVIRON SCI-CHINA	137	0.255	0.014	140	4.3
56	APPL MATH MECH	422	0.251	0.086	152	5.1
57	SCI CHINA SER A	722	0.247	0.024	85	7.3
57	ACTA METALL SIN	569	0.247	0.097	258	4.8
57	J INORG MATER ¹	346	0.247	0.030	234	4.0
60	J IRON STEEL RES INT	40	0.245	0.000	43	
61	PROG BIOCHEM BIOPHYS ¹	206	0.241	0.048	145	3.0
62	CHINESE J ANAL CHEM ¹	971	0.224	0.036	389	5.2
63	J INFRARED MILLIM W	107	0.160	0.019	105	3.5
64	J COMPUT MATH	188	0.153	0.013	79	>10.0
65	CHINESE ASTRON ASTR	57	0.149	0.000	57	
66	J COMPUT SCI TECHNOL	50	0.140	0.040	99	
67	ACTA MATH SCI	119	0.127	0.000	50	>10.0

¹Chinese.

Impact factors and citation times of Chinese scientific journals covered by ISI JCR (2000-2003)

Abbreviated journal title	Impact factor				Citation time			
	2000	2001	2002	2003	2000	2001	2002	2003
ACTA BIOCH BIOPH SIN ¹	0.289	0.399	0.596	0.524	150	217	377	386
ACTA BOT SIN	0.434	0.284	0.376	0.321	698	516	1 336	712
ACTA CHIM SINICA ¹	0.435	0.530	0.536	0.643	844	990	1 298	1 375
ACTA GEOL SIN	1.000	0.271	0.531	1.040	323	234	316	467
ACTA MATH SCI			0.104	0.127			108	119
ACTA MATH SIN	0.234	0.324	0.407	0.297	212	275	299	327
ACTA MECH SINICA	0.575	0.734	0.726	0.587	180	242	265	270
ACTA MECH SOLIDA SIN	0.215	0.191	0.226	0.389	68	70	78	115
ACTA METALL SIN				0.247				569
ACTA PETROL SINICA ¹			0.534	1.078			289	444
ACTA PHARMACOL SIN	0.485	0.631	0.688	0.884	854	958	1 575	1 586
ACTA PHYS SIN ¹		0.657	1.182	1.130		1 227	2 277	2 410
ACTA PHYS SIN	0.210	0.369			100	176		
ACTA PHYS-CHIM SIN ¹	0.192	0.269	0.361	0.468	119	283	350	516
ACTA POLYM SIN		0.377	0.288	0.351		314	358	410
ADV ATMOS SCI		0.327	0.288	0.449		146	172	231
ALGEBR COLLOQ	0.089	0.188	0.150	0.274	25	84	94	106
APPL MATH MECH	0.166	0.155	0.199	0.251	250	267	354	422
ASIAN J ANDROL			0.827	1.064			99	188
BIOMED ENVIRON SCI	0.400	0.437	0.500	0.609	359	332	390	387
CELL RES		2.102	1.958	1.729		244	308	354
CHEM J CHINESE U ¹	0.590	0.904	0.830	0.796	1 421	1 959	2 189	2 391
CHEM RES CHINESE U	0.260	0.223	0.229	0.370	125	106	131	175
CHINA OCEAN ENG	0.137	0.206	0.196	0.413	24	46	41	95
CHINESE ANN MATH B	0.153		0.296	0.343	116		146	169
CHINESE ASTRON ASTR	0.164	0.144	0.181	0.149	49	47	60	57
CHINESE CHEM LETT	0.229	0.289	0.347	0.342	536	603	733	717
CHINESE J ANAL CHEM ¹		0.288	0.240	0.224		992	949	971
CHINESE J ASTRON AST			0.879	1.768		1	65	229
CHINESE J CATAL				0.542				396
CHINESE J CHEM	0.707	0.663	0.558	0.592	318	369	413	578
CHINESE J CHEM	0.124	0.223	0.222	0.357	55	101	117	172
CHINESE J GEOPHYS ¹	0.097	0.155	0.122	0.375	13	34	45	278
CHINESE J INORG CHEM ¹		0.301	0.494	0.535		141	280	481
CHINESE J ORG CHEM ¹		0.294	0.377	0.497		271	338	430
CHINESE J STRUCT CHEM ¹		0.184	0.324	0.548		168	260	319
CHINESE MED J ¹	0.107	0.108	0.182	0.393	752	807	909	1 245
CHINESE PHYS		0.828	1.185	1.347	39	200	542	855
CHINESE PHYS LETT	0.638	0.813	1.036	1.095	761	1 215	1 644	1 955
CHINESE SCI BULL	0.414	0.511	0.570	0.593	1 321	1 628	2 030	2 302
COMMUN THEOR PHYS	0.302	0.397	0.453	0.666	350	479	577	727
EPISODES				1.020				411
FUNGAL DIVERS				1.437				207
HIGH ENERG PHYS NUC ¹	0.264	0.324	0.248	0.285	225	271	248	293
J ASIAN NAT PROD RES	0.294	0.508			16	54		
J CENT SOUTH UNIV T			0.052	0.299			6	80
J COMPUT MATH	0.250	0.168	0.135	0.153	175	155	173	188
J COMPUT SCI TECHNOL			0.154	0.140			53	50
J ENVIRON SCI-CHINA				0.255				137
J INFRARED MILLIM W ¹	0.146	0.198	0.121	0.160	39	68	85	107
J INORG MATER ¹		0.131	0.222	0.247		77	260	346
J IRON STEEL RES INT	0.195	0.171	0.083	0.245	18	21	31	40
J MATER SCI TECHNOL	0.241	0.269	0.239	0.275	164	220	271	318
J RARE EARTH	0.125	0.236	0.287	0.486	57	117	147	263
J UNIV SCI TECHNOL B	0.118	0.099	0.397	0.437	38	37	100	145
J WUHAN UNIV TECHNOL	0.185	0.140	0.376	0.356	41	56	119	139
PROG BIOCHEM BIOPHYS ¹	0.077	0.112	0.160	0.241	95	109	140	206
PROG CHEM				0.319				121
PROG NAT SCI	0.249	0.288	0.264	0.335	167	279	309	360
RARE METAL MAT ENG ¹	0.242	0.319	0.225	0.329	103	151	223	435
RARE METALS		0.142	0.284	0.274		60	69	98
SCI CHINA SER A	0.309	0.340	0.295	0.247	528	627	682	722
SCI CHINA SER B	0.751	0.840	0.702	0.541	799	925	895	838
SCI CHINA SER C	0.291	0.396	0.358	0.440	155	171	180	228
SCI CHINA SER D	0.475	0.610	0.688	0.801	236	369	580	737
SCI CHINA SER E	0.309	0.376	0.412	0.355	91	140	197	210
SPECTROSC SPECT ANAL ¹		0.250	0.293	0.298		280	377	427
T NONFERR METAL SOC	0.294	0.340	0.293	0.322	221	306	374	413
WORLD J GASTROENTERO	0.993	1.445	2.532	3.318	327	722	1 535	2 387
TOTAL					13 557	20 957	28 866	35 842

¹Chinese.